UNIVERSITAT DE BARCELONA

Estudi teòric del magnetisme en cristalls moleculars: mecanismes d'interacció i empaquetament

Mercè Deumal i Solé

ADVERTIMENT. La consulta d'aquesta tesi queda condicionada a l'acceptació de les següents condicions d'ús: La difusió d'aquesta tesi per mitjà del servei TDX (**www.tdx.cat**) i a través del Dipòsit Digital de la UB (**diposit.ub.edu**) ha estat autoritzada pels titulars dels drets de propietat intel·lectual únicament per a usos privats emmarcats en activitats d'investigació i docència. No s'autoritza la seva reproducció amb finalitats de lucre ni la seva difusió i posada a disposició des d'un lloc aliè al servei TDX ni al Dipòsit Digital de la UB. No s'autoritza la presentació del seu contingut en una finestra o marc aliè a TDX o al Dipòsit Digital de la UB (framing). Aquesta reserva de drets afecta tant al resum de presentació de la tesi com als seus continguts. En la utilització o cita de parts de la tesi és obligat indicar el nom de la persona autora.

ADVERTENCIA. La consulta de esta tesis queda condicionada a la aceptación de las siguientes condiciones de uso: La difusión de esta tesis por medio del servicio TDR (**www.tdx.cat**) y a través del Repositorio Digital de la UB (**diposit.ub.edu**) ha sido autorizada por los titulares de los derechos de propiedad intelectual únicamente para usos privados enmarcados en actividades de investigación y docencia. No se autoriza su reproducción con finalidades de lucro ni su difusión y puesta a disposición desde un sitio ajeno al servicio TDR o al Repositorio Digital de la UB. No se autoriza la presentación de su contenido en una ventana o marco ajeno a TDR o al Repositorio Digital de la UB (framing). Esta reserva de derechos afecta tanto al resumen de presentación de la tesis como a sus contenidos. En la utilización o cita de partes de la tesis es obligado indicar el nombre de la persona autora.

WARNING. On having consulted this thesis you're accepting the following use conditions: Spreading this thesis by the TDX (**www.tdx.cat**) service and by the UB Digital Repository (**diposit.ub.edu**) has been authorized by the titular of the intellectual property rights only for private uses placed in investigation and teaching activities. Reproduction with lucrative aims is not authorized nor its spreading and availability from a site foreign to the TDX service or to the UB Digital Repository. Introducing its content in a window or frame foreign to the TDX service or to the UB Digital Repository is not authorized (framing). Those rights affect to the presentation summary of the thesis as well as to its contents. In the using or citation of parts of the thesis it's obliged to indicate the name of the author.

UNIVERSITAT DE BARCELONA. FACULTAT DE CIÈNCIES QUÍMIQUES

DEPARTAMENT DE QUÍMICA FÍSICA

Programa de Doctorat de Química Fonamental. Química Física

Bienni 1994-1996

ESTUDI TEÒRIC DEL MAGNETISME EN CRISTALLS MOLECULARS: MECANISMES D'INTERACCIÓ I EMPAQUETAMENT

per

MERCÈ DEUMAL i SOLÉ

Memòria presentada per a optar al grau de
Doctor en Ciències Químiques

Barcelona, Octubre del 1998

DIRECTOR DE LA TESI

Prof. Juan J. Novoa Vide

AUTORA

Mercè Deumal i Solé

CARLES MÜLLER i JEVENOIS, Cap del Departament de Química Física de la Universitat de Barcelona,

CERTIFICA :

que el treball "Estudi Teòric del Magnetisme en Cristalls Moleculars: Mecanismes d'Interacció i Empaquetament" que presenta Mercè Deumal i Solé, per tal d'aspirar al grau de Doctor en Ciències Químiques corresponent al programa de doctorat *"Química Fonamental: Química Física"* (bienni 1994-1996), ha estat realitzat en el Departament de Química Física de la Universitat de Barcelona.

Barcelona, octubre 1998

Dr. Carles Müller i Jevenois

Al Xavier

Als meus pares

(i a McConnell !)

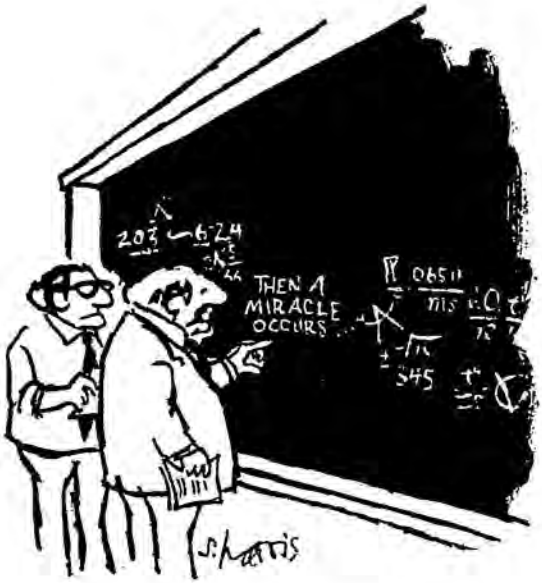

"I THINK YOU SHOULD BE MORE EXPLICIT HERE IN STEP TWO."

AGRAÏMENTS

"L'experiència ens demostra que l'obtenció d'una ferromagnetotesi no és una tasca fàcil.

La presència d'un director magnètic $\mu_{J,J}$ és la primera condició requerida perquè una tesi exhibeixi comportament magnètic. Ara bé, aquest $\mu_{J,J}$ haurà de ser persistent (tot i que moltes vegades es pot deslocalitzar) i formar agregats supraGEM² estables. Així doncs, una tesi molecular magnètica està constituïda per doctorands lliures, ions de mota's de transició, ions de terres rares *(majoritàriament, Robbi i Carmi) i lligands ICMABnètics.*

Una segona condició és que els moments magnètics μ de tots aquests constituents han d'interaccionar entre ells mateixos, via reunió directa, super-congrés, email indirecte, estada itinerant ...

I, un tercer requisit és que la disposició dels μ ha de ser tal que aquestes interaccions puguin propagar-se arreu de la tesi."

Voldria agrair a tots el fer possible l'obtenció d'aquesta ferromagnetotesi a una T_c prou alta com per poder estar escribint ara aquestes ratlles ...

Gràcies al "jef", el Juan, per haver sabut despertar la meva curiositat científica i haver guiat el meu spin i fer-me costat al llarg d'aquests quatre anys. Ell m'ha ensenyat la gran importància que *científicament* té l'art de la deslocalització, la dialèctica i la *diplomàcia*. Al Juan també li he d'agrair el fet d'haver estat el responsable de què, fa uns quants anyets, *photo*-interaccionés amb el Mike.

I'd like to thank Mike for giving me so many times the chance to work with him. Oops ... I must admit he's been the first person to teach me about the theory of the relativity : his world-wide known *"5 seconds"* is a relative concept, it never means less than 5 seconds, but it doesn't necessarily mean *"just"* 5 seconds ;) . I must thank Mike's group as well ... all of them have been really friendly with me.

Al Jaume i als seus nois els he de donar les gràcies per molts mals de cap estadístics i moltes bones estones en congressos.

Parlar de Fernando i de paciència sembla impossible, però ... jo li he d'agrair la *paciència* que ha tingut amb mi, no només en fer d'okupa del *seu* MAC mentre escribia aquesta

memòria, sinó també en totes aquelles ocasions en què les seves concises explicacions m'han solucionat més d'un problema.

Al Marc "the best", al Ramon "el surfista" i al Jesús, els he de donar gràcies per ampliar, de manera tant efectiva, el meu vocabulari *científic*. A ells tres, a la Carme "la Frau Rovira", a la Pilar "companya d'exili" i al Toni "l'home gol" els dec el bon ambient en què he estat treballant aquest temps i ... els cafès.

A tots els membres del Departament de Química Física, professors i *currantes*, els dec bones hores de ciència, de pràctiques i de *passadís*.

Al Raimon, als electrònics: en Pep, en Martí, el José Luís, el Sisco ... els he d'agrair la companyia a *l'hora* de dinar i les tertúlies.

Als Pyrex —amb una nova incorporació, la del Pau—, l'amistat.

A la Montserrat, a la Pilar i al Manel els vull donar gràcies per al seu recolzament incondicional i per les moltes pizzes que hem compartit.

To Dirk, Ulli, Ramón, Leti, Malar and Deepak thanks to be my King's family.

Als meus pares, Martí i Ma. Àngels, a la Montserrat, i a la iaia Antonieta els dec el ser com sóc i l'estar on estic. Bé, no es pot negar que el Xavier també té el seu mèrit ... ;)
Hmnn ... no ens oblidem de la família política, la Isa, el Manuel i el Carlos ...

Finalment, vull agrair al Sr. McConnell l'haver estat tant críptic en proposar el seu primer model ... sense ell, aquesta tesi no hauria estat el que és.

INDEX

INTRODUCCIÓ

Els materials magnètics són molt importants en el desenvolupament de la tecnologia actual. Durant molts anys, la recerca científica en magnetisme ha estat dirigida a l'estudi de les propietats magnètiques dels elements i dels seus aliatges en funció de la temperatura, amb l'objectiu d'optimitzar el cost i la densitat magnètica utilitzable tecnològicament. El progrés en aquest camp ha estat obstaculitzat pel fet que el magnetisme a nivell molecular no s'entén d'un manera adequada. Aquest és el motiu per al qual, avui en dia, hi ha una clara tendència a estudiar els fenòmens magnètics a nivell microscòpic. El per què d'aquesta tendència és molt senzill: si es controlessin els principis *moleculars* que regeixen el magnetisme, seria factible el disseny i la síntesi de nous materials magnètics.

La presència de moments magnètics és la primera condició requerida perquè un material exhibeixi comportament magnètic. Així doncs, un sòlid molecular magnètic pot estar format per radicals lliures, ions de metalls de transició, ions de terres rares i lligands diamagnètics. Qualsevol combinació d'aquests ingredients és possible, sempre i quan les entitats que són portadores d'spin siguin persistents, i els seus agregats supramoleculars siguin estables. Per aquest motiu, els ions de metalls de transició i de terres rares s'han de combinar amb lligands, magnètics o diamagnètics, per a ser un sistema molecular estable. Una segona condició és que aquests moments magnètics han d'interaccionar entre ells mateixos. I, un tercer requisit és que la seva disposició ha de ser tal que aquestes interaccions puguin propagar-se arreu del cristall. Així doncs, depenent de l'ordenament de les molècules i/o ions, les interaccions magnètiques donaran lloc a una rica varietat de fenòmens magnètics molt interessants com el ferromagnetisme [1], ferrimagnetisme [2], ferromagnetisme dèbil [3], metamagnetisme [4], i propietats de vidre d'spin [5].

Desenvolupament tecnològic, control molecular, síntesi ... obviament, el camp dels Materials Moleculars Magnètics és multidisciplinari. La Química Orgànica i Inorgànica s'encarrega de la síntesi d'aquests materials, la Física i Química Física contribueixen teòricament i experimental al seu estudi, i les Enginyeries participen en l'aplicació pràctica tecnològica dels nous materials. Els resultats obtinguts en aquesta àrea són molt prometedors, sobretot si es té en compte que és una àrea relativament jove. S'han obtingut materials magnètics purament orgànics, que presenten magnetització espontània per sota de certa temperatura crítica de l'ordre de 1-2K, i en alguns casos *bulk* ferromagnetisme [6]. Fins ara, les temperatures crítiques d'aquests materials són molt baixes. Per tant, actualment, la recerca està orientada al disseny racional de radicals persistents, els cristalls dels quals presentin un ordre ferromagnètic a temperatures crítiques més altes. D'altra banda, s'han aconseguit materials magnètics organometàl.lics que són ferromagnètics fins a temperatura ambient (per exemple, el cas dels derivats de les sals del blau de Prússia) [7].

També s'han sintetitzat materials amb propietats magneto-òptiques i magneto-superconductores mixtes [8].

Ara bé, d'entre tots els materials magnètics, el camp dels materials magnètics purament orgànics de base molecular [6] és el més interessant des del punt de vista teòric, donat el grau de control que s'ha assolit en la seva síntesi i a la dificultat per entendre el mecanisme de la seva interacció magnètica. Aquest tipus de materials combinaran les propietats innherents dels compostos orgànics amb propietats magnètiques. Així doncs, es podran usar en aparells òptics per manipular la llum polaritzada o com a interruptors magneto-òptics. D'altra banda, els materials orgànics són aïllants elèctrics, per tant, es podran sintetitzar magnets que no siguin conductors elèctrics. A més, seran fàcilment processables, donades les característiques de plasticitat, flexibilitat i solubilitat que presenten els compostos orgànics/polimèrics. També cal destacar les possibles aplicacions biomèdiques, per exemple com a agents de contrast selectiu en RMN o per dirigir l'aplicació de certs medicaments.

Totes aquestes propietats i possibles aplicacions van motivar l'estudi d'una de les famílies de compostos més interessants i millor documentades en el camp del ferromagnetisme orgànic: la família dels derivats *α-nitronil nitròxid* [9]. La seva fòrmula general és

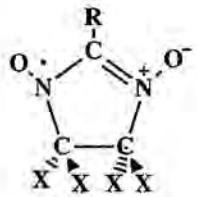

on R és un grup funcional que pot ser des d'un àtom d'hidrogen fins a grups aromàtics substituïts, i X és un grup metil (no s'han aconseguit estabilitzar els radicals amb grups més petits). Totes aquestes molècules tenen electrons desaparellats (en general, són doblets), fet que permetrà que, en agrupar-se formant un sòlid, aquest sòlid pugui presentar magnetisme. Depenent de com s'agrupin, l'estat electrònic resultant serà d'alt spin (ferromagnètic) o de baix spin (antiferromagnètic). Així doncs, l'empaquetament cristal.lí d'aquests radicals lliures persistents *decidirà* si les interaccions ferromagnètiques intermoleculars es poden propagar arreu del cristall [10, 11]. En conseqüència, el primer objectiu d'aquest treball ha estat posar a punt un procediment sistemàtic per racionalitzar l'estructura de qualsevol cristall molecular. Aquesta racionalització implica, alhora, un estudi adequat a nivell MP2 [12] de l'energia d'interacció dels contactes intermoleculars existents dins dels cristalls.

En el Capítol 1 es proposa un procediment qualitatiu sistemàtic, l'anàlisi de l'empaquetament cristal.lí en base als seus grups funcionals (CPFGA), per tal d'identificar i caracteritzar energèticament les estructures primària, secundària i d'ordre superior de qualsevol cristall molecular. El tractament CPFGA —seguit en tota racionalització de l'empaquetament d'un cristall— està descrit en els articles 1, 2, 3a, 4 i 6a. La seva aplicació s'exemplificarà racionalitzant l'empaquetament cristal.lí experimental del 2-hidro nitronil nitròxid, l'HNN [13], en la seva fase α (articles 1 i 2). Finalment, s'estudiarà l'empaquetament de les fases α i β de l'HNN i la transició cristal.lina d'α a β, per tal de justificar la irreversibilitat d'aquesta transició (articles 5 i 4).

Un cop familiaritzats amb el procediment CPFGA de racionalització de l'empaquetament de cristalls moleculars, estudiarem com es pot interpretar el magnetisme en aquest tipus de cristalls. D'entre tots els models qualitatius de predicció de propietats magnètiques, ens hem centrat en el model de McConnell-I (basat en densitats d'spin) [14] perquè, donada la seva simplicitat, és el més usat. Segons aquest model, les propietats magnètiques dels cristalls de radicals α-nitronil nitròxid es racionalitzen generalment en funció dels contactes NO···ON i NO···C(sp^2) més curts presents entre els grups ONCNO de l'anell de 5 membres, degut a què la major part de la distribució electrònica d'spin hi està localitzada. Altres autors, en canvi, han proposat la utilització de contactes H···ON en la racionalització del magnetisme [15]. En el Capítol 2, aquest model s'aplicarà per a predir el caràcter ferro- o antiferromagnètic de cinc cristalls de la família dels α-nitronil nitròxids (en l'article 6c se n'estudien dos) amb l'objectiu de comprovar la validesa del model de McConnell-I. D'aquesta aplicació en resulten algunes inconsistències en quan a la predicció del comportament magnètic dels cinc cristalls estudiats. Aquest fet questiona la validesa del model de McConnell-I, i en motiva un estudi més detallat. L'aplicabilitat del primer model proposat per McConnell per tal de racionalitzar la naturalesa de les interaccions magnètiques en cristalls moleculars purament orgànics s'estudiarà en els Capítols 3, 4 i 5.

En el Capítol 3 es presentarà la comparació formal del model de McConnell-I amb una implementació rigorosa de l'Hamiltonià d'spin de Heisenberg en un espai VB (article 7). En aquest capítol, usant l'Hamiltonià de Heisenberg rigorós implementat en el mètode MMVB (Molecular Mechanics - Valence Bond) [16], es duran a terme càlculs numèrics amb un dels exemples més usats per a exemplificar la correcta predicció del magnetisme per part del model de McConnell-I. Així doncs, s'estudiarà l'estabilitat singlet / quintet en el cas dels isòmers pseudo-orto-, -meta- i -para-bis(fenilmetilenil)[2.2]paraciclofans [17] (simulats amb els estats singlet / triplet dels corresponents isòmers bis(metil)[2.2]paraciclofans).

D'altra banda, un dels punts més importants en l'estudi de cristalls moleculars ferromagnètics és poder reconèixer els possibles ordenaments relatius de dues molècules

veïnes que donin lloc a interaccions intermoleculars ferro- o antiferromagnètiques. Així doncs, paral.lelament a l'estudi teòric dut a terme en el Capítol 3, s'ha realitzat una anàlisi estadística de cristalls α-nitronil nitròxids amb propietats ferro- o antiferromagnètiques ben caracteritzades. L'objectiu d'aquesta anàlisi (Capítol 4) és poder associar l'existència d'estructures primàries específiques d'aquests cristalls amb interaccions dominants ferro- o antiferromagnètiques (articles 8, 9 i 3b). Segons McConnell-I, contactes curts NO···ON intermoleculars estan associats a interaccions antiferromagnètiques. Per tant, en aquest capítol interessarà definir el rol magnètic que realment tenen aquest tipus de contactes en compostos de la família dels α-nitronil nitròxids. Tanmateix, amb aquest estudi també es pretén comprovar el valor de qualsevol correlació magneto-estructural feta examinant aquests contactes individualment. Finalment, s'estudiarà si el comportament magnètic d'aquests cristalls depèn d'interaccions del tipus C-H···ON [15]. Així doncs, aquesta anàlisi estadística servirà per tal de comprovar de manera exhaustiva si hi ha orientacions característiques de grups funcionals que es poden associar unívocament a interaccions ferro- o antiferromagnètiques.

Finalment, en el Capítol 5 es presentaran els resultats de l'estudi ab initio CASSCF [18] dut a terme amb sistemes simples amb uns contactes intermoleculars que tenen un comportament magnètic *"pre-assignat"*, d'acord amb el model de McConnell-I (article 10). Els sistemes escollits són el dímer d'H_2NO i del sistema radicalari metil-allil perquè, segons McConnell-I, tindran caràcter antiferro- i ferromagnètic, respectivament. D'altra banda, el càlcul de l'estabilitat singlet / triplet en el dímer del 3-OHPNN —el qual ha estat aïllat experimentalment [19]— permetrà comprovar la idoneïtat del mètode DFT [20] en reproduir la constant d'acoblament magnètic J. Finalment, es proposaran diferents sistemes model per estudiar els dímers dels dos cristalls obtinguts amb l'anàlisi estadística del Capítol 4 [21] que presentaven els contactes O···O més curts. Amb aquests càlculs es vol fer una estimació de la J d'aquests dos dímers a nivell ab initio CASSCF i DFT.

ARTICLES

Article 1
M. Deumal, J. Cirujeda, J. Veciana, M. Kinoshita, Y. Hosokoshi, J.J Novoa
"Theoretical Analysis of the Crystal Packing of Nitronyl Nitroxide Radicals : The Packing of the α-2-hydro nitronyl nitroxide radical", *Chem. Phys. Lett.*, **1997**, *265*, 190-199.

Article 2
J.J Novoa, M. Deumal
"Theoretical Analysis of the Packing and Polimorphism of Molecular Crystals using Quantum Mechanical Methods: The Packing of the 2-hydro nitronyl nitroxide", *Mol. Cryst. Liq. Cryst.* **1997**, *305*, 143-156.

Article 3a (pp. 3-8); *3b* (pp. 9-18)
J. Veciana, J.J Novoa, M. Deumal, J. Cirujeda
"Supramolecular Architectures and Magnetic Interactions in Crystalline α-Nitronyl Nitroxide Radicals", *Magnetic Properties of Organic Materials*, P. Lahti (ed.), Marcel Dekker, New York (**1998**). (en premsa)

Article 4
J.J Novoa, M. Deumal, J. Veciana
"Architecture of Purely Organic Molecular Magnets : Crystal Packing Rationalization of some α-Nitronyl Nitroxides using the Crystal Packing Functional Group Analysis", *Synthetic Met.*, **1998** (en premsa). (acceptat, comunicació congrés invitada)

Article 5
J.J. Novoa, M. Deumal, M. Kinoshita, Y. Hosokoshi, J. Veciana, J. Cirujeda
"A Theoretical Analysis of the Packing and Polymorphism of the 2-hydro nitronyl nitroxide Crystal", *Mol. Cryst. Liq. Cryst.*, **1997**, *305*, 129-141.

Article 6a (pp. 3-11); *6b* (pp. 11-16); *6c* (pp. 16-17)
J.J. Novoa, J. Veciana, M. Deumal
"Crystal Engineering of Purely Organic Molecular Magnets : What Ab Initio Computations can tell us?", *Supramolecular Engineering of Synthetic Materials : Conductors and Magnets*. J. Veciana (ed.) Kluwer, Dordrecht (**1998**). (pg. 105-126)

Article 7
M. Deumal, J.J. Novoa, M.J. Bearpark, P. Celani, M. Olivucci, M.A. Robb
"On the Validity of the McConnell-I Model of Ferromagnetic Interactions : The [2.2]paracyclophane Example", *J. Phys. Chem.*, **1998** (en premsa)

Article 8
M. Deumal, J. Cirujeda, J. Veciana, J.J. Novoa
"Structure-Magnetism Relationships in α-Nitronyl Nitroxide Radicals : Pitfalls and Lessons to be learned", *Adv. Mater.* **1998** (en premsa)

Article 9
M. Deumal, J. Cirujeda, J. Veciana, J.J. Novoa
"Structure-Magnetism Relationships in α-Nitronyl Nitroxide Radicals", *Chem. Eur. J.* **1998** (enviat)

Article 10
J.J. Novoa, M. Deumal, P. Lafuente, M.A. Robb
"Does the McConnell-I Model really work?. An Ab Initio Study of the Magnetic Character of some Intermolecular Contacts", *Mol. Cryst. Liq. Cryst.*, **1998** (acceptat, comunicació congrés invitada)

BIBLIOGRAFIA

[1] (a) M. Tamura, Y. Nakazawa, D. Shiomi, K. Nozawa, Y. Hosokoshi, M. Ishikawa, M. Takahashi, M. Kinoshita, *Chem. Phys. Lett.* **1991**, *186*, 401; (b) R. Chiarelli, M.A. Novak, A. Rassat, J.L. Tholence, *Nature* **1993**, *363*, 147; (c) A. Caneschi, F. Ferraro, D. Gatteschi, A. le Lirzin, M. Novak, E. Rentscher, R. Sessoli, *Adv. Mater.* **1995**, *7*, 476; (d) T. Nogami, T. Ishida, H. Tsuboi, H. Yoshikawa, H. Yamamoto, M. Yasui, F. Iwasaki, H. Iwamura, N. Takeda, M. Ishikawa, *Chem. Lett.* **1995**, 635; (e) F.M. Romero, R. Ziessel, M. Drillon, J.L. Tholence, C. Paulsen, N. Kyritsakas, J. Fisher, *Adv. Mater.* **1996**, *8*, 826; (f) J. Cirujeda, M. Mas, E. Molins, F.L. de Panthou, J. Laugier, J.G. Park, C. Paulsen, P. Rey, C. Rovira, J. Veciana, *J. Chem. Soc., Chem. Commun.* **1995**, 709.

[2] (a) A. Izuoka, M. Fukada, R. Kumai, M. Itakura, S. Hikami, T. Sugawara, *J. Am. Chem. Soc.* **1994**, *116*, 2609; (b) A. Izuoka, R. Kumai, T. Sugawara, *Adv. Mater.* **1995**, *7*, 672; (c) D. Shiomi, M. Nishizawa, K. Sato, T. Takui, K. Itoh, H. Sakurai, A. Izuoka, T. Sugawara, *J. Phys. Chem. B* **1997**, *101*, 3342.

[3] (a) S. Mitra, A.K. Gregson, W.E. Hatfield, R.R. Weller, *Inorg. Chem.* **1983**, *22*, 1729; (b) A.J. Banister, N. Bricklebank, I. Lavender, J.M. Rawson, C.I. Gregory, B.K. Tanner, W. Clegg, M.R.J. Elsegood, F. Palacio, *Angew. Chem. Int. Ed. Engl.* **1996**, *35*, 2533; (c) P. Yu, O. Kahn, M.A. Aebersold, L. Ouahab, F. Le Berre, L. Pardi, J.L. Tholence, *Adv. Mater.* **1994**, *6*, 681.

[4] (a) G. Chouteau, C. Veyret-Jeandey *J. Phys. (Paris)* **1981**, *42*, 1441; (b) G.A. Candela, L. Swartzendruber, J.S. Miller, M.J. Rice, *J. Am. Chem. Soc.* **1979**, *101*, 2755.

[5] P. Zhou, B.G. Morin, J.S. Miller, A.J. Epstein, *Phys. Rev. B* **1993**, *48*, 1325.

[6] (a) ref. 1a. (b) P.M. Allemand, K.C. Khemani, A. Koch, F. Wudl, K. Holczer, S. Donovan, G. Grüner, J.D. Thompson, *Science*, **1991**, *253*, 301. (c) ref. 1b. (d) O. Kahn, *Molecular Magnetism*, VCH Publishers, New York, **1993**. (e) T. Sugawara, M.M. Matsushita, A. Izuoaka, N. Wada, N. Takeda, M. Ishikawa, *J. Chem. Soc., Chem. Commun.*, **1994**, 1081. (f) ref. 3c. (g) J.S. Miller, A.J. Epstein, *Angew. Chem. Int. Ed. Engl.* **1994**, *33*, 385. (h) M. Kinoshita, *Jpn. J. Appl. Phys.* **1994**, *33*, 5718. (i) ref. 1f. (j) ref. 1c. (k) K. Togashi, K. Imachi, K. Tomioka, H. Tsuboi, T. Ishida, T. Nogami, N. Takeda, M. Ishikawa, *Bull. Chem. Soc. Jpn.* **1996**, *69*, 2821. (l) E. Coronado, P. Delhaes, D. Gatteschi, J.S. Miller, (eds.) *Molecular Magnetism: From Molecular Assemblies to Devices*, Kluwer Academic Publishers, Dordretch, **1996**. (m) O. Kahn, (ed.) *Magnetism: A Supramolecular Function*, Kluwer Academic Publishers, Dordretch, **1996**. (n) K. Itoh, J.S. Miller, T. Takui, (eds.) *Mol. Cryst. Liq. Cryst.* **1997**, *305/306*, 1-586/1-520.

[7] (a) S. Ohkoshi, T. Iyoda, A. Fujishima, K. Hashimoto, *Phys. Rev. B - Conds. Matter*, **1997**, *56*, 11642; (b) Z.Z. Gu, O. Sato, T. Iyoda, K. Hashimoto, A. Fujishima, *Chem. Mat.* **1997**, *9*, 1092.

[8] (a) F. Manders, K.J. Veenstra, A. Kirilyuk, T. Rasing, H.A.M. Vandenberg, N. Persat, *IEEE Trans. Magn.* **1998**, *34*, 855; (b) B. Briat, T.V. Panchenko, H.B. Rjeily, A. Hamri, *J. Opt. Soc. Am. B - Opt. Phys.* **1998**, *15*, 2147; (c) I. Felner, U. Asaf, *Physica C*, **1997**, *292*, 97.

[9] α-Nitronil nitròxid és el nom abreviat més àmpliament usat per indicar 4,4,5,5-tetrametil-4,5-dihidro-1*H*-imidazol-1-oxil-3-*N*-òxid, el nom correcte segons la IUPAC.

[10] En general, *bulk* ferromagnetisme requereix la presència d'interaccions ferromagnètiques al llarg de tres (o dues) direccions del sòlid, depenent de si l'anisotropia magnètica és baixa o alta. Donat que els radicals lliures orgànics tenen una anisotropia magnètica molt petita, la presència d'interaccions ferromagnètiques en tres dimensions és un requisit per tal d'assolir *bulk* ferromagnetisme. Consultar: F. Palacio, *From Ferromagnetic Interactions to Molecular Ferromagnets: An Overview of Models and Materials*, pg. 1-40 (Eds.: D. Gatteschi, O. Kahn, J.S. Miller, F. Palacio, in "*Magnetic Molecular Materials*"), Kluwer Academic Publishers : Dorderecht, **1991**.

[11] La no compensació dels moments magnètics dels spins acoblats antiferromagnèticament pot també produir un moment magnètic net —*spin canting*— que, quan es propaga arreu del sòlid, produeix una magnetització espontània. Per a un exemple recent, consultar ref. 3b.

[12] (a) C. Møller, M.S. Plesset, *Phys. Rev.* **1934**, *46*, 61. (b) M. Head-Gordon, J.A. Pople, M.J. Frisch, *Chem. Phys. Lett.* **1988**, *153*, 503. (c) S. Saebo, J. Almlof, *ibid.* **1989**, *154*, 83. (d) M.J. Frisch, M. Head-Gordon, J.A. Pople, *ibid.* **1990**, *166*, 281. (e) M. Head-Gordon, T. Head-Gordon, *ibid.* **1994**, *220*, 122.

[13] (a) D.G.B. Boocock, R. Darey, E.F. Ullman, *J. Am. Chem. Soc.*, **1968**, *90*, 5945; (b) Y. Hosokoshi, M. Tamura, K. Nozawa, S. Suzuki, H. Sawa, R. Kato, M. Kinoshita., *Mol. Cryst. Liq. Cryst.*, **1995**, *115*, 271; (c) E. Molins, resultats no publicats (refinament posterior a 13b de l'estructura β-HNN); (d) J. Cirujeda, Tesi Doctoral, Univ. Ramon Llull, **1997**.

[14] H.M. McConnell, *J. Chem. Phys.*, **1963**, *39*, 1910.

[15] Consultar: (a) J. Veciana, J. Cirujeda, C. Rovira, J. Vidal-Gancedo, *Adv. Mater.* **1995**, *7*, 221. (b) J. Cirujeda, E. Hernàndez, C. Rovira, P. Turek, J. Veciana, *New Organic Magnetic Materials. The Use of Hydrogen Bonds as a Crystalline Design Element of Organic Molecular Solids with Intermolecular Ferromagnetic Interactions*, pp 262-272, in "*New Organic Materials*", (Eds.: C. Seoane, N. Martin); Universidad Complutense de Madrid: Madrid, **1994**. (c) J. Cirujeda, E. Hernàndez, C. Rovira, J.-L. Stanger, P. Turek, J. Veciana, *J. Mater. Chem.* **1995**, *5*, 243-252. (d) J. Cirujeda, E. Hernàndez, C. Rovira, J.-L. Stanger, P. Turek, J. Veciana, *J. Mater. Chem.* **1995**, *5*, 243-252. (e) J. Cirujeda, C. Rovira, J.-L. Stanger, P. Turek, J. Veciana, *The Self-Assembly of Hydroxylated Phenyl a-Phenyl Nitronyl Nitroxide Radicals*, pp 219-248, in "*Magnetism. A Supramolecular Function*"; (Ed.: O. Kahn); Kluwer Academic Publishers: Amsterdam, **1996**. (f) J. Cirujeda, E. Hernàndez, F. Lanfranc de Panthou, J. Laugier, M. Mas, E. Molins, C. Rovira, J.-J. Novoa, P. Rey, J. Veciana, *Mol. Cryst. Liq. Cryst.* **1995**, *271*, 1-12.

[16] (a) M.J. Bearpark, F. Bernardi, M. Olivucci, M.A. Robb, *Chem. Phys. Lett.*, **1994**, *217*, 513; (b) F. Bernardi, M. Olivucci, J.J. McDouall, M.A. Robb, *J. Chem. Phys.*, **1988**, *89*, 6365; (c) F. Bernardi, M. Olivucci, M.A. Robb, *J. Am. Chem. Soc.*, **1992**, *114*, 1606.

[17] (a) C.J. Brown, *J. Chem. Soc.*, **1953**, 326;. (b) K. Lonsdale, H.J. Milledge, K.V.K. Rao, *Proc. R. Soc. London, Ser. A*, **1960**, *555*, 82; (c) D.J. Cram, J.M. Cram, *Acc. Chem. Res.*, **1971**, *4*, 204. (d) A. Izuoka, S. Murata, T. Sugawara, H. Iwamura, *J. Am. Chem. Soc.*, **1985**, *107*, 1786; (e) A. Izuoka, S. Murata, T. Sugawara, H. Iwamura, *ibid.*, **1987**, *109*, 2631.

[18] (a) D. Hegarty, M.A. Robb, *Mol. Phys.* **1979**, *38*, 1795. (b) R.H.E. Eade, M.A. Robb, *Chem. Phys. Lett.* **1981**, *83*, 362. (c) H.B. Schlegel, M.A. Robb, *ibid.* **1982**, *93*, 43. (d) F. Bernardi, A. Bottini, J.J.W. McDougall, M.A. Robb, H.B. Schlegel, *Far. Symp. Chem. Soc.* **1984**, *19*, 137. (e) M.J. Frisch, I.N. Ragazos, M.A. Robb, H.B. Schlegel, *Chem. Phys. Lett.* **1992**, *189*, 524.

[19] J. Veciana et al., resultats no publicats.

[20] (a) P. Hohenberg, W. Kohn, *Phys. Rev.* **1964**, *136*, B864. (b) W. Kohn, L.J. Sham, *Phys. Rev.* **1965**, *140*, A1133. (c) R.G. Parr, W. Yang, *Density-functional theory of atoms and molecules*, Oxford Univ. Press : Oxford, **1989**.

[21] (a) LICMIT: T. Sugawara, M.-M. Matsushita, A. Izuoka, N. Wada, N. Takeda, M. Ishikawa, *J. Chem. Soc., Chem. Commun.* **1994**, 1723; (b) WILVIW10: K. Awaga, A. Yamaguchi, T. Okuno, T. Inabe, T. Nakamura, M. Matsumoto, Y. Maruyama, *J. Mater. Chem.* **1994**, *4*, 1377

CAPÍTOL 1:

Racionalització de l'Empaquetament de Cristalls

1.1. ANÀLISI DE L'EMPAQUETAMENT CRISTAL.LÍ EN BASE ALS SEUS GRUPS FUNCIONALS, UN MÈTODE QUALITATIU DE RACIONALITZACIÓ.

1.1.1.- Predicció teòrica d'empaquetaments en funció d'interaccions intermoleculars energèticament dominants.

D'acord amb les tendències actuals de disseny de cristalls moleculars [1a], no és possible predir un únic empaquetament del cristall amb una anàlisi teòrica; és d'esperar que es trobarà un conjunt d'estructures, entre les quals hi haurà les experimentals. Cadascuna d'aquestes estructures, que corresponen a mínims locals [1], és un dels polimorfs que el cristall pot presentar. Sovint, la diferència d'energia entre l'estructura més estable i la resta de polimorfs no arriba a ser ni de 2 kcal mol^{-1} [1a, d-e]. Així doncs, hom s'enfronta amb un problema de múltiples mínims (cada polimorf) separats per diferents barreres d'energia. Les estructures experimentals no tenen perquè ser les més estables, ja que factors cinètics, termodinàmics o d'altre tipus poden jugar un rol important en la manera que té el cristall de créixer en una solució saturada.

Computacionalment, el problema de trobar un mínim per a un cristall molecular en qüestió es redueix a localitzar l'ordenament geomètric de les molècules que minimitza l'energia potencial de l'empaquetament del cristall. Aquesta energia s'escriu normalment com una suma sobre tots els parells possibles d'interaccions intermoleculars [1a, d-e]

$$E = \sum E_{ij}(r_{ij}) \tag{1.1}$$

on $E_{ij}(r_{ij})$ és qualsevol de les interaccions intermoleculars entre àtoms i, j situats a una distància r_{ij}. Per tal de disminuir el cost computacional, en molts casos la geometria de les molècules interaccionants es considera fixada. Aquesta aproximació està basada en el fet que, en el cas d'interaccions intermoleculars febles, les distorsions geomètriques en les molècules interaccionants són petites.

La forma del potencial intermolecular $E_{ij}(r_{ij})$ és el resultat de sumar les seves components repulsiva (V_{rep}), electrostàtica (V_{ele}), inductiva (V_{ind}) i dispersiva (V_{dis}). L'única component repulsiva V_{rep} és proporcional al solapament de les distribucions electròniques. És únicament important a distàncies curtes i és responsable d'evitar el col.lapse d'un àtom en un altre. La resta de components són atractives i tenen la forma

$$V_{ele} = -\frac{1}{4\pi\varepsilon_0}\frac{q_i q_j}{r_{ij}} - \frac{2}{3kT(4\pi\varepsilon_0)^2}\frac{\mu_i^2\mu_j^2}{r_{ij}^6} \tag{1.2}$$

$$V_{ind} = -\frac{1}{(4\pi\varepsilon_0)^2}\frac{(\mu_i^2\alpha_j + \mu_j^2\alpha_i)}{r_{ij}^6} \tag{1.3}$$

$$V_{dis} = -\frac{3}{4(4\pi\varepsilon_0)^2}\frac{\alpha_i\alpha_j}{r_{ij}^6}\frac{I_iI_j}{(I_i + I_j)} \tag{1.4}$$

El terme V_{ele} és el dominant si les molècules tenen càrrega neta i en sistemes amb moments dipolars importants, com són els membres de la família dels α-nitronil nitròxids. En general, $V_{ele} > V_{ind} > V_{dis}$.

En conseqüència, l'anàlisi teòrica de l'empaquetament de tot cristall es pot simplificar centrant l'atenció en les interaccions energèticament dominants entre molècules (no cal examinar tots els parells d'interaccions àtom-àtom existents entre les diferents molècules d'un mateix cristall). Aquestes interaccions intermoleculars dominants [2] són el resultat de combinar adequadament grups de molècules veïnes; per exemple, entre molècules neutres es poden establir enllaços de tipus pont d'hidrogen i van der Waals. Un enllaç d'hidrogen intermolecular A-H···B requereix la presència d'un grup donador de protons o àcid A-H en una de les molècules i d'un grup acceptor de protons o bàsic B en l'altra de les molècules [3]. Aquests grups es poden identificar fàcilment analitzant els mapes de potencial electrostàtic molecular (MEP) [4] de la molècula o agregat. És, per tant, una interacció molt específica, que serà més forta a mesura que els àtoms A i B siguin més electronegatius ja que la component electrostàtica és la dominant ($X^{\delta-}$-$H^{\delta+}$···$Y^{\delta-}$). L'enllaç d'hidrogen és de curt abast (proporcional a $1/r_{ij}^6$ —segon terme de l'equació (1.2)—) i direccional. La força de les interaccions per pont d'hidrogen pren valors en l'interval 0.5-5 kcal mol^{-1}. D'altra banda, els enllaços de van der Waals A:···:B són el resultat d'interaccions dispersives V_{dis} entre els parells solitaris dels àtoms A i B. Són interaccions de curt abast (proporcional a $1/r_{ij}^6$ —en l'equació (1.4)—) i no massa direccionals. La força dels enllaços de van der Waals és proporcional a la polaritzabilitat dels àtoms A, B i, en general, el seu valor és menor de 0.5 kcal mol^{-1}. En canvi, en sòlids iònics, a més de les anteriors interaccions intermoleculars, també hi ha interaccions Coulòmbiques dirigides per V_{ele} que són de llarg abast (proporcionals a $1/r_{ij}$ —primer terme de l'equació (1.2)—) i isotròpiques (és a dir, el camp creat per cada àtom no depèn de cap dels angles). La seva força pot arribar a ser de 20 kcal mol^{-1}.

Des d'un punt de vista microscòpic, l'empaquetament cristal.lí vindrà, per tant, determinat per les interaccions intermoleculars energèticament dominants descrites en el paràgraf anterior. Concretament, en el cas de cristalls derivats de l'α-nitronil nitròxid, les interaccions per pont d'hidrogen seran les responsables de la formació de l'estructura primària de l'empaquetament cristal.lí (*primary packing pattern*). Cal tenir en compte el fet

que no totes les interaccions presents en aquesta estructura primària han de ser necessàriament atractives; n'hi pot haver de repulsives que quedin compensades per les atractives. A més, donat que per a un mateix cristall a vegades es poden definir vàries estructures primàries, caldrà seleccionar aquelles que energèticament siguin més estables i que puguin ser compatibles amb la propagació tridimensional necessària per a la formació del cristall. D'altra banda, estructures d'ordre superior (secundària, terciària,...) podran tenir lloc gràcies a la participació tant d'enllaços d'hidrogen com de van der Waals.

Així doncs, per tal de definir les interaccions intermoleculars responsables de les estructures primària i secundària de l'empaquetament cristal.lí caldrà (1) identificar la naturalesa dels grups funcionals presents en les interaccions intermoleculars energèticament dominants, i (2) conèixer la força relativa de totes les possibles interaccions intermolecular que l'agregat molecular pot establir. Aquesta informació es pot obtenir mitjançant la combinació de tres mètodes : anàlisi de distàncies d'enllaç intermoleculars del cristall, anàlisi de mapes de potencial electrostàtic molecular (MEP) de la molècula o agregat presents en les interaccions, i càlculs ab initio d'energies d'interacció.

L'anàlisi de distàncies d'enllaç intermoleculars és la forma més "artesanal" de determinació dels motius (*motifs*) presents en un cristall. Donat que la forma de tota interacció intermolecular atractiva $E_{ij}(r_{ij})$ és una corba de Morse, les interaccions amb una contribució energètica més important es localitzen en la regió propera al mínim de la corba. Es tracta, per tant, de contactes intermoleculars curts que són escasos i estan estadísticament localitzats en l'espai, al llarg de les direccions en què la interacció és més estable. En incrementar-se la distància, el número de contactes augmenta, i es distribueixen al llarg de totes les direccions de l'espai. A distàncies molt llargues, es pot considerar que els contactes estan distribuïts uniformement en l'espai creant un camp isomòrfic de Madelung. Així doncs, l'anàlisi de distàncies d'enllaç intermoleculars es basa en el fet que les interaccions intermoleculars energèticament dominants són també moltes vegades les que presenten distàncies d'enllaç més curtes. Per tant, interessarà caracteritzar aquelles interaccions intermoleculars que presentin distàncies d'enllaç més petites que un cert valor de tall d_0 —e.g., d_0=[Σ radis Van der Waals dels àtoms entre els quals s'estableix el contacte + 0.5Å].

Els MEP's [4] són una representació de les regions on una càrrega puntual +1 és atreta o repel.lida en funció de la seva posició en l'espai entorn la molècula. Les regions amb acumulació de densitat electrònica tendeixen a ser atractives (MEP negatiu), mentre que aquelles on hi hagi una disminució tenen tendència a ser repulsives (MEP positiu). El solapament de regions amb el mateix signe de dos mapes MEP donarà lloc a una contribució energètica electrònica repulsiva. Ara bé, si els MEP solapats són de signe contrari, les

contribucions seran atractives. Aquest procediment s'anomena "anàlisi del solapament de mapes MEP". Donat que les interaccions electrostàtiques són, en la majoria dels casos, el tipus d'enllaç dominant [5], aquesta anàlisi és una bona aproximació a les interaccions intermoleculars que donen lloc a l'estructura primària de l'empaquetament cristal.lí. Aquesta anàlisi comporta un únic problema: en ser una aproximació, prediu massa estructures primàries. Serà necessari, per tant, discriminar les que donaran lloc als polimorfs més estables d'entre totes les estructures primàries predites. Això implica que s'ha de determinar la força de les interaccions intermoleculars presents en l'empaquetament. Caldrà, doncs, dur a terme càlculs ab initio de les energies d'interacció dels enllaços intermoleculars dominants.

Els mètodes ab initio de mecànica quàntica permeten estimar la força dels que es postulen com a enllaços intermoleculars que dirigeixen la formació de l'estructura primària (o d'ordre superior) del cristall. Amb aquests càlculs, a més de la força també es pot tenir una idea de la direccionalitat dels enllaços intermoleculars d'interès. Com a primera aproximació, podem considerar que la força es pot obtenir sumant l'energia d'interacció de cadascun dels enllaços intermoleculars que l'estructura primària en qüestió pot presentar. Per tant, s'assumeix que es pot calcular per separat l'energia d'interacció de cada enllaç intermolecular amb un sistema model. Aquest sistema model haurà de ser prou petit per tal de fer possible el càlcul i prou gran per a incloure tots els efectes inductius i de polarització induïts pels grups funcionals que hi ha al voltant de la interacció que s'està estudiant. Ara bé, en cas de ser factible, és millor dur a terme els càlculs ab initio en l'agregat molecular complet (per tal de tenir en compte els possibles efectes cooperatius).

1.1.2.- Anàlisi de l'empaquetament cristal.lí en base als seus grups funcionals (CPFGA).

Seguint els arguments exposats anteriorment, podem proposar un procediment qualitatiu per tal de racionalitzar l'estructura de l'empaquetament de qualsevol cristall, el qual anomenarem "anàlisi de l'empaquetament cristal.lí en base als seus grups funcionals" (*crystal packing functional group analysis, CPFGA*). Aquest procediment consta de les següents etapes:

1) Caracterització dels grups funcionals segons el seu caràcter àcid / bàsic mitjançant l'estudi d'un mapa MEP, buscant regions on hi hagi disminució o concentració de densitat electrònica.

2) Identificació de les estructures primàries d'empaquetament generades a partir

dels grups caracteritzats en (1), o bé mitjançant una anàlisi del solapament de mapes MEP o bé gràcies a l'examen de les interaccions intermoleculars més curtes. En aquesta etapa no s'obté cap informació sobre l'estabilitat relativa de les estructures primàries identificades.

3) Càlcul de la força de les estructures primàries d'interès usant mètodes ab initio en sistemes model adequats o en l'agregat molecular complet en cas de ser factible.

4) Racionalització de l'estructura. Usant la informació obtinguda en les tres etapes anteriors, es pot definir les estructures primària, secundària i d'ordre superior presents en el cristall.

L'anàlisi de l'empaquetament cristal.lí en base als seus grups funcionals CPFGA s'ha aplicat a diferents cristalls moleculars i ha permès racionalitzar amb èxit tots els empaquetaments [6]. A continuació, es presenta la racionalització de l'empaquetament de l'HNN [7], i es justifica la transició de fase α- a β-HNN.

1.2. L'EMPAQUETAMENT DEL 2-HIDRO NITRONIL NITRÒXID (HNN), UNA APLICACIÓ DEL MÈTODE CPFGA

Dins de la família dels α-nitronil nitròxids, hem seleccionat el radical HNN (R=H) com a exemple per a l'aplicació d'un nou procediment qualitatiu de racionalització de l'empaquetament de cristalls en base als seus grups funcionals. L'HNN va ser primer sintetitzat per Ullman et al. [7a], i un estudi recent [7b-c] ha permès trobar dues fases cristal.lines (α-HNN i β-HNN) antiferromagnètiques. Una anàlisi tèrmica de la fase α-HNN [7b, d] en el rang 40-160°C indica la presència d'una transició endotèrmica irreversible a 63±2 °C versus la fase més estable β-HNN. A 105.4°C el cristall d'α-HNN inicia descomposició tèrmica. Cal dir que s'ha escollit aquest radical (i no pas un altre amb comportament ferromagnètic), en primer lloc, per la mida de la molècula: és prou petita com per permetre l'ús de mètodes ab initio d'alta precisió a baix cost computacional. A més, aquest radical presenta un polimorfisme molt ben documentat que és interessant d'estudiar. Finalment, la molècula d'HNN és un bon model per tal d'entendre les propietats de l'empaquetament de l'anell de 5 membres que tenen tots els α-nitronil nitròxids. Aquesta informació es podrà combinar amb la que es tingui sobre l'empaquetament del grup R per tal de predir l'empaquetament esperat per a qualsevol molècula que pertanyi a la família dels α-nitronil nitròxids.

1.2.1.- Caracterització dels grups funcionals.

Les dues fases antiferromagnètiques, α i β, de l'HNN serviran d'exemple per a il.lustrar l'aplicació del mètode CPFGA. El cristall α-HNN conté quatre molècules per cel.la unitat i pertany al grup espacial $P2_1/n$ [7b]. Els paràmetres cristal.logràfics de la cel.la són: a=11.879Å, b=11.611Å, c=6.332Å i β=104.48°. El cristall β-HNN té setze molècules per cel.la unitat i el grup espacial és el mateix que per a la fase α, el $P2_1/n$ [7c]. En aquest cas, els paràmetres cristal.logràfics valen: a=12.133Å, b=14.080Å, c=19.991Å i β=92.96°.

La molècula d'HNN és neutra, per tant, només es poden establir interaccions intermoleculars del tipus pont d'hidrogen o van der Waals. Els enllaços de tipus van der Waals són més dèbils, de manera que no seran la força directriu de l'empaquetament molecular, excepte en aquelles situacions en què hi hagi ponts d'hidrogen molt dèbils. Aquest no és el cas de l'HNN ja que té un important moment dipolar permanent de 3.872 Debyes (calculat a nivell HF/ 6-31G(d, p)).

Així doncs, per tal de racionalitzar l'empaquetament del cristall d'HNN caldrà localitzar els seus enllaços d'hidrogen mitjançant la identificació dels grups donadors (àcids) i acceptors (bàsics) de protons. El mapa MEP de l'HNN (FIGURA 1.1) mostra que els grups N-O són bàsics, mentre que els C-H són àcids. A més, s'observa l'existència de dos mínims sobre cada oxigen (FIGURA 1.1). Aquests mínims indiquen la possibilitat que té cada oxigen d'establir dos enllaços d'hidrogen acceptant dos grups C-H.

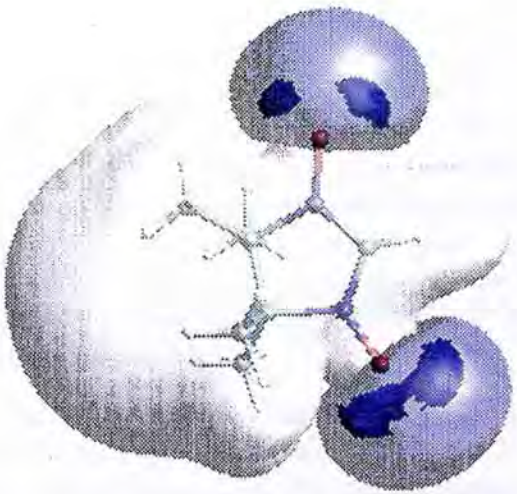

FIGURA 1.1.- Mapa MEP de la molècula d'HNN calculat a nivell HF / 6-31G(d, p) [blau intens: -45 kcal mol^{-1}; blau cel: -20 kcal mol^{-1}; gris: +10 kcal mol^{-1}].

1.2.2.- Possibles estructures primàries d'empaquetament.

El fet de conèixer el caràter àcid-bàsic dels grups de l'HNN permet fer una anàlisi del solapament de mapes MEP. Amb l'aplicació d'aquest procediment i tenint cura que les estructures obtingudes presentin ordre a llarg abast, s'obtenen els possibles ordenaments de molècules d'HNN dins del pla, il.lustrats esquemàticament en la FIGURA 1.2. Cada molècula està identificada per un cercle amb línies que representen els grups àcid-bàsic: els grups àcids tenen una fletxa al seu extrem, i els bàsics n'hi tenen una d'invertida. Les línies estan disposades de tal manera que es mantenen les orientacions relatives que els grups tenen en respecte al centre de massa de la molècula.

L'ordenament **a** correspon a aquella situació en què els grups metil estan enllaçats als grups NO. La propagació d'aquest motiu estructural dóna lloc a un pla perfectament ordenat (línees de puntets) amb possibilitats de crear una estructura tridimensional, 3-D (ordre a llarg abast). L'ordenament **b** és similar a **a**, però amb les molècules de la segona columna rotades 120°, per tal d'establir els contactes metil···ON presents en **a** i nous contactes $C(sp^2)$-H···ON. En aquesta ocasió, la propagació de l'ordenament **b** dóna lloc a cadenes (línees de puntets) sense possibilitats de propargar-se al llarg d'una segona direcció en el pla. Aquest no és el cas dels quatre ordenaments restants, els quals han estat seleccionats perquè presenten un ordre bidimensional a llarg abast. L'ordenament **c** és un dels possibles polimorfs d'**a**: dues cadenes paral.leles en forma de zig-zag connectades a través de ponts $(metil)_2$···ON. En canvi, els ordenaments **d**, **e** i **f** són tres possibilitats obtingudes per associació de dímers. Els casos **d** i **f** s'obtenen a partir del mateix dímer quan es modifica la seva orientació relativa: un triangle en el primer cas i un quadrat en el segon. El dímer que intervé en aquests dos ordenaments s'obté amb la formació de dos contactes $C(sp^2)$-H···ON. D'altra banda, el dímer de l'ordenament **e** és el resultat de formar simultàneament un contacte $C(sp^2)$-H···ON i un altre de metil···ON. Aquests sis ordenaments són només un exemple de les múltiples opcions possibles. Evidentment, a un nivell tridimensional la situació és encara molt més complicada. Per tant, no ens hem de sorprendre de trobar molts polimorfs en un petit rang d'energies. Ara bé, el número de possibilitats es pot reduir amb relativa facilitat un cop hàgim calculat la força de les interaccions intermoleculars presents en els diferents ordenaments ja que només estem interessats en els polimorfs més estables.

Acabem de proposar a nivell teòric uns possibles ordenaments de molècules d'HNN. El nostre objectiu, però, és racionalitzar l'empaquetament de les fases α i β de l'HNN. Així doncs, caldrà proposar uns ordenaments *reals*, és a dir, cal caracteritzar els motius que permeten l'empaquetament tridimensional de les molècules d'HNN en les fases α i β. Prenent com a referència els ordenaments geomètrics de la FIGURA 1.2, es fa una búsqueda

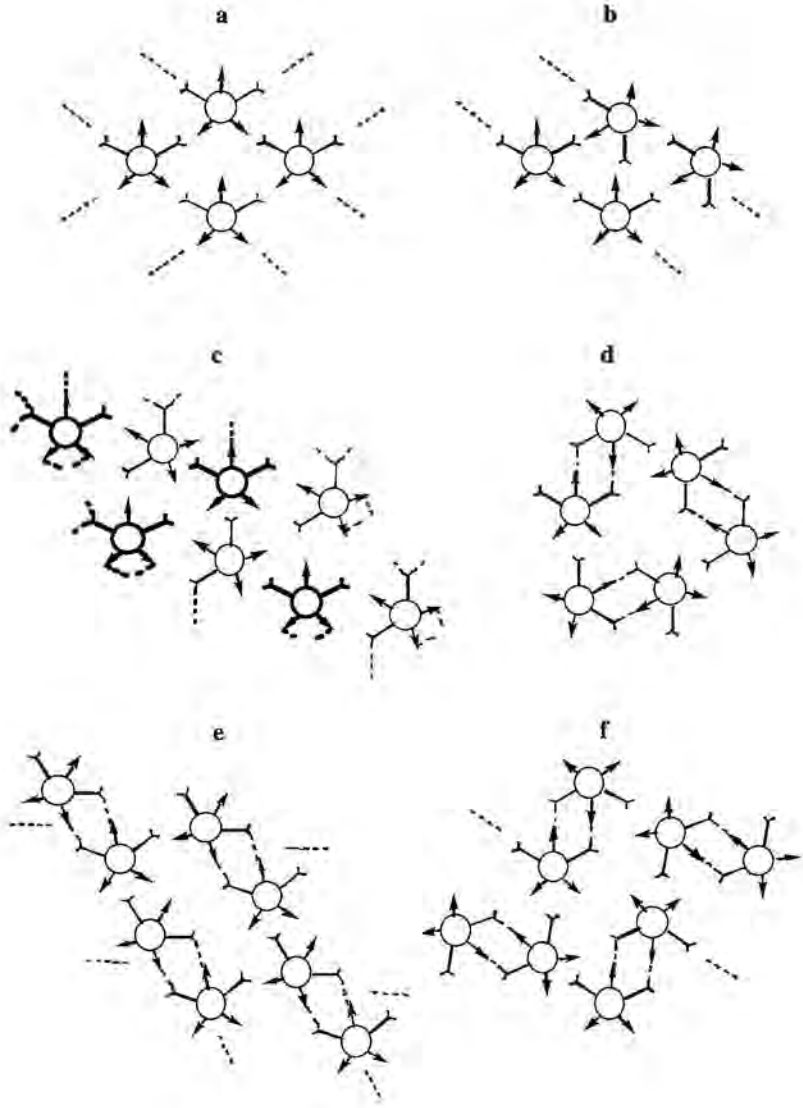

Figura 1.2.- Possibles ordenaments de molècules d'HNN per a formar plans.

en els cristalls d'α-HNN i β-HNN. Els diferents ordenaments trobats s'il.lustren en la FIGURA 1.3. Els ordenaments 1, 2, 5 i 6 corresponen a conformacions presents dins dels plans, mentre que els 3 i 4 corresponen a conformacions entre plans. Ara ja s'està en condicions de calcular les energies d'interacció associades a aquests ordenaments.

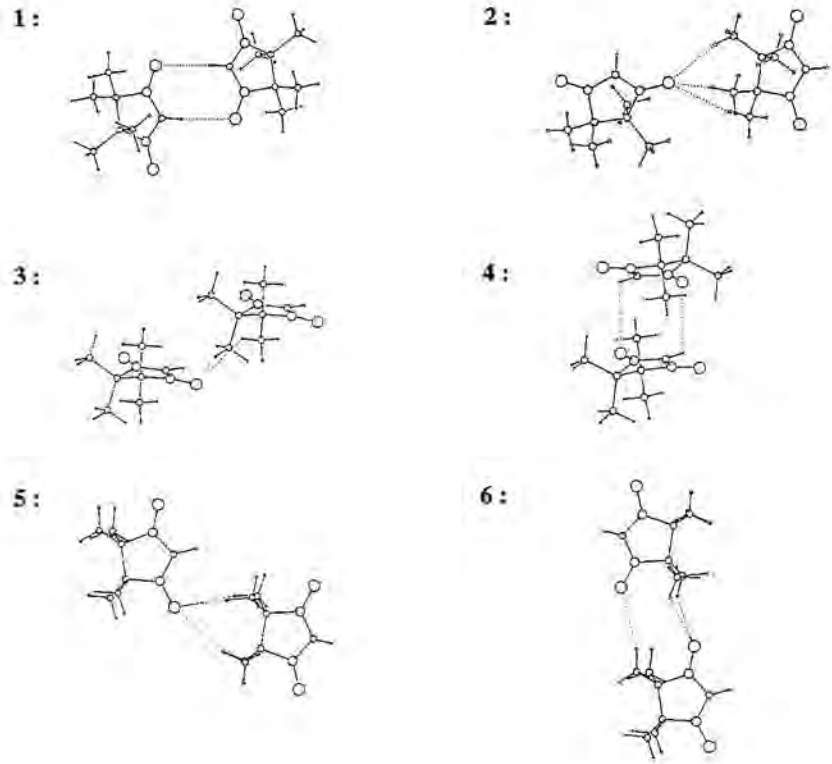

FIGURA 1.3.- Ordenaments presents en els cristalls α-HNN i β-HNN.

1.2.3.- Càlcul de la força de les estructures primàries d'interès a nivell ab initio.

L'experiència acumulada en el càlcul d'enllaços d'hidrogen i d'interaccions de van der Waals [9] ens indica que, per tal d'obtenir resultats precisos, cal usar mètodes amb correlació. En tots els càlculs d'energies d'interacció s'ha usat el mètode Moller-Plesset de segon ordre MP2 [8], conjuntament amb bases adequades [9a-b]. Aquestes bases han de ser prou extenses i equilibrades per tal de descriure correctament totes les interaccions existents en el sistema. Un cop calculada l'energia d'aquestes interaccions, cal corregir l'error de superposició de base (BSSE) [9a, d-f] mitjançant el mètode de counterpoise [9g]. Amb aquesta metodologia, els valors d'energies d'interacció calculats per a enllaços de van der Waals [9b-c] i d'hidrogen [9e-f] tenen menys d'un 10% d'error amb respecte als valors experimentals. Tots el càlculs ab initio han estat fets usant Gaussian 94 [10].

La manera més correcta d'obtenir les energies d'interacció que ens interessen seria calculant-les en cada un dels agregats moleculars que intervenen en les interaccions intermoleculars, per tal de quantificar la seva energia i estructura òptima. A més, aquests càlculs també donarien informació sobre les barreres que separen els diferents mínims per a cadascun dels agregats, és a dir, sobre la cinètica del polimorfisme. Ara bé, aquest tipus de càlculs té un cost massa alt fins i tot per a molècules "petites" com l'HNN. Per tant, caldrà modelitzar els agregats moleculars que interessen amb un sistema model adequat i, llavors, calcular l'energia dels contactes a nivell ab initio. Tal com ja s'ha vist, en el cas de l'HNN, els contactes més importants a l'hora de definir la seva estructura primària són els enllaços d'hidrogen, tot i la possibilitat d'establir interaccions de van der Waals del tipus NO···ON.

En primer lloc, doncs, ens ocuparem dels enllaços d'hidrogen, modelitzant els contactes $C(sp^2)$-H···ON i $C(sp^3)$-H···ON presents en els ordenaments de la FIGURA 1.3. S'ha d'assumir que l'energia d'interacció d'aquests ordenaments es pot calcular com a suma de les energies d'interacció associades a cadascun dels contactes del tipus $C(sp^2)$-H···ON i $C(sp^3)$-H···ON presents en aquests ordenaments i calculats prèviament en sistemes model. Amb el càlcul de les seves energies d'interacció s'aconseguirà una descripció més quantitativa de l'empaquetament dels cristalls, ja que es podrà establir l'estabilitat relativa dels ordenaments reals presents en les fases α i β de l'HNN. Començarem avaluant l'energia de la interacció $C(sp^2)$-H···ON usant el Model I (FIGURA 1.4). En aquest model, la geometria de cada fragment ha estat escollida deliberadament per tal de reproduir la de les molècules d'HNN en la seva fase α (r=2.416Å, θ=142.1°). No s'ha seleccionat un sistema model més petit, com per exemple el dímer $H_2NO\cdots CH_3$, perquè càlculs previs a nivell MP2/6-311++G(2d, 2p) amb aquest sistema indiquen que la inclusió dels dos grups NO duplica la força de la interacció. Així doncs, el valor de l'energia d'interacció obtingut després de corregir l'BSSE a nivell MP2/6-311++G(2d, 2p) per a interaccions $C(sp^2)$-H···ON (Model I) és de -3.71 kcal mol^{-1}. Ara ja estem en condicions de calcular l'energia associada a l'ordenament 1. En aquest ordenament s'estableixen dos contactes $C(sp^2)$-H···ON, per tant, l'energia d'interacció serà de 2 x (-3.71) = -7.42 kcal mol^{-1}. S'ha comprovat la validesa d'aquest resultat amb el càlcul de l'energia d'interacció del dímer optimitzat en fase gas i el valor obtingut és de -7.20 kcal mol^{-1}. La diferència entre el valor calculat (-7.20 kcal mol^{-1}) i l'aproximat (-7.42 kcal mol^{-1}) posa de relleu la importància dels efectes de polarització que un enllaç indueix en l'altre. Ara bé, també cal tenir en compte el fet que les geometries dels dímers en els cristalls α-HNN i β-HNN no són la mateixa que la calculada òptima en fase gas. Això es posa de manifest quan calculem l'energia d'interacció per al dímer de la fase α amb la geometria que presenta en el cristall. En aquest cas, a un nivell MP2/6-311++G(2d, 2p), el valor amb correcció BSSE és de -5.53 kcal mol^{-1}, és a dir, menys del doble de l'energia de dos contactes $C(sp^2)$-H···ON aïllats. Tot i aquesta diferència, podem considerar que l'aproximació que es fa en sumar les energies d'interacció

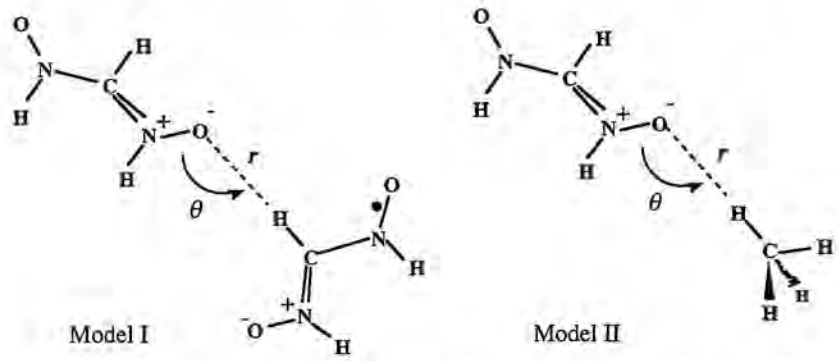

FIGURA 1.4.- Sistemes model usats en la modelització d'interaccions C(sp^2)-H···ON (Model I) i C(sp^3)-H···ON (Model II) presents en el cristall d'HNN.

dels contactes aïllats és adequada, i que és aplicable a la resta d'ordenaments.

L'energia d'interacció dels contactes C(sp^3)-H···ON s'ha calculat usant el Model II (FIGURA 1.4) a nivell MP2/6-311++G(2d, 2p), on r=2.637Å i θ=128.7°. El seu valor amb correcció BSSE és de només -0.40 kcal mol^{-1}, és a dir, una desena part de l'energia d'interacció obtinguda per a un contacte C(sp^2)-H···ON aïllat. En aquest cas també s'ha comprovat que cal tenir en compte l'efecte inductiu dels grups NO. Per aquest motiu, models del tipus H_2NO···CH_4 no descriuen bé la interacció C(sp^3)-H···ON. Coneixent el valor d'aquesta interacció ja es poden discutir els ordenaments 2, 3, 5 i 6 (FIGURA 1.3). L'ordenament 3 presenta dos enllaços C(sp^3)-H···ON i la seva energia serà de 2 x (-0.40) = -0.80 kcal mol^{-1}. En canvi, en l'ordenament 2 participen tres enllaços del tipus C(sp^3)-H···ON; la seva energia es pot calcular com 3 x (-0.40) = -1.2 kcal mol^{-1}. De la mateixa manera, els ordenaments 5 i 6 també presenten tres contactes C(sp^3)-H···ON i, per tant, l'estimació de l'energia serà també de -1.2 kcal mol^{-1}. Ara bé, donat que les distàncies intermoleculars són més curtes en l'ordenament 2, és d'esperar que sigui el més estable dels tres. Possiblement, els efectes de polarització seran els responsables de diferenciar els ordenaments 5 i 6, tot i que la diferència d'energies no serà massa significativa.

Finalment, l'ordenament 4 (FIGURA 1.3) correspon a una interacció entre plans mitjançant contactes C(sp^2)-H···ON, situació que encara no s'havia contemplat. El sistema model usat en el càlcul de l'energia d'interacció de l'ordenament 4 és similar al Model I (en FIGURA 1.4) però orientat per tal de simular la geometria d'aquest dímer dins del cristall ($d_{H\cdots O}$=3.331Å, $\theta_{CH\cdots O}$=85.3°, $\theta_{H\cdots ON}$=80.5°, $\theta_{CH\cdots ON}$=106.3° i 253.8°). S'ha calculat l'energia d'interacció amb correcció BSSE a nivell MP2 i una base 6-311++G(2d, 2p) i el seu valor és de -1.38 kcal mol^{-1}, és a dir, -0.69 kcal mol^{-1} per a cada contacteC(sp^2)-H···ON entre plans. Aquest valor és molt interessant perquè, fins i tot a llargues distàncies, el

contacte $C(sp^2)$-H···ON és més fort que un de $C(sp^3)$-H···ON aïllat calculat amb la seva geometria òptima. Així doncs, tot i que el número d'enllaços del tipus $C(sp^3)$-H···ON serà més gran, no es pot descartar la influència de l'ordenament 4 en la determinació de l'empaquetament del cristall d'α-HNN.

Podem dir que els càlculs ab initio mostren que els ordenaments il.lustrats en la FIGURA 1.3 són estabilitzants, en concordança amb les prediccions fetes amb l'anàlisi del solapament de mapes MEP. A més, tots ells tenen una energia d'interacció molt més gran que els contactes del tipus $C(sp^3)$-H···H (-0.12 kcal mol^{-1} [11]), també presents en els cristalls d'HNN. Les seves forces relatives són: $1 >> 2 > 5 \equiv 6 > 4 > 3$ (FIGURA 1.3).

Si ens fixem atentament en els ordenaments de la FIGURA 1.3, veurem que no hi ha cap interacció de van der Waals NO···ON curta. Aquest fet ens dóna una idea del possible caràter repulsiu d'aquest tipus de contacte. Amb tot i això, estudiarem les interaccions de van der Waals entre grups N-O colineals. El sistema model està constituit, en aquesta ocasió, per dues molècules planes d'H_2NO amb els grups NO enfrontats. Trobem que l'energia d'interacció d'aquest sistema a nivell MP2 i amb una base 6-31+G(2d, 2p) és repulsiva per a qualsevol distància intermolecular. El seu valor és de +1 kcal mol^{-1} a la distància de van der Waals (amb correcció de BSSE, l'energia encara és més repulsiva). Així doncs, donat que els grups NO tendiran a evitar-se, tots els ordenaments presents en els cristalls d'HNN (FIGURA 1.3) disposaran les molècules d'HNN de tal manera que els enllaços d'hidrogen compensin la repulsió entre grups NO (que són els portadors d'electrons desaparellats).

Arribats a aquest punt, sabem —gràcies a les dades ab initio anteriors— que les forces directrius de l'estructura primària de l'empaquetament de l'HNN són les interaccions $C(sp^2)$-H···ON dins dels plans (-3.71 kcal mol^{-1}). Les interaccions NO···ON són, en canvi, repulsives (+1 kcal mol^{-1} a la distància de van der Waals). D'altra banda, les $C(sp^2)$-H···ON entre plans conjuntament amb les $C(sp^3)$-H···ON són prou atractives com per poder ser considerades responsables de l'estructura secundària i d'ordre superior de l'empaquetament de l'HNN.

1.2.4.- Racionalització de l'estructura d'α-HNN i β-HNN amb dades ab initio.

A continuació, s'aplicarà la informació ab initio anterior sobre energies d'interacció ($1 >> 2 > 5 \equiv 6 > 4 > 3$ en FIGURA 1.3) en el cas dels cristalls de les fases α-HNN i β-HNN [7b-c] per tal d'entendre el seu empaquetament i, per tant, el seu polimorfisme.

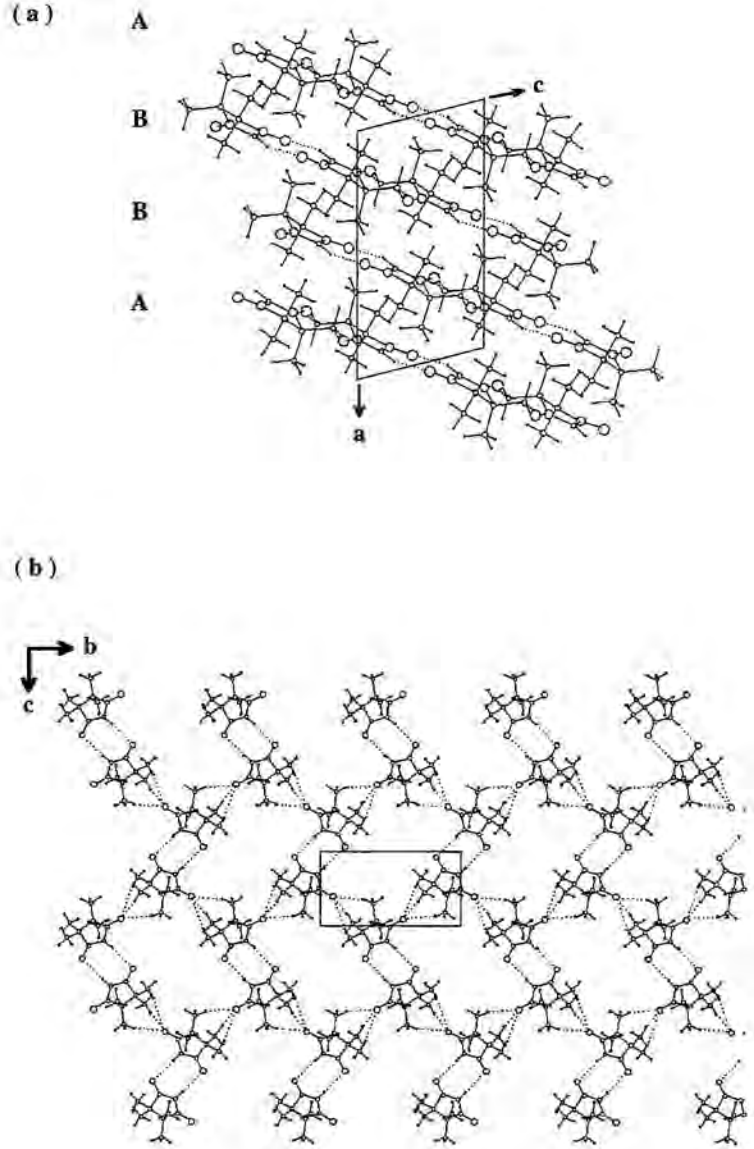

FIGURA 1.5.- Empaquetament d'α-HNN mostrant els contactes C-H···O ≤3.20Å ; (a) vista extesa al llarg de l'eix b on veiem quatre capes (ABBA) dins de la cel.la unitat; (b) vista de la capa A (pla bc)

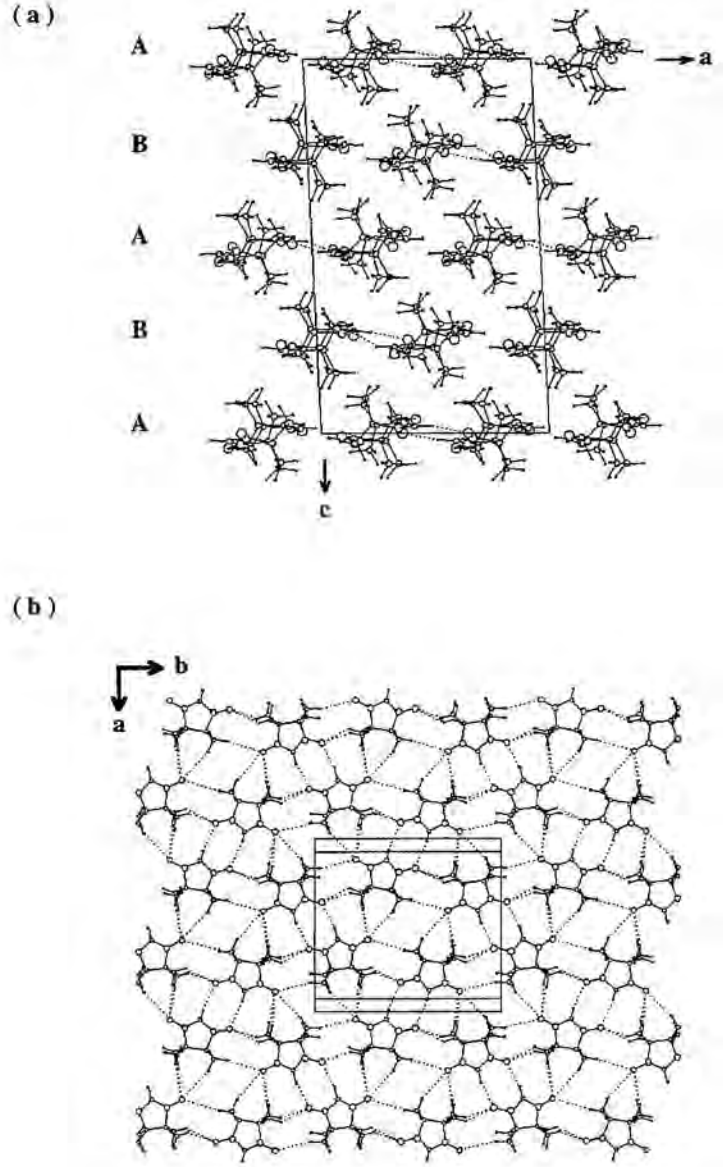

FIGURA 1.6.- Empaquetament de β-HNN mostrant els contactes C-H···O ≤3.20Å : (a) vista extesa al llarg de l'eix b on veiem cinc capes (ABABA) dins de la cel.la unitat; (b) vista de la capa A (pla ab)

Per tal d'entendre l'empaquetament d'aquests sistemes és millor tenir un esquema més detallat de la seva estructura, on es dibuixaran els contactes intermoleculars més curts que una certa distància de tall d_0. En aquest estudi, d_0 és la suma dels radis de van der Waals dels dos àtoms entre els quals s'estableix el contacte més 0.50Å, és a dir, per a un enllaç d'hidrogen O···H ($r_{vw}(O) = 1.50Å$, $r_{vw}(H) = 1.20Å$) d_0 serà 3.20Å. La FIGURA 1.5 (1.6) mostra una vista de l'estructura del cristall d'α-HNN (β-HNN), on les interaccions intermoleculars C-H···O menors de 3.20Å estan indicades amb una línia discontínua.

En ambdós casos, l'empaquetament està caracteritzat per l'apilament de capes. Cada capa és el resultat de l'agregació de dímers d'HNN. La formació de capes no és sorprenent perquè és la manera més estable d'ordenar moments dipolars, i la molècula d'HNN té un moment dipolar important originat pels seus dos grups NO. Dins de cada cristall les capes incloses en la cel.la unitat es diferencien per la seva posició relativa deguda als elements de simetria del grup espacial al qual el cristall pertany. Cristal.logràficament, dins de la cel.la unitat de l'α-HNN podem distingir dos tipus de capes, identificades com A i B, ordenades seguint la seqüencia ABBA (les capes B són les més properes al centre d'inversió situat en el centre de la cel.la unitat). En canvi, en la cel.la unitat del β-HNN hi ha cinc capes disposades com ABABA (la capa A central passa pel centre d'inversió de la cel.la unitat).

L'estructura interna de les capes (TAULA 1.1) és diferent depenent de la fase α o β del cristall de l'HNN , tot i que els dímers que donen lloc a aquesta estructura són similars.

TAULA 1.1. Distàncies intermoleculars —enllaços d'hidrogen i interaccions de van der Waals— més curtes dels cristalls α-HNN i β-HNN.

		distància / Å	
classe	tipus de contacte	α-HNN	β-HNN
dins del pla	$C(sp^2)$-H···O	2.416	2.202
	$C(sp^3)$-H···O	2.554	2.479
	$C(sp^2)$-H···H-$C(sp^2)$	2.689	3.027
	$C(sp^3)$-H···H-$C(sp^3)$	2.790	2.830
	N-O···O-N	4.271	3.645
entre plans	$C(sp^3)$-H···O	2.535	2.718
	$C(sp^2)$-H···H-$C(sp^3)$	2.660	2.812
	$C(sp^3)$-H···H-$C(sp^3)$	2.548	2.428
	N-O···O-N	3.798	4.209

En ambdós cristalls, els dímers es formen gràcies a contactes del tipus C(sp^2)-H···ON (ordenaments del tipus 1 en la FIGURA 1.3). Ara bé, mentre en l'α-HNN només hi ha un dímer, *dim1* ($d_{H\cdots O}$=2.416Å, $\theta_{CH\cdots O}$=162°), que es repeteix en l'estructura interna de les capes, en la fase β-HNN n'hi ha dos, dim2 ($d_{H\cdots O}$=2.202Å, $\theta_{CH\cdots O}$=165°) i dim3 ($d_{H\cdots O}$=2.431Å, $\theta_{CH\cdots O}$=159°) que s'alternen (FIGURA 1.7). D'altra banda, les fases α i β de l'HNN també es diferencien en termes de coplanaritat (FIGURA 1.7): en *dim2*, les dues molècules d'HNN són quasi coplanars ($\theta_{CH\cdots ON}$=30°), mentre que en els dos dímers restants aquesta coplanaritat no es manté (*dim1*: $\theta_{CH\cdots ON}$=266°, i *dim3*: $\theta_{CH\cdots ON}$=75°). Càlculs ab initio [12] indiquen que la conformació plana del dímer és la més estable (en fase gas, la distància H···O òptima és 2.154Å mentre que l'angle és 133.1°). Aquest resultat es pot prendre com a referència per tal d'entendre les distorsions geomètriques induïdes per les molècules veïnes en el dímer estudiat. Així doncs, els dímers en la fase α-HNN *dim1* prefereixen relaxar la seva planaritat, i així maximitzar la força i/o el número de contactes amb les molècules de capes veïnes. En canvi, en la fase β-HNN, els dímers *dim2* adopten una distància molt similar a l'òptima en fase gas per tal de maximitzar el grau d'interpenetració de l'estructura dins de les capes, mentre que els *dim3* es comportaran com els de la fase α.

Un cop discutida la geometria interna pròpia de cada dímer, es passarà a parlar de les possibles maneres que tenen aquests dímers de combinar-se entre si i donar lloc a les capes esmentades anteriorment. Cada dímer d'HNN té encara dos grups NO i vuit grups metil per a establir contactes intermoleculars amb d'altres dímers (TAULA 1.1) via ponts d'hidrogen o interaccions de van der Waals. Els contactes entre dímers C-H···O ($d_{H\cdots O} \leq 3.20$Å) que s'observen en la fase α-HNN (FIGURA 1.5) són del tipus C(sp^3)-H···ON (ordenaments del tipus 2 en la FIGURA 1.3): cada dímer estableix 12 contactes, 6 com a àcid i 6 com a base. En la fase β-HNN (FIGURA 1.6) els contactes entre dímers són també del tipus C(sp^3)-H···ON ($d_{H\cdots O} \leq 3.20$Å) (ordenaments del tipus 5 i 6 en la FIGURA 1.3), però són molt més nombrosos: 23 en total. Així doncs, donat que els dímers de les fases α i β de l'HNN s'estableixen via contactes C(sp^2)-H···ON, seria d'esperar que les capes del cristall β-HNN fossin energèticament més estables . Ara bé, aquest no és el cas : l'efecte desestabilitzant de la tensió creada per una major interpenetració entre cadenes de dímers adjacents (FIGURA 1.8) fa que les capes dels cristalls α- i β-HNN tinguin una estabilitat similar.

Finalment, només ens resta explicar l'apilament d'aquestes capes (TAULA 1.1). En aquest cas, únicament s'ha de tenir en compte que encara hi ha grups metil amb C(sp^3)-H lliures, els quals s'usen en la formació de contactes entre plans del tipus C(sp^3)-H···ON (ordenaments del tipus 3 i 4 en la FIGURA 1.3). Aquest tipus d'ordenaments són els adequats per maximitzar l'energia d'interacció entre capes i només els trobarem estabilitzant l'apilament de capes quan aquestes capes ja s'han format.

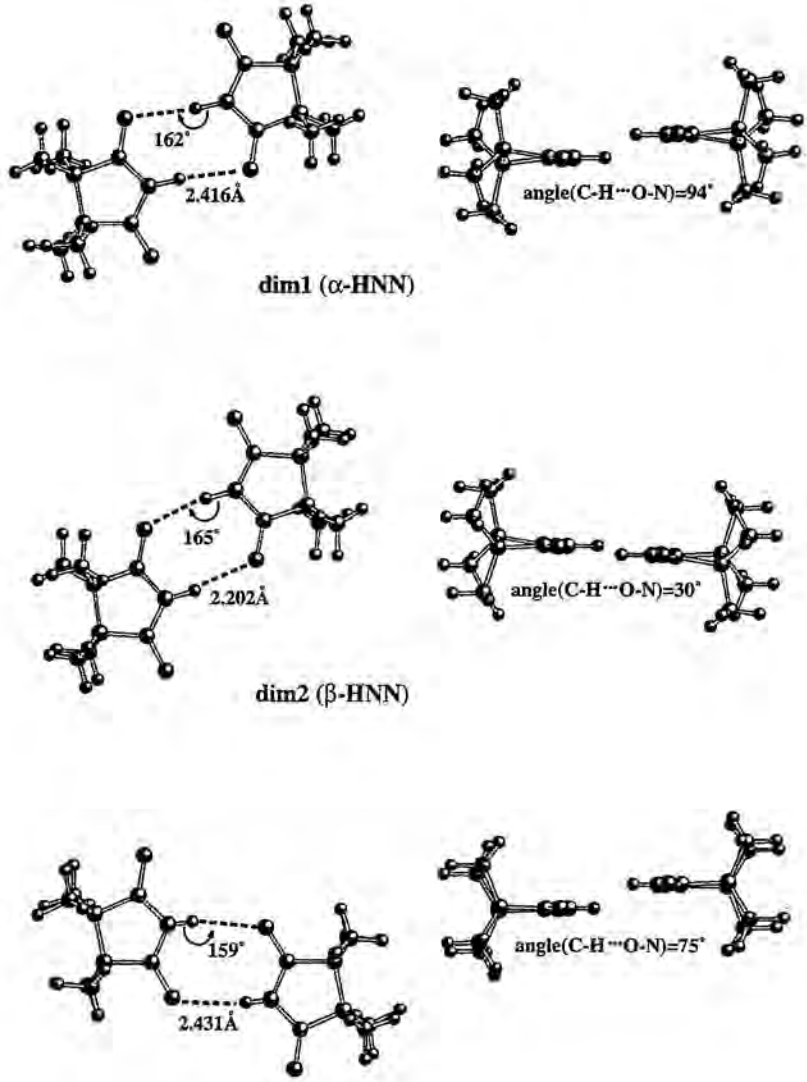

FIGURA 1.7.- Estructura dels dímers dels cristalls α-HNN (*dim1*) i β-HNN (*dim2* i *dim3*) (en la FIGURA s'indiquen els valors de la distància H···O, de l'angle C-H···O i del dihedre C-H···O-N)

1.2.5.- El mètode CPFGA : Etapes seguides en la racionalització de l'empaquetament de les fases α i β de l'HNN.

En ambdues fases α i β de l'HNN les molècules formen capes de dímers, apilades per tal de formar el cristall. Els dímers són el resultat de la formació simultànea de dos contactes $C(sp^2)$-H···ON entre molècules participants. Com podem racionalitzar aquests empaquetaments usant el mètode CPFGA ?

(1) El mapa MEP de la molècula d'HNN amb la geometria que presenta en el cristall (FIGURA 1.1) mostra dues regions amb acumulació de càrrega, localitzades en els grups NO (les regions negatives del MEP). Així doncs, els grups NO actuen com a acceptors de grups C-H que poden ser $C(sp^2)$-H i $C(sp^3)$-H.

(2) El solapament dels mapes MEP de dues molècules d'HNN dóna lloc a diferents ordenaments (FIGURA 1.3), que s'han buscat en els cristalls d'α-HNN i β-HNN en base als ordenaments teòrics proposats en la FIGURA 1.2.

(3) Càlculs ab initio mostren que les energies de contactes $C(sp^2)$-H···O-N (-3.71 kcal mol^{-1} dins de la capa i -0.69 kcal mol^{-1} entre capes) i $C(sp^3)$-H···O-N (-0.40 kcal mol^{-1}) són atractives. En conseqüència, aquelles estructures primàries de l'empaquetament de l'HNN on hi hagi enllaços del tipus $C(sp^2)$-H···O-N seran molt estables. Un cop estudiades les diferents possibilitats, s'arriba a la conclusió de què, tenint en compte el tipus d'interaccions intermoleculars, l'estabilitat dels ordenaments il.lustrats la FIGURA 1.3 és: $1 >> 2 > 5 \equiv 6 > 4 > 3$.

(4) Ara ja es té informació suficient per tal de racionalitzar l'empaquetament de l'HNN (FIGURA 1.5-1.6). L'HNN té una forta tendència a formar dímers del tipus 1 (FIGURA 1.3), els quals constitueixen l'estructura primària d'aquest empaquetament cristal.lí. Aquests dímers encara tenen grups N-O i C-H capaços d'establir més enllaços d'hidrogen $C(sp^3)$-H···O-N. Així doncs, els dímers es poden agregar per tal de formar plans mitjançant ordenaments del tipus 2 i 5-6 (FIGURA 1.3), donant lloc a l'estructura secundària dels polimorfs α i β respectivament. Si hom es fixa en les distàncies NO···ON de la TAULA 1.1, observa que dins d'una capa no hi ha contactes curts d'aquest tipus, conseqüència de la repulsió que existeix entre grups NO. L'únic canvi entre ambdós polimorfs resideix en les orientacions relatives d'aquestes capes [7b-c], tal i com s'explicarà en l'apartat 1.2.6 [13]. Aleshores, aquestes capes s'apilen formant l'estructura terciària del cristall (ABBA en α-HNN , ABABA en β-HNN) gràcies a l'ús dels

grups C-H que encara hi ha disponibles per tal d'establir contactes amb grups N-O de capes veïnes a través de contactes del tipus 3 i 4 (FIGURA 1.3).

1.2.6.- Transicions polimòrfiques entre les fases α i β de l'HNN.

Un cop racionalitzada l'estructura dels cristalls α-HNN i β-HNN, ens podem centrar en les transformacions polimòrfiques entre les fases α i β de l'HNN. Es pot entendre l'essència del procés mirant la FIGURA 1.8, on l'empaquetament en una de les capes ha estat esquematitzat usant els dímers com a unitat d'empaquetament.

En la fase α, cada capa està constituïda per fileres de dímers, paral.leles unes a les altres, però apuntant en direccions diferents, tal que els dímers d'una de les fileres estan disposats quasi perpendicularment als de les fileres adjacents. La filera ***n*** està enllaçada a les fileres *n-1* i *n+1* mitjançant contactes del tipus 2 (FIGURA 1.3). Cada dímer forma dos d'aquests contactes amb altres dos dímers que pertanyen a la filera adjacent. Cada molècula del dímer d'HNN fa contacte amb només una de les molècules del dímer al qual està enllaçat. D'altra banda, en la fase β, el contacte entre dímers és tal que els dímers de la filera ***n*** poden establir ponts d'hidrogen del tipus 5 i 6 (FIGURA 1.3) amb dímers de les fileres *n-1* i *n+1*, però alhora estan suficientment a prop dels de les fileres ***n-2*** i ***n+2*** com per establir contactes de van der Waals $C(sp^3)$-H···H-$C(sp^3)$ estables. En conseqüència, l'empaquetament dels dímers de la fase β és molt més dens que el de l'α, tal com es pot veure en la FIGURA 1.7.

Si es pren la filera ***n*** com a referència, és possible transformar la fase α en β amb el desplaçament simultani dels dímers de les fileres *n-1* i *n+1* cap al centre dels dímers de la filera ***n***. Així doncs, en aquesta transformació es fa variar el grau d'interpenetració de les fileres *n-1* i *n + 1* en direcció cap a la filera ***n***. En principi, també es podria fer la transformació inversa: convertir la fase β en α. Aquesta transformació serà espontània o no en funció del valor de la seva energia lliure de Gibbs ($\Delta G=\Delta H-T\Delta S$). Experimentalment [9d] s'ha determinat que la transició de fase $\alpha \rightarrow \beta$ és endotèrmica i irreversible (63±2 °C). La irreversibilitat ens indica que el terme $\Delta G(\beta \rightarrow \alpha)$ és positiu i gran : el procés no serà espontani. El fet que la transició $\alpha \rightarrow \beta$ és endotèrmica (0.4±0.1 kcal mol^{-1}), indica que l'entalpia del procés invers $\Delta H(\beta \rightarrow \alpha)$ serà petita però negativa. De manera que el factor determinant de la irreversibilitat en passar d'$\alpha \rightarrow \beta$ sembla ser el terme entròpic. Aquesta apreciació concorda amb el fet que, donat el gran número de contactes a establir en la fase β, la fase β sembla presentar una major flexibilitat a l'hora d'establir-los, la qual cosa es tradueix en què la fase β sembla tenir més entropia que l'α-HNN.

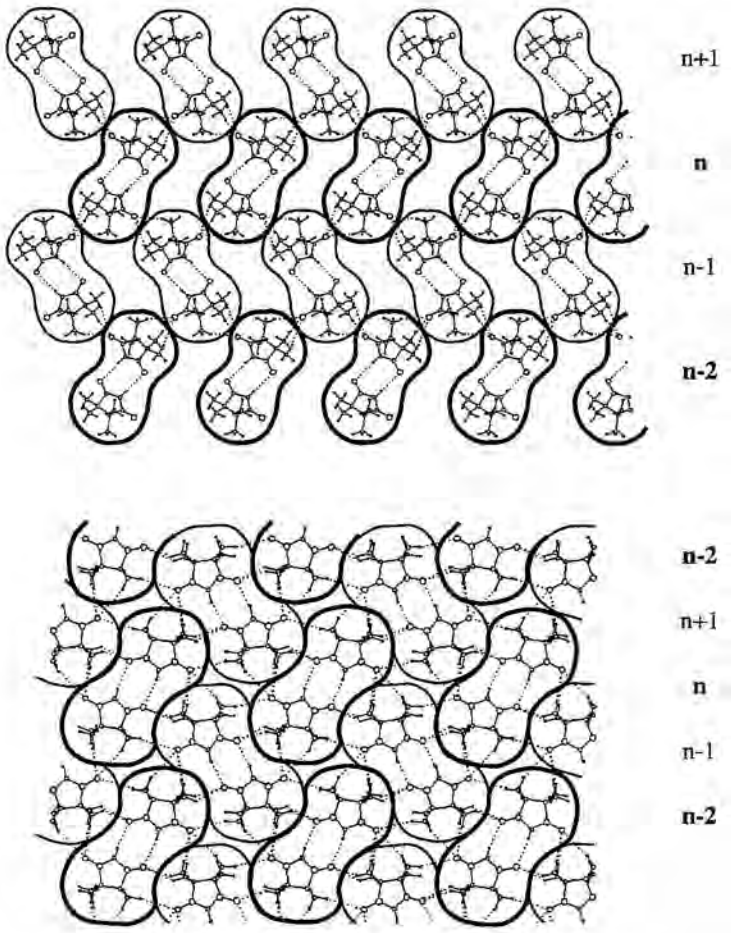

FIGURA 1.8.- Representació esquemàtica de les capes dels cristalls α-HNN (pla bc) i β-HNN (pla ab) (part superior i inferior de la FIGURA, respectivament)

Finalment, només cal dir que els canvis en l'estructura secundària de l'empaquetament produïts en la transició d'α-HNN a β-HNN es veuran reflectits en les respectives estructures terciàries. Així doncs, les variacions en l'estructura interna de les capes de l'empaquetament (estructura secundària) en passar d'α-HNN a β-HNN són les responsables de què l'apilament d'aquests plans (estructura terciària) també s'hagi d'adaptar. Això, però, no serà cap problema donat el gran número de grups metil disponibles perpendiculars als plans que s'apilen.

1.3. CONCLUSIONS.

L'anàlisi de l'empaquetament cristal.lí en base als seus grups funcionals (CPFGA) ha demostrat ser un procediment adequat per tal de racionalitzar l'estructura de qualsevol cristall. Aquesta tècnica es basa en (1) la caracterització del caràcter àcid-bàsic dels grups funcionals dels radicals constituents del cristall, (2) la identificació de les estructures primàries de l'empaquetament cristal.lí, i (3) el càlcul de la força de les estructures primàries d'interès. La informació obtinguda amb el mètode CPFGA no només serveix per a racionalitzar estructures de cristalls sinó que també permet *entendre* els canvis microscòpics que tenen lloc en una transició polimòrfica entre diferents fases.

Gràcies a l'estudi de l'HNN i tenint en compte que la molècula d'HNN és l'*esquelet* de la resta de membres de la família d'α-nitronil nitròxids (R=H), podem concloure que, en tots els membres d'aquesta família, els contactes intermoleculars que dirigeixen i estabilitzen l'empaquetament d'aquests cristalls són del tipus C-H···O-N. Càlculs ab initio a nivell MP2/6-311++G(2d, 2p) han permès estimar l'energia d'interacció d'aquest tipus de contactes. D'altra banda, aquestes estimacions ens han permès justificar l'existència experimental d'una transició de fase α a β irreversible en el cristall d'HNN.

BIBLIOGRAFIA.

[1] (a) A. Gavezzotti, *Acc. Chem. Res.*, **1994**, *27*, 309; (b) J. Bernstein, *J. Phys. D: Appl. Phys.*, **1993**, *26*, B66; (c) J.D. Dunitz, J. Bernstein, *Acc. Chem. Res.*, **1995**, *28*, 193; (d) H.R Karfunkel,. R.J. Gdanitz, *J. Comput. Chem.*, **1992**, *13*, 1171; (e) J. Bernstein, *J. Am. Chem. Soc.*, **1994**, *116*, 455.

[2] G.C. Maitland, M. Rigby, E. Brian Smith, W.A. Wakeham, *Intermolecular Forces*, Clarendon Press, Oxford, **1981**.

[3] J. Bernstein, M.C. Etter, L. Leiserowitz, *Structure Correlation*, edited by H.-B. Burgi and J.D. Dunitz, VCH, Weinheim, **1994**. Chap. 11.

[4] (a) E. Scrocco, J. Tomasi, *Adv. Quantum Chem.*, **1978**, *11*, 115; (b) P. Politzer, J.S. Murray, *Rev. Comput. Chem.*, **1991**, *2*, 273.

[5] A.J. Stone, *The theory of intermolecular forces*, Clarendon Press,Oxford, **1996**.

[6] (a) J.J. Novoa, M. Deumal, *Mol. Cryst. Liq. Cryst.* **1997**, *305*, 143. (b) M. Deumal, J. Cirujeda, J. Veciana, M. Kinoshita, Y. Hosokoshi, J.J. Novoa. *Chem. Phys. Lett.*, **1997**, *265*, 190. (c) J.J. Novoa, F. Allen, J. Howard (eds.) *Implications of Molecular and Materials Structure for New Technologies*, Kluwer Academic Publishers, Dordretch, (in press).

[7] (a) D.G.B. Boocock, R. Darey, E.F. Ullman, *J. Am. Chem. Soc.*, **1968**, *90*, 5945; (b) Y. Hosokoshi, M. Tamura, K. Nozawa, S. Suzuki, H. Sawa, R. Kato, M. Kinoshita., *Mol. Cryst. Liq. Cryst.*, **1995**, *115*, 271; (c) E. Molins, resultats no publicats (refinament posterior a 7b de l'estructura β-HNN); (d) J. Cirujeda, Tesi Doctoral, Univ. Ramon Llull, **1997**.

[8] (a) C. Møller, M.S. Plesset, *Phys. Rev.* **1934**, *46*, 61. (b) M. Head-Gordon, J.A. Pople, M.J. Frisch, *Chem. Phys. Lett.* **1988**, *153*, 503. (c) S. Saebo, J. Almlof, *ibid.* **1989**, *154*, 83. (d) M.J. Frisch, M. Head-Gordon, J.A. Pople, *ibid.* **1990**, *166*, 281. (e) M. Head-Gordon, T. Head-Gordon, *ibid.* **1994**, *220*, 122.

[9] (a) J.H. van Lenthe, J.G.C.M. van Duijneveldt-van de Rijdt, R.F. van Duijneveldt, *Ab Initio Methods in Quantum Chemistry*, Vol. II, K.P. Lawley, ed.,Wiley, New York, **1987**; (b) F.B. van Duijneveldt, J.G.C.M. van Duijneveldt-van der Rijdt, J.H. van Lenthe, *Chem. Rev.* **1994**, *94*, 1873; (c) F.-M. Tao, Y.-K. Pan, *J. Phys. Chem.*, **1991**, *95*, 3582; (d) P. Hobza, R. Zahradnik, *Chem. Rev.*, **1988**, *88*, 871; (e) J.J. Novoa, M. Planas, M.-H. Whangbo, *Chem. Phys. Lett.*, **1994**, *225*, 240; (f) J.J. Novoa, M. Planas, M. C. Rovira, *Chem. Phys. Lett.*, **1996**, *251*, 33; (g) S.F. Boys, F. Bernardi, *Mol. Phys.*, **1970**, *19*, 553.

[10] Gaussian 94, Revision C.3, M.J.Frisch, G.W. Trucks, H.B. Schlegel, P.M.W. Gill, B.G. Johnson, M.A. Robb, J.R. Cheeseman, T. Keith, G.A. Peterson, J.A. Montgomery, K. Raghavachari, M.A. Al-Laham, V.G. Zakrzewski, J.V. Ortiz, J.B. Foresman, J. Ciolowski, B.B. Stefanov, A. Nanayakkara, M. Challacombe, C.Y. Peng, P.Y. Ayala, W. Chen, M.W. Wong, J.L. Andres, E.S. Replogle, R. Gomperts, R.L. Martin, D.J. Fox, J.S. Binkley, D.J. Defrees, J. Baker, J.J.P. Stewart, M. Head-Gordon, C. Gonzalez, J.A. Pople, Gaussian, Inc., Pittsburgh PA, **1995**.

[11] J.J. Novoa, M.-H. Whangbo, J. M Williams, *J. Chem. Phys.*, **1991**, *94*, 4835.

[12] M. Deumal, J.J. Novoa, resultats no publicats.

[13] J.J. Novoa, M. Deumal, M. Kinoshita, Y. Hosokoshi, J. Veciana, J. Cirujeda, *Mol. Cryst. Liq. Cryst.*, **1997**, *305*, 129.

"Se non è vero,
è ben trovato"
Dante Alighieri

CAPÍTOL 2:

Validesa del Model de McConnell-I

2.1. Models Qualitatius Magnètics.

El fet que fases cristal.lines diferents constituïdes a partir d'un mateix radical presentin propietats magnètiques diferents suggereix que el magnetisme molecular d'un cristall està fortament relacionat amb l'ordenament geomètric relatiu dels radicals dins del cristall [1]. Així doncs, per a un disseny racional de materials magnètics purament orgànics amb temperatures crítiques altes es necessiten teories que relacionin magnetisme i estructura cristal.lina.

Actualment, hi ha un gran número de models pensats per tal de correlacionar magnetisme i estructura [1a, 2]. Molts d'aquests models estan dissenyats per explicar el magnetisme en derivats polinuclears de compostos de metalls de transició. El model que primer va aparèixer per racionalitzar qualitativament aquest magnetisme anomenat "a través d'enllaç" (*through bond*) va ser proposat per Anderson [3], seguit després pels suggerits per Kahn [1b], i Hay-Thibeault-Hoffmann [4]. Les dues darreres aproximacions donen resultats similars i prediuen correctament la presència d'interaccions ferro- i antiferromagnètiques [5]. Ara bé, aquestes aproximacions no tenen en compte els efectes de correlació electrònica necessaris per tal de descriure correctament algunes propietats de compostos magnètics [6]. Aquesta mancança ha afavorit el desenvolupament d'aproximacions més precises per a aquests sistemes, pensades per al estudi quantitatiu de propietats magnètiques. Aquesta nova metodologia està basada en mètodes pertorbatius [7] i d'interacció de configuracions com el DDCI (*difference dedicated configuration interaction method*) [8]. D'altra banda, l'aproximació de simetria trencada introduïda per Noodleman, en el context de la metodologia del funcional de la densitat [9a], també sembla donar bons resultats en alguns casos [9b-c]. Els mètodes que s'usen per a explicar l'ordenació dels estats d'alt i baix spin en molècules diradicalàries [10] estan força relacionats amb l'anterior aproximació.

Hi ha models particularment interessants que es van dissenyar per a explicar el magnetisme "a través d'espai" (*through space*) en sistemes moleculars purament orgànics [11]. Aquest magnetisme s'anomena així per a diferenciar-se del magnetisme "a través d'enllaç". Els mètodes que s'usen amb més freqüència per aquest tipus de sistemes es basen en els models proposats per McConnell, I [11a] i II [11b]. El model II va ser proposat per a explicar el magnetisme en compostos de transferència de càrrega. Kollmar i Kahn [11g], però, van demostrar que aquest mecanisme no era adequat. En canvi, el model més usat per a l'estudi del magnetisme de cristalls neutres —per exemple, els de la família dels α-nitronil nitròxids— és el model de McConnell-I. Aquest model, que introduirem en l'apartat 2.1.1, és considerat la millor eina qualitativa que es té en estat sòlid a l'hora d'esbrinar quin és el magnetisme d'un cristall molecular. Per aquest motiu, al llarg d'aquest capítol, pretenem comprovar la seva validesa.

2.1.1.- El model de McConnell-I.

L'any 1963, McConnell [11a] va proposar que la interacció magnètica entre dos radicals *aromàtics* A i B es podia aproximar amb un Hamiltonià de Heisenberg d'spin del tipus:

$$\hat{H}^{AB} = -\sum_{i\in A, j\in B} J_{ij}^{AB} \hat{\mathbf{S}}_i^A \cdot \hat{\mathbf{S}}_j^B \qquad (2.1)$$

on $\hat{S}_i^A, \hat{S}_j^B$ és el producte dels operadors d'spin en els àtoms i, j dels fragments A, B i J_{ij}^{AB} són integrals de bescanvi bielectròniques. Cal puntualitzar que la notació utilitzada per McConnell pot donar lloc a confusió, ja que el que ell anomena "integrals de bescanvi bielectròniques J_{ij}^{AB}" prenen el nom genèric de *paràmetres d'acoblament de bescanvi* J_{ij} en el context dels Hamiltonians de Heisenberg d'spin. En aquest context, el paràmetre d'acoblament de bescanvi J_{ij} s'interpreta en termes de distribució electrònica com el bescanvi de Heitler-London

$$J_{ij} = [ij|ij] + 2s_{ij} < i|h|j > \qquad (2.2)$$

on $[ij|ij]$ és un valor petit i positiu corresponent a l'energia de bescanvi bielectrònica, i $< i|h|j >$ està dominat per l'atracció electrònica nuclear, essent un valor gran i negatiu. Així doncs, J_{ij} és negatiu generalment. La quantitat s_{ij} és el solapament dels orbitals i, j, per tant J_{ij} serà un terme positiu només quan el solapament d'orbitals tendeixi a zero.

L'Hamiltonià corresponent a l'equació (2.1), però, no ha estat avaluat mai, sinò que és substituït per una simplificació "ad hoc" donada per

$$\hat{H}^{AB} = -\hat{\mathbf{S}}^A \cdot \hat{\mathbf{S}}^B \sum_{i\in A, j\in B} J_{ij}^{AB} \rho_i^A \rho_j^B \qquad (2.3)$$

on $\hat{S}^A, \hat{S}^B$ són els operadors totals d'spin dels fragments A i B, J_{ij}^{AB} són altre cop les integrals de bescanvi bielectròniques, i ρ_i^A, ρ_j^B són les densitats d'spin dels àtoms i, j dels fragments A i B, respectivament.

Sempre en el *context de molècules aromàtiques apilades una al damunt de l'altra en cristalls*, McConnell afirma textualment que "la tendència dominant per un acoblament d'spin antiparal.lel en radicals lliures en estat sòlid és deguda al fet que les densitats d'spin ρ_i^A, ρ_j^B són normalment positives, i que els valors més grans de les integrals de bescanvi J_{ij}^{AB} són negatius". Així doncs, en assumir que les J_{ij}^{AB} són negatives, el model de McConnell-I està associant la presència d'interaccions intermoleculars ferromagnètiques amb l'existència de contactes curts entre àtoms i, j que tenen una població d'spin ρ_i, ρ_j considerable amb

signe contrari. Donat que la distribució d'spin és una propietat que es pot obtenir a nivell experimental [12] i teòric [12, 13], els usuaris de McConnell-I *s'obliden* del valor de les J_{ij}^{AB}, i *amplien* el rang d'aplicabilitat d'aquest model a qualsevol tipus de sistema. El resultat és que, en l'ús normal del model de McConnell-I[1], el caràcter magnètic d'un cristall molecular donat es pot racionalitzar calculant la distribució d'spin en els àtoms de les molècules que donen lloc a aquest cristall i mirant el seu solapament.

En el següent apartat es racionalitzarà el magnetisme de 5 cristalls que pertanyen a la família dels α-nitronil nitròxids en base al model de McConnell-I per tal de determinar l'abast de la seva validesa i el seu rang d'aplicabilitat.

2.2. Interpretació del Magnetisme de 5 Cristalls de la Família dels α-Nitronil Nitròxids segons el Model de McConnell-I.

Els cristalls estudiats en aquest apartat són : (1) PNN [14], (2) les fases α i β del 2-OHPNN [15], (3) 4-OHPNN [16] i (4) β-p-NPNN [17] en la FIGURA 2.1. Experimentalment, la fase α-2-OHPNN, el 4-OHPNN i el β-p-NPNN són ferromagnets, mentre que el PNN i la fase β-2-OHPNN són antiferromagnets.

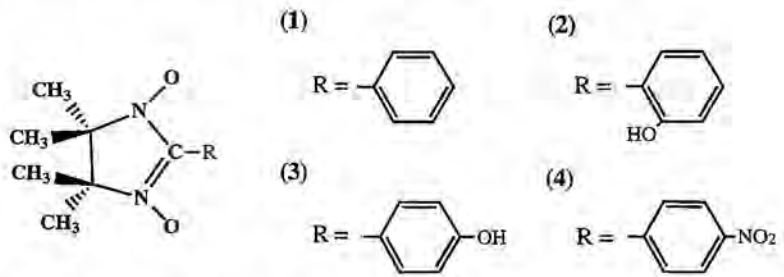

FIGURA 2.1.- Estructura dels radicals (1) PNN, (2) 2-OHPNN, (3) 4-OHPNN i (4) β-p-NPNN.

El model de McConnell-I es basa en què electrons desaparellats en àtoms/fragments que pertanyen a molècules veïnes s'acoblen ferromagnèticament només si els respectius àtoms/fragments presenten densitats d'spin de diferent signe que es poden solapar. Així doncs, la interpretació del magnetisme dels cristalls anteriors segons el model de McConnell-I requereix dues etapes prèvies: (1) el càlcul de les densitats electròniques d'spin

[1] A partir d'aquest moment, quan es parli de "model de McConnell-I" s'haurà d'entendre *"l'ús qualitatiu normal del model de McConnell-I"*

en els àtoms dels radicals α-nitronil nitròxid constituents, i (2) una anàlisi CPFGA del seu empaquetament cristal.lí.

2.2.1.- Densitats electròniques d'spin.

Els radicals α-nitronil nitròxid analitzats tenen un electró desaparellat, per tant es comporten electrònicament com a doblets. Totes les densitats d'spin s'han calculat a nivell DFT amb el funcional BLYP i la base 6-31G(2d, 2p). Les densitats electròniques d'spin resultants es mostren en la FIGURA 2.2. Cal esmentar que les densitats d'spin tenen simetria π : existeix un pla nodal que conté l'anell de cinc que apareix en tots els derivats α-nitronil nitròxid. Experimentalment, la densitat d'spin en els radicals de derivats α-nitronil nitròxid està localitzada majoritàriament en la unitat ONCNO, independentment del substituent enllaçat en α. La FIGURA 2.2 suggereix que el resultat dels càlculs de densitats d'spin concorda amb el que s'ha mesurat experimentalment: la major part de la densitat d'spin està localitzada en els grups NO. S'ha detectat també una petita densitat negativa en el C(sp^2) en α de la unitat ONCNO, i una alternació en el signe de la densitat en l'anell de benzè. D'altra banda, l'O dels grups OH i NO_2 i alguns C dels grups metil tenen una petita densitat d'spin positiva. Ara bé, tot i que els espectres d'ESR indiquen l'existència d'una petita densitat en tots els H, els càlculs a nivell BLYP/6-31G(2d, 2p) no han detectat cap densitat d'spin en els àtoms d'H.

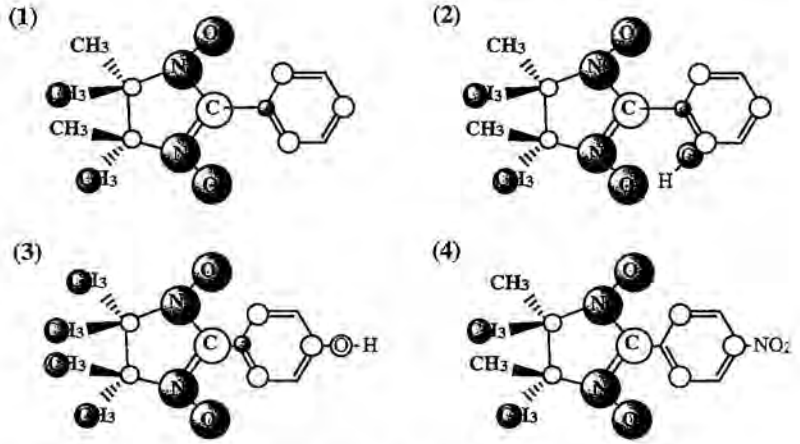

FIGURA 2.2.- Representació de les densitats electròniques d'spin dels radicals (1) PNN, (2) 2-OHPNN, (3) 4-OHPNN i (4) β-p-NPNN a nivell BLYP/6-31G(2d, 2p).

Així doncs, tal com ja s'ha dit, la densitat electrònica d'spin es concentra en la unitat ONCNO, la qual cosa significa que l'electró desaparellat es pot associar a aquesta unitat. L'acoblament de dos electrons desaparellats que pertanyin a dues de les unitats anteriors, ONCNO, podrà donar lloc a un estat resultant singlet o triplet. Segons el model de McConnell-I, un singlet s'obtindrà si dues unitats ONCNO interaccionen a través dels grups NO ja que són aquests grups els que concentren la major part de la densitat d'spin de signe positiu. Contràriament, si els electrons s'acoblen de manera paral.lela l'estat resultant serà triplet i requerirà, segons McConnell, la interacció NO $\leftrightarrow$ C(sp^2) (densitat d'spin positiva $\leftrightarrow$ negativa) de dues unitats ONCNO. Així doncs, el model de McConnell-I proposa com a responsable de l'existència d'un estat fonamental singlet (o triplet) l'orientació que pren la unitat ONCNO dins del cristall (sempre i quan la distància NO···ON / NO···C(sp^2) sigui suficientment curta com perquè la interacció no sigui negligible).

2.2.2.- McConnell-I aplicat a l'empaquetament de les unitats ONCNO.

Per tal de determinar el tipus de magnetisme dels cristalls formats a partir dels radicals de la FIGURA 2.1 necessitem aplicar els arguments exposats en el paràgraf anterior. Abans, però, hem fet una anàlisi CPFGA de l'empaquetament que presenten els 5 cristalls que volem estudiar. Aquest procediment ja ha estat exposat i exemplificat en el Capítol 1, per tant, passarem a interpretar directament el magnetisme segons McConnell-I en base a l'empaquetament, analitzat amb el mètode CPFGA, de les unitats ONCNO. S'estudiaran, doncs, les orientacions del tipus O···O i O···C(sp^2), on O pot pertànyer als grups ONCNO, NO_2, i OH.

El cristall PNN és un antiferromagnet, AFM [14]. Aquest cristall pertany al grup espacial $P2_1/c$ (a=21.14Å, b=10.14Å, c=12.22Å i β=108.1°) i té vuit molécules per cel.la unitat. La disposició que adopten els radicals dins de la cel.la unitat és en capes del tipus ABBA al llarg d'a (FIGURA 2.3a), amb les capes A i B empaquetades de diferent manera. Dins d'ambdues capes A i B (pla bc), la distància més curta entre grups NO provinents d'unitats ONCNO és de 5.02Å i 6.65Å, respectivament (FIGURA 2.3b). A aquestes distàncies el solapament de densitats electròniques d'spin és negligible. De la mateixa manera, tampoc n'existeix entre NO···C(sp^2) en α dels grups ONCNO perquè les distàncies més curtes són 5.13Å (capa A) i 6.69Å (capa B). Per tant, és d'esperar que no hi hagi cap interacció magnètica significativa en cap de les capes. En la FIGURA 2.3c es presenten les interaccions NO···ON i NO···C(sp^2) entre capes. Els contactes intermoleculars NO···ON són relativament curts: 3.68Å en l'apilament de capes B···B, 4.05 i 5.10Å en el B···A, i 4.51Å en el A···A. En canvi, dels NO···C(sp^2) només cal destacar els contactes entre B···A a 3.93 i

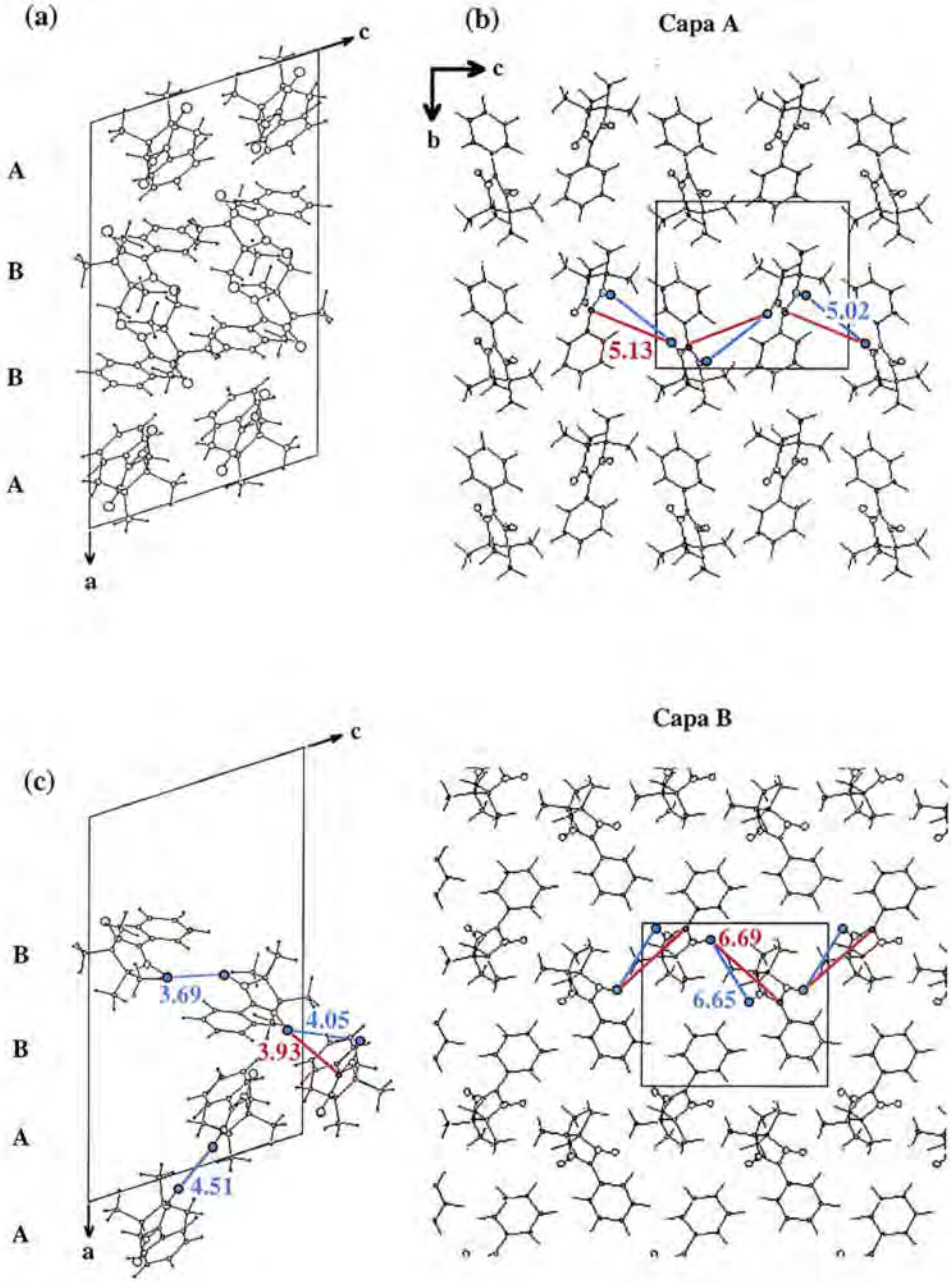

FIGURA 2.3.- Estructura del cristall PNN

5.79Å (6.84Å en B···B, 6.16Å en A···A). En base a McConnell-I i donat el solapament dels grups NO de les unitats ONCNO, els contactes B···B i A···A tindran un caràcter antiferromagnètic, però en B···A hi haurà una competició entre interaccions ferro- (3.93Å) i antiferromagnètiques (4.05Å). Ara bé, tot i existir interaccions magnètiques al llarg de l'apilament entre capes B···B···A···A, és d'esperar que aquestes interaccions no es propagaran ja que seran molt dèbils entre capes A···A, degut a la distància. Així doncs, d'acord amb el model de McConnell-I, el cristall PNN es comportarà com un paramagnet. En aquest cas, el model de McConnell-I no ha predit correctament el caràter antiferromagnètic del PNN.

El cristall α-2-OHPNN (2) experimentalment és un ferromagnet tridimensional (FM 3D) [15a]. Aquest cristall pertany al grup espacial Pbca (a=12.957Å, b=13.584Å, c=14.772Å) i té vuit molécules per cel.la unitat. Aquest cristall s'empaqueta de tal manera que la cel.la unitat presenta capes idèntiques A al llarg de c (FIGURA 2.4a). L'estructura de cada capa (pla ab) és força complicada, però es pot racionalitzar en base a cadenes alternades a dreta i esquerra formades per la propagació de "dímers moleculars" al llarg de b (FIGURA 2.4a). En cada capa A (FIGURA 2.4b), dins de cada cadena hi ha contactes ONCNO···ONCNO a 3.97Å i ONCNO···OH a 4.94Å, i entre cadenes aquests contactes estan a 5.73 i 5.50Å, respectivament. En quan a contactes del tipus NO···C(sp^2) presents en A, només cal dir que no n'hi ha per sota de 5Å (dins de cada cadena a 5.61Å, i entre cadenes a 5.89Å). Així doncs, cada capa A tindrà, al llarg de b, cadenes antiferromagnètiques . D'altra banda, les distàncies ONCNO···OH més curtes entre dues capes A són de 4.79 i 5.54Å (FIGURA 2.4c) (no hi ha contactes NO···C(sp^2) per sota de 5Å: el més curt està a 6.48Å). Per tant, entre capes les interaccions magnètiques seran negligibles. Segons McConnell-I, el cristall α-2-OHPNN serà un antiferromagnet monodimensional (1D) i no un ferromagnet 3D.

El cristall β-2-OHPNN (2) és experimentalment un antiferromagnet 1D amb interaccions FM febles entre cadenes [15b]. Aquest cristall pertany al grup espacial C2/c (a=18.372Å, b=7.294Å, c=20.088Å i β=106.56°) i té vuit molécules per cel.la unitat. En aquest cristall hi ha quatre capes per cel.la unitat del tipus ABBA al llarg d'a (FIGURA 2.5a). Dins de cada capa (pla bc, FIGURA 2.5b), trobem cadenes antiferromagnètiques al llarg de b, donat que hi ha contactes ONCNO···ONCNO a 3.82Å (també n'hi ha d'ONCNO···OH a 5.01Å que són magnèticament negligibles). Aquestes cadenes, però, no es propaguen al llarg de c perquè no existeixen contactes O···O a distàncies suficientment curtes. D'altra banda, dins d'aquestes capes no hi ha contactes del tipus NO···C(sp^2) per sota de 5.18Å. Entre capes (FIGURA 2.5c), hi ha força contactes O···O ja que cada molècula de 2-OHPNN estableix interaccions ONCNO···ONCNO a 3.84, 5.08Å (B···B) i 3.74, 4.84Å (B···A); ONCNO···OH a 3.98Å (B···A) i 5.38Å (B···B); i HO···OH entre B···A a 5.88Å. A més,

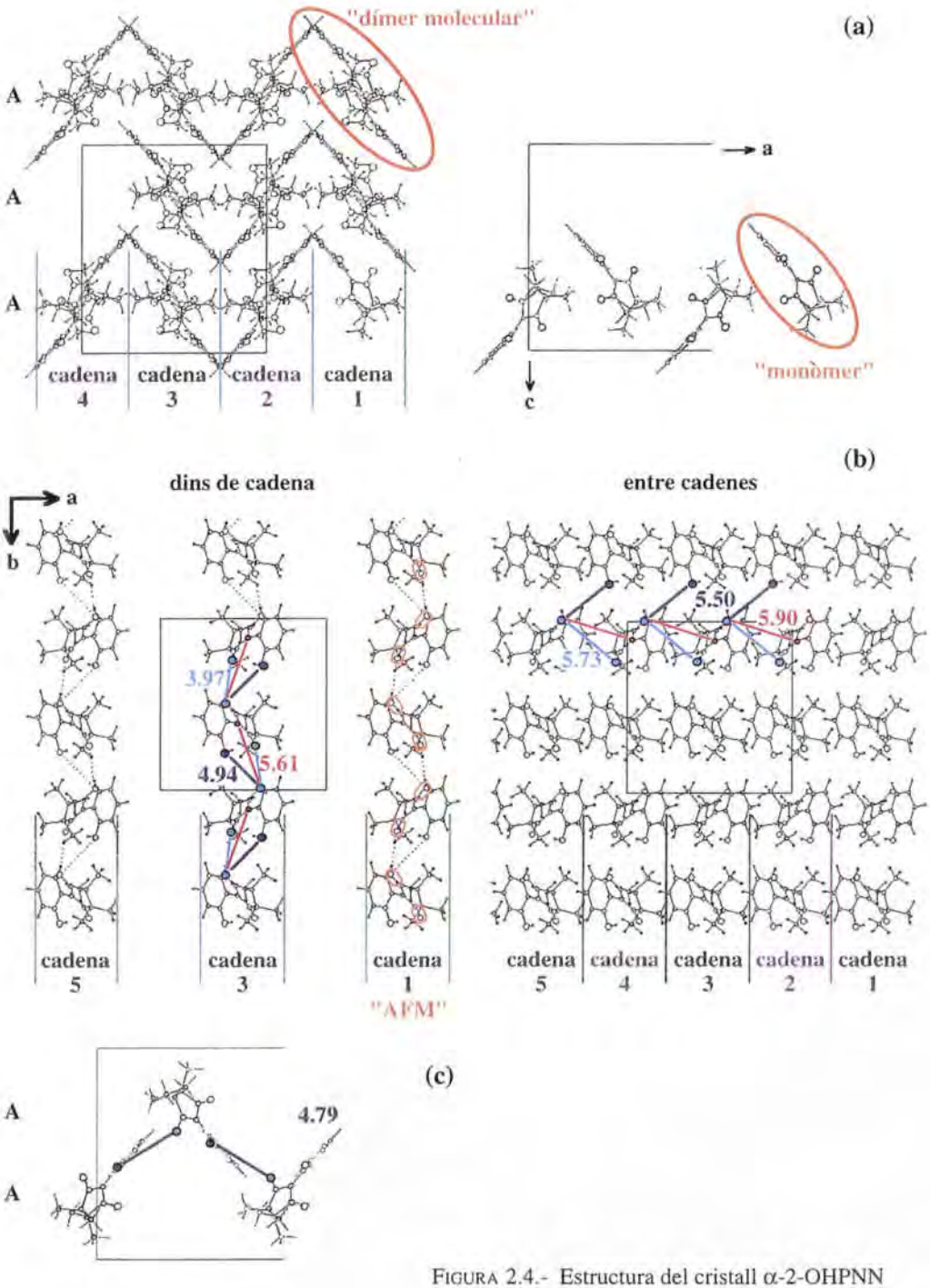

FIGURA 2.4.- Estructura del cristall α-2-OHPNN

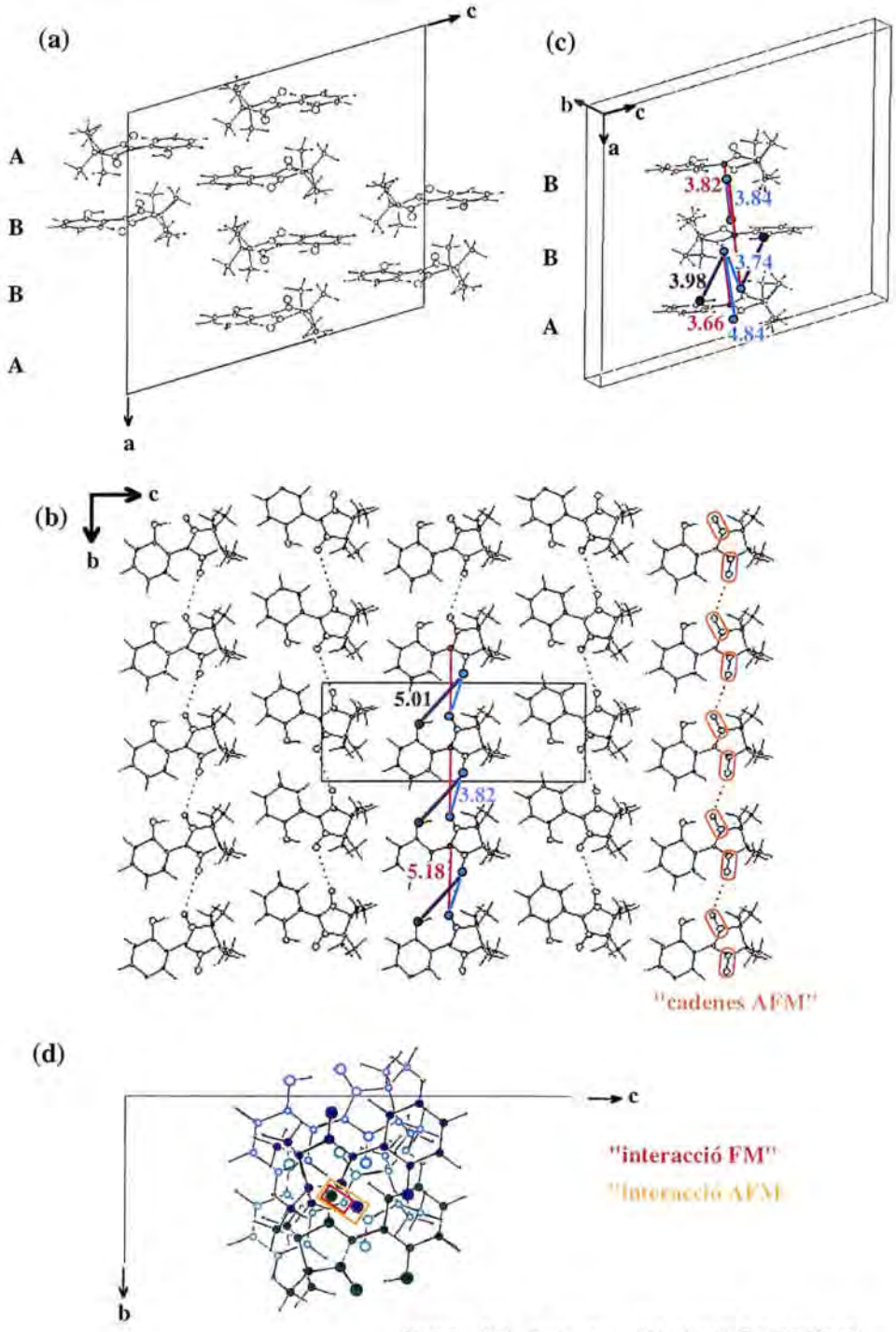

FIGURA 2.5.- Estructura del cristall β-2-OHPNN

també s'estableixen contactes NO···C(sp^2) a 3.66Å (B···A) i 3.82Å (B···B). En aquest cas, doncs, no és fàcil predir el signe de la interacció magnètica ja que existeixen múltiples contactes de signe diferent (O···O vs. O···Csp^2) que estan competint entre ells mateixos (FIGURA 2.5d). Ara bé, en ser les distàncies NO···C(sp^2) més curtes, podríem concloure que entre capes les interaccions ferromagnètiques seran febles, però predominants. Així doncs, segons McConnell-I, el cristall β-2-OHPNN serà un antiferromagnet monodimensional (1D) amb interaccions ferromagnètiques febles entre cadenes; predicció que concorda amb els resultats experimentals.

El cristall 4-OHPNN (4) es comporta experimentalment com a un ferromagnet 2D [16]. Aquest cristall pertany al grup espacial $Pca2_1$ (a=11.765Å, b=12.726Å, c=17.601Å) i té vuit molécules per cel.la unitat. La disposició que adopten aquestes molècules dins de la cel.la és en capes ABBA al llarg de c (FIGURA 2.6a). Dins de cada capa (pla ab, FIGURA 2.6b), hi ha contactes ONCNO···OH a 2.69 i 5.66Å (també existeixen interaccions del tipus C(sp^2)···OH a 4.47Å). Tanmateix, però, tot i existir contactes NO···OH i C(sp^2)···OH, els grups ONCNO estan suficientment separats com per considerar que estan "aïllats". Entre capes (FIGURA 2.6c), s'estableixen contactes ONCNO···ONCNO (5.16Å en B···B i 4.91Å en B···A) i ONCNO···OH (5.29Å en B···B i 4.38 i 4.40Å en B···A). De la mateixa manera, les interaccions C(sp^2)···ONCNO i C(sp^2)···OH només són significatives entre B···A a 4.63 i 4.83Å, respectivament (entre B...B, C(sp^2)···ONCNO a 5.07Å i C(sp^2)···OH a 5.66Å). Ara bé, tal com passava dins de les capes, tot i establir contactes NO···O i C(sp^2)···O, les distàncies intermoleculars són prou grans com per a poder negligir totes aquestes interaccions. El resultat és que el cristall 4-OHPNN es comportarà com un paramagnet d'acord amb McConnell-I i no com un ferromagnet 2D.

El cristall β-p-NPNN (5) es comporta experimentalment com a un ferromagnet 3D [17]. Aquest cristall pertany al grup espacial F2dd (a=10.960Å, b=19.350Å, c=12.347Å) i té vuit molécules per cel.la unitat. La disposició que adopten els radicals dins de la cel.la és en capes del tipus ABABA al llarg de b (FIGURA 2.7a). Dins de cada capa (pla ac), la distància entre grups NO provinents de fragments ONCNO és aproximadament d'uns 6.00Å (FIGURA 2.7b). Aquesta distància és massa llarga com perquè dos grups ONCNO estableixin una interacció antiferromagnètica entre ells. Tampoc n'existeixen de ferromagnètiques perquè la distància ONCNO···C(sp^2) en α dels grups ONCNO és encara més llarga. D'altra banda, els O dels grups nitro (ONO) han estat proposats com a part activa en les interaccions entre unitats ONCNO [18]. En aquest cas, cada monòmer estableix 8 contactes del tipus ONCNO···ONO (a 3.44 i 3.68 Å) i 4 del tipus ONC(sp^2)···ONO (a 5.49 i 5.68 Å) (FIGURA 2.7b). Ara bé, tot i que el número de contactes és important, l'orientació és l'adequada i la distància intermolecular prou curta en el primer cas, la densitat electrònica d'spin dels grups nitro és quasi negligible. Per tant, d'acord amb McConnell-I, dins d'una mateixa capa hi

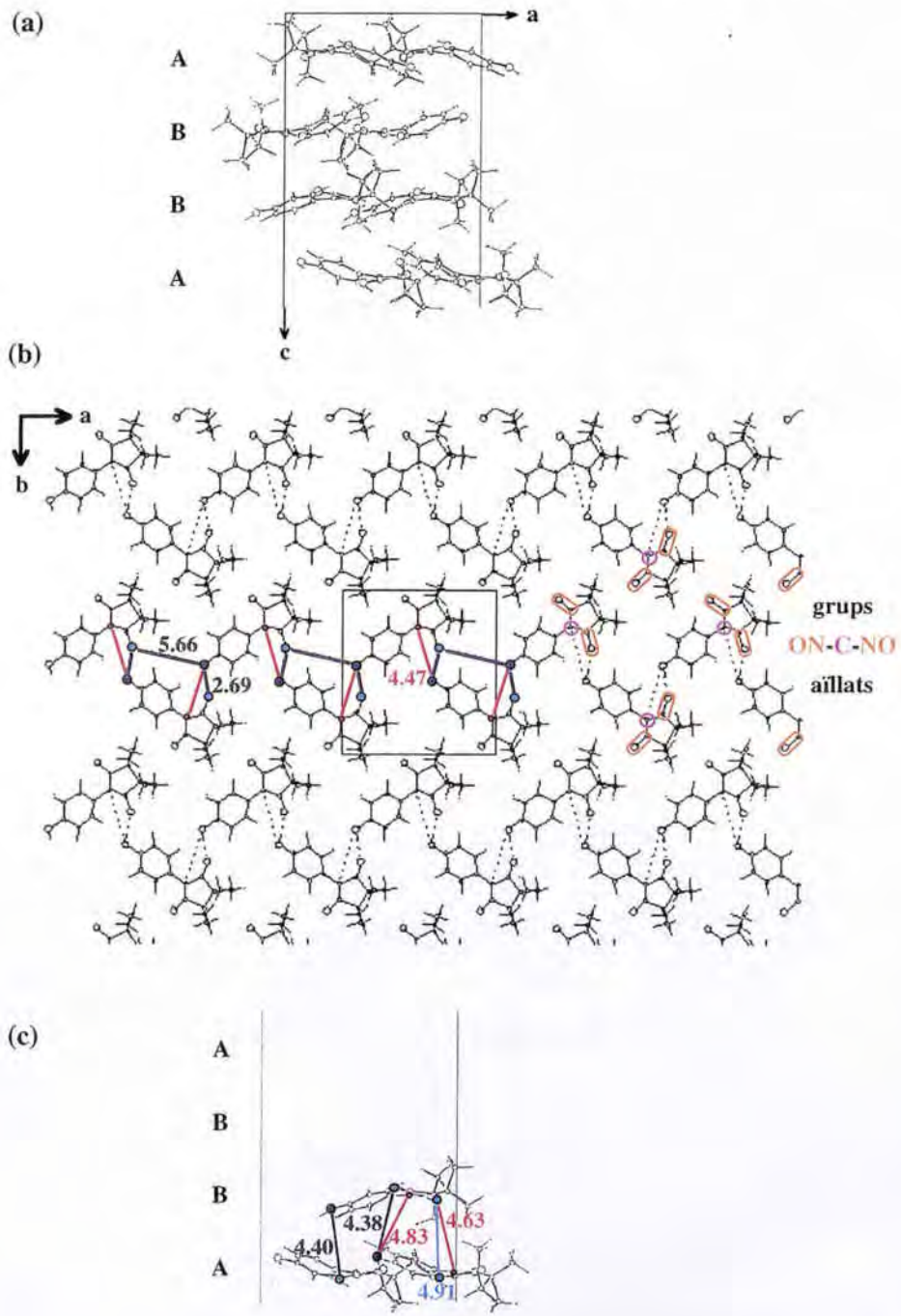

FIGURA 2.6.- Estructura del cristall 4-OHPNN

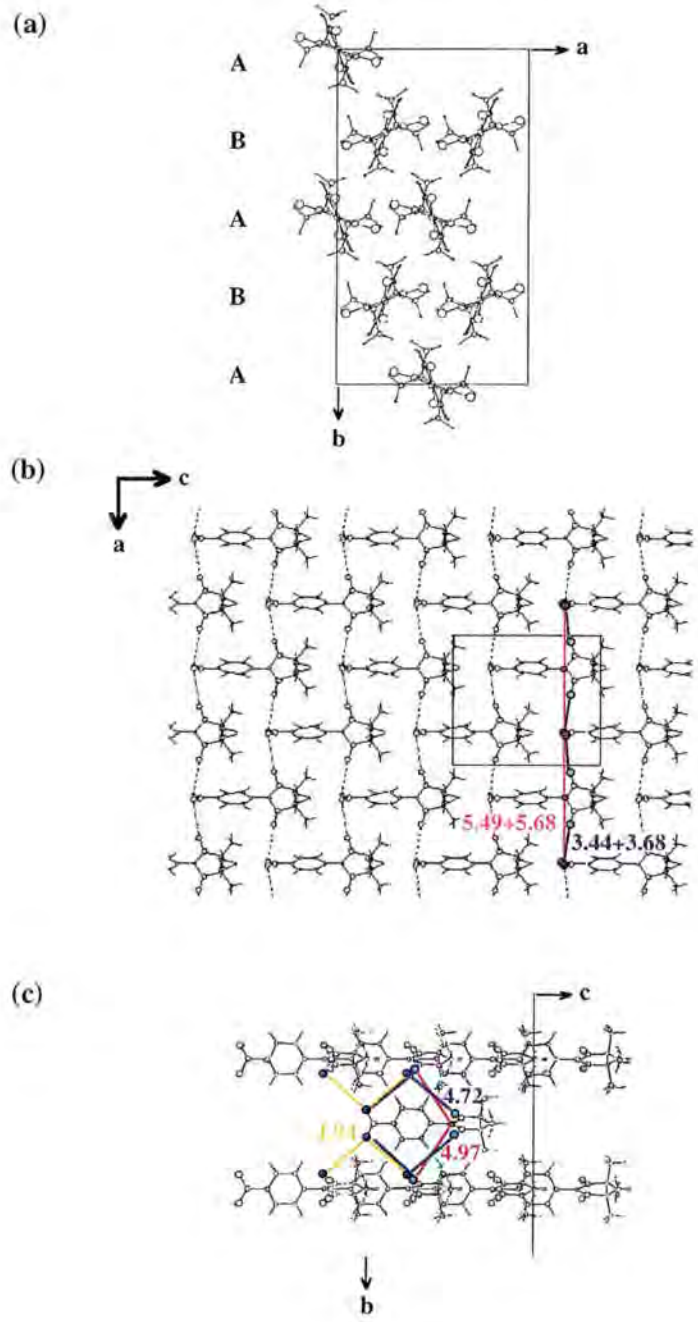

FIGURA 2.7.- Estructura del cristall β-p-NPNN

haurà interaccions antiferromagnètiques molt dèbils a través de contactes ONCNO···ONO, mentre que les ferromagnètiques seran negligibles. Entre capes, i fent participar els O dels grups nitro, també veiem l'existència de contactes ONCNO···ONO (4.72 Å), ONO···ONO (4.94 Å) i ONC(sp^2)···ONCNO (4.97 Å) (FIGURA 2.7c). Tenint només en compte la densitat electrònica d'spin dels grups que estableixen aquests contactes i donat que la quasi totalitat de la densitat d'spin està localitzada en els grups ONCNO (FIGURA 2.2), és d'esperar que una interacció del tipus ONC(sp^2)···ONCNO sigui més forta. En conseqüència, les interaccions dominants entre capes serien dèbilment ferromagnètiques d'acord amb McConnell-I. Ara bé, les distàncies intermoleculars associades a aquestes interaccions són massa llargues i, per tant, aquestes interaccions seran negligibles entre capes. Resumint, segons el model de McConnell-I, el β-p-NPNN està format per capes amb interaccions dèbils antiferromagnètiques; capes que no interaccionen entre elles mateixes. Evidentment, la predicció feta pel model de McConnell-I i les dades experimentals no coincideixen en el cas del β-p-NPNN.

Els resultats anteriors mostren que hi ha inconsistències entre les prediccions fetes pel model de McConnell-I en base a interaccions O···O i O···C(sp^2) i les dades experimentals sobre el magnetisme d'aquests cristalls. Així doncs, donat que hi ha bibliografia [19] que proposa els enllaços per pont d'hidrogen H···O com a responsables del magnetisme, s'ha dut a terme el mateix estudi per a aquest tipus d'interaccions. Les prediccions fetes pel model de McConnell-I[2] sobre el signe de les interaccions H···O depenen del tipus d'H. Els H metílics i aromàtics en posició meta tenen una densitat d'spin calculada experimentalment negativa i, per tant, donen lloc a interaccions ferromagnètiques. En canvi, la densitat d'spin dels H aromàtics en orto i para és positiva, donant lloc a interaccions antiferromagnètiques. En base a aquests criteris, s'ha estudiat el magnetisme dels 5 cristalls anteriors. Els resultats tornen a no ajustar-se amb el magnetisme experimental d'aquests cristalls. En el cas dels cristalls α-2-OHPNN, β-2-OHPNN, 4-OHPNN i β-p-NPNN s'obté que són ferromagnets d'alta dimensionalitat, mentre que per al PNN es prediu un comportament ferromagnètic de baixa dimensionalitat (recordem que l'α-2-OHPNN és un FM 3D, β-2-OHPNN un AFM 1D amb interaccions FM febles entre cadenes, 4-OHPNN un FM 2D, β-p-NPNN un FM 3D i PNN un AFM). Tots els cristalls es comporten, segons la interpretació en base a interaccions H···O, com a ferromagnets. De fet, aquest resultat era d'esperar perquè les interaccions intermoleculars que dirigeixen l'empaquetament cristal.lí són els ponts d'hidrogen; de manera que n'hi haurà arreu del cristall. Així doncs, torna a haver inconsistències entre les prediccions fetes pel model de McConnell-I sobre el magnetisme

[2] S'ha d'assumir que el model de McConnell-I es pot aplicar a interaccions on hi ha participació de densitats d'spin de tipus σ; per exemple, interaccions H···ON.

dels 5 cristalls anteriors i les dades experimentals que es tenen sobre aquests cristalls. Donades aquestes inconsistències, la revisió del model de McConnell-I es creu necessària.

2.3. CONCLUSIONS.

S'ha comprovat que sense tenir explícitament en compte el valor de les J_{ij}^{AB}, el model de McConnell-I no és capaç de predir correctament el comportament magnètic dels cristalls PNN, α-2-OHPNN, β-2-OHPNN, 4-OHPNN i β-p-NPNN ni en base a contactes O···O / O···C(sp^2) ni en base a contactes O···H. Conseqüentment, les prediccions fetes pel model de McConnell-I sobre el magnetisme dels cinc cristalls anteriors qüestionen la validesa de l'aplicació qualitativa d'aquest model en funció de les densitats d'spin. Validesa que no només s'ha de qüestionar en cristalls d'α-nitronil nitròxid, sinò en general per a qualsevol tipus de cristall amb comportament magnètic.

L'aplicabilitat del primer model proposat per McConnell per tal de racionalitzar la naturalesa de les interaccions magnètiques en cristalls moleculars purament orgànics s'estudiarà a nivell de comparació teòrica, d'anàlisi estadística, i d'estudi ab initio de contactes intermoleculars en els Capítols 3, 4 i 5, respectivament.

BIBLIOGRAFIA.

[1] Per a una revisió, consultar: a) J.S. Miller, A.J. Epstein, *Angew. Chem. Int. Ed. Engl.* **1994**, *33*, 385-415. b) O. Kahn, *Molecular Magnetism*, VCH Publishers: New York, **1993**. c) M. Kinoshita, *Jpn. J. Appl. Phys.* **1994**, *33*, 5718. d) D. Gatteschi, O. Kahn, J.S. Miller, F. Palacio, Eds.; *Molecular Magnetic Materials*, Kluwer Academic Publishers: Dordretch, **1991**. e) H. Iwamura, J.S. Miller, Eds., *Mol. Cryst. Liq. Cryst.*, **1993**, *232/233*, 1-360/1-366. f) J.S. Miller, A.J. Epstein, Eds.; *Mol. Cryst. Liq. Cryst.*, **1995**, *272-274*. g) K. Itoh, J.S. Miller, T. Takui, Eds.; *Mol. Cryst. Liq. Cryst.*, **1997**, *305-306*.. h) E. Coronado, P. Delhaes, D. Gatteschi, J.S. Miller, Eds.; *Molecular Magnetism: From Molecular Assemblies to Devices*, Kluwer Academic Publishers: Dordretch, **1996**. i) O. Kahn, Ed.; *Magnetism: A Supramolecular Function*, Kluwer Academic Publishers: Dordretch, **1996**.

[2] Unes quantes apareixen en: O. Kahn, D.N. Hendreickson, H. Iwamura, J. Veciana, *Molecular Magnets*, D. Gatteschi, O. Kahn, J.S. Miller, F. Palacio, Eds., Kluwer Academic Publishers: Dordrecht, **1991**, p. 385

[3] P.W. Anderson, *In Magnetism* , G.T. Rado, H. Shul, Eds., Academic Press: New York, **1963**; vol. 1, pg. 25.

[4] P.J. Hay, J.C. Thibeault, R. Hoffmann, *J. Am. Chem. Soc.*, **1975**, *97*, 4884.

[5] Consultar, per exemple: M.F. Charlot, O. Kahn, S. Jeannin, Y. Jeannin, *Inorg. Chem.* **1980**, *19*, 1410.

[6] Per a un exemple, veure: O. Kahn, J. Galy, Y. Journaux, I. Morgenstern-Badarau, *J. Am. Chem. Soc.* **1982**, *104*, 2165.

[7] (a) P. de Loth, P. Cassoux, J.P. Daudey, J.P. Malrieu, *J. Am. Chem. Soc.*, **1981**, *103*, 4007; (b) J.P. Daudey, P. De Loth, J. P. Malrieu, *Magneto structural correlations in exchange coupled systems*, R.D. Willet, D. Gatteschi, O. Kahn, (eds.), Nato Adv. Studies Ser. C, vol 140, Reidel, Dordrecht (**1985**); (c) P. De Loth, P. Karafiloglou, J. P. Daudey, O. Kahn, *J. Am. Chem. Soc.* **1988**, *110*, 5676.

[8] (a) J. Miralles, O. Castell, R. Caballol, J.P. Malrieu, *Chem. Phys.*, **1993**, *172*, 33; (b) O. Castell, R. Caballol, R. Subra, A. Grand, *J. Phys. Chem.* **1995**, *99*, 154.

[9] (a) L. Noodleman, D.A. Case, *Adv. Inorg. Chem.*, **1992**, *38*, 423; (b) E. Ruiz, P. Alemany, S. Alvarez, J. Cano, *J. Am. Chem. Soc.* **1997**, *119*, 1297; (c) R. Caballol, O. Castell, F. Illas, I. de P. R. Moreira, J.P. Malrieu, *J. Phys. Chem. A*, **1997**, *101*, 7860.

[10] (a) W.T. Borden, E.R. Davidson, *Acc. Chem. Res.*, **1981**, *14*, 69; (b) W.T. Borden, H. Iwamura, J.A. Berson, *Acc. Chem. Res.*, **1994**, *27*, 109; (c) A. A. Ovchinnikov, *Theor. Chim. Acta* **1978**, *47*, 297.

[11] (a) H.M. McConnell, *J. Chem. Phys.*, **1963**, *39*, 1910; (b) H.M. McConnell, *Proc. Robert A. Welch Found. Conf. Chem. Res.*, **1967**, *11*, 144; (c) R. Breslow, *Pure and Appl. Chem.*, **1982**, *54*, 927; (d) K. Yamaguchi, H. Fukui, T. Fueno, *Chem. Lett.*, **1986**, 625; (e) T. Kawakami, S. Yamanaka, D. Yamaki, W. Mori, K. Yamaguchi, **1996**, *ACS Symp. Ser.* , *# 644*, M. M. Turnbull, T. Sugimoto, L.K. Thompson, (eds.), ch. 3; (f) K. Awaga, T. Sugano, M. Kinoshita, *Chem. Phys. Lett.*, **1987**, *141*, 540; (g) C. Kollmar, O. Kahn, *Acc. Chem. Res.*, **1993**, *26*, 259.

[12] A. Zheludev, V. Barone, M. Bonnet, B. Delley, A. Grand, E. Ressouche, R. Subra, J. Schweizer, *J. Am. Chem. Soc.*, **1994**, *116*, 2019.

[13] J.J. Novoa, F. Mota, J. Veciana, J. Cirujeda, *Mol. Cryst Liq. Cryst.*, **1995**, *271*, 79.

[14] (a) ref. 12; (b) K. Awaga, Y. Maruyama, *J. Chem. Phys.*, **1989**, *91*, 2743.

[15] (a) J. Cirujeda, M. Mas, E. Molins, F. Lanfranc de Panthou, J. Laugier, J.G. Park, C. Paulsen, P. Rey, C. Rovira, J. Veciana, *J. Chem. Soc., Chem. Commun.*, **1995**, 709; (b) J. Cirujeda, Tesi Doctoral, Univ. Ramon Llull, **1997**.

[16] (a) E. Hernández, M. Mas, E. Molins, C. Rovira, J. Veciana, *Angew. Chem. Int. Ed. Engl.*, **1993**, *32*, 882; (b) J. Cirujeda, E. Hernández-Gasio, C. Rovira, J.L. Stanger, P. Turek, J. Veciana, *J. Mat. Chem.*, **1995**, *5*, 243; (c) J.L. García-Muñoz, J. Cirujeda, J. Veciana, S.F.J. Cox, *Chem. Phys. Lett.*, **1998**, *293*, 560.

[17] (a) K. Awaga, T. Inabe, U. Nagashima, Y. Maruyama, *J. Chem. Soc., Chem. Commun.*, **1989**, 1617; (b) M. Tamura, Y. Nakazawa, D. Shiomi, K. Nozawa, Y. Hosokoshi, M. Ishikawa, M. Takahashi, M. Kinoshita, *Chem. Phys. Lett.*, **1991**, *186*, 401; (c)Y. Nakazawa, M. Tamura, N. Shirakawa, D. Shiomi, M. Takahashi, M. Kinoshita, M. Ishikawa, *Phys. Rew. B* **1992**, *46*, 8906.

[18] P. Turek, K. Nozawa, D. Shiomi, K. Awaga, T. Inabe, Y. Maruyama, M. Kinoshita, *Chem. Phys. Lett.* **1991**, *180*, 327.

[19] Per a exemples, consultar: (a) J. Veciana, J. Cirujeda, C. Rovira, J. Vidal-Gancedo, *Adv. Mater.* **1995**, *7*, 221; (b) J. Cirujeda, E. Hernàndez, C. Rovira, P. Turek, J. Veciana, *New Organic Magnetic Materials. The Use of Hydrogen Bonds as a Crystalline Design Element of Organic Molecular Solids with Intermolecular Ferromagnetic Interactions*, pp 262-272, in *"New Organic Materials"*, (Eds.: C. Seoane, N. Martin); Universidad Complutense de Madrid: Madrid, **1994**; (c) J. Cirujeda, E. Hernàndez, C. Rovira, J.-L. Stanger, P. Turek, J. Veciana, *J. Mater. Chem.* **1995**, *5*, 243-252; (d) J. Cirujeda, E. Hernàndez, C. Rovira, J.-L. Stanger, P. Turek, J. Veciana, *J. Mater. Chem.* **1995**, *5*, 243-252; (e) J. Cirujeda, C. Rovira, J.-L. Stanger, P. Turek, J. Veciana, *The Self-Assembly of Hydroxylated Phenyl α-Phenyl Nitronyl Nitroxide Radicals*, pp 219-248, in *"Magnetism. A Supramolecular Function"*; (Ed.: O. Kahn); Kluwer Academic Publishers: Amsterdam, **1996**; (f) J. Cirujeda, E. Hernàndez, F. Lanfranc de Panthou, J. Laugier, M. Mas, E. Molins, C. Rovira, J.-J. Novoa, P. Rey, J. Veciana, *Mol. Cryst. Liq. Cryst.* **1995**, *271*, 1-12.

CAPÍTOL 3:

Estudi Teòric del Model de McConnell-I

La comparació formal del model de McConnell-I amb una implementació rigorosa de l'Hamiltonià d'spin de Heisenberg en un espai VB ens permetrà desenvolupar un formalisme general aplicable a tot sistema magnètic. Aquest formalisme ens permetrà conèixer el rang d'aplicabilitat de la teoria de McConnell-I.

3.1. L'HAMILTONIÀ DE HEISENBERG VS. L'HAMILTONIÀ DE MCCONNELL-I.

3.1.1.- L'Hamiltonià de Heisenberg.

El magnetisme és una propietat d'estat sòlid que està relacionada amb la presència d'electrons desaparellats: l'acoblament dels spins d'aquests electrons donarà lloc a un estat d'alt o de baix spin. Per tal d'estudiar aquest problema podem substituir l'Hamiltonià real $\hat{H}$ del sistema magnètic per un Hamiltonià "efectiu" $\hat{H}_{eff}$, que conté operadors d'spin i paràmetres numèrics escollits per tal de reproduir correctament les energies i valors propis del sistema estudiat. Aquest Hamiltonià d'spin $\hat{H}^S$, anomenat Hamiltonià de Heisenberg, redueix el problema de l'enllaç químic a acoblaments entre spins electrònics. Acoblaments que, un cop descartats els petits efectes relativístics, no tenen una existència física real. Un Hamiltonià de Heisenberg de bescanvi d'spin genèric es pot, per tant, escriure com

$$\hat{H}^S = Q - \sum_{i,j} J_{ij}\left(2\hat{S}_i \cdot \hat{S}_j + \tfrac{1}{2}\hat{I}_{ij}\right) \tag{3.1}$$

on Q és el terme de Coulomb, J_{ij} és el paràmetre d'acoblament de bescanvi, $\hat{S}_i$ és l'operador d'spin associat amb el centre i, i $\hat{I}_{ij}$ és l'operador d'spin identitat.

Anderson [1a] va ser el primer en reconèixer que els Hamiltonians de Heisenberg es podien entendre com a Hamiltonians efectius calculats a partir d'un Hamiltonià *full CI* exacte, usant un espai model de determinants VB neutres formats per n electrons en n AO. L'ús d'aquest tipus d'espais en química quàntica va ser proposat per primer cop en aquest context per l'Escola de Toulouse [1], ja que la base física de la teoria VB és que un enllaç químic s'associa amb l'aparellament dels spins dels electrons en els orbitals de valència (d'ocupació 1) dels àtoms implicats. Des d'aleshores, aquest tipus d'Hamiltonians s'han pogut implementar amb èxit en mètodes com l'MMVB [2] on els paràmetres Q i J es deriven a partir de càlculs CASSCF.

Així doncs, per a una rigorosa (és a dir, fidel) implementació de l'equació (3.1), s'ha de poder associar un electró i en el centre i amb un orbital atòmic (AO) en el centre i [per a discussió ref. 3]. Això implica que els orbitals han d'estar localitzats en centres atòmics (és a dir, són AO localitzats). A més, gràcies a l'operador $\hat{H}^S$ (3.1), les complexitats de la funció

d'ona queden descrites pels paràmetres Q i J_{ij}. Finalment, $\hat{H}^S$ està únicament definit per espais de funcions multielectròniques expandides per una base on la part espacial de totes les configuracions és la mateixa, de manera que aquestes configuracions només es diferencien en la part d'spin. Aquest fet implica que l'espai on $\hat{H}^S$ actua és l'espai de determinants VB, en el qual cada orbital espacial participa una vegada, és a dir, l'espai de determinants VB neutres.

Els arguments anteriors són suficients per a justificar el per què de la comparació formal entre un Hamiltonià d'spin de Heisenberg (3.1) en un espai VB i el model de McConnell-I, en voler establir el rang d'aplicabilitat d'aquest darrer. Ara, doncs, procedirem a clarificar el significat de l'equació (3.1) amb un exemple, tenint en compte que el valor esperat del producte escalar d'spin $\left\langle 2\hat{S}_i \cdot \hat{S}_j \right\rangle$ és simplement $S(S+1)-\frac{3}{2}$. En el cas de dos electrons, el valor esperat de $\left\langle \hat{S}_1 \cdot \hat{S}_2 \right\rangle$ pels estats singlet i triplet resulta $-\frac{3}{4}$ i $+\frac{1}{4}$, respectivament. Així doncs, a partir de (3.1), l'energia dels estats bielectrònics singlet i triplet es pot escriure com a

$$E^{S/T} = Q \pm J_{12} \tag{3.2}$$

donat que per a dos electrons s'obté

$$-\left\langle \left(2\hat{S}_1 \cdot \hat{S}_2 + \tfrac{1}{2}\hat{I}_{12} \right) \right\rangle^{S/T} = \pm 1 \tag{3.3}$$

Cal destacar que l'expressió (3.2) de l'energia en el cas de dos electrons (calculada a partir d'un Hamiltonià de Heisenberg) coincideix amb la de l'energia aproximada proposada pels mateixos Heitler i London en resoldre el problema de la molècula d'hidrogen. En conseqüència, no és d'extranyar que, en aplicar Hamiltonians de Heisenberg, el paràmetre d'acoblament de bescanvi J_{ij} s'interpreti en termes de distribució electrònica com el bescanvi de Heitler-London

$$J_{ij} = [ij|ij] + 2s_{ij} < i|h|j > \tag{3.4}$$

on $[ij|ij]$ és un valor petit i positiu corresponent a l'energia de bescanvi bielectrònica, i $< i|h|j >$ està dominat per l'atracció electrònica nuclear, essent un valor gran i negatiu. Així doncs, J_{ij} és negatiu generalment. La quantitat s_{ij} és el solapament dels orbitals i, j, per tant J_{ij} serà un terme positiu només quan el solapament d'orbitals tendeixi a zero. Clarament, en fer aquesta interpretació estem associant un electró i en el centre i amb un orbital atòmic (AO) en el centre i.

Ara, caldrà escriure l'equació (3.1) adientment per tal d'implementar-la en química quàntica. Assumim que tenim una base d'orbitals AO que es poden identificar amb centres i,

j en l'equació (3.1). En segona quantització, (3.1) es pot escriure com

$$\hat{H}^S = Q - \sum_{i,j}^{N} J_{ij} \left\langle i(1)\, j(2) \left| \hat{S}(1)\cdot\hat{S}(2) + \frac{1}{4}\hat{I}(1,2) \right| i(1)\, j(2) \right\rangle a_i^+ a_j^- a_j a_i \qquad (3.5)$$

on N és el número total d'spin-orbitals, a_i^+, a_i són operadors creació i anihilació i *i(1), j(2)* són AO localitzats en els centres i, j. En la pràctica, però, l'Hamiltonià (3.5) es pot reescriure [2a, derivació en Annex 1] en termes dels generadors estàndard $\hat{E}_{ij}^{\sigma\sigma} = a_{i\sigma}^+ a_{j\sigma}$ del grup unitari U(n) on $\sigma = \alpha, \beta$ com

$$\hat{H}^S = Q + \sum_{i,j}^{M} J_{ij} \frac{1}{2}\left(\hat{E}_{ij}^{\alpha\alpha}\hat{E}_{ji}^{\beta\beta} + \hat{E}_{ij}^{\beta\beta}\hat{E}_{ji}^{\alpha\alpha} + \left[\hat{E}_{ij}^{\alpha\alpha}\hat{E}_{ji}^{\alpha\alpha} - \hat{E}_{ii}^{\alpha\alpha}\right] + \left[\hat{E}_{ij}^{\beta\beta}\hat{E}_{ji}^{\beta\beta} - \hat{E}_{ii}^{\beta\beta}\right] \right) \qquad (3.6)$$

on M és el número d'orbitals espacials. L'equació (3.6) és la base de la implementació de l'equació (3.1) en química quàntica, donat que els valors esperats de les formes bilinears de (3.6) són els d'operadors densitat genèrics de dues partícules (*"symbolic" density matrices*) en un càlcul *CI*. Cal dir, també, que els operadors de l'equació (3.6) únicament connecten configuracions que tenen la mateixa part espacial però diferent part d'spin. Així doncs, l'Hamiltonià de Heisenberg actua en un espai de determinants VB on cada orbital espacial participa un únic cop. Tal com s'ha demostrat en la literatura [2b], tot Hamiltonià *full CI* es pot projectar en l'espai anterior i reproduir exactament un subconjunt dels seus valors propis. Per tant, la representació matricial de l'equació (3.6) en un espai de determinants VB neutres constitueix una implementació completament rigorosa de l'Hamiltonià de Heisenberg.

Per tal de després comparar aquest Hamiltonià amb el proposat pel model de McConnell-I, és convenient introduir la matriu densitat de bescanvi d'spin [veure referència 2c]. Els elements de la matriu densitat de bescanvi d'spin P_{ij} poden expressar-se com

$$P_{ij} = \left\langle -\left(2\hat{S}_i \cdot \hat{S}_j + \frac{1}{2}\hat{I}_{ij} \right) \right\rangle \qquad (3.7)$$

o (en la pràctica) com

$$P_{ij} = \left\langle \frac{1}{2}\left(\hat{E}_{ij}^{\alpha\alpha}\hat{E}_{ji}^{\beta\beta} + \hat{E}_{ij}^{\beta\beta}\hat{E}_{ji}^{\alpha\alpha} + \left[\hat{E}_{ij}^{\alpha\alpha}\hat{E}_{ji}^{\alpha\alpha} - \hat{E}_{ii}^{\alpha\alpha}\right] + \left[\hat{E}_{ij}^{\beta\beta}\hat{E}_{ji}^{\beta\beta} - \hat{E}_{ii}^{\beta\beta}\right] \right) \right\rangle \qquad (3.8)$$

Així doncs, podem escriure l'energia com el següent valor esperat

$$\left\langle \hat{H}^S \right\rangle = Q + \sum J_{ij} P_{ij} \qquad (3.9)$$

L'equació (3.8) és un element de la matriu densitat de dues partícules [2a] que podem obtenir a partir de qualsevol càlcul *CI*. La densitat de bescanvi ha de satisfer la relació [4]

$$S(S+1) = -\tfrac{1}{4}N(N-4) - \sum_{i,j} P_{ij} \qquad (3.10)$$

on N és el número d'electrons.

Aquesta densitat de bescanvi P_{ij}, obtinguda a partir d'un càlcul usant determinants VB neutres, té una interpretació molt senzilla i és un indicatiu de la naturalesa de l'acoblament d'spin entre electrons en orbitals i, j. Usant una funció de Rumer [5] (és a dir, una *single configuration perfectly paired VB wavefunction*), P_{ij} té valor +1 per spins aparellats antiparal.lelament per donar un singlet, −1 per dos electrons acoblats de manera paral.lela donant lloc a un triplet, i $-½$ per spins no-acoblats (és a dir, i, j pertanyen a *diferents* funcions "*spin-paired*") [veure la *perfect pairing formula* en ref. 5]. Evidentment, les P_{ij} calculades a partir de l'equació (3.8) tindran valors diferents als valors "ideals" anteriors degut a la interacció de configuracions. Així doncs, des d'un punt de vista numèric, després de la interacció de configuracions, no podem distingir entre "acoblament triplet" i "spins no-acoblats". Per tant, ens referirem a P_{ij} positives com a "acoblament singlet", i P_{ij} negatives com a "acoblament triplet". Donat que J_{ij} és normalment negativa, les P_{ij} negatives (acoblament triplet o electrons no-acoblats) estan associades amb interaccions desestabilitzants via equació (3.9). Els avantatges que implica la introducció de la densitat de bescanvi P_{ij} en l'expressió de l'energia són, per tant, obvis ja que no només ens simplifica moltíssim el seu càlcul, sinó que també ens permet una ràpida interpretació dels fenòmens d'acoblament que tenen lloc entre els centres i, j. Aquests factors fan que l'expressió (3.9) sigui una candidata immillorable a l'hora de fer comparacions amb el model de McConnell-I.

3.1.2.- L'Hamiltonià de Heisenberg del model de McConnell.

L'any 1963, McConnell [6] va suggerir que la interacció magnètica entre dos radicals aromàtics A i B podia aproximar-se amb un Hamiltonià de Heisenberg tal que:

$$\hat{H}^{AB} = -\sum_{i\in A, j\in B} J_{ij}^{AB} \hat{\mathbf{S}}_i^A \cdot \hat{\mathbf{S}}_j^B \qquad (3.11)$$

on J_{ij}^{AB} són integrals de bescanvi de dos centres, i $\hat{S}_i^A, \hat{S}_j^B$ és el producte d'operadors d'spin en els àtoms i, j dels fragments A i B. Aquest Hamiltonià es pot fàcilment relacionar amb la forma de l'Hamiltonià (3.5). És evident, però, que aquest Hamiltonià negligeix els termes dins de cada fragment i, a més, elimina l'operador identitat (la qual cosa significa un canvi en el zero d'energies). Així doncs, la primera assumpció fonamental del model de McConnell-I és que *les contribucions dins de cada fragment són les mateixes en cada estat on l'Hamiltonià actua*.

Ara bé, l'Hamiltonià corresponent a l'equació (3.11) mai s'usa, sinó que és substituït per una simplificació "ad hoc" donada per

$$\hat{H}^{AB} = -\hat{\mathbf{S}}^{A} \cdot \hat{\mathbf{S}}^{B} \sum_{i \in A, j \in B} J_{ij}^{AB} \rho_i^A \rho_j^B \tag{3.12}$$

on J_{ij}^{AB} són integrals de bescanvi de dos centres, i ρ_i^A, ρ_j^B són densitats d'spin en els àtoms i, j dels fragments A i B. Els termes $\hat{S}^A, \hat{S}^B$ són els operadors d'spin total pels fragments A, B, i el valor esperat del seu producte ve donat per

$$\left\langle \hat{\mathbf{S}}^{A} \cdot \hat{\mathbf{S}}^{B} \right\rangle = \frac{1}{2}[S(S+1) - S_A(S_A+1) - S_B(S_B+1)] \tag{3.13}$$

És important destacar que l'Hamiltonià (3.12) actua únicament en un espai model (normalment de dimensió dos) expandit per estats de diferent multiplicitat d'spin (per exemple, un singlet i un triplet). Així doncs, aquest Hamiltonià tindrà només elements diagonals. Cal afegir, també, que l'equació (3.12) és purament fenomenològica: no hi ha cap sèrie sistemàtica d'aproximacións que permeti passar de l'equació (3.11) a (3.12).

En el cas de tenir dos doblets acoblats triplet s'obté $\left\langle \hat{S}^A \cdot \hat{S}^B \right\rangle^T = ¼$, i si s'acoblen singlet obtindrem $\left\langle \hat{S}^A \cdot \hat{S}^B \right\rangle^S = -¾$. Per tant

$$E^{\frac{S}{T}} = \begin{Bmatrix} ¾ J \\ -¼ J \end{Bmatrix} \tag{3.14}$$

Aquest resultat és el mateix que l'obtingut en l'equació (3.2), exceptuant el canvi en el zero d'energies. La constant d'acoblament efectiva J ve donada per

$$J = \sum_{i \in A, j \in B} J_{ij}^{AB} \rho_i^A \rho_j^B \tag{3.15}$$

Ara només resta relacionar la teoria proposada per l'equació (3.11) amb el model basat en el rigorós Hamiltonià de Heisenberg presentat en l'equació (3.1).

3.1.3.- Comparació entre el model de McConnell-I i el model basat en un rigorós Hamiltonià de Heisenberg.

Per tal de comparar el model de McConnell-I amb un rigorós desenvolupament de Heisenberg cal que considerem diferències d'energia. A tall d'exemple (i per clarificar les idees) considerarem la diferència d'energia existent entre un singlet i un triplet. A partir de l'equació (3.14) (model de McConnell-I) tenim

$$E^S - E^T = \sum_{i \in A, j \in B} J_{ij}^{AB} \rho_i^A \rho_j^B \tag{3.16}$$

En canvi, partint de (3.9) (model d'Hamiltonià de Heisenberg) tenim

$$E^S - E^T = \sum_{i,j} J_{ij} \Delta P_{ij} \tag{3.17}$$

on definim ΔP_{ij} com

$$\Delta P_{ij} = P_{ij}^S - P_{ij}^T \tag{3.18}$$

Cal emfasitzar que P_{ij}^S i P_{ij}^T són les matrius densitat de bescanvi singlet i triplet obtingudes a partir de vectors propis singlet i triplet (és a dir, P_{ij}^S i P_{ij}^T s'han calculat separadament per als estats singlet i triplet, respectivament). En canvi, $\rho_i^A \rho_j^B$ és el producte de la diferència de densitats d'spin avaluades a partir de dos fragments doblet. Comparant equacions (3.16) i (3.17) veiem clarament que la relació de McConnell és vàlida només si fem l'associació

$$\Delta P_{ij} \Leftrightarrow \rho_i^A \rho_j^B \tag{3.19}$$

Ara bé, la relació (3.19) és heurística, ja que no hi ha cap raó òbvia per la qual $\rho_i^A \rho_j^B$ i ΔP_{ij} hagin d'estar relacionats entre si. Aquesta relació, per tant, constitueix l'assumpció més fonamental del model de McConnell-I, la qual mai ha estat comprovada numèricament.

Segons el model de McConnell-I, per a tenir estabilitat triplet, la constant d'acoblament efectiva J de l'equació (3.15) ha de ser positiva. Així doncs, donat que s'assumeix que les J_{ij}^{AB} són negatives, el producte $\rho_i^A \rho_j^B$ haurà de ser negatiu també. Associarem, per tant, "acoblament ferromagnètic" amb aquells casos en què $\rho_i^A \rho_j^B$ sigui negatiu. *(És important tenir en compte que en l'equació (3.16) cal prendre els fragments A i B tal que* $S_z^A = ½$, $S_z^B = ½$*).* D'altra banda, les contribucions ΔP_{ij} entre centres i, j "més propers" que pertanyen a diferents fragments també hauran de ser negatives —corresponent a estabilitat triplet via equació (3.17). S'obtindran ΔP_{ij} negatives en tres casos: (1) si P_{ij}^T és negativa, P_{ij}^S haurà de ser negativa i $|P_{ij}^S\rangle|P_{ij}^T|$ forçadament; en canvi, si P_{ij}^T és positiva, P_{ij}^S podrà ser (2) negativa o (3) positiva i $P_{ij}^T > P_{ij}^S$. En el primer cas, segons $|P_{ij}^S\rangle|P_{ij}^T|$, els centres "més propers en l'espai" en l'estat singlet presentaran un acoblament triplet més fort que el que presenten els centres "més propers" en l'estat triplet. La situació s'inverteix en el segon i tercer casos. Donada l'argumentació anterior i el fet que $\rho_i^A \rho_j^B$ i ΔP_{ij} estan relacionades heurísticament, caldrà posar en dubte des d'un punt de vista conceptual l'associació de $\rho_i^A \rho_j^B$ negatiu amb el concepte "d'acoblament ferromagnètic". Per tal de solucionar el dubte conceptual anterior i discriminar quina de les tres opcions proporciona el signe a ΔP_{ij}, ens cal desenvolupar un formalisme prou general com per poder descomposar la diferència d'energia obtinguda amb el model d'Hamiltonià de Heisenberg (3.17) en termes de l'obtinguda amb el model de McConnell-I (3.16).

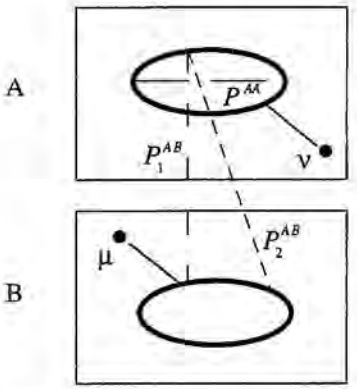

FIGURA 3.1.- Representació esquemàtica de la partició de la densitat de bescanvi per a dues estructures doblet aromàtiques.

3.2. Esquema Pràctic per a Descomposar la Separació d'Energia Singlet / Triplet en termes de McConnell-I.

Per a il.lustrar l'aproximació que usarem, ens cal considerar l'acoblament d'spin de dos fragments doblets A i B amb centres radicalaris ν i μ (FIGURA 3.1). En general, hi ha dos tipus d'interaccions entre fragments: un primer tipus que s'estableix entre centres que estan "propers en l'espai", i un segon tipus format per la resta de contactes. En el model de la FIGURA 3.1, el primer tipus correspon a interaccions directes entre àtoms de C alineats, i el segon a interaccions indirectes entre àtoms de C no-alineats. Aquesta partició serà útil a l'hora d'exemplificar la descomposició de la separació d'energia singlet / triplet en termes de la separació obtinguda amb el model de McConnell-I en el cas dels isòmers pseudo-orto-, -meta-, i -para-bis(fenilmetilenil)[2.2]paraciclofans. Ara bé, aquesta divisió dependrà en general dels sistema que es vulgui estudiar.

El sumatori de l'equació (3.16) està restringit a interaccions entre fragments $i \in A, j \in B$, mentre que el sumatori de l'equació (3.17) s'extén sobre tots els àtoms. Així doncs, per tal de comparar les prediccions obtingudes a partir de l'equació (3.17) amb la teoria de McConnell, haurem de particionar la suma de l'equació (3.17) en contribucions dins de cada fragment $ii' \in A$, i.e. $\{\Delta P_{ii'}\}_{ii' \in A}$, i en contribucions entre fragments $\{\Delta P_{ij}\}_{i \in A, j \in B}$. Separarem, per tant, els termes P_{ij} i ΔP_{ij} de l'equació (3.18), en termes que contribueixen dins de cada fragment $\{\Delta P^{AA}\} = \{\Delta P_{ii'}\}_{ii' \in A}$, i entre fragments $\{\Delta P^{AB}\} = \{\Delta P_{ij}\}_{i \in A, j \in B}$ (FIGURA 3.1). A més, és convenient separar els termes de contribució entre fragments en tres conjunts:

i) $\{P_1^{AB}\}$ i $\{\Delta P_1^{AB}\}$, el conjunt d'interaccions directes entre àtoms de C alineats,

ii) $\{P_2^{AB}\}$ i $\{\Delta P_2^{AB}\}$, el conjunt d'interaccions indirectes entre àtoms de C no-alineats, i

iii) $\{P_3^{AB}\}$ i $\{\Delta P_3^{AB}\}$, el conjunt d'interaccions que resulten en acoblar els centres radicalaris ν amb els centres del fragment B, els centres radicalaris μ amb els centres del fragment A, i els mateixos centres radicalaris ν, μ. Així doncs, les interaccions que pertanyen a aquest tercer conjunt són $\{\Delta P_3^{AB}\}=\{\Delta P_{i\mu}\bigcup\Delta P_{j\nu}\bigcup\Delta P_{\mu\nu}\}_{i\in A,j\in B,j\neq\mu,i\neq\nu}$

Arribats a aquest punt, és necessari definir la notació que utilitzarem. Amb la notació $\{P_r^{AB}\}$, $\{\Delta P_r^{AB}\}$ ens referirem al conjunt d'elements de la matriu densitat i de la matriu diferència de densitats del tipus r ($r=1,2,3$), respectivament. Usarem P_r^{AB} i ΔP_r^{AB} per indicar que s'ha sumat sobre tots els elements dels conjunts $\{P_r^{AB}\}$ i $\{\Delta P_r^{AB}\}$. Les corresponents contribucions a l'energia s'expressaran com a ΔE_r^{AB}. A tall d'exemple si $r=3$ aleshores

$$\Delta P_3^{AB}=\sum_{\substack{i\in A,j\in B,\\ j\neq\mu,i\neq\nu}}(\Delta P_{i\mu}+\Delta P_{j\nu}+\Delta P_{\mu\nu}) \quad , \tag{3.20}$$

$$\Delta E_3^{AB}=\sum_{\substack{i\in A,j\in B,\\ j\neq\mu,i\neq\nu}}(J_{i\mu}\Delta P_{i\mu}+J_{j\nu}\Delta P_{j\nu}+J_{\mu\nu}\Delta P_{\mu\nu}) \quad , \tag{3.21}$$

Finalment, usarem ΔP i ΔE per a indicar la suma sobre tots els tipus r de contribucions.

Després de presentar la partició de la diferència d'energia proposada pel nou formalisme d'Hamiltonians de Heisenberg que acabem de descriure i d'introduir la nova notació, exposarem una sèrie de relacions aproximades que s'han de verificar per tal que el model de McConnell-I tingui validesa qualitativa.

3.2.1.- Relacions necessàries entre el formalisme d'Hamiltonians de Heisenberg proposat i el model de McConnell-I.

Primer de tot, cal que l'acoblament d'spin dins de cada fragment es correspongui a un doblet (és a dir, el valor propi de l'operador S^2 ha de ser ¾). Així doncs, partint de l'equació (3.10), la següent relació s'haurà de verificar aproximadament en el cas del fragment A (o B)

$$S_A(S_A+1)=-\frac{N_A(N_A-4)}{4}-\sum_{ii'\in A}P_{ii'}=-\frac{N_A(N_A-4)}{4}-P^{AA}\approx\frac{3}{4} \tag{3.22}$$

on N_A és el número d'electrons associat al fragment A.

En segon lloc, la teoria de McConnell-I negligeix l'acoblament dins de cada fragment. Això significa que per a obtenir $\Delta E^{AA} = 0$ tots els elements del conjunt $\{\Delta P^{AA}\}$ haurien de ser aproximadament zero. El model de McConnell-I serà vàlid, si $\rho_i^A \rho_j^B$ i ΔP_{ij} es comporten qualitativament de manera similar. Per tant, totes les contribucions del conjunt $\{\Delta P^{AA}\}$ hauran de ser aproximadament zero.

D'altra banda, en el límit en què els dos fragments no interaccionen, tindrem dos electrons "localitzats" en els centres radicalaris ν i μ, els quals podran acoblar-se donant lloc a un estat singlet o triplet. Així doncs, d'acord amb la *perfect pairing formula* [5], el valor de $\Delta P_{\mu\nu}$ vindrà donat per

$$\Delta P_{\mu\nu} = P_{\mu\nu}^S - P_{\mu\nu}^T = 1 - (-1) = 2.0 \tag{3.23}$$

En aquest límit, la contribució dels conjunts $\{\Delta P_1^{AB}\}$ i $\{\Delta P_2^{AB}\}$, i totes les contribucions a $\{\Delta P_3^{AB}\}$ (excepte les que provenen dels electrons "localitzats" en els centres radicalaris ν i μ, $P_{\mu\nu}$) seran zero. Ara bé, aquesta és una situació ideal, ja que els fragments estaran realment interaccionant de manera molt feble, $\Delta P^{AA} \approx 0$ i $\Delta P \approx \Delta P^{AB} \approx 2$, per tant

$$\Delta P_3^{AB} \approx 2 - \delta \tag{3.24}$$

i

$$\Delta P_{1+2}^{AB} = \Delta P_1^{AB} + \Delta P_2^{AB} \approx \delta \tag{3.25}$$

on δ és una petita quantitat positiva que prové de la interacció entre fragments A, B.

Finalment, cal destacar que el model de McConnell-I sempre s'usa qualitativament. Les J_{ij}^{AB} individuals mai s'avaluen (però s'assumeixen negatives) i únicament $\rho_i^A \rho_j^B$ s'usa per fer prediccions. Així doncs, hi ha algunes assumpcions adicionals, relacionades amb les J_{ij}^{AB} individuals, que són innherents fins i tot en l'aplicació qualitativa del model de McConnell-I.

1) Les contribucions que provenen de centres "propers en l'espai" no-alineats, $\{\Delta P_3^{AB}\}$, s'ignoren completament. Ara bé, és d'esperar que les $\{\Delta P_3^{AB}\}$ siguin grans d'acord amb l'equació (3.24), per tant la validesa de l'aproximació de McConnell depèn de què tots els membres del conjunt $J_{\mu\nu}, \{J_{i\mu} \bigcup J_{j\nu}\}_{i\in A, j\in B, j\neq\mu, i\neq\mu}$ siguin zero (la qual cosa és raonable sempre i quan els centres radicalaris estiguin suficientment allunyats).

2) Les aplicacions qualitatives de la teoria de McConnell-I en molècules aromàtiques que s'apilen una damunt de l'altra formant cristalls tenen en compte la contribució que prové dels centres alineats $\{\Delta P_1^{AB}\}$, mentre que la contribució provinent de $\{\Delta P_2^{AB}\}$ és ignorada. Efectivament, doncs, la teoria de McConnell fa una estimació qualitativa de ΔE_1^{AB}. A partir de l'equació (3.25), sabem que ΔP_{1+2}^{AB} és

un valor petit δ que s'obté sumant ΔP_1^{AB} i ΔP_2^{AB}. Així doncs, les contribucions ΔP_1^{AB} i ΔP_2^{AB} hauran de tenir una magnitud similar però de signe oposat. Les aplicacions qualitatives seran només vàlides si les J_{ij} que es corresponen amb els termes $\{\Delta P_2^{AB}\}$ són molt petites. Si aquestes condicions es verifiquen, la geometria i l'estabilitat relativa singlet / triplet estaran controlades pels elements $\{\Delta P_1^{AB}\}$. Així doncs, si els termes $\{\Delta P_1^{AB}\}$ són tots negatius, l'acoblament d'spin serà triplet, en concordança amb el model de McConnell-I, el qual requereix $\rho_i^A \rho_j^B < 0$. Cal esmentar també que les J_{ij} corresponents a $\{\Delta P_1^{AB}\}$ seran molt sensibles a la distància perquè depenen del solapament directe entre orbitals p^{π} de l'àtom de C.

Ara només ens resta aplicar aquest nou formalisme d'Hamiltonians de Heisenberg a un sistema real, el magnetisme del qual hagi estat predit correctament amb el model de McConnell-I.

3.3. EL CAS DELS [2.2]PARACICLOFANS.

3.3.1.- Dades experimentals.

Els [2.2]paraciclofandicarbens han estat proposats per tal de proporcionar un bon model en examinar les interaccions intermoleculars magnètiques segons el model de McConnell-I [7], ja que dues molècules de difenilcarbè amb electrons desaparellats estan apilades una al damunt de l'altra en l'esquelet d'un [2.2]paraciclofà. En la FIGURA 3.2 mostrem els isòmers (a) pseudo-orto-, (b) pseudo-meta-, i (c) pseudo-para-bis(fenilmetilenil)[2.2]paraciclofà (bPhMenyl). Les dades experimentals del sistema bPhMenyl indiquen que, d'entre els isòmers amb diferent orientació dels dos substituents fenilmetilenil, només els isòmers pseudo-orto i -para presenten un estat fonamental quintet, mentre que el singlet és l'estat fonamental de l'isòmer pseudo-meta [7]. Ara bé, estrictament parlant, el model no és pas ideal : els dos anells de benzè incorporats en l'estructura del

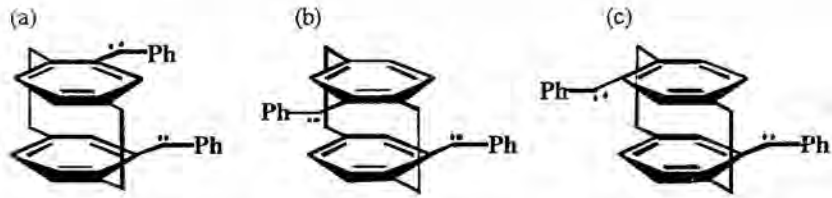

FIGURA 3.2.- Estructura dels isòmers pseudo- (a) -orto-, (b) -meta-, i (c) -para-bis(fenilmetilenil)[2.2]paraciclofà

difenilcarbè radical difenilmetil

FIGURA 3.3.- Estructura π-electrònica de difenilcarbè i radical difenilmetil

[2.2]paraciclofà no són plans, sinó que tenen forma de vaixell amb distàncies entre anells que no són iguals (~ 2.8 - 3.1 Å), i amb els dos anells de-eclipsats 3.2° per a evitar l'eclipsament de tipus età en les cadenes laterals [8].

Un estudi recent [9] ha demostrat que l'estructura π-electrònica del difenilcarbè és molt similar a la del radical difenilmetil, tal com s'indica en la FIGURA 3.3. L'important estat triplet del carbè té un sol electró en el sistema π conjugat. Així doncs, és raonable modelitzar aquest sistema amb un radical metil, en el lloc del carbè. Per tant, en el cas dels bis(fenilmetil)[2.2]paraciclofans s'obtindrà un estat fonamental singlet per l'isòmer pseudo-meta, i un estat fonamental triplet pels pseudo-orto i -para. A més, donat que el fenil enllaçat al radical metil no està implicat en la reorganització π-electrònica relacionada amb els estats singlet / triplet [9], el radical fenilmetil es pot substituir per un simple radical metil, donant lloc al bis(metil)[2.2]paraciclofà (bMe).

3.3.2.- Interpretació qualitativa del magnetisme dels [2.2]paraciclofans segons el model de McConnell-I.

En l'apartat 3.1.3 ja s'ha esmentat que el model de McConnell-I —equació (3.12)— divideix el sistema magnètic que està estudiant en dos fragments A i B, tal que el valor de S_z en cada fragment sigui positiu i el més gran possible. Així doncs, en aplicar McConnell-I al cas dels isòmers bis(metil)[2.2]paraciclofans (bMe), caldrà prendre com a fragment A (B) un dels dos fenils amb el seu radical metil corresponent. En aquest cas, s'haurà d'avaluar el producte $\rho_i^A \rho_j^B$ a partir de dos fragments doblet, és a dir, dos fragments amb $S_z^A = ½$ i $S_z^B = ½$. En la FIGURA 3.4 s'exemplifica el cas dels isòmers (a) pseudo-orto- i (b) pseudo-meta-bMe (per a una major claretat, s'obviarà l'esquelet del bMe). En aquesta FIGURA s'han representat les densitats d'spin associades a cada àtom de C del sistema π dels isòmers pseudo-orto- i pseudo-meta-bMe. Tal com era d'esperar, els àtoms de C directament alineats de l'isòmer pseudo-orto-bMe (FIGURA 3.4a) presentaran un producte $\rho_i^A \rho_j^B$ de signe negatiu;

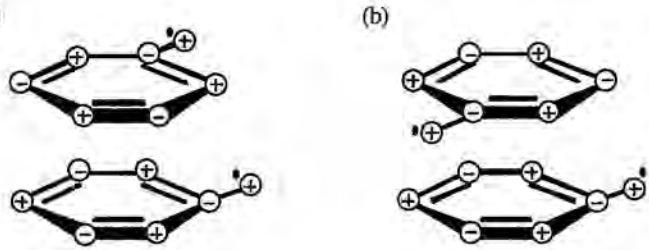

FIGURA 3.4.- Model de McConnell-I aplicat als isòmers pseudo- (a) -orto- i (b) -meta-bis(metil)[2.2]paraciclofà (els signes + i - representen la densitat d'spin en cada àtom de C del sistema π)

fet que, segons McConnell-I, s'ha d'associar a una interacció ferromagnètica entre els centres i, j dels fragments A, B. Per tant, l'estat fonamental de l'isòmer pseudo-orto-bMe serà triplet (el mateix passa en aplicar McConnell-I a l'isòmer pseudo-para-bMe). En canvi, l'isòmer pseudo-meta-bMe (FIGURA 3.4b) presenta els C directament alineats amb densitats d'spin del mateix signe. El resultat serà un producte $\rho_i^A \rho_j^B$ de signe positiu; de manera que entre i, j s'estableix una interacció antiferromagnètica. Així doncs, en el cas de l'isòmer pseudo-meta-bMe, l'estat fonamental serà singlet d'acord amb la predicció del model de McConnell-I.

El model de McConnell-I prediu correctament l'estabilitat singlet / triplet en el cas dels [2.2]paraciclofans. Ara, la pregunta que cal respondre és *per què*.

3.3.3.- Detalls metodològics.

El càlcul de les energies i l'optimització geomètrica dels sistemes model pseudo-orto-, -meta- i -para-bis(metil)[2.2]paraciclofà (bMe) s'han realitzat amb el mètode *Molecular Mechanics - Valence Bond* (MMVB). En aquest apartat no pretenem fer una descripció exhaustiva de l'MMVB, només volem esmentar els punts més rellevants d'aquest mètode.

L'Hamiltonià de Heisenberg implementat en l'MMVB és una fidel representació de les equacions (3.5) i (3.6), i actua sobre un conjunt de base format per estats VB multielectrònics neutres construïts a partir d'orbitals actius que estan ocupats per un sol electró (*singly occupied*). Els elements de matriu P_{ij} s'obtenen a partir de vectors *CI* de l'Hamiltonià MMVB [2c] i proporcionen una partició de $\hat{S}(1)\cdot\hat{S}(2)$ en forma d'interaccions entre aquests centres.

En el mètode MMVB [2], les parts actives dels sistema, és a dir, aquelles on hi ha una reorganització electrònica estan descrites per la teoria VB. La mecànica molecular (MM), en

canvi, s'encarrega de descriure la resta d'àtoms electrònicament inactius, així com l'esquelet covalent de tot el sistema. Per tant, l'MMVB és un mètode *híbrid* en el sentit que cada àtom està modelitzat o bé amb MM, o bé gràcies a una combinació de MM i VB. Originalment, l'MMVB va ser creat per a l'estudi de reaccions amb hidrocarburs[1]. Qualsevol hidrocarbur es pot visualitzar com a un conjunt d'interaccions de dos centres C-C. L'estructura electrònica de cadascuna d'aquestes components serà similar a la de l'etilè o a la de l'età, amb certes modificacions degudes a interaccions entres parells veïns. Així doncs, aquestes molècules són el punt inicial lògic per a construir el potencial MMVB. Per tant, en comptes de dur a terme una descripció VB rigorosa de cada un dels sistemes estudiats, l'MMVB usa les superfícies d'energia potencial ab initio de l'etilè i de l'età per tal de generar un potencial VB parametritzat, el qual és llavors modificat per a modelitzar sistemes més complexos. Els paràmetres Q i J_{ij} —equació (3.6)— seran, doncs, funcions de l'estat d'hibridació (sp^2/sp^3) i de la distància interatòmica.

L'MMVB és un mètode que ha estat parametritzat mitjançant un Hamiltonià efectiu [per discussió ref. 2b]. El punt més important del mètode és el fet que els paràmetres de bescanvi estan ajustats amb un Hamiltonià efectiu CASSCF. Aquests paràmetres es poden interpretar en termes d'una expansió que implica una sèrie de potències en funció del solapament [2b]. Ara bé, a la pràctica les integrals de solapament no es calculen. Així doncs, l'equació (3.4) únicament s'usa amb un propòsit explicatiu. A més, per definició, l'Hamiltonià efectiu CASSCF reprodueix estats covalents neutres de qualsevol multiplicitat d'spin, de manera que la parametrització no depèn de l'spin.

3.3.4.- Resultats a nivell Molecular Mechanics - Valence Bond.

En el sistema model bis(metil)[2.2]paraciclofà (bMe), l'optimització MMVB [2] dels isòmers pseudo-orto, pseudo-meta i pseudo-para es va dur a terme per ambdós estats, singlet i triplet. A més, també es van caracteritzar i localitzar les geometries del creuament singlet / triplet. La FIGURA 3.5 il.lustra les geometries dels mínims i del creuament singlet/triplet. Amb les estructures optimitzades de mínima energia (triplet en el cas dels isòmers en orto i para, i singlet en el cas del meta) es va dur a terme una descomposició de la diferència d'energia singlet / triplet en funció de $\left\{\Delta P_r^{AB}\right\}$ (TAULES 3.1 i 3.2) [les contribucions $P_{ij}^{S/T}$ de ΔP per a tots tres isòmers bMe avaluades amb la geometria de l'estat fonamental i les corresponents J_{ij} es llisten en l'Annex 2].

[1] Actualment s'està treballant en la parametrització dels àtoms de N i O.

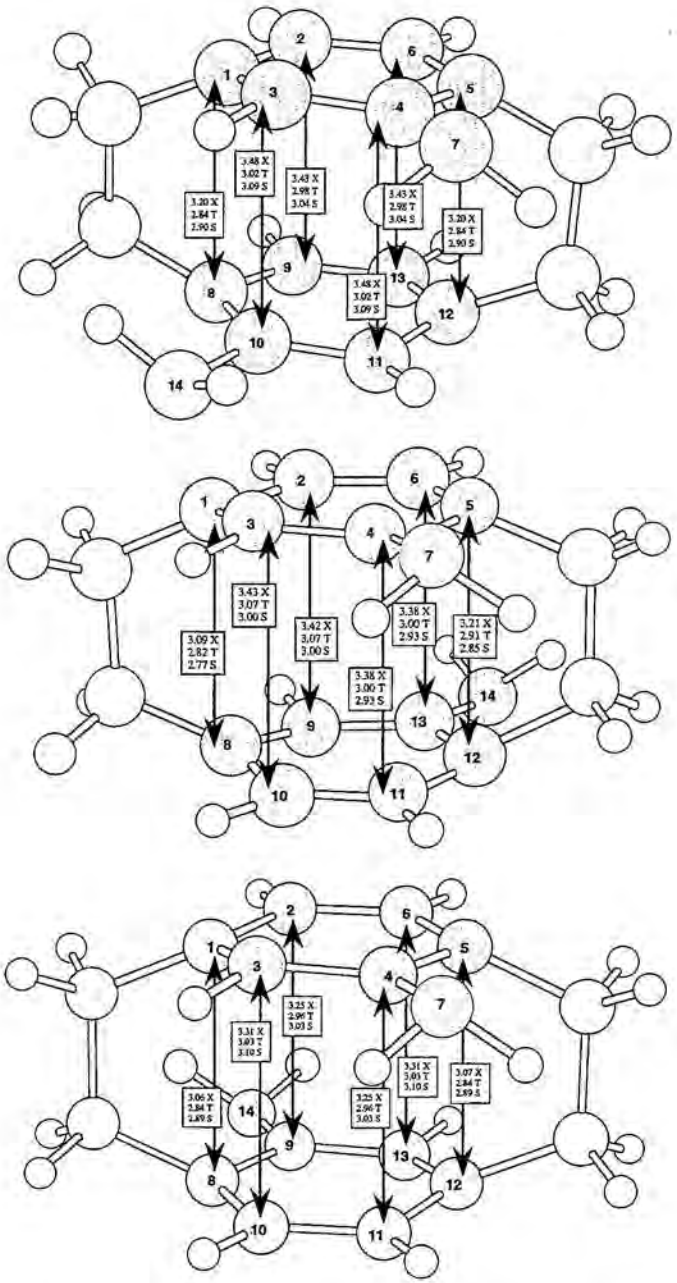

FIGURA 3.5.- Distàncies entre fragments optimitzades via MMVB dels isòmers pseudo- (a) -orto-, (b) -meta-, i (c) -para-bis(metil)[2.2]paraciclofans (S = singlet, T = triplet, X = creuament S-T)

TAULA 3.1.- Diferències de matrius densitat de bescanvi entre fragments ΔP_r^{AB} i contributions a l'energia total ΔE_r^{AB}. Totes les diferències d'energia en kcal mol^{-1}.

Isòmer	Estructura	ΔE^{AB}	ΔP_3^{AB} ΔE_3^{AB}	ΔP_1^{AB} ΔE_1^{AB}	ΔP_2^{AB} ΔE_2^{AB}	ΔP_{1+2}^{AB}
pseudoorto	T_{min}	2.9493	1.834 0.0006	-1.355 0.0060	1.508 -0.0019	0.153
pseudometa	S_{min}	-2.1963	1.666 -0.0002	1.264 -0.0057	-0.942 0.0024	0.322
pseudopara	T_{min}	2.6983	1.831 0.0000	-1.370 0.0064	1.525 -0.0021	0.155

3.3.4.1.- Geometria MMVB.

Començarem discutint breument les geometries optimitzades de la FIGURA 3.5. Les geometries dels estats singlet i triplet difereixen només uns 0.001-0.07 Å amb respecte a les longituds d'enllaç C-C entre fragments. Així doncs, els factors principals que controlen l'estabilitat singlet / triplet són d'origen electrònic, i no pas geomètric. Aquesta conclusió es reforça quan considerem les geometries en què els estats singlet i triplet es creuen. En cada cas, el creuament té lloc quan les distàncies d'enllaç entre fragments s'incrementen des d'uns 2.9Å a uns 3.3Å, de manera que la J_{ij} entre fragments tendeix a zero. Així doncs, en augmentar les distàncies entre fragments l'estabilitat relativa del singlet i triplet persisteix, fins que les interaccions entre fragments es fan zero. Les distàncies anell-anell entre fragments per als estats singlet i triplet calculades concorden amb les dades experimentals disponibles (2.8Å i 3.1Å en bPhMenyl [8]). Així doncs, el sistema bMe sembla modelitzar correctament el sistema bPhMenyl (tal com era d'esperar donat que cap dels fenils enllaçats al carbè està implicat en la reorganització π-electrònica [7]).

L'estabilitat relativa singlet / triplet s'indica en la columna 2 de la TAULA 3.1, i concorda amb l'observada experimentalment per als isòmers de baix-spin pseudo-meta i alt-spin pseudo-orto / para bPhMenyl [7]. El valor absolut de la diferència d'energia entre els estats singlet i triplet calculada amb les geometries optimitzades és similar en tots tres isòmers (3 kcal mol^{-1}). Per tal de confirmar que les conclusions relatives a l'estabilitat triplet versus singlet provenen majoritàriament de l'orientació dels grups benzil en el paraciclofà, es van realitzar sèries de càlculs amb dos radicals benzil orientats en orto, meta i para situats a una distància de 3Å. Els resultats són qualitativament similars als resultats presentats en el cas dels paraciclofans optimitzats i, per tant, ens indiquen que el mètode MMVB els descriu correctament.

TAULA 3.2.- Diferències de matrius densitat de bescanvi entre fragments $\{\Delta P^{AB}\}$ per als mínims. (ΔP_1^{AB} negreta cursiva; ΔP_2^{AB} normal; ΔP_3^{AB} negreta). La numeració (#) dels àtoms es correspon a la de la FIGURA 3.5.

a) pseudoorto (mínim triplet)

# d'àtom	1	2	3	4	5	6	7
8	***-.236***	.320	.326	-.299	.388	-.231	**.609**
9	.137	***-.198***	-.194	.175	-.231	.138	**-.356**
10	.175	-.245	***-.258***	.230	-.299	.175	**-.467**
11	-.190	.267	.273	***-.258***	.326	-.194	**.509**
12	.132	-.188	-.190	.175	***-.236***	.137	**-.352**
13	-.188	.262	.267	-.246	.320	***-.198***	**.497**
14	**-.352**	**.496**	**.509**	**-.467**	**.609**	**-.355**	**.957**

b) pseudometa (mínim singlet)

8	***.121***	-.172	-.171	.146	-.198	.116	**-.292**
9	-.171	***.270***	.259	-.221	.303	-.174	**.445**
10	-.172	.263	***.269***	-.225	.306	-.174	**.359**
11	.116	-.174	-.174	***.158***	-.205	.119	**-.301**
12	-.198	.307	.303	-.264	***.370***	-.205	**.531**
13	.146	-.226	-.221	.192	-.264	***.158***	**-.387**
14	**-.292**	**.452**	**.445**	**-.387**	**.531**	**-.301**	**.785**

c) pseudopara (mínim triplet)

8	***-.239***	.326	.329	-.305	.397	-.233	**.613**
9	.176	***-.260***	-.249	.230	-.305	.179	**-.465**
10	.137	-.192	***-.199***	.179	-.233	.137	**-.356**
11	-.190	.267	.268	***-.260***	.326	-.192	**.501**
12	.132	-.190	-.189	.176	***-.239***	.137	**-.351**
13	-.189	.268	.268	-.250	.329	***-.199***	**.503**
14	**-.350**	**.501**	**.502**	**-.465**	**.613**	**-.356**	**.948**

3.3.4.2.- Anàlisi de la separació d'energia singlet / triplet.

A continuació, analitzarem la diferència d'energia singlet / triplet ΔE^{AB} en termes de les components de ΔP^{AB} donades en la TAULA 3.1. Les components individuals de ΔP^{AB} per a totes les interaccions entre fragments es llisten en la TAULA 3.2. Cal destacar que aquesta anàlisi és només raonable si $\Delta E^{AA} = \Delta E^{BB} = 0$. En tots tres isòmers, aquesta contribució és

menor de 0.2 kcal mol^{-1}. A més, les P^{AA} i P^{BB} dins de cada un dels fragments tenen un valor de -6.0 (corresponent a un doblet via equació (3.22) amb $N_A = N_B = 7$), independentment de què l'acoblament d'spin global sigui triplet o singlet, de manera que $\Delta P^{AA}\left(\Delta P^{BB}\right)$ és zero.

D'acord amb McConnell-I, el terme $\rho_i^A \rho_j^B$ [7] haurà de ser negatiu per a les espècies pseudo-orto i -para donant lloc a un estat fonamental triplet, i positiu per a la pseudo-meta amb un estat fonamental singlet. Els valors calculats de $\left\{\Delta P_1^{AB}\right\}$ són els elements en la diagonal de la TAULA 3.2 (en negreta i cursiva), i concorden amb el model qualitatiu de McConnell-I. Així doncs, les components $\left\{\Delta P_1^{AB}\right\}$ són negatives en els isòmers pseudo-orto i -para (els quals tenen un estat fonamental triplet), i positives en l'isòmer pseudo-meta (el qual té un estat fonamental singlet). La relació (3.19) sembla, per tant, verificar-se numèricament.

Finalment ens ocuparem de $\left\{\Delta P_2^{AB}\right\}$ i $\left\{\Delta P_3^{AB}\right\}$. Les contribucions de $\left\{\Delta P_2^{AB}\right\}$ i $\left\{\Delta P_3^{AB}\right\}$ s'ignoren en el model de McConnell; ara bé, en la TAULA 3.2 veiem clarament que els seus valors no són zero. És més, tenen elements amb valors positius i negatius grans. En primer lloc i d'acord amb l'equació (3.24), cal destacar que $\Delta P_3^{AB} \approx 2$, però $\Delta E_3^{AB} \approx 0.0$ (TAULA 3.1). Aquest resultat està associat amb el fet que les J_{ij} (Annex 2) corresponents a cada $\left\{\Delta P_3^{AB}\right\}$ són petites, de manera que aquest terme no contribueix a l'estabilitat singlet versus triplet. En segon lloc, a partir de la TAULA 3.1 obtenim que $\Delta P_{1+2}^{AB} \approx \delta$ (d'acord amb (3.25)) donat que ΔP_2^{AB} i ΔP_1^{AB} tenen signe oposat. Ara bé, ΔE_2^{AB} no és negligible. Per tant, l'estabilitat del singlet relativa a la del triplet és el resultat de la competició existent entre ΔE_1^{AB} i ΔE_2^{AB}. En tots els exemples estudiats $\left|\Delta E_1^{AB}\right| > \left|\Delta E_2^{AB}\right|$, de manera que el terme ΔE_1^{AB} per si sol dóna la predicció qualitativa correcta, que concorda amb la predicció feta pel model de McConnell-I. Aquesta situació és conseqüència del fet que la magnitud de les J_{ij} (Annex 2) que estan combinades amb $\left\{\Delta P_2^{AB}\right\}$ és, en general, més petita que la magnitud de les J_{ij} que s'associen amb $\left\{\Delta P_1^{AB}\right\}$.

3.4. ORIGEN DE LA CONCORDANÇA EN LES PREDICCIONS FETES PELS MODELS DE HEISENBERG I MCCONNELL-I.

En comparar les equacions (3.16) i (3.17), es veu clarament que l'estabilitat singlet / triplet depèn del signe i la magnitud de $\rho_i^A \rho_j^B$ / ΔP_{ij}, i de la magnitud de les J_{ij} que es combinen amb $\rho_i^A \rho_j^B$ / ΔP_{ij}. En aquest treball, s'han inclós ambdós efectes en el sistema bMe, el qual modelitza el sistema real bPhMenyl que normalment s'usa per comprovar la validesa de la relació de McConnell-I. Cal remarcar que les prediccions obtingudes amb l'Hamiltonià de Heisenberg definit en l'equació (3.17) concorden amb les prediccions qualitatives fetes a partir de l'equació (3.16) degut a cancel.lacions fortuïtes. Aquesta

concordança és conseqüència del fet que els signes de $\rho_i^A \rho_j^B$ i ΔP_{ij} són els mateixos i que moltes J_{ij} valen zero. Ens interessa, però, discutir l'origen d'aquest efecte més detalladament.

És evident que la concordança entre les prediccions fetes pel model de McConnell-I (3.16) i el nostre Hamiltonià de Heisenberg (3.17) és deguda a què la partició en $\{\Delta P_1^{AB}\}$, $\{\Delta P_2^{AB}\}$, i $\{\Delta P_3^{AB}\}$ és possible, i a què la contribució dominant és la provinent de $\{\Delta P_1^{AB}\}$. Cada un dels termes $\{\Delta P_2^{AB}\}$ i $\{\Delta P_3^{AB}\}$ té un valor gran que pot ser tant positiu com negatiu; ara bé, aquesta contribució no és important perquè les J_{ij} corresponents són molt petites. Així doncs, el model de McConnell-I prediu correctament el magnetisme en el cas del nostre model de paraciclofans per casualitat, ja que $|\Delta E_1^{AB}| > |\Delta E_2^{AB}|$. En general, si els àtoms no estan perfectament alineats, caldrà esperar que el terme ΔE_2^{AB} no sigui negligible. En aquest cas, una predicció qualitativa usant el model de McConnell és impossible sense conèixer a priori el valor de les J_{ij}. A més, és evident que les J_{ij} tenen unes propietats que depenen fortament de l'orientació i direcció. Per tant, quan ΔE_1^{AB} i ΔE_2^{AB} tinguin magnituds similars (però de signe oposat) la qüestió de l'estabilitat singlet / triplet dependrà de detalls molt subtils en l'orientació que es manifestaran en les J_{ij}.

La discussió anterior oculta un greu problema conceptual. Els acoblaments calculats entre centres "propers en l'espai" $\{P_1^{AB}\}$ (Annex 2) són *sempre* negatius, independentment de si l'estat fonamental és triplet o singlet. Així doncs, una ΔP_1^{AB} negativa (corresponent a estabilitat triplet) es pot obtenir si $|P_1^{AB}|^S > |P_1^{AB}|^T$. (En el cas "ideal" en què la funció d'ona fos simplement una funció de Rumer [5], les P_{ij} valdrien -1 per dos electrons acoblats paral.lels en triplet, i $-½$ per spins no-acoblats). Donat que la funció de Rumer dominant en la funció d'ona implica parells d'spins acoblats dins de cada fragment (*spin-paired function*), l'acoblament entre fragments és principalment del tipus d'electrons no-acoblats. Així doncs, és d'esperar que les P_{ij} de centres "propers en l'espai" tinguin un valor aproximat de $-½$. De fet, aquests acoblaments calculats a nivell MMVB són tots negatius i el seus valors pertanyen a l'interval de -0.3 a -0.6, la qual cosa concorda amb l'observació anterior. D'acord amb McConnell-I, aquells casos on el producte $\rho_i^A \rho_j^B$ és negatiu estan associats amb "acoblament ferromagnètic". Alhora, una ΔP_1^{AB} negativa està també associada amb estabilitat triplet. Així doncs, només ens cal explicar per què l'estabilitat triplet implica que els centres "més propers en l'espai" en l'estat singlet presentin un acoblament triplet més fort (és a dir, amb P_1^{AB} negatives) que el que presenten els centres "més propers" en l'estat triplet. La resposta ha resultat ser curiosament simple, tal i com ara discutirem.

En la FIGURA 3.6 il.lustrem els determinants principals de les funcions d'ona singlet i triplet que s'usen per calcular les P_{ij}. Els signes + i - en la FIGURA indiquen l'spin (α o β) de l'orbital en el seu corresponent centre per al singlet (S) i triplet (T). Curiosament, els ordenaments d'spin en el triplet ($|S_z| = 1$) (FIGURA 3.6b, d, f) concorden amb els suggerits pel

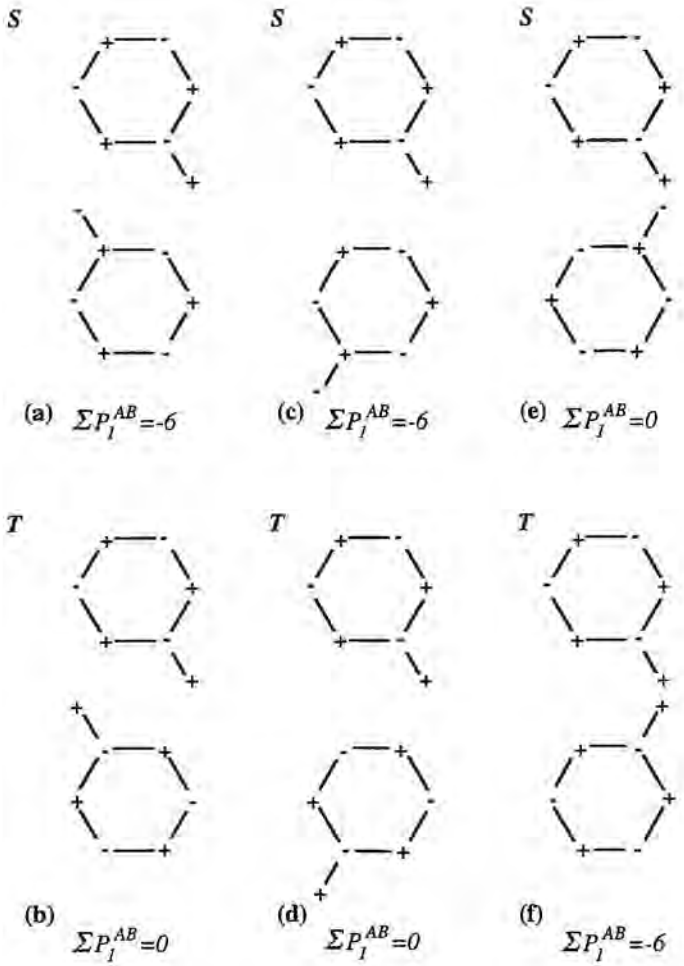

FIGURA 3.6.- Determinants principals de les funcions d'ona singlet (S) i triplet (T) que s'usen en el càlcul de les P_{ij} per als isòmers pseudo- (a/b) -para-, (c/d) -orto- i (e/f) -meta-bMe.

model de McConnell-I en interpretar el magnetisme dels paraciclofans (apartat 3.3.2). A partir de l'equació (3.8) per a un únic determinant, obtenim $P_{ij}=-1$ per electrons amb el mateix spin i $P_{ij}=0$ amb diferent spin. En la FIGURA 3.6, hem donat el valor de la suma de les P_{ij} ideals entre els centres "més propers en l'espai" com a $\sum P_1^{AB}$. En les FIGURES 3.6 a/b i c/d s'observa que, en el primer terme de la funció d'ona, les P_{ij} del singlet entre centres "propers" en un estat fonamental triplet són negatives, mentre que la situació s'inverteix en el cas d'un estat fonamental singlet (FIGURA 3.6 e/f). L'estabilitat triplet implica veritablement

que centres "propers" s'acoblin més ferromagnèticament en l'estat singlet que en el triplet en el cas de tenir un estat fonamental triplet. Així doncs, la magnitud de les ΔP_1^{AB} és predictible toscament a partir del terme principal de la funció d'ona. Per tant, donat que el model de McConnell sembla predir adequadament l'estabilitat dels termes principals en la funció d'ona VB en el cas dels paraciclofans, prediu també correctament el seu magnetisme. Ara bé, no hi ha cap raó per esperar que aquesta situació es verifiqui en general.

3.5. CONCLUSIONS.

En aquest Capítol, s'ha desenvolupat un formalisme prou general com per poder descomposar la diferència d'energia obtinguda amb el model de l'Hamiltonià de Heisenberg en termes de l'obtinguda amb el model de McConnell-I, en base a particionar la densitat de bescanvi d'spin P_{ij}, i la diferència de densitats de bescanvi ΔP_{ij}. Cal destacar que la introducció de P_{ij} simplifica moltíssim el càlcul de l'energia i permet una ràpida interpretació dels fenòmens d'acoblament que tenen lloc entre els centres i, j.

Gràcies a aquest formalisme, s'ha comprovat que el model de McConnell-I prediu correctament l'estabilitat singlet / triplet en l'exemple del bis(metil)[2.2]paraciclofà. En el cas dels [2.2]paraciclofans, el seu esquelet rígid permet que molts dels àtoms estiguin perfectament alineats. En conseqüència, moltes J_{ij} són negligibles; curiosament, aquelles J_{ij} que el model de McConnell ignora. D'altra banda, el model de McConnell sembla predir correctament l'estabilitat dels determinants principals de la funció d'ona VB. Aquests fets fan que l'associació $\Delta P_{ij} \Leftrightarrow \rho_i^\alpha \rho_j^\beta$ sigui raonable. Ara bé, en general, el valor predictiu del model de McConnell és força limitat donat que mai s'estudia la dependència orientacional del model via les J_{ij}. Per tant, una predicció qualitativa usant el model de McConnell-I no serà factible, sense conèixer a priori el valor de les J_{ij}, en aquells casos que no presentin sistemes amb àtoms fortament alineats.

Finalment, cal dir que el formalisme usat en aquest estudi es pot aplicar de manera general a altres problemes relacionats amb el magnetisme. Un exemple és el cas del ferrimagnetisme, el qual és el resultat de l'acoblament d'spins de diferents magnituds de tal manera que mai es té un acoblament amb S=0. McConnell-I és un mecanisme a través de l'espai, mentre que el mecanisme en ferrimagnets és sovint a través d'enllaç. Un altre exemple de mecanisme a través d'enllaç és el model de Dougherty [10a], al qual s'ha aplicat amb èxit un tractament similar [10b]. Així doncs, el formalisme descrit en aquest Capítol és vàlid per a descriure tant mecanismes magnètics a través de l'espai —com és el cas dels isòmers [2.2]paraciclofans [11]—, com mecanismes a través d'enllaç —com és el cas de Dougherty [10b].

BIBLIOGRAFIA.

[1] (a) P.W. Anderson, *Phys. Rev.*, **1959**, *115*, 2; (b) M Sai, D. Maynau, J.P. Malrieu, M.A.G. Bach, *J. Am. Chem. Soc.*, **1984**, *106*, 571; (c) D. Maynau, Ph. Durand, J.P. Daudey, J.P. Malrieu, *Phys. Rev. A*, **1983**, *28*, 3193; (d) Ph. Durand, J.P. Malrieu, *Adv. Chem. Phys.*, **1987**, *68*, 931.

[2] (a) M.J. Bearpark, F. Bernardi, M. Olivucci, M.A. Robb, *Chem. Phys. Lett.*, **1994**, *217*, 513; (b) F. Bernardi, M. Olivucci, J.J. McDouall, M.A. Robb, *J. Chem. Phys.*, **1988**, *89*, 6365; (c) F. Bernardi, M. Olivucci, M.A. Robb, *J. Am. Chem. Soc.*, **1992**, *114*, 1606.

[3] R. McWeeny, B.T. Sutcliffe, *Methods of Molecular Quantum Mechanics*, Academic Press : New York, **1969**.

[4] R. Pauncz, *Spin eigenfunctions* , Plenum Press: New York, **1979**.

[5] R. McWeeny, *Spins in Chemistry* , Academic Press Inc.: New York, **1970**.

[6] H.M. McConnell, *J. Chem. Phys.*, **1963**, *39*, 1910.

[7] (a) A. Izuoka, S. Murata, T. Sugawara, H. Iwamura, *J. Am. Chem. Soc.*, **1985**, *107*, 1786; (b) A. Izuoka, S. Murata, T. Sugawara, H. Iwamura, *ibid.*, **1987**, *109*, 2631.

[8] (a) C.J. Brown, *J. Chem. Soc.*, **1953**, 326;. (b) K. Lonsdale, H.J. Milledge, K.V.K. Rao, *Proc. R. Soc. London, Ser. A*, **1960**, *555*, 82; (c) D.J. Cram, J.M. Cram, *Acc. Chem. Res.*, **1971**, *4*, 204.

[9] K. Yoshizawa, R. Hoffmann, *J. Am. Chem. Soc.*, **1995**, *117*, 6921.

[10] (a) D.A. Dougherty, *Acc. Chem. Res.*, **1991**, *24*, 88; (b) P. Lafuente, J.J. Novoa, M.J. Bearpark, P. Celani, M. Olivucci, M.A. Robb, *Theoretical Chem. Acc.* **1998** (en premsa).

[11] M. Deumal, J.J. Novoa, M.J. Bearpark, P. Celani, M. Olivucci, M.A. Robb, *J. Phys. Chem.*, **1998** (en premsa).

CAPÍTOL 4:

Tractament Estadístic de Cristalls α-Nitronil Nitròxid

L'estudi de la disposició geomètrica dels contactes intermoleculars NO···ON i CH···ON en cristalls de la família dels α-nitronil nitròxid ens permetrà trobar d'una manera sistemàtica i inequívoca la possible relació entre la presència de ferromagnetisme (o antiferromagnetisme) i l'orientació relativa d'aquests contactes. Cal destacar que aquests contactes han estat seleccionats perquè és d'esperar que siguin els que controlin energèticament i magnètica l'empaquetament dels cristalls α-nitronil nitròxids.

4.1. Bases de Dades Ferromagnètica i Antiferromagnètica.

Per a aquest estudi es van seleccionar 143 cristalls de la família dels α-nitronil nitròxid amb propietats magnètiques conegudes, dels quals es van descartar tots els que tenien un factor R més gran que 0.10, els que havien estat determinats a partir d'un número de dades molt limitat i els que presentaven desordre o distorsions moleculars grans. De les 117 estructures restants, se'n van descartar 45 més que contenien metalls de transició o molècules orgàniques capes tancades co-cristal.litzades, ja que podien presentar mecanismes magnètics a través dels àtoms metàl.lics o les molècules capes tancades i les unitats radicalàries. Finalment, d'entre les 72 que quedaven, es van eliminar totes aquelles que no presentaven un comportament *dominantment* ferro- o antiferromagnètic [1]. La naturalesa de les interaccions magnètiques *dominants* es manifesta clarament en la dependència en la temperatura de la susceptibilitat magnètica, χ, en el rang de temperatures de 2-300K [2]. Així doncs, radicals amb interaccions dominantment ferromagnètiques mostren el característic increment de χT quan T disminueix en graficar χT vs. T. En canvi, els radicals amb interaccions dominants antiferromagnètiques tenen la tendència oposada. No s'han inclós cristalls amb un comportament magnètic mixte (amb interaccions ferro- i antiferromagnètiques alhora), perquè haguessin dificultat la identificació dels possibles ordenaments associats a l'empaquetament ferro- o antiferromagnètic. Aquesta última criba ens deixa amb un conjunt de 47 cristalls α-nitronil nitròxid purament orgànics, 23 [3] dels quals presenten interaccions ferromagnètiques, FM, i 24 [4] en presenten d'antiferromagnètiques, AFM. Les FIGURES 4.1 i 4.2 mostren l'estructura molecular dels radicals, els cristalls dels quals presenten interaccions intermoleculars dominantment FM i AFM, respectivament (el *refcode* —generat o bé per la Cambridge Structural Database, CSD [5], o bé per nosaltres— que permet identificar els cristalls FM/AFM s'ha indicat a sota de cada estructura).

Els 47 cristalls seleccionats pertanyen als següents grups espacials: P-1 (3), $P2_1$ (2), Cc (2), $P2_1/c$ (25), C2/c (2), $P2_12_12_1$ (2), $Pca2_1$ (1), Ib2a (1), Pbca (4), Fdd2 (1), $I4_1/a$ (1),

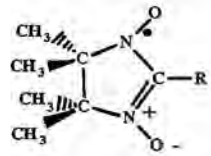

where **R ≡**

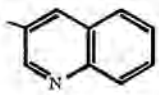

0003QN

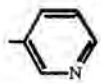

000MPY

000PPY

00DPNP (δ-phase)
00GPNP (γ-phase)

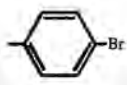

0PBRPH

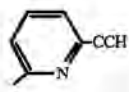

MACOPY

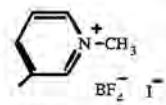

MMEPYB

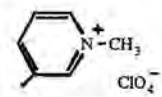

MMEPYC

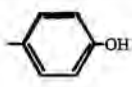

HAFXOB

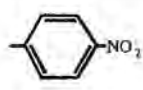

KAXHAS (β-phase)

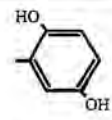

LICMIT (α-phase)

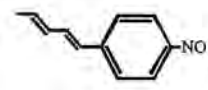

PEFMES

PEYPUA

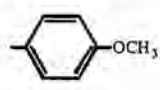

YISCEI

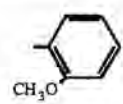

YISCOS

YISNIX

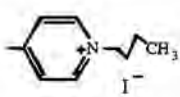

YIWSEC

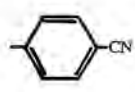

YODBUO

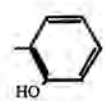

YOMYII (α-phase)

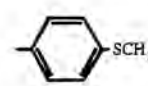

YUJNEW10

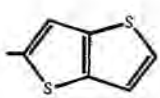

YULPOK

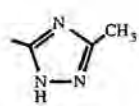

ZORHIX

FIGURA 4.1.- Fórmula dels substituents R dels radicals α-nitronil nitròxid inclosos en la base de dades FM (en la part inferior apareixen aquells cristalls, les estructures dels quals han estat dipositades en la CSD).

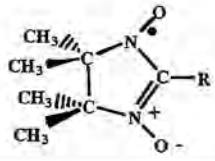

where R ≡

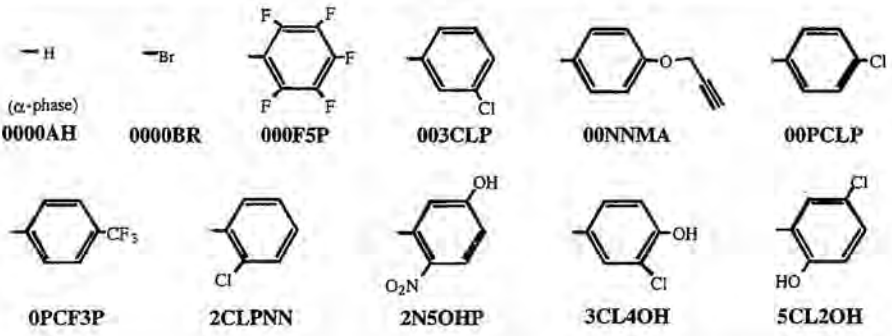

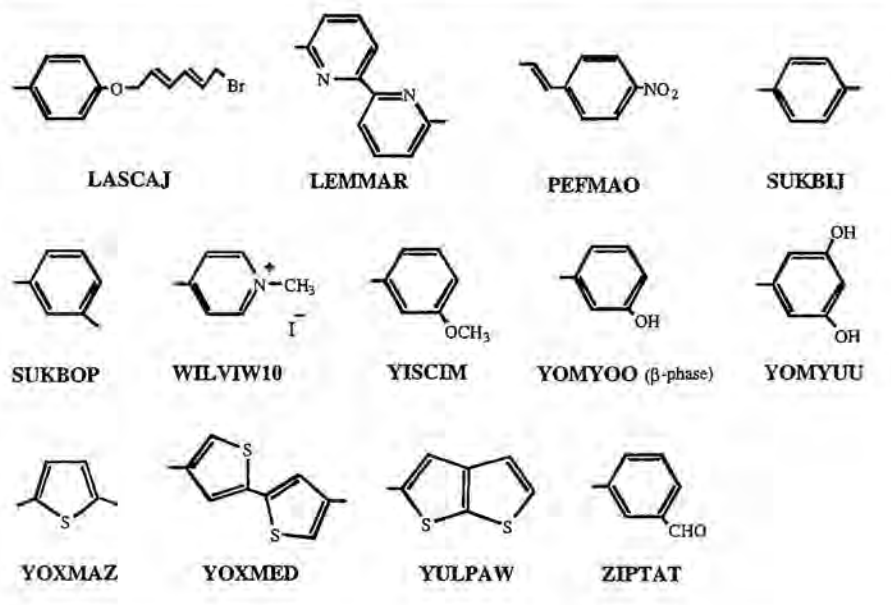

FIGURA 4.2.- Fórmula dels substituents R dels radicals α-nitronil nitròxid inclosos en la base de dades AFM (en la part inferior apareixen aquells cristalls, les estructures dels quals han estat dipositades en la CSD).

$P4_2bc$ (1), i P3c1 (2). Com era d'esperar, la majoria dels cristalls s'empaqueten segons el grup espacial $P2_1/c$ [6].

Cal destacar que la major part de les estructures analitzades han estat determinades a temperatura ambient, on l'energia tèrmica sobrepassa la força de les interaccions magnètiques intermoleculars. Així doncs, volem correlacionar una propietat física, la magnitud de la qual només es pot observar a temperatures baixes, amb l'empaquetament cristal.lí que existeix a temperatura ambient. Aquesta correlació és molt usual en Magnetisme Molecular ja que, desafortunadament, s'han determinat molt pocs cristalls a temperatures baixes. Ara bé, exceptuant els casos que presenten transicions de fase estructurals de primer ordre [7], l'empaquetament cristal.lí de cristalls moleculars mostra només petits canvis amb la temperatura deguts a contracció tèrmica. Aquests canvis, però, no fan variar la disposició relativa de les molècules (la informació que ens interessa) tant com per invertir la naturalesa de les interaccions magnètiques intermoleculars dominants [8]. Així doncs, tot i que els valors de les distàncies i angles que defineixen cada contacte poden canviar lleugerament, es pot assumir que l'empaquetament cristal.lí serà similar a baixes i altes temperatures. Per tant, les similituds i diferències entre la distribució de contactes en els conjunts de cristalls FM i AFM seran significatives en la nostra anàlisi estadística.

4.1.1.- Metodologia.

La distribució de contactes intermoleculars en les bases de dades FM i AFM de la família dels α-nitronil nitròxid s'ha analitzat amb el paquet de programes de la CSD [5]. En ambdues bases de dades hi ha cristalls que provenen directament de la CSD i d'altres que no. El mòdul PREQUEST s'ha fet servir per a generar les estructures adequades per al seu posterior processament amb el mòdul QUEST de tots aquells cristalls que no pertanyien a la CSD. La localització dels contactes intermoleculars NO···ON i CH···ON en aquests cristalls s'ha realitzat mitjançant QUEST. Gràcies al mòdul VISTA, s'ha fet una primera visualització i un tractament estadístic preliminar de les dades obtingudes via QUEST. El tractament definitiu s'ha dut a terme amb uns programes de *factor* i *cluster analysis* escrits com a part d'aquesta tesi [9, 10] (Annex 3).

L'anàlisi dels contactes intermoleculars presents en els 47 cristalls provinents de les bases de dades FM i AFM dóna com a resultat la presència de 1312 contactes NO···ON, i de 6039 / 2286 contactes $C(sp^3$ / $sp^2)$-H···O-N dins d'un rang de distàncies O···O i H···O menors de 10Å. El número de contactes és prou gran com per fer possible una anàlisi

estadística de la distribució geomètrica dels paràmetres que defineixen els tres tipus de contactes anteriors.

4.2. ANÀLISI D'INTERACCIONS INTERMOLECULARS DEL TIPUS NO···ON.

4.2.1.- Definició de l'orientació relativa de contactes NO···ON.

Per tal d'analitzar les orientacions relatives de contactes NO···ON entre radicals veïns en les bases de dades FM i AFM, s'ha de definir la posició relativa dels grups ONCNO que participen en el contacte. Una anàlisi estadística prèvia de la geometria en radicals α-nitronil nitròxids va demostrar que els àtoms ONCNO de l'anell de cinc membres estan disposats en un mateix pla i que la seva geometria és aproximadament la mateixa [11]. Aquest comportament es pot atribuir a la hibridació sp^2 de l'àtom de C en α, que permet la deslocalització dels electrons π arreu del grup ONCNO a través de vàries formes ressonants. Així doncs, no cal preocupar-nos per petites distorsions en la geometria del grup ONCNO ni de la resta d'àtoms de l'anell imidazòlic, inclosos els quatre grups metil. Per tant, la geometria interna d'aquests grups es pot considerar fixada. Conseqüentment, usant coordenades internes, la posició relativa d'un contacte del tipus NO···ON, $N_{11}O_{11}\cdots O_{21}N_{21}$, establert entre els grups $O_{12}N_{12}C_1N_{11}O_{11}$ i $O_{21}N_{21}C_2N_{22}O_{22}$ es pot definir mitjançant sis coordenades: tres per definir la posició de l'àtom O_{21} relativa al grup $O_{12}N_{12}C_1N_{11}O_{11}$ (la distància $O_{11}\cdots O_{21}$, l'angle N_{11}-$O_{11}\cdots O_{21}$ i el dihedre N_{11}-$O_{11}\cdots O_{21}$-N_{21}), dos per determinar la de l'àtom N_{21} per a una distància N-O fixada (l'angle $O_{11}\cdots O_{21}$-N_{21} i el dihedre N_{11}-$O_{11}\cdots O_{21}$-N_{21}), i un per fixar el pla dels grup $O_{12}N_{12}C_1N_{11}O_{11}$ (el dihedre $O_{11}\cdots O_{21}$-N_{21}-C_2 ja que la distància C_2-N_{21} i l'angle C_2-N_{21}-O_{21} estan fixats). Simplifiquem la notació identificant els paràmetres intermoleculars anteriors com D, A_1, A_2, T_1, T_2 i T_3 (FIGURA 4.3). Tot i existir altres opcions per a definir l'espai de sis coordenades, el conjunt de paràmetres seleccionat permet una fàcil visualització i una clara interpretació física dels paràmetres geomètrics.

En el processament d'aquests sis paràmetres s'han evitat duplicitats de valors amb l'eliminació d'aquells valors que eren quasi idèntics. També s'han evitat distribucions espacials a l'atzar forçant que els valors dels angles A_1 i A_2 fossin menors que 180° i, alhora, imposant la condició $A_1 \geq A_2$. Aquesta darrera restricció es va haver d'imposar perquè no hi ha cap altra manera de definir que un dels grups ONCNO sigui el grup número 1 i l'altre el grup 2 en l'anàlisi duta a terme amb el mòdul QUEST. A part de les ja esmentades, no hi ha cap altra restricció en l'anàlisi de les dades corresponents a contactes intermoleculars en cristalls FM i AFM.

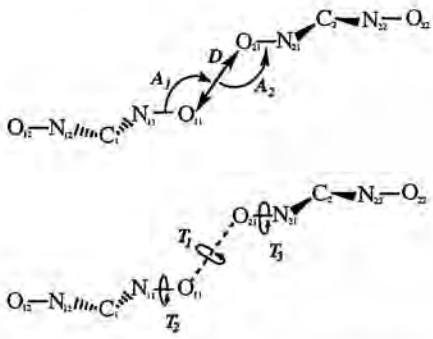

$D = O_{21} \cdots O_{11}$

$A_1 = O_{21} \cdots O_{11} - N_{11}$

$A_2 = N_{21} - O_{21} \cdots O_{11}$

$T_1 = N_{21} - O_{21} \cdots O_{11} - N_{11}$

$T_2 = O_{21} \cdots O_{11} - N_{11} - C_1$

$T_3 = C_2 - N_{21} - O_{21} \cdots O_{11}$

FIGURA 4.3.- Paràmetres geomètrics que defineixen la posició relativa de dos grups ONCNO.

4.2.2.- Distribució de contactes NO···ON en funció de la distància O···O.

Podem iniciar l'anàlisi de la geometria dels contactes NO···ON en els conjunts FM i AFM examinant el seu número en funció de la distància O···O (el paràmetre D). Hi ha un número similar de contactes en ambdós conjunts en l'interval de distàncies 0-n (n≤10) Å analitzat (TAULA 4.1). En aquesta anàlisi es va seleccionar una distància de tall de 10Å per tal d'incloure ordenaments en què el contacte NO···ON més curt entre dues molècules veïnes implica distàncies O···O considerables; per exemple, els contactes que s'estableixen entre un substituent R gran (un anell aromàtic) d'una molècula i un grup ON de la segona molècula. La proporció de contactes en els conjunts FM i AFM (TAULA 4.1) és quasi constant per n ≤ 10 Å (en promig, un 44% dels contactes provenen de la base de dades FM, amb un 39% i 47% com a valors mínim i màxim). Aquests valors són sempre molt similars al percentatge de cristalls que pertanyen al conjunt FM (49%). Aquest fet ens suggereix que el número de contactes ONCNO···ONCNO que cada grup NO està establint és similar en ambdós conjunts de cristalls, FM i AFM. Conseqüentment, no és veritat que la presència de contactes NO···ON curts sigui un indicatiu de cristalls antiferromagnètics, tal i com s'afirma a vegades en la literatura [12]. La TAULA 4.1 mostra que hi ha un número similar de cristalls FM i AFM que presenten contactes NO···ON curts. El valor més curt que trobem en el conjunt de cristalls FM és de 3.158Å, mentre que en el de cristalls AFM és de 3.159Å. La FIGURA 4.4 mostra la disposició relativa de molècules amb les distàncies O···O més curtes d'ambdós conjunts de dades. L'ordenament és del tipus *up-down* (a) en el cas FM, mentre que en l'AFM n'hi ha d'*up-up* (b) i *up-down* (c). Així doncs, *és impossible definir el caràcter*

TAULA 4.1.- Llistat de contactes ONCNO···ONCNO (i percentatges) en cristalls dels conjunts FM i AFM en el rang de distàncies indicat.

		conjunt FM		conjunt AFM	
rang de distàncies (Å)	número total de contactes	número de contactes	%	número de contactes	%
[0,3]	0	0	0	0	0
[0,4]	24	10	42	14	58
[0,5]	92	36	39	56	61
[0,6]	204	90	44	114	56
[0,7]	378	167	44	211	56
[0,8]	608	274	45	334	55
[0,9]	901	416	46	485	54
[0,10]	1312	611	47	701	53

magnètic d'un cristall basant-se únicament en la presència o absència de contactes NO···ON curts.

4.2.3.- Distribució angular de contactes del tipus NO···ON.

Fins ara, únicament s'han estudiat les distàncies O···O, sense tenir en compte explícitament les distribucions angulars associades a cada distància. McConnell-I [13a] prediu que contactes curts que resultin del solapament directe entre dos grups ONCNO poden donar lloc a interaccions ferro- o antiferromagnètiques. El tipus d'interacció dependrà de l'orientació relativa dels grups ONCNO: si el solapament dominant és entre dos grups NO (les dues densitats d'spin [14] tenen el mateix signe) la interacció serà antiferromagnètica, mentre que si és entre un grup NO i l'àtom de C central serà ferromagnètica [13]. Així doncs, cal comprovar si la distribució angular dels contactes NO···ON presents en cristalls FM té orientacions angulars particulars que són excloents del conjunt de contactes AFM. Amb aquest propòsit, s'ha fet una primera anàlisi de la distribució angular que presenten ambdós conjunts de cristalls en l'interval de 3-5Å. Aquest interval ha estat seleccionat perquè és el rang de distàncies més important si el mecanisme responsable de la interacció magnètica és el solapament directe dels grups que contenen la densitat d'spin, els dos grups NO. La FIGURA 4.5a mostra els scattergrames dels valors de D i T_2 per als conjunts FM i AFM en el rang 3-10Å. Tal com es veu en aquesta FIGURA, hi

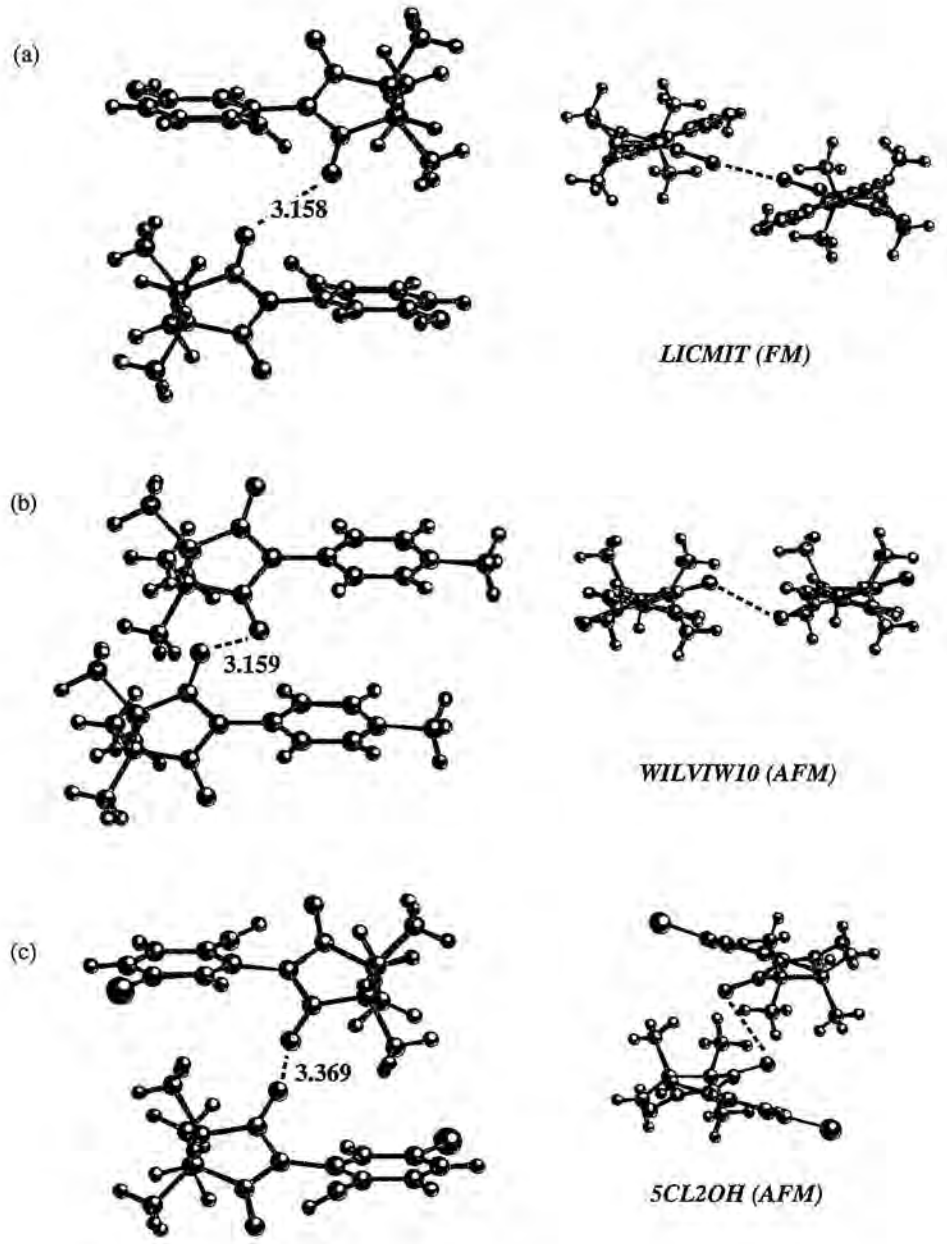

FIGURA 4.4.- Disposició geomètrica dels dímers que presenten els contactes NO···ON més curts dins dels conjunts FM (a: conformació *up-down*) i AFM (b: conformació *up-up*; c: conformació *up-down*).

(a)

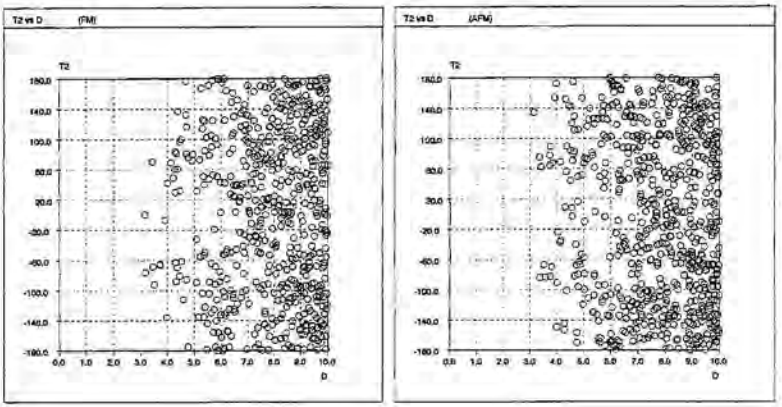

(b)

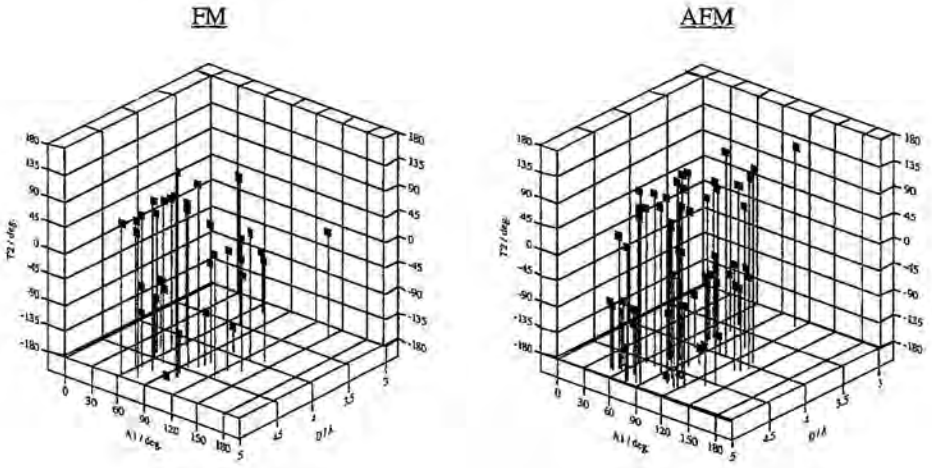

FIGURA 4.5.- (a) Scattergrames del parell de paràmetres indicat que caracteritzen els contactes NO···ON dels conjunts FM (esquerra) i AFM (dreta). (b) Posició de l'àtom O_{21} relativa al grup O_{11}-C_{11}-C_1 en l'interval de distàncies 3-5 Å per als conjunts de cristalls FM (esquerra) i AFM (dreta).

ha una similitud remarcable entre les dues distribucions al llarg de tot l'interval seleccionat i, en particular, en el rang de distàncies de 3 a 5 Å. Scattergrames d'altres parells de variables mostren un comportament similar al de la FIGURA 4.5a. Per comprovar que aquesta semblança no és un artefacte del parell de variables seleccionat, s'ha dibuixat (FIGURA 4.5b) la posició de l'àtom O_{21} relativa al grup N_{11}-O_{11} per a tots els contactes dels conjunts FM i AFM en l'interval de distàncies de 3-5Å. Si observem la FIGURA 4.5b, veurem (1) que l'àtom O_{21} està situat arreu de l'espai, i (2) que no hi ha diferències apreciables entre les distribucions espacials dels contactes FM i AFM, és a dir, per un mateix rang de distàncies i angles és possible trobar contactes NO···ON curts en ambdós conjunts, FM i AFM (fet que ja ha estat exemplificat en la FIGURA 4.4). Aquestes similituds en la distribució geomètrica dels contactes NO···ON FM i AFM també s'aprecien en l'anàlisi feta en el rang de 0-10Å; interval on s'obtenen scattergrames molt semblants als de la FIGURA 4.5 (però amb molts punts més).

Tanmateix, aquesta similitud torna a posar-se de manifest en comparar els valors promig dels sis paràmetres que defineixen l'orientació dels contactes NO···ON en cada un dels conjunts FM i AFM en els intervals de 0-10Å i de 0-4Å. En l'interval de 0-10Å, els valors promig dels paràmetres D, A_1, A_2, T_1, T_2 i T_3 en el conjunt FM són 7.9Å, 74°, 115°, 13°, 3° i -5°, mentre que en el conjunt AFM els seus valors corresponents són 7.8Å, 73°, 113°, 8°, -6° i 2° (la diferència entre aquests valors i els anteriors és menor que les seves desviacions estàndards [15]). De la mateixa manera, quan aquesta anàlisi és duta a terme en el rang de 0-4Å, la diferència entre els valors promig FM i AFM en aquest interval torna a ser menor que les seves desviacions estàndards (3.6Å, 92°, 137°, 18°, -22° i -37° (FM); 3.6Å, 88°, 93°, 32°, 44° i 10° (AFM)); valors promig que són molt semblants als de l'interval 0-10Å.

Així doncs, l'estudi realitzat fins ara demostra clarament que, fins i tot tenint en compte l'orientació angular dels contactes NO···ON, la presència de contactes curts d'aquest tipus (associats a interaccions antiferromagnètiques segons McConnell-I) no implica que el cristall tingui interaccions dominants antiferromagnètiques. Per tant, *no és possible definir la naturalesa de les interaccions intermoleculars magnèticament dominants analitzant únicament la disposició geomètrica dels contactes NO···ON més curts.*

4.2.4.- *Factor* i *Cluster Analysis* de la geometria dels contactes NO···ON.

Arribats a aquest punt, hem decidit realitzar una anàlisi estadística detallada dels 611 i 701 contactes del tipus ONCNO···ONCNO que hem trobat en els conjunts FM i AFM,

respectivament. En aquesta nova anàlisi buscarem possibles tendències, inconsistències, o variables amagades en les dades [9, 16]. A més, també s'ha dut a terme un *cluster analysis* [10] per tal de determinar, d'una manera numèrica i matemàticament ben definida, si hi ha clústers presents en la distribució geomètrica dels sis paràmetres que defineixen la geometria NO···ON.

Primer de tot, ens interessa saber si totes les conclusions anteriors han estat una conseqüència del conjunt de coordenades seleccionat per a l'anàlisi estadística. Per demostrar que aquest no és el cas, s'ha dut a terme un test en cada una de les bases de dades per separat. En ambdues bases, hem considerat cada contacte NO···ON com un vector V de sis components, una per a cada un dels sis paràmetres definits en la Figura 4.3. Així doncs, V(1)=D, V(2)=A1, etc. Cal destacar, també, que els valors de V referents a angles i dihedres van ser renormalitzats, expressant-se en radians, per tal que tinguessin un pes similar al de la distància. Amb aquestes dades, es va calcular la matriu de correlació [16], la qual mostra una petita correlació de 0.36 entre els paràmetres A_1 i A_2 (probablement deguda a la tendència que tenen aquests radicals d'empaquetar-se formant plans). El valor absolut dels elements no-diagonals d'aquesta matriu és sempre menor que 0.17, exceptuant el que correlaciona A_1 i A_2. El promig del valor absolut dels elements no-diagonals és 0.07 pels contactes ONCNO···ONCNO presents en el conjunt FM, i 0.06 pels de l'AFM. Així doncs, exceptuant la petita correlació existent entre els angles A_1 i A_2, no n'hi ha cap altra entre qualsevol altre parell de paràmetres usat en aquest estudi.

S'ha realitzat, també, un *factor analysis* de les sis coordenades internes que defineixen la posició relativa de dos grups ONCNO [9, 16]. Aquest procediment es basa en calcular els valors propis de la matriu de covariància 6x6 obtinguda a partir de la premultiplicació de la matriu de dades (611x6 en la base de dades FM i 701x6 en l'AFM) per la seva matriu transposada. La matriu covariància FM inicial és quasi diagonal, i els seus valors propis són 4.096, 3.479, 3.246, 2.590, 0.374 i 0.177. Els tres primers valors propis estan majoritàriament associats als tres angles dihedres, el quart a la distància D, i els dos darrers als angles A_1 i A_2. Trobem conclusions similars quan apliquem el *factor analysis* en el conjunt AFM: la matriu de covariància i els valors i vectors propis són molt semblants als obtinguts en el conjunt FM. Aquest fet indica que els conjunts de dades inicials FM i AFM, és a dir, les geometries dels contactes FM i AFM, són molt similars. Resultat que concorda amb el que havíem conclòs prèviament. *Aquests números indiquen que sis és el número de paràmetres independents necessari per tal de tractar les dades geomètriques que determinen els contactes NO···ON*, i que no és possible reduir aquest número. Aquesta conclusió també demostra que l'ús de tres o, fins i tot, dos paràmetres geomètrics en analitzar sèries de radicals α-nitronil nitròxids i establir relacions magneto-estructurals no és correcte.

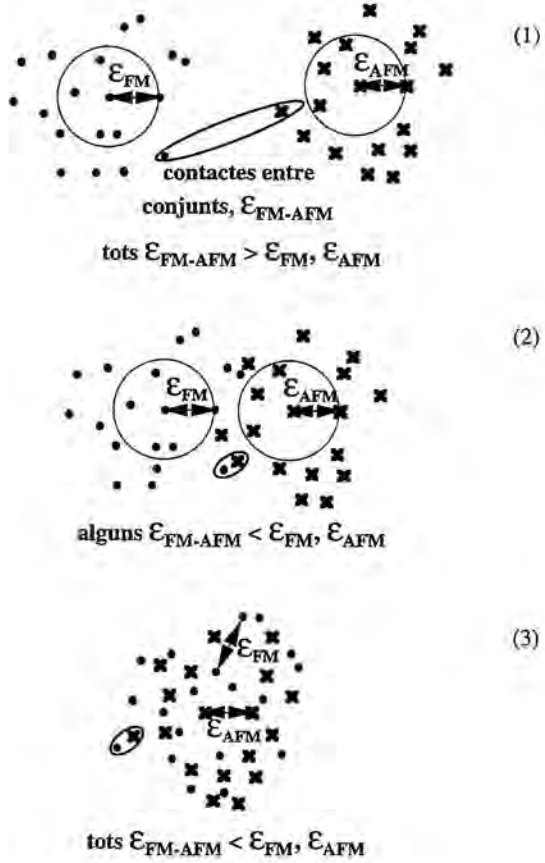

FIGURA 4.6.- Tipus de clústers possibles en l'anàlisi dels conjunts de cristalls FM i AFM.

Finalment, s'ha dut a terme un *cluster analysis* [10] de les dades geomètriques NO···ON dels contactes intermoleculars en els conjunts FM i AFM. Amb aquesta tècnica es pretenia determinar si els contactes ONCNO···ONCNO dels conjunts FM i AFM estaven localitzats en regions diferents de l'espai de coordenades de dimensió sis. El criteri de clusterització que s'ha usat és el *single linkage method* [10], també conegut com a tècnica dels veïns més propers. Segons aquest criteri, un clúster es defineix com un conjunt d'elements connectats. Un element i es diu que està connectat al seu veí més proper j quan la distància entre ambdós elements, d_{ij} [17], és igual o menor que un valor llindar, ε, és a dir,

$d_{ij} \leq \varepsilon$. Aquest tipus de connexió és de tipus directe. Si l'element j està també connectat a un altre element k, aleshores i i k estan connectats indirectament i el clúster està constituït pels elements i, j i k. Així doncs, un nou element l és afegit a aquest clúster quan la distància més curta a qualsevol element del cluster és menor que el valor llindar ε. Conseqüentment, ε és un paràmetre que caracteritza els possibles clústers que hi ha en un determinat conjunt de dades. Donat un conjunt de dades, tenim dos clústers A i B (caracteritzats per dos valors llindar diferents, ε_A i ε_B) completament diferenciats si, i només si, la distància més curta entre elements de clústers diferents ($\varepsilon_{A\text{-}B}$) és més llarga que qualsevol dels dos valors llindars ε_A i ε_B. En aplicar aquesta argumentació al cas en què A=FM i B=AFM, tenim que cada element és un vector en el conjunt de vectors V sis dimensional que únicament està associat a un tipus de contacte: o bé és FM o bé és AFM. El *cluster analysis* no depèn de les components del vector V (les coordenades D, A_1, A_2, T_1, T_2, T_3) ja que la distància Cartesiana entre dos vectors (ε_{FM}, ε_{AFM} i $\varepsilon_{FM\text{-}AFM}$ [110, ref.30]) és invariant respecte al conjunt de coordenades que representen a aquests vectors. Per tant, un canvi en l'eix de coordenades és equivalent, en el nostre cas, a un canvi en les coordenades internes que estem usant, la qual cosa és en principi arbitrària.

Tres situacions extremes són possibles amb aquest tipus d'anàlisi (FIGURA 4.6). En (1), els conjunts FM i AFM són disjunts, és a dir, no comparteixen cap element perqué estan perfectament separats: els cristalls FM estableixen contactes que són completament diferents dels que estableixen els AFM. En (2), hi ha elements en comú compartits pels dos conjunts de contactes, és a dir, els dos conjunts són no-disjunts. En (3), els dos conjunts estan totalment interpenetrats i són indistinguibles; de fet, són un únic conjunt. Matemàticament, les tres situacions es diferencien si comparem la distància més curta dins de cada conjunt FM i AFM (ε_{FM} i ε_{AFM}) amb la distància més curta entre parells d'elements que pertanyen a diferents conjunts ($\varepsilon_{FM\text{-}AFM}$). Si $\varepsilon_{FM\text{-}AFM} > \varepsilon_{FM}$ i alhora $\varepsilon_{FM\text{-}AFM} > \varepsilon_{AFM}$, els dos conjunts són disjunts (1), mentre que si una d'aquestes condicions no es verifica hi haurà un solapament entre els dos conjunts i no serà possible diferenciar -los amb un *cluster analysis*. Seria interessant, però, poder distingir entre els casos (2) i (3). Ambdós tenen un número d'elements en comú tal que $\varepsilon_{FM\text{-}AFM}$ és menor que ε_{FM} i ε_{AFM}, si aquest número és igual al número global d'elements en els conjunts FM i AFM ens trobem en la situació (3), altrament és el cas (2). L'anàlisi de les dades corresponents a ambdós conjunts FM i AFM indica que ε_{FM} i ε_{AFM} valen 1.980 i 2.130, respectivament. D'altra banda, $\varepsilon_{FM\text{-}AFM} < \varepsilon_{FM}$ i $\varepsilon_{FM\text{-}AFM} < \varepsilon_{AFM}$. Conseqüentment, el nostre conjunt de contactes està distribuït d'acord amb la tercera possibilitat, és a dir, els dos conjunts són quasi idèntics i interpenetrats, essent indistingibles. Així doncs, matemàticament trobem que *no hi ha cap diferència estadísticament significant en la disposició relativa de contactes NO···ON dins de les bases de dades FM i AFM*.

4.3. ANÀLISI D'INTERACCIONS INTERMOLECULARS DEL TIPUS C-H···ON.

4.3.1.- Altres contactes magnèticament relevants.

Fins ara, d'acord amb McConnell-I i donat que la major part de la densitat d'spin està localitzada en el grup ONCNO [14], hem assumit que els únics contactes intermoleculars relevants, des d'un punt de vista magnètic, són aquells que contenen grups ONCNO. Ara bé, tots els resultats obtinguts en estudiar els contactes NO···ON de manera individual indiquen que no hi ha cap connexió general entre la geometria d'aquests contactes i la presència d'interaccions dominants ferro- o antiferromagnètiques. Aquest fet es podria entendre fàcilment si els contactes NO···ON curts no fossin els únics magnèticament relevants. En la Figura 4.4 es veu clarament que l'existència de contactes NO···ON curts és conseqüència de contactes C-H···ON curts (repulsius els primers, atractius els segons) [18]. Així doncs, interessa investigar si les interaccions C-H···ON tenen algun rol magnètic que complementi les NO···ON, possibilitat que ja ha estat esmentada en la literatura [19]. Cal destacar, però, el fet que la densitat d'spin en els hidrògens [20], a més de ser de tipus σ, és molt més petita que la dels grups NO; de manera que, assumint que McConnell-I és aplicable en el cas H···ON —equació (3.12)—, el valor del producte de densitats d'spin ($\rho_H \cdot \rho_O$, $\rho_H \cdot \rho_N$) serà molt petit. Ara bé, segons l'equació (3.12), la corresponent integral de bescanvi magnètica J_{ij} —que depèn principalment de la distància entre els àtoms i, j— podria compensar aquest petit valor, i fer que contactes del tipus C-H···ON tinguin un pes magnètic important.

4.3.2.- Definició de l'orientació relativa de contactes C-H···ON.

Donada la possible importància de les interaccions C-H···ON per tal d'entendre la relació magneto-estructural en els α-nitronil nitròxids, s'ha fet una anàlisi —similar a la duta a terme amb els contactes NO···ON— de la geometria d'aquest tipus d'interaccions en els conjunts FM i AFM. Concretament, ens hem centrat en contactes del tipus C(sp^3)-H···O-N i C(sp^2)-H···O-N, perquè constitueixen la major part de contactes CH···O i, experimentalment, s'han localitzat petites quantitats de densitat d'spin en els àtoms d'H dels grups aromàtics i metílics.

Per tal de definir la geometria d'un contacte genèric C-H···O-N calen sis coordenades internes independents (com en el cas anterior, FIGURA 4.3). Ara bé, donada la simetria quasi cilíndrica de la densitat electrònica entorn el grup C-H, d'entre aquests sis paràmetres en podem descartar dos, i usar els quatre il.lustrats en la FIGURA 4.7a en el cas C(sp^3)-H···O-N

(a)

$$D = H\cdots O_{21}$$

$$A_1 = H\cdots O_{21}\text{-}N_{21}$$

$$A_2 = C_{111}\text{-}H\cdots O_{21}$$

$$T_1 = C_{111}\text{-}H\cdots O_{21}\text{-}N_{21}$$

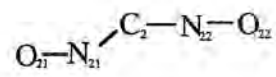

(b)

$$D_i = H_j\cdots O_{21}$$

$$A_{1i} = H_j\cdots O_{21}\text{-}N_{21}$$

$$A_{2i} = C_i\text{-}H_j\cdots O_{21}$$

$$T_{1i} = C_i\text{-}H_j\cdots O_{21}\text{-}N_{21}$$

$$(i=o,\ m,\ p)$$

$$(H_j = H_{orto},\ H_{meta},\ H_{para})$$

FIGURA 4.7.- Paràmetres geomètrics usats per definir la posició relativa d'un grup (a) C(sp^3)-H i (b) C(sp^2)-H en respecte a un grup ONCNO.

o els de la FIGURA 4.7b pels contactes C(sp^2)-H···O-N. Per simplificar la notació els anomerarem D, A_1, A_2 i T_1. En el cas C(sp^2)-H···O-N, caldrà a més distingir entre *orto*, *meta* i *para* contactes depenent de la posició que ocupi el C(sp^2) relativa al C en α de l'anell de cinc membres. Els identificarem afegint el sufix o, m i p: A_{1o}, A_{1m} i A_{1p} per exemple.

4.3.3.- Distribució de contactes CH···ON en funció de la distància H···O i de la seva angularitat.

Tots els cristalls inclosos en ambdós conjunts magnètics FM i AFM tenen 12 hidrògens enllaçats a C(sp^3) metílics. Hi ha, per tant, un 49% vs. un 51% de grups C(sp^3)-H amb possibilitat d'establir contactes intermoleculars amb grups NO en els conjunts de cristalls FM i AFM, respectivament. Ara bé, no tots els cristalls analitzats tenen grups funcionals aromàtics com a substituents R, i la proporció de grups C(sp^2)-H que poden

TAULA 4.2.- Número i proporció de contactes $C(sp^3)$-H···ON i $C(sp^2)$-H···ON (separats en contribucions orto, meta i para) en cristalls dels conjunts FM i AFM (distàcia H···O ≤ 3.8Å).

Tipus de contacte	número total de contactes	conjunt FM número de contactes	conjunt FM %	conjunt AFM número de contactes	conjunt AFM %
$C(sp^3)$-H··· ON	364	157	43	207	57
$C(sp^2)$-H··· ON					
orto	35	20	57	15	43
meta	51	32	63	19	37
para	16	6	38	10	62

interaccionar amb grups NO dependrà de la disponibilitat d'hidrògens en posició orto, meta i para. Una búsqueda de distàncies H···O menors o iguals que 3.8Å [21] en els conjunts FM i AFM obté 364 contactes $C(sp^3)$-H···ON i 102 contactes $C(sp^2)$-H···ON (TAULA 4.2). En la TAULA 4.2 també s'indica la proporció FM/AFM per a cada tipus de contacte: dels 364 contactes $C(sp^3)$-H···ON, un 43% pertanyen al conjunt FM i un 57% a l'AFM. Aquesta proporció és molt similar al percentatge de grups $C(sp^3)$-H amb possibilitat d'establir contactes intermoleculars amb grups NO donat anteriorment: 49% (FM) vs. 51% (AFM). De la mateixa manera, les proporcions de contactes $C(sp^2)$-H···ON en posició orto, meta i para també es corresponen amb el percentatge de grups $C(sp^2)$-H disponibles en posicitó orto, meta i para.

Podem tenir una idea de la distribució d'aquests contactes en l'espai observant els scattergrames de les FIGURES 4.8 i 4.9, els quals representen els valors dels paràmetres D, A_1 i A_2 en contactes C-H···O-N trobats en els conjunts FM i AFM. Tot i que el número de contactes en aquestes FIGURES no és prou gran com per permetre generalitzacions, els contactes C-H···O-N estan distribuïts de manera similar en ambdós conjunts, dins dels intervals 80-180° pels angles i 2.2-3.8Å per les distàncies [21]. S'observa el mateix tipus de comportament quan es grafiquen altres parells de paràmetres. Així doncs, es pot concloure que *no s'han trobat diferències en la distribució geomètrica de contactes C-H···ON en els conjunts FM i AFM*.

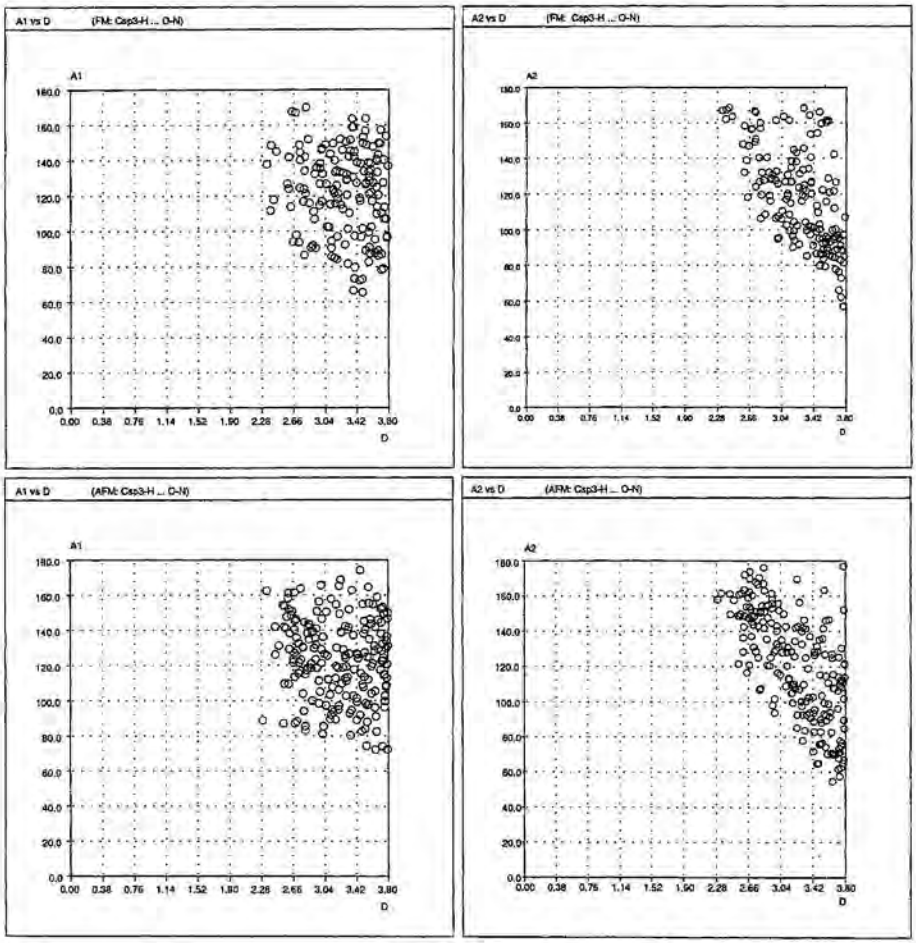

FIGURA 4.8.- Scattergrames de D vs. A_1 i D vs. A_2 per contactes $C(sp^3)$-H···ON dels conjunts FM (inferior) i AFM (superior).

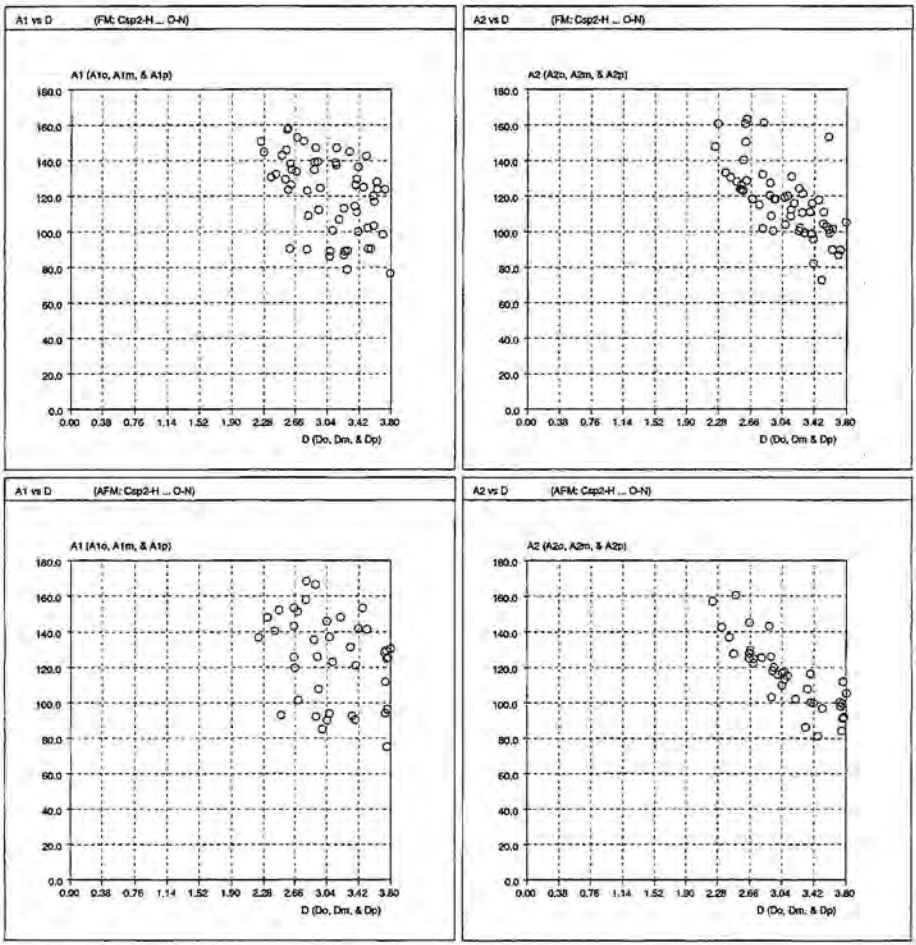

FIGURA 4.9.- Scattergrames de D vs. A_1 i D vs. A_2 per contactes $C(sp^2)$-H···ON en orto, meta i para dels conjunts FM (inferior) i AFM (superior).

4.4. CONCLUSIONS.

La nostra anàlisi indica que estadísticament no hi ha diferències significants en la disposició relativa dels contactes NO···ON i C-H···O-N que s'estableixen en els cristalls FM i AFM. Aquesta observació experimental és consistent amb el fet que l'empaquetament de radicals α-nitronil nitròxid està dirigit per les mateixes forces intermoleculars en cristalls FM i AFM. Així doncs, no serà possible determinar la naturalesa (ferro- o antiferromagnètica) de les interaccions magnèticament dominants en un cristall amb únicament l'estudi de la geometria d'un sol tipus de contacte intermolecular. Aquesta afirmació trenca amb algunes idees molt exteses, com per exemple la d'associar el caràcter magnètic dominant d'un cristall amb la presència de distàncies curtes NO···ON. A més, també s'ha de concloure que es necessiten sis paràmetres per tal de representar NO···ON; de manera que l'ús de tres o dos paràmetres geomètrics en buscar relacions magneto-estructurals no és vàlid.

Ara bé, si els cristalls de la base de dades FM (AFM) han de tenir les interaccions dominants d'aquesta base de dades, i aquestes interaccions clarament depenen de l'ordenament geomètric relatiu dels radicals, per què no es veuen aquestes diferències en l'anàlisi estadística prèvia ? Hi ha dues respostes diferents. En primer lloc, el model de McConnell-I pot no ser vàlid i podria ser una simplificació massa aproximada del mecanisme operatiu experimental [22]. I en segon lloc, podria ser que en examinar els contactes intermoleculars individualment, s'hagi assumit que el magnetisme en aquests sòlids està associat a la posició relativa d'un sol tipus de contacte, mentre que les interaccions intermoleculars experimentals són col.lectives, és a dir, associades a la disposició relativa de *tots* els grups funcionals magnèticament actius. Aquesta segona idea es pot il.lustrar mirant les diferències en els ordenaments de la FIGURA 4.4 : les orientacions relatives dels contactes NO···ON no són prou diferents en aquests ordenaments geomètrics, però la disposició geomètrica de les molècules i de *tots* els seus grups funcionals sí és molt diferent. Aquesta anàlisi, però, no pot determinar quina de les dues respostes és la correcta i caldrà dur a terme altres estudis per tal de determinar-la. Alguns d'aquests estudis es basen en la búsqueda de similaritats en els ordenaments presents en cristalls que tenen propietats magnètiques semblants, mentre que d'altres estan dirigits a entendre el fonament teòric del model de McConnell-I [23].

BIBLIOGRAFIA I NOTES.

[1] Si la susceptibilitat magnètica mostra la típica signatura de la presència d'interaccions ferro- i antiferromagnètiques que estan competint, es considera que una d'elles és dominant només quan la seva força —deduïda a partir de l'ajust de les dades magnètiques a diferents models magnètics— és, com a mínim, un ordre de magnitud més gran que la de l'altra interacció. S'han descartat, per tant, les estructures de tots aquells cristalls en què les magnituds són comparables.

[2] En alguns casos la susceptibilitat magnètica només es pot mesurar fins a 4K.

[3] Els 23 cristalls ferromagnètics seleccionats (identificats amb els seus refcodes) són : 0003QN: T. Sugano, M. Tamura, M. Kinoshita, Y. Sakai, Y. Ohashi, *Chem. Phys. Lett.* **1992**, *200*, 235; 000MPY: F. Lanfranc de Panthou, PhD Thesis, Univ. J. Fourier Grenoble I (**1994**); 000PPY: K. Awaga, T. Inabe, Y. Maruyama, *Chem. Phys. Lett.* **1992**, *190*, 349; 00DPNP: Prof. M. Kinoshita, unpublished results; 00GPNP: P. Turek, K. Nozawa, D. Shiomi, K. Awaga, T. Inabe, Y. Maruyama, M. Kinoshita, *Chem. Phys. Lett.* **1991**, *180*, 327; 0PBRPH: Y. Hosokoshi, PhD Thesis, Univ. of Tokyo (**1995**); MACOPY: F.M. Romero, R. Ziessel, A. De Cian, J. Fischer, P. Turek, *New J. Chem.* **1996**, *20*, 919; MMEPYB: K. Awaga, T. Inabe, Y. Maruyama, T. Nakamura, M. Matsumoto, *Chem. Phys. Lett.* **1992**, *195*, 21; MMEPYC: K. Awaga, T. Okuno, A. Yamaguchi, M. Hasegawa, T. Inabe, Y. Maruyama, N. Wada, *Phys. Rev. B* **1994**, *49*, 3975; HAFXOB: E. Hernández, M. Mas, E. Molins, C. Rovira, J. Veciana, *Angew. Chem., Int. Ed. Engl.* **1993**, *32*, 882; KAXHAS: K. Awaga, T. Inabe, U. Nagashima, Y. Maruyama, *J. Chem. Soc., Chem. Commun.* **1989**, 1617; LICMIT: T. Sugawara, M.-M. Matsushita, A. Izuoka, N. Wada, N. Takeda, M. Ishikawa, *J. Chem. Soc., Chem. Commun.* **1994**, 1723; PEFMES: H. Wang, D. Zhang, M. Wan, D. Zhu, *Solid State Commun.* **1993**, *85*, 685; PEYPUA: F. Lanfranc de Panthou, D. Luneau, J. Laugier, P. Rey, *J. Am. Chem. Soc.* **1993**, *115*, 9095; YISCEI: L. Angeloni, A. Caneschi, L. David, A. Fabretti, F. Ferraro, D. Gatteschi, A. le Lirzin, R. Sessoli, *J. Mater. Chem.* **1994**, *4*, 1047; YISCOS: L. Angeloni, A. Caneschi, L. David, A. Fabretti, F. Ferraro, D. Gatteschi, A. le Lirzin, R. Sessoli, *J. Mater. Chem.* **1994**, *4*, 1047; YISNIX: Y. Hosokoshi, M. Tamura, M. Kinoshita, H. Sawa, R. Kato, Y. Fujiwara, Y. Ueda, *J. Mater. Chem.* **1994**, *4*, 1219; YIWSEC: K. Awaga, A. Yamaguchi, T. Okuno, T. Inabe, T. Nakamura, M. Matsumoto, Y. Maruyama, *J. Mater. Chem.* **1994**, *4*, 1377; YODBUO: Y. Hosokoshi, M. Tamura, H. Sawa, R. Kato, M. Kinoshita, *J. Mater. Chem.* **1995**, *5*, 41; YOMYII: J. Cirujeda, M. Mas, E. Molins, F. Lanfranc de Panthou, J. Laugier, J. Geun Park, C. Paulsen, P. Rey, C. Rovira, J. Veciana, *J. Chem. Soc., Chem. Commun.* **1995**, 709; YUJNEW10: A. Caneschi, F. Ferraro, D. Gatteschi, A. le Lirzin, E. Rentschler, *Inorg. Chim. Acta* **1995**, *235*, 159; YULPOK: T. Akita, Y. Mazaki, K. Kobayashi, N. Koga, H. Iwamura, *J. Org. Chem.* **1995**, *60*, 2092; ZORHIX: A. Lang, Y. Pei, L. Ouahab, O. Kahn, *Adv. Mater.* **1996**, *8*, 60.

[4] Els 24 cristalls antiferromagnètics seleccionats (identificats amb els seus refcodes) són : 0000AH: Y. Hosokoshi, PhD Thesis, Univ. of Tokyo (**1995**); 0000BR: Y. Hosokoshi, PhD Thesis, Univ. of Tokyo (**1995**); 000F5P: Y. Hosokoshi, PhD Thesis, Univ. of Tokyo (**1995**); 003CLP: O. Jürgens, J. Cirujeda, M. Mas, I. Mata, A. Cabrero, J. Vidal-Gancedo, C. Rovira, E. Molins, J. Veciana, *J. Mater. Chem.* **1997**, *7*, 1723; 00NNMA: E. Hernández, PhD Thesis, Univ. of Barcelona (**1995**); 00PCLP: Y. Hosokoshi, PhD Thesis, Univ. of Tokyo (**1995**); 0PCF3P: Y. Hosokoshi, PhD Thesis, Univ. of Tokyo (**1995**); 2CLPNN: O. Jürgens, J. Cirujeda, M. Mas, I. Mata, A. Cabrero, J. Vidal-Gancedo, C. Rovira, E. Molins, J. Veciana, *J. Mater. Chem.* **1997**, *7*, 1723; 2N5OHP: J. Cirujeda, PhD Thesis, Univ. Ramon Llull (**1997**); 3CL4OH: O. Jürgens, J. Cirujeda, M. Mas, I. Mata, A. Cabrero, J. Vidal-Gancedo, C. Rovira, E. Molins, J. Veciana, *J. Mater. Chem.* **1997**, *7*, 1723; 5CL2OH: O. Jürgens, J. Cirujeda, M. Mas, I. Mata, A. Cabrero, J. Vidal-Gancedo, C. Rovira, E. Molins, J. Veciana, *J. Mater. Chem. i***1997**, *7*, 1723; LASCAJ: D. Zhang, W. Zhou, D. Zhu, *Solid State Commun.* **1993**, *86*, 291; LEMMAR: D. Luneau, J. Laugier, P. Rey, G. Ulrich, R. Ziessel, P. Legoll, M. Drillon, *J. Chem. Soc., Chem. Commun.* **1994**, 741; PEFMAO: H. Wang, D. Zhang, M. Wan, D. Zhu, *Solid State Commun.* **1993**, *85*, 685; SUKBIJ: A. Caneschi, P. Chiesi, L. David, F. Ferraro, D. Gatteschi, R. Sessoli, *Inorg. Chem.* **1993**, *32*, 1445; SUKBOP: A. Caneschi, P. Chiesi, L. David, F. Ferraro, D. Gatteschi, R. Sessoli, *Inorg. Chem.* **1993**, *32*, 1445; WILVIW10: K. Awaga, A. Yamaguchi, T. Okuno, T. Inabe, T. Nakamura, M. Matsumoto, Y. Maruyama, *J. Mater. Chem.* **1994**, *4*, 1377; YISCIM: L. Angeloni, A. Caneschi, L. David, A. Fabretti, F.

Ferraro, D. Gatteschi, A. le Lirzin, R. Sessoli, *J. Mater. Chem.* **1994**, *4*, 1047; YOMYOO: J. Cirujeda, M. Mas, E. Molins, F. Lanfranc de Panthou, J. Laugier, J. Geun Park, C. Paulsen, P. Rey, C. Rovira, J. Veciana, *J. Chem. Soc., Chem. Commun.* **1995**, 709; YOMYUU: J. Cirujeda, M. Mas, E. Molins, F. Lanfranc de Panthou, J. Laugier, J. Geun Park, C. Paulsen, P. Rey, C. Rovira, J. Veciana, *J. Chem. Soc., Chem. Commun.* **1995**, 709; YOXMAZ: T. Mitsumori, K. Inoue, N. Koga, H. Iwamura, *J. Am. Chem. Soc.* **1995**, *117*, 2467; YOXMED: T. Mitsumori, K. Inoue, N. Koga, H. Iwamura, *J. Am. Chem. Soc.* **1995**, *117*, 2467; YULPAW: T. Akita, Y. Mazaki, K. Kobayashi, N. Koga, H. Iwamura, *J. Org. Chem.* **1995**, *60*, 2092; ZIPTAT: A. Caneschi, D. Gatteschi, E. Rentschler, R. Sessoli, *Gazzetta Chim. Ital.* **1995**, *125*, 283.

[5] (a) F.-H. Allen, S. Bellard, M.-D. Brice, B.-A. Cartwright, A. Doubleday, H. Higgs, T. Hummelink, B.-G. Hummelink-Peters, O. Kennard, W.D.S. Motherwell, J.-R. Rodgers, D.-G. Watson, *Acta Crystallogr.* **1979**, *B35*, 2331.

[6] (a) A.-D. Mighell, V.-L. Himes, J.-R. Rodgers, *Acta Cryst.* **1983**, *A39*, 737-740; (b) A.J.C. Wilson, *Acta Cryst.* **1988**, *A44*, 715-724.

[7] Aquest tipus de transicions de primer-ordre generalment produeixen canvis abruptes en les gràfiques χT vs. T, els quals es poden detectar amb facilitat.

[8] Aquest fet ha estat molt ben documentat per a cristalls superconductors orgànics, les temperatures crítiques dels quals són també molt més baixes que la temperatura ambient. Consultar, per exemple, J.-M. Williams, J.-R. Ferraro, R.-J. Thorn, K.-D. Carlson, U. Geiser, H.-H. Wang, A.-M. Kini, M.-H. Whangbo, "*Organic Superconductors*", Prentice Hall, Englewood Cliffs, **1992**. El magnetisme és una propietat física diferent que la superconductivitat, tot i que ambdós estan íntimament relacionats amb l'ordenament relatiu de les molècules en el cristall. Les propietats d'empaquetament de sòlids moleculars i, en particular, la seva variació amb la temperatura, estan determinades pels contactes intermoleculars, i són independents de les propietats físiques electròniques presents en el cristall.

[9] E.-R. Malinowski, D.-G. Howery, "*Factor Analysis in Chemistry*", Wiley Interscience: New York, **1980**.

[10] B.-S. Everitt, "*Cluster Analysis*", 3rd edition, Edward Arnold: London, **1993**.

[11] Les desviacions estàndards de les distàncies atòmiques i angles d'enllaç d'aquest anell de cinc membres són més petites que el 2% de les seves respectives magnituds. Consultar: J. Cirujeda, Tesi doctoral, Univ. Ramon Llull, Barcelona, **1997**.

[12] Per exemple, consultar: (a) K. Awaga, T. Inabe, Y. Maruyama, T. Nakamura, M. Matsumoto, *Chem. Phys. Letters* **1992**, *195*, 21-24; (b) K. Awaga, T. Inabe, T. Nakamura, M. Matsumoto, Y. Maruyama, *Mol. Cryst. Liq. Cryst.* **1993**, *232*, 69-78; (c) K. Awaga, T. Okuno, A. Yamaguchi, M. Hasegawa, T. Inabe, Y. Maruyama, N. Wada, *Phys. Rev. B* **1994**, *49*, 3975-3981; (d) K. Awaga, A. Yamaguchi, T. Okuno, T. Inabe, T. Nakamura, M. Matsumoto, Y. Maruyama, *J. Mater. Chem.* **1994**, *4*, 1377-1385; (e) K. Awaga, T. Okuno, A. Yamaguchi, M. Hasegawa, T. Inabe, Y. Maruyama, N. Wada, *Synth. Met.* **1995**, *71*, 1807-1808.

[13] (a) H.-M. McConnell, *J. Chem. Phys.* **1963**, *39*, 1910; (b) C. Kollmar, O. Kahn, *Acc. Chem. Res.* **1993**, 26, 259. (c) K. Yamaguchi, Y. Toyoda, T. Fueno, *Chem. Phys. Lett.* **1989**, 159, 459. (d) K. Yoshizawa, R. Hoffmann, *J. Am. Chem. Soc.* **1995**, *117*, 6921. (e) P. M. Lahti, *ACS Symp. Series*, # 644, (Eds. M. M. Turnbull, T. Sugimoto, L. K. Thompson), **1996**, Ch. 14.

[14] S'ha demostrat experimentalment i teòrica que la major part de la densitat d'spin està localitzada en el grup ONCNO (el grup NO és portador de densitat d'spin positiva). Consultar, per exemple, A. Zheludev, V. Barone, M. Bonnet, B. Delley, A. Grand, E. Ressouche, P. Rey, R. Subra, J. Schweizer, *J. Am. Chem. Soc.* **1994**, *116*, 2019-2027; J.-J. Novoa, F. Mota, J. Veciana, J. Cirujeda, *Mol. Cryst. Liq. Cryst.* **1995**, *271*, 79-90.

[15] Les desviacions estàndards dels paràmetres geomètrics per als conjunts FM i AFM són també similars. Els seus valors són més grans per als angles que per a la distància D i, d'entre els angles, són més grans per als paràmetres T_i que per als A_i. Aquesta tendència és només conseqüència de la forma suau de les corbes de l'energia potencial dels dihedres T_i, comparada amb la dels angles A_i i dels stretchings D.

[16] R. Barlow, "*Statistics*", John Wiley and Sons: Chichester, **1989**.

[17] La distància entre dos elements i, j en l'espai definit per sis coordenades ve donada per

$$d_{ij} = \sum_{k=1}^{6} \left[V(k)_i^2 - V(k)_j^2 \right]^{1/2}$$

[18] (a) M. Deumal, J. Cirujeda, , J. Veciana, M. Kinoshita, Y. Hosokoshi, J.J. Novoa, *Chem. Phys. Lett.* **1997**, 265, 190. (b) J.J. Novoa, M. Deumal *Mol. Cryst. Liq. Cryst.*, **1997**, *305*, 143. (c) J.J. Novoa, M. Deumal, M. Kinoshita, Y. Hosokoshi, J. Veciana, J. Cirujeda, *Mol. Cryst. Liq. Cryst.*, **1997**, *305*, 129.

[19] Consultar: (a) J. Veciana, J. Cirujeda, C. Rovira, J. Vidal-Gancedo, *Adv. Mater.* **1995**, *7*, 221. (b) J. Cirujeda, E. Hernàndez, C. Rovira, P. Turek, J. Veciana, *New Organic Magnetic Materials. The Use of Hydrogen Bonds as a Crystalline Design Element of Organic Molecular Solids with Intermolecular Ferromagnetic Interactions*, pp 262-272, in "*New Organic Materials*", (Eds.: C. Seoane, N. Martin); Universidad Complutense de Madrid: Madrid, **1994**. (c) J. Cirujeda, E. Hernàndez, C. Rovira, J.-L. Stanger, P. Turek, J. Veciana, *J. Mater. Chem.* **1995**, *5*, 243-252. (d) J. Cirujeda, E. Hernàndez, C. Rovira, J.-L. Stanger, P. Turek, J. Veciana, *J. Mater. Chem.* **1995**, *5*, 243-252. (e) J. Cirujeda, C. Rovira, J.-L. Stanger, P. Turek, J. Veciana, *The Self-Assembly of Hydroxylated Phenyl a-Phenyl Nitronyl Nitroxide Radicals*, pp 219-248, in "*Magnetism. A Supramolecular Function*"; (Ed.: O. Kahn); Kluwer Academic Publishers: Amsterdam, **1996**. (f) J. Cirujeda, E. Hernàndez, F. Lanfranc de Panthou, J. Laugier, M. Mas, E. Molins, C. Rovira, J.-J. Novoa, P. Rey, J. Veciana, *Mol. Cryst. Liq. Cryst.* **1995**, *271*, 1-12.

[20] La densitat d'spin d'un H metílic és negativa, mentre que la dels H d'un fenil enllaçat al C en α de l'anell de cinc membres alterna el seu signe, essent positiva per als H orto i para, i negativa per als meta. Consultar: (a) M.-S. Davis, K. Morokuma, R.-W. Kreilich, *J. Am. Chem. Soc.*, **1972**, *94*, 5588-5592. (b) J.-W. Neely, G.-F. Hatch, R.-W. Kreilich, *ibid*, **1974**, *96*, 652-656. (c) A. Zheludev, V. Barone, M. Bonnet, B. Delley, A. Grand, E. Ressouche, P. Rey, R. Subra, J. Schweizer, *ibid*, **1994**, *116*, 2019-2027. (d) Ref [19a].

[21] Un interval de distàncies típic en anàlisis recents d'enllaços d'hidrogen C-H...O. Consultar: G.A. Jeffrey, W. Saenger, *"Hydrogen Bonding in Biological Structures"*, Springer-Verlag, Berlin, **1991**.

[22] Un mecanisme alternatiu, basat en interaccions magnètiques dipol-dipol, ha estat proposat per tal d'explicar les interaccions magnètiques intermoleculars dèbils entre radicals orgànics (J.-S. Miller, A.-J. Epstein, *Angew. Chem. Int. Ed. Engl.* **1994**, *33*, 385-415). Aquest mecanisme podria explicar l'absència de diferències significants estadísticament en el cas de contactes NO···ON i C-H···O. Ara bé, alguns estudis indiquen que la magnitud de les interaccions dipolars magnètiques és molt més petita que la de les interaccions de bescanvi magnètiques (K. Takeda, K. Konishi, M. Tamura, M. Kinoshita, *Mol. Cryst. Liq. Cryst.*, **1995**, *273*, 57).

[23] M. Deumal, J.J. Novoa, M.J. Bearpark, P. Celani, M. Olivucci, M.A. Robb, *J. Phys. Chem.* **1998** (en premsa).

CAPÍTOL 5:

Determinació de l'Estabilitat Singlet / Triplet a nivell Ab Initio

L'ús de sistemes simples amb unes interaccions magnètiques *esperades* ens servirà per a comprovar, des d'una nova perspectiva, la validesa del model de McConnell-I. D'altra banda, el càlcul de l'estabilitat singlet / triplet en el dímer de 3-OHPNN —el qual ha estat aïllat experimentalment— ens permetrà comprovar la idoneïtat del mètode DFT en reproduir la constant d'acoblament magnètic J. Finalment, es proposaran diferents sistemes model per estudiar els dímers dels cristalls que presenten els contactes O···O més curts (obtinguts amb l'anàlisi estadística del Capítol 4). Amb aquests càlculs —realitzats usant Gaussian 94—volem fer una estimació de la J d'aquests dos dímers.

5.1. Càlculs Ab Initio de Sistemes Simples.

Per tal de comprovar la validesa del model de McConnell-I [1], hem estudiat la diferència d'energies d'alt spin - baix spin en diferents orientacions de dos dímers molt simples, el dímer d'H_2NO i el sistema radicalari metil - al.lil. El dímer d'H_2NO ha estat seleccionat perquè és un prototipus senzill per a estudiar les interaccions magnètiques entre dos grups nitronils. Per tant, les conclusions obtingudes a partir d'aquest estudi són d'interès per tal d'entendre les interaccions magnètiques en els cristalls α-nitronil nitròxids. El segon dímer, metil - al.lil, ha estat escollit perquè va ser un dels sistemes model prèviament seleccionats per a provar la validesa del model de McConnell-I. La Figura 5.1 esquematitza qualitativament la distribució d'spin per als fragments aïllats, calculada a nivell ab initio CASSCF [2] amb bases exteses (la més petita era una base 6-31+G(d)).

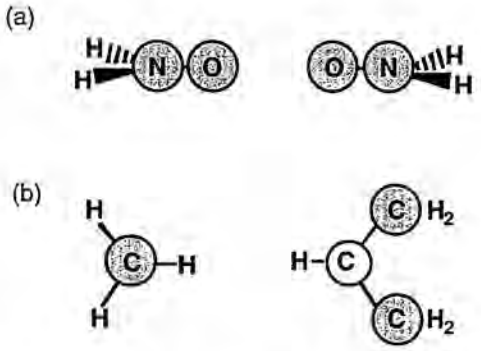

Figura 5.1.- Densitats d'spin dels fragments aïllats en (a) el dímer d'H_2NO, i (b) els radicals metil i al.lil (àtoms ombrejats: densitat d'spin positiva, àtoms no-ombrejats: negativa)

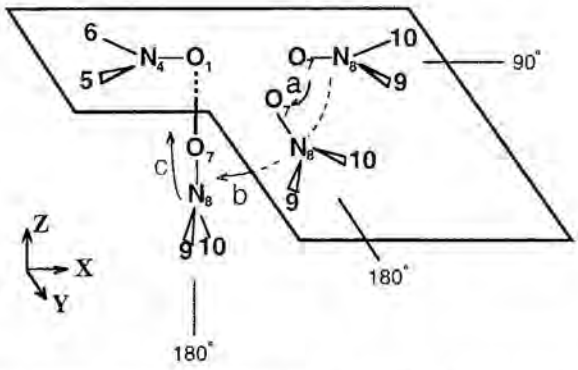

FIGURA 5.2.- Scans duts a terme amb el dímer d'H_2NO. Les dues configuracions extremes estan marcades com a 90° i 180°.

5.1.1.- El dímer d'H_2NO.

S'ha avaluat la diferència d'energies singlet - triplet per al dímer d'H_2NO mitjançant tres scans angulars, tal com s'indica en la FIGURA 5.2. En el primer scan (a) es mantenen tots els àtoms en el mateix pla XY (pla ombrejat en la FIGURA), mentre que en els altres dos traiem una de les molècules fora d'aquest pla. L'scan (b) s'encarrega d'explorar el pla XZ, mentre que el (c) l'YZ. En tots els casos el contacte més curt és la distància O···O, la qual està fixada a 3Å. Hem seleccionat aquests ordenaments geomètrics perquè són característics de moltes orientacions NO···ON que es troben en alguns dels cristalls α-nitronil nitròxids. Segons el model de McConnell-I, en tots els punts dels scans estem solapant àtoms amb densitats d'spin del mateix signe (FIGURA 5.1a). Així doncs, aquest model prediu que l'estat d'spin més estable hauria de ser sempre singlet (l'estat antiferromagnètic).

5.1.1.1.- Selecció del mètode i la base.

Abans, però, de fer aquests tres scans, s'han realitzat càlculs preliminars per tal de seleccionar l'espai actiu i la base més adequats per a descriure el sistema format pel dímer d'H_2NO. En primer lloc, s'ha dut a terme el càlcul de la diferència d'energia singlet / triplet, ΔE(S-T), a nivell CASSCF/3-21G amb diferents espais actius per al cas de l'scan XY (FIGURA 5.2, scan a). En la TAULA 5.1 es donen els valors de ΔE(S-T) per a un interval de 179-139°. En aquesta TAULA es veu com amb tots quatre espais actius s'obtenen valors molt similars de ΔE(S-T). A més, si comparem els elements diagonals de la matriu densitat (TAULA 5.2) —ens dóna la densitat electrònica en els orbitals actius— veiem que la introducció d'un espai actiu més gran no significa una major correlació entre electrons de

TAULA 5.1.- Diferències d'energia singlet / triplet, $\Delta E(S-T)$, a nivell CASSCF/3-21G amb diferents espais actius (scan XY). Totes les diferències d'energia en cm^{-1}.

angle d'scan	CAS (2, 2)	CAS (6, 4)	CAS (6, 6)	CAS (10, 8)
179.	-0.2	-0.2	-0.2	-0.0
169.	-1.5	-1.5	-1.5	-1.3
159.	-2.2	-2.3	-2.3	-2.1
149.	-2.6	-2.7	-2.7	-2.6
139.	-2.8	-3.0	-2.9	-2.8

TAULA 5.2.- Elements diagonals de la matriu densitat electrònica per als estats singlet, S, i triplet, T per als angles d'scan XY 179° i 139° (entre parèntesi s'especifica l'espai actiu; correlació π en **negreta**, correlació σ en *cursiva*).

angle d'scan XY = 179°

S (2, 2)	T (2, 2)	S (6, 4)	T (6, 4)	S (6, 6)	T (6, 6)	S(10, 8)	T(10, 8)
1.00583	**1.00000**	**1.99999**	**1.99999**	*1.97550*	*1.97552*	*1.96472*	*1.96474*
0.99417	**1.00000**	**2.00000**	**1.99999**	*1.97552*	*1.97554*	*1.96479*	*1.96481*
		1.00602	**1.00001**	**1.00595**	**1.00000**	**1.98370**	**1.98371**
		0.99400	**1.00001**	**0.99405**	**1.00000**	**1.98369**	**1.98369**
				0.02447	*0.02445*	**1.02091**	**1.01544**
				0.02451	*0.02449*	**1.01008**	**1.01552**
						0.03601	*0.03599*
						0.03609	*0.03607*

angle d'scan XY = 139°

S (2, 2)	T (2, 2)	S (6, 4)	T (6, 4)	S (6, 6)	T (6, 6)	S(10, 8)	T(10, 8)
0.98875	**1.00000**	**1.99998**	**1.99998**	*1.97541*	*1.97541*	*1.96482*	*1.96480*
1.01126	**1.00000**	**1.99998**	**1.99998**	*1.98385*	*1.98385*	*1.96476*	*1.96478*
		1.01179	**1.00002**	**1.01162**	**1.00000**	**1.98390**	**1.98390**
		0.98825	**1.00002**	**0.98838**	**0.99999**	**1.98389**	**1.98389**
				0.02459	*0.02459*	**1.02707**	**1.01530**
				0.01615	*0.01615*	**1.00354**	**1.01531**
						0.03597	*0.03597*
						0.03605	*0.03606*

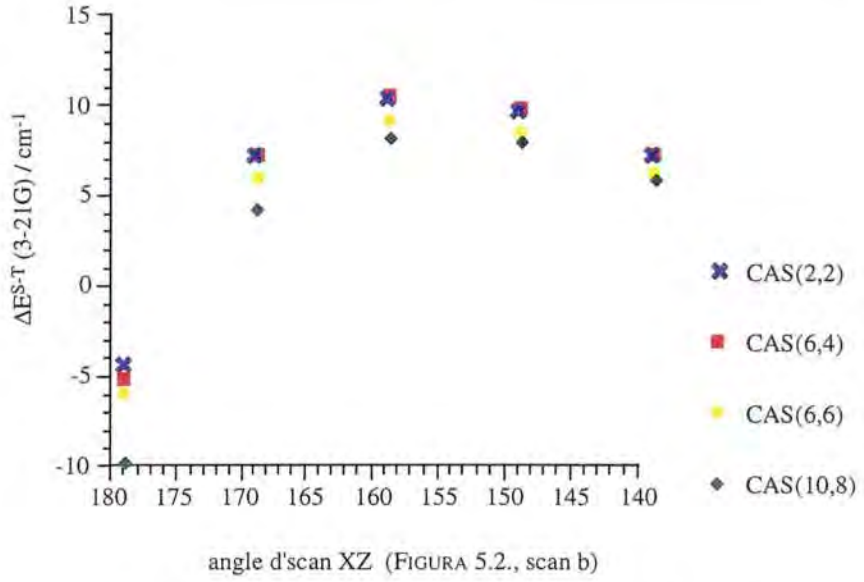

FIGURA 5.3.- Diferències d'energia singlet / triplet, ΔE(S-T), a nivell CASSCF/3-21G usant diferents espais actius en l'interval 180°-140°.

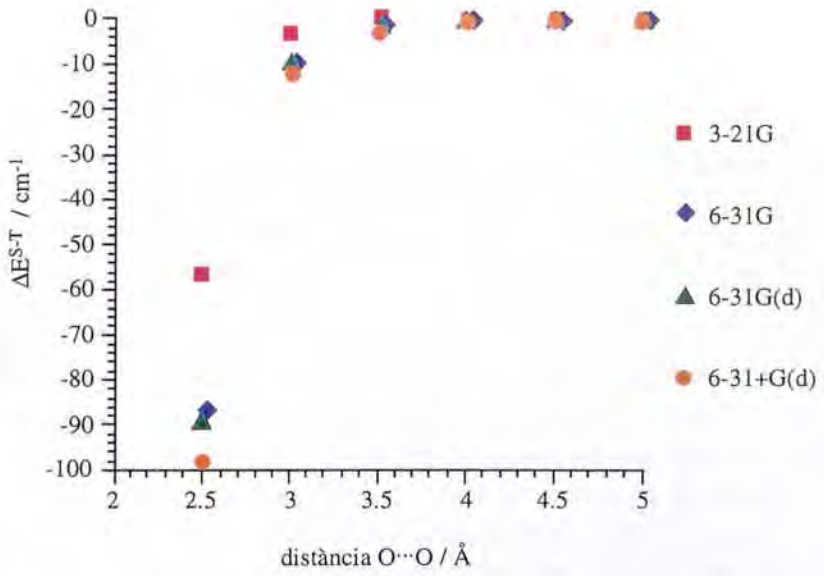

FIGURA 5.4.- Diferències d'energia singlet / triplet, ΔE(S-T), a nivell CAS (2, 2) usant bases de diferent qualitat en l'interval de distàncies 2-5Å.

tipus π (en **negreta**) o de tipus σ (en *cursiva*). Els mateixos càlculs realitzats per a l'scan XZ (FIGURA 5.2, scan b) es mostren gràficament en la FIGURA 5.3. Altre cop, s'observa una clara concordança de resultats, independentment de l'espai actiu amb què es treballa. En fer els mateixos càlculs preliminars amb el tercer scan YZ (FIGURA 5.2, scan c) s'obté un resultat similar. Així doncs, un petit (2, 2) format per dos orbitals i dos electrons —un electró desaparellat provinent de cada un dels fragments i el seu respectiu orbital π on està localitzat— sembla capaç de descriure el sistema format pel dímer d'H_2NO.

Un cop s'ha seleccionat l'espai actiu més adequat només queda determinar la base que s'usarà en tots tres scans. Amb aquesta finalitat, s'han fet scans variant la distància O···O entre grups H_2NO amb bases de diferent qualitat (FIGURA 5.4). El resultat d'aquests scans és que per a distàncies inferiors a 3.0Å és necessari introduir funcions difoses i de polarització per tal de donar una bona descripció del sistema (6-31+G(d)). També s'observa que per a distàncies més grans que 4.0Å la diferència d'energia tendeix ràpidament a zero. En l'interval de 3.0 a 4.0Å, però, s'observa que bases de qualitat 6-31G(d) i 6-31+G(d) es comporten similarment (fins i tot, una base de qualitat 6-31G sembla donar resultats adequats). Donat que el nostre objectiu final és fer una estimació de constants d'acoblament J d'α-nitronil nitròxids i que en l'anàlisi estadística del Capítol 4 no s'han obtingut distàncies O···O per sota de 3Å, tots tres scans es duran a terme fixant la distància O···O a 3Å. Per a càlculs a aquesta distància hem seleccionat una base de qualitat 6-31+G(d), ja que el sistema és prou petit com per poder fer càlculs CASSCF amb una base d'aquesta qualitat.

5.1.1.2.- Resultats a nivell CASSCF / 6-31+G(d).

Hem calculat la diferència d'energies singlet / triplet usant el mètode CASSCF i la base 6-31+G(d). L'espai actiu CAS és un petit (2, 2) format per dos orbitals i dos electrons: un electró desaparellat provinent de cada un dels fragments i el seu respectiu orbital π on està localitzat. La diferència d'energia singlet / triplet obtinguda es mostra en la FIGURA 5.5. En aquesta FIGURA mostrem juntament amb l'angle d'scan, la conformació geomètrica dels dímers en alguns punts representatius de la corba. S'observa que, quan fem l'scan en el pla XY (FIGURA 5.2, scan a), l'estat fonamental és singlet: la interacció serà, per tant, antiferromagnètica en concordança amb el que prediu el model de McConnell-I. També, en l'scan YZ (FIGURA 5.2, scan c) observem, aproximadament, el mateix comportament. Ara bé, aquest no és el cas de l'scan en el pla XZ (FIGURA 5.2, scan b). Es veu clarament que hi ha una regió on el dímer es comporta ferromagnèticament, en contra de les prediccions de McConnell-I. L'interval que abasta aquesta regió és des d'uns 119° a 175°, amb un "màxim ferromagnètic" al voltant d'un angle d'scan de 149°.

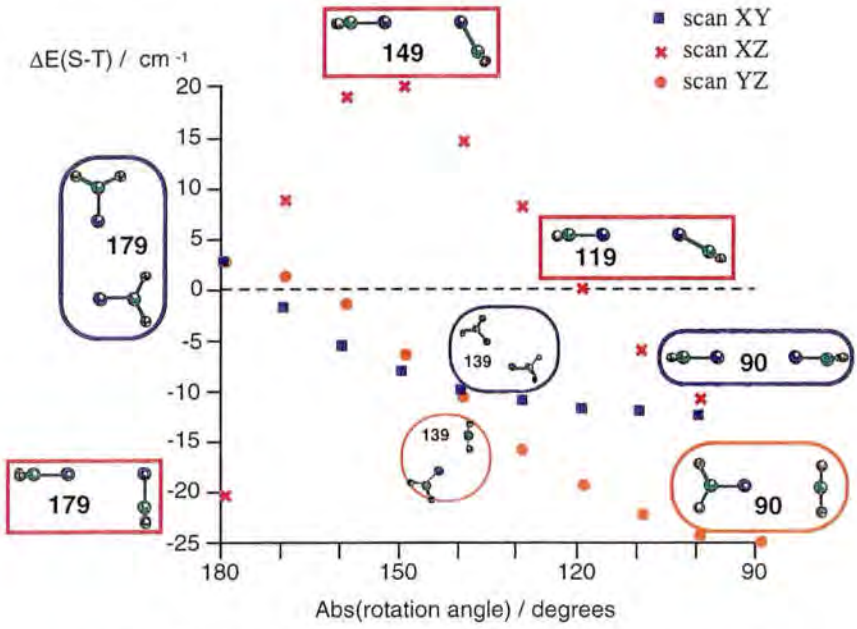

FIGURA 5.5.- Variació de la diferència d'energia singlet / triplet en els scans duts a terme amb el dímer d'H_2NO.

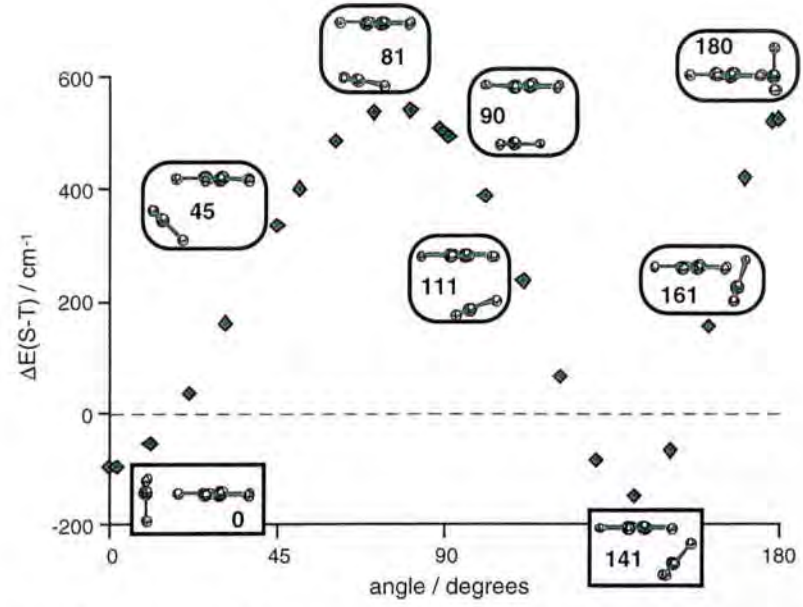

FIGURA 5.6.- Variació de la diferència d'energia singlet / triplet en els scans de l'angle $H\text{-}C_{al.lil}\cdots C_{metil}$ amb el dímer metil - al.lil.

5.1.2.- El sistema metil - al.lil.

Per comprovar si les limitacions en la predicció del magnetisme per al dímer d'H_2NO segons McConnell-I són degudes al comportament excepcional d'aquest dímer o bé a mancances del model, hem realitzat un estudi similar amb el dímer metil - al.lil. En aquest sistema hem avaluat la diferència d'energia singlet / triplet en fer rotar l'àtom de C metílic (C_{metil}) entorn l'àtom de C central ($C_{al.lil}$) del fragment al.lílic, forçant que C_{metil} estigui en el pla C_s perpendicular al pla C-C-C de l'al.lil (mirar FIGURA 5.4 per algunes instàntanees). L'angle de variació és l'H-$C_{al.lil}$···C_{metil}. A 0°, el C_{metil} està en el pla C-C-C de l'al.lil, situat a l'extrem H de l'eix C_{2v}, que passa a través de l'àtom de C central ($C_{al.lil}$) de l'al.lil i de l'àtom d'H enllaçat a ell. A 90°, el metil i l'al.lil estan situats en plans paral.lels. A 180°, el C_{metil} torna a situar-se en el pla C-C-C al.lílic, però a l'extrem C de l'eix C_{2v}. La distància $C_{al.lil}$···C_{metil} es va fixar a 3Å. Tots els càlculs s'han realitzat a nivell CASSCF / 6-31G(d). L'espai actiu CAS és un (4, 4), per tal d'incloure tots els orbitals π i els electrons corresponents dels fragments aïllats metil i al.lil.

Segons el model de McConnell-I, l'estat fonamental en el cas H-$C_{al.lil}$···C_{metil} = 90° hauria de ser triplet (ferromagnètic); predicció que concorda amb les dades resultants ab initio per a aquesta orientació. Ara bé, l'estabilitat de l'estat triplet no hauria de canviar per variacions petites de l'angle H-$C_{al.lil}$···C_{metil} quan mantenim la distància constant (ja que les densitats d'spin dels àtoms no variaran). S'observa, però, que entorn 90° hi ha grans oscil.lacions de l'energia (tot i que el signe es conserva); fet que no hauria de tenir lloc d'acord amb el model de McConnell-I. En la FIGURA 5.6 es mostra, també, que entorn 141° hi ha la màxima estabilització de l'estat fonamental singlet per al sistema metil - al.lil com a conseqüència de possibles interaccions amb els C al.lílics dels extrems. Així doncs, el model de McConnell-I no prediu correctament el caràcter magnètic en certes regions de la superfície d'energia potencial del sistema metil - al.lil.

Es pot argumentar que les regions en què el model de McConnell-I fracassa estan fora del propòsit original de McConnell, qui va dissenyar el seu primer model per a interpretar el magnetisme en sistemes π-π. Ara bé, tal com s'ha vist amb anterioritat en el Capítol 3 [3], el seu èxit aparent en el cas π-π és conseqüència d'una cancel.lació fortuïta de termes associats a l'alta simetria del problema; situació que no es verifica en general. Hi ha prou motius, doncs, per pensar que McConnell-I no és un bon model per tal de dur a terme anàlisis de les propietats magnètiques de cristalls moleculars.

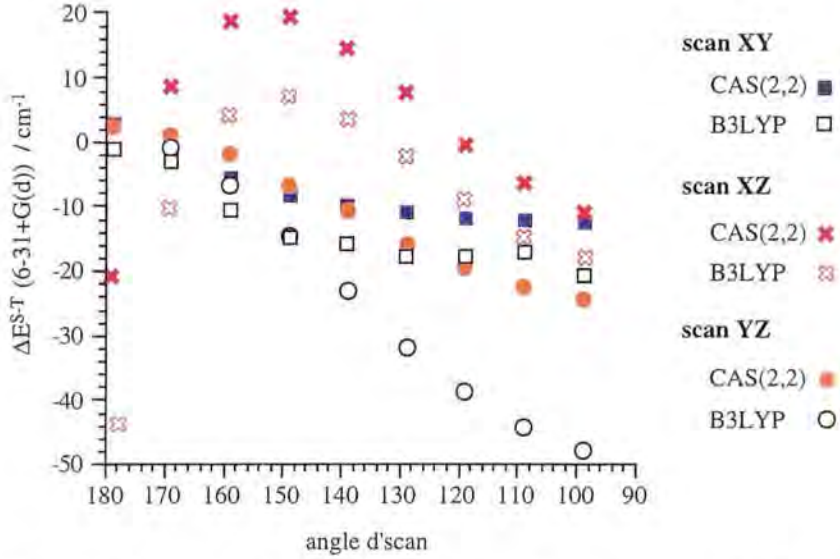

FIGURA 5.7.- Variació de la diferència d'energia singlet / triplet per als scans XY, XZ i YZ a nivell CASSCF i B3LYP *broken symmetry*.

5.1.3.- Comparació de resultats a nivell CASSCF i DFT.

Amb el sistema metil - al.lil, s'ha comprovat que les limitacions en la predicció del magnetisme per al dímer d'H_2NO segons McConnell-I no són degudes al comportament excepcional d'aquest dímer, sinó a mancances del model de McConnell-I. S'ha d'esmentar, també, que càlculs a nivell CASSCF no són massa costosos per a sistemes relativament petits, com els dímers d'H_2NO o metil - al.lil. Ara bé, el nostre objectiu és poder descriure adequadament sistemes reals, en els quals intervenen molts més àtoms. Un tractament CASSCF d'aquests sistemes seria massa car, de manera que cal buscar alternatives. Els mètodes DFT [4] constitueixen una clara alternativa per a calcular l'estabilitat relativa singlet / triplet. Cal, però, contrastar els resultats a nivell DFT amb dades CASSCF. Amb aquesta finalitat, s'han repetit els tres scans duts a terme amb el dímer d'H_2NO a nivell B3LYP *broken symmetry* [5] amb una base 6-31+G(d). La FIGURA 5.7 mostra com les dades a nivell CAS (2, 2) i B3LYP *broken symmetry* segueixen la mateixa tendència en tots tres scans. Això, ens permet concloure que el mètode B3LYP *broken symmetry* sembla ser adient per tal de calcular diferències d'energia singlet / triplet.

5.2. DETERMINACIÓ DE LA CONSTANT D'ACOBLAMENT MAGNÈTIC J PER AL DÍMER DEL 3-OHPNN.

5.2.1.- Determinació experimental del caràcter ferromagnètic o antiferromagnètic d'un cristall.

En tot cristall, l'existència d'un moment angular d'spin en les seves unitats moleculars juntament amb la possibilitat d'interacció entre elles dóna lloc als diferents tipus de comportaments magnètics que s'observen a nivell macroscòpic. En concret, si la interacció més estable és la que alinea paral.lelament tots els moments d'spin es parla de l'existència de ferromagnetisme, mentre que si l'ordenament més estable és antiparal.lel parlem d'antiferromagnetisme.

A nivell microscòpic, hi haurà, doncs, un acoblament entre els spins de les unitats constituents del cristall. Ara bé, cap mètode experimental és capaç d'estimar el valor d'aquests acoblaments microscòpics J_{ij} (definició en Capítol 3, equació (3.4)) ni tampoc de conèixer les direccions en què aquests acoblaments tenen lloc dins del cristall. Els mètodes experimentals únicament són capaços d'obtenir el valor promig dins d'un model d'interacció magnètica.

Experimentalment, només es pot mesurar com varia el magnetisme en funció de la temperatura. En dibuixar la corba χT vs. T, sabem que un material té interaccions ferromagnètiques dominants perquè χT augmenta en disminuir T; en canvi, si les interaccions dominants són antiferromagnètiques s'obté la tendència oposada (cal recordar que χ és la constant de proporcionalitat que relaciona la magnetització amb la intensitat del camp magnètic). El valor de la constant (o constants) d'acoblament magnètic J no s'obté directament amb cap experiment, sinó que és el resultat d'ajustar les dades experimentals de la corba χT vs. T a una sèrie de models establerts mitjançant el conegut mètode "d'assaig i error". El número d'aquests models és força gran, ja que depenen de la dimensionalitat d'spin (models d'Ising, XY i Heisenberg) i de la xarxa cristal.lina (model 1-, 2-, ó 3-dimensional). Així doncs, podrem obtenir més d'una constant d'acoblament magnètic J en funció de l'anisotropia del material; constants que en cap moment podrem relacionar amb les J_{ij} microscòpiques. Conseqüentment, en molts casos no es pot associar la J determinada experimentalment a un tipus de contacte intermolecular o intramolecular en qüestió. Aquest fet limita moltíssim el desenvolupament de mètodes i models teòrics microscòpics que siguin adequats per a reproduir els resultats experimentals en el camp del magnetisme molecular.

5.2.2.- Càlcul de la constant d'acoblament magnètic J a nivell DFT.

Actualment, les constants d'acoblament magnètic J s'estudien a nivell teòric des de dos punts de vista diferents. En primer lloc, per al càlcul de propietats termodinàmiques de xarxes infinites, s'han desenvolupat mètodes aproximats com l'expansió a alta temperatura de la funció de partició [6], la tècnica DMRG (*density matrix renormalization group approach*) [7] i simulacions Monte Carlo clàssiques (sistemes amb $S \geq 2$) [8] i quàntiques (sistemes amb $S < 2$) [9] de χT vs. T. Ara bé, d'entre aquestes tres tècniques proposades, només l'última és prou general i relativament fàcil d'implementar. D'altra banda, la segona manera d'enfocar l'estudi de J en cristalls és intuitiva i juga amb l'experiència de l'investigador. Es tracta de proposar els candidats que tindran una millor relació "control de l'empaquetament cristal.lí / pes magnètic dins del cristall a estudiar", i assumir que la J calculada en aquests candidats és la que es manifesta macroscòpicament. Aquesta assumpció serà més o menys aproximada depenent de les possibilitats de propagació de la interacció magnètica que s'ha proposat. Tal com ja s'ha dit en el Capítol 4, en la família dels α-nitronil nitròxids l'empaquetament està dominat energèticament i magnètica per contactes NO···ON i C-H···ON. Per tant, en aquesta família, un candidat raonable serà tot aquell dímer amb distàncies O···O i H···O prou curtes. Des del punt de vista metodològic, els mètodes DFT [4] han estat proposats com a tècniques adequades per al càlcul de les constants d'acoblament J. Ens interessa, per tant, trobar un sistema on poder comprovar la idoneïtat del DFT.

El candidat ideal és el dímer del 3-OHPNN perquè ha estat aïllat en dissolució. Aquest dímer es comporta ferromagnèticament ($J = 2.69 \pm 0.75$ cm^{-1}) [10a]. A més, s'ha comprovat que la seva geometria optimitzada és molt similar a la que presenten els dímers del 3-OHPNN en la fase cristal.lina α amb distància O···H de 1.63Å [10b] (FIGURA 5.8). El cristall α-3-OHPNN pertany al grup espacial C2/c (a = 25.08Å, b = 8.315Å, c = 12.840Å, β = 105.35°) i presenta vuit molècules per cel.la unitat. La fase α d'aquest cristall, a més, es comporta com a un ferromagnet.

TAULA 5.1.- Resultats a nivell B3LYP *broken symmetry* de la constant d'acoblament magnètic J en el cas del dímer del 3-OHPNN (FIGURA 5.8). La J s'ha calculat com a $\Delta E^{S-T} / 2$.

base	J / cm^{-1}
6-31G	+0.2
6-31G(d)	+0.2
6-31+G(d)	+0.5

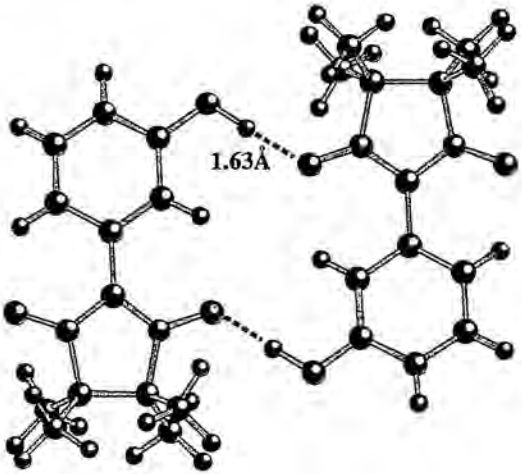

FIGURA 5.8.- Geometria del dímer (distància O···H de 1.63Å) de la fase α del cristall 3-OHPNN.

Les dades obtingudes a nivell B3LYP *broken symmetry* [5] amb bases de diferent qualitat es llisten en la TAULA 5.1. Tots els resultats presenten el mateix ordre de magnitud i tenen el mateix signe que el resultat experimental de J (2.69±0.75 cm^{-1}). S'ha d'esmentar que no pretenem que els càlculs reprodueixin exactament el valor experimental de J, només volem reproduir el signe i l'ordre de magnitud del resultat experimental. Signe i ordre de magnitud que amb el mètode B3LYP *broken symmetry* són reproduïts en el cas del dímer del 3-OHPNN. Així doncs, aquest mètode sembla ser adequat per al calcul de J en sistemes α-nitronil nitròxids.

5.3. LICMIT I WILVIW: ESTIMACIÓ DE J MITJANÇANT SISTEMES MODEL.

En el Capítol 4, s'han trobat contactes entorn una distància O···O de 3.2Å en dos cristalls que magnèticament tenen comportaments oposats (FIGURA 5.9). Es tracta dels cristalls LICMIT i WILVIW [11], els quals estan dipositats a la CSD [12].

El cristall LICMIT és un ferromagnet. Aquest cristall pertany al grup espacial $P2_1/n$ (a=15.142Å, b=12.320Å, c=7.196Å, β=99.18°) i té 4 molècules per cel.la unitat. En canvi, el cristall WILVIW es comporta experimentalment com a un antiferromagnet. WILVIW pertany al grup espacial P-1 (a=11.843Å, b=12.695Å, c=9.532Å, α=95.53°, β=90.55°, γ=146.89°) i té 2 molècules per cel.la unitat.

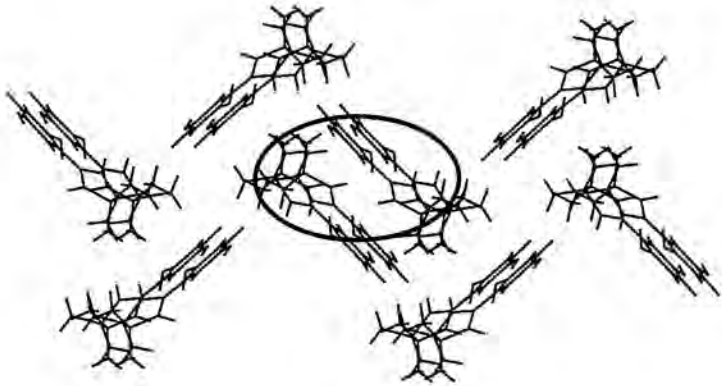

FIGURA 5.9.- Vista del cristall LICMIT. Extensió de la capa de molècules ab al llarg de c.

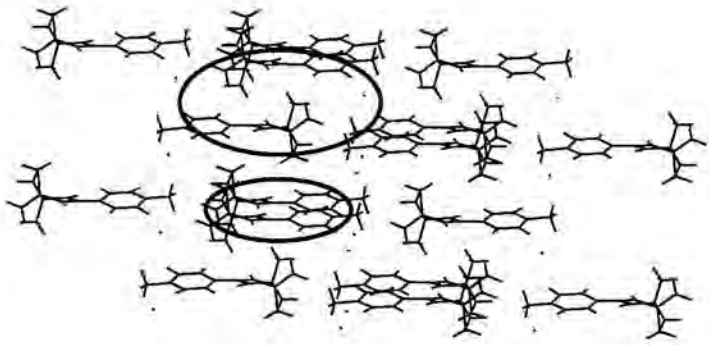

FIGURA 5.10.- Vista del cristall WILVIW. Extensió de la capa de molècules bc al llarg d'a.

En les FIGURES 5.9 i 5.10 es mostren dues vistes dels cristalls LICMIT i WILVIW. LICMIT s'empaqueta formant cadenes en zig-zag en el pla ab. En la part central de la FIGURA 5.9 veiem que hi ha un "dímer" format per molècules que pertanyen a diferents cadenes. En aquest "dímer" és on es troben els únics contactes NO···ON per sota de 4Å. En la FIGURA 5.11*a* es pot apreciar millor la disposició espacial d'aquest contacte. En canvi, WILVIW s'empaqueta formant plans paral·lels al llarg d'a. Aquest cristall presenta

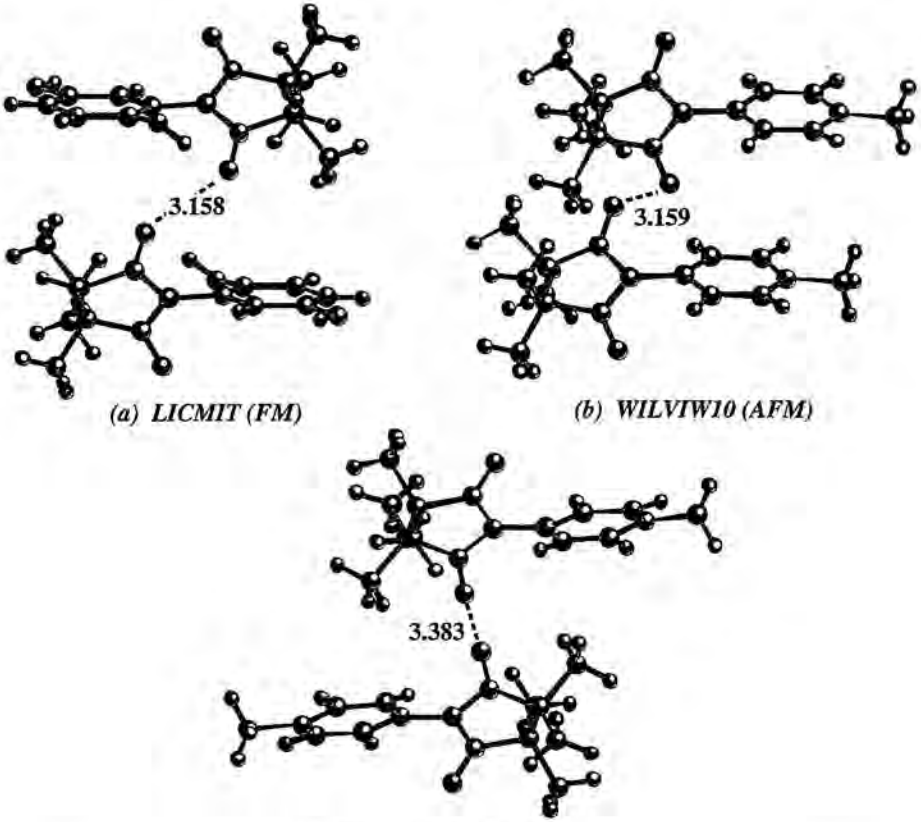

(a) LICMIT (FM) *(b) WILVIW10 (AFM)*

(c) WILVIW10 (AFM)

FIGURA 5.11.- Contactes en els cristalls LICMIT i WILVIW que presenten distàncies O···O per sota de 4.0Å.

dos ordenaments diferents on la distància NO···ON és menor que 4Å. Un d'ells s'estableix entre molècules que pertanyen a un mateix pla (FIGURA 5.11*b*), mentre que en l'altre el contacte s'estableix entre plans (FIGURA 5.11*c*).

Segons el model de McConnell-I [1], sembla lògic pensar que el comportament magnètic dels cristalls α-nitronil nitròxids estarà dirigit per aquells contactes que presentin les interaccions NO···ON més curtes. Dins del marc de McConnell-I, contactes NO···ON curts seran sinònim d'interaccions antiferromagnètiques. Així doncs, sembla interessant estudiar el caràcter d'aquests contactes en dos cristalls que presenten interaccions dominants de diferent magnetisme (ferro- o antiferromagnètiques) i en els quals s'estableixen contactes NO···ON de la mateixa distància.

Tal com ja s'ha esmentat, estudis de l'empaquetament d'aquests cristalls mostren que els únics contactes NO···ON que s'estableixen en el cristall LICMIT per sota de 4Å són els representats en la FIGURA 5.11*a* a 3.158Å (el següent contacte es troba a 4.594Å). En canvi, en el cristall WILVIW se'n troben dos: un a 3.159Å (FIGURA 5.11*b*) i l'altre a 3.383Å (FIGURA 5.11*c*) (el següent contacte es troba a 4.370Å). Donat que per sobre de 4Å les possibles interaccions magnètiques NO···ON són quasi negligibles, s'haurà de proposar el dímer 5.11*a* com a únic responsable del magnetisme del cristall LICMIT, si acceptem el mecanisme de McConnell-I sobre grups NO. D'altra banda, en una primera aproximació, prendrem el dímer que presenta una distància O···O més curta 5.11*b* com a responsable del magnetisme en el cas del cristall WILVIW.

Curiosament, aquests contactes NO···ON curts, il.lustrats en la FIGURA 5.11*a-b*, presenten un entorn força similar. Així doncs, ens trobem davant d'un problema molt interessant : el dímer (5.11*b*) hauria de ser el responsable del caràcter antiferromagnètic que presenta el cristall WILVIW, però ... què passa amb el dímer (5.11*a*)? Aquest dímer no pot ser el responsable del comportament antiferromagnètic del cristall LICMIT, perquè aquest cristall és un ferromagnet. En tot cas, sembla més *factible* creure que el dímer (5.11*a*) hauria de ser el responsable del caràcter ferromagnètic mostrat per LICMIT (recordem que no hi ha cap altre contacte NO···ON inferior a 4.594Å). Així doncs, ens interessarà estudiar el tipus de resposta magnètica que presenten el contactes mostrats en la FIGURA 5.11.

En primer lloc, ens centrarem únicament en els grups que hom pren com a responsables del caràcter antiferromagnètic en un cristall, els grups NO [1]. Amb aquesta finalitat hem modelitzat els centres magnètics NO amb les estructures il.lustrades esquemàticament en la FIGURA 5.12. Aquests sistemes model han estat seleccionats tal que reprodueixin la geometria que presenten els dímers en els respectius cristalls. Amb la comparació dels resultats obtinguts per al càlcul de la constant d'acoblament magnètic J amb

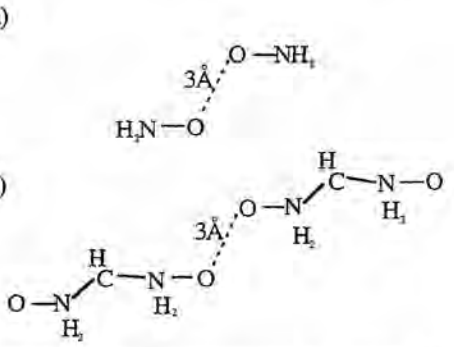

FIGURA 5.12.- Sistemes model usats en l'estudi dels dímers LICMIT i WILVIW.

TAULA 5.2.- Resultats a nivell CASSCF i B3LYP *broken symmetry* de la constant d'acoblament magnètic J en el cas dels sistemes model de la FIGURA 5.12 (a = $H_2NO\cdots ONH_2$; b = ONCNO···ONCNO). La J s'ha calculat com a ΔE^{S-T} / 2.

sistema model	cristall	base	J^{CAS} / cm^{-1}	J^{B3LYP} / cm^{-1}
$H_2NO\cdots ONH_2$	LICMIT	6-31G	-1.7	-2.3
(model 5.12a)		6-31G(d)	-2.1	-2.2
		6-31+G(d)	-2.1	-4.0
	WILVIW	6-31G	-4.6[1] / -30.2[2]	-7.1[1] / -49.8[2]
		6-31G(d)	-3.7[1] / -35.4[2]	-6.9[1] / -51.3[2]
		6-31+G(d)	-3.7[1] / -42.1[2]	-5.9[1] / -59.9[2]
ONCNO···ONCNO	LICMIT	6-31G	-0.4	-1.0
(model 5.12b)		6-31G(d)	-0.5	-0.9
	WILVIW	6-31G	-1.1[1] / -8.2[2]	-2.7[1] / -7.0[2]
		6-31G(d)	-0.9[1] / -8.8[2]	-2.6[1] / -7.5[2]

[1] dímer corresponent a la FIGURA 5.11*b*; [2] dímer corresponent a 5.11*c*

les estructures 5.12a i 5.12b es podrà comprovar els possibles efectes de tenir en compte la deslocalització electrònica en 5.12b. El model 5.12a s'ha estudiat a nivell ab initio CASSCF amb un espai actiu (2, 2) que correspon als electrons i orbitals del sistema π d'aquest dímer (tal i com ja s'ha fet en l'apartat 5.1.1). De la mateixa manera, l'estudi del model 5.12b s'ha dut a terme a nivell CAS treballant amb un espai actiu (6, 6) que també representa el sistema π del dímer de la FIGURA 5.12b. Amb aquests dos models es pretén, per tant, estudiar *individualment* l'efecte dels contactes NO···ON en el càlcul de la constant d'acoblament magnètic J del dímers LICMIT i WILVIW.

Els resultats obtinguts es llisten en la TAULA 5.2 discriminant el tipus de base que s'ha usat. Per al model 5.12a, tots els valors de J calculats tenen el mateix signe i són del mateix ordre de magnitud, independentment de si la geometria NO···ON prové del dímer 5.11*a* o 5.11*b*. D'altra banda, hem tornat a comprovar que per a distàncies O···O d'uns 3Å bases de qualitat 6-31G(d) i 6-31+G(d) donen els mateixos resultats. Aquest fet no és important en el cas del sistema model 5.12a, però constituirà un gran *estalvi* en el cas del model 5.12b. Així doncs, en aquest darrer sistema model, no caldrà fer càlculs a nivell CAS(6, 6) / 6-31+G(d) perquè amb bases de qualitat 6-31G(d) (i fins i tot, 6-31G) ja s'obtenen resultats adequats.

Cal destacar que en ambdós models, 5.12a i 5.12b, s'obté la mateixa tendència en el signe. Criteris de predicció de magnetisme basats en la presència de grups NO···ON establint distàncies curtes són, per tant, incorrectes. Així doncs, una vegada més s'ha de concloure que no es pot associar la presència de contactes curts NO···ON amb l'existència de *bulk* antiferromagnetisme, pràctica força habitual com a conseqüència d'un abús en *"l'ús qualitatiu normal del model de McConnell-I"*.

S'ha estudiat, a més, el dímer 5.11*c* ja que estableix contactes O···O a una distància prou curta com per presentar interaccions magnètiques no negligibles. Els resultats a nivell CASSCF en modelitzar aquest dímer amb els sistemes 5.12a i 5.12b es presenten en la TAULA 5.2. En aquest cas, hi ha clares diferències entre els valors obtinguts amb el model 5.12a i 5.12b. Per buscar el *per què* cal fixar-se en la geometria del dímer 5.11*c* : els dos grups NO estan disposats quasi un al damunt de l'altre en plans paral.lels. Aquest és el motiu per al qual és més adient usar el model 5.12b, ja que és necessari introduir l'efecte degut a la deslocalització electrònica en el grup ONCNO. Cal puntualitzar que en el cas dels dímers 5.11*a-b* la introducció de l'efecte de la deslocalització no produïa canvis tant notables, perquè els grups NO d'aquests dímers estan disposats en un mateix pla. Els resultats a nivell CAS(6, 6) indiquen, també, que grups NO situats aproximadament un al damunt de l'altre en plans paral.lels (dímer 5.11*c*) interaccionen amb més força que aquests mateixos grups situats aproximadament en el mateix pla però a una distància menor (dímer 5.11*b*). Per tant, interaccions d'aquest tipus no es poden negligir.

En la TAULA 5.2 també es presenten els valor de J calculats a nivell B3LYP *broken symmetry* [5] amb bases de diferent qualitat. Amb aquests càlculs preteniem comprovar que aquest mètode reprodueix correctament tant el signe com l'ordre de magnitud dels valors obtinguts a nivell CASSCF. Aquest fet és molt important ja que el principal avantatge d'aquest mètode és que tots els càlculs són molt més econòmics. Aquest avantatge per si sol constitueix un gran pas endavant en l'estudi de sistemes *reals*, ja que la metodologia DFT permetrà fer càlculs de sistemes complexos que mètodes com el CASSCF no són capaços de dur a terme.

Així doncs, per a poder discriminar el tipus de magnetisme, caldrà tenir en compte tots els grups magnèticament actius dels dímers 5.11*a-c*. En aquests moments, estem duent a terme càlculs a nivell B3LYP *broken symmetry* amb bases de diferent qualitat amb els dímers complets 5.11*a-c*. Donada la longitud i el grau de dificultat d'aquests càlculs, no ha estat possible incloure'ls en aquesta memòria i es presentaran en treballs posteriors.

5.4. CONCLUSIONS.

L'estudi dels dímers d'H_2NO i metil - al.lil dóna com a resultat noves inconsistències en relació a les prediccions fetes amb *"l'ús qualitatiu normal del model de McConnell-I"*. Hi ha prou motius, doncs, per pensar que McConnell-I no és un bon model per tal de dur a terme anàlisis de les propietats magnètiques de cristalls moleculars.

D'altra banda, càlculs realitzats a nivell B3LYP *broken symmetry* —en el cas del dímer del 3-OHPNN— semblen ser adequats per tal de reproduir el signe i l'ordre de magnitud del resultat experimental de la constant d'acoblament magnètic J.

Finalment, amb l'estudi dels dímers dels cristalls LICMIT i WILVIW s'ha comprovat que la modelització dels contactes NO···ON més curts no és suficient per a descriure el magnetisme dominant que presenten aquests cristalls. Serà, doncs, necessari tenir en compte les interaccions intermoleculars de tots els grups funcionals magnèticament actius.

BIBLIOGRAFIA.

[1] H. M. McConnell. *J. Chem. Phys.* **1963**, *39*, 1910.

[2] (a) D. Hegarty, M.A. Robb, *Mol. Phys.* **1979**, *38*, 1795. (b) R.H.E. Eade, M.A. Robb, *Chem. Phys. Lett.* **1981**, *83*, 362. (c) H.B. Schlegel, M.A. Robb, *ibid.* **1982**, *93*, 43. (d) F. Bernardi, A. Bottini, J.J.W. McDougall, M.A. Robb, H.B. Schlegel, *Far. Symp. Chem. Soc.* **1984**, *19*, 137. (e) M.J. Frisch, I.N. Ragazos, M.A. Robb, H.B. Schlegel, *Chem. Phys. Lett.* **1992**, *189*, 524.

[3] M. Deumal; J.J. Novoa; M.J. Bearpark; P. Celani; M. Olivucci; M.A. Robb, *J. Phys. Chem.* **1998** (en premsa).

[4] (a) P. Hohenberg, W. Kohn, *Phys. Rev.* **1964**, *136*, B864. (b) W. Kohn, L.J. Sham, *Phys. Rev.* **1965**, *140*, A1133. (c) R.G. Parr, W. Yang, *Density-functional theory of atoms and molecules*, Oxford Univ. Press : Oxford, **1989**.

[5] B3LYP és un funcional híbrid: funcional Becke88 per al bescanvi [A.D. Becke, *Phys. Rev. A* **1988**, *38*, 3098]; funcional de Lee, Yang, Parr per a la correlació [(a) C. Lee, W. Yang, R.G. Parr, *Phys. Rev. B* **1988**, *37*, 785; (b) B. Miehlich, A. Savin, H. Stoll, H. Preuss, *Chem. Phys. Lett.* **1989**, *157*, 20]).
Cal puntualitzar que el càlcul de l'energia en els estats singlet s'ha fet amb *broken symmetry*.

[6] (a) E. Langmann, M. Wallin, *Europhysics-Lett.* **1997**, *37*, 219; (b) E. Langmann, M. Wallin, *Phys. Rev. B - Condens. Matter* **1997**, *55*, 9439; (c) J. Curely, *Physica B* **1998**, *245*, 263.

[7] (a) R. Arita, K. Kuroki, H. Aoki, M. Fabrizio, *Phys. Rev. B - Conds. Matter* **1998**, *57*, 10324; (b) S.R. White, D.J. Scalapino, *Phys. Rev. Lett.* **1998**, *80*, 1272; (c) G. Fano, F. Ortolani, L. Ziosi, *J. Chem. Phys.* **1998**, 108, 9246.

[8] (a) J.E. Hirsch, R.L. Sugar, D.J. Scalapino, R. Blankenbecler, *Phys. Rev. B*, **1982**, *26*, 5033; (b) A. Oguchi, Y. Tsuchida, *Prog. Theor. Phys.* **1976**, *56*, 1976.

[9] (a) M.S. Makivic, H.-Q. Ding, *Phys. Rev B*, **1991**, *43*, 3562; (b) E. Dagotto, T.M. Rice, *Science*, **1996**, *271*, 618.

[10] (a) J.Veciana et al., resultats no publicats. (b) J. Cirujeda, M. Mas, E. Molins, F. Lanfranc de Panthou, J. Laugier, J.G. Park, C. Paulsen, P. Rey, C. Rovira, J. Veciana, *J. Chem. Soc., Chem. Commun.*, **1995**, 709.

[11] (a) LICMIT: T. Sugawara, M.-M. Matsushita, A. Izuoka, N. Wada, N. Takeda, M. Ishikawa, *J. Chem. Soc., Chem. Commun.* **1994**, 1723; (b) WILVIW10: K. Awaga, A. Yamaguchi, T. Okuno, T. Inabe, T. Nakamura, M. Matsumoto, Y. Maruyama, *J. Mater. Chem.* **1994**, *4*, 1377.

[12] F.-H. Allen, S. Bellard, M.-D. Brice, B.-A. Cartwright, A. Doubleday, H. Higgs, T. Hummelink, B.-G. Hummelink-Peters, O. Kennard, W.D.S. Motherwell, J.-R. Rodgers, D.-G. Watson, *Acta Crystallogr.* **1979**, *B35*, 2331.

CONCLUSIONS

CONCLUSIONS

L'anàlisi de l'empaquetament cristal.lí en base als seus grups funcionals (CPFGA) ha demostrat ser un procediment adequat per tal de racionalitzar l'estructura dels cristalls de la família dels α-nitronil nitròxid. La informació obtinguda amb el mètode CPFGA no només serveix per a racionalitzar estructures de cristalls sinó que també permet *entendre* els canvis microscòpics que tenen lloc en una transició polimòrfica entre diferents fases.

Els contactes intermoleculars que dirigeixen i estabilitzen l'empaquetament de cristalls de la família d'α-nitronil nitròxids són del tipus C-H···O-N. S'ha observat també que l'empaquetament tendeix a minimitzar contactes NO···ON directes perquè són repulsius.

Calen sis paràmetres per a definir les relacions magneto-estructurals dels contactes de tipus NO···ON. En el cas de contactes CH···ON, aquest número es redueix a quatre donada la simetria quasi cilíndrica de la densitat electrònica entorn el grup C-H.

No hi ha diferències significatives en la disposició relativa dels contactes NO···ON i NO···HC per a cristalls amb comportament dominant ferro- o antiferromagnètic.

El model de McConnell-I no està ben fonamentat teòricament i, quan *"el seu ús qualitatiu normal"* prediu el magnetisme correctament ho fa per compensació d'errors.

S'ha proposat un formalisme alternatiu per a predir estats d'alt - baix spin que és generalitzable a mecanismes magnètics *a través d'espai* i mecanismes *a través d'enllaç*.

El magnetisme s'ha de relacionar amb ordenaments (*patterns*), no amb contactes individuals.

És impossible distingir les característiques magnètiques d'un *pattern* únicament amb l'anàlisi de contactes NO···ON i NO···HC. A més, càlculs a nivell CASSCF i B3LYP *broken symmetry* mostren que amb la modelització dels contactes NO···ON no és possible reproduir el caràcter magnètic d'aquests *patterns*.

Càlculs realitzats a nivell B3LYP *broken symmetry* amb bases adequades dels *patterns* complets semblen reproduir correctament el signe i l'ordre de magnitud de la constant d'acoblament magnètic J.

ANNEX 1

Derivació d'un Hamiltonià de Heisenberg de bescanvi d'spin en termes de generadors estàndard del grup unitari U(n) [equació (3.6)].

En segona quantització, un Hamiltonià de Heisenberg de bescanvi d'spin genèric es pot escriure com

$$\hat{H}^S = Q - \sum_{i,j,k,l}^{N} J_{ij} \left\langle i(1)\, j(2) \left| \hat{S}(1)\cdot\hat{S}(2) + \frac{1}{4}\hat{I}(1,2) \right| k(1)\, l(2) \right\rangle a_i^+ a_j^+ a_l a_k \quad , \tag{A1.1}$$

el qual només depèn de les coordenades dels electrons (1, 2) en els spin-orbitals i, j, k, l (N és el número total d'spin-orbitals).

Donat que es treballarà en un espai de determinants VB covalents (és a dir, tots els orbitals espacials tenen ocupació 1), interessa saber quins termes de l'expressió (A1.1) contribuiran en aquest espai. Així doncs, serà necessari avaluar els elements de la matriu de valors propis de l'Hamiltonià (A1.1). Amb aquesta finalitat, cal definir $\hat{S}(1)\cdot\hat{S}(2)$ en termes d'operadors d' $\hat{S}^+$, $\hat{S}^-$, i $\hat{S}_z$ com

$$\hat{S}(1)\cdot\hat{S}(2) = \frac{1}{2}\left[\hat{S}^+(1)\hat{S}^-(2) + \hat{S}^-(1)\hat{S}^+(2)\right] + \hat{S}_z(1)\hat{S}_z(2) \tag{A1.2}$$

Cal recordar que els operadors d'spin només actuen sobre les coordenades d'spin dels electrons i no sobre les coordenades espacials. Interessa escriure els spin-orbitals com a productes de funcions espacials i d'spin *pures*

$$i(1) = i(1_{Spat})\sigma(1_{Spin}) \tag{A1.3}$$

En l'expressió anterior, 1_{Spat} s'usa per significar Coordenades Espacials de l'electró 1 i 1_{Spin} per significar Coordenades d'Spin de l'electró 1. Les funcions $i(1_{Spat})$ i $\sigma(1_{Spin})$ representen un orbital espacial (no hi ha contribució d'spin) i la seva funció d'spin associada α o β, respectivament.

Avaluant els elements de matriu entre els spin-orbitals i els operadors d'spin de (A1.1), s'obté

$$\langle \Psi | \hat{H}^S | \Psi \rangle = Q - \sum_{i,j}^{N} J_{ij} \left\{ \begin{array}{l} \frac{1}{2}\langle i(1)\, j(2) | \hat{S}^+(1)\hat{S}^-(2) | k(1)\, l(2) \rangle \\ + \frac{1}{2}\langle i(1)\, j(2) | \hat{S}^-(1)\hat{S}^+(2) | k(1)\, l(2) \rangle \\ + \langle i(1)\, j(2) | \hat{S}_z(1)\hat{S}_z(2) | k(1)\, l(2) \rangle \\ + \frac{1}{4}\langle i(1)\, j(2) | \hat{I}(1,2) | k(1)\, l(2) \rangle \end{array} \right\} \langle \Psi | a_i^+ a_j^+ a_l a_k | \Psi \rangle \tag{A1.4}$$

Introduint (A1.3) en l'expressió (A1.4), podem factoritzar les integrals en una part d'spin —amb participació d'operadors i funcions d'spin— i en una integral de solapament *pura* entre orbitals espacials —no implica la participació de cap operador. Aquest últim terme sempre es resol en una delta de Kroneker entre orbitals espacials perquè els orbitals VB són ortonormals. Així doncs, podem expressar el primer terme de l'equació (A1.4), mitjançant l'ús de (A1.3), com a

$$\sum_{i,j,k,l}^{M} \sum_{\mu,\eta,\gamma,\pi} \frac{1}{2}\left(\begin{array}{l}\langle i(1_{Spat})\mu(1_{Spin})\, j(2_{Spat})\eta(2_{Spin})|\hat{S}^{+}(1_{Spin})\hat{S}^{-}(2_{Spin})|\, k(1_{Spat})\gamma(1_{Spin})l(2_{Spat})\pi(2_{Spin})\rangle \\ \langle \Psi|a_{i\mu}^{+}a_{j\eta}^{+}a_{l\pi}a_{k\gamma}|\Psi\rangle\end{array}\right)$$

on M és el número total d'orbitals espacials. Separant les integrals i reorganitzant, l'expressió anterior es converteix en

$$\sum_{i,j,k,l}^{M} \delta_{ik}\delta_{jl} \sum_{\mu,\eta,\gamma,\pi} \frac{1}{2}\left(\begin{array}{l}\langle \mu(1_{Spin})\eta(2_{Spin})|\hat{S}^{+}(1_{Spin})\hat{S}^{-}(2_{Spin})|\, \gamma(1_{Spin})\pi(2_{Spin})\rangle \\ \langle \Psi|a_{i\mu}^{+}a_{j\eta}^{+}a_{l\pi}a_{k\gamma}|\Psi\rangle\end{array}\right) = \qquad \text{(A1.5)}$$

$$= \sum_{i,j}^{M} \sum_{\mu,\eta,\gamma,\pi} \frac{1}{2}\left(\begin{array}{l}\langle \mu(1_{Spin})|\hat{S}^{+}(1_{Spin})|\, \gamma(1_{Spin})\rangle \\ \langle \eta(2_{Spin})|\hat{S}^{-}(2_{Spin})|\pi(2_{Spin})\rangle\end{array}\right)\langle \Psi|a_{i\mu}^{+}a_{j\eta}^{+}a_{j\pi}a_{i\gamma}|\Psi\rangle \qquad \text{(A1.6)}$$

Cal destacar que, un cop s'ha integrat sobre tot l'espai, l'expressió (A1.6) s'escriu únicament en funció dels orbitals i, j (no apareix cap terme en funció de k, l). [Aquesta expressió és la que s'ha donat en el Capítol 3 com a equació (3.5)].

A continuació, caldrà avaluar els termes de dins del parèntesi, els quals poden ser zero degut al solapament entre funcions d'spin diferents. Tenint en compte que les funcions d'spin $\mu(1_{Spin})$, $\eta(1_{Spin})$, $\gamma(1_{Spin})$, $\pi(1_{Spin})$ només poden ser α o β, s'haurà d'estudiar el comportament d'aquestes funcions d'spin quan es combinen amb els operadors $\hat{S}^{+}$, i $\hat{S}^{-}$. La TAULA 1 sumaritza totes les possibilitats de combinació.

$\hat{X}$	$\langle\alpha\|\hat{X}\|\alpha\rangle$	$\langle\alpha\|\hat{X}\|\beta\rangle$	$\langle\beta\|\hat{X}\|\alpha\rangle$	$\langle\beta\|\hat{X}\|\beta\rangle$
$\hat{S}^{+}$	$\langle\alpha\|0\rangle = 0$	$\langle\alpha\|\alpha\rangle = 1$	$\langle\beta\|0\rangle = 0$	$\langle\beta\|\alpha\rangle = 0$
$\hat{S}^{-}$	$\langle\alpha\|\beta\rangle = 0$	$\langle\alpha\|0\rangle = 0$	$\langle\beta\|\beta\rangle = 1$	$\langle\beta\|0\rangle = 0$

Els resultats de la TAULA 1 ens indiquen que només hi ha una combinació en què l'equació (A1.6) és no nul.la :

$$\mu(1_{Spin}) = \alpha;\ \gamma(1_{Spin}) = \beta;\ \eta(2_{Spin}) = \beta;\ \pi(2_{Spin}) = \alpha \qquad \text{(A1.7)}$$

Ara, caldrà repetir el mateix procediment per als tres termes restants de l'equació (A1.4).

En el segon terme també participen els operadors $\hat{S}^+$ i $\hat{S}^-$. Usant les relacions que apareixen en la TAULA 1, aquest terme contribueix únicament en el cas en què

$$\mu(1_{Spin}) = \beta;\ \gamma(1_{Spin}) = \alpha;\ \eta(2_{Spin}) = \alpha;\ \pi(2_{Spin}) = \beta \tag{A1.8}$$

Per tal d'avaluar el tercer terme, caldrà introduir la TAULA 2.

$\langle\alpha\lvert\,\hat{S}_z\rvert\alpha\rangle$	$\langle\alpha\lvert\,\hat{S}_z\rvert\beta\rangle$	$\langle\beta\lvert\,\hat{S}_z\rvert\alpha\rangle$	$\langle\beta\lvert\,\hat{S}_z\rvert\beta\rangle$
$\langle\alpha\lvert\tfrac{1}{2}\alpha\rangle = \tfrac{1}{2}$	$\langle\alpha\lvert-\tfrac{1}{2}\beta\rangle = 0$	$\langle\beta\lvert\tfrac{1}{2}\alpha\rangle = 0$	$\langle\beta\lvert-\tfrac{1}{2}\beta\rangle = -\tfrac{1}{2}$

Cal destacar que l'operador $\hat{S}_z$ (TAULA 2) no modifica la funció d'spin —només la multiplica per ½ si la funció d'spin és α i per $-\tfrac{1}{2}$ si és β—, mentre que els operadors $\hat{S}^+$ i $\hat{S}^-$ (TAULA 1) sí canvien l'spin de la funció sobre la qual actuen —permeten la combinació de funcions de diferent spin.

Els termes tercer i quart permeten que les funcions d'spin es combinin amb més llibertat. Així doncs, tot i que amb diferents factors i signes, les mateixes quatre combinacions són possibles

$$\begin{aligned}
&\mu(1_{Spin}) = \alpha;\ \gamma(1_{Spin}) = \alpha;\ \eta(2_{Spin}) = \alpha;\ \pi(2_{Spin}) = \alpha\\
&\mu(1_{Spin}) = \alpha;\ \gamma(1_{Spin}) = \alpha;\ \eta(2_{Spin}) = \beta;\ \pi(2_{Spin}) = \beta\\
&\mu(1_{Spin}) = \beta;\ \gamma(1_{Spin}) = \beta;\ \eta(2_{Spin}) = \alpha;\ \pi(2_{Spin}) = \alpha\\
&\mu(1_{Spin}) = \beta;\ \gamma(1_{Spin}) = \beta;\ \eta(2_{Spin}) = \beta;\ \pi(2_{Spin}) = \beta
\end{aligned} \tag{A1.9}$$

Integrant sobre les funcions d'spin, l'expressió (A1.4) es converteix en

$$\sum_{i,j}^{M}\left[\begin{pmatrix}
\tfrac{1}{2}\langle\Psi|a_{i\alpha}^{+}a_{j\beta}^{+}a_{j\alpha}a_{i\beta}|\Psi\rangle\\
+\tfrac{1}{2}\langle\Psi|a_{i\beta}^{+}a_{j\alpha}^{+}a_{j\beta}a_{i\alpha}|\Psi\rangle\\
+\tfrac{1}{4}\langle\Psi|a_{i\alpha}^{+}a_{j\alpha}^{+}a_{j\alpha}a_{i\alpha}|\Psi\rangle\\
-\tfrac{1}{4}\langle\Psi|a_{i\alpha}^{+}a_{j\beta}^{+}a_{j\beta}a_{i\alpha}|\Psi\rangle\\
-\tfrac{1}{4}\langle\Psi|a_{i\beta}^{+}a_{j\alpha}^{+}a_{j\alpha}a_{i\beta}|\Psi\rangle\\
+\tfrac{1}{4}\langle\Psi|a_{i\beta}^{+}a_{j\beta}^{+}a_{j\beta}a_{i\beta}|\Psi\rangle
\end{pmatrix}+\begin{pmatrix}
\tfrac{1}{4}\langle\Psi|a_{i\alpha}^{+}a_{j\alpha}^{+}a_{j\alpha}a_{i\alpha}|\Psi\rangle\\
+\tfrac{1}{4}\langle\Psi|a_{i\alpha}^{+}a_{j\beta}^{+}a_{j\beta}a_{i\alpha}|\Psi\rangle\\
+\tfrac{1}{4}\langle\Psi|a_{i\beta}^{+}a_{j\alpha}^{+}a_{j\alpha}a_{i\beta}|\Psi\rangle\\
+\tfrac{1}{4}\langle\Psi|a_{i\beta}^{+}a_{j\beta}^{+}a_{j\beta}a_{i\beta}|\Psi\rangle
\end{pmatrix}\right]= \tag{A1.10}$$

Després de sumar termes en l'equació (A1.10), permutarem els operadors creació / anihilació d'acord amb les regles d'anticommutació per tal d'obtenir

$$= \sum_{i,j}^{M} \begin{pmatrix} -\frac{1}{2}\langle \Psi | a_{i\alpha}^{+} a_{j\alpha} a_{j\beta}^{+} a_{i\beta} | \Psi \rangle \\ -\frac{1}{2}\langle \Psi | a_{i\beta}^{+} a_{j\beta} a_{j\alpha}^{+} a_{i\alpha} | \Psi \rangle \\ +\frac{1}{2}\langle \Psi | a_{i\alpha}^{+} a_{i\alpha} | \Psi \rangle - \frac{1}{2}\langle \Psi | a_{i\alpha}^{+} a_{j\alpha} a_{j\alpha}^{+} a_{i\alpha} | \Psi \rangle \\ +\frac{1}{2}\langle \Psi | a_{i\beta}^{+} a_{i\beta} | \Psi \rangle - \frac{1}{2}\langle \Psi | a_{i\beta}^{+} a_{j\beta} a_{j\beta}^{+} a_{i\beta} | \Psi \rangle \end{pmatrix} = \tag{A1.11}$$

Usant la nomenclatura $E_{ij}^{\alpha\alpha} = a_{i\alpha}^{+} a_{j\alpha}$, l'expressió anterior es pot escriure com a

$$= \sum_{i,j}^{M} \begin{pmatrix} -\frac{1}{2}\langle \Psi | \hat{E}_{ij}^{\alpha\alpha} \hat{E}_{ji}^{\beta\beta} | \Psi \rangle \\ -\frac{1}{2}\langle \Psi | \hat{E}_{ij}^{\beta\beta} \hat{E}_{ji}^{\alpha\alpha} | \Psi \rangle \\ +\frac{1}{2}\langle \Psi | \hat{E}_{ii}^{\alpha\alpha} | \Psi \rangle - \frac{1}{2}\langle \Psi | \hat{E}_{ij}^{\alpha\alpha} \hat{E}_{ji}^{\alpha\alpha} | \Psi \rangle \\ +\frac{1}{2}\langle \Psi | \hat{E}_{ii}^{\beta\beta} | \Psi \rangle - \frac{1}{2}\langle \Psi | \hat{E}_{ij}^{\beta\beta} \hat{E}_{ji}^{\beta\beta} | \Psi \rangle \end{pmatrix} \tag{A1.12}$$

Així doncs, els elements de matriu de l'equació (A1.4) són

$$\langle \Psi | \hat{H}^{S} | \Psi \rangle = Q + \sum_{i,j}^{M} J_{ij} \frac{1}{2} \langle \Psi | \begin{pmatrix} \hat{E}_{ij}^{\alpha\alpha} \hat{E}_{ji}^{\beta\beta} + \hat{E}_{ij}^{\beta\beta} \hat{E}_{ji}^{\alpha\alpha} \\ +\left[\hat{E}_{ij}^{\alpha\alpha} \hat{E}_{ji}^{\alpha\alpha} - \hat{E}_{ii}^{\alpha\alpha} \right] \\ +\left[\hat{E}_{ij}^{\beta\beta} \hat{E}_{ji}^{\beta\beta} - \hat{E}_{ii}^{\beta\beta} \right] \end{pmatrix} | \Psi \rangle \tag{A1.13}$$

A partir de l'expressió (A1.13), podem derivar l'Hamiltonià de Heisenberg de bescanvi d'spin $\hat{H}^{S}$ en termes de generadors estàndard del grup unitari U(n) [equació (3.6)].

$$\hat{H}^{S} = Q + \sum_{i,j}^{M} J_{ij} \frac{1}{2} \left(\hat{E}_{ij}^{\alpha\alpha} \hat{E}_{ji}^{\beta\beta} + \hat{E}_{ij}^{\beta\beta} \hat{E}_{ji}^{\alpha\alpha} + \left[\hat{E}_{ij}^{\alpha\alpha} \hat{E}_{ji}^{\alpha\alpha} - \hat{E}_{ii}^{\alpha\alpha} \right] + \left[\hat{E}_{ij}^{\beta\beta} \hat{E}_{ji}^{\beta\beta} - \hat{E}_{ii}^{\beta\beta} \right] \right)$$

ANNEX 2

TAULA 1.- Coordenades cartesianes per a les geometries dels isòmers pseudo-orto-, -meta-, i -para-bis(metil)[2.2]paraciclofans (bMe) optimitzades a nivell MMVB del singlet, triplet i creuament singlet / triplet.

SINGLET (pseudo-orto-bMe optimitzat)

6	0.000000	0.000000	0.000000
6	0.000000	0.000000	1.547428
6	1.244068	0.000000	2.258155
6	-1.165742	0.325942	2.267342
6	-1.069054	0.979327	3.544687
6	0.199831	1.102461	4.222169
6	1.333518	0.558396	3.546370
1	2.177697	-0.290991	1.723829
1	-2.121327	0.406656	1.702678
1	2.341119	0.653910	4.012717
6	0.459628	1.363475	-0.644870
1	-1.029574	-0.241598	-0.352289
1	0.648613	-0.831862	-0.361585
6	0.519440	2.573288	0.327709
1	-0.168492	1.611133	-1.531464
1	1.482262	1.219886	-1.064963
6	1.732749	2.753169	1.058005
6	-0.681838	3.080038	0.947745
6	-0.633911	3.741026	2.223968
6	0.541767	3.703346	2.998237
6	1.758300	3.321457	2.344744
6	-1.919795	3.056603	0.248215
1	-2.736250	3.035832	1.003319
1	-1.988125	2.103087	-0.315472
1	-1.593598	3.957661	2.744135
1	2.710952	3.319507	2.922929
6	0.472031	3.714201	4.543971
1	-0.449728	4.260452	4.851356
1	1.326338	4.311419	4.940117
6	0.465095	2.280216	5.199698
1	-0.249158	2.241619	6.054233
1	1.462295	2.109246	5.667937
6	-2.272196	1.381970	4.187362
1	2.684143	2.353533	0.637283
1	-2.073968	2.315669	4.753481
1	-3.008735	1.643554	3.395975

TRIPLET (pseudo-orto-bMe optimitzat)

6	0.000000	0.000000	0.000000
6	0.000000	0.000000	1.545975
6	1.242982	0.000000	2.256455
6	-1.169582	0.309410	2.265826
6	-1.081763	0.937711	3.559322
6	0.190338	1.051216	4.243338
6	1.326593	0.536971	3.558167
1	2.179240	-0.277816	1.719774
1	-2.125743	0.386767	1.701838
1	2.332530	0.628759	4.028808
6	0.420512	1.385109	-0.620085

1	-1.021270	-0.269278	-0.356571
1	0.677212	-0.807098	-0.365204
6	0.478951	2.555046	0.398093
1	-0.234975	1.649037	-1.481641
1	1.434911	1.274795	-1.069287
6	1.692627	2.717768	1.123306
6	-0.726298	3.037638	1.041116
6	-0.669314	3.669838	2.334436
6	0.515409	3.628762	3.093708
6	1.726669	3.261659	2.424315
6	-1.961505	3.032830	0.349637
1	-2.778205	2.993960	1.103747
1	-2.033833	2.100889	-0.248687
1	-1.624363	3.878358	2.866150
1	2.685198	3.256570	2.992636
6	0.463938	3.635639	4.638988
1	-0.445871	4.192414	4.962846
1	1.333765	4.213221	5.030396
6	0.443124	2.191188	5.265760
1	-0.287499	2.133391	6.105088
1	1.431471	2.003572	5.746304
6	-2.283984	1.306174	4.209457
1	2.642692	2.333945	0.685244
1	-2.100674	2.221552	4.809611
1	-3.028466	1.578129	3.429075

CREUAMENT SINGLET / TRIPLET (pseudo-orto-bMe optimitzat)

6	0.000000	0.000000	0.000000
6	0.000000	0.000000	1.555394
6	1.258798	0.000000	2.267617
6	-1.139978	0.390813	2.279667
6	-0.995437	1.181109	3.473031
6	0.274285	1.369150	4.100173
6	1.387148	0.670731	3.475445
1	2.176708	-0.351164	1.741986
1	-2.091099	0.489096	1.709878
1	2.408616	0.790789	3.904768
6	0.624720	1.236199	-0.774923
1	-1.056641	-0.118970	-0.332775
1	0.511835	-0.931988	-0.336355
6	0.692896	2.645518	-0.103353
1	0.129653	1.340132	-1.768481
1	1.674734	0.957393	-1.024211
6	1.909625	2.948958	0.635500
6	-0.496444	3.250231	0.403949
6	-0.486335	4.063191	1.591471
6	0.643768	4.068857	2.425725
6	1.895525	3.643508	1.835754
6	-1.738778	3.112093	-0.304608
1	-2.558704	3.194582	0.442368
1	-1.791889	2.076853	-0.699411
1	-1.466062	4.293467	2.066923
1	2.824203	3.684074	2.450591
6	0.493594	4.092454	3.973736
1	-0.492562	4.554920	4.208363
1	1.247709	4.811699	4.370883
6	0.611001	2.733466	4.783420
1	0.017832	2.812371	5.724165
1	1.665938	2.658287	5.135483
6	-2.184659	1.731151	4.063744

1	2.870413	2.493864	0.301021
1	-1.932031	2.732510	4.468482
1	-2.912434	1.909092	3.241708

SINGLET (pseudo-meta-bMe optimitzat)

6	0.000000	0.000000	0.000000
6	0.000000	0.000000	1.546807
6	1.248675	0.000000	2.249710
6	-1.160803	0.338541	2.264241
6	-1.062002	0.959839	3.563175
6	0.218309	1.064584	4.236661
6	1.343549	0.529239	3.553975
1	2.179640	-0.298130	1.714734
1	-2.117798	0.423028	1.701691
6	-2.255621	1.334328	4.219133
1	2.351335	0.602944	4.023147
6	0.236477	1.434344	-0.609620
1	-0.968977	-0.413963	-0.364608
1	0.792540	-0.697563	-0.358355
6	0.428210	2.521083	0.474295
1	-0.629060	1.718326	-1.252526
1	1.130407	1.422419	-1.275927
6	1.685079	2.724377	1.070864
6	-0.721802	3.079318	1.121857
6	-0.626727	3.624614	2.419393
6	0.600618	3.666512	3.134254
6	1.780229	3.201477	2.429784
1	-2.062447	2.241977	4.827900
1	-1.725968	2.962634	0.653021
1	-1.563308	3.953657	2.925076
6	3.063306	3.335321	3.005163
6	0.520150	3.627330	4.681968
1	-0.410055	4.158255	4.990720
1	1.342937	4.228272	5.133232
6	0.487481	2.175106	5.284248
1	-0.243305	2.108871	6.122869
1	1.474023	1.967575	5.759789
1	-3.002120	1.617533	3.444581
1	2.567698	2.220207	0.616734
1	2.993083	3.128757	4.093364
1	3.721506	2.551488	2.569548

TRIPLET (pseudo-meta-bMe optimitzat)

6	0.000000	0.000000	0.000000
6	0.000000	0.000000	1.547819
6	1.247260	0.000000	2.253169
6	-1.160798	0.343535	2.265829
6	-1.057826	0.985219	3.550627
6	0.217418	1.099759	4.222321
6	1.343560	0.547172	3.546950
1	2.178265	-0.299983	1.719260
1	-2.116389	0.429805	1.701202
6	-2.254714	1.385534	4.200071
1	2.352280	0.629357	4.012878
6	0.277122	1.418530	-0.632989
1	-0.981898	-0.387215	-0.359359
1	0.767621	-0.726233	-0.355708

6	0.455904	2.542094	0.416336
1	-0.561367	1.696977	-1.313123
1	1.190626	1.373973	-1.270741
6	1.707793	2.770480	1.017609
6	-0.699677	3.116323	1.038949
6	-0.617669	3.685582	2.324286
6	0.605353	3.740807	3.052783
6	1.786845	3.268316	2.366253
1	-2.051205	2.309947	4.779340
1	-1.700150	2.980389	0.567369
1	-1.560108	4.018140	2.816805
6	3.069553	3.405836	2.957985
6	0.506715	3.695256	4.600631
1	-0.436096	4.211571	4.895340
1	1.311442	4.316169	5.057671
6	0.492592	2.249907	5.226903
1	-0.221557	2.196238	6.080789
1	1.487596	2.061907	5.692681
1	-2.993482	1.659454	3.414894
1	2.594842	2.253754	0.586872
1	2.981747	3.202616	4.045435
1	3.725427	2.611420	2.538408

CREUAMENT SINGLET / TRIPLET (pseudo-meta-bMe optimitzat)

6	0.000000	0.000000	0.000000
6	0.000000	0.000000	1.554650
6	1.261522	0.000000	2.259113
6	-1.137982	0.390706	2.276911
6	-0.994701	1.137133	3.497944
6	0.276737	1.314153	4.124784
6	1.386985	0.624565	3.493459
1	2.179926	-0.344891	1.730260
1	-2.093973	0.478885	1.713364
6	-2.184192	1.669222	4.107402
1	2.407505	0.737896	3.926771
6	0.347294	1.349588	-0.763424
1	-1.005349	-0.347151	-0.334617
1	0.707709	-0.793701	-0.335431
6	0.555521	2.649610	0.064511
1	-0.455120	1.555680	-1.509745
1	1.270403	1.187728	-1.367503
6	1.801995	2.951455	0.627288
6	-0.599012	3.334174	0.608666
6	-0.516379	4.021755	1.808952
6	0.717361	4.093632	2.574120
6	1.877299	3.575881	1.923705
1	-1.931642	2.662005	4.533749
1	-1.600211	3.151789	0.154336
1	-1.459322	4.398072	2.268630
6	3.173105	3.707849	2.535621
6	0.577351	4.030013	4.127524
1	-0.395049	4.513952	4.376519
1	1.331294	4.715616	4.579645
6	0.615131	2.634312	4.885504
1	-0.029214	2.695331	5.793230
1	1.643496	2.509167	5.295971
1	-2.910192	1.868782	3.288837
1	2.677586	2.360006	0.276808
1	3.049967	3.540137	3.625554
1	3.795033	2.862291	2.167927

SINGLET (pseudo-para-bMe optimitzat)

6	0.000000	0.000000	0.000000
6	1.547371	0.000000	0.000000
6	2.252977	1.249850	0.000000
6	2.272377	-1.160269	0.323123
6	3.558874	-1.055443	0.961752
6	4.224938	0.219921	1.093900
6	3.534816	1.351319	0.566132
1	1.715629	2.182015	-0.288993
1	1.710957	-2.118311	0.403335
6	4.215644	-2.254842	1.350325
1	3.990476	2.363235	0.668065
6	-0.652243	0.069882	1.433963
1	-0.362793	-0.904173	-0.542552
1	-0.346452	0.874046	-0.598988
6	0.331939	0.344614	2.603827
1	-1.148887	-0.907478	1.636795
1	-1.489354	0.805003	1.450548
6	0.998912	1.619395	2.736933
6	1.021357	-0.787229	3.131198
6	2.303345	-0.686813	3.697381
6	3.009913	0.562360	3.697632
6	2.285408	1.723311	3.375525
6	0.343320	2.819888	2.349806
1	0.564730	-1.798740	3.029528
1	2.840421	-1.619361	3.985675
1	2.847423	2.681071	3.296131
6	4.557211	0.561070	3.697800
1	4.902830	-0.316053	4.292750
1	4.921135	1.462619	4.243934
6	5.209116	0.495837	2.263436
1	6.048881	-0.236217	2.244210
1	5.701689	1.475540	2.062062
1	1.127614	3.563375	2.086364
1	-0.229785	2.624301	1.419631
1	4.787363	-2.057744	2.281053
1	3.432498	-2.999590	1.613604

TRIPLET (pseudo-para-bMe optimitzat)

6	0.000000	0.000000	0.000000
6	1.545994	0.000000	0.000000
6	2.251975	1.249292	0.000000
6	2.269812	-1.163704	0.307833
6	3.570387	-1.067451	0.925829
6	4.245172	0.210255	1.045203
6	3.548184	1.343721	0.543163
1	1.714141	2.183502	-0.280985
1	1.706793	-2.120703	0.389315
6	4.231280	-2.265700	1.284502
1	4.010251	2.353311	0.638917
6	-0.624684	0.074521	1.443643
1	-0.367199	-0.907576	-0.533792
1	-0.351331	0.872910	-0.597806
6	0.402806	0.337722	2.576726
1	-1.126813	-0.897175	1.659788
1	-1.450116	0.821823	1.481213
6	1.078670	1.615049	2.696709
6	1.098462	-0.796374	3.078220

6	2.394580	-0.703230	3.622181
6	3.101971	0.545093	3.622327
6	2.379500	1.709757	3.314376
6	0.419200	2.814023	2.337861
1	0.635470	-1.805492	2.981931
1	2.931406	-1.638088	3.902935
1	2.943587	2.666181	3.233510
6	4.647955	0.543554	3.622711
1	4.998096	-0.333705	4.214803
1	5.017042	1.447811	4.160818
6	5.272008	0.474431	2.178565
1	6.100754	-0.269100	2.138214
1	5.770008	1.448748	1.964701
1	1.193576	3.563997	2.063583
1	-0.186526	2.631104	1.425943
1	4.837034	-2.081872	2.196227
1	3.457880	-3.016578	1.559054

CREUAMENT SINGLET / TRIPLET (pseudo-para-bMe optimitzat)

6	0.000000	0.000000	0.000000
6	1.552599	0.000000	0.000000
6	2.260543	1.254759	0.000000
6	2.277567	-1.148109	0.362504
6	3.524490	-1.021803	1.063835
6	4.162747	0.248155	1.237989
6	3.495443	1.375120	0.634217
1	1.726460	2.180424	-0.315639
1	1.718727	-2.108118	0.436743
6	4.161396	-2.221476	1.534079
1	3.934584	2.392774	0.750890
6	-0.737618	0.071892	1.401266
1	-0.348457	-0.901608	-0.556149
1	-0.332604	0.870081	-0.612434
6	0.110598	0.362012	2.675793
1	-1.235802	-0.911562	1.567325
1	-1.589153	0.788878	1.350407
6	0.760400	1.626584	2.856554
6	0.762530	-0.771756	3.275390
6	1.998366	-0.666225	3.915312
6	2.717523	0.580647	3.922830
6	2.003925	1.738796	3.563825
6	0.137312	2.834219	2.388190
1	0.314044	-1.784242	3.149627
1	2.522066	-1.598917	4.227654
1	2.572276	2.693764	3.497200
6	4.270477	0.564140	3.920585
1	4.592987	-0.341632	4.484644
1	4.630770	1.432266	4.520735
6	5.002584	0.553815	2.515063
1	5.883280	-0.128322	2.550184
1	5.453778	1.562641	2.368401
1	0.951365	3.561786	2.175993
1	-0.336219	2.616205	1.408270
1	4.639472	-1.992926	2.509296
1	3.355815	-2.955815	1.755206

TAULA 2.- Contribucions individuals $P_{ij}^{S/T}$'s a ΔP per a tots tres isòmers bis(metil) [2.2]paraciclofans avaluats amb la geometria de l'estat fonamental (GS). Contactes "més propers" entre veïns en negreta. La numeració dels àtoms correspon a la de la FIGURA 3.5.

C atom		ortho (T_{GS})		meta (S_{GS})		para (T_{GS})	
i	j	P_{ij}^{T}	P_{ij}^{S}	P_{ij}^{T}	P_{ij}^{S}	P_{ij}^{T}	P_{ij}^{S}
2	1	0.304	0.308	0.302	0.295	0.285	0.296
3	1	0.551	0.551	0.555	0.560	0.568	0.562
3	2	-0.909	-0.907	-0.909	-0.911	-0.907	-0.905
4	1	-0.856	-0.856	-0.854	-0.854	-0.856	-0.855
4	2	-0.158	-0.149	-0.154	-0.163	-0.158	-0.150
4	3	0.170	0.187	0.170	0.152	0.157	0.176
5	1	-0.102	-0.099	-0.105	-0.110	-0.107	-0.100
5	2	-0.934	-0.931	-0.934	-0.936	-0.936	-0.932
5	3	-0.862	-0.864	-0.860	-0.858	-0.858	-0.862
5	4	0.189	0.214	0.195	0.172	0.189	0.217
6	1	-0.861	-0.863	-0.859	-0.857	-0.856	-0.861
6	2	0.437	0.450	0.439	0.431	0.446	0.461
6	3	-0.129	-0.125	-0.131	-0.133	-0.135	-0.128
6	4	-0.833	-0.834	-0.832	-0.832	-0.831	-0.832
6	5	0.455	0.445	0.455	0.462	0.450	0.436
7	1	-0.168	-0.200	-0.184	-0.156	-0.168	-0.201
7	2	-0.796	-0.778	-0.789	-0.803	-0.797	-0.777
7	3	-0.881	-0.861	-0.871	-0.886	-0.876	-0.860
7	4	0.470	0.419	0.456	0.503	0.477	0.427
7	5	-0.899	-0.887	-0.893	-0.904	-0.900	-0.889
7	6	-0.196	-0.226	-0.210	-0.182	-0.197	-0.226
8	**1**	**-0.379**	**-0.608**	**-0.452**	**-0.346**	**-0.378**	**-0.610**
8	2	-0.638	-0.320	-0.525	-0.685	-0.638	-0.312
8	3	-0.636	-0.312	-0.527	-0.685	-0.638	-0.312
8	4	-0.385	-0.679	-0.484	-0.348	-0.380	-0.680
8	5	-0.644	-0.263	-0.510	-0.696	-0.646	-0.254
8	6	-0.391	-0.617	-0.470	-0.366	-0.394	-0.623
8	7	-0.679	-0.080	-0.473	-0.754	-0.682	-0.079
9	1	-0.588	-0.458	-0.527	-0.685	-0.592	-0.423
9	**2**	**-0.386**	**-0.580**	**-0.495**	**-0.237**	**-0.375**	**-0.633**
9	3	-0.402	-0.594	-0.502	-0.254	-0.395	-0.643
9	4	-0.583	-0.412	-0.495	-0.706	-0.594	-0.369
9	5	-0.391	-0.616	-0.516	-0.224	-0.380	-0.680
9	6	-0.590	-0.459	-0.521	-0.682	-0.593	-0.420
9	7	-0.378	-0.729	-0.570	-0.136	-0.358	-0.815
9	8	0.455	0.444	0.555	0.560	0.189	0.216
10	1	-0.591	-0.422	-0.525	-0.685	-0.587	-0.457
10	2	-0.396	-0.642	-0.507	-0.252	-0.403	-0.594
10	**3**	**-0.384**	**-0.639**	**-0.496**	**-0.238**	**-0.393**	**-0.588**
10	4	-0.595	-0.371	-0.504	-0.718	-0.593	-0.420
10	5	-0.385	-0.679	-0.517	-0.221	-0.394	-0.623
10	6	-0.583	-0.412	-0.513	-0.677	-0.577	-0.445
10	7	-0.357	-0.816	-0.565	-0.123	-0.373	-0.724
10	8	0.190	0.215	0.302	0.295	0.451	0.437
10	9	-0.833	-0.834	-0.909	-0.911	-0.831	-0.832
11	1	-0.405	-0.593	-0.470	-0.366	-0.401	-0.589
11	2	-0.616	-0.345	-0.513	-0.677	-0.619	-0.347
11	3	-0.619	-0.343	-0.520	-0.682	-0.622	-0.351
11	**4**	**-0.384**	**-0.639**	**-0.469**	**-0.325**	**-0.375**	**-0.633**
11	5	-0.636	-0.313	-0.515	-0.706	-0.638	-0.312

11	6	-0.402	-0.593	-0.473	-0.366	-0.403	-0.594
11	7	-0.664	-0.156	-0.481	-0.768	-0.669	-0.167
11	8	-0.862	-0.864	-0.859	-0.857	-0.936	-0.932
11	9	-0.129	-0.125	-0.131	-0.133	-0.158	-0.149
11	10	0.170	0.187	0.440	0.431	0.445	0.460
12	1	-0.579	-0.452	-0.510	-0.696	-0.579	-0.452
12	2	-0.402	-0.588	-0.517	-0.220	-0.401	-0.589
12	3	-0.405	-0.593	-0.516	-0.224	-0.406	-0.592
12	4	-0.591	-0.422	-0.496	-0.746	-0.592	-0.423
12	**5**	**-0.379**	**-0.607**	**-0.519**	**-0.165**	**-0.378**	**-0.610**
12	6	-0.588	-0.458	-0.515	-0.706	-0.587	-0.457
12	7	-0.374	-0.720	-0.585	-0.069	-0.373	-0.718
12	8	-0.102	-0.099	-0.105	-0.109	-0.107	-0.100
12	9	-0.861	-0.863	-0.860	-0.858	-0.856	-0.855
12	10	-0.856	-0.856	-0.934	-0.936	-0.856	-0.861
12	11	0.551	0.552	0.454	0.461	0.286	0.297
13	1	-0.402	-0.588	-0.484	-0.348	-0.406	-0.593
13	2	-0.627	-0.362	-0.505	-0.719	-0.622	-0.351
13	3	-0.616	-0.345	-0.495	-0.706	-0.612	-0.341
13	4	-0.396	-0.641	-0.502	-0.320	-0.395	-0.643
13	5	-0.638	-0.320	-0.496	-0.746	-0.638	-0.311
13	**6**	**-0.386**	**-0.580**	**-0.469**	**-0.325**	**-0.393**	**-0.588**
13	7	-0.657	-0.157	-0.441	-0.815	-0.657	-0.155
13	8	-0.934	-0.931	-0.854	-0.854	-0.858	-0.862
13	9	0.438	0.451	0.170	0.152	0.158	0.176
13	10	-0.158	-0.149	-0.154	-0.163	-0.135	-0.128
13	11	-0.909	-0.907	-0.832	-0.832	-0.907	-0.905
13	12	0.303	0.308	0.195	0.172	0.567	0.561
14	1	-0.374	-0.720	-0.473	-0.754	-0.374	-0.718
14	2	-0.657	-0.157	-0.565	-0.123	-0.669	-0.168
14	3	-0.664	-0.156	-0.570	-0.136	-0.657	-0.155
14	4	-0.357	-0.817	-0.441	-0.815	-0.358	-0.815
14	5	-0.679	-0.080	-0.585	-0.069	-0.682	-0.079
14	6	-0.378	-0.729	-0.481	-0.768	-0.373	-0.723
14	7	-0.741	0.192	-0.675	0.091	-0.738	0.184
14	8	-0.899	-0.887	-0.184	-0.156	-0.900	-0.889
14	9	-0.196	-0.226	-0.871	-0.886	0.478	0.427
14	10	0.469	0.419	-0.789	-0.803	-0.197	-0.226
14	11	-0.881	-0.861	-0.210	-0.182	-0.797	-0.777
14	12	-0.168	-0.200	-0.893	-0.904	-0.168	-0.201
14	13	-0.796	-0.778	0.456	0.504	-0.877	-0.860

TAULA 3.- J_{ij} per a tots tres isòmers bis(metil)[2.2]paraciclofans avaluades amb la geometria de l'estat fonamental (GS). La numeració dels àtoms correspon a la de la FIGURA 3.5.

C atom		ortho (T_{GS})	meta (S_{GS})	para (T_{GS})
i	j	J_{ij}	J_{ij}	J_{ij}
2	1	-.06096	-.06080	-.06030
3	1	-.06492	-.06536	-.06563
3	2	-.00413	-.00411	-.00412
4	1	-.00371	-.00361	-.00370
4	2	-.00058	-.00058	-.00059
4	3	-.06127	-.06085	-.06082
5	1	-.00015	-.00016	-.00015
5	2	-.00275	-.00292	-.00279
5	3	-.00201	-.00210	-.00197
5	4	-.05722	-.05718	-.05704
6	1	-.00332	-.00321	-.00333
6	2	-.06719	-.06721	-.06758
6	3	-.00056	-.00055	-.00054
6	4	-.00404	-.00401	-.00404
6	5	-.06176	-.06240	-.06205
7	1	-.00002	-.00002	-.00002
7	2	.00000	.00000	.00000
7	3	-.00211	-.00224	-.00213
7	4	-.05856	-.05912	-.05869
7	5	-.00199	-.00209	-.00197
7	6	.00000	.00000	.00000
8	1	-.00408	-.00649	-.00417
8	2	-.00050	-.00123	-.00034
8	3	-.00008	-.00057	-.00016
8	4	-.00002	-.00009	-.00003
8	5	-.00001	.00000	-.00001
8	6	-.00001	-.00004	.00000
8	7	.00000	-.00001	-.00001
9	1	-.00115	-.00058	-.00195
9	2	-.00497	-.00363	-.00611
9	3	.00000	.00000	-.00003
9	4	-.00002	-.00001	-.00004
9	5	.00000	.00000	-.00003
9	6	.00000	-.00062	-.00170
9	7	-.00129	.00000	.00000
9	8	-.06172	-.06535	-.05701
10	1	-.00217	-.00123	-.00135
10	2	-.00007	-.00002	-.00002
10	3	-.00429	-.00360	-.00344
10	4	-.00202	-.00182	-.00170
10	5	-.00002	.00000	.00000
10	6	-.00002	-.00001	-.00001
10	7	-.00002	-.00007	-.00005
10	8	-.05721	-.06079	-.06212
10	9	-.00404	-.00410	-.00403
11	1	.00000	-.00004	-.00002
11	2	.00000	-.00001	.00000
11	3	-.00016	-.00062	-.00045
11	4	-.00431	-.00713	-.00610
11	5	-.00009	-.00068	-.00033

11	6	-.00020	-.00004	-.00002
11	7	.00000	-.00001	-.00005
11	8	-.00201	-.00321	-.00279
11	9	-.00056	-.00055	-.00059
11	10	-.06127	-.06722	-.06755
12	1	.00000	.00000	.00000
12	2	-.00002	.00000	-.00002
12	3	.00000	.00000	.00000
12	4	-.00217	-.00133	-.00196
12	5	-.00410	-.00322	-.00417
12	6	-.00011	-.00068	-.00134
12	7	-.00115	-.00016	-.00010
12	8	-.00015	-.00016	-.00015
12	9	-.00332	-.00210	-.00370
12	10	-.00371	-.00292	-.00333
12	11	-.06493	-.06238	-.06032
13	1	-.00002	-.00009	.00000
13	2	-.00092	-.00182	-.00045
13	3	.00000	-.00001	.00000
13	4	-.00007	-.00014	-.00003
13	5	-.00051	-.00134	-.00017
13	6	-.00498	-.00714	-.00345
13	7	-.00001	.00000	-.00001
13	8	-.00275	-.00361	-.00197
13	9	-.06720	-.06084	-.06083
13	10	-.00058	-.00058	-.00054
13	11	-.00413	-.00401	-.00412
13	12	-.06095	-.05716	-.06561
14	1	-.00011	-.00001	-.00010
14	2	-.00001	-.00007	-.00005
14	3	-.00020	.00000	-.00001
14	4	-.00002	.00000	.00000
14	5	-.00001	-.00016	-.00001
14	6	.00000	-.00001	-.00005
14	7	-.00018	.00000	.00000
14	8	-.00199	-.00002	-.00197
14	9	.00000	-.00224	-.05869
14	10	-.05855	.00000	.00000
14	11	-.00211	.00000	.00000
14	12	-.00002	-.00210	-.00002
14	13	.00000	-.05912	-.00213

ANNEX 3

```
C*************************************************************************
C*                                                                       *
C*                        FACTOR  ANALYSIS                               *
C*                        ~~~~~~~~~~~~~~~~                               *
C*                                                                       *
C*     Pm  =>  PARAMETER (NF=650,NC=650,Ndata=611,Nvar=6,iin=5,iout=6)   *
C*     APm =>  PARAMETER (NF=710,NC=710,Ndata=701,Nvar=6,iin=5,iout=6)   *
C*                                                                       *
C*************************************************************************
C
C   Nvar  num. de "variables" mesurades
C   Ndata num. d'experiments mesurats
C   Ndnr  num. de Ndata no repetides !!
C
C   Dini   matriu de dades inicial           (Ndnr x Nvar)
C   D      matriu de dades en radians        (Ndnr x Nvar)
C   Dtras  matriu transposta de D            (Nvar x Ndnr)
C   Z      matriu de dades D z-transformada  (Ndnr x Nvar)
C   Ztras  matriu transposta de Z            (Nvar x Ndnr)
C   dIDENT matriu ID x IDtras                (Ndnr x Ndnr)
C   Corr   matriu correlacio                 (Nvar x Nvar)
C   C      matriu covariancia                (Nvar x Nvar)
C   Cdiag  matriu covariancia diagonalitzada (Nvar x Nvar)
C   dLanda matriu de VAP's elevada a 1/2     (Nvar x Nvar)
C   FACT   matriu de factors                 (Nvar x Nvar)
C   S      matriu de factor scores           (Nvar x Nvar)
C
C
      IMPLICIT REAL*8 (A-H,O-Z)
C     PARAMETER (NF=650,NC=650,Ndata=611,Nvar=6,iin=5,iout=6)
      PARAMETER (NF=710,NC=710,Ndata=701,Nvar=6,iin=5,iout=6)
      DIMENSION SIMBOL(NF),NUMCOD(NF),REFCOD(NF),Dini(NF,NC),
     *          D(NF,NC),Z(NF,NC),Dtras(NC,NF),Ztras(NC,NF),
     *          dIDENT(NF,NF),Corr(NC,NC),C(NC,NC),
     *              Cdiag(NC,NC),dLanda(NC,NC),FACT(NC,NC),S(NF,NC)
 CHARACTER SIMBOL(NF)*8,NUMCOD(NF)*8,REFCOD(NF)*6
C
C
C llegim el fitxer .tab de dades VISTA (provinent de la CSD)
      write(iout,*) "VISTA"
      call VISTA(SIMBOL,NUMCOD,REFCOD,Dini)
      write(iout,*) "VISTA"
C
C busquem dades redundants i construccio de matriu de dades D
      write(iout,*) "REDUN"
      call REDUN(REFCOD,Dini,Ndnr,D)
      write(iout,*) Ndnr
      write(iout,*) "REDUN"
C
C bescanviem els angles A1 per A2 i T2 per T3 si A1 es > que A2
      write(iout,*) "PERM"
      call PERM(Ndnr,D)
      write(iout,*) "PERM"
C
C*************************************************************************
C*                                                                       *
C*           "z-transformation" de la matriu de dades D --> Z            *
C*           calcul de covariancia = correlacio a partir de Z            *
C*                                                                       *
C*************************************************************************
C
C "z-transformation" de la matriu de dades D -aquesta transformacio
C expressa una *observation as the number of standard deviations
C from the mean*-.
      write(iout,*) "Ztransf"
      call ZTRANSF(D,Ndnr,Z)
      write(iout,*) "Ztransf"
```

```
C
C calcul de la matriu covariancia = correlacio Corr a partir de la
C matriu de dades Z
      write(iout,*) "Corr"
      call COVAR(Z,Ndnr,Corr)
      write(iout,*) "Corr"
C
C*************************************************************************
C*                                                                       *
C*      calcul de matriu de Covariancia i diagonalitzacio posterior      *
C*               per a obtenir els seus VAP's i VEP's                    *
C*                                                                       *
C*************************************************************************
C
C calculem la matriu de covariancia C a partir de la matriu de dades D
      write(iout,*) "COVAR"
      call COVAR(D,Ndnr,C)
      write(iout,*) "COVAR"
C
C diagonalitzacio de la matriu de covariancia Cdiag
      write(iout,*) "DIAGO"
      call DIAGO(Ndnr,C,Cdiag)
      write(iout,*) "DIAGO"
C
C calculem matriu dLanda = SQRT(C)
      write(iout,*) "SQROOT"
      call SQROOT(C,dLanda)
      write(iout,*) "SQROOT"
C
C calculem la matriu factor FACT(Nvar,Nvar)
      write(iout,*) "FACT"
      call PROMAT(Cdiag,dLanda,FACT,Nvar,Nvar,Nvar)
C escribim matriu FACT
      call WRIMAT(FACT,Nvar,Nvar)
      write(iout,*) "FACT"
C
C calculem la matriu de "factor scores" S
      write(iout,*) "SCORES"
      call PROMAT(D,FACT,S,Ndnr,Nvar,Nvar)
C escribim matriu de "factor scores" S
      call WRIMAT(S,Ndnr,Nvar)
      write(iout,*) "SCORES"
C
C*************************************************************************
C*                                                                       *
C*   calcul de la mitjana i de la desviacio standard de les 6 variables  *
C*                          de la matriu de dades D                      *
C*                                                                       *
C*************************************************************************
C
C trobem la mitjana i la desviacio standard de la matriu de dades D
      write(iout,*) "mitdev"
      call MITDEV(D,Ndnr)
      write(iout,*) "mitdev"
C
      stop
      end
C
C-----------------------------------------------------------------------
      SUBROUTINE VISTA(SIMBOL,NUMCOD,REFCOD,Dini)
C-----------------------------------------------------------------------
      IMPLICIT REAL*8 (A-H,O-Z)
C     PARAMETER (NF=650,NC=650,Ndata=611,Nvar=6,iin=5,iout=6)
      PARAMETER (NF=710,NC=710,Ndata=701,Nvar=6,iin=5,iout=6)
      DIMENSION SIMBOL(NF),NUMCOD(NF),REFCOD(NF),Dini(NF,NC)
      CHARACTER SIMBOL(NF)*8,NUMCOD(NF)*8,REFCOD(NF)*6
C
```

```
      DO i=1,Ndata
        read(iin,100) SIMBOL(i)
        read(iin,100) NUMCOD(i)
        read(iin,200) REFCOD(i)
        DO j=1,Nvar
          read (iin,300) Dini(i,j)
          if (j.ne.1) then
            Dini(i,j)=RAD(Dini(i,j))
          end if
        END DO
      END DO
C
      return
  100 FORMAT (A8)
  200 FORMAT (A6)
  300 FORMAT (F8.3)
      end
C
C-----------------------------------------------------------------------
      FUNCTION RAD(x)
C-----------------------------------------------------------------------
      IMPLICIT REAL*8 (A-H,O-Z)
      RAD=x*3.14159265359/180.
      return
      end
C
C-----------------------------------------------------------------------
      SUBROUTINE REDUN(REFCOD,Dini,Ndnr,D)
C-----------------------------------------------------------------------
      IMPLICIT REAL*8 (A-H,O-Z)
C     PARAMETER (NF=650,NC=650,Ndata=611,Nvar=6,iin=5,iout=6,
C    *           EPSILON=1.D-2)
      PARAMETER (NF=710,NC=710,Ndata=701,Nvar=6,iin=5,iout=6,
     *           EPSILON=1.D-2)
      DIMENSION REFCOD(NF),Dini(NF,NC),D(NF,NC)
      CHARACTER REFCOD(NF)*6
C
      k=1
      DO i=1,Ndata-1
        igual=0
        j=i+1
        DO WHILE ((igual.eq.0).and.(j.le.Ndata))
          if (REFCOD(i).eq.REFCOD(j)) then
            do=0
            m=1
            DO WHILE ((do.eq.0).and.(m.le.Nvar))
              if (DABS(Dini(i,m)-Dini(j,m)).lt.EPSILON) then
                igual=igual+1
              else
                if (DABS(Dini(i,m)-Dini(j,m)).ge.EPSILON) then
                  do=1
                  igual=0
                end if
              end if
              if ((m.eq.Nvar).and.(igual.ne.Nvar)) igual=0
              m=m+1
            END DO
          end if
          j=j+1
        END DO
          if (igual.eq.0) then
            REFCOD(k)=REFCOD(i)
            DO mm=1,Nvar
              D(k,mm)=Dini(i,mm)
            END DO
            k=k+1
          end if
```

```
      END DO
      REFCOD(k)=REFCOD(Ndata)
      DO mm=1,Nvar
        D(k,mm)=Dini(Ndata,mm)
      END DO
      Ndnr=k
C
      return
      end
C
C-----------------------------------------------------------------------
      SUBROUTINE PERM(Ndnr,D)
C-----------------------------------------------------------------------
      IMPLICIT REAL*8 (A-H,O-Z)
C     PARAMETER (NF=650,NC=650,Ndata=611,Nvar=6,iin=5,iout=6)
      PARAMETER (NF=710,NC=710,Ndata=701,Nvar=6,iin=5,iout=6)
      DIMENSION D(NF,NC)
C
      DO i=1,Ndnr
        ang=0.
        dih=0.
        if (D(i,2).gt.D(i,3)) then
          ang=D(i,2)
            D(i,2)=D(i,3)
            D(i,3)=ang
          dih=D(i,5)
            D(i,5)=D(i,6)
            D(i,6)=dih
        endif
      END DO
C
      return
      end
C
C-----------------------------------------------------------------------
      SUBROUTINE ZTRANSF(D,Ndnr,Z)
C-----------------------------------------------------------------------
C
C "z-transformation" de la matriu de dades Z -aquesta transformacio
C
C expressa una *observation as the number of standard deviations Sj
C
C from the mean dj*-.
C
C           Dij-dj                    _   SUM(i=1,Ndnr) Dij
C     Zij= --------   where       dj= ------------------
C             Sj                            Ndnr
C                                                        _  2
C                                    2   SUM(i=1,Ndnr) (Dij-dj)
C                                  Sj= ----------------------
C                                            Ndnr - 1
C
      IMPLICIT REAL*8 (A-H,O-Z)
C     PARAMETER (NF=650,NC=650,Ndata=611,Nvar=6,iin=5,iout=6)
      PARAMETER (NF=710,NC=710,Ndata=701,Nvar=6,iin=5,iout=6)
      DIMENSION D(NF,NC),Z(NF,NC),COLMEAN(Nvar),STANDEV(Nvar)
C
C
      DO j=1,Nvar
C
        DO i=1,Ndnr
          COLMEAN(j)=COLMEAN(j)+D(i,j)
        END DO
        COLMEAN(j)=COLMEAN(j)/Ndnr
        write(iout,*)  'mitjana de variable ',j,' = ',COLMEAN(j)
C
        DO i=1,Ndnr
```

```
          STANDEV(j)=STANDEV(j)+(D(i,j)-COLMEAN(j))**2
        END DO
        STANDEV(j)=DSQRT(STANDEV(j)/(Ndnr-1))
        write(iout,*) "desv. stand. de var.",j," = ",STANDEV(j)
      write(iout,*)
C
        DO i=1,Ndnr
          Z(i,j)=(D(i,j)-COLMEAN(j))/STANDEV(j)
        END DO
C
      END DO
C
C escribim les matrius de dades abans i despres de la z-transformacio
      write(iout,*) 'matriu de dades D'
      call WRIMAT(D,Ndnr,Nvar)
      write(iout,*)
      write(iout,*) 'matriu de dades Z'
      call WRIMAT(Z,Ndnr,Nvar)
      write(iout,*)
C
      return
      end
C
C-----------------------------------------------------------------------
      SUBROUTINE COVAR(D,Ndnr,C)
C-----------------------------------------------------------------------
C Formula de la matriu de covariancia C
C
C            1                    1
C     C = ------- ( Dtras*D - ------ Dtras*I*Itras*D )
C          Ndnr-1               Ndnr
C
C
      IMPLICIT REAL*8 (A-H,O-Z)
C     PARAMETER (NF=650,NC=650,Ndata=611,Nvar=6,iin=5,iout=6)
      PARAMETER (NF=710,NC=710,Ndata=701,Nvar=6,iin=5,iout=6)
      DIMENSION D(NF,NC),Dtras(NC,NF),dIDENT(NF,NF),C(NC,NC),
     *          DtD(NC,NC),DtI(NC,NF),DtID(NC,NC)
C
C fem transposta de matriu de dades D
      write(iout,*) "Dtras"
      call TRANSP(Ndnr,D,Dtras)
      write(iout,*) "Dtras"
C
C calculem "mat.identitat x transposta mat.ident." (NdataxNdata)
      write(iout,*) "dIDENT"
      call IDxIDt(Ndnr,dIDENT)
      write(iout,*) "dIDENT"
C
      write(6,*) "DtD"
      call PROMAT(Dtras,D,DtD,Nvar,Ndnr,Nvar)
      write(6,*) "DtI"
      call PROMAT(Dtras,dIDENT,DtI,Nvar,Ndnr,Ndnr)
      write(6,*) "DtID"
      call PROMAT(DtI,D,DtID,Nvar,Ndnr,Nvar)
C
      DO k=1,Nvar
        DO j=1,Nvar
          C(k,j)=(1./(Ndnr-1))*(DtD(k,j)-(1./Ndnr)*DtID(k,j))
        END DO
      END DO
C
C escribim la matriu de covariance C
      call WRIMATSIM(C,Nvar)
C
      return
      end
```

```
C
C-----------------------------------------------------------------------
      SUBROUTINE TRANSP(Ndnr,D,Dtras)
C-----------------------------------------------------------------------
      IMPLICIT REAL*8 (A-H,O-Z)
C     PARAMETER (NF=650,NC=650,Ndata=611,Nvar=6,iin=5,iout=6)
      PARAMETER (NF=710,NC=710,Ndata=701,Nvar=6,iin=5,iout=6)
      DIMENSION D(NF,NC),Dtras(NC,NF)
C
      DO i=1,Nvar
        DO j=1,Ndnr
          Dtras(i,j)=D(j,i)
        END DO
      END DO
C
      return
      end
C
C-----------------------------------------------------------------------
      SUBROUTINE IDxIDt(Ndnr,dIDENT)
C-----------------------------------------------------------------------
      IMPLICIT REAL*8 (A-H,O-Z)
C     PARAMETER (NF=650,NC=650,Ndata=611,Nvar=6,iin=5,iout=6)
      PARAMETER (NF=710,NC=710,Ndata=701,Nvar=6,iin=5,iout=6)
      DIMENSION dIDENT(NF,NF)
C
      DO i=1,Ndnr
        DO j=1,Ndnr
          dIDENT(i,j)=1.D0
        END DO
      END DO
C
      return
      end
C
C-----------------------------------------------------------------------
      SUBROUTINE PROMAT(A,B,AB,NFA,NCA,NCB)
C-----------------------------------------------------------------------
C     PRODUCTE DE DUES MATRIUS A(NFAxNCA) I B(NFBxNCB)
C     A i B SON LES MATRIUS A MULTIPLICAR.
C     AB ES LA MATRIU RESULTAT (NFAxNCB)
C
      IMPLICIT REAL*8 (A-H,O-Z)
C     PARAMETER (NF=650,NC=650,Ndata=611,Nvar=6,iin=5,iout=6)
      PARAMETER (NF=710,NC=710,Ndata=701,Nvar=6,iin=5,iout=6)
      DIMENSION A(NF,NC),B(NF,NC),AB(NC,NF)
C
      DO i=1,NFA
        DO j=1,NCB
          AB(i,j)=0.D0
          DO k=1,NCA
            AB(i,j)=AB(i,j)+A(i,k)*B(k,j)
          END DO
        END DO
      END DO
C
      return
      end
C
C-----------------------------------------------------------------------
      SUBROUTINE DIAGO(Ndnr,C,Cdiag)
C-----------------------------------------------------------------------
C   PROGRAMA PER CALCULAR ELS VALORS I VECTORS PROPIS D'UNA MATRIU
C   EL METODE DE DIAGONALITZACIO ES UN JACOBI.
C
      IMPLICIT REAL*8 (A-H,O-Z)
C     PARAMETER (NF=650,NC=650,Ndata=611,Nvar=6,iin=5,iout=6)
```

```
      PARAMETER (NF=710,NC=710,Ndata=701,Nvar=6,iin=5,iout=6)
      DIMENSION C(NC,NC),Cdiag(NC,NC)
C
C comprovem que la matriu C(Nvar,Nvar) de dades es simetrica
      CALL TESTM(C,Nvar)
C
C es diagonalitza la matriu C
      CALL JACOBI(Nvar,C,Cdiag)
C
C s'escriuen els valors propis despres d'haver fet 0's els
C valors d'exponent < 1.D-4 !!!!!
      DO i=1,Nvar
        DO j=1,Nvar
          if (DABS(C(i,j)).lt.(1.D-4)) then
            C(i,j)=0.D0
          end if
        END DO
      END DO
C
C s'escriuen els valors propis
      write(iout,100)
      CALL WRIMAT(C,Nvar,Nvar)
C
C s'escriuen els vectors propis
      write(iout,101)
      CALL WRIMAT(Cdiag,Nvar,Nvar)
      write(iout,*)' *** FI DEL CALCUL ***'
C
      return
  100 FORMAT(/1H ,'VALORS PROPIS')
  101 FORMAT(/1H ,'VECTORS PROPIS')
      end
C
C-----------------------------------------------------------------------
      SUBROUTINE JACOBI(N,F,V)
C-----------------------------------------------------------------------
C     PROGRAMA PER DIAGONALITZAR UNA MATRIU REAL I SIMETRICA D'ORDRE N
C
C     F ES LA MATRIU A DIAGONALITZAR. EN FINALITZAR ELS ELEMENTS
C       DIAGONALS SON ELS VALORS PROPIS.
C     V ES LA MATRIU DE VECTORS PROPIS (CADA COLUMNA UN VECTOR)
C     RHO ES EL CRITERI DE CONVERGENCIA. EL PROCES FINALITZA SI TE<RHO
C       ON TE ES LA NORMA DELS ELEMENTS NO DIAGONALS.
C
      IMPLICIT REAL*8 (A-H,O-Z)
C     PARAMETER (Ndim=650,Ndata=611,iin=5,iout=6,RHO=1.D-4)
      PARAMETER (Ndim=710,Ndata=701,iin=5,iout=6,RHO=1.D-4)
      DIMENSION F(Ndim,Ndim),V(Ndim,Ndim)
C
C inicialitzacio de la matriu de vectors propis
      DO 20 I=1,N
       DO 21 J=1,N
   21  V(I,J)=0.0D0
      V(I,I)=1.0D0
   20 CONTINUE
C
C inicialitzacio de les variables de la iteracio
      MA=0
      A=N
      ITER=0
C
C proces iteratiu
    2 CONTINUE
C
      CALL RMS(TE,F,N)
      TEN=TE/A
      IF(TE.LT.RHO)GO TO 17
```

```
      ITER=ITER+1
C
    3 DO 14 II=2,N
      IJ=II-1
      DO 14 JJ=1,IJ
      IF(DABS(F(II,JJ))-TEN)14,4,4
    4 MA=1
      V1=F(JJ,JJ)
      V2=F(II,JJ)
      V3=F(II,II)
      U=.5*(F(JJ,JJ)-F(II,II))
      IF(DABS(U)-.000001)5,6,6
    5 OMEGA=-1.0
      GO TO 7
    6 OMEGA=-F(II,JJ)/DSQRT(F(II,JJ)*F(II,JJ)+U*U)
      Z=1.
      IF(U.LT.0.)Z=-Z
      OMEGA=OMEGA*Z
    7 SINT=OMEGA/DSQRT(2.*(1.+DSQRT(1.-OMEGA*OMEGA)))
      COST=DSQRT(1.-SINT*SINT)
      DO 13 I=1,N
      IF(I-II)9,8,8
    8 TEM=F(I,JJ)*COST-F(I,II)*SINT
      F(I,II)=F(I,JJ)*SINT+F(I,II)*COST
      F(I,JJ)=TEM
      GO TO 12
    9 IF(I-JJ)10,11,11
   10 TEM=F(JJ,I)*COST-F(II,I)*SINT
      F(II,I)=F(JJ,I)*SINT+F(II,I)*COST
      F(JJ,I)=TEM
      GO TO 12
   11 TEM=F(I,JJ)*COST-F(II,I)*SINT
      F(II,I)=F(I,JJ)*SINT+F(II,I)*COST
      F(I,JJ)=TEM
   12 TEM=V(I,JJ)*COST-V(I,II)*SINT
      V(I,II)=V(I,JJ)*SINT+V(I,II)*COST
   13 V(I,JJ)=TEM
      F(JJ,JJ)=V1*COST*COST+V3*SINT*SINT-2.*V2*SINT*COST
      F(II,II)=V1*SINT*SINT+V3*COST*COST+2.*V2*SINT*COST
      F(II,JJ)=2.*U*SINT*COST+V2*(COST*COST-SINT*SINT)
   14 CONTINUE
      IF(MA-1)16,15,15
   15 MA=0
      GO TO 3
   16 IF(TE-RHO)17,17,2
   17 CONTINUE
      DO 30 I=2,N
      II=I-1
      DO 31 J=1,II
   31 F(J,I)=F(I,J)
   30 CONTINUE
      write(iout,*)' *** FI DE LA DIAGONALITZACIO ***'
C
      return
      end
C
C-----------------------------------------------------------------------
      SUBROUTINE TESTM(A,N)
C-----------------------------------------------------------------------
      IMPLICIT REAL*8 (A-H,O-Z)
C     PARAMETER (Ndim=650,Ndata=611,iin=5,iout=6,EPSILON=1.D-5)
      PARAMETER (Ndim=710,Ndata=701,iin=5,iout=6,EPSILON=1.D-5)
      DIMENSION A(Ndim,Ndim)
C
      DO i=2,N
        II=i-1
        DO j=1,II
```

```
          if(DABS(A(i,j)-A(j,i)).gt.EPSILON) then
            go to 5
          else
            A(i,j)=A(j,i)
          end if
        END DO
      END DO
C
      return
    5 write(iout,*)' ERROR: LA MATRIU A DIAGONALITZAR NO ES SIMETRICA'
      write(iout,*)'        S''ATURA L''EXECUCIO.'
      stop
C
      end
C
C-----------------------------------------------------------------------
      SUBROUTINE RMS(TE,F,N)
C-----------------------------------------------------------------------
      IMPLICIT REAL*8 (A-H,O-Z)
C     PARAMETER (Ndim=650,Ndata=611,iin=5,iout=6)
      PARAMETER (Ndim=710,Ndata=701,iin=5,iout=6)
      DIMENSION F(Ndim,Ndim)
C
      TE=0.0D0
      DO 1 I=2,N
        K=I-1
        DO 1 J=1,K
    1     TE=TE+2.*F(I,J)*F(I,J)
          TE=DSQRT(TE)
C
      return
      end
C
C-----------------------------------------------------------------------
      SUBROUTINE SQROOT(C,dLanda)
C-----------------------------------------------------------------------
      IMPLICIT REAL*8 (A-H,O-Z)
C     PARAMETER (NF=650,NC=650,Ndata=611,Nvar=6,iin=5,iout=6)
      PARAMETER (NF=710,NC=710,Ndata=701,Nvar=6,iin=5,iout=6)
      DIMENSION C(NC,NC),dLanda(NC,NC)
C
      DO i=1,Nvar
        DO j=1,Nvar
          dLanda(i,j)=0.D0
          dLanda(i,i)=DSQRT(C(i,i))
        END DO
      END DO
C
      return
      end
C
C-----------------------------------------------------------------------
      SUBROUTINE MITDEV(D,Ndnr)
C-----------------------------------------------------------------------
C
C     -   SUM(i=1,Ndnr) Dij
C     dj= ----------------                    mitjana de la variable j
C            Ndnr
C                          _  2
C      2  SUM(i=1,Ndnr) (Dij-dj)
C     Sj= ----------------------              desviacio standard de j
C              Ndnr - 1
C
      IMPLICIT REAL*8 (A-H,O-Z)
C     PARAMETER (NF=650,NC=650,Ndata=611,Nvar=6,iin=5,iout=6)
      PARAMETER (NF=710,NC=710,Ndata=701,Nvar=6,iin=5,iout=6)
      DIMENSION D(NF,NC),COLMEAN(Nvar),STANDEV(Nvar)
```

```
C
C
      DO j=1,Nvar
C
        DO i=1,Ndnr
          COLMEAN(j)=COLMEAN(j)+D(i,j)
        END DO
        COLMEAN(j)=COLMEAN(j)/Ndnr
        write(iout,*)  'mitjana de variable ',j,' = ',COLMEAN(j)
C
        DO i=1,Ndnr
          STANDEV(j)=STANDEV(j)+(D(i,j)-COLMEAN(j))**2
        END DO
        STANDEV(j)=DSQRT(STANDEV(j)/(Ndnr-1))
        write(iout,*) "desv. stand. de var.",j," = ",STANDEV(j)
      write(iout,*)
C
      END DO
C
      return
      end
C
C-----------------------------------------------------------------------
      SUBROUTINE WRIMAT(A,Nfil,Ncol)
C-----------------------------------------------------------------------
      IMPLICIT REAL*8 (A-H,O-Z)
C     PARAMETER (Ndim=650,iin=5,iout=6)
      PARAMETER (Ndim=710,iin=5,iout=6)
      DIMENSION A(Ndim,Ndim)
C
c     write (iout,100)(j,j=1,Ncol)
      DO i=1,Nfil
        write(iout,101) (A(i,j),j=1,Ncol)
      END DO
C
      return
c 100 FORMAT(1H ,6X,5(7X,I2,8X))
  101 FORMAT(10(F7.3,1X))
      end
C
C-----------------------------------------------------------------------
      SUBROUTINE WRIMATSIM(A,Nfil)
C-----------------------------------------------------------------------
      IMPLICIT REAL*8 (A-H,O-Z)
C     PARAMETER (Ndim=650,iin=5,iout=6)
      PARAMETER (Ndim=710,iin=5,iout=6)
      DIMENSION A(Ndim,Ndim)
C
      DO i=1,Nfil
        write(iout,101) (A(i,j),j=1,i)
      END DO
C
      return
  101 FORMAT(10(F7.3,1X))
      end
```

```
C*************************************************************************
C*                                                                       *
C*                        CLUSTER  ANALYSIS                              *
C*                        ~~~~~~~~~~~~~~~~~                              *
C*                                                                       *
C*      busquem la matriu de "distancies Euclidianes" per obtenir :      *
C*        1) els radis de les boles F-F i AF-AF                          *
C*        2) les dist. INTERclusters menors que els radis de les boles   *
C*         - amb aixo sabrem si els 2 clusters formen 2 cj's disjunts -  *
C*                                                                       *
C*************************************************************************
C
C   Nvar  num. de "variables" mesurades
C   Ndata num. d'experiments mesurats
C   Ndnr  num. de Ndata no repetides !!
C
C   Dini  matriu de dades inicial            (Ndata x Nvar)
C   D     matriu de dades en radians         (Ndnr x Nvar)
C   Eucl  matriu de distancies Euclidianes   (Ndnr x Ndnr)
C
C
      IMPLICIT REAL*8 (A-H,O-Z)
      PARAMETER (NF=1312,NC=1312,Ndata=1312,Nvar=6,
     *           Nfm=611,Nafm=701,iin=5,iout=6)
      DIMENSION SIMBOL(NF),NUMCOD(NF),REFCOD(NF),
     *            Dini(NF,NC),D(NF,NC),Eucl(NF,NF)
      CHARACTER SIMBOL(NF)*8,NUMCOD(NF)*8,REFCOD(NF)*6
C
C llegim el fitxer .tab de dades VISTA (provinent de la CSD)
      write(iout,*) "VISTA"
      call VISTA(SIMBOL,NUMCOD,REFCOD,Dini)
      write(iout,*) "VISTA"
C
C busquem de dades redundants i construccio de matriu de dades D
      write(iout,*) "REDUN"
      call REDUN(REFCOD,Dini,Ndnr,D)
      write(iout,*) "REDUN"
C
C bescanviem els angles A1 per A2 i T2 per T3 si A1 es > que A2
      write(iout,*) "PERM"
      call PERM(Ndnr,D)
      write(iout,*) "PERM"
C
C busquem la matriu de "distancies Euclidianes" vs D
      write(iout,*) "EUCLIDIAN"
      call DEUCL(D,Eucl,Ndnr)
      write(iout,*) "EUCLIDIAN"
C
      stop
      end
C
C-------------------------------------------------------------------------
      SUBROUTINE VISTA(SIMBOL,NUMCOD,REFCOD,Dini)
C-------------------------------------------------------------------------
      IMPLICIT REAL*8 (A-H,O-Z)
      PARAMETER (NF=1312,NC=1312,Ndata=1312,Nvar=6,
     *           Nfm=611,Nafm=701,iin=5,iout=6)
      DIMENSION SIMBOL(NF),NUMCOD(NF),REFCOD(NF),Dini(NF,NC)
      CHARACTER SIMBOL(NF)*8,NUMCOD(NF)*8,REFCOD(NF)*6
C
      DO i=1,Ndata
        read(iin,100) SIMBOL(i)
        read(iin,100) NUMCOD(i)
        read(iin,200) REFCOD(i)
        DO j=1,Nvar
          read (iin,300) Dini(i,j)
          if (j.ne.1) then
```

```
            Dini(i,j)=RAD(Dini(i,j))
          end if
        END DO
      END DO
C
      return
  100 FORMAT (A8)
  200 FORMAT (A6)
  300 FORMAT (F8.3)
      end
C
C-----------------------------------------------------------------------
      FUNCTION RAD(x)
C-----------------------------------------------------------------------
      IMPLICIT REAL*8 (A-H,O-Z)
      RAD=x*3.14159265359/180.
      return
      end
C
C-----------------------------------------------------------------------
      SUBROUTINE REDUN(REFCOD,Dini,Ndnr,D)
C-----------------------------------------------------------------------
      IMPLICIT REAL*8 (A-H,O-Z)
      PARAMETER (NF=1312,NC=1312,Ndata=1312,Nvar=6,
     *           Nfm=611,Nafm=701,iin=5,iout=6,EPSILON=1.D-2)
      DIMENSION REFCOD(NF),Dini(NF,NC),D(NF,NC)
      CHARACTER REFCOD(NF)*6
C
      k=1
      DO i=1,Ndata-1
        igual=0
        j=i+1
        DO WHILE ((igual.eq.0).and.(j.le.Ndata))
          if (REFCOD(i).eq.REFCOD(j)) then
            do=0
            m=1
            DO WHILE ((do.eq.0).and.(m.le.Nvar))
              if (DABS(Dini(i,m)-Dini(j,m)).lt.EPSILON) then
                igual=igual+1
              else
                if (DABS(Dini(i,m)-Dini(j,m)).ge.EPSILON) then
                  do=1
                  igual=0
                end if
              end if
              if ((m.eq.Nvar).and.(igual.ne.Nvar)) igual=0
              m=m+1
            END DO
          end if
          j=j+1
        END DO
          if (igual.eq.0) then
            REFCOD(k)=REFCOD(i)
            DO mm=1,Nvar
              D(k,mm)=Dini(i,mm)
            END DO
            k=k+1
          end if
      END DO
      REFCOD(k)=REFCOD(Ndata)
      DO mm=1,Nvar
        D(k,mm)=Dini(Ndata,mm)
      END DO
      Ndnr=k
C
      return
      end
```

```
C
C-----------------------------------------------------------------------
      SUBROUTINE PERM(Ndnr,D)
C-----------------------------------------------------------------------
      IMPLICIT REAL*8 (A-H,O-Z)
      PARAMETER (NF=1312,NC=1312,Ndata=1312,Nvar=6,
     *           Nfm=611,Nafm=701,iin=5,iout=6)
      DIMENSION D(NF,NC),DNORM(NF)
C
      DO i=1,Ndnr
        ang=0.
        dih=0.
        if (D(i,2).gt.D(i,3)) then
          ang=D(i,2)
          D(i,2)=D(i,3)
          D(i,3)=ang
          dih=D(i,5)
          D(i,5)=D(i,6)
          D(i,6)=dih
        endif
      END DO
C
C norma de cada un dels elements
      DO i=1,Ndnr
        DNORM(i)=0.
        DO j=1,6
          DNORM(i)=DNORM(i)+D(i,j)*D(i,j)
        END DO
          DNORM(i)=DSQRT(DNORM(i))
      END DO
C
C escribim la matriu de dades tq. # mesura, 6 variables, norma 6 var.
      write(iout,100)
      DO i=1,Ndnr
        write(iout,101) i,(D(i,j),j=1,6),DNORM(i)
      END DO
C
      return
  100 FORMAT(1X,'Mesura',4X,'Dist',6X,'A1',7X,'A2',7X,'T1',7X,'T2',
     *       7X,'T3',6X,'Norm')
  101 FORMAT(3X,I4,3X,7(F7.3,2X))
      end
C
C-----------------------------------------------------------------------
      SUBROUTINE DEUCL(D,Eucl,Ndnr)
C-----------------------------------------------------------------------
C calcul de la matriu de distancies Euclidianes entre 2 contactes
C qualssevol de la matriu D
C                        2    Nvar                    2
C             Eucl(k,l) = SUMatori [D(k,j)-D(l,j)] = SQEucl(k,l)
C                            j=1
C
C  D      matriu de dades en radians
C  SQEucl matriu SUMatori de diferencia de contactes al quadrat
C  Eucl   matriu de distancies Euclidianes
C  kpos   matriu q indica entre quins contactes (k,l) es calcula la
C           distancia Euclidiana -mateixa formula q en MMVB ;-)
C  VEC    matriu q usarem per ordenar les distancies de la matriu
C           Eucl de menor a major
C  FERRO  matriu dist INTERcluster menors que els radis de bola
C           obtinguts per a F-F --> en 1st col acumula el
C           VEC(1,1) i en 2nd la kpos(1,1) on l=Nfm+1,Ndnr
C  ANTIFE matriu dist INTERcluster menors que els radis de bola
C           obtinguts per a AF-AF --> en 1st col acumula el
C           VEC(1,1) i en 2nd la kpos(1,1) on l=1,Nfm
C
      IMPLICIT REAL*8 (A-H,O-Z)
```

```
      PARAMETER (NF=1312,NC=1312,Nvar=6,Nfm=611,Nafm=701,iin=5,iout=6,
     *           PI=3.14159265359)
      DIMENSION D(NF,NC),SQEucl(NF,NF),Eucl(NF,NF),kpos(NF,NF),
     *          VEC(NF,NF),FERRO(NF,2),ANTIFE(NF,2)
C
C k,l CONTROLEN LES FILES I j LES COLUMNES ... FEM (1a fila-1a fila),
C (2a fila-1a fila), (2a fila-2a fila), (3a fila-1a fila) ... as RESTA!
C ... ESTEM RESTANT ENTRE SI ELS CONTACTES QUE PERTANYEN A LA DIAGONAL
C INFERIOR DE LA MATRIU DE DADES Dij
C
      DO k=1,Ndnr
        DO l=1,k
          kpos(k,l)=0
          SQEucl(k,l)=0.
          DO j=1,Nvar
            RESTA=DABS(D(k,j)-D(l,j))
C
C corregim dihedres en aquells casos en que tenen signe negatiu
            if ((j.ge.4).and.(RESTA.gt.PI)) RESTA=2*PI-RESTA
            SQEucl(k,l)=SQEucl(k,l)+(RESTA)**2
          END DO
          Eucl(k,l)=DSQRT(SQEucl(k,l))
          kpos(k,l)=((k*(k-1))/2)+l
        END DO
      END DO
C
C ordenem de dist. mes petita a mes gran dins d'una mateixa columna "l"
C (k,l)=(fila,columna)
      DO l=1,Ndnr
        DO k=1,Ndnr
          if (k.lt.l) then
            VEC(k,l)=Eucl(l,k)
            kpos(k,l)=((l*(l-1))/2)+k
          else
            VEC(k,l)=Eucl(k,l)
            kpos(k,l)=kpos(k,l)
          end if
        END DO
        DO m=1,Ndnr-1
          if (m.le.Nfm) then
            N=Nfm
          else
            if (m.ge.(Nfm+1)) N=Ndnr
          end if
          DO n=m+1,N
            if (VEC(n,l).lt.VEC(m,l)) then
              aux=VEC(m,l)
                VEC(m,l)=VEC(n,l)
                VEC(n,l)=aux
              npos=kpos(m,l)
                kpos(m,l)=kpos(n,l)
                kpos(n,l)=npos
            end if
          END DO
        END DO
C
C Escribim les distancies min+max Fm-Fm/AFm-AFm i les Fm-AFm.
C Dins del "cluster" Fm la 1st. sera = 0.; dins del AFm ho sera
C la Nfm+1
C
        if (l.le.Nfm) then
          write(iout,100) kpos(1,1),VEC(2,1),kpos(2,1),VEC(Nfm,1),
     *                    kpos(Nfm,1),VEC(Nfm+1,1),kpos(Nfm+1,1),
     *                    VEC(Ndnr,1),kpos(Ndnr,1)
        else
          write(iout,100) kpos(Nfm+1,1),VEC(1,1),kpos(1,1),VEC(Nfm,1),
     *                    kpos(Nfm,1),VEC(Nfm+2,1),kpos(Nfm+2,1),
```

```
     *                          VEC(Ndnr,1),kpos(Ndnr,1)
          end if
        END DO
C
C busquem el radi max de la bola que *conte* 2 interaccions del
C mateix *signe* (ie. F-F o AF-AF) dins de cada un dels "cluster"'s
C ==> traduccio : d'entre les dist. min's INTRAcluster buscar la
C max !
        DO l=1,Ndnr-1
          if (l.le.Nfm) then
            Ncol=Nfm
            Nfila=2
          else
            Ncol=Ndnr
            Nfila=Nfm+2
          end if
          DO n=l+1,Ncol
            if (VEC(Nfila,n).gt.VEC(Nfila,l)) then
              aux=VEC(Nfila,l)
              VEC(Nfila,l)=VEC(Nfila,n)
              VEC(Nfila,n)=aux
              npos=kpos(Nfila,l)
            kpos(Nfila,l)=kpos(Nfila,n)
            kpos(Nfila,n)=npos
          end if
          END DO
        END DO
        write(6,101) 'RADI de *bola* Fm ',VEC(2,1),'  (i,j)=',kpos(2,1)
        write(6,101) 'RADI de *bola* AFm',VEC(Nfm+2,Nfm+1),'  (i,j)=',
     *                kpos(Nfm+2,Nfm+1)
C
C buscar les dist INTERcluster menors que els radis de bola obtinguts
C per a F-F i AF-AF
        NUMfm=0
        DO l=Nfm+1,Ndnr
          if (VEC(1,l).lt.VEC(2,1)) then
            NUMfm=NUMfm+1
            FERRO(NUMfm,1)=VEC(1,l)
            FERRO(NUMfm,2)=kpos(1,l)
          end if
        END DO
        NUMafm=0
        DO l=1,Nfm
          if (VEC(Nfm+1,l).lt.VEC(Nfm+2,Nfm+1)) then
            NUMafm=NUMafm+1
            ANTIFE(NUMafm,1)=VEC(Nfm+1,l)
            ANTIFE(NUMafm,2)=kpos(Nfm+1,l)
          end if
        END DO
        write(6,102) 'NUMfm =',NUMfm
        DO k=1,NUMfm
          write(6,103) FERRO(k,1),FERRO(k,2)
        END DO
        write(6,102) 'NUMafm=',NUMafm
        DO k=1,NUMafm
          write(6,103) ANTIFE(k,1),ANTIFE(k,2)
        END DO
        write(6,102) 'NUMfm =',NUMfm
        write(6,102) 'NUMafm=',NUMafm
C
        return
  100 FORMAT(I6,2X,4(F7.3,2X,I6,2X))
  101 FORMAT(A18,2X,F8.3,2X,A8,I6)
  102 FORMAT(A7,I4)
  103 FORMAT(F8.3,2X,F8.0)
        end
```

PUBLICACIONS

ARTICLE 1

Chem. Phys. Lett. **1997**, *265*, 190-199

Reprinted from

CHEMICAL PHYSICS LETTERS

Chemical Physics Letters 265 (1997) 190–199

Theoretical analysis of the crystal packing of nitronyl nitroxide radicals: the packing of the α-2-hydro nitronyl nitroxide radical

M. Deumal [a], J. Cirujeda [b], J. Veciana [b], M. Kinoshita [c], Y. Hosokoshi [d], Juan J. Novoa [a,*]

[a] *Departament de Química Física, Facultat de Química, Universitat de Barcelona, Av. Diagonal 647, 08028 Barcelona, Spain*
[b] *Institut de Ciencia de Materials de Barcelona, 08193 Bellaterra, Barcelona, Spain*
[c] *Science University of Tokyo in Yamaguchi, Daigaku-dori 1–1–1, Onoda-shi, Yamaguchi 756, Japan*
[d] *Institute for Solid State Physics, University of Tokyo, Roppongi, Minato-ku, Tokyo 106, Japan*

Received 17 June 1996; in final form 22 November 1996

ELSEVIER

EDITORS: A.D. BUCKINGHAM, D.A. KING, A.H. ZEWAIL
Assistant Editor: Dr. R. Kobayashi, Cambridge, UK

FOUNDING EDITORS: G.J. HOYTINK, L. JANSEN
FORMER EDITORS: R.B. BERNSTEIN, D.A. SHIRLEY, R.N. ZARE

ADVISORY EDITORIAL BOARD

Australia
B.J. ORR, Sydney

Canada
P.A. HACKETT, Ottawa
J.W. HEPBURN, Waterloo
C.A. McDOWELL, Vancouver

Czech Republic
Z. HERMAN, Prague

Denmark
F. BESENBACHER, Aarhus
G.D. BILLING, Copenhagen

France
E. CLEMENTI, Strasbourg
J. DURUP, Toulouse
J.-M. LEHN, Strasbourg
J.-L. MARTIN, Palaiseau
B. SOEP, Orsay

Germany
R. AHLRICHS, Karlsruhe
V.E. BONDYBEY, Garching
W. DOMCKE, Dusseldorf
G. ERTL, Berlin
G. GERBER, Würzburg
G.L. HOFACKER, Garching
D.M. KOLB, Ulm
J. MANZ, Berlin
M. PARRINELLO, Stuttgart
S.D. PEYERIMHOFF, Bonn
R. SCHINKE, Göttingen
E.W. SCHLAG, Garching
J. TROE, Göttingen
H.C. WOLF, Stuttgart
W. ZINTH, Munich

India
C.N.R. RAO, Bangalore

Israel
J. JORTNER, Tel Aviv
R.D. LEVINE, Jerusalem

Italy
V. AQUILANTI, Perugia

Japan
H. HAMAGUCHI, Tokyo
M. ITO, Okazaki
T. KOBAYASHI, Tokyo
K. KUCHITSU, Sakado
H. NAKATSUJI, Kyoto
K. TANAKA, Tokyo
K. YOSHIHARA, Okazaki

People's Republic of China
C.-H. ZHANG, Beijing

Poland
Z.R. GRABOWSKI, Warsaw

Russian Federation
A.L. BUCHACHENKO, Moscow
V.S. LETOKHOV, Troitzk
Yu.N. MOLIN, Novosibirsk

Spain
A. GONZÁLEZ UREÑA, Madrid

Sweden
P.E.M. SIEGBAHN, Stockholm
V. SUNDSTRÖM, Lund

Switzerland
M. CHERGUI, Lausanne-Dorigny
R.R. ERNST, Zurich
M. QUACK, Zurich

Taiwan, ROC
Y.T. LEE, Taipei

The Netherlands
A.J. HOFF, Leiden
A.W. KLEYN, Amsterdam
D.A. WIERSMA, Groningen

United Kingdom
M.N.R. ASHFOLD, Bristol
G.S. BEDDARD, Leeds
M.S. CHILD, Oxford
D.C. CLARY, London
R. FREEMAN, Cambridge
R.H. FRIEND, Cambridge
N.C. HANDY, Cambridge
A.C. LEGON, Exeter
R.M. LYNDEN-BELL, Belfast
J.P. SIMONS, Oxford
I.W.M. SMITH, Birmingham

USA
P. AVOURIS, Yorktown Heights, NY
A.J. BARD, Austin, TX
A.W. CASTLEMAN Jr., University Park, PA
S.T. CEYER, Cambridge, MA
D. CHANDLER, Berkeley, CA
F.F. CRIM, Madison, WI
A. DALGARNO, Cambridge, MA
C.E. DYKSTRA, Indianapolis, IN
K.B. EISENTHAL, New York, NY
M.A. EL-SAYED, Atlanta, GA
M.D. FAYER, Stanford, CA
G.R. FLEMING, Chicago, IL
R.M. HOCHSTRASSER, Philadelphia, PA
J.L. KINSEY, Houston, TX
S.R. LEONE, Boulder, CO
M.J. LESTER, Philadelphia, PA
W.C. LINEBERGER, Boulder, CO
B.V. McKOY, Pasadena, CA
W.H. MILLER, Berkeley, CA
K. MOROKUMA, Atlanta, GA
S. MUKAMEL, Rochester, NY
A. PINES, Berkeley, CA
A.R. RAVISHANKARA, Boulder, CO
S.A. RICE, Chicago, IL
P.J. ROSSKY, Austin, TX
R.J. SAYKALLY, Berkeley, CA
H.F. SCHAEFER III, Athens, GA
G.C. SCHATZ, Evanston, IL
R.E. SMALLEY, Houston, TX
W.C. STWALLEY, Storrs, CT
D.G. TRUHLAR, Minneapolis, MN
J.J. VALENTINI, New York, NY
G.M. WHITESIDES, Cambridge, MA
C. WITTIG, Los Angeles, CA
P.G. WOLYNES, Urbana, IL
J.T. YATES Jr., Pittsburgh, PA
R.N. ZARE, Stanford, CA

Contributions should, preferably, be sent to a member of the Advisory Editorial Board (addresses are given in the first issue of each volume) who is familiar with the research reported, or to one of the Editors:

A.D. BUCKINGHAM
D.A. KING
Editor of Chemical Physics Letters
University Chemical Laboratory
Lensfield Road
Cambridge CB2 1EW, UK
FAX 44-1223-336362

A.H. ZEWAIL
Editor of Chemical Physics Letters
A.A. Noyes Laboratory of Chemical Physics
California Institute of Technology
Mail Code 127-72
Pasadena, CA 91125, USA
FAX 1-818-4050454

After acceptance of the paper for publication, all further correspondence should be sent to the publishers (Ms. S.A. Hallink, Issue Management (Chemistry), Elsevier Science B.V., P.O. Box 2759, 1000 CT Amsterdam, The Netherlands; telephone 31-20-4852664, FAX 31-20-4852775, telex 10704 espom nl; electronic mail X400: C=NL; A=400NET; P=SURF; O=ELSEVIER; S=HALLINK, I=S or RFC822: S.HALLINK@ELSEVIER.NL).

Publication information: Chemical Physics Letters (ISSN 0009-2614). For 1997, volumes 264–280 are scheduled for publication. Subscription prices are available upon request from the publisher. Subscriptions are accepted on a prepaid basis only and are entered on a calendar year basis. Issues are sent by surface mail except to the following countries where Air delivery via SAL is ensured: Argentina, Australia, Brazil, Canada, Hong Kong, India, Israel, Japan, Malaysia, Mexico, New Zealand, Pakistan, PR China, Singapore, South Africa, South Korea, Taiwan, Thailand, USA. For all other countries airmail rates are available upon request. Claims for missing issues must be made within six months of our publication (mailing) date.

Copyright © 1997, Elsevier Science B.V. All rights reserved

0009-2614/1997/$17.00

US mailing notice – Chemical Physics Letters (ISSN 0009-2614) is published weekly by Elsevier Science B.V., Molenwerf 1, P.O. Box 211, 1000 AE Amsterdam. Annual subscription price in the USA US$ 7818.00, including air speed delivery, valid in North, Central and South America only. Periodicals postage paid at Jamaica, NY 11431. USA POSTMASTERS: Send address changes to Chemical Physics Letters, Publications Expediting, Inc., 200 Meacham Avenue, Elmont, NY 11003. Airfreight and mailing in the USA by Publication Expediting.

Printed in The Netherlands

Published weekly

Library of Congress Catalog Card Number 68-26532

ELSEVIER

31 January 1997

Chemical Physics Letters 265 (1997) 190–199

CHEMICAL PHYSICS LETTERS

Theoretical analysis of the crystal packing of nitronyl nitroxide radicals: the packing of the α-2-hydro nitronyl nitroxide radical

M. Deumal [a], J. Cirujeda [b], J. Veciana [b], M. Kinoshita [c], Y. Hosokoshi [d], Juan J. Novoa [a,*]

[a] *Departament de Química Física, Facultat de Química, Universitat de Barcelona, Av. Diagonal 647, 08028 Barcelona, Spain*
[b] *Institut de Ciencia de Materials de Barcelona, 08193 Bellaterra, Barcelona, Spain*
[c] *Science University of Tokyo in Yumaguchi, Daigaku-dori 1-1-1, Onoda-shi, Yamaguchi 756, Japan*
[d] *Institute for Solid State Physics, University of Tokyo, Roppongi, Minato-ku, Tokyo 106, Japan*

Received 17 June 1996; in final form 22 November 1996

Abstract

The crystal packing of the simplest member of the nitronyl nitroxide family of compounds, the 2-hydro nitronyl nitroxide radical in its α phase, is analyzed by means of a combination of distance analysis and accurate ab initio computations using correlated methods and extended basis sets. The packing is found to be driven by two types of intermolecular interactions, the $C(sp^2)$–H · · · O–N and $C(sp^3)$–H · · · O–N interactions, both of them found to be stable by ab initio computations (by −3.71 and −0.40 kcal/mol, respectively). The packing can be rationalized as planes kept together by $C(sp^2)$–H · · · O–N interactions. The planes are then linked by $C(sp^3)$–H · · · O–N interactions.

1. Introduction

The design of purely organic ferromagnetic materials has received considerable attention after the observation of bulk ferromagnetism in several nitronyl nitroxide radicals and C_{60} charge transfer salts [1–6]. The existence of this property in a crystal, successfully rationalized by various models [7–11], is a consequence of the way the unpaired electrons of adjacent molecules interact. Consequently, the presence of ferromagnetic interactions is affected by the distance and relative spatial orientation of the molecules in the crystal. In consequence, small variations in the molecular structure can create enough changes in the crystal packing as to severely modify the macroscopic magnetic properties. Therefore, it seems worthwhile to identify the key factors which determine the packing within the crystal of the molecules which are already known to present interesting magnetic properties as a step towards a better understanding of the magnetic properties of these systems and, hopefully, for the design of new organic ferromagnets with higher transition temperatures.

Due to the importance of nitronyl nitroxide radicals in the field of organic ferromagnets we will first

* Corresponding author.

0009-2614/97/$17.00 Copyright © 1997 Elsevier Science B.V. All rights reserved.
PII S0009-2614(96)01431-5

focus our attention on understanding the main factors controlling the packing of this family of free radicals with a general formula:

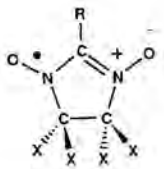

The crystal packing of these radicals is a compromise among all the possible intermolecular interactions that one molecule can make with all the adjacent ones. Rationalizing the whole packing implies understanding the effect created by each functional group which constitutes the molecule. Given the complexity of the problem one possible strategy of addressing it is by breaking down the molecule into chemically significant building units and studying the crystal packing of each of these parts separately and as they add up. One of the building units in the nitronyl nitroxide molecules is the five-membered ring where the two NO groups are located. The simplest persistent radical molecule associated to this five-membered ring would be that with R = H, i.e. the 2-hydro nitronyl nitroxide radical (or HNN) [12,13].

Besides the previous facts, the packing of HNN presents some extra interesting features. First of all, this molecule crystallizes into two polymorphs [15–18], identified as phases α and β. A thermal analysis performed with the α phase in the 40 to 160°C range shows an irreversible transition to the more stable β phase at 60.2°C and a thermal decomposition at 105.4°C. As a first step toward a better understanding of the key factors influencing the crystal packing of this family of compounds in this Letter we have centered our attention in finding the main factors directing the packing of the 2-hydro nitronyl nitroxide radical, using as reference system the so called α-phase (hereafter α-HNN) and a combination of short contacts analysis and quantum mechanical ab initio computations.

2. Methodology

The experimental packing structure of a crystal is one of the geometrical arrangements of the molecules of the crystal for which the packing energy is a minimum [15–18]. It is not necessarily the most stable one because the formation of a crystal is determined by thermodynamic and kinetic factors. Each minimum-energy structure corresponds, in principle, to one of the thermodynamically possible polymorphs. For a given polymorph, the optimum structure is a compromise between all the intermolecular interactions which can be made for the molecules constituting the crystal. Consequently, it is possible that some of the intermolecular interactions are not in their minimum conformation and optimum energy. The set of more stable polymorphs, among which one expects to find the experimental structures, corresponds to crystal packings that maximize the number of contacts within the set of stronger interactions. For these polymorphs, the energetically dominant interactions are within the set of shortest intermolecular distances. Thus, we can understand the main factors governing the packing of a low energy polymorph by (1) systematically identifying the shortest intermolecular interactions, (2) accurately computing the nature of these interactions (strength and directionality) using quantum mechanical ab initio methods and (3) by using the information from the previous two steps to rationalize the packing.

To locate the shortest intermolecular interactions in the α-HNN crystal one has to identify the functional groups capable of forming hydrogen bonds or van der Waals contacts, the only two types of contacts that the neutral HNN molecules can make. This can be done in a systematic way using the information included in the molecular electrostatic potential map. Then, an accurate study of the strength and directionality of the interaction energy of a given intermolecular contact is done using an appropriate model complex where the interaction of interest is present in a chemical environment as close as possible to the one present in the crystal. The model system has to be small to make the computation possible but big enough to include all the important inductive and polarization effects induced by nearby functional groups of the HNN molecule.

In these model systems, the interaction energy is computed using extended basis sets of so called adequate class [19] and second-order or fourth-order Møller–Plesset methods (MP2 and MP4, respectively). Previous tests have shown that one can obtain with these methods accurate descriptions of the intermolecular interactions in neutral hydrogen bonds and van der Waals complexes [19–21] once the interaction energy is corrected from the possible basis set superposition error [19,22,23] using the full counterpoise method [24]. All the quantum mechanical computations reported here were done using the procedures implemented in the Gaussian 94 suite of programs [25].

3. Results and discussion

The crystal of the α phase of the HNN molecule, belongs to the $P2_1/n$ space group and has the following crystallographic parameters: $a = 11.879$ Å, $b = 11.611$ Å, $c = 6.332$ Å, $\beta = 104.48°$, being $Z = 4$. The packing of this crystal is shown in Fig. 1 in an extended view, indicating by broken lines the shortest H ··· O contacts. The shortest contacts are the most likely candidates to be the driving forces of the packing due to the Morse shape of the intermolecular potentials. However, the crystal packing is just a compromise among all the possible interactions and long-range intermolecular contacts can be

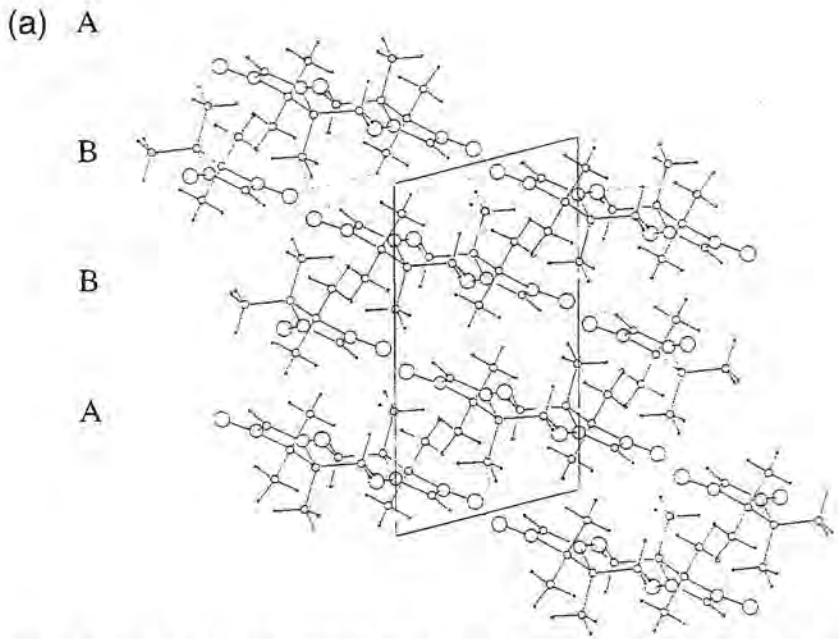

Fig. 1. Plots of the packing of the α-HNN crystal showing the shortest C–H ··· O contacts. (a) extended view along the *b* axis showing the four planes (ABBA) which lie within the unit cell; (b) view of the plane along the *a* axis; (c) stereoview showing the shortest contacts of a dimer belonging to the A shell with the molecules of the same plane and one of the closest B planes.

more attractive than short ones and short ones can be repulsive if they allow the formation of other strong attractive contacts. Consequently, one has to complement the distance analysis with information on the energetics of each short contact.

To localize the dominant contacts in α-HNN, we looked at the H···H, H···O and O···O contacts, which totally determine the packing, as discussed below. The results are collected in Table 1 and can be summarized as follows: the crystal can be visualized as a set of dimeric units oriented to maximize their short contacts. Each dimer presents two intradimer $C(sp^2)$–H···O–N bonds. However, it still has two more N–O groups and eight methyl groups to interact with other dimers. The shortest interdimer contacts are two $C(sp^2)$–H···O–N hy-

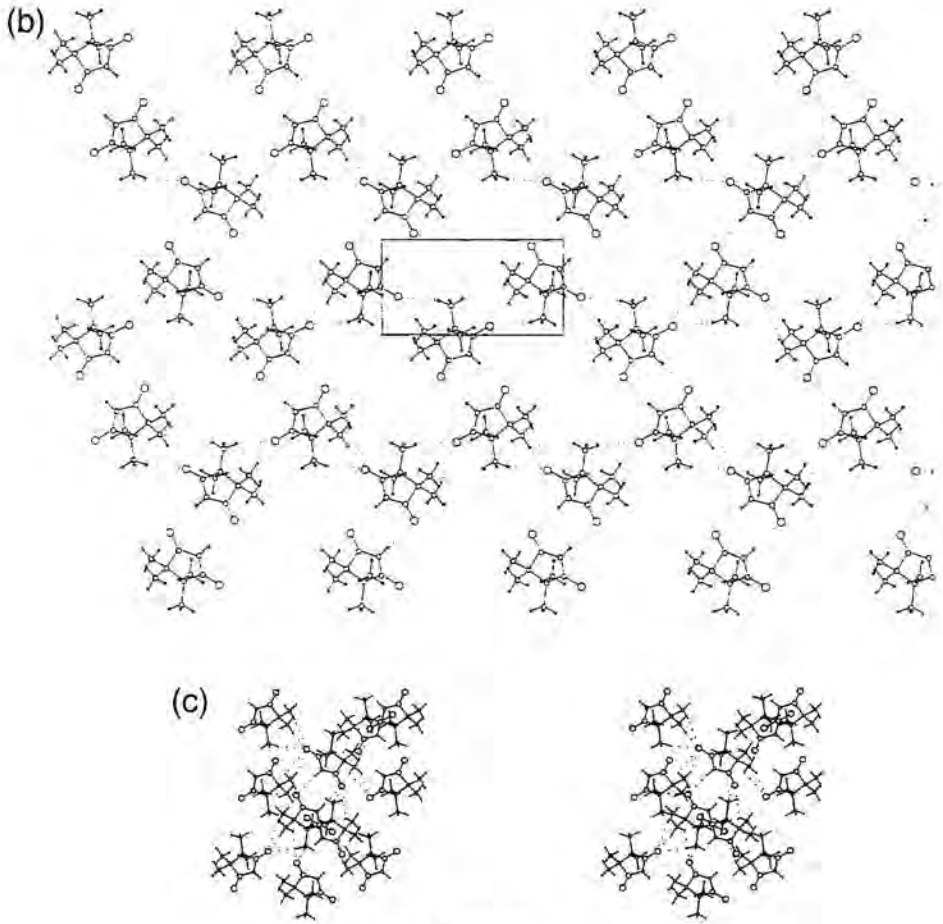

Fig. 1. Continued.

Table 1
Shortest intermolecular distances within the α-HNN crystal

Class	Contact type	Distance [a]	Number of contacts [b]
muraplane	$C(sp^2)$–H · · · O	2.416	2
	$C(sp^3)$–H · · · O	2.554	4
		2.636	4
		2.844	4
	$C(sp^2)$–H · · · H–$C(sp^2)$	2.689	1
	$C(sp^3)$–H · · · H–$C(sp^3)$	2.790 [c]	4
	N–O · · · O–N	4.271	1
interplane	$C(sp^3)$–H · · · O	2.535	2
		2.663	2
		2.833	2
	$C(sp^2)$–H · · · H–$C(sp^3)$	2.660	2
		2.829	2
	$C(sp^3)$–H · · · H–$C(sp^3)$	2.548	2
		2.640	2
		2.646	2
		2.649	2
	N–O · · · O–N	3.798	2

[a] In Å.
[b] Per dimer.
[c] The next contact is at a distance > 3.20 Å.

drogen bonds and two sets of three $C(sp^3)$–H · · · O–N bonds. The resulting pattern when these two types of contacts are combined is a plane of dimers in which each dimer makes four contacts in perpendicular directions. This pattern is like a two-dimensional square network and leaves rectangular holes between the dimers. Each pair of connected dimers make only one contact between them.

Once the planes are formed, interplane $C(sp^3)$–H · · · O–N bonds can be made using the C–H and NO groups of the neighboring planes not employed in the in-plane contacts. Alternatively, the planes can be connected by long distance $C(sp^2)$–H · · · O–N contacts. To maximize the number and strength of these contacts there is a relative displacement by two cell units of one of the planes. Besides this displacement, the planes are identical in structure. Within each unit cell there are four planes related by the center of inversion located in the (0.5, 0.5, 0.5) crystallographic position. Due to the relative displacement of the planes we can distinguish between two different planes, A and B. The ordering of the four planes within the cell is ABBA, with the B planes closer to the inversion center, as shown in Fig. 1a.

A justification of the packing described above is possible looking at the way the HNN molecules aggregate. The α-HNN crystal can be visualized as a progressive build up of packing units. Thus, by looking at the energetics of formation of small aggregates one can localize the driving forces of the packing. Large aggregates can present new minima by combining the ones from two or more units and/or modifying the strength of the minima already present in the small ones. However, giving the distances among the packing units this second effect is not expected to be large. Therefore, if one maps the attractive and repulsive energetic regions for the interaction between two units one has a good starting idea of how the packing motifs between these units can be. In many cases, as in the one studied here, this mapping can be done by looking at the molecular electrostatic map (MEP) of the isolated molecule [26,27], sometimes even by simplistic considerations about the orientation of their charge distributions. The MEP maps plot the regions around the molecule where a positive unit charge is attracted (negative regions) or repelled (positive regions) and the strength of such an interaction. The HNN molecule has no net charge and has a strong dipole moment of 3.872 D at the Hartree–Fock/6-31G(d,p) level, resulting from the two bond dipoles located on each NO group. Therefore, one can expect the presence of strong dipole–dipole electrostatic interactions between the dimers. A simple dipole–dipole model for the interaction justifies the preference of this molecule to form planes, as this is the most stable arrangement of the two dipoles. However, this simple model does not give much information on the fine details of the packing. A better idea can be obtained by analyzing the molecular electrostatic map of the isolated HNN molecule (Fig. 2a, computed using the Hartree–Fock method and 6-31g(d,p) basis set). For systems where the electrostatic components of the interaction energy are dominant, as in the HNN case, the MEP map is close to the interaction energy map.

The most energetically favorable orientations of the HNN dimer can be located by overlapping the MEP maps of each HNN molecule: the overlap of positive and negative regions is energetically favored, while the overlap of regions of the same sign

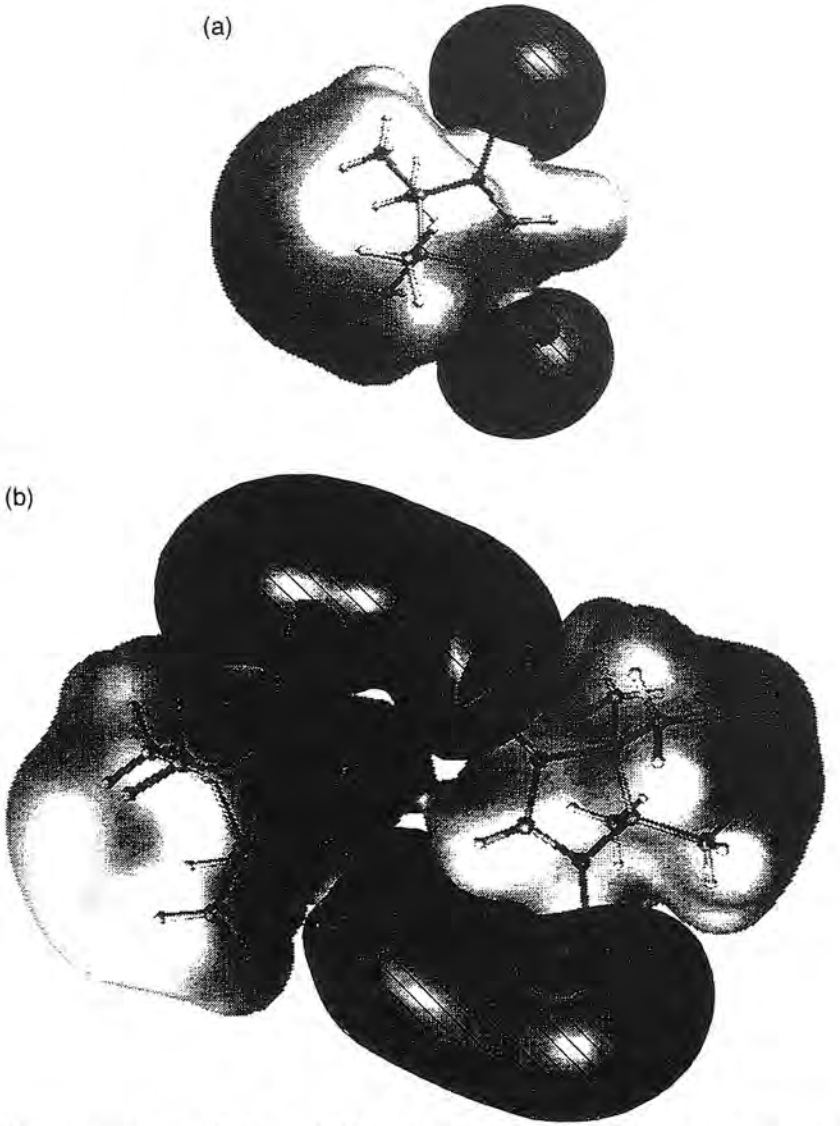

Fig. 2. Molecular electrostatic maps: (a) HNN molecule, (b) HNN dimer. The color code is the following: in black, at a potential of −48 kcal/mol, are indicated the four regions where the absolute minima are located (at −56 kcal/mol for the monomer and −61 kcal/mol for the dimer); the regions of −10 kcal/mol are shaded and the regions of +10 kcal/mol are light.

is not. The process can easily be extended to higher aggregates. The MEP map of each HNN molecule (Fig. 2a) shows a strong attractive area over the two oxygens, with the minima located in the N–C–N plane in the same spatial positions where the two sp^2 lone pair electrons of each oxygen would be located. At the same time, one finds free positive regions (i.e. not surrounded by negative regions) in the $C(sp^2)$ carbon hydrogen and in the methyl hydrogens.

The overlap analysis of two HNN maps allows the identification of many types of stable geometrical arrangements for the HNN dimer, five of which (the most interesting ones in the light of the previous packing analysis) are shown in Fig. 3. Arrangements 1–3 are the main in-plane contacts. Arrangement 1 is an eight-membered ring resulting from the formation of two $C(sp^2)$–H · · · O–N intradimer contacts. Arrangement 2 is a non-dimeric $C(sp^2)$–H · · · O–N contact (the two molecules are not necessarily placed in the same plane). Arrangement 3 is due to the presence of three $C(sp^3)$–H · · · O–N contacts. The most interesting out-of-plane arrangements found after analyzing the interplane contacts (see Fig. 1) are Arrangements 4 and 5. The first one consists of $C(sp^3)$–H · · · O–N contacts in a different spatial conformation than Arrangement 3. Arrangement 5 is characterized by the formation of two $C(sp^2)$–H · · · O–N interplane contacts. Notice that this MEP overlap analysis does not give any information on the relative stability of each arrangement, information which can be computed using ab initio methods.

Once the dimer is formed, the next HNN molecule (or new dimer) will be attached to the first dimer following the same overlap rules described for the dimer. The MEP map of the dimer (see Fig. 2b) is nearly an addition of the two MEP maps of each monomer, with an almost negligible potential in the places where the two monomers are contacting. It shows two strong attractive regions on the non-bonded NO groups and positive regions on the terminal methyls. Consequently, it is possible to make new $C(sp^3)$–H · · · O–N contacts between dimeric units. Its number is maximized if the dimers form planes. The MEP overlap analysis also shows that the conformations with short N–O · · · O–N contacts are not very likely because they imply the overlap of strongly negative areas, and this is highly unstable energetically. We have estimated the nature of the

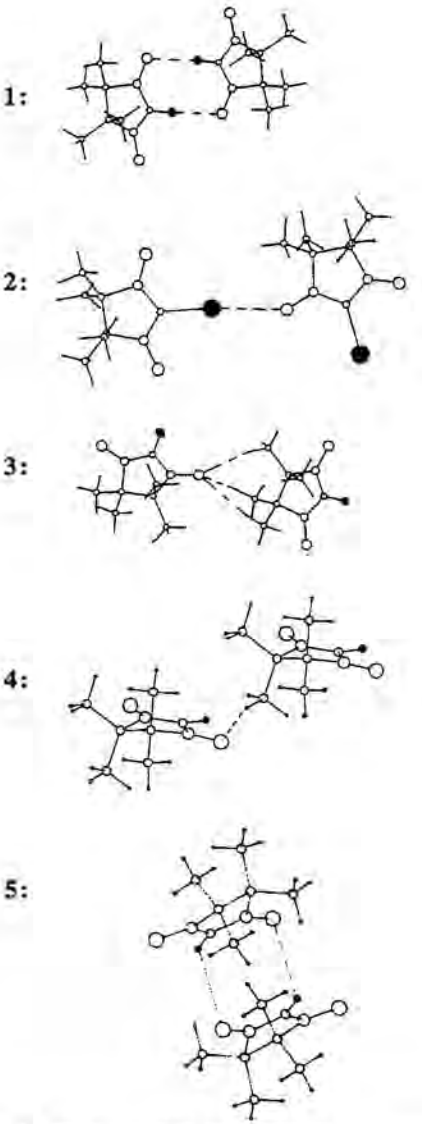

Fig. 3. Types of energetically stable geometrical arrangements predicted by the MEP overlap analysis.

N–O · · · O–N interaction using as model system a H_2NO dimer with the two NO groups pointing to each other at 180°. The interaction energy is repulsive at all distances, being about +1 kcal/mol at the sum of the oxygens van der Waals radii. This is key for the design of nitronyl nitroxide magnets because it is in the NO groups where most of the spin is located.

To give a more quantitative description of the packing of the α-HNN crystal we have to compute the strength of the previous arrangements. We began by evaluating the energy of the $C(sp^2)$–H · · · O–N interaction. This was done at the MP2/6-311 + + G(2d,2p) level using Model I (see Scheme 1). In this model the geometry of each fragment is the one found for the HNN molecules in the α-HNN crystal, and the values of r and θ (2.416 Å and 142.1°, respectively) are also the values in the crystal. The methyl groups have been deleted and the remaining $C(sp^3)$ atom attached to the N atoms have been substituted by hydrogen atoms located at 1.11 Å. It is possible to select smaller fragments of the HNN which also contain the interaction of interest for the models, as the $H_2NO \cdots CH_3$ dimer. However, there is an important inductive effect created by the NO groups which these smaller models do not describe: MP2/6-311 + + G(2d,2p) computations on the $H_2NO \cdots CH_3$ dimer and $H_2NO \cdots CH(NO)_2$ dimer indicated that the inclusion of the two NO groups doubles the strength of the interaction. The optimum orientation for the latter dimers is with the CH in the H_2NO plane and around the direction of the $O(sp^2)$ lone pairs, as predicted by the MEP maps.

The BSSE-corrected MP2/6-311 + + G(2d,2p) interaction energy obtained using Model I is −3.71 kcal/mol, our estimate for the strength of the $C(sp^2)$–H · · · O–N interactions and of Arrangement 2. Arrangement 1 has two contacts $C(sp^2)$–H · · · O–N and its strength should be twice the previous value, assuming that the fragments are located at their optimum geometry. A more correct estimate of the strength of Arrangement 1 can be obtained using a variation of Model I in which the monomers are oriented as in this arrangement. The BSSE-corrected MP2/6-311 + + G(2d,2p) interaction energy obtained in this case is −5.53 kcal/mol, i.e. less than twice the energy of an isolated $C(sp^2)$–H · · · O–N contact. This is an indication that in the crystal the dimer is not in its optimum geometry, probably due to the distortions induced by other interactions.

The strength of the $C(sp^3)$–H · · · O–N interaction was computed using Model II at the MP2/6-311 + G(2d,2p) level in which the r and θ values are 2.637 Å and 128.7°, typical values of the $C(sp^3)$–H · · · O–N contacts found in Arrangements 3 and 4 within the α-HNN crystal. Our best BSSE-corrected interaction energy for the $C(sp^3)$–H · · · O–N contact is −0.40 kcal/mol, i.e., about

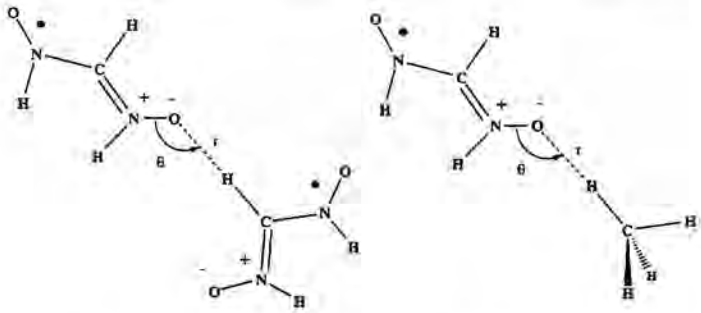

Model I Model II

Scheme 1.

one tenth of the interaction energy of an isolated $C(sp^2)$–H ··· O–N contact, a key factor for understanding the packing of the α-HNN crystal. Computations with smaller model systems, such as the $H_2NO \cdots CH_4$ dimer, gave optimum values of r and θ of 2.544 Å and 84.7°, and a BSSE-corrected interaction energy of −0.667 kcal/mol, smaller than that computed using Model II due to the inductive effect of the NO group. With these values we can directly estimate the strength of Arrangement 4, which has only one $C(sp^3)$–H ··· O–N contact. We have also estimated the strength associated to Arrangement 3. The latter presents three $C(sp^3)$–H ··· O–N contacts which can be considered as independent due to the small polarizability of a C atom. Consequently, its total strength is about three times the energy of a $C(sp^3)$–H ··· O–N interaction. The energy associated to Arrangement 5 was computed using a model dimer similar to Model I but oriented adequately to mimic the geometry of this arrangement within the crystal (i.e. with the H ··· O located at 3.331 Å and the C–H ··· O angle being 85.3°). The BSSE-corrected energy for such a contact is −1.38 kcal/mol at the MP2/6-311 + + G(2d,2p) level, i.e. −0.69 kcal/mol per $C(sp^2)$–H ··· O–N bond. This is interesting because even at such a large distance the $C(sp^2)$–H ··· O–N contact is a bit stronger than an isolated $C(sp^3)$–H ··· O–N one at their optimum geometry. Although the number of $C(sp^3)$–H ··· O–N bonds that the HNN molecules can make is larger, one cannot discard the influence of Arrangement 5 in determining the packing of the α-HNN crystal.

4. Concluding remarks

Ab initio computations show that all the arrangements included in Fig. 3 are stabilizing, in good agreement with predictions from the overlap of MEP maps. All the arrangements are constituted by C–H ··· O–N intermolecular interactions. This is just a class of the more general C–H ··· O intermolecular contact, found to be attractive from statistical analysis and ab initio computations [28,29]. Our results provide an estimate of the $C(sp^3)$–H ··· O–N and $C(sp^2)$–H ··· O–N interactions (−0.40 and −3.71, respectively) not far from the values for the $C(sp^3)$–H ··· OH_2 and $C(sp^2)$–H ··· OH_2 interactions (−0.40 and −1.01 kcal/mol, respectively [29]). All of them are larger than the $C(sp^3)$–H ··· H contacts, also present in the α-HNN crystal, whose strength is −0.12 kcal/mol [30]. We have also computed the relative strength for the five types of arrangements found in the crystal ($1 \gg 2 > 3 \cong 5 > 4$).

Using the data from the ab initio computations, we can reanalyze the structure of the α-HNN crystal These results explain the strong tendency of HNN to form dimers (see Arrangement 1). Once these dimers are formed, they can aggregate making as many as possible Arrangement 3 tetramers. As the number of their contacts is maximized by keeping the molecules in the same plane, they do so. The connection between consecutive planes is done by the $C(sp^3)$–H ··· O–N contacts present in Arrangement 4 and also by $C(sp^2)$–H ··· O–N contacts of the type involved in Arrangement 5. The $C(sp^3)$–H ··· H contacts also present in the crystal just stabilize the crystal in a non-directional way. The spatial combination of these arrangements is not unique.

Acknowledgements

This work was supported by the CICYT (Grant No. MAT94-0797), the DGICYT (Project No. PB92-0655-C02-02 and PB95-0848-C02-02), CIRIT (GRP94-1077 and GRQ93-8028), the NEDO (Grant Organic Magnets) and CESCA and CEPBA. MD and JC acknowledge CIRIT for their doctoral grants.

References

[1] H. Tamura, Y. Nakazawa, D. Shiomi, K. Nozawa, Y. Hosokoshi, M. Ishikawa, M. Takahashi and M. Kinoshita, Chem. Phys. Lett. 186 (1991) 401.
[2] P.-M. Allemand, K.C. Khemani, A. Koch, F. Wudl, K. Holezer, S. Donovan, G. Guner and J.D. Thompson, Science 253 (1991) 301.
[3] R. Chiarelli, M.A. Novak, A. Rassat and J.L. Tholence, Nature (London) 363 (1993) 147.
[4] T. Tomioka, H. Ishida, H. Yoshikawa, M. Yami, F. Iwasaki, H. Iwamura, N. Takeda and M. Ishikawa, Chem. Lett. 29 (1994).
[5] T. Sugawara, M.M. Matsushita, A. Izouka, N. Wada, N. Takeda and M. Ishikawa, J. Chem. Soc. Chem. Commun. (1994) 1723.
[6] J. Cirujeda, M. Mas, E. Molins, F. Lanfranc de Panthou, J.

Laugier, J.-G. Park, C. Paulsen, P. Rey, C. Rovira and J. Veciana, J. Chem. Soc. Chem. Commun. (1995) 709.
[7] H.M. McConnell, J. Chem. Phys. 39 (1963) 1910.
[8] H.M. McConnell, Proc. Robert A. Welch Found. Conf. Chem. Res. 11 (1967) 144.
[9] M. Kinoshita, Jpn. J. Appl. Phys. 33 (1994) 5718 and references cited therein.
[10] O. Kahn, Molecular magnetism (VCH, New York, 1993).
[11] J.S. Miller and A.J. Epstein, Angew. Chem. Int. Ed. Engl. 33 (1994) 385.
[12] D.G.B. Boocock, R. Darey and E.F. Ullman, J. Am. Chem. Soc. 90 (1968) 5945.
[13] Y. Hosokoshi, M. Tamura, K. Nozawa, S. Suzuki, H. Sawa, R. Kato and M. Kinoshita, Mol. Cryst. Liq. Cryst. 115 (1995) 271.
[15] A. Gavezzotti, Acc. Chem. Res. 27 (1994) 309.
[16] J. Bernstein, J. Phys. D: Appl. Phys. 26 (1993) B66.
[17] J.D. Dunitz and J. Bernstein, Acc. Chem. Res. 28 (1995) 193.
[18] H.R. Karfunkel and R.J. Gdanitz, J. Comput. Chem. 13 (1992) 1171
[19] F.B. van Duijneveldt, J.G.C.M. van Duijneveldt-van der Rijdt and J.H. van Lenthe, Chem. Rev. 94 (1994) 1873.
[20] J.H. van Lenthe, J.G.C.M. van Duijneveldt-van de Rijdt and R.F. van Duijneveldt, in: Ab initio methods in quantum chemistry, Vol. II, ed. K.P. Lawley (Wiley, New York, 1987).
[21] P. Hobza and R. Zahradnik, Chem. Rev. 88 (1988) 871.
[22] J.J. Novoa, M. Planas and M.-H. Whangbo, Chem. Phys. Lett. 225 (1994) 240.
[23] J.J. Novoa, M. Planas and M.C. Rovira, Chem. Phys. Lett. 251 (1996) 33 and references therein
[24] S.F. Boys and F. Bernardi, Mol. Phys. 19 (1970) 553.
[25] M.J.Frisch, G.W. Trucks, H.B. Schlegel, P.M.W. Gill, B.G. Johnson, M.A. Robb, J.R. Cheeseman, T. Keith, G.A. Petersson, J.A. Montgomery, K. Raghavachari, M.A. Al-Laham, V.G. Zakrzewski, J.V. Ortiz, J.B. Foresman, J. Cioslowski, B.B. Stefanov, A. Nanayakkara, M. Challacombe, C.Y. Peng, P.Y. Ayala, W. Chen, M.W. Wong, J.L. Andres, E.S. Replogle, R. Gomperts, R.L. Martin, D.J. Fox, J.S. Binkley, D.J. Defrees, J. Baker, J.J.P. Stewart, M. Head-Gordon, C. Gonzalez and J.A. Pople, Gaussian 94, Revision C.3 (Gaussian, Pittsburgh, PA, 1995).
[26] E. Scrocco and J. Tomasi, Adv. Quantum Chem. 11 (1978) 115.
[27] P. Politzer and J.S. Murray, Rev. Comput. Chem. 2 (1991) 273.
[28] G. Desiraju, Acc. Chem. Res. 24, (1991) 290, and references therein.
[29] M.C. Rovira, J.J. Novoa, M.-H. Whangbo and J.M. Williams, Chem. Phys. 200 (1995) 319. and references therein.
[30] J.J. Novoa, M.-H. Whangbo, and J.M. Williams, J. Chem. Phys. 94 (1991) 4835.

Orders, claims, and product enquiries: please contact the Customer Support Department at the Regional Sales Office nearest to you:

New York
Elsevier Science
P.O. Box 945
New York, NY 10159-0945
USA
Tel. (+1)212-633-3730
[Toll free number for North American customers: 1-888-4ES-INFO (437-4636)]
Fax (+1)212-633-3680
e-mail: usinfo-f@elsevier.com

Amsterdam
Elsevier Science
P.O. Box 211
1000 AE Amsterdam
The Netherlands
Tel. (+31)20-4853757
Fax (+31)20-4853432
e-mail: nlinfo-f@elsevier.nl

Tokyo
Elsevier Science
9-15 Higashi-Azabu 1-chome
Minato-ku, Tokyo 106
Japan
Tel. (+81)3-5561-5033
Fax (+81)3-5561-5047
e-mail: kyf04035@niftyserve.or.jp

Singapore
Elsevier Science
No. 1 Temasek Avenue
#17-01 Millenia Tower
Singapore 039192
Tel. (+65)434-3727
Fax (+65)337-2230
e-mail: asiainfo@elsevier.com.sg

Advertising information: Advertising orders and enquiries may be sent to: **International:** Elsevier Science, Advertising Department, The Boulevard, Langford Lane, Kidlington, Oxford OX5 1GB, UK, Tel. (+44)(0)1865 843565, Fax (+44)(0)1865 843976. **USA and Canada:** Weston Media Associates, Daniel Lipner, P.O. Box 1110, Greens Farms, CT 06436-1110, USA, Tel. (+1)(203)261-2500, Fax (+1)(203)261-0101. **Japan:** Elsevier Science Japan, Marketing Services, 1-9-15 Higashi-Azabu, Minato-ku, Tokyo 106, Japan, Tel. (+81)3-5561-5033, Fax (+81)3-5561-5047.

Electronic manuscripts: Electronic manuscripts have the advantage that there is no need for the rekeying of text, thereby avoiding the possibility of introducing errors and resulting in reliable and fast publication.

Your disk plus three, final and exactly matching printed versions should be submitted together. Double density (DD) or high density (HD) diskettes ($3^1/2$ or $5^1/4$ inch) are acceptable. It is important that the file saved is in the native format of the wordprocessor program used. Label the disk with the name of the computer and wordprocessing package used, your name, and the name of the file on the disk. Further information may be obtained from the Publisher.

Authors in Japan please note: Upon request, Elsevier Science Japan will provide authors with a list of people who can check and improve the English of their paper (*before submission*). Please contact our Tokyo office: Elsevier Science Japan, 1-9-15 Higashi-Azabu, Minato-ku, Tokyo 106; Tel. (03)-5561-5032; Fax (03)-5561-5045.

Chemical Physics Letters has no page charges.

For a full and complete Instructions to Authors, please refer to *Chemical Physics Letters*, Vol. 264, No. 6, pp. 700–701. The instructions can also be found on the World Wide Web: access under http://www.elsevier.nl or http://www.elsevier.com.

♾ The paper used in this publication meets the requirements of ANSI/NISO Z39.48-1992 (Permanence of Paper)

ARTICLE 2

Mol. Cryst. Liq. Cryst. **1997**, *305*, 143-156

Mol. Cryst. Liq. Cryst., 1997, Vol. 305, pp. 143–156
Reprints available directly from the publisher
Photocopying permitted by license only

© 1997 OPA (Overseas Publishers Association)
Amsterdam B.V. Published in The Netherlands
under license by Gordon and Breach Science Publishers
Printed in India

THEORETICAL ANALYSIS OF THE PACKING AND POLIMORPHISM OF MOLECULAR CRYSTALS USING QUANTUM MECHANICAL METHODS: THE PACKING OF THE 2-HYDRO NITRONYL NITROXIDE

JUAN J. NOVOA AND MERCE DEUMAL
Departament de Química Física, Facultat de Química, Universitat de Barcelona,
Av. Diagonal 647, 08028-Barcelona (Spain)

Abstract The crystal packing of molecular crystals can be rationalized using quantum mechanical ab initio methods. This work describes the principles in which this approach is based, applying the basic principles to the 2-hydro nitronyl nitroxides. Two forms of packing analysis using ab initio methods are described. The first one is based on the use of the molecular electrostatic maps for the molecules. The second one uses the information about the strength of the molecular interactions present in the crystal provided by accurate ab initio computations from model systems. Using this information it is possible to rationalize the packing in terms of primary, secondary and so on structures. For the 2-hydro nitronyl nitroxide radical the $C(sp^2)$-H···O contacts should be the driving force behind the primary structure of the packing, while the $C(sp^3)$-H···O contacts should be responsible of the secondary structure. The N-O···O-N contacts are found to be repulsive.

INTRODUCTION

It is commonly accepted that the presence of magnetism in a molecular crystal and its dimensionality depends on the way the crystal packs, that is, on the distance and relative spatial orientation of the molecules which constitute the crystal.[1] Small changes in the molecular structure create changes in the crystal packing which give rise to a modification in the macroscopic observed magnetic properties. This is the commonly accepted justification for the wide variation of magnetic properties found within families of compounds. Therefore, understanding and controlling the factors which govern the packing of these crystals is a key step towards the design of molecular magnetic crystals. This is the aim of

this work, where our attention is focused in rationalizing the packing of the simplest member of the nitronyl nitroxide family of radicals, the 2-hydro nitronyl nitroxide radical (hereafter identified as HNN), using the information from ab initio quantum mechanical methods and from the distance analysis of the crystal.

The nitronyl nitroxide radicals is one of the most interesting families in the field of organic ferromagnetism. Their general formula is:

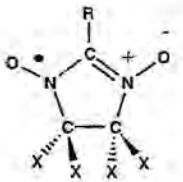

In this rather large family, the HNN radical is the member with R=H. It was first synthesized by Ullman et al.[2] and a recent study[3] has allowed to find two crystal phases (thereafter identified as the α-HNN and β-HNN phases) which show an antiferromagnetic behavior. A thermal analysis of the α-HNN phase[3,4] in the 40-160 °C range shows the presence of an irreversible transition to the more stable β-HNN phase at 60.2 °C. At 105.4 °C the α-HNN crystals begins thermal decomposition.

Why to select the HNN radical as the focus of our study and not another member of the nitronyl family showing ferromagnetism?. There are various reasons for this choice, the first one being the size of the molecule, which allows to use highly accurate ab initio methods and test options at a lower computational cost. Furthermore, this radical presents an interesting and well documented polymorphism which it is interesting to study. Last but not least, the HNN molecule is a good model to understand the packing properties of the five member ring part of the nitronyl nitroxide family. This information can then be combined with the packing behavior of the R group to predict the expected packing of any molecule of the nitronyl nitroxide family.

PACKING STRUCTURE AND INTERMOLECULAR FORCES

According to the modern ideas about the design of molecular crystals,[5] except in some simple cases, it is possible to predict only one packing structure from a theoretical analysis. Instead one should expect to find a set of structures, which hopefully contains the experimental ones. Each of these minimum structures is one of the polymorphs the crystal

can present, often a set of 10 structures which differ by less than 2 kcal/mol from the most stable one for each symmetry group of the crystal. Consequently, we are facing a problem of multiple minima (each polymorph) separated by small or large energetic barriers. The experimental structures are not necessarily the most stable ones, as kinetic and other factors can play an important role in the way the crystal grows in a saturated solution. The problem is similar to that of finding the minimum structures in a molecule or molecular aggregate.

Computationally, the problem of finding one minimum for the molecular crystal is one of locating the geometrical arrangement of the molecules which minimizes the packing potential energy of the crystal, which is normally written as a sum over all the pairs of the possible pair intermolecular interactions:

$$E = \sum' E_{ij}(r_{ij})$$

being $E_{ij}(r_{ij})$ any of the intermolecular interactions between atoms i and j located at a distance r_{ij}. To lower the computational cost, in many cases the geometry of the interacting molecules is considered to be frozen, based on the fact that for weak intermolecular interactions the geometrical distortions in the interacting molecules is small.

The shape of the $E_{ij}(r_{ij})$ intermolecular potential results from the addition of the following four components: repulsive (V_{rep}), electrostatic (V_{ele}), induction (V_{ind}) and dispersion (V_{dis}). The first one is always repulsive and is proportional to the overlap of the electron distributions. It is only important at short distance and is responsible for the so called repulsive wall which avoids the collapse of one atom atoms into another. The remaining three components are all attractive and have the following form:

$$V_{ele} = -\frac{1}{4\pi\varepsilon_o}\frac{q_i q_j}{r_{ij}} - \frac{2}{3kT(4\pi\varepsilon_o)^2}\frac{\mu_i^2\mu_j^2}{r_{ij}^6}$$

$$V_{ind} = -\frac{1}{(4\pi\varepsilon_o)^2}\frac{(\mu_i^2\alpha_j + \mu_j^2\alpha_i)}{r_{ij}^6}$$

$$V_{dis} = -\frac{3}{4(4\pi\varepsilon_o)^2}\frac{\alpha_i\alpha_j}{r_{ij}^6}\frac{I_i I_j}{(I_i + I_j)}$$

V_{ele} is the dominant term if the molecules have net charge. In the other case is also important and, in general, $V_{ele} > V_{ind} > V_{dis}$. This is specially true for systems with strong dipole moments, as the many nitronyl nitroxides.

One can simplify the analysis centering our attention in the energetically dominant interactions. As the shape of the $E_{ij}(r_{ij})$ intermolecular interactions is a Morse curve, the most important energetic contributions come from interactions located close to the minimum of the curve. The shortest intermolecular contacts to any given atom are small in number and are statistically located in the space along the directions in which the interaction is more stable. This is the base of the statistical analysis of intermolecular interactions. As one increases the distance, the number of contacts increases, but they are located in all the directions of the space. At very large distances, they can be considered as uniformly distributed in the space, thus creating an isotropic Madelung field. This field is the one created by the rest of the crystal in any given atom in its interior and works like the external field in a particle in a box model and stabilizes the energetic levels of the overall system and, in this way, the $E_{ij}(r_{ij})$ interactions. As all intermolecular interactions will feel a similar Madelung field, probably it is not going to change the relative stability of the various minima or the barrier connecting them.

The next step is to understand the nature of each dominant intermolecular interactions present in the crystal. One can classify the intermolecular contacts that a molecule can make in three not always well defined different classes:[6]

1) Ionic interactions: Formed when the atoms i and j are charged. In these interactions the dominant term is the first one in the V_{ele} component. These interactions are long range (they are proportional to $1/r_{ij}$) and isotropic (i.e., the field created by each atom does not depend on the any of the angles). Their strength can be as large as 20 kcal/mol.

2) Hydrogen bonds: A functional definition is one that associates this bonds to the presence of a short X-H···Y interaction, with the X-H group pointing to the lone pairs of the Y atom.[7] The X-H group is called the proton donor or acid group, while the Y atom is the proton acceptor or basic group. It becomes stronger as the atoms X and Y become more electronegative. In these cases the interaction is dominated by the electrostatic component and can be easily visualized as $X^{\delta-}$-$H^{\delta+}$···$Y^{\delta-}$. It is short range (proportional to $1/r_{ij}^6$) and directional. It is also very specific: it requires the presence of two complementary groups with potential acid (X-H) and basic (Y) characters. These groups can be easily identified, as we will see later by inspection or, more systematically, analyzing the molecular electrostatic potential (MEP) maps[7] of the molecule or aggregate. The optimum strength normally is between 5 and 0.5 kcal/mol.

3) van der Waals interactions: Linked to the presence of short contacts between the lone pairs of two atoms which have no dangling bond, as the oxygen atom in a carbonyl

group. It can be represented by the X:···:Y symbol and is the weakest of the three types of intermolecular interactions. It just shows up when all except the V_{dis} component become negligible, being its size proportional to the polarizability of the X and Y atoms. It is also short range (proportional to $1/r_{ij}^6$) and not very directional. The optimum values are smaller than 0.5 kcal/mol in general.

If the molecule is non ionic, as is the HNN case, the only two possible types of intermolecular interactions are of the hydrogen bond or van der Waals type. Both types of bonds are formed when the adequate complementary groups are close to each other. The second type is weaker and is not going to be the driving force of the packing, except when very weak hydrogen bonds are present. Thus we can center our attention in localizing hydrogen bonds by looking at the potential as acid or basic hydrogen bond groups of the most external atoms of the molecule. In the HNN case, these atoms are all except the $C(sp^3)$ atoms attached to the nitrogens. Once this character has been established, one has to find ways of attaching the acid and basic groups to form dimers, trimers, and higher aggregates. Previous experiences with high order aggregates shows that the most stable aggregate is that which makes the higher number of intermolecular contacts even if the geometry is not the most stable one for the dimer. This trend was long time ago recognized by Etter[6] and is implied in the maximum density packing principle suggested by Kitaigorodsky.[8] The various stable options correspond to the different polymorphs. The barrier to go from one to other polymorph is, like in the case of the covalent bonds, associated to the energy involved in the breaking the intermolecular bonds of one polymorph while the news ones of the other polymorph are being created.

How to define in a systematic and precise way the acid or basic capabilities of a part of a molecule, in particular, of the HNN molecule ?. This can be done with the help of the MEP maps,[7] which not only indicate the nature of the functional group present in the molecule but give some indications about their relative strength. It is not well established at the present moment the issue of the maximum number of contacts one functional group can accept but a rule of thumb commonly accepted is that the maximum number of X-H···Y contacts that can be made to an atom Y is equal to the number of lone pairs on this atom.

The MEP map of a molecule is a representation of the regions where a +1 point charge is attracted or repelled as a function of its position in the space around the molecule.[7] Regions of large accumulation of electron density trend to be attractive, while these regions where the electron density has been depleted have the tendency of being repulsive. A simple way of locating these regions is by inspection of the atomic charges located on each atom. This is not a quantum observable and various methods have been devised to compute this property, not all arriving to the same result for the HNN molecule. Figure 1 shows the

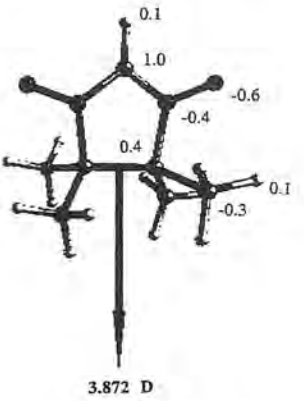

FIGURE 1.- Net charges (in atomic units) located on the atoms according to Bader's Atoms-in-Molecules algorithm. The dipole moment is also shown by an arrow.

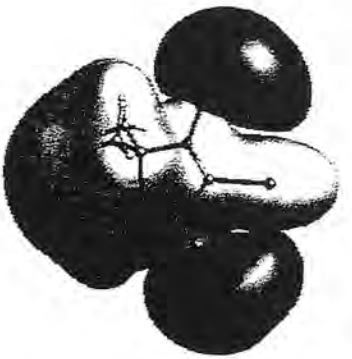

FIGURE 2.- MEP map of the HNN molecule.

values obtained by doing a numerical integration of the atomic region, defined according Bader criteria. Thus, one can expect the C-H groups to be acid groups and the N-O groups to be basic. These conclusions are in total agreement with these obtained analyzing the MEP map (see Figure 2). This map shows the presence of a strong attractive region in the same positions where one would expect to find the lone pairs of the oxygen atoms, and a positive region over the C-H bonds and over the five member ring. Therefore, the C-H bonds are expected to be acid groups in the hydrogen bond and the N-O groups basic groups. Two minimum are found over each oxygen, indicating the possibility of accepting two C-H bonds each.

The combination of an acid and basic group always gives an stable contact when isolated in gas phase and the minimum of this contact is at the optimum intermolecular distance for that acid-base combination. The presence of other groups in nearby positions can affect the formation of this bond or even make it impossible. To find the possible orientations in which attractive hydrogen bonds can be made for dimer one just has to overlap the attractive and repulsive regions of the MEP maps (which correspond to electron excess or deficient regions). This procedure can be extended to find the possible stable conformations of aggregates of any size. The process is very similar to that of finding all the topologies to connect bonds of different type following a lock-and-key rule. Notice that for crystals one requires that the structures obtained present long range order. When all of these things are combined, the number of ways the molecules can be associated is very small compared with all the possible combinations of dimers.

APPLICATION TO THE PACKING OF THE 2-HYDRO NITRONYL NITROXIDE RADICAL

The application of the previous ideas can be illustrated for the HNN case, looking at the possible ways of forming planes of long range ordered molecules. Figure 3 shows some possible arrangements of HNN molecules in the plane. Each molecule is represented by a circle with lines attached to it, which represent the acid and basic groups: the acid groups have an arrow at their end, while the basic groups have an inverted arrow at their end. The lines are placed along the same relative orientations in which the groups are located respect to the center of mass of the molecule. Arrangement **a** corresponds to a situation in which the methyl groups are linked to the NO groups. The propagation of this structural motif gives rise to a perfectly ordered plane with long range order. This is not the case or arrangement **b**, similar to the previous one but with the molecules of the second column rotated 120°, in order to make news $C(sp^2)$-H···ON contacts and the methyl···ON

also present in **a**. When the packing motif is propagated along one direction gives rise to strips but there is no obvious way to propagate along a second direction in the plane without introducing disorder, that is, no long order is found for arrangement **b**. This is not the case of the other four arrangements, which have been selected among many others because present two dimensional long range order. For arrangement **c** we represent two parallel strips, each with the shape the letter z, and connected by $(methyl)_2$···NO bridges. This is just a possible polymorph of **a**. Arrangements **d**, **e** and **f** are just three possibilities obtained by association of dimers. cases **d** and **f** are obtained from the same dimer modifying the relative orientation, a triangle in the first case and a pentangle in the second. The dimer used in arrangement **d** and **f** is obtained after forming two $C(sp^2)$-H···ON contacts. The dimer used in arrangement **e** is the result of forming simultaneously one $C(sp^2)$-H···ON contact and one methyl ···ON contact. This is just a pale reflection of the multiple possibilities open. Obviously, at the three dimensional level the situation is even more complex, so one does not have to be surprised of finding many polymorphs within a small energetic range.

The number of possibilities to deal with can be greatly reduced if one is interested in the most stable polymorphs. This implies that one has to determine the strength of the intermolecular interactions present in the packing. If this is the case, one can select only these arrangements which maximize the number of strong contacts. The aggregate which saturates all the strong bonds is the primary structure of the packing. These aggregates sometimes still have the possibility of forming more intermolecular contacts with other aggregates using its weaker intermolecular bonds. In this case, we have an association of aggregates or secondary structure of the packing. Higher order structures (tertiary and so on) could be formed in some cases via the intermolecular contacts which have not been used up to now. As one goes to higher level structures of the packing, the hydrogen bonds still not used are weaker and their strength can be similar to that for typical van der Waals interactions. So, while hydrogen bonds and ionic interactions are expected to be the main forces controlling the primary structure and probably the secondary, higher orders can be influenced in some cases by the possible van der Waals interactions.

As mentioned above, defining the intermolecular interactions responsible of the primary and secondary structures of the packing implies a knowledge of the relative strength of the possible intermolecular interactions the molecular aggregates can make. This information can be obtained from various sources: MEP analysis, statistical analysis of crystals, ab initio computations. The MEP maps, can give us a first preliminary idea about relative strengths and type of bonds of the possible hydrogen bonds, but if reliable predictions are wished one has to obtain more accurate values. The statistical analysis of the

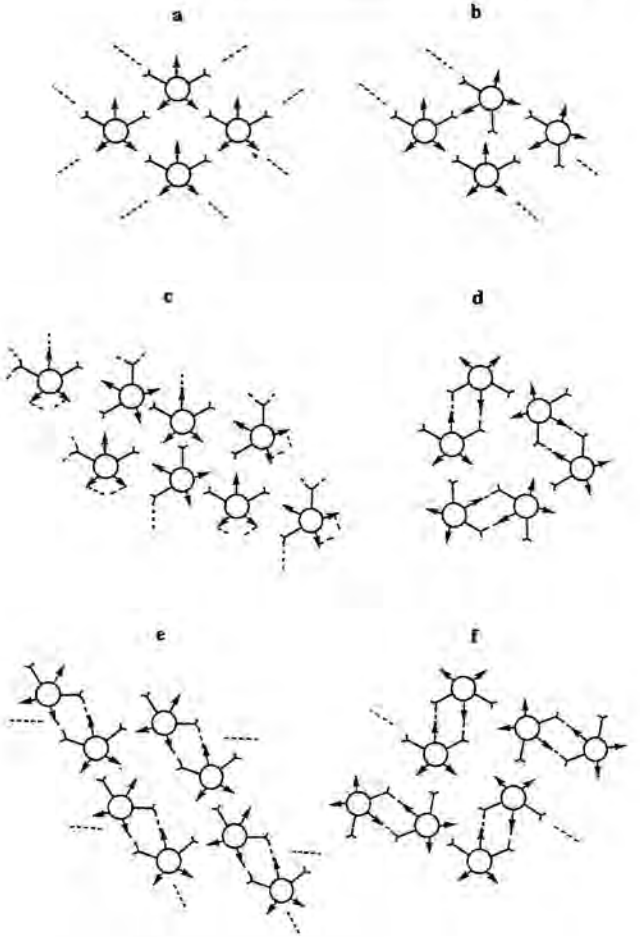

FIGURE 3.- Possible arrangements of HNN molecules to form planes.

intermolecular interactions over a large range of molecules of the same family gives the probability distribution of finding atoms around a given intermolecular contact point. One can then do a connection between the probability of finding short distances and the strength of the interaction. One can also define the anisotropy of each intermolecular contact by looking at the angular probability distribution. The results, although reliable in general, can be misleading in some cases, as short interactions in a similar family of compounds can be due to the presence of strong attractive interactions close to the one of interest, therefore modifying the distribution one would obtain in another environment.

One can also resort to ab initio computations in which, using the appropriate model systems and methodology, one can compute the strength and anisotropy of any intermolecular interaction. The accumulated experience in the computation of hydrogen bonds and van der Waals interactions[9,10] shows that accurate results are obtained if correlated methods are used (at least second order and sometimes fourth order Moller Plesset (MP2 and MP4, respectively)[11] in conjunction with adequate basis sets[12-13] (that is large and well balanced basis sets as to properly describe all the physical forces). Then, one has to correct the basis set superposition error (BSSE)[9,10] of the computed interaction energy using the counterpoise method.[14] Using this methodology one can decrease the errors to less than 10% of the experimental interaction energy for hydrogen bonds[15,16] and van der Waals interactions.[12,13]

How to carry out ab initio computations and use the information obtained in them to understand the packing of the crystals ?. The first and obvious way would be computing the interaction energy of each pair of molecules and of other higher aggregates, to quantify the energies and the optimum structure of the dimers and other aggregates. This can also give information about the kinetics of polymorphism, through the barriers which separate the various minima for each aggregate. However, even for molecules of the size of the HNN this computation is too expensive for the present generation of computers and software, if accurate results are wanted. Therefore, one can to resort to a more practical approach based on identifying the possible contacts that the molecule of interest can make in the crystal, and then compute the energy of these contacts using ab initio methods and the appropriate model system. We show how this process can be carried out in the following paragraphs.

The possible intermolecular interactions to compute at the ab initio level can be selected using the information from the MEP maps to localize complementary parts of hydrogen bond contacts. For the HNN molecule, good candidates for hydrogen bond contacts from the MEP map are the $C(sp^2)$-H···O and the $C(sp^3)$-H···O interactions, while the lone pairs of the oxygen atoms or the π network of the N-O bonds are good candidates for van der Waals interactions. These two are two orientations of N-O···O-N interactions.

Alternatively, one can select the intermolecular interactions to compute after analyzing the shortest contacts within the crystal or from statistical distributions of contacts carried out for a similar family of crystals. The shortest contacts are the most relevant energetically, for the reasons described above, and are good candidates for being the most attractive ones. Obviously, both approaches can be used in a complementary way.

Once the interactions of interest have been selected, one can compute their strength and directional properties using a dimer which presents the same interaction in an environment as close as possible to the one find in the crystal for the same contact. This means, to use the same substituents in the α and, maybe, in the β positions. In some cases it could be important to include the Madelung field created by the other molecules of the crystal, even in an approximate way, although more studies are under way to define the relative importance of this field.

Good models to describe the $C(sp^2)$-H···O and the $C(sp^3)$-H···O interactions in the HNN molecules are the ones represented in Model I and Model II, respectively, with r = 2.416 Å and θ = 142.1° in Model I and r = 2.637 Å and θ = 128.7° in Model II. The geometry of each fragment is selected in such a way that mimics that of the HNN units in the α-HNN crystal. We have substituted the $C(sp^3)$ groups attached to the N atoms by H atoms located at 1.1 Å to lower the computational cost as the effect of these groups on the O atoms is negligible. For the same reasons the $C(sp^3)$ atom attached to the C in the methyl group has been substituted by a H at the same distance it has in methane. The relative orientation of the two monomers have deliberately been chosen to reproduce the geometry of the two intermolecular contacts in the crystals. One can optimize the geometry to find the most favorable geometry when the monomers are isolated, to compare such a value with the crystal geometry and in this way understand the importance of the other groups present in the vicinity or other environmental effects.

Using Models I and II, one can compute the interaction energy, using the MP2 method and the 6-311++G(2d,2p) basis set. The BSSE-corrected interaction energy for the $C(sp^2)$-H···O interaction becomes -3.71 kcal/mol, while that for the $C(sp^3)$-H···O interaction is just -0.40 kcal/mol. That is, we have a strong and a weak hydrogen bond.

In relation to the N-O...O-N interactions, we did a simple computation for the case in which the two NO groups are pointing to each other colinearly. The model system was two H_2NO planar molecules in which the NO groups are facing each other with the C_{2v} axis of each monomer lying one on top of the other. The interaction energy computed using the MP2 method and the 6-31+G(2d,2p) basis set is repulsive at all distances, being at the van der Waals distance about +1 kcal/mol. After correcting the BSSE this energy becomes even a bit more repulsive. Therefore, the NO groups will try to avoid each other as much as

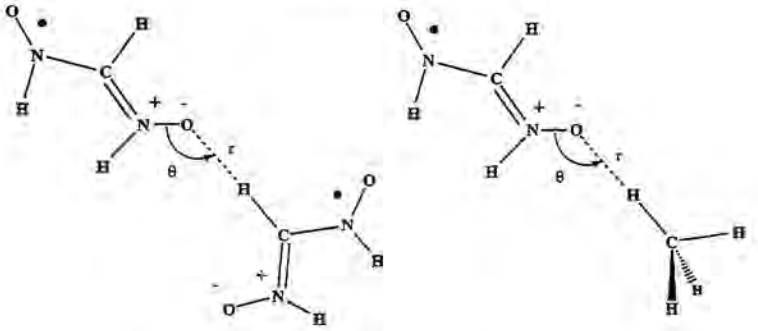

FIGURE 4.- Possible model systems employed to compute the interaction energy of the $C(sp^2)$-H···O and the $C(sp^3)$-H···O interactions present in the HNN crystals.

possible if isolated. To increase the size of the magnetic interactions between the HNN molecules one has to make a network of attractive contacts around the NO groups to compensate this trend and approach the unpaired electrons sitting preferentially in these groups.

With the previous ab initio data, one can analyze the structures proposed in Figure 3 and select the most stable ones looking at the number of contacts of each class within the structures. One can, alternatively, do the same analysis on the experimental X-ray structure of the crystal to understand why the crystal packs the way it does it once all the intermolecular interactions are combined and, in this way, understand the packing. What can be concluded up to know from our study is that the primary driving forces of the packing are the $C(sp^2)$-H···O interactions (-3.71 kcal/mol). On the other hand, the N-O···O-N interaction are repulsive (+1 kcal/mol at the van der Waals distance), while the $C(sp^3)$-H···O interactions are weakly attractive and can be considered as responsible for the secondary structure. To illustrate the use of the previous ideas in a practical way, in the accompanying article we will show how using these ideas and data is possible to rationalize the packing and polymorphism of the two packing forms of the HNN crystals.

ACKNOWLEDGMENTS

This work was supported by the DGICYT (Project No. PB92-0655-C02-02) and CIRIT (GRP94-1077). The use of computer time made available by CESCA and CEPBA is also acknowledged. M.D. thanks CIRIT for her doctoral grant.

REFERENCES

1.- (a) H. M. McConnell, J. Chem. Phys. 39, 1910 (1963)
(b) McConnell, H. M. Proc. Robert A. Welch Found. Conf. Chem. Res. 11, 144(1967).
(c) M. Kinoshita, Jpn. J. Appl. Phys., 33, 5718 (1994) and references therein.
(d) O. Kahn, Molecular Magnetism, (VCH Publishers, New York, 1993).
(e) J. S.Miller; A. J. Epstein, Angew. Chem. Int. Ed. Engl., 33, 385 (1994).

2.- D. B. G. Boocock, R. Darey, E. F. Ullman, J. Am. Chem. Soc., 90, 5945 (1968)

3.- Y. Hosokoshi, M. Tamura, K. Nozawa, S. Suzuki, H. Sawa, R. Kato and M. Kinoshita., Mol. Cryst. and Liq. Cryst., 115, 271 (1995).

4.- J. J. Novoa, M. Deumal, M. Kinoshita, J. Cirujeda and J. Veciana, Mol. Cryst. and Liq. Cryst., this issue.

5.- A. Gavezzotti, Acc. Chem. Res., 27, 309 (1994).

6.- G. C. Maitland, M. Rigby, E. Brian Smith and W. A. Wakeham, Intermolecular Forces, (Clarendon Press, Oxford, 1981).

6.- J. Bernstein, M. C. Etter and L. Leiserowitz, in Structure Correlation, edited by H.-B. Burgi and J. D. Dunitz (VCH, Weinheim, 1994), Chap. 11.

7.- (a) E. Scrocco, J. Tomasi, Adv. Quantum Chem., 11, 115 (1978).
(b) P. Politzer, J. S. Murray, Rev. Comput. Chem., 2, 273 (1991).

8.- A. I. Kitaigorodsky, Molecular Crystals and Molecules (Academic Press, New York, 1973).

9.- J. H. van Lenthe, J. G. C. M. van Duijneveldt-van de Rijdt and R. F. van Duijneveldt, "Ab Initio Methods in Quantum Chemistry", Vol. II, K. P. Lawley, ed.,Wiley, New York (1987).

10.- P. Hobza and R. Zahradnik, Chem. Rev., 88 (1988) 871.

11.- A. Szabo and N. S. Ostlund, Modern Quantum Chemistry, (MacMillan, New York, 1982).

12.- F.-M. Tao and Y.-K. Pan, J. Phys. Chem., 95, 3582 (1991).

13.- F. B. van Duijneveldt, J. G. C. M. van Duijneveldt-van der Rijdt and J. H. van Lenthe, Chem. Rev. 94, 1873 (1994).

14.- S. F. Boys and F. Bernardi, Mol. Phys., 19, 553 (1970).

15.- J. J. Novoa, M. Planas, M.-H. Whangbo, Chem. Phys., Letters 225, 240 (1994).

16.- J. J. Novoa, M. Planas and M. C. Rovira, Chem. Phys. Letters 251, 33 (1996).

ARTICLE 3

Magnetic Properties of Organic Materials
P. Lahti (ed.), Marcel Dekker, New York
(1998)

UNIVERSITY OF MASSACHUSETTS
AMHERST

Department of Chemistry

Lederle Graduate Research Center
Box 34510
Amherst, MA 01003-4510
(413) 545-2291
FAX: (413) 545-4490

PHONE: 413-545-4890 or 2291
FAX: 413-545-4490
INTERNET: lahti@grond.chem.umass.edu

23 July 1998

Professor Juan J. Novoa,
Departament de Quimica Fisica,
Facultat de Quimica Universitat de Barcelona,
Av. Diagonal 647
E-08028 Barcelona, SPAIN

Dear Prof. Novoa:

I have now received most of the book chapters for ***Magnetic Properties of Organic Materials*** (title tentative). The chapters are now in the hands of Marcel Dekker, and are being converted into proofs for your approval. Please find attached a tentative ordering of chapters based on those that I have received to date.

The chapters have been superb, and a joy to read. I believe that you will be pleased to have your chapter included in this series of monographs. I am presently engaged in doing everything I can to get this book produced and ready for market, since I am well aware of the pace at which science moves forward nowadays. I shall keep you advised of progress.

Best regards,

Paul M. Lahti
Professor of Chemistry

cc: Ms. Jeanne McFadden, Marcel Dekker Publishers

The University of Massachusetts is an Affirmative Action/Equal Opportunity Institution

Supramolecular architectures and magnetic interactions in crystalline α-nitronyl nitroxide radicals.

Jaume Veciana,[‡*] Juan J. Novoa,[†*] Mercè Deumal,[†] and Joan Cirujeda,[‡]

[‡] *Institut de Ciència de Materials de Barcelona (CSIC), Campus UAB, E-08913 Bellaterra (Spain).*

[†] *Departament de Química Física. Facultat de Química, Universitat de Barcelona, Av. Diagonal 647, E-08028 Barcelona (Spain)*

Introduction

The design of purely organic magnetic materials has been the goal of many research groups during the last decade.[1] As result of a systematic synthetic effort, it has been possible to obtain different kinds of crystalline organic free radicals that show relevant magnetic properties and, in very exceptional cases, even bulk ferromagnetism.[2] The number of these compounds is now large enough as to make possible to look at the general trends of the structure-magnetism relationship, even in an statistical form, that is, one can look at the connections between the crystal packing of the material and its magnetic properties. Understanding the driving forces behind the already known compounds will be very useful for the design of new purely organic magnetic materials in which the magnetic properties are enhanced. As the packing of a given molecular system can be strongly influenced by the functional groups present in the molecule, we have to look at data in families of compounds. We have chosen to focus our analysis in just one uniform family of magnetic compounds, that of the so called α-nitronyl nitroxide (or α-nitronyl aminoxyl) radicals,[3] whose general formula is shown in Figure 1, and characterized by the presence of a five-membered ring with two nitronyl groups attached in an alpha position to a C(sp^2) carbon.

-Figure 1-

This is the most extensively studied family of persistent radicals in the purely organic molecular magnets. Within this family, there are many different packings and magnetic behaviors due to the effect of other functional groups present in the compounds. The latter fact reflects the strong influence induced on the packing by the functional groups attached to the five-membered ring. Sometimes, even small changes on a large group, as a functionalized phenyl, can give rise to remarkable changes in the packing. It is well established that the presence of bulk ferromagnetism in a crystal of this family is strongly related to the relative disposition of the spin containing molecules within the crystal. This result is consistent with the most commonly accepted ideas based on the already existing theoretical models about intermolecular magnetic interactions.[1,2,4] For instance, within the very popular McConnell I model,[4] probably the most employed one today due to its simplicity, in which intermolecular ferromagnetic interactions are only possible when short contacts are found between atoms bearing a considerable atomic spin population of opposite spin. Otherwise, the interaction would be antiferromagnetic or negligible.

The presence of magnetism in a compound relies on three facts: the ability to prepare a persistent free radical, the possibility to grow a crystalline supramolecular organization with such a radical, and the ability of radicals in such crystals to interact magnetically with each other. The preparation of molecular organic crystals showing a spontaneous magnetization below a certain critical temperature, T_C, is possible for persistent free radicals capable of presenting a crystalline packing which allows for the presence of intermolecular ferromagnetic interactions propagating all over the crystal.[5,6] This is only possible if each spin containing molecule is capable of having one or more ferromagnetic interactions with one or more of its first neighbor molecules, and their strengths overcome the thermal energy at T_C; i.e., with an energy larger than $k \cdot T_C$.[7] Consequently, one of the most important points in this field is to recognize among all the possible relative arrangements of two neighbor molecules that produce intermolecular ferromagnetic interactions, as well as those responsible for the antiferromagnetic ones.[8] In general, the limited geometrical layouts of crystalline molecular

solids received the name of *crystal packing patterns*,[10] although recently these geometrical packing have been also called *synthons*,[11] stressing their role as crystal building units in the supramolecular entity constituted by the crystal.

Packing patterns and crystal structure

From the microscopic point of view, a *crystal packing pattern* is the result of the intermolecular interaction between some or all of the functional groups of the molecules which conform the pattern. One can define many patterns within a crystal, but the most relevant to understand the crystal structure of molecular crystals are those that describe the way in which two molecules bonded through intermolecular bonds are linked. These patterns describe the topology of the synthons and can be called primary patterns, to distinguish them from the other types. Except when otherwise noted we will just concentrate on them and drop the primary adjective.

From a microscopic perspective, a pattern is a particular geometrical distribution of a set of intermolecular interactions. Not all the interactions in the pattern are necessarily attractive in nature, but we can assume that to obtain stable crystals we need energetically stable patterns. When for a given crystal one can sometimes define more than one pattern, we will select those that are energetically stable. One can predict possible patterns looking at the forms in which one can obtain stable small aggregates (dimers, trimers, ...). These patterns are easy to design if one knows the nature of the interactions involved in the pattern, since many interactions are highly directional, as the hydrogen bonds, π stacking, etc.[9] In these cases, one only has to look at the complementarity of the functional groups of the molecule, as shown schematically in Figure 2 for a molecule with more than one complementary groups for intermolecular interactions.

Not all the packing patterns are going to be relevant for the analysis of the crystal packing due to energetical, and symmetrical factors. The energetical factor implies that among all possible patterns only the most stable ones are the most likely to be found in any molecular aggregate, due to statistical reasons, when the energy difference between the energetically

adjacent patterns is large. In this case, the most stable pattern is likely to be the dominant one in presence probability. Furthermore, due to the translational symmetry inherent to the nature of the crystal, some of these geometrical arrangements (that is, relative orientations) of two radicals are not possible in the crystal, because they do not allow for a propagation of the packing pattern, or this propagation is not energetically stable (see Figure 2). The combined effect of these two factors is to limitate the number of relevant packing patterns present in the packing an organic molecule. When the molecules are persistent free radicals, some of the *crystal packing patterns* could produce dominant ferromagnetic interactions and others yielding dominant antiferromagnetic interactions, allowing for this reason to be identified as *ferro- and antiferromagnetic patterns.*

- Figure 2 -

Why the primary packing patterns are so relevant to establish the crystal packing?. Because one can define in a precise way the packing by looking at all the primary packing patterns present in the crystal. The crystal is just a repetition by application of the symmetry operations of its spatial group, of the primary packing patterns along the three directions of the space. This fact was first realized by Etter and coworkers,[10] who introduced a graph set analysis to identify the crystal packing patterns established by hydrogen bonds. Within their method, the packing patterns are identified in terms of motifs.[12] This topological analysis of a crystal is very useful to distinguish between polymorphs of hydrogen bonded crystals in terms of its first and higher order graph sets.[10] The graph set idea could be easily extended to other type of bonds or contacts. The main problem for complex systems relies in the automatic identification of the patterns, which requires of the previous identification of all the intermolecular bonds present. The latter has been done up to now using a geometrical criteria based upon estimated van der Waals radii,[13,14] although there have been recent suggestions of more systematic methods.[15]

Can we predict the shape and stability of the relevant primary patterns formed by a molecule? We can using theoretical ab initio methods to compute and localize the minimum energy conformations for a dimer of the molecule of interest. Looking at the relative stability

of these minimum energy conformers we can have an idea on the statistical probability of each conformer. We can even study the barrier for the transformation from one conformer to another, which can give us a first idea of the dynamics of the polymorphic transformation. This is a first approximation to the primary packing patters, as we have not included the effect induced by the crystal environment and the restrictions induced by the periodicity of the patterns, but we can investigate them by simple introspection or by improving our model using higher order aggregates. If the molecule is too large as to be able to do such geometrical search study even with dimers, we can have a good qualitative idea by studying the potential intermolecular contacts that each molecule could do in a dimer. Using adequate models, one can compute, for instance, the strength of the $C(sp^2)$-H···O-N, N-O···O-N, and $C(sp^3)$-H···O-N contacts in the α-nitronyl nitroxides. Using this information, one can study the relative stability of the possible primary packing patterns present in the crystal of namely the hydro-α-nitronyl nitroxide (or HNN, for short), and rationalize the packing in this crystal.[16] A first guess of the possible orientations in which the packing patterns can be minimum energy structures is obtained in the case of crystals dominated by electrostatic interactions or hydrogen bonds looking at the molecular electrostatic potential (MEP) maps,[17] which give information on where a positive charge will have a more stable electrostatic interaction. The interaction energy of a hydrogen bonded crystal will be dominated by the electrostatic component and, thus, the MEP maps give useful information on how two molecules can approach to each other in stable orientations: if in the approach they overlap regions of the MEP map of opposite sign the interaction is attractive, otherwise is repulsive. We can call this qualitative approach, the MEP overlap analysis method. It gives a good starting point for the identification of primary packing patterns, which, can be useful for the rationalization of very large molecules crystals. We have successfully used this method to rationalize the packing of many crystals[16] and large molecular clusters.[18] We will show later in this work some examples of application. Finally, one can obtain primary packing patterns by analyzing the regularities in the packing of a crystal. The structure can come from a crystal grown up experimentally. Alternatively, if no experimental crystal is available one can use computed crystal structures obtained using any of the programs published in the literature for crystal prediction[19] or optimization.[20]

The MEP overlap analysis directly provides candidates for primary packing patterns. Each conformation obtained in this way is the result of overlapping complementary parts (positive with negative) of the same molecule. Thus a C-H···O-N bond results in an α-nitronyl nitroxide radical from the combination of an acid part (the C-H groups) and a basic one (the O-N group). We can read their acid-basic character by their positive and negative MEP potential. The MEP overlap analysis does not give energetic information. However, it is known that the interaction is most energetic as more acid or basic is the group. This character is manifested by more positive and negative regions in the MEP maps. Therefore, the strongest intermolecular contacts are those between the same acid groups and the most basic groups. This gives us a qualitative ordering of the conformations obtained in the MEP overlap analysis. A better information on the energy ordering comes from ab initio computation of the interaction energy of each intermolecular contact present in the conformation or, when possible, from the interaction energy of the dimer. The accurate evaluation of the interaction energy of each interaction can be carried out by the adequate ab initio methodology.[21-24] Thus, following the MEP overlap analysis we have ended in a functional group analysis of the crystal packing in which we combine complementary functional groups.

What is the connection between the MEP overlap analysis, or the group functional analysis, and the structure of the crystal? The answer to this question was put down by Kitaigorodsky in its *Aufbau Principle*.[25] Such a principle simply states that when organic molecules pack to form a molecular crystal, it tries to minimize the total energy of the crystal. This is an energetic criterion, that is, a thermodynamic criterion. If one defines the packing energy E_p as a sum over all possible different pairs of atoms,

$$E_p = \Sigma' E_{ij}(r_{ij}) \qquad (1)$$

where $E_{ij}(r_{ij})$ is the intermolecular interaction energy between atoms i and j located at a distance r_{ij}, and the prime indicates the lack of repetitions. Notice that this function has many local minima, each corresponding to a different crystal structure or polymorph that a given compound is able to show. The experimental crystal is not necessarily the most stable one or the most densely packed, as was assumed by Kitaigorodsky. In some cases, one can find

many local minima in a small energy range.[26] According to this principle, the most stable crystals satisfy the strongest intermolecular contacts first, and then the remaining contacts, in order of decreasing strengths. It is possible, depending on the way the crystal is grown, to lie in local minima. On the other hand, one should keep in mind that the crystal packing depends also on kinetic factors, although we will not consider them explicitly in our treatment.

Normally, the real crystal is the result of the progressive association of molecules within the solution in which they are grown. In solution, when the molecules form aggregates (molecular clusters) they do it employing the most stable primary packing patterns, in an statistical distribution. They form as many as the most primary patterns as possible to build the first order aggregates. At this point, when they have saturated this kind of patterns, if they want to further aggregate and thus build up the crystal, they have to use other patterns linking the first order aggregates. The higher order aggregates can be ribbons, planes, or other motifs. They can build the crystal or further aggregate using other patterns in order to build the bulk crystal. Therefore, we have an ordering in the crystal structure, associated to the stability of the different packing patterns. We can thus differentiate a *primary structure* of the crystal, associated to the most stable primary packing patterns, a *secondary structure* of the crystal, also presenting its associated patterns, and even *tertiary* or *quaternary structures*, formed by packing patterns which employ previously unused functional groups.

Using the methodological approach described above it is possible to carry out the analysis of any crystal structure following the next steps:

1) Characterization of the functional groups. This can be done by simple inspection, extrapolating the already known information on the same groups, or by studying the nature of the MEP map, which allows regions of concentration and depletion of the electronic density, and the acid-basic character of the functional groups. We thus can identify the potential nature of any intermolecular contact which can be done form the functional groups present in the molecule.

2) Identification of the primary packing patterns. This can be done from a experimental determined crystal structure by looking at the shortest intermolecular contacts, normally assumed to be attractive and responsible for the packing structure. Alternatively, one can carry out the same analysis on any structure obtained after a computational optimization of the

crystal. Note here that not every short contact is always attractive, but can be a consequence of the presence in nearby positions of two attractive interactions. We should also use relaxed cutoffs in the distances to avoid problems.[13,14]

3) MEP overlap analysis. To identify the possible relative geometry dispositions in which the functional groups can be associated in energetically stable conformations. This is sometimes done intuitively by associating complementary groups but is more systematic in terms of MEP maps obtained from ab initio computations.

4) Computation of the strength of the primary patterns by ab initio computations. This allows to define an energetic order for all the patterns (that is, $E_1 < E_2 < \ldots$) required to understand the presence or absence of some patterns in the first step.

5) Rationalization of the structure. Using the information obtained in the previous steps, the crystal packing can be justified in terms of a primary structure, secondary and so on.

Examples of the application of the previous methodology to the family of the α-nitronyl nitroxide family have been recently published[16,27,28] and will not discussed here in detail. We just will mention that these studies allow to rationalize the packing oh the hydro α-nitronyl nitroxide (HNN, for short), the simplest member of the nitronyl nitroxide in which R=H. This crystal has a primary structure of dimers, each involving the formation of two strong $C(sp^2)$-H···O-N contacts (-3.71 kcal/mol each one). The dimers then aggregate among themselves through weaker $C(sp^3)$-H···O-N contacts (-0.40 kcal/mol of interaction energy each one) forming planes (in this way the number of these contacts is maximized). This is the secondary structure of the HNN crystal. No short NO···ON distances are found in this crystal because the NO groups repel each other when coplanar and in a collinear or near arrangement. Once the planes are formed, there are still some unused intermolecular groups. For instance, the methyl groups can still make contacts against the NO groups involved in the $C(sp^2)$-H···O-N contacts, although this is not the only possibility. Using these groups the planes can be linked to each other. The result is the formation of ordered stacks of planes, piled up in such a way that they maximize the interplane interaction energy. This is the tertiary structure of the crystal. Thus, the whole crystal has been rationalized.

Statistical analysis of the packing patterns in ferro and antiferro α-nitronyl nitroxides: are there ferro and antiferro packing patterns?

The previous analysis can be extended to any α-nitronyl nitroxide crystal. This will allow to obtain generalities of their crystalline packings. Nevertheless, such kind of analysis does not provide any information about the relationship between the magnetic properties and the crystallographic structure.

The most common way of obtaining structural information about *ferro-* and *antiferromagnetic patterns* is by a detailed inspection of the molecular packing in individual crystals that show well-characterized magnetic behaviors, searching for packing patterns which are specific of ferromagnetic crystals. Usually, this kind of analysis implies that once that it is known the magnetic behavior of the crystal one searches for the packing pattern responsible for it, under the light shed by the use of a theoretical model capable of associate a magnetic character to a given crystal pattern, normally the so called McConnell I model. Most of these analysis have been performed on crystals of the α-nitronyl nitroxide radicals. Although qualitative, several interesting conclusions have been achieved with this methodology. For instance, close contacts between NO groups of neighboring molecules, the groups that support the largest spin density on these radicals, have been associated to *antiferromagnetic patterns*.[1,29] At the same time, those contacts among one NO group of one radical and certain H atoms of neighboring ones have been ascribed to *ferromagnetic patterns*, in particular when the H atoms are located on aromatic substituents or on CH_3 groups.[1,30] However, this approach has some drawbacks, because the structural information achieved on the *magnetic patterns* is very limited and occasionally the conclusions are contaminated by preconceptions.[31] For this reason, a more systematic and quantitative approach, as the one we describe here, is required.

Magneto-structural information can be obtained by performing an statistical analysis of a large set of crystals. We can look in these analysis at the key information defining the packing and then relate the type of packing and the ferro or antiferromagnetic properties of the crystal. At this point, it is interesting to note that the packing of the magnetic crystals is driven

only by the intermolecular interactions and not affected by the magnetic interactions, as these interactions are much weaker in magnitude than the hydrogen bonds or van der Waals interactions. According to the McConnell I model the presence of a ferromagnetic interaction requires the overlap of significant positive and negative spin densities. It is well known, both experimentally and theoretically,[1,30a,32] that the major part of the spin density in α-nitronyl nitroxide radicals is located on the ONCNO part of the five-membered ring, being the density on the central C atom opposite to that in the N and O atoms. Thus, the nature of the magnetic interactions present in the crystal of α-nitronyl nitroxide is expected to be directly related to the spatial orientation and proximity of the atoms of the ONCNO group. Thus, the statistical analysis of the geometry of the shortest ONCNO···ONCNO contacts in crystals whose magnetic properties are well characterized can help to understand the packing-magnetism properties in α-nitronyl nitroxides. We have performed such analysis for radicals that clearly belong to one of the following two different magnetic classes or subsets: those that show *dominant* ferromagnetic intermolecular interactions and those exhibiting *dominant* antiferromagnetic interactions. We did not want to include in our study crystals whose magnetic behavior is not clearly defined, as they would be of no help to identify the possible patterns associated to a ferro or antiferromagnetic packing. The analysis of the two subsets can give rise to totally different *crystal packing patterns* in each subset or, instead, one can find similar patterns in both subsets. The second case would indicate the statistical presence of *ferro-* and *antiferromagnetic patterns* in both magnetic classes, combined in such a way that their number and strength results on a magnetic character for the crystal compatible with the subset in which this crystal is included.

The total number of crystals analyzed in this study, 47 crystals, is large enough to make feasible a statistical analysis of the most relevant intermolecular contacts they present. The crystallographic data used in the survey were, in part retrieved from the Cambridge Structural Database (CSD),[33] and the rest from our own research or were directly found in the literature or supplied to us by other authors. A total of 143 crystal structures containing substituted α-nitronyl nitroxide radical units were initially used.[34] The criteria employed to select the final set of structures were as follows: (1) Structures with R factors greater than 0.10, or which were determined from very limited data, or which exhibit disorder or large

molecular distortions, were excluded remaining 117 crystal structures. (2) All of the structures containing both transition metal atoms and large closed-shell organic molecules co-crystallized (45 structures) were discarded for the present analysis since intermolecular magnetic interactions between radicals could be complicated in these cases by the existence of other magnetic pathways through the metal atoms or the closed-shell molecule and the radical units. This criterion left 72 crystal structures of purely organic compounds. (3) We discarded in our statistical analysis all the crystals whose magnetic interactions are not clearly dominated by ferro- or antiferromagnetic interactions. The nature of the dominant magnetic interactions is clearly manifested by the temperature dependence of the magnetic susceptibility, χ, in the temperature range of 2-300 K. Thus, radicals with dominant ferromagnetic interactions, grouped in the subset named as FM, show the characteristic signature in the χT vs. T plot of a continuous increasing of χT when T decreases. By contrast radicals with dominant antiferromagnetic interactions have the opposite trend and were classified in the AFM subset. It is convenient to exclude the crystals with non dominating signature because, by construction, they can show both types of *crystal packing patterns* and, in consequence, it would make impossible a clear identification of the *ferro-* and *antiferromagnetic patterns*. Their exclusion left us with only 47 purely organic crystals. Of these, the dominant intermolecular magnetic interactions were ferromagnetic in 23 cases and antiferromagnetic in the remaining 24 ones. The total number of crystals which fulfill the previous conditions and are suitable for their statistical analysis belong to the following spatial groups: P-1 (3), $P2_1$ (2), Cc (2), $P2_1/c$ (25), C2/c (2), $P2_12_12_1$ (2), $Pca2_1$ (1), Ib2a (1), Pbca (4), Fdd2 (1), $I4_1/a$ (1), $P4_2bc$ (1), and P3c1 (2).

The statistical analysis of the packing of both magnetic subsets can be done by looking at the geometry of the shortest intermolecular contacts of the N-O···O-N, C(sp^3)-H···ON and C(sp^2)-H···ON types present in each crystal. We selected these contacts, first because they are the most relevant ones according to the McConnell I model and the literature,[4] and, second, because they are the ones that at the light of the analysis of the previous section, are the energetically dominant ones. There are 1312 NO···ON contacts at O···O distances smaller than 10 Å. Also present are 6039 C(sp^3)-H···ON contacts and 2286 C(sp^2)-H···ON contacts at H···O distances smaller than 10 Å. These three sets of contacts are large enough to make

feasible a statistical analysis of their geometrical parameters searching for differences which are signature of different packing patterns.

It is important to mention here that most of the analyzed structures in both magnetic subsets were determined at room temperature where the thermal energy largely overcome the strengths of the intermolecular magnetic interactions. This means that we are trying to correlate a physical property, whose magnitude is only clearly observed at low temperatures, with the crystal packing patterns existing at room temperature. This is a common practice in *Molecular Magnetism* that, unfortunately, cannot be avoided since only very few crystal structures have been determined at low temperatures. At first glance the above mentioned objection may look serious but a detailed analysis of this problem revealed that it has minor consequences for our magneto-structural correlations. Actually, except for those cases where a first-order structural phase transition occur, the *crystal packing patterns* of molecular crystals show only small changes with the temperature due to the thermal contraction. These changes do not turn the relative disposition of the molecules to such extension as to reverse the nature of the dominant intermolecular magnetic interaction.[35] Therefore, it can be assumed without too much risk that similar *crystal packing patterns* exist at low and high temperatures in the 47 crystals selected here.

Spatial distributions of the N-O···O-N contacts

A preliminary analysis of the geometry of the α-nitronyl nitroxide molecules in the 47 crystals analyzed, and in others with no definite or relevant or complex magnetic behaviors, showed that the spatial distribution of the atoms in the five-membered ring is nearly the same, and that the five ONCNO atoms lie in the same plane. This behavior can be attributed to the delocalization of the π electrons over the five ONCNO atoms through various resonant forms. Given this fact, we do not have to worry about small distortions in the geometry of the ONCNO group and all the atoms of the imidazolidine ring, including the four methyl groups. This simplifies considerably our analysis, as we can consider the internal geometry of ONCNO groups as fixed. Consequently, given a ONCNO group in a certain crystal, whose atoms are labeled as $O_{12}N_{12}C_1N_{11}O_{11}$, the relative geometrical position of another similar

group labeled as $O_{22}N_{22}C_2N_{21}O_{21}$ (obviously identical in geometry due to the above mentioned behavior and the translation symmetry present in the crystal), is completely defined by six internal coordinates, as occurs for any two rigid asymmetrical objects in a Cartesian space. There are many possible choices for this six coordinate space, all of them correlated by a linear transformation among themselves. Among these choices, the one selected here is the one shown in Figure 3, chosen because it allows an easy visualization and physical interpretation of the geometrical parameters. We first define the position of the terminal O_{21} atom relative to the $O_{12}N_{12}C_1N_{11}O_{11}$ group using three parameters, the $O_{21}\cdots O_{11}$ distance, the $O_{21}\cdots O_{11}$-N_{11} angle, and the $O_{21}\cdots O_{11}$-N_{11}-C_1 torsion angle. Then, the position of the N_{21} atom for a fixed N-O distance is defined giving the value of the N_{21}-$O_{21}\cdots O_{11}$ angle and the N_{21}-$O_{21}\cdots O_{11}$-N_{11} torsional angle. Finally, the plane on which the $O_{22}N_{22}C_2N_{21}O_{21}$ group lies is fully defined giving the C_2-N_{21}-$O_{21}\cdots O_{11}$ torsional angle, as the C_2-N_{21} distance and the C_2-N_{21}-O_{21} angle are fixed. Once this plane is known, the position of the N_{22} and O_{22} atoms are automatically established due to the fixed geometry of all ONCNO groups. To simplify the notation, we will identify the previous six intergroup geometrical parameters as D, A_1, A_2, T_1, T_2 and T_3 (see Figure 3 for a proper visualization).

-Figure 3-

Using the previous six parameters, as a first step in our research on the spatial distribution of the ONCNO groups, we studied the number of contacts as a function of the O···O distance; i.e., of the D parameter. The results indicate that there are no contacts in none of the subsets at distances shorter that 3 Å. The shortest value of D (the NO···ON distance) is 3.158 Å within the FM subset and 3.159 Å in the AFM one. The number of contacts in the FM and AFM subsets increases as the third power of the distance in the 3-10 Å range. The proportion of contacts in the FM and AFM subsets is nearly constant for all the distance ranges tested (in average, 44% are from the FM subset and 56% from the AFM one). These values are close to the percentage of crystals in the FM and AFM subsets (49% and 51%, respectively), although the percentage of contacts in the AFM subset is slightly larger . This

result suggests that the number of ONCNO···ONCNO contacts that each NO group is making is similar in both subsets and does not strongly depend on its magnetic properties.

The previous values also indicate that the cutoff employed in analyzing the ONCNO···ONCNO contacts is not in principle a key factor. Therefore, given the large sizes of the R groups in many α-nitronyl nitroxide molecules, it seems adequate to begin by performing an analysis in the 0-10 Å range, to allow the possibility of unusual crystal packing patterns. Within this range, the average values of the parameters D, A_1, A_2, T_1, T_2 and T_3 for the AFM subset are 7.8 Å, 73°, 113°, 8°, -6°, 2°, while the equivalent ones for the FM subset differ in less than their standard deviation, namely, 7.9 Å, 74°, 115°, 13°, 3°, -5°. It is interesting to note that when the analysis is carried out in the 0-4 Å range (the range for which the intermolecular contacts are supposed to be stronger and more determinant to determine the FM or AFM character) the average values for the previous six parameters in the FM subset are 3.6 Å, 92°, 137°,18°,-22°, and -37°, while for the AFM subset are 3.6Å, 88°, 93°, 32°, 44°, and 10°. Once again, the average values for the two subsets differ in less than their standard deviations. Concerning the previous values, it is interesting to note the 190° value for the average of $A_1 + A_2$, an indication of the trend of the NO···ON groups of being parallel. It is also worth pointing out the similarity in the average values of the six geometrical parameters for the two magnetic subsets, an indication that the FM and AFM packing patterns are similar. This can be better appreciated plotting the position of the O_{21} atom for a representative sample of the FM and AFM subsets (see Figure 4, where the values of the parameters D, A_1 and T_2 are plotted for a random selection of 100 contacts within each subset). We see in Figure 4 that the O_{21} atom is distributed over the whole Cartesian space in a smooth and similar form in both magnetic subsets. The similarity in the relative position distributions of the ONCNO groups in the FM and AFM subsets is also shown in the scattergrams of pairs of parameters for the FM and AFM subsets (Figure 5). Therefore, we can safely conclude that there are no characteristic patterns present in the FM subset excluded in the AFM subset and viceversa. Instead, the two subsets present very similar or identical *crystal packing patterns*.

-Figure 4 and 5-

The scattergrams mentioned above, also show that there is no relationship between the presence of magnetism and the values of D. This is important because it goes against some commonly accepted ideas about the relationship between magnetism and crystal packing in α-nitronyl nitroxides, as the idea associating the presence of short NO···ON contacts to crystals with dominant antiferromagnetic interactions: According to the McConnell I model,[4] when two ONCNO groups approach in such a way that their closest oxygen atoms lie in the same plane with A_1 angles between 90° and -90°, they will directly overlap the positive electron spin densities[36] of the two closest O atoms and, consequently, should give rise to a strong antiferromagnetic interaction, more important as the O···O distance gets shorter. That situation is found in our set of parameters when T_2 is equal to 0° or 180°, for values of the A_1 angles between 90° and -90°. Consequently, if the simple association between short NO···ON distance and dominant antiferromagnetic interactions is valid, one should find at these values a decrease in the number of ONCNO···ONCNO contacts in the FM subset and an increase in the contacts of the AFM subset. This is not found in the scattergrams shown in Figure 5. We have explored if this conclusion was a consequence of a particular distance range employed in the analysis with no change in the conclusions: The proportion of contacts in the ferro and antiferromagnetic subsets is nearly independent on the range of distances selected. Even at very short distance ranges, where the overlap of the spin densities is maximum and the magnetic strength associated to the NO···ON contact is the largest, one also finds contacts within the FM subset. It is clear from such data the similar values of all parameters for the shortest contacts within the FM and AFM subsets. Therefore, *the presence of short NO···ON contacts, classically considered antiferromagnetic according to the McConnell I model , does not imply that the crystal has dominant antiferromagnetic interactions*. Does the latter conclusion means that the McConnell I model is not working properly for the α-nitronyl nitroxide radicals? Strictly speaking, we cannot conclude at this stage this possibility. The failure in correlating the presence of expectedly large antiferromagnetic interactions with particular crystal packing patterns in these systems could be due to the failure of the theoretical model or to the simultaneous presence of other interactions whose strengths or number can overcome the magnetic effect of the NO···ON contact. However, even in the second case, it

changes the way in which the structure-magnetism correlation analysis of these crystals has to be carried out from now on.

We have also carried out[34] a correlation analysis[37] of the data to search for better sets of coordinates or linear dependencies. Besides a small correlation found between the A_1 and A_2 angles, not surprising given their definition, there is no correlation for any other pair of parameters employed in this study. A factor analysis[38] concluded[34] that six is the number of parameters required to treat the geometrical data of the ONCNO···ONCNO contacts and that it is not possible to reduce this number.[39] Similar conclusions are found for the contacts of the AFM subset when the factor analysis is done. Finally, a cluster analysis[40] of ONCNO···ONCNO contacts geometrical data, using as criteria to define a cluster the single linkage method,[40] on the set composed by the addition of the FM and AFM subsets, indicated that the FM and AFM sets of contacts are nearly identical and interpenetrated, thus being *indistinguishable*. Consequently, there is no statistically significant difference in the relative positions of the NO groups for the two magnetic subsets. This is equivalent to say that there are no different *crystal packing patterns* in these subsets attending to the relative positions of the NO groups. This is reasonable if one realizes that the interactions responsible for the packing of these crystals, which are rationalizable in terms of NO···ON and C-H···ON contacts, as already mentioned, are very similar in both subsets of crystals and stronger than the magnetic intermolecular interactions.

Spatial distributions of the C(sp³)-H···O-N and C(sp²)-H···O-N contacts

The C(sp³)-H···O-N and the C(sp²)-H···O-N contacts, together with the X-H···O-N ones (X = heteroatom) when they are possible, are the contacts responsible for the formation of hydrogen bonds within the crystals of α-nitronyl nitroxide radicals. Therefore, in case there is a general ferro or antiferromagnetic pattern associated with these hydrogen bonds in the packing it must be reflected in the analysis of these types of bonds. Given the small amount of spin density localized in the H atoms of methyl and aromatic groups, these contacts can only produce very weak magnetic interactions, according to the McConnell I model.[4] These contacts are ferromagnetic if the spin density on such H atoms is negative and

antiferromagnetic if this is positive, as the oxygen of the NO group is always positive. In principle, due to their weakness this kind of contacts should not be the determinant ones in establishing the dominant magnetic interaction in a given crystal, although if their number is large enough, they could compensate the stronger ones.

To carry out a systematic search on the geometry of a general C-H···O-N contact, we need, as for any two asymmetrical rigid objects in a three dimensional Cartesian space, six independent internal coordinates: the H···O distance and the H···O-N angle, to define the position of the hydrogen, the C-H···O angle and the C-H···O-N dihedral, to define the position of the C atom, and the R-C-H angle and R-C-H···O dihedral to define the position of the R group attached to the C-H. Among these parameters, the two used to define the position of the functional group R do not play a determinant role to define the geometry of the C-H···O-N contacts due to the quasi cylindrical symmetry of the electron density on the C-H group. So we will not consider them further. For simplicity, as before, we will identify the remaining four parameters as D, A_1, A_2 and T_1. Figure 6 shows these parameters for the C(sp^3)-H···O-N contacts present in the α-nitronyl nitroxide radicals, while Figure 7 shows their definition for the aromatic C(sp^2)-H···O-N contacts. In the later case, one can distinguish between *ortho*, *meta* and *para* aromatic carbons of C(sp^2)-H···O-N contacts respect to the *alpha* C atom of the five-membered ring. We will identify them by adding the suffix *o*, *m* and *p* after the name of the parameter (for instance A_{1o}, A_{1m} and A_{1p}). All crystals included in the two magnetic subsets have 12 hydrogens bonded to C(sp^3) atoms which have negative spin sitting on them.[41] Therefore, a proportion of 49% ferro- vs. 51% antiferromagnetic C(sp^3)-H···O-N contacts should be expected according to the number of crystals in the FM and AFM subsets. However, not all the analyzed crystals have functionalized aromatic groups as the *R* substituent, and the proportion of ferro vs. antiferromagnetic C(sp^2)-H···O-N contacts will depend not only on the number of analyzed crystals belonging to each magnetic subset but also on the available number of hydrogens in *ortho*, *meta* or *para* positions.

-Figures 6 and 7-

A search within the FM and AFM subsets for H···O distances smaller or equal to 3,8 Å gives the 364 C(sp^3)-H···O-N contacts and 102 C(sp^2)-H···O-N contacts. Of the 364 C(sp^3)-H···O-N contacts, 43% belong to the FM subset and 57% to the AFM one, a proportion similar to the number of crystals in each subset. Similarly, the proportion of C(sp^2)-H···O-N contacts in the FM and AFM subsets for hydrogens in the *ortho*, *meta* and *para* positions are in clear accordance with the number of crystals pondered by the number of hydrogens in each of those positions. In conclusion, the number of C-H···O contacts does not depend on the dominant magnetic interactions present in the crystal.

-Figures 8 and 9-

One can have an idea of the distribution of these contacts by looking at Figures 8 and 9, which represent the values of the D, A_1, and T_1 parameters for the C-H···O-N contacts found in the two magnetic subsets. In the C-H···O-N case, the points are spread in a smooth and in a similar way over the whole range of values represented. Consequently, there seem to be no excluded regions, specific for the crystals belonging to FM and AFM subsets. Instead, the similarity of geometries in the intermolecular contacts of the two subsets is manifested, making impossible to distinguish between the crystals showing dominant ferro- and antiferromagnetic interactions just by a direct inspection of the geometry of a particular intermolecular contact.

Concluding remarks

We have shown how the packing of molecular crystals can be analyzed in terms of primary packing patterns, geometrical constructions equivalent to the synthons introduced by Desiraju.[11] Using these patterns and with the help of the MEP overlap analysis, is possible to rationalize the crystal packing of any molecular crystal. In particular, the packing of the HNN crystal can be rationalized in terms of C(sp^2)-H···O-N and C(sp^3)-H···O-N contacts, being

the first stronger.[16,27,28] The N-O···O-N contacts present in the HNN and other α-nitronyl nitroxide crystals are repulsive.[16,27,28]

We have then carried out an statistical analysis of the crystal packing of α-nitronyl nitroxide radicals. For such a purpose, we have selected only crystals having dominant ferro- or antiferromagnetic intermolecular interactions, and they have grouped in a FM subset and an AFM one. We have found that these two subsets do not present different *crystal packing patterns*, that is, it is not possible to identify specific packing patterns for the ferro- and antiferromagnetic interactions. This experimental observation agrees with the fact that the packing of the α-nitronyl nitroxide radicals is driven by intermolecular forces which are identical in both FM and AFM subsets of crystals.

Given the fact that all the crystals of a magnetic subset must have the dominant interactions of the subset type and that these interactions clearly depend on the geometry of the relative arrangements of radicals, the obvious question is: why are these differences not seen in the statistical analysis? The only possible explanation, after all the statistical tests carried out on the data, is the simultaneous presence of *ferro-* and *antiferromagnetic patterns* in each magnetic subset. Consequently, it is impossible to guess the dominant intermolecular magnetic interactions of a given molecular crystal just by looking at some particular detail of its crystal *packing pattern* such as the relative orientation of the N-O···O-N, $C(sp^3)$-H···O-N or $C(sp^2)$-H···O-N contacts. It is, instead, necessary have a look at the whole packing pattern of the neighboring molecules to guess the dominant magnetic character associated to such *packing pattern*. Experimentally this is not an easy task, since it requires to generate isolated clusters of molecules in solution (dimer, trimers, regular chains, ...) having a fixed and known geometry and then being able to determine the involved magnetic interaction. Otherwise, one can use solid samples to extract this information, although it requires the use of more elaborated techniques with oriented single crystals (magnetic and heat capacity measurements, EPR spectroscopic measurements, muon spin rotation experiments, etc) in order to identify and anticipate the nature and directionality of the intermolecular magnetic interactions in a given molecular crystal. Alternatively, high level *ab-initio* computations on model clusters could also give the same information, although given their cost they have not

been carried out, for the moment, on realistic α-nitronyl nitroxide molecules at the adequate computational level as to provide accurate results.

Finally, there are no simple structural features characteristic of a ferro or antiferromagnetic pattern. In this line, we have found that some commonly accepted ideas on the magnetic character of the NO···ON contacts are not completely correct. For instance, it is not true that short in-plane NO···ON contacts are always a signature that the dominant magnetic interactions in the crystal are antiferromagnetic, as one would expect just by using the McConnell I model. All this information indicates that one has to analyze each crystal in detail to deduce the nature and strength of the magnetic interactions associated to all the *crystal packing patterns* present in it.

References and notes.

1. For a recent overview see: a) Gatteschi D, Kahn O., Miller JS., Palacio F, eds., Molecular Magnetic Materials, Kluwer Academic Publishers, Dordretch, 1991. b) Iwamura H, Miller, J. S. eds. Mol. Cryst. Liq. Cryst. 1993; 232/233: 1-360/1-366. c) Miller J. S. and Epstein A.J. Angew. Chem. Int. Ed. Engl. 1994; 33: 385-415. d) Kahn O. Molecular Magnetism, VCH Publishers, New York, 1993. e) Rajca A. Chem. Rev. 1994; 94: 871-893. f) Miller JS, Epstein AJ, eds. Mol. Cryst. Liq. Cryst., 1995; 272-274. g) Kinoshita M. Jpn. J. Appl. Phys. 1994; 33: 5718. h) Coronado E, Delhaes P, Gatteschi D, Miller JS, eds. Molecular Magnetism: From Molecular Assemblies to Devices, Kluwer Academic Publishers, Dordretch, 1996. i) Kahn O. ed., Magnetism: A Supramolecular Fucntion, Kluwer Academic Publishers, Dordretch, 1996.

2. a) Tamura M, Nakazawa Y, Shiomi D, Nozawa K, Hosokoshi Y, Isjikawa M, Takahashi M, Kinoshita M. Chem. Phys. Lett. 1991, 186, 401. b) Allemand PM, Khemani KC, Koch A., Wudl F, Holczer K, Donovan S, Grüner G, Thompson J.D. Science, 1991; 253: 301. c) Chiarelli R, Novak MA, Rassat A, Tholance JL. Nature, 1993; 363: 147. d) Sugawara T, Matsushita MM, Izuoaka A, Wada N, Takeda N, Ishikawa M. J. Chem. Soc., Chem. Commun. 1994; 1081. e) Cirujeda J, Mas M, Molins E, Lanfranc de Panthou F, Laugier J, Geun Park J, Paulsen C, Rey P, Rovira

C, Veciana J. J. Chem. Soc., Chem .Comm. 1995; 709-710. f) Caneschi A, Ferraro F, Gatteschi D, leLirzin A, Novak MA, Rentsecheler E, Sessoli R. Adv. Mater. 1995; 7: 476. g) Pei Y, Kahn O, Aebersold MA, Ouahab L, Le Berre F, Pardi L, Tholance JL. Adv. Mater. 1994; 6: 681. h) Togashi K, Imachi K, Tomioka K, Tsuboi H, Ishida T, Nogami T, Takeda N, Ishikawa M. Bull. Chem. Soc. Jpn., 1996; 69: 2821 and papers cited therein.

3. α-Nitronyl nitroxide is the abbreviated name most wealthy employed and it is here used to indicate 4,5-dihydro-4,4,5,5-tetramethyl-3-oxido-1H-imidazol-3-ium-1-oxyl, the correct IUPAC name.

4. McConnell HM. J. Chem. Phys. 1963; 39: 1910.

5. In general, bulk ferromagnetism requires the presence of ferromagnetic interactions along three (or two) directions of the solid depending if there is a low (or high) magnetic anisotropy. Since organic free radicals have in general very small magnetic anisotropy, the requirement of the presence of ferromagnetic interactions in 3 dimensions is completely necessary for achieving such a macroscopic property. See: Palacio F. From Ferromagnetic Interactions to Molecular Ferromagnets: An Overview of Models and Materials, Gatteschi D, Kahn O, Miller JS, and Palacio F. eds. in Magnetic Molecular Materials, Kluwer Academic Publishers, Dorderecht, 1991, p.1-40.

6. A lack of compensation of the magnetic moments of spins coupled antiferromagnetically can also produce a net magnetic moment -spin canting- that, when propagates over the solid, produce a spontaneous magnetization. For a recent organic example of this situation, see: Banister AJ, Bricklebank N, Lavender I, Rawson JM, Gregory CI, Tanner BK, Clegg W, Elsegood RRJ, Palacio F. Angew. Chem. Int. Ed. Engl. 1996; 35: 2533.

7. For molecular organic crystals with high symmetry, namely rhombic or cubic, the presence of just one intermolecular ferromagnetic interaction among the neighbor units is enough in order to guarantee the propagation of magnetic interactions along two or three spatial directions. By contrast for crystals with lower symmetries it is necessary the existence of more than one intermolecular ferromagnetic interaction for

each crystallographically independent radical molecule in order to achieve a bulk ferromagnetism.

8. Another important facets to be developed in this field are the different ways to enhance the strengths of intermolecular magnetic interactions. Only increasing these strengths it will be possible to increase the T_C of purely organic ferromagnets that nowadays are still very low, most of them in the mK region.

9. a) Mighell AD, Himes VL, Rodgers JR. Acta Cryst. 1983; A39: 737-740. b) Wilson AJC. Acta Cryst. 1988; A44: 715-724. c) Baur WH, Kassner D. Acta Cryst. 1992; A48: 356-369.

10. Etter MC. Acc. Chem. Res. 1990; 23: 120-126, Bernstein J, Davis RE., Shimoni L, Chang N-L. Angew. Chem. Int. Ed. Engl. 1995; 34: 1555-1573.

11. Desiraju G. Angew. Chem. Int. Ed. Engl. 1995; 34: 2311-2327.

12. A motif is a pattern containing only one type of hydrogen bond. Note that some motifs can extend over more than one molecule.

13. This has been a controversial criteria, because depending on which radii are taken some interactions are visualized as hydrogens bonds or not (see reference 14 for a detailled discussion).

14. Jeffrey GA, Saenger W, Hydrogen Bonding in Biological Structures, Springer Verlag, Berlin, 1991.

15. Novoa JJ, Lafuente P, Mota F, submitted.

16. See for instance: Deumal M, Cirujeda J, Veciana J, Kinoshita M, Hosokoshi Y, Novoa JJ, Chem. Phys. Lett., 1997; 265: 190.

17. a) Scrocco E, Tomasi J. Adv. Quant. Chem., 1978; 11: 115. b) Politzer P, Murray JS. Rev. Comp. Chem., 1991; 2: 273.

18. Novoa JJ, Mota F, Perez del Valle C, Planas M. J. Phys. Chem. A, 1997; 101: 7842.

19. For a review see: Ckaka AM, Zaniewski R, Youngs W, Tessier C, Klopman G. Acta Cryst., 1996; B52: 165. See also: a) Gavezzotti A. J. Am. Chem. Soc., 1991; 113: 4622, b) Gdanitz RJ, Chem. Phys. Lett., 1992; 190: 391, c) Karfunkel HR, Gdanitz R.J. J. Comp. Chem., 1992; 13: 1170.

20. Williams DE, PCK83, QCPE # 41, 1983.

21. Such methodology requires the use of methods capable of including the electron correlation (as the second order or fourth order Moller-Plesset methods, better known by their acronyms, MP2 and MP4, respectively), the use of very extended basis sets of the adequate class (see reference 22), and correcting the basis set superposition error (BSSE) using the counterpoise method (reference 23). With this methodology is possible to reproduce the interaction energy and main characteristics of the potential energy surface of hydrogen bonded and van der Waals dimers very accurately (see reference 24).

22. van Duijneveldt FB, van Duijneveldt-van de Rijdt JGCM, van Lenthe JH. Chem. Rev., 1994; 94: 1873.

23. Boys SF, Bernardi F. Mol. Phys., 1970; 19: 553.

24. a) Novoa JJ, Planas M, Whangbo M-H. Chem. Phys. Lett., 1994; 225: 240. b) Novoa JJ, Planas M, Rovira MC. Chem. Phys. Lett., 1996; 251: 33. c) Novoa JJ, Planas M. Chem. Phys. Lett. In press.

25. Kitaigorodsky A.I. Molecular Crystals and Molecules, Academic Press, London, 1973.

26. See, for instance: Gavezzotti A. Acc. Chem. Res., 1994; 27: 309. See also reference 19.

27. Novoa JJ, Deumal M. Mol. Cryst. Liq. Cryst., 1997; 305: 143.

28. Novoa JJ, Deumal M, Kinoshita M, Hosokoshi Y, Veciana J, Cirujeda J. Mol. Cryst. Liq. Cryst., 1997; 305, 129.

29. For examples see: a) Awaga K, Inabe T, Maruyama Y, Nakamura T, Matsumoto M. Chem. Phys. Letters 1992; 195: 21-24, b) Awaga K, Inabe T, Nakamura T, Matsumoto M, Maruyama Y. Mol. Cryst. Liq. Cryst. 1993; 232: 69-78, c) Awaga K, Okuno T, Yamaguchi A, Hasegawa M, Inabe T, Maruyama Y, Wada N. Phys. Rev. B 1994; 49: 3975-3981, d) Awaga K, Yamaguchi A, Okuno T, Inabe T, Nakamura T, Matsumoto M, Maruyama Y. J. Mater. Chem. 1994; 4: 1377-1385, e) Awaga K, Okuno T, Yamaguchi A, Hasegawa M, Inabe T, Maruyama Y, Wada N. Synth. Met. 1995; 71: 1807-1808.

30. For some examples see: a) Veciana J, Cirujeda J, Rovira C, Vidal-Gancedo J. Adv. Mater. 1995; 7: 221. b) Cirujeda J, Hernàndez E, Rovira C, Turek P, Veciana, J. New Organic Magnetic Materials. The Use of Hydrogen Bonds as a Crystalline Design Element of Organic Molecular Solids with Intermolecular Ferromagnetic Interactions, in New Organic Materials, Seoane C, Martin N, eds. Universidad Complutense de Madrid, Madrid, 1994, pp 262-272. c) Cirujeda J, Hernàndez E, Rovira C, Stanger JL, Turek P, Veciana J. J. Mater. Chem. 1995; 5: 243-252. d) Cirujeda J, Hernàndez E, Rovira C, Stanger JL, Turek P, Veciana J. J. Mater. Chem. 1995; 5: 243-252. e) Cirujeda J, Rovira C, Stanger JL, Turek P, Veciana J. The Self-Assembly of Hydroxylated Phenyl a-Phenyl Nitronyl Nitroxide Radicals, in Magnetism. A Supramolecular Function, Kahn O., ed. Kluwer Academic Publishers, Amsterdam, 1996, pp 219-248. f) Cirujeda J, Hernàndez E, Lanfranc de Panthou F, Laugier J, Mas M, Molins E, Rovira C, Novoa JJ, Rey P, Veciana J. Mol. Cryst. Liq. Cryst. 1995; 271: 1-12.

31. When no angular data are taken into account and only intermolecular distances are considered in a given magnetostructural correlation, one is always tempted to ascribe the observed ferromagnetic intermolecular interaction to the contacts between atoms of the two interacting molecules that have opposite spin densities and are at the closest distances. However, in some molecular layouts there could be other atoms at longer distances that are more favorable to interact ferromagnetically due to angular reasons.

32. See, for instance: a) Zheludev A, Barone V, Bonnet M, Delley B, Grand A, Ressouche E, Rey P, Subra R, Schweizer J. J. Am. Chem. Soc. 1994; 116: 2019-2027, b) Novoa JJ, Mota F, Veciana J, Cirujeda J. Mol. Cryst. Liq. Cryst. 1995; 271: 79-90.

33. Allen FH, Bellard S, Brice MD, Cartwright BA, Doubleday A, Higgs H, Hummelink T, Hummelink-Peters BG, Kennard O, Motherwell WDS, Rodgers JR, Watson DG. Acta Crystallogr. 1979; B35: 2331.

34. Deumal M, Cirujeda J, Veciana J, Novoa JJ, submitted.

35. This fact has been well documented for organic superconducting crystals, whose critical temperatures are also much lower than the room temperature. See, for

instance: Williams JM, Ferraro JR, Thorn RJ, Carlson KD, Geiser U, Wang HH, Kini AM, Whangbo M-H. Organic Superconductors, Prentice Hall, Englewood Cliffs, 1992. Magnetism is a different physical property than superconductivity, although both are intimately related with the relative arrangement of molecules in the crystal. The packing properties of molecular solids and, in particular, its variation with temperature, are determined by the intermolecular contacts, characteristic of the intermolecular contact and independent of the electronic physical property present in the crystal.

36. The presence of a positive density on the O atom has been shown by experimental and theoretical methods. See for instance, Ref. [32].

37. Barlow R. Statistics, John Wiley and Sons, Chichester, 1989.

38. Malinowski ER, Howery DG. Factor Analysis in Chemistry, Wiley Interscience, New York, 1980.

39. This conclusion shows that the use of three or even two geometrical parameters, a practice performed by some authors for analyzing series of α-nitronyl nitroxide radicals, is not correct.

40. Everitt BS. Cluster Analysis, 3rd edition, Edward Arnold, London, 1993.

41. The spin density on the H atom of the four CH_3 groups is negative, whereas these on the H atoms of a phenyl ring linked to the α carbon of the five membered ring are alternated in their sign, being positive for *ortho* and *para* H atoms and negative for the *meta* ones. See: a) Davis MS, Morokuma K, Kreilich RW. J. Am. Chem. Soc., 1972; 94: 5588-5592, b) Neely JW, Hatch GF, Kreilich RW. ibid, 1974; 96: 652-656, and Ref [32].

Figure captions

Figure 1. General structure of α-nitronyl nitroxide radicals (R is a substituent).

Figure 2. Examples of patterns compatible with the formation of infinite planes (a,c, e) and incompatible with that formation (b, d, f)

Figure 3. Geometrical parameters employed to define the relative position of two ONCNO groups in the space.

Figure 4. Tridimensional positions of the O_{21} atom relative to a $O_{12}N_{12}C_1N_{11}O_{11}$ group (as given by the values of D, A_1 and T_2) for a random selection of 100 contacts within the FM (upper) and AFM (lower) subsets of α-nitronyl nitroxide crystals.

Figure 5. Scattergram showing the dependence of D versus T_2 and A_1 versus T_2 for all the contacts of the FM (upper) and AFM (lower) subsets of α-nitronyl nitroxide crystals.

Figure 6. Geometrical parameters employed to define the relative position of one ONCNO group relative to the $C(sp^3)$-H group of the methyl groups attached to the five-membered rings of α-nitronyl nitroxide radicals.

Figure 7. Geometrical parameters employed to define the relative position of one ONCNO group relative to a $C(sp^2)$-H group located in *ortho*, *meta* or *para* position of an aromatic ring attached to the five-membered ring of an α-nitronyl nitroxide radical.

Figure 8. Tridimensional positions of the H atom relative to a $O_{12}N_{12}C_1N_{11}O_{11}$ group (as given by the values of D, A_1 and T_1) for all the $C(sp^3)$-H···O-N contacts

within the FM (upper) and AFM (lower) subsets of α-nitronyl nitroxide crystals.

Figure 9. Tridimensional positions of the H atom relative to a $O_{12}N_{12}C_1N_{11}O_{11}$ group (as given by the values of D, A_1 and T_1) for all the $C(sp^2)$-H···O-N contacts within the FM (upper) and AFM (lower) subsets of α-nitronyl nitroxide crystals.

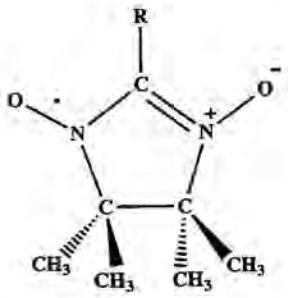

Fig. 1

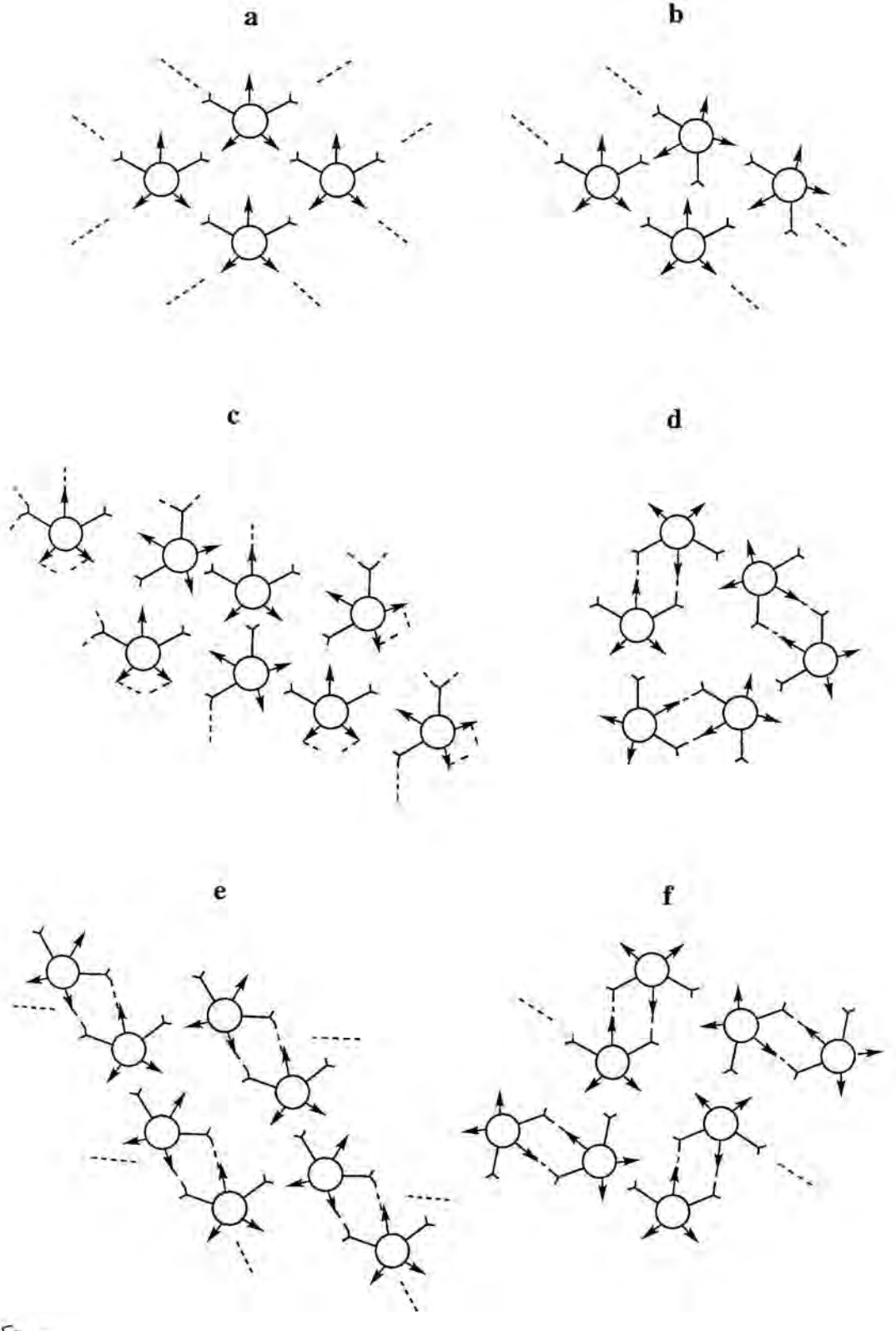

Fig. 2

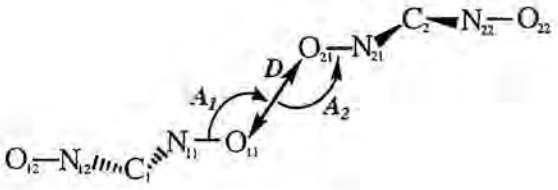

$D = O_{21} \cdots O_{11}$

$A_1 = O_{21} \cdots O_{11} - N_{11}$

$A_2 = N_{21} - O_{21} \cdots O_{11}$

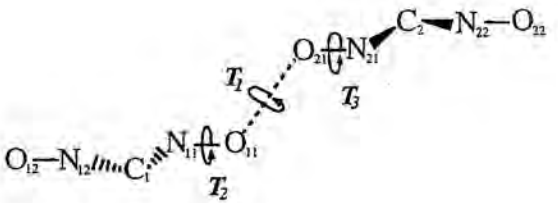

$T_1 = N_{21} - O_{21} \cdots O_{11} - N_{11}$

$T_2 = O_{21} \cdots O_{11} - N_{11} - C_1$

$T_3 = C_2 - N_{21} - O_{21} \cdots O_{11}$

Fig 3

FM subset of crystals

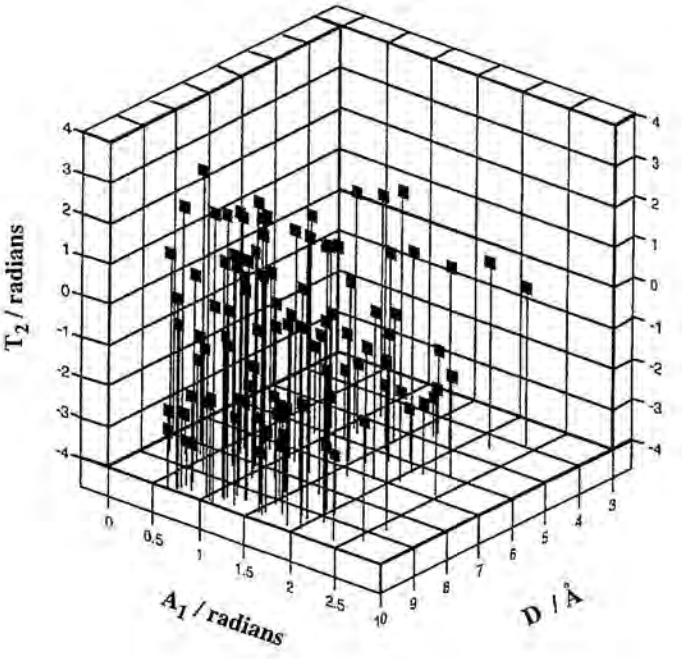

AFM subset of crystals

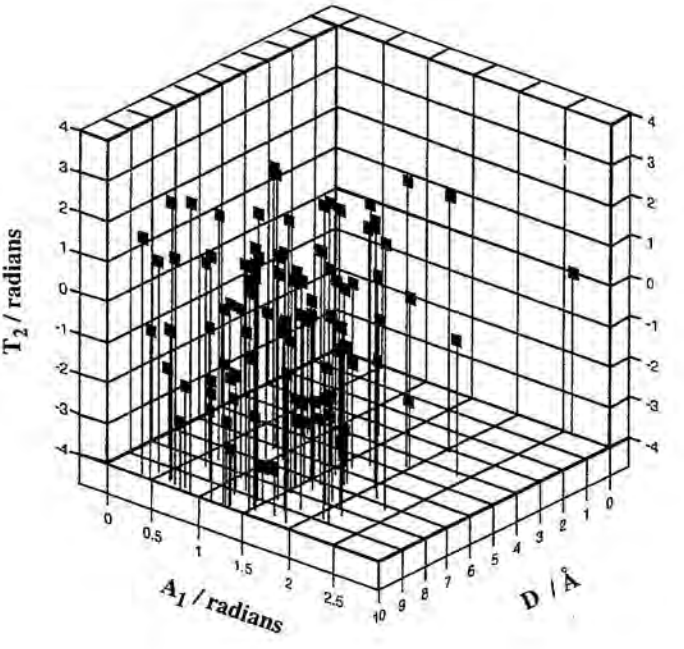

Figure 2

F5.4

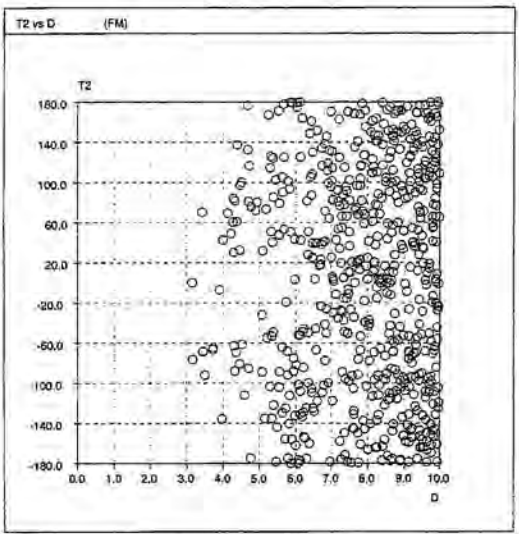
T2 vs D (FM)
T2
180.0
140.0
100.0
60.0
20.0
-20.0
-60.0
-100.0
-140.0
-180.0
0.0 1.0 2.0 3.0 4.0 5.0 6.0 7.0 8.0 9.0 10.0
D

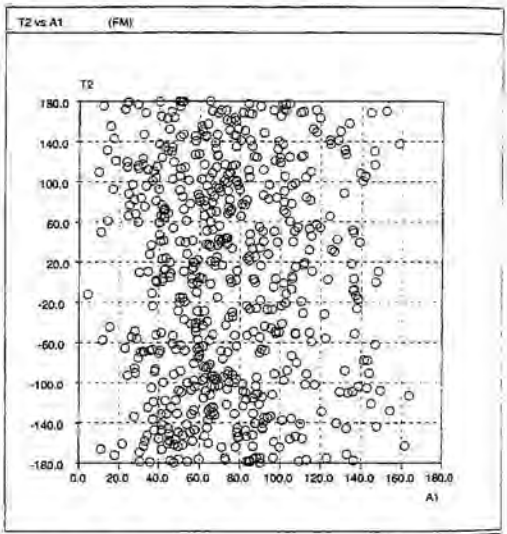
T2 vs A1 (FM)
T2
180.0
140.0
100.0
60.0
20.0
-20.0
-60.0
-100.0
-140.0
-180.0
0.0 20.0 40.0 60.0 80.0 100.0 120.0 140.0 160.0 180.0
A1

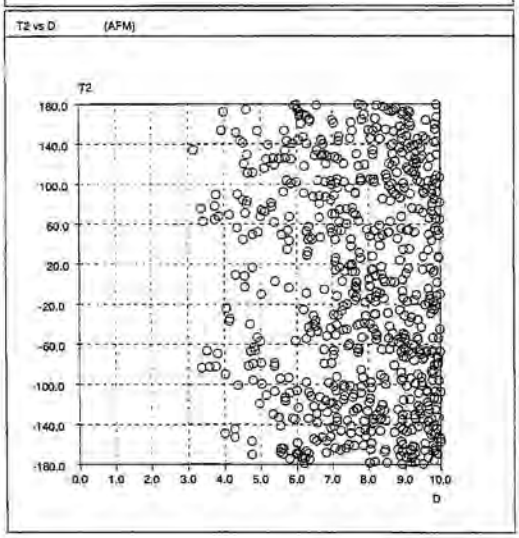
T2 vs D (AFM)
T2
180.0
140.0
100.0
60.0
20.0
-20.0
-60.0
-100.0
-140.0
-180.0
0.0 1.0 2.0 3.0 4.0 5.0 6.0 7.0 8.0 9.0 10.0
D

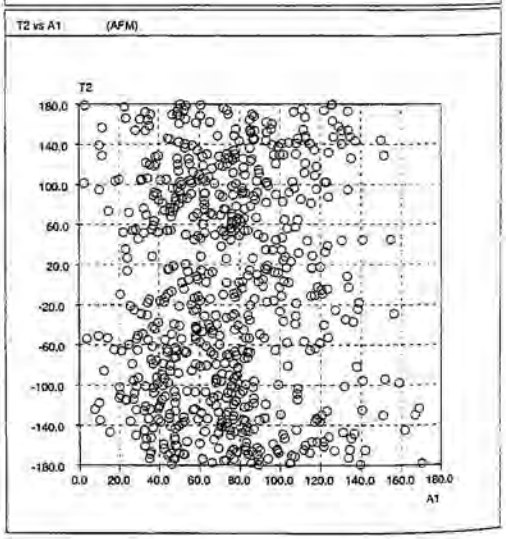
T2 vs A1 (AFM)
T2
180.0
140.0
100.0
60.0
20.0
-20.0
-60.0
-100.0
-140.0
-180.0
0.0 20.0 40.0 60.0 80.0 100.0 120.0 140.0 160.0 180.0
A1

Fig 5

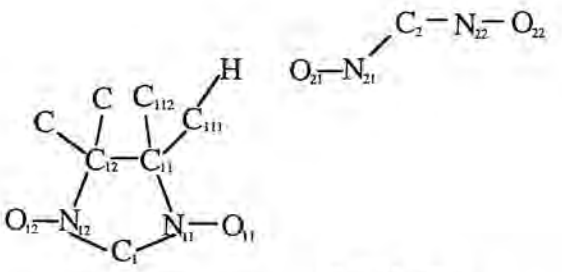

$D = H\cdots O_{21}$

$A_1 = H\cdots O_{21}\text{-}N_{21}$

$A_2 = C_{111}\text{-}H\cdots O_{21}$

$T_1 = C_{111}\text{-}H\cdots O_{21}\text{-}N_{21}$

Fig 6

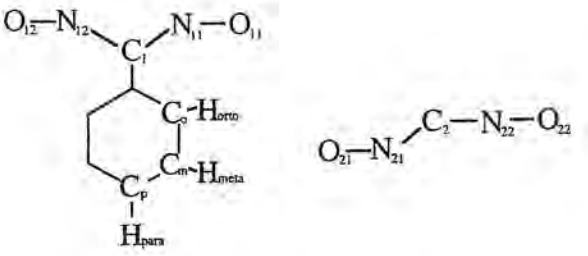

$D_o = H_{orto} \cdots O_{21}$

$D_m = H_{meta} \cdots O_{21}$

$A_{1o} = H_{orto} \cdots O_{21} - N_{21}$

$A_{1m} = H_{meta} \cdots O_{21} - N_{21}$

$A_{2o} = C_o\text{-}H_{orto} \cdots O_{21}$

$A_{2m} = C_m\text{-}H_{meta} \cdots O_{21}$

$T_{1o} = C_o\text{-}H_{orto} \cdots O_{21} - N_{21}$

$T_{1m} = C_m\text{-}H_{meta} \cdots O_{21} - N_{21}$

$D_p = H_{para} \cdots O_{21}$

$A_{1p} = H_{para} \cdots O_{21} - N_{21}$

$A_{2p} = C_p\text{-}H_{para} \cdots O_{21}$

$T_{1p} = C_p\text{-}H_{para} \cdots O_{21} - N_{21}$

Fig 7

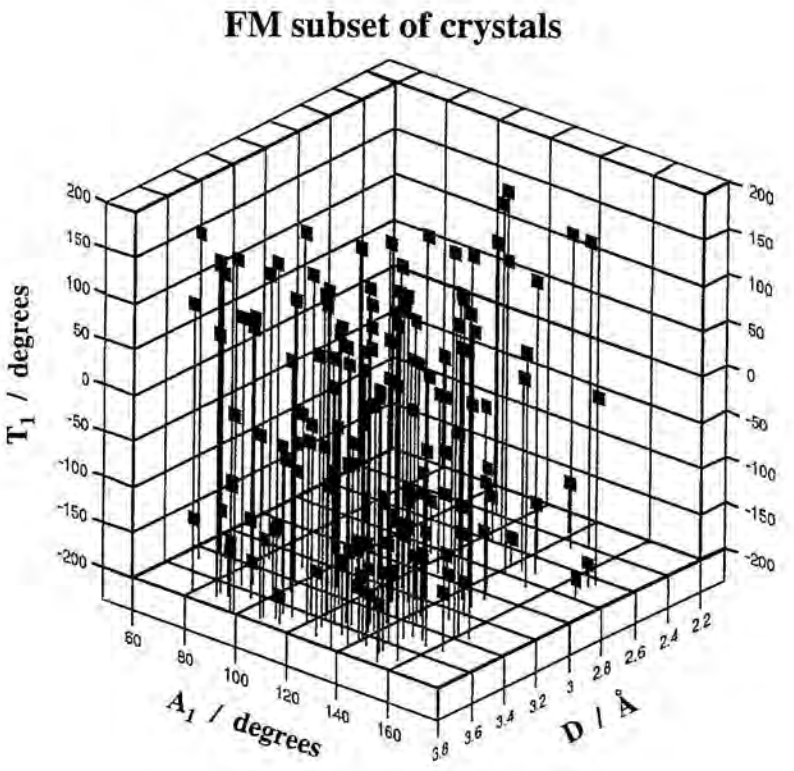
FM subset of crystals
T_1 / degrees
200
150
100
50
0
-50
-100
-150
-200
60
80
100
120
140
160
A_1 / degrees
3.8
3.6
3.4
3.2
3
2.8
2.6
2.4
2.2
D / Å

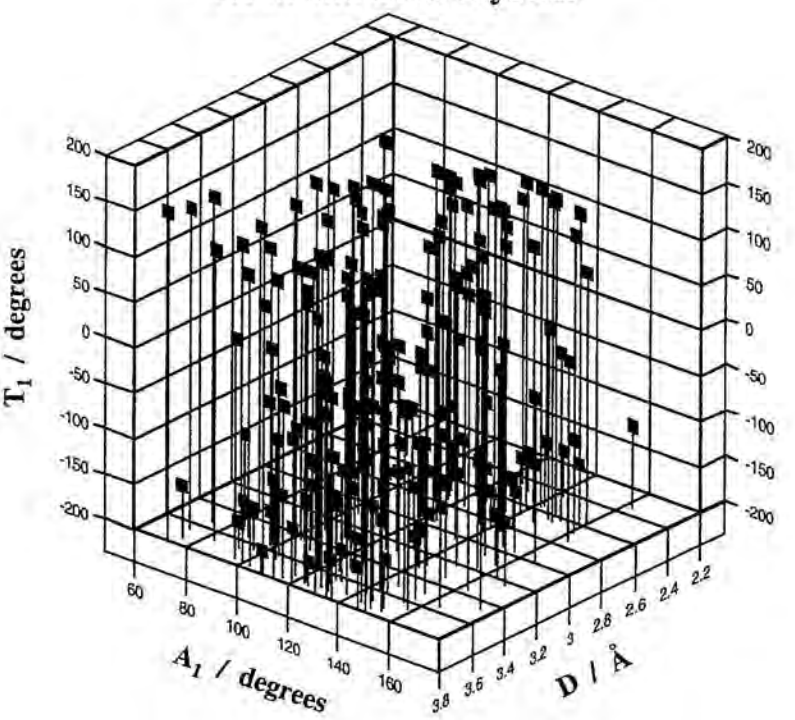
AFM subset of crystals
T_1 / degrees
200
150
100
50
0
-50
-100
-150
-200
60
80
100
120
140
160
A_1 / degrees
3.8
3.6
3.4
3.2
3
2.8
2.6
2.4
2.2
D / Å

Fig. 8

FM subset of crystals

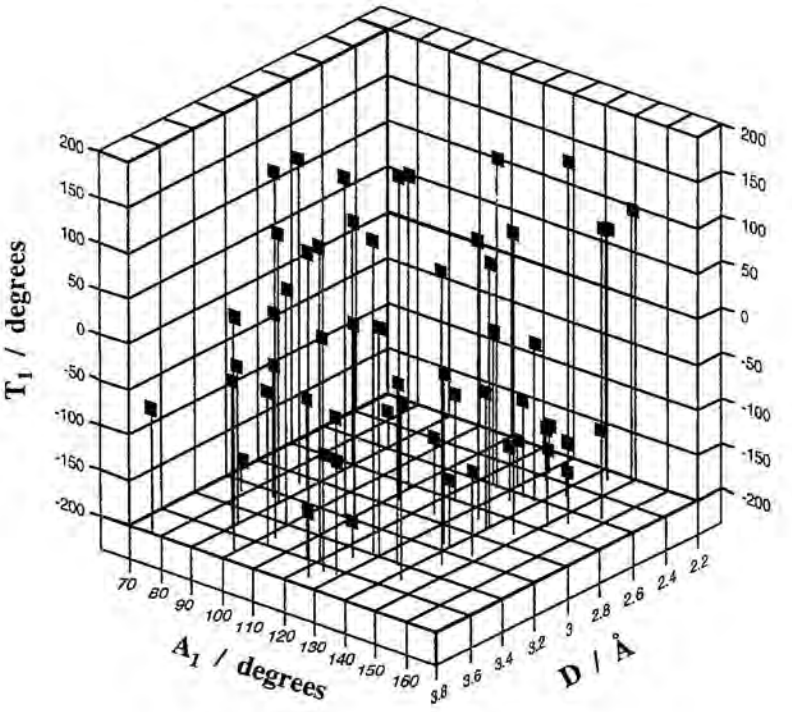

AFM subset of crystals

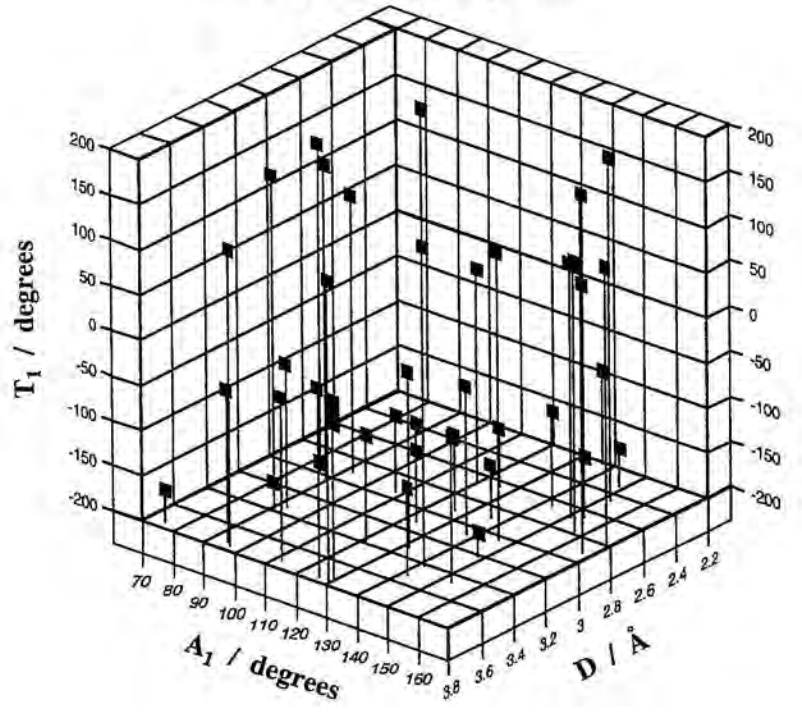

Fig. 9

ARTICLE 4

Synthetic Met. **1998**

Architecture of purely organic molecular magnets: Crystal packing rationalization of some α-nitronyl nitroxides using the crystal packing functional group analysis.

J. J. Novoa,[a*] Mercè Deumal,[a] J. Veciana[b]

[a]*Departament de Química Física, Universitat de Barcelona, Av. Diagonal, 08028-Barcelona (Spain)*

[b]*Institut de Ciència de Materials (CSIC), Caumpus Universitari de Bellaterra, 08913-Cerdanyola (Spain)*

Abstract

The main ideas of a method aimed at the rationalization of the crystal packing of molecular crystals in qualitative terms, called the crystal packing functional analysis, are presented. This method uses the information obtained from quantum chemical ab initio computations on the isolated molecule and some of its small aggregates. Its application is illustrated here to rationalize the experimental crystal packing of some α-nitronyl nitroxide radicals presenting interesting magnetic properties.

Keywords: Computer simulations; Ab initio quantum chemical methods and calculations; Molecular magnetic crystals.

1. Introduction

The α-nitronyl nitroxide (or α-nitronyl aminoxyl) radicals,[1,2] whose general formula is shown in Figure 1, are

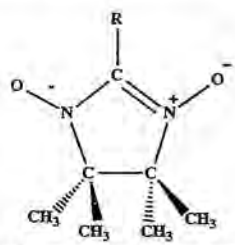

Fig 1. Molecular structure of the α-nitronyl nitroxides. R is any substituent.

one of the purely organic persistent radicals whose crystals show spontaneous magnetization below a certain critical temperature, in some cases, even bulk ferromagnetism.[1,3] However, up to now, the critical temperatures found in these materials are very low. Consequently, there is nowadays in the field of the molecular magnetism a strong research effort directed to improve our understanding of the factors controlling the magnetism in these materials, as an intermediate step towards the rational design of persistent radicals whose crystals could present ferromagnetic ordering at higher critical temperatures.

To achieve such objective, one needs to have a sounding structure-magnetism relationship which could tell us the relative orientations of the nearby radicals for which ferro or antiferromagnetic interactions are present. Once this is known, one also needs to understand the factors which control the crystal packing of the radicals of interest. In this form, it will be possible to design radicals whose crystal packing could present the relative geometrical arrangements between radicals which are required for the presence of the magnetic interaction of interest . A very popular structure-magnetism relationship has been the McConnell-I model,[4] in which the magnetic properties of the α-nitronyl nitroxide radicals are commonly rationalized looking at the closest NO...ON and NO...C(sp^2) contacts present among the ONCNO groups of the five-membered ring, the reason being that these are atoms in which most of the electronic spin distribution is located.[5] However, although the computation of minimum energy crystal packings of molecular crystals is nowadays well established, the rationalization of the experimental or computed packing structures was not achieved at the degree of comprehension required for its practical use as a tool, due to the lack of the adequate methodology. In this work, we will present a qualitative method developed in our laboratory, [6] called the crystal packing functional group analysis, aimed at rationalizing in qualitative terms any crystal packing structure. It uses the quantum chemical ab initio data from the isolated molecule and some of its small aggregates. Hereafter, we describe the basics of the method and its application to rationalize the experimental crystal packing of some α-nitronyl nitroxides showing magnetic properties.

2. The crystal packing functional group analysis

The experimentally seen molecular crystals are just one of minimum energy structures for that crystal. Many of the computed minimum energy structures, also called polymorphs, are never found experimentally, although computationally one can obtain many of these minimum in a small window of 2 kcal/mol.[7] In general, the experimentally observed structure (or structures) lye within the set of most stable minima, although it is not always the most stable one.

To rationalize these minimum energy structures one has to understand the driving force behind the existence of the crystal. The forces responsible for the existence of molecular crystal are the intermolecular interactions among the molecules. At low enough temperature, the molecules aggregate to form, first a liquid and, after more cooling, a solid. Under special conditions this solid presents long range order, and we talk about a crystal. The crystal interaction energy can be seen as the result of adding the contribution of all the different pairs of molecules.[7] From this point of view, it is a compromise between all possible pairs, but the driving forces behind the packing are easily appreciated by looking at how molecules aggregate to form a dimer or other small aggregates.

When two molecules are brought together all the atoms of these two molecules interact among each other. However, some of these interactions are much stronger than the rest and in fact, only a few dominate the packing. The idea is similar to that behind the bond concept in the molecules: They represent the strongest (and dominant) interactions within the molecules. Similarly, the strongest intermolecular interactions acting between molecules are the dominant forces and can be called intermolecular bonds. By doing this, we do not have to look at all the pair interactions between the atoms (within a pair approximation to the total interaction energy) but instead we look for the possible intermolecular bonds.

Intermolecular bonds are formed as a result of combining the adequate groups of two neighboring molecules. For instance, an intermolecular A-H...B hydrogen bond is formed by combining an A-H donor group of one molecule with a B acceptor group, from the second molecule. In neutral molecules, the other relevant although weaker intermolecular bond is the A...B van der Waals bond, resulting from the dispersive interaction of the lone pairs of the A and B atoms. In ionic solids, the Coulombic interactions (X(+)...Y(+), for instance) are the dominant ones and must be taken into account.

The nature of the functional groups present in the molecule can be identified by computing its molecular electrostatic map (MEP map).[8] This map represents the strength of the interaction energy between the molecule and a +1 charge in every region of the space. Regions of accumulation of electronic density will have negative MEP, while regions of decrease in the electronic density will have positive MEP. Therefore, the overlap of two MEP maps of the same molecule directly talks about the sign of the electrostatic energy between two molecules: the overlap of regions of the same sign have a repulsive electronic energy contribution, while overlap of opposite MEP regions give rise to attractive electronic energy contributions. We called this procedure a MEP map overlap analysis. As the electrostatic interaction is in most of the cases the dominant one,[9] this is a good approximation to the interaction between molecules.

Therefore, we can rationalize the interaction between molecules in terms of the intermolecular bonds they form, according to the following rules:

(1) Molecules aggregate using their functional groups to form intermolecular bonds, thus increasing their stability;
(2) We can predict these bonds by looking at the molecular electrostatic map to establish the nature of the functional groups each molecule has; the bonds are located by doing a MEP overlap analysis;
(3) There are many possible minimum energy aggregates (not necessarily dimeric), each can be called a *primary packing pattern*, as these are the blocks that make the crystal packing, or also synthons;
(4) The relative energy of each primary packing pattern is important to know its relative statistical probability of presence;
(5) The most stable crystals are grown up by using the most stable primary packing patterns. The primary packing patterns (for instance, a dimer) associate to for a secondary packing pattern (for instance, a plane of dimers), which can further associate to form higher structures or the crystal (stacks of planes). This allows to describe the crystal in terms of primary, secondary, and so on structure, according to their energetic stability.

Once the primary packing patterns have been found, one has to discard those not compatible with the tridimensional propagation required for the formation of a crystal. Therefore, only a few are relevant to understand the crystal structures of the molecule of interest. Notice that each relevant primary packing pattern (also called synthon) is one of the relative geometries of these dimers which (a) are compatible with the crystal structure, and (b) are minimum energy structures (energetically stable, of course).

From the previous ideas, it is possible to define a procedure to rationalize the structure of any molecular crystal, which we have called crystal packing functional group analysis,[6] because rationalizes the crystal packing by looking at the bonds made by the functional groups present in the molecule. It consists of the following steps:

1) *Characterization of the functional groups.* This can be done by simple inspection, extrapolating the behavior already obtained from other compounds, or by studying the MEP map, searching in it for the regions of concentration or depletion of electronic density.
2) *Identification of the primary packing patterns generated from these groups.* This can be done by a MEP map overlap analysis. The results from this analysis can be compared with the primary packing patterns present in the crystal. One can also identify these primary packing patterns by looking at the shortest intermolecular contacts.
3) *Computation of the strength of the primary packing patterns of interest.* Using ab initio computations on the adequate model systems, one can obtain the strength and directionality of the intermolecular bonds of interest. A first approximation of the strength of the primary packing pattern can be obtained by adding the energy of all the intermolecular bonds it presents. When possible, one can carry out the ab initio computation on pairs of dimers or the whole aggregate.
4) *Rationalization of the structure.* Using the information from the previous steps, one can define the primary, secondary and other higher structures present in the crystal .

We have successfully applied these rules to various molecular crystals [6,10]. In the next section we will describe its

application to some crystals of the α-nitronyl nitroxide family presenting magnetic properties.

3. Crystal packing analysis: the HNN case

The simplest crystal of the α-nitronyl nitroxide family is that of the 2-hydro nitronyl nitroxide (hereafter abbreviated as HNN), corresponding to the R = H case. This radical crystallizes in two polymorphic phases, identified as α and β, both of them antiferromagnetic in character.[11] In both phases the molecules form planes of dimers, piled up to give rise to the crystal. The dimers result from the simultaneous formation of two C(sp2)-H...ON contacts between the participating molecules. How can one rationalize these packings using the crystal packing functional group analysis?.

Following the previously mentioned steps, we computed the MEP map for the HNN molecule at the geometry of the crystal (see Figure 2). The MEP map clearly shows two regions of accumulation of charge, located on the NO groups (the negative regions of the MEP map). So, the NO groups serve as acceptors to the C-H groups, of which one can differentiate between the C(sp2)-H and C(sp3)-H groups.

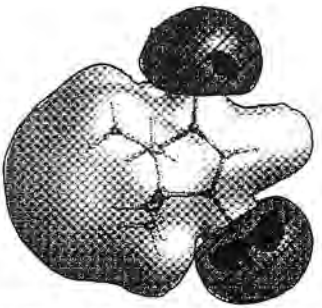

Fig. 2. MEP map of the HNN molecule, showing the negative regions (deep dark: -45 kcal/mol, shaded dark: -20 kcal/mol) and positive regions of +10 kcal/mol

The overlap of the MEP of two HNN molecules gives various minimum energy conformations, like those three shown in Figure 3. Quantum mechanical ab initio computations shows that the energy of a C(sp3)-H...O-N contact is -0.40 kcal/mol attractive, a C(sp2)-H...O-N contact is -3.71 kcal/mol stable.[6] Thus, the primary packing patterns involving the second are likely to be much more stable, as computations on the dimer quickly confirm. There are also other primary packing patterns, but a detailed study shows that the one identified as **1** in Figure 3 is the most stable one. The other lye much higher in energy and statistically are less likely to be found.

Using the previous information on the primary packing patterns stability one can rationalize the structure. The HNN has a strong tendency to form dimers of the type identified as 1, therefore, it constitutes the primary structure of the HNN molecules in the HNN crystal. These dimers still have N-O and C-H groups capable of forming more C-H...O-N hydrogen bonds, so they can aggregate to form planes, thus forming in the α and β polymorphs their secondary structure. The only change between these two polymorphic forms is their different relative orientation.[11,12] These planes then pile-up to form the tridimensional crystal structure using their still unused C(sp3)-H groups, making contacts with the N-O groups of the nearby planes (each N-O group can accept two C-H contacts using the two oxygen lone pairs).

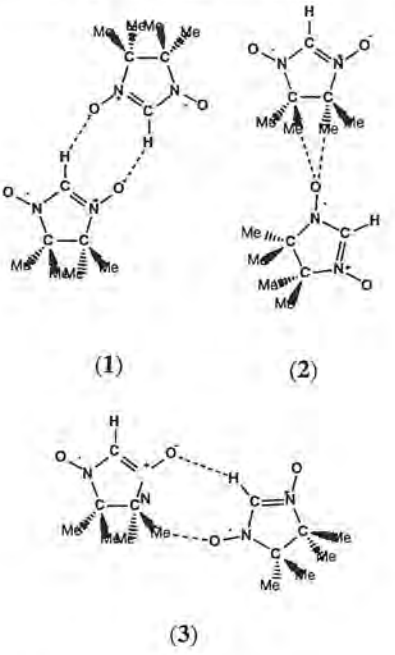

(1) (2) (3)

Fig. 3. Some of the minimum energy conformations of the HNN dimer found by doing a MEP map overlap analysis.

The previous example illustrates the use of the crystal packing functional group analysis. We have successfully applied the same procedure to other crystals of the α-nitronyl nitroxide family, and also to crystals of other families. [13]

4. Statistical analysis of the crystal packing of the α-nitronyl nitroxide ferromagnetic crystals

We have seen that the crystal packing of the α-nitronyl nitroxide family of radicals can be understood and their primary packing patterns identified. So, can we design new members of this family which likely will show better magnetic properties?.

The answer is not afirmative yet, as the identification of the ferromagnetic or antiferromagnetic nature of the primary packing patterns is not fully achieved at the present moment. We have seen[14] that the use of the McConnell-I model gives sometimes inconsistent results. Thus, an alternative solution seems to be an statistical analysis of all the crystal packing of the α-nitronyl nitroxide crystals showing dominant ferro or antiferromagnetic interactions, selected from the literature and from our own crystals. From an initial set of 143 crystals, we discarded those presenting R factors

greater than 0.10, those presenting disorder or large molecular distortions, those with metal atoms, and those co-crystallized with large closed-shell organic molecules. This left 72 crystals, but only 47 of them have clear dominating ferro (a subset of 23) or antiferromagnetic (a subset of 24) interactions.

The geometry of these crystals was analyzed within each subset. We did the analysis by looking at the geometry of the NO...ON and C-H...O-N contacts, trying to find the similitudes and differences in the geometrical distribution of these contacts in each subset. According to the McConnell-I model, one can expect that the crystals of the ferromagnetic subset will present, for instance, larger NO...ON distances and different angular orientation. However, our results show that the geometrical distribution of the NO...ON and C-H...O-N contacts is similar for the ferromagnetic and antiferromagnetic subsets. This fact questions the validity of any magneto-structural correlation made looking at the geometry of an individual contact. Further details on this will be published elsewhere and are not given here.[15]

From the previous results we conclude that new analysis using different perspectives or methods are needed to find sounding magneto-structural correlations which will be helpful to design new molecular magnets based on purely organic radicals.

5. References

[1] (a) M. Tamura, Y. Nakazawa, D. Shiomi, K. Nozawa, Y. Hosokoshi, M. Isjikawa, M. Takahashi, M. Kinoshita, Chem. Phys. Lett. 186 (1991) 401. (b) P.M. Allemand, K. C. Khemani, A. Koch, F. Wudl, K. Holczer, S. Donovan, G. Grüner, J. D. Thompson, Science, 253 (1991) 301. (c) R. Chiarelli, M. A. Novak, A. Rassat, J. L. Tholance, Nature, , 363 (1993) 147. (d) T. Sugawara, M. M. Matsushita, A. Izuoaka, N. Wada, N. Takeda, M. Ishikawa, J. Chem. Soc., Chem. Commun., (1994)1081. (e) J. Cirujeda, M. Mas, E. Molins, F. Lanfranc de Panthou, J. Laugier, J. Geun Park, C. Paulsen, P. Rey, C. Rovira, J. Veciana, J. Chem. Soc., Chem .Comm. (1995) 709. (f) A. Caneschi, F. Ferraro, D. Gatteschi, A. leLirzin, M. A. Novak, E. Rentsecheler, R. Sessoli, Adv. Mater. 7 (1995) 476. (g) Y. Pei. O. Kahn, M. A. Aebersold, L. Ouahab, F. Le Berre, L. Pardi, J. L. Tholance, Adv. Mater. 6 (1994) 681. (h) K. Togashi, K. Imachi, K. Tomioka, H. Tsuboi, T. Ishida, T. Nogami, N. Takeda, M. Ishikawa, Bull. Chem. Soc. Jpn. 69 (1996) 2821 and references therein.

[2]. α-nitronyl nitroxide is the abbreviated name commonly employed for the 4,5-dihydro-4,4,5,5-tetramethyl-3-oxido-1*H*-imidazol-3-ium-1-oxyl compounds, the correct IUPAC name.

[3] (a) O. Kahn, Molecular Magnetism, VCH Publishers, New York, 1993. (b) J. S. Miller, A. J. Epstein, *Angew.* Chem. Int. Ed. Engl. 33 (1994) 385. (c) M. Kinoshita, Jpn. J. Appl. Phys. 33 (1994) 5718. (d) E. Coronado, P. Delhaes, D. Gatteschi, J. S. Miller, (eds.) Molecular Magnetism: From Molecular Assemblies to Devices, Kluwer Academic Publishers, Dordretch, 1996. (e) O. Kahn, (ed.) Magnetism: A Supramolecular Function, Kluwer Academic Publishers, Dordretch, 1996. (f) K. Itoh, J. S. Miller, T. Takui, (eds.) Mol. Cryst. Liq. Cryst. 305/306 (1997)1-586/1-520.

[4] H. M. McConnell, J. Chem. Phys. 39 (1963) 1910.

[5] (a) A. Zheludev, V. Barone, M. Bonnet, B. Delley, A. Grand, E. Ressouche, P. Rey, R. Subra, J. Schweizer, J. Am. Chem. Soc. 116 (1994) 2019. (b) J. J. Novoa, F. Mota, J. Veciana, J. Cirujeda, Mol. Cryst. Liq. Cryst. 271 (1995) 79.

[6] (a) J. J. Novoa, M. Deumal, Mol. Cryst. Liq. Cryst. 305 (1997) 143. (b) M. Deumal, J. Cirujeda, J. Veciana, M. Kinoshita, Y. Hosokoshi, J. J. Novoa, Chem. Phys. Lett., 165 (1997) 190. (c) J. J. Novoa, F. Allen, J. Howard (eds.) Implications of Molecular and Materials Structure for New Technologies, Kluwer Academic Publishers, Dordretch, (in press).

[7] (a) H. R. Karfunkel, R. J. Gdanitz, J. Comput. Chem. 13 (1992) 1171. (b) J. Perlstein, J. Am. Chem. Soc. 116 (1994) 455. (c) A. Gavezzotti, Acc. Chem. Res. 27 (1994) 309.

[8] E. Scrocco, J. Tomasi, Adv. Quantum Chem. 11 (1978) 115.

[9] Stone, A. J. The theory of intermolecular forces, Clarendon Press,Oxford (1996).

[10] M. Deumal, J. J. Novoa (unpublished results)

[11] Y. Hosokoshi, M. Tamura, K. Nozawa, S. Sizuki, H. Sawa, R. Kato, M. Kinoshita, Mol. Cryst. Liq. Cryst. 115 (1995) 271.

[12] J. J. Novoa, M. Deumal, M. Kinoshita, Y. Hosokoshi, J. Veciana, J. Cirujeda, Mol. Cryst. Liq. Cryst. 305 (1997) 129.

[13] D. Braga, F. Grepioni, E. Tagliavini, J. J. Novoa, F. Mota, New. J. Chem. (in press).

[14] J. J. Novoa, J. Vecian, M. Deumal, J. Veciana (ed.), Supramolecular Emgineering of Synthetic Materials: Conductors and Magnets, Kluwer, Dordrecht (in press).

[15] M. Deumal, J. Cirujeda, J. Veciana, J. J. Novoa, Adv. Mater. (in press).

ARTICLE 5

Mol. Cryst. Liq. Cryst. **1997**, *305*, 129-141

Mol. Cryst. Liq. Cryst., 1997, Vol. 305, pp. 129–141
Reprints available directly from the publisher
Photocopying permitted by license only

© 1997 OPA (Overseas Publishers Association)
Amsterdam B.V. Published in The Netherlands
under license by Gordon and Breach Science Publishers
Printed in India

A THEORETICAL ANALYSIS OF THE PACKING AND POLYMORPHISM OF THE 2-HYDRO NITRONYL NITROXIDE CRYSTAL

JUAN J. NOVOA,[a] MERCE DEUMAL,[a] MINORU. KINOSHITA,[b] YUKO HOSOKISHI,[c] JAUME VECIANA[d] AND JOAN CIRUJEDA[d]

[a] Departament de Química Física, Facultat de Química, Universitat de Barcelona, Av. Diagonal 647, 08028-Barcelona, Spain

[b] Science University of Tokyo in Yamaguchi, Daigaku-dori 1-1-1, Onoda-shi, Yamaguchi 756, Japan

[c] Institute for Solid State Physics, University of Tokio, Roppongi, Minato-ku, Tokio 106, Japan.

[c] Institut de Ciencia de Materials de Barcelona, 08193-Bellaterra, Barcelona, Spain

Abstract The packing of the two crystallographics forms the 2-hydro nitronyl nitroxide (HNN) molecule has been studied. Using the ab initio methodology described in the accompanying paper, the packing is rationalized. In both crystals the primary structure are the HNN dimers linked trough C(sp2)-H...O-N contacts. These dimers form planes of molecules, which constitute the secondary structure. The structure and stability of the planes are different in the two crystals. Finally, the planes form stacks, the tertiary and last structure in both crystals. The forces involved in each type of structure have been quantified. The relationship between the two polymorph crystal forms have been analyzed and rationalized.

INTRODUCTION

The presence of magnetism in a molecular crystal and its dimensionality depends on the way the crystal packs, that is, on the distance and relative spatial orientation of the molecules which constitute the crystal.[1] Therefore, understanding and controlling the factors which govern the packing of these crystals is a key step towards the design of

molecular magnetic crystals. In the previous paper,[2] we have described how the packing of a molecular crystal can be analyzed using the data from ab initio computations. This is the aim of this work is to apply the previous methodology to rationalize the packing of the simplest member of the nitronyl nitroxide family of radicals, the 2-hydro nitronyl nitroxide radical (hereafter identified as HNN), using the information from ab initio quantum mechanical methods and from the distance analysis of the crystal.

The HNN radical is the simplest member of the nitronyl nitroxide radicals,[1,3] whose general formula is :

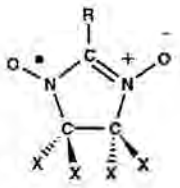

being HNN the member in which R=H. A recent study[4] has allowed to find two crystal phases (thereafter identified as the α-HNN and β-HNN phases), both showing an antiferromagnetic behavior. A thermal analysis of the α-HNN phase in the 40-160 °C range shows the presence of an irreversible transition to the more stable β-HNN phase at 60.2 °C. At 105.4 °C the α-HNN crystals begin thermal decomposition. This paper is devoted to rationalize these two packing structures using the analytical the methods described in detail in the accompanying article. These results should also help to understand the packing motifs generated by the five member ring common to other members of the nitronyl nitroxides family.

METHODOLOGY

The packing of a molecular system is one of the minima found in the total interacting energy of the crystal, that is, is influenced by all the intermolecular interactions present in the crystal. However, this energy can be analyzed looking at its components and at how the dimers and other small aggregates are formed: the crystal is a progressive built up of packing units and the possible minima in these aggregates can be rationalized knowing the properties of the possible intermolecular interactions, and in particular, of the strongest

ones. In the most stable packing structures the molecules aggregate maximizing the number of strongest interactions. The packing motifs generated by the strongest bonds is the primary structure of the crystal (for instance, planes of molecules), while the weaker bonds are responsible for the secondary one. In a crystal, the aggregation process must be done in such a way that the long range order is preserved, a fact that limits the number of packing forms.

From the above discussion it is clear that to rationalize the packing one has to understand the nature of the intermolecular interactions present in it. Any given crystal can present three types of intermolecular interactions: ionic, hydrogen bonds, and van der Waals, being diffuse in some cases the separation between these classes.[5] The ionic interactions are present when the crystal has ions in it, so they are not possible in the HNN case. Hydrogen bond interactions are found whenever a contact of the type X-H···Y is produced between two molecules of the crystal.[6] They have a strong electrostatic character and are expected to be important in the HNN crystal because this molecule has a strong permanent dipole moment of 3.872 Debyes. Finally, van der Waals interactions are the weak short range found between atoms with no dangling bonds and whose lone pair electrons are at a short distance of each other. This situation that can be represented as X:···:Y, where the symbol : represents the lone pair electrons. The van der Waals interactions are expected to be weaker than the hydrogen bond interactions in the HNN molecule. The information from ab initio computations can help us to determine the possible contacts and their strength.

To identify the possible arrangements of the molecules which will generate the packing motifs, one can use the molecular electrostatic (MEP) maps.[7] The one for the HNN molecule[2] shows two strongly attractive region located on each oxygen and repulsive regions over the C-H bonds. Thus, one can expect that the C-H bonds will act as acid groups and the O of the NO groups as basic in the formation of the C-H···O-N hydrogen bond. One can distinguish between two types of carbons according to their hybridization: the methyl carbons are C(sp^3), while the carbon in between the two NO groups is a C(sp^2). Using the MP2 method and the 6-311++G(2d,2p) basis set on the adequate model systems we have computed the strength of the C(sp^2)-H···O-N and C(sp^2)-H···O-N contacts.[2] They are attractive with a strength of -3.71 and -0.40 kcal/mol, respectively. At the same time, using the same methodology and the adequate model system the N-O···O-N is found to be repulsive by about +1 kcal/mol at the van der Waals distance.[2] In the rest of the paper we will show how this information can be used to understand the packing and polymorphism of the α-HNN and β-HNN crystals.

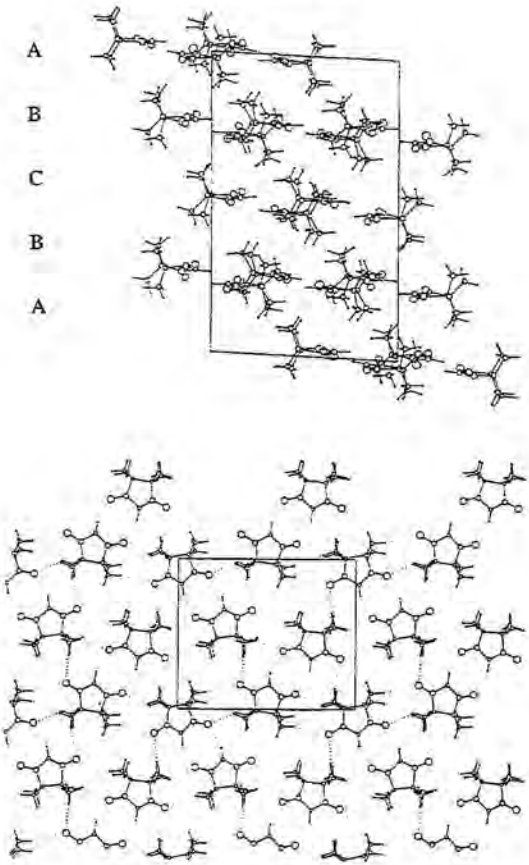

FIGURE 1.- Packing of the α-HNN crystal showing the shortest C-H···O contacts: (a) Extended view along the **b** axis showing the four planes (ABBA) within the unit cell; (b) view of the A plane along the **a** axis.

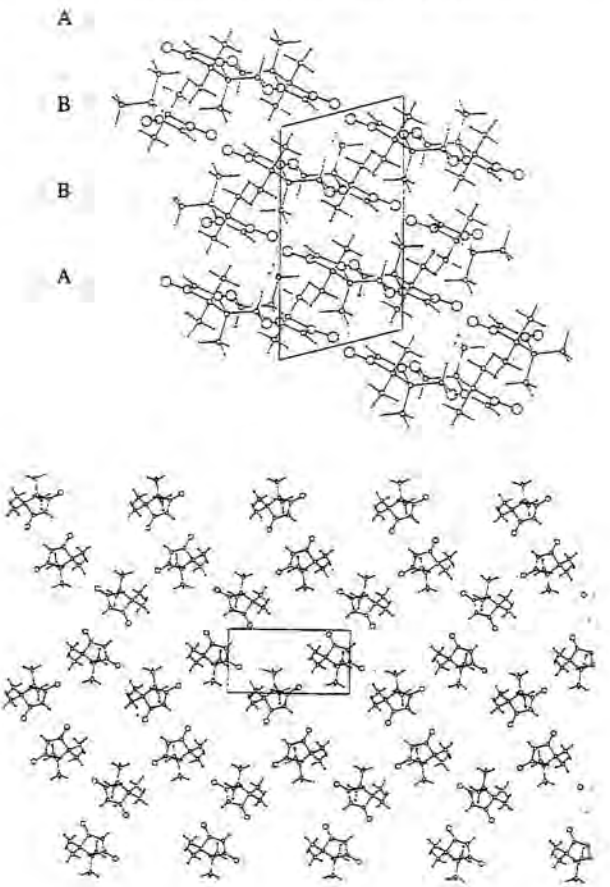

FIGURE 2.- Packing of the β-HNN crystal showing the shortest C-H···O contacts: (a) Extended view along the **b** axis showing the five planes (ABCBA) within the unit cell; (b) view of the A plane along the **a** axis.

RESULTS AND DISCUSSION

The packing of the α and β phases of the HNN crystal

The α-HNN crystal contains four molecules per unit cell arranged in such a way that the crystal belongs to the $P2_1/n$ spatial group.[4] The unit cell has the following crystallographic parameters: a = 11.879 Å, b = 11.611 Å, c = 6.332 Å and β = 104.48°. The β-HNN crystal has sixteen molecules per unit cell packed in such a way that the space group is the $P2_1$ one.[4] The crystallographic parameters of the second crystal are: a = 19.991 Å, b = 14.091 Å, c = 12.144 Å and β = 92.92°.

For an in depth understanding of the packing of these systems is better to have a more exhaustive picture of their packing. We can plot, in an extended way, the shortest contacts between the molecules of the crystal (i.e., those contacts whose distance is around the sum of the van der Waals radii of the two atoms making the contact). Figure 1 shows a view of the structure of the α-HNN crystal in which the intermolecular C-H···O contacts smaller than 3.5 Å have been indicated by broken lines, while Figure 2 shows, indicating also the C-H···O contacts, a view of the structure of the β-HNN crystal. In both cases the packing is characterized by the superposition of planes, each resulting from the aggregation of HNN dimers. The formation of planes is not surprising because is the most stable way of ordering dipole moments and the HNN molecule has a strong dipole moment originated by his two NO groups. At a first look, the previous structural consideration could indicate that the planes constitute the primary structure of the crystal, while the stacking of these planes the secondary one.

Within each crystal all the planes included in the unit cell are identical but differ by their relative position, sometimes by an inversion center, sometimes by a relative displacement along some symmetry element. Consequently, within the unit cell of the α-HNN crystal we can distinguish crystallographically two types of planes, identified as A and B, ordered in a sequence ABBA, with the B planes closer to the inversion center located in the center of the cell. Within the unit cell of the β-HNN crystal there are five planes, ordered in a sequence ABCBA, with the C plane passing through the inversion center located in the middle of the unit cell.

The internal structure of the planes in the α-HNN and β-HNN crystals is different although the dimers which constitute the planes have a similar structure. In both crystals the dimers are made by means of two $C(sp^2)$-H···O-N contacts (see Figures 1 and 2). However, the geometries of the two types of dimers, although similar, is slightly different: The $C(sp^2)$-H···O angle is 162° in the α-HNN crystal to be compared with the 156° value for the β-HNN crystal; The shortest H···O distance is 2.416 Å in the α-HNN crystal and 2.256 Å in the β-HNN crystal, while the H···H distances are 2.688 and 3.085 Å in the α-

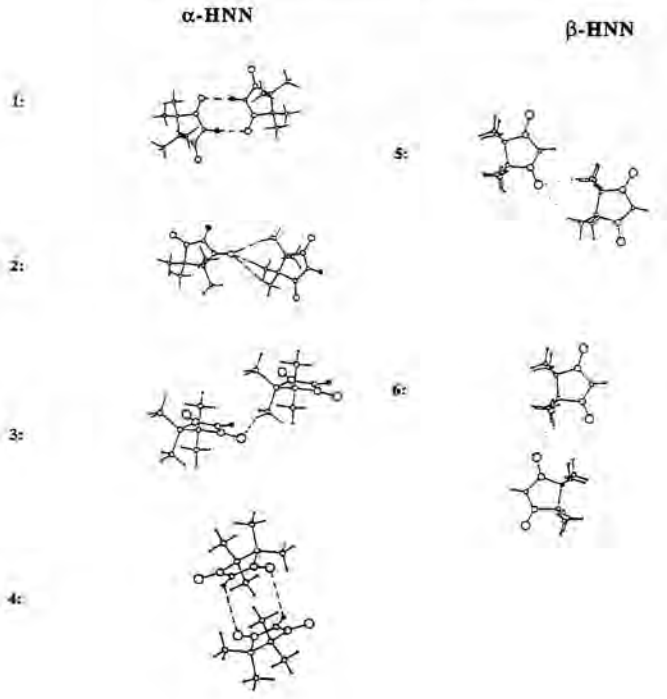

FIGURE 3.- Types of arrangements found in the α-HNN and β-HNN crystals.

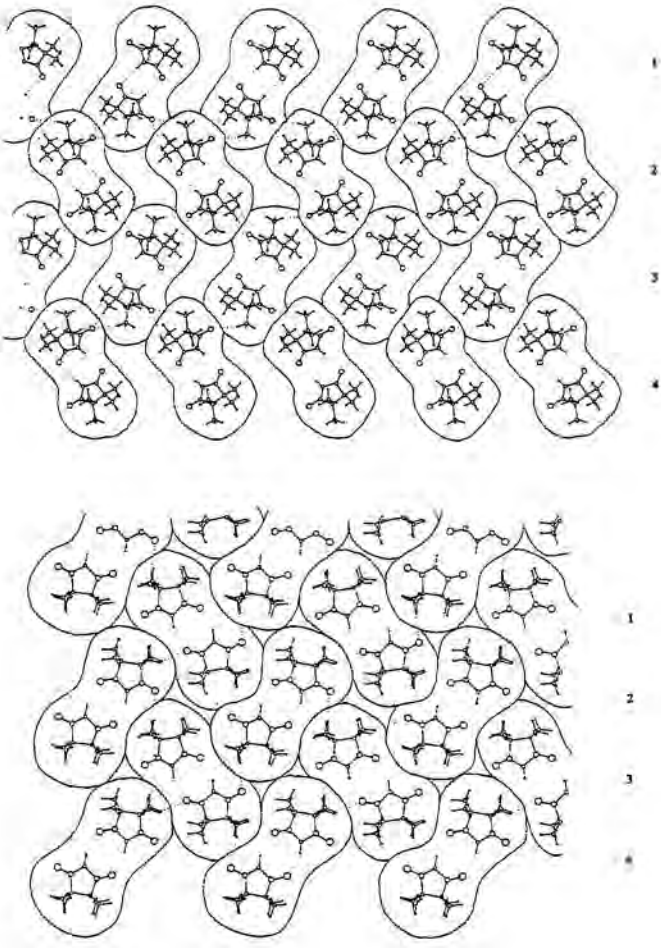

FIGURE 4.- Schematic representation of the planes of the α-HNN and β-HNN crystals (upper and lower part of the Figure, respectively).

HNN and β-HNN crystals, respectively; Finally, the dimers are not strictly coplanar in the α-HNN crystal while they are coplanar in the β-HNN crystal. Ab initio computations[8] have showed that the planar conformation of the dimer is the most stable one but that slight displacements from the planarity are not expensive energetically and the dimer can relax its planarity if in this way it maximizes the number of contacts with the surrounding molecules or the strength of the contacts. The optimum H···O distances in gas phase[8] are both 2.154 Å while the angle is 133.1°. This result can be taken as reference to understand the geometrical distortions induced by the surrounding molecules in the dimer geometry .

The HNN dimer has still two NO groups and eight methyl groups which can be used to make intermolecular contacts with other dimers via hydrogen bonds or van der Waals interactions. Using these contacts, the dimers can make links with their neighboring dimers to form the above mentioned planes. A close look at Figures 1 reveals that in the α-HNN crystal all the interdimer contacts are of the $C(sp^3)$-H···O-N type, with each dimer making 12 contacts, 6 as acid and 6 as base. The interdimer contacts in the β-HNN crystal are also of the $C(sp^3)$-H···O-N type, but the number is larger (24 in total, eighteen of whom are shown in Figure 2). As the two dimers make two $C(sp^2)$-H···O-N intradimer contacts at about the same geometry, one can expect that the planes in the β-HNN crystal are more stable. The formation of planes maximizes the number of contacts and is the most stable conformation for systems with strong dipole moments, as the HNN. Once the planes are formed, the methyl groups still have $C(sp^3)$-H bonds which are unused and can be used to form $C(sp^3)$-H···O-N interplane contacts (one has to keep in mind that each oxygen has two lone pairs and only one has been used in the in-the-plane contacts.

Table I lists the shortest intermolecular distances within the planes and between the planes for the two crystals. The numbers indicate that the contacts are similar in the two crystals, with small variations. On the other hand, the various types of geometrical arrangements that the dimers can make in the α-HNN and β-HNN crystals are shown in Figure 3. Arrangements 1, 2, 5 and 6 correspond to in-the-plane conformations, while 3 and 4 correspond to between-planes conformations, found in the α-HNN and β-HNN crystals. Obviously, arrangement 1 is also found in the β-HNN crystal but is not duplicated in the list.

One can compute the energy associated to each of these geometrical arrangements using the ab initio data for the model $C(sp^2)$-H···O-N and $C(sp^3)$-H···O-N contacts, after multiplying this number by the number of contacts which each arrangement makes. Thus arrangement 1, which makes two $C(sp^2)$-H···O-N contacts, and its interaction energy should be 2x(-3.71) = -7.42 kcal/mol. We tested the validity of this result by computing the interaction energy of the optimized dimer in gas phase and we obtained a value of -7.20 kcal/mol. The difference between this number and the previous one reflect the importance

TABLE I. Shortest intermolecular distances within the α-HNN and β-HNN crystals.

Class	Contact type	distance[a] α-HNN	distance[a] β-HNN
Intraplane	$C(sp^2)$-H···O	2.416	2.193
	$C(sp^3)$-H···O	2.554	2.431
	$C(sp^2)$-H···H-$C(sp^2)$	2.689	3.085
	$C(sp^3)$-H···H-$C(sp^3)$	2.790[c]	2.741
	N-O···O-N	4.271	3.642
Interplane	$C(sp^3)$-H···O	2.535	2.637
	$C(sp^2)$-H···H-$C(sp^3)$	2.660	2.781
	$C(sp^3)$-H···H-$C(sp^3)$	2.548	2.491
	N-O···O-N	3.798	4.226

[a] in Å

[b] per dimer

[c] the next contact is at a distance >3.20 Å

of the polarization effects that one bond induces in the other. However, the geometry of the dimers in the crystal is not the same that the gas phase optimum geometry and, consequently, the interaction energy of each dimers of the α-HNN and β-HNN crystals is -5.53 and -5.44 kcal/mol, respectively. The energy of arrangement 2 can be computed as three times that for a $C(sp^3)$-H···O-N contact, that is, 3 x (-0.40) = - 1.2 kcal/mol, while that for arrangement 3, in which only one $C(sp^3)$-H···O-N contact is made, is -0.40 kcal/mol. Arrangement 4 corresponds to an inter-plane interaction and was computed using a model system similar to Model I but oriented to mimic the geometry of this arrangement in the crystal (that is, the H···O distance was 3.331 Å and the C-H...O angle 85.3°). The BSSE-corrected interaction energy computed using the MP2 method and the 6-311++G(2d,2p) basis set is -1.38 kcal/mol, that is, -0.69 kcal/mol per each long range $C(sp^2)$-H···O-N contact. Arrangement 5 shows two $C(sp^3)$-H···O-N contacts against the same NO groups with an estimated total interaction energy of -0.80 kcal/mol, the same. Finally, arrangement 6, which presents also the same number of $C(sp^3)$-H···O-N contacts,

but connected in a different way, has an estimated interaction energy of -0.80 kcal/mol. Probably the polarization effects will make the energy of the last two arrangements slightly different but not significantly, as was seen above.

How can one characterize the packing of the two crystals at the light of the previous results ?. These values indicate that there are strong and weak hydrogen bonds. The strong $C(sp^2)$-H···O-N contacts are used to form HNN dimers, by large, the most stable geometrical arrangement. Therefore, the HNN molecules will have a strong energetic preference to form dimers and this is the main motif of the primary structure. When the dimers are formed, no new strong $C(sp^2)$-H···O-N contacts can be made as no free $C(sp^2)$-H bonds are left. In the crystals studied here the dimers make contacts among themselves according to one of the types indicated in arrangements 2-6. Arrangement 4 is not a minimum energy structure of the dimer and, if left alone, the two molecules will become coplanar as in arrangement 1. So, arrangement 4 will only be find once the planes are formed. Among arrangements 2, 5 and 6, the first is the most stable one. By making use of it, the crystal will grow one of the planes (making planes always maximizes the number of these contacts) to form the packing motif typical of the α-phase. Using a combination of 5 and 6, the planes of the β-phase are obtained. As the number of contacts to be made is larger and requires a more ordered structure, entropically the growth of the β-phase planes is more difficult, although energetically is more favorable. So, we have justified the secondary structure of the two crystals, the molecular planes. As the NO groups repel each other in the plane, no short NO···ON distances are found in these crystals. Once the planes are formed, there are still some unused intermolecular interactions. The first type is located in the methyl groups, which can still make contacts against the NO groups involved in the $C(sp^2)$-H···O-N contacts, arrangement 3, as only one intermolecular interaction is made there. Otherwise, using arrangement 4, the planes can be attached to each other. The result is the formation of ordered stacks of planes, piled up in such a way that they maximize the interplane interaction energy. This is the tertiary structure of the crystal.

Polymorphic transformations between the α and β phases.

The previous analysis fully rationalizes the structure of the α-HNN and β-HNN crystals and gives clues on the effect that the five member ring can induce in the packing of other similar molecules of the nitronyl nitroxide family. Now we can have a look at the polymorphic α -β transformations.

We can understand the essence of the process looking at Figure 4, where the packing in one of the planes has been schematized using the dimers as packing units. In the α-phase each plane is constituted by rows of dimers, parallel to each other, but pointing in different directions, in such a way that the dimers of one row are nearly perpendicular to

these of the adjacent rows. The n row is liked with the n-1 and n+1 rows by means of arrangement 2 contacts. Each dimer makes two of these contacts to two different dimers of the adjacent row. Each molecule of the HNN dimer is liked to only one molecule of the dimer to which is linked. On the other hand, in the β-phase the contact between the dimers are made in such a way that the dimers in the nth row makes hydrogen bond contacts with these of the n-1 and n+1 rows and, at the same time, "touch" the dimers in the n+2 and n-2 rows, thus allowing the formation of stable $C(sp^3)$-H···H-$C(sp^3)$ van der Waals contacts. Consequently, the dimers in the β-phase are more tightly packed. It is possible to go from the α to the β phase by a collective displacement of the dimers of the n-1 and n+1 rows in the opposite direction towards the center of the dimers of the nth row. The shift is structurally reversible and one can in principle go from the β to the α phase by reversing the it. However, as was mentioned before, the β-phase is much more stable and the barrier to leave the potential well associated to this phase can be much more important than the one needed to enter in it, making irreversible the b to a pathway for thermodynamic or kinetic reasons. Finally, due to the change of structure in the planes, the stacking has to adapt its structure, but this should be no problem as a large number of methyl groups is always available perpendicular to the planes.

In summary, we have seen that one can explain the known properties of the packing of the HNN crystal by a careful use of the MEP maps and the strength of the intermolecular interactions, both data obtained from ab initio computations. The extension to larger systems has been already tested. The results are also satisfactory and will be presented elsewhere.

ACKNOWLEDGMENTS

This work was supported by the CICYT (Grant No. MAT94-0797), the DGICYT (Project No. PB92-0655-C02-02), CIRIT (GRP94-1077 and GRQ93-8028), the NEDO (Grant Organic Magnets). We also thank CESCA and CEPBA for generous allocations of computer time. M.D. and J. C. acknowledge CIRIT for their doctoral grants.

REFERENCES

1.- (a) H. M. McConnell, J. Chem. Phys. 39, 1910 (1963)
(b) McConnell, H. M. Proc. Robert A. Welch Found. Conf. Chem. Res. 11, 144(1967).

(c) M. Kinoshita, Jpn. J. Appl. Phys., 33, 5718 (1994) and references therein.
(d) O. Kahn, Molecular Magnetism, (VCH Publishers, New York, 1993).
(e) J. S.Miller; A. J. Epstein, Angew. Chem. Int. Ed. Engl., 33, 385 (1994).

2.- J. J. Novoa and M. Deumal, Mol. Cryst. and Liq. Cryst., this issue.

3.- (a) H. Tamura, Y. Nakazawa, D. Shiomi, K. Nozawa, Y. Hosokoshi, M. Ishikawa, M. Takahashi, M. Kinoshita, Chem. Phys. Lett., 186, 401 (1991).
(b) R. Chiarelli, M. A. Novak, A. Rassat, J. L. Tholence, J. L. Nature (London), 363, 147 (1993).
(c) T. Tomioka, H. Ishida, H. Yoshikawa, M. Yami, F. Iwasaki, H. Iwamura, N. Takeda, M. Ishikawa, Chem. Lett., 29 (1994).
(d) T. Sugawara, M. M. Matsushita, A. Izouka, N. Wada, N. Takeda, M. Ishikawa, J. Chem. Soc., Chem. Commun., 1723 (1994).
(e) J. Cirujeda, M. Mas, E. Molins, F. Lanfranc de Pauthou, J. Laugier, J.-G. Park, C. Paulsen, P. Rey, C. Rovira, J. Veciana, J. Chem. Soc., Chem. Commun., 709 (1995).

4.- Y. Hosokoshi, M. Tamura, K. Nozawa, S. Suzuki, H. Sawa, R. Kato and M. Kinoshita., Mol. Cryst. and Liq. Cryst., 115, 271 (1995).

5.- G. C. Maitland, M. Rigby, E. Brian Smith and W. A. Wakeham, Intermolecular Forces, (Clarendon Press, Oxford, 1981).

6.- J. Bernstein, M. C. Etter and L. Leiserowitz, in Structure Correlation, edited by H.-B. Burgi and J. D. Dunitz (VCH, Weinheim, 1994), Chap. 11.

7.- (a) E. Scrocco, J. Tomasi, Adv. Quantum Chem., 11, 115 (1978).
(b) P. Politzer, J. S. Murray, Rev. Comput. Chem., 2, 273 (1991).

8.- J. J. Novoa and M. Deumal, unpublished computations.

ARTICLE 6

Supramolecular Engineering of Synthetic Materials: Conductors and Magnets
J. Veciana (ed.), Kluwer, Dordrecht (**1998**)

CRYSTAL ENGINEERING OF PURELY ORGANIC MOLECULAR MAGNETS: WHAT AB INITIO COMPUTATIONS CAN TELL US?

J. J. NOVOA,[1*] J. VECIANA,[2*] AND M. DEUMAL[1]

[1] *Departament de Química Física. Facultat de Química, Universitat de Barcelona, Av. Diagonal 647, E-08028 Barcelona (Spain)*

[2] *Institut de Ciència de Materials de Barcelona (CSIC), Campus UAB, E-08913 Bellaterra (Spain).*

1. Introduction

Molecular ferromagnetism [1] is only possible for persistent radicals capable of presenting a crystalline packing which allows for the presence of intermolecular ferromagnetic interactions propagating all over the crystal. It is only possible if each spin containing molecule is capable of having one or more magnetic interactions with one or more of its first neighbor molecules, and their strengths overcome the thermal energy at T_C; i.e., with an energy larger than kT_C[2]. Thus, the presence of ferromagnetism in a purely organic compound relies on three facts: the ability to prepare a persistent free radical, the possibility to grow a crystalline supramolecular organization with such a radical, and the ability of radicals in such crystals to interact ferromagnetically with each other [3]. These materials are characterized by the presence of a spontaneous magnetization below a certain critical temperature, T_C, as detected by the shape of the χT *vs* T or M *vs* T curves in a temperature range as close as possible to the 0-300K range.

As result of a systematic synthetic effort, it has been possible to obtain different kinds of crystals of organic free radicals that show relevant magnetic properties [1]. In very exceptional cases, even bulk ferromagnetism has been achieved [4,5]. The critical temperatures of the already known compounds are still low [6]. Consequently, there is a drift towards the design of compounds presenting ferromagnetism at higher critical temperatures. This requires, besides the synthetic effort essential to create new permanent radical molecules, a better understanding of the driving forces behind the already known compounds, that is, of the methodologies required to control the crystal packing of molecular materials, and of the factors that govern the magnetic interactions between purely organic molecules. In this work we will show how the results from ab initio computations [7] can help us to understand the crystal engineering and our understanding of the magnetic interaction in purely organic crystals. We will show how using ab initio methods one can improve our knowledge on the following three important questions for the design of purely organic ferromagnetic compounds: 1) Can we rationalize and/or predict the crystal packing of purely organic molecular magnets?, 2) Are there specific crystal packing patterns associated to the ferro and antiferromagnetic crystals of the already known compounds?, and 3) Does the McConnell-I model work in predicting the magnetic behavior of a molecular crystal?.

We will address the previous questions looking into the α-nitronyl nitroxide [8] family of radicals (also called α-nitronyl aminoxyl), whose general formula is shown in Figure 1a. This family of radicals is characterized by the presence of a five-membered ring with two

nitronyl groups attached in an alpha position to a C(sp^2) carbon. We will pay a special attention to the properties of two members of this family whose magnetic properties are well characterized, the phenylnitronyl nitroxide (PhNN for short, see Figure 1b) and the α phase of the 2-hydroxy-nitronyl nitroxide (α-2OHNN, see Figure 1c). The PhNN crystals show an antiferromagnetic behavior [9], while the α-2OHNN crystals show ferromagnetic interactions along the three directions of the space [10]. Here we will try to understand why a small change in the chemical structure induces such a large modification in the magnetic properties.

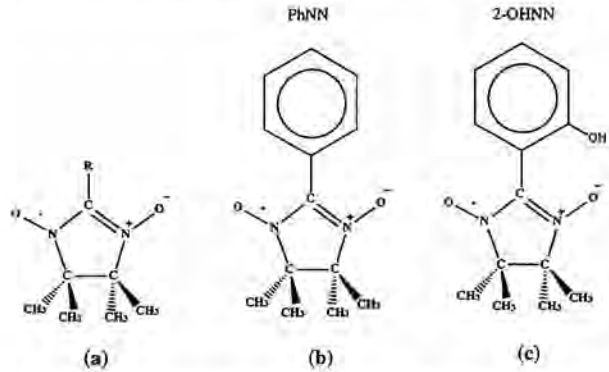

Figure 1. (a) General nitronyl nitroxide; (b) the PhNN radical; (c) the 2-OHNN radical

The α-nitronyl nitroxides is the most extensively studied family of persistent radicals in the purely organic molecular magnets. Within this family, there are many different packings and magnetic behaviors due to the effect of other functional groups present in the compounds. The latter fact reflects the strong influence induced on the packing by the functional groups attached to the five-membered ring: even small changes on a large group, as the insertion of a OH group on a phenyl, can give rise to remarkable changes in the packing. So, it is important to rationalize and predict the changes in the packing of the crystals if a better degree of control on the design of molecular magnets is desired, our first question. Also recognizing if there are some special orientations of the molecules associated to the presence of ferromagnetism is important, and is the main point of our second question. On the other hand, it is well established that the presence of bulk ferromagnetism in a crystal of this family is strongly related to the relative disposition of the spin containing molecules within the crystal. This result is consistent with the most commonly accepted ideas based on the already existing theoretical models about intermolecular magnetic interactions [1,11]. For instance, within the very popular McConnell-I model [11], probably the most employed magnetic model nowadays due to its simplicity. It predicts the existence of intermolecular ferromagnetic interactions when short contacts are present between atoms bearing a considerable atomic spin population of opposite spin. Otherwise, the interaction would be antiferromagnetic or negligible. However, we will see later that one cannot explain the magnetic properties of the PhNN and α-2OHNN crystals using the McConnell-I model in the usual way done up to now.

2. Crystal packing of molecular magnets: can we rationalize and predict it?

When molecular crystals pack they form characteristic tridimensional networks of intermolecular contacts, called *motifs* [12], a fact first recognized by Etter [13] and employed as a classification tool by Bernstein, for instance [14]. Alternatively, one can look at the crystal from a supramolecular point of view and notice that it is made of basic building units called *primary packing patterns* [15] or *synthons* [16], each of them obtained by associating groups of molecules (normally dimers) through intermolecular bonds, not necessarily of the same kind [17]. In purely organic molecular magnets, the intermolecular contacts are of the hydrogen bond and van der Waals type. They can be differentiated by their topology: Hydrogen bonds are contacts in which an A-H···:B topology is present, that is a A-H group points to a high electronic density region of the B atom created by a lone pair, for instance, while van der Waals contacts are A:···:B contacts in which the lone pairs of the A atom are close to the lone pair of the B atom.

If we want to be able to rationalize and predict crystal packing we have to include in our model the basic property which makes to exist the synthons and dictates their structural preferences, the energy. It was long recognized that crystals pack in such a way that minimize their total packing energy, E_T, a fact that has been used by many to compute the crystal packings of molecules with remarkable good results [18-20]. The total packing energy is normally defined as a sum over all different pair interactions, $E_{ij}(r_{ij})$, that is,

$$E_T = \sum' E_{ij}(r_{ij}) \qquad (1)$$

Of all of the pair interactions, only the strongest ones play a key role in defining the geometry of the motifs and synthons. The most likely important ones are those whose atom-atom distances are close to the sum of the van der Waals radii of the atoms involved in the contact, and we generally associate these to the presence of an intermolecular bond [21]. Doing only the sum over the important contacts in Equation (1), is equivalent to substitute the atom-atom summation of that equation by an intermolecular bond summation [17]. In purely organic molecular magnets, the energetically important interactions are necessarily hydrogen bonds or van der Waals bonds, as these are the only ones present in neutral molecules. Normally, one expects the hydrogen bonds to be the key ones.

The formulation of Equation (1) as sum over intermolecular bonds is a very useful tool to rationalize the packing of molecular crystals. One just has to look at the crystal as a supramolecular aggregate and realize that the main difference between any gas phase molecular aggregate and a crystal is the presence of periodic boundary conditions, which restricts the geometry of the aggregate. Now we just need to identify the structure within these repeating aggregates. These are just the *primary packing patterns* or *synthons*, whose propagation along the symmetry elements of the crystal generates the crystal, characterized by its *pattern* (described in terms, for instance, of *motifs*). Thus, we can understand the way the crystal pack looking at why molecules aggregate at the molecular level, that is, we look at it as a supramolecular aggregate [22]. *Primary packing patterns* describe the topology of the *synthons*. The most relevant to understand the crystal structure are those that describe the way in which two neighbor molecules are linked through intermolecular bonds. Understanding the reasons for the existence of these *primary packing patterns* is the key to understand the structure of the molecular crystals.

At the dimer level, a primary packing pattern is one stable geometrical orientation of two molecules. This stability is just the result of the formation of intermolecular bonds between their functional groups. So, if we identify the functional groups, their ability to

participate in the formation of hydrogen bonds and van der Waals contacts, and their geometrical distribution, we can search for possible primary packing patterns by looking at the ways in which the complementary functional groups can be associated. Once this is done, one has to identify what intermolecular bonds it really presents. This can be done using some geometrical criteria based in cutoff distances [21], or using more precise methods, like those based on locating the bond critical points in the electronic density, which are characteristic of the formation of the intermolecular bonds [23,24]. These ideas are very powerful to identify intermolecular bonds in molecular aggregates and crystals [25], or to define the type of intermolecular bond [23,26].

Notice that not all the intermolecular interactions within the pattern are necessarily attractive, but we can assume that to obtain stable crystals we need energetically stable primary patterns. The generation of dimeric primary packing patterns from a molecule by molecular association is illustrated in Figure 2 for a hypothetical molecule presenting five functional groups, three capable of acting as hydrogen donors (A-H groups, in general) and two acting as hydrogen bond acceptors (:B groups). Different primary patterns can have different energetic stability, computed in an approximate form as the addition of the energy of the intermolecular bonds present in them or from accurate ab initio computations of the dimer. The most stable patterns are those maximizing the number of most stable intermolecular contacts. The most stable crystals are those obtained by using the most stable patterns.

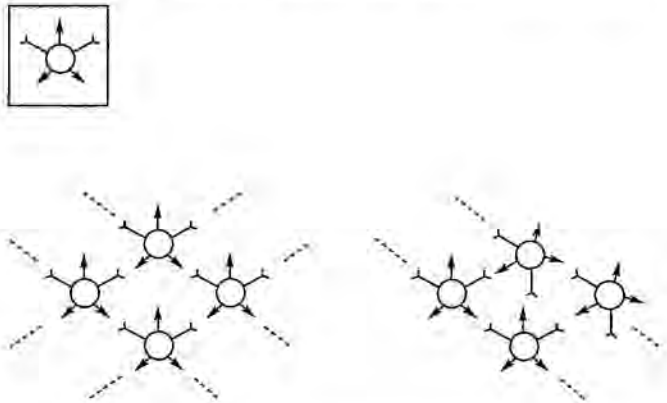

Figure 2. Two possible packing patterns for a molecule with three donor and two acceptor hydrogen bond groups.

Molecules in crystals can associate in many stable primary pattern, but not all the primary packing patterns are going to be relevant for the analysis of the crystal packing due to energetical, and symmetrical factors. The energetical factor, the different stability primary packing patterns, is responsible for the higher statistical probability of presence of the most stable primary packing patterns. If the energy difference between the energetically adjacent

patterns is not large there is no statistical preference, but in some cases the most stable primary packing pattern or a small group is more stable than the rest and becomes dominant in terms of probability of presence. The symmetrical factor is due to the translational symmetry inherent to the nature of the crystal: some patterns are not possible in the crystal, because they cannot propagate, or this propagation is not energetically stable. This is illustrated for two dimensions in Figure 2: while pattern **a** is suitable for its 2D propagation, pattern **b** is not. When the molecules are persistent free radicals, some of the primary packing patterns can produce dominant ferromagnetic interactions and others yield dominant antiferromagnetic interactions, allowing for this reason to be identified as *ferro- and antiferromagnetic patterns*.

Can we predict the shape and stability of the relevant primary packing patterns formed by a molecule? The answer is affirmative: using ab initio methods one can localize the minimum energy conformations for a dimer of the molecule of interest (or higher aggregate, if needed) and estimate its energy. This can be done in two ways (a) by solving the Schrödinger equation of the dimer or aggregate to find the optimum geometry and associated energy, or, when this is too expensive computationally, (b) estimating in a qualitative form the primary packing patterns and then computing its energy by adding the estimate for the interaction energy of each intermolecular bond present in it. In the second case, one can obtain good estimates of the optimum geometry of the aggregate by a *MEP maps overlap analysis*. In this analysis, one looks at the overlap between the regions of attractive and repulsive molecular electrostatic potentials (MEP) maps [27,28]: overlapping MEP regions of opposite sign gives rise to attractive interactions, otherwise they are repulsive. We can also have a first guess of the geometry of the primary packing patterns by a geometrical overlap of the complementary groups of the molecule with their functional groups oriented as they are in the molecule (see Figure 2). Finally, if one just wants to rationalize the structure of a given crystal, then one can obtain the primary packing patterns by analyzing the regularities in the packing of a crystal. The crystal structure can come from a crystal grown up experimentally or, if no experimental crystal is available, one can use computed crystal structures obtained from any of the programs for crystal optimization [18-20].

The ab initio computation of the optimum geometry and energy of primary packing patterns requires of a careful selection of the model system, basis set and ab initio method. Such methodology requires the use of methods capable of including the electron correlation (as the second order or fourth order Moller-Plesset methods, better known by their acronyms, MP2 and MP4, respectively), the use of very extended basis sets of the adequate class [29], and correcting the basis set superposition error (BSSE) using the counterpoise method [30]. With this methodology is possible to reproduce the interaction energy and main characteristics of the potential energy surface of hydrogen bonded and van der Waals dimers very accurately [31]. To optimize the whole aggregate, one uses its crystal geometry or other starting geometry. However, this approach is very expensive and normally one has to resort to add the strength of the bonds using realistic model systems (the second approach mentioned above). One can compute, for instance, the strength of the $C(sp^2)$-H···O-N, N-O···O-N, and $C(sp^3)$-H···O-N contacts present in many primary patterns of the α-nitronyl nitroxides using substituted dimers in which these interactions are present. We have successfully used this method to rationalize the packing of many crystals [32] and large molecular clusters [25].

Normally, the real crystal is the result of the progressive association of molecules within the solution in which they grow. They do so forming as many as the most primary patterns as possible, to build the first order aggregates. At this point, when this kind of patterns are saturated, if they want to further aggregate they have to use other patterns to link the first order aggregates, like ribbons and planes, for instance. To build the crystal these second order aggregates have to further aggregate using other primary packing patterns. Therefore, we can

define an ordering in the crystal structure, associated to the stability of the different packing patterns: we can differentiate a *primary structure* of the crystal, associated to the most stable primary packing patterns, a *secondary structure*, and even a *tertiary* or *quaternary structures*, in some cases. When the primary packing patterns have similar energy, it is not so easy to talk about these levels of structure, or they are not uniquely defined.

Using the methodological approach described above it is possible to carry out the analysis of any crystal structure by following the next sequence of steps:

1) Characterization of the functional groups. This can be done by simple inspection, extrapolating the already known information on the same groups, or by studying the nature of the MEP map, which defines regions of concentration and depletion of the electronic density, and the acid-basic character of the functional groups. Thus, we can assign an acid character for a C-H group in an α-nitronyl nitroxide radical looking at their positive MEP, and a basic character for a N-O group due to their negative MEP.
2) Identification of the primary packing patterns. This can be done from a experimental determined crystal structure by looking at the shortest intermolecular contacts, normally assumed to be attractive and responsible for the main issues of the packing structure. Alternatively, one can carry out the same analysis on any structure obtained after a computational optimization of the crystal. Note here that not every short contact is always attractive, but can be a consequence of the presence in nearby positions of two attractive interactions. We should also use relaxed cutoffs in the distances to avoid problems [21], or carry out a bond critical point analysis [23-26]. A *MEP overlap analysis* can also help to identify the possible relative geometry dispositions in which the functional groups can be associated in energetically stable conformations. This is sometimes done intuitively by associating complementary groups but is more systematic in terms of MEP maps obtained from ab initio computations.
3) Definition of the strength of the primary patterns. Ab initio computations allow to define an energetic order for all the primary packing patterns, required to understand the presence or absence of some patterns in the crystal due to statistical reasons.
4) Rationalization of the structure. Using the information obtained in the previous steps. The crystal packing can be justified in terms of a primary structure, secondary and so on.

This is a ***crystal packing functional group analysis***, as the primary patterns are obtained looking at the different forms in which the groups can be associated (using MEP overlap analysis or other alternative approach).

We can apply the crystal packing functional groups analysis to rationalize the structure of the PhNN and α-2OHNN crystals shown in Figure 3. These two crystals, although only differ in the presence of a OH group in the 2 position relative to the five membered ring C(sp^2) atom, present totally different crystal packing and magnetic properties (see above) [9,10]. The PhNN crystal has four planes, in a ABBA disposition, with the A planes packed in a different form that the B ones (Figure 3a). At the same time, the α-2OHNN crystal packs in such a form that three identical A planes are present in the unit cell. The structure of these planes is quite complicated, but can be rationalized in terms of alternating right-left chains made of a propagated molecular dimers (see Figure 3b). So, it seems worth a detailed study of these two crystals to understand what causes these differences.

Following the above mentioned steps, we begun by computing the MEP maps of the two molecules at their crystal geometry (Figure 4). The PhNN molecule presents a strong basic region (of -36 kcal/mol) located on the two NO groups, and a less basic region (of -15 kcal/mol) located above and below the benzene ring. At the same time, there are positive regions along all the C-H bonds (computations show that a C(sp^2)-H bond is more acidic than a C(sp^3)-H one).

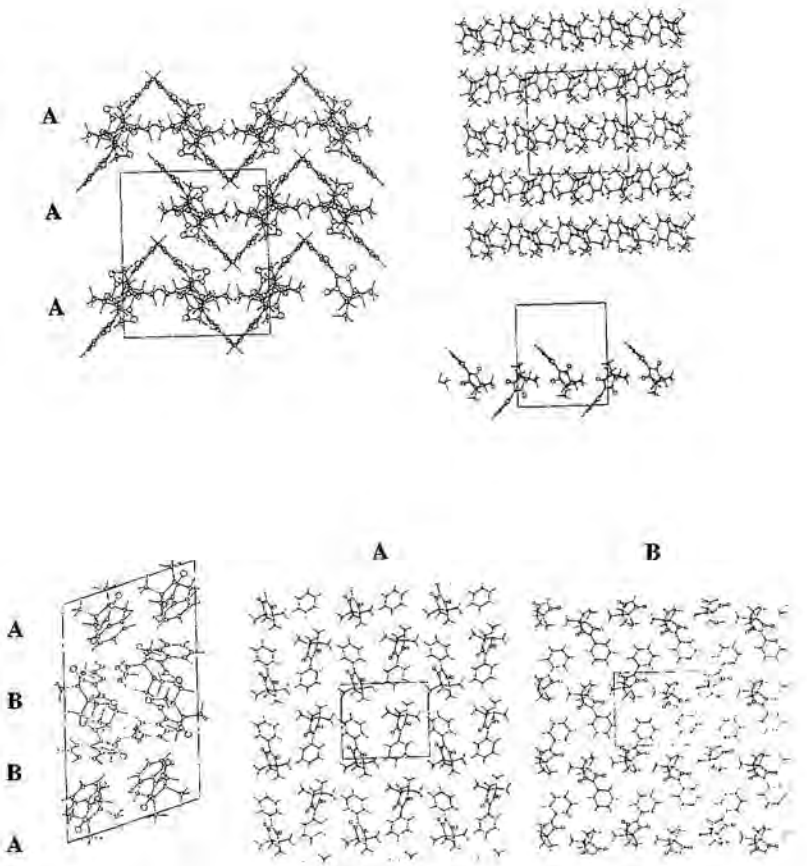

Figure 3. Up: Packing of the PhNN crystal. Down: Packing of the α-2OHNN crystal.

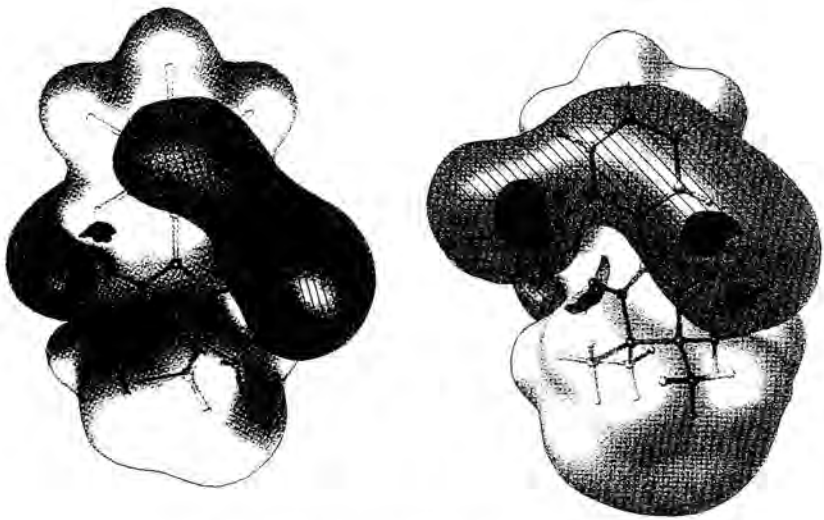

Figure 4. MEP map of the PhNN (left) and α-2OHNN molecules (right).

The overlap of the MEP maps of these two molecules allows the identification of many primary patterns constituted by C-H···ON contacts. Stable C-H···π contacts are also possible, but they are predicted by the MEP map to be much weaker than the C-H···ON contacts and should evolve to them, if no geometrical restrictions are present. A detailed analysis of the PhNN crystal packing (Figure 3a) allows to identify three primary packing patterns within the A and B planes (see Figure 5), all showing D-type packing motifs [13,14]. More informative is to know that each molecule of the A plane makes four $C(sp^2)$-H···ON contacts, while the molecules of the B plane make four $C(sp^3)$-H···ON contacts and two $C(sp^2)$-H···ON contacts (Figure 5). These planes are linked together using some of the seven interplane primary packing motifs, all of them presenting $C(sp^3)$-H···ON and $C(sp^2)$-H···ON bonds. Notice the absence of C-H···π contacts. So, we have seen that the contacts present in the PhNN crystal are compatible with the ones expected according to our MEP map overlap analysis, although this analysis predicts the presence of other primary patterns not seen in the crystal.

Intra-plane

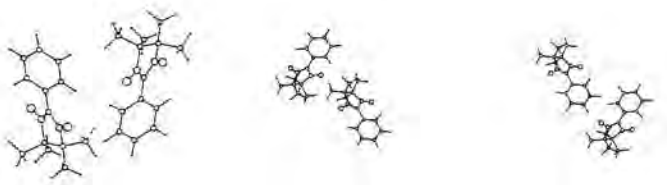

Inter-plane

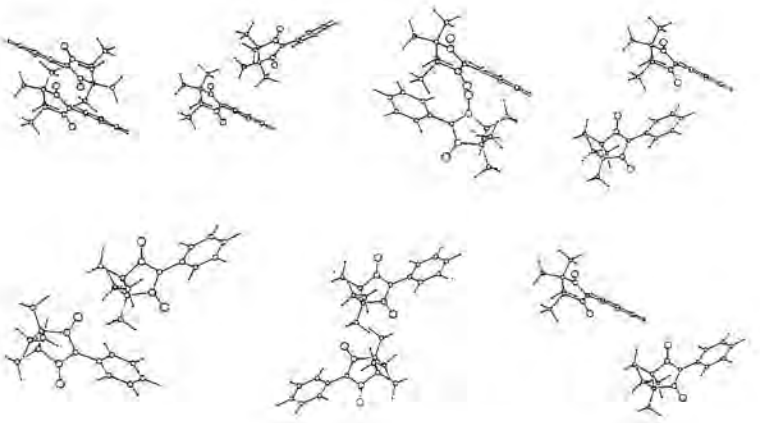

Figure 5. Primary packing patterns present in the PhNN crystal.

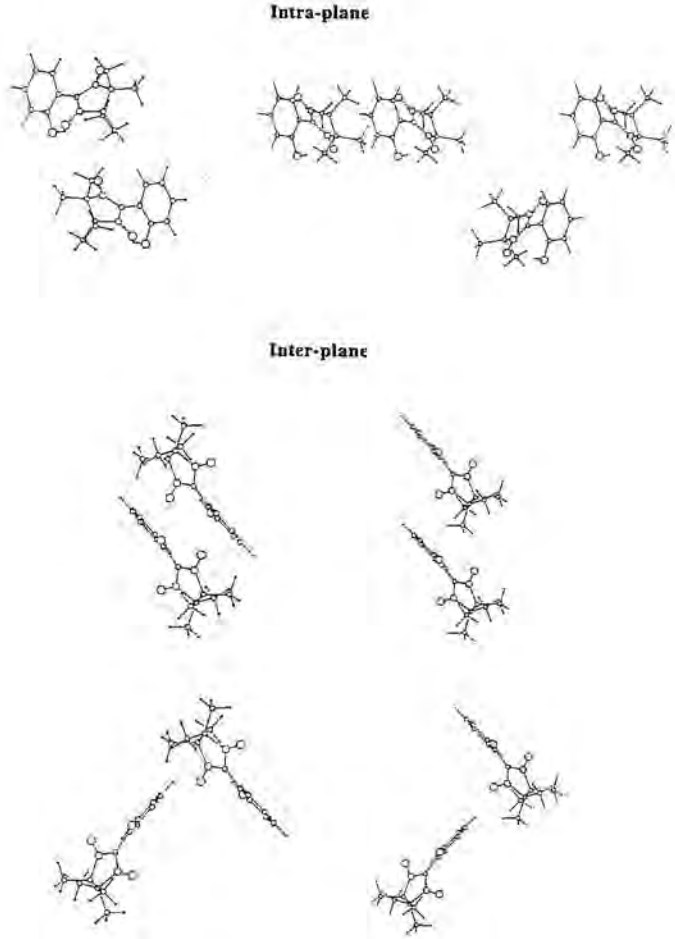

Figure 6. Primary packing patterns of the α-2OHNN crystal.

The same procedure can be employed on the α-2OHNN crystal. The presence of the OH group in this molecule creates a new region of negative MEP (-50 kcal/mol), stronger than the negative region located on the NO groups (-35 kcal/mol) (see Figure 4). The negative potential also spans above and below the benzene ring (-15 kcal/mol). So the O atom of the OH groups is the stronger basic group, followed by the two NO groups and then by the benzene rings. The C-H groups act, once again, as acid groups, while the hydrogen of the hydrogen of the OH group does not show acid character, as it is involved in the intramolecular OH···ON contact. From the MEP map overlap analysis one can expect stronger C-H···OH contacts and weaker C-H···ON ones. For the same reasons stated above, the C-H···π contacts will be only found when the other basic groups have been saturated. The analysis of the crystal packing shows three intraplane and four interplane primary packing patterns (see Figure 6). The three intraplane primary patterns present at least one C-H···OH contact, together with C-H···ON contacts, in two of the cases. The interplane primary patterns follow a parallel disposition in two of the cases and a T shape in the other two. They allow the NO groups of one molecule to overlap the positive regions of the CH benzenes. The shortest contacts are of the C-H···ON type, although a C-H···OH contact is also present in one of the cases. Once again, these primary packing patterns are consistent with the MEP map overlap analysis results. The energy of these primary packing patterns can be estimated from their intermolecular bonds. Ab initio computations are currently under progress to accurate define the energy of these contacts.

The previous analysis show that one can fully rationalize the packing patterns of purely organic magnetic crystals and understand the dramatic changes induced by the presence of just one different group, like the OH group, in the structure of the molecule. One might find many possibilities of for other possible crystal patterns based on the MEP map overlap analysis, some of them not seen experimentally in crystals, an indication of the possibility of polymorphism in these systems.

3. Are there ferro and antiferromagnetic primary packing patterns?. An statistical analysis of the packing patterns in ferro and antiferro α-nitronyl nitroxides.

The success in rationalizing analysis of the packing of the purely organic molecular magnets present us with a new problem: what kind of structures should one try to obtain?. We mean by this that if there are primary packing patterns associated to the presence of ferromagnetism one should try to design the crystals in such a form that these primary packing patterns are present. Similarly, of some primary packing patterns should be associated to an antiferromagnetic character, we should avoid their presence in a ferromagnetic material or induce their presence in an antiferromagnetic one.

To locate the presence of primary packing patterns in the ferromagnetic crystals in an unbiased form we have performed an statistical analysis of the already known ferromagnetic crystals showing dominant ferromagnetic properties. The same was done for the antiferromagnetic crystals showing dominant antiferromagnetic properties. Ideally, the characteristic patterns in one subgroup should be absent in the other.

According to the McConnell I model [11] the presence of a ferromagnetic interaction requires the overlap of significant positive and negative spin densities. It is well known, both experimentally and theoretically, that the major part of the spin density in α-nitronyl nitroxide radicals is located on the ONCNO part of the five-membered ring, being the density on the central C atom opposite to that in the N and O atoms [1,33]. Thus, the nature of the magnetic interactions present in the crystal of α-nitronyl nitroxide is expected to be directly related to the

spatial orientation and proximity of the atoms of the ONCNO groups [34]. Ferromagnetic patterns, if present, are probably associated to specific orientations of the shortest ONCNO···ONCNO contacts, although could be associated to contacts between the ONCNO groups and other atomic groups. These contacts should be geometrically different than the equivalent ones present in antiferromagnetic patterns. Consequently, the statistical analysis of the geometry of the shortest ONCNO···ONCNO or ONCNO···other-group contacts in crystals whose magnetic properties are well characterized should help to find the existing packing-magnetism relationships in α-nitronyl nitroxides.

We have performed such analysis for radicals that clearly belong to one of the following two different magnetic classes or subsets: those that show *dominant* ferromagnetic intermolecular interactions and those exhibiting *dominant* antiferromagnetic interactions. We did not want to include in our study crystals whose magnetic behavior is not clearly defined, as they would be of no help to identify the possible patterns associated to a ferro or antiferromagnetic packing. The total number of crystals analyzed in this study, 47 crystals [35], is large enough to make feasible a statistical analysis of the most relevant intermolecular contacts they present. The crystallographic data used in the survey were, in part retrieved from the Cambridge Structural Database (CSD) [36], and the rest from our own research or were directly found in the literature or supplied to us by other authors. A total of 143 crystal structures containing substituted α-nitronyl nitroxide radical units were initially used [35]. The criteria employed to select the final set of structures were as follows: (1) Structures with R factors greater than 0.10, or which were determined from very limited data, or which exhibit disorder or large molecular distortions, were excluded remaining 117 crystal structures. (2) All of the structures containing both transition metal atoms and large closed-shell organic molecules co-crystallized (45 structures) were discarded for the present analysis since intermolecular magnetic interactions between radicals could be complicated in these cases by the existence of other magnetic pathways through the metal atoms or the closed-shell molecule and the radical units. This criterion left 72 crystal structures of purely organic compounds. (3) We discarded in our statistical analysis all the crystals whose magnetic interactions are not clearly dominated by ferro- or antiferromagnetic interactions. It is convenient to exclude the crystals with non dominating signature because, by construction, they can show both types of *crystal packing patterns* and, in consequence, it would make impossible a clear identification of the *ferro-* and *antiferromagnetic patterns*. Their exclusion left us with only 47 purely organic crystals. Of these, the dominant intermolecular magnetic interactions were ferromagnetic (FM) in 23 cases and antiferromagnetic (AFM) in the remaining 24 ones. The nature of the dominant magnetic interactions is clearly manifested by the temperature dependence of the magnetic susceptibility, χ, in the temperature range of 2-300 K that is easily accessible in the literature. Thus, radicals with dominant FM interactions show the characteristic signature in the χT vs. T plot of a continuous increasing of χT when T decreases. By contrast radicals with dominant AFM interactions have the opposite trend. The total number of crystals which fulfill the previous conditions and are suitable for their statistical analysis belong to the following spatial groups: P-1 (3), $P2_1$ (2), Cc (2), $P2_1/c$ (25), C2/c (2), $P2_12_12_1$ (2), $Pca2_1$ (1), Ib2a (1), Pbca (4), Fdd2 (1), $I4_1/a$ (1), $P4_2bc$ (1), and P3c1 (2). A search in the two subgroups looking for the shortest NO···ON contacts whose O···O distances are smaller than 10 Å gives as result 1312 contacts. There are also 6039 C(sp^3)-H···ON contacts and 2286 C(sp^2)-H···ON contacts at H···O distances smaller than 10 Å. These three sets of contacts are large enough to make feasible a statistical analysis of their geometrical parameters searching for differences which are signature of different packing patterns.

It is important to mention here that most of the analyzed structures in both magnetic subsets were determined at room temperature where the thermal energy largely overcome the strengths of the intermolecular magnetic interactions. This means that we correlate a physical

property whose magnitude is only clearly observed at low temperatures with the crystal packing patterns existing at room temperature. This is a common practice in *Molecular Magnetism* that, unfortunately, cannot be avoided since only very few crystal structures have been determined at low temperatures. At first glance the above mentioned objection may look serious but a detailed analysis of this problem revealed that it has minor consequences for our magneto-structural correlations. Actually, except for those cases where a first-order structural phase transition occur, the *crystal packing patterns* of molecular crystals show only small changes with the temperature due to the thermal contraction. These changes do not turn the relative disposition of the molecules to such extension as to reverse the nature of the dominant intermolecular magnetic interaction [37]. Therefore, it can be assumed without too much risk that similar *crystal packing patterns* exist at low and high temperatures in the 47 crystals selected here.

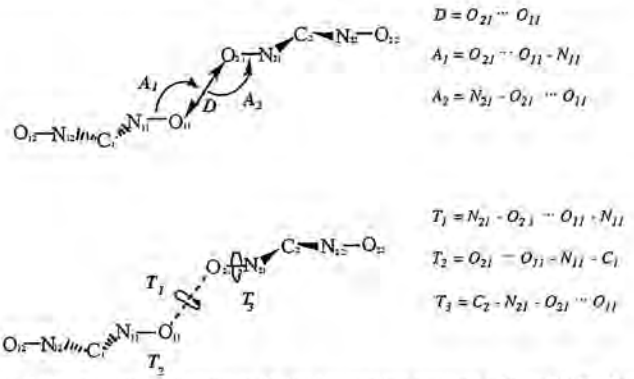

Figure 7. Coordinates employed to define the relative position of two ONCNO groups

A preliminary analysis of the geometry of the α-nitronyl nitroxide molecules in the 47 crystals analyzed, and in others with no definite or relevant or complex magnetic behaviors, showed that the spatial distribution of the atoms in the five-membered ring is nearly the same, and that the five ONCNO atoms lie in the same plane. Given this fact, we can consider the internal geometry of ONCNO groups as fixed. Consequently, the relative position of two ONCNO groups in a certain crystal, whose atoms are labeled as $O_{12}N_{12}C_1N_{11}O_{11}$ and $O_{22}N_{22}C_2N_{21}O_{21}$ (identical in geometry due to the translation symmetry present in the crystal and the mentioned similarity), is completely defined by six internal coordinates, as occurs for any two rigid asymmetrical objects in a Cartesian space. There are many possible choices for this six coordinate space, all of them correlated by a linear transformation among themselves. Among these choices, the one selected here is the one shown in Figure 7, chosen because it allows an easy visualization and physical interpretation of the geometrical parameters. First, one establishes the position of the terminal O_{21} atom relative to the $O_{12}N_{12}C_1N_{11}O_{11}$ group defining the $O_{21}\cdots O_{11}$ distance, the $O_{21}\cdots O_{11}$-N_{11} angle, and the $O_{21}\cdots O_{11}$-N_{11}-C_1 dihedral.

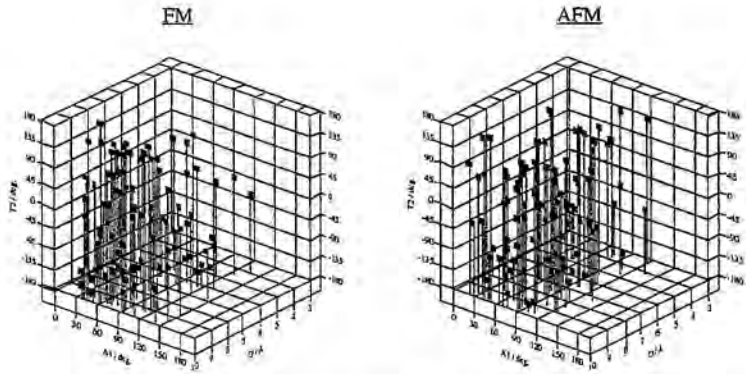

Figure 8. Tridimensional position of the O_{21} atom relative to a $O_{12}N_{12}C_1N_{11}O_{11}$ group (as a function of D, A_1 and T_2) within the FM (left) and AFM (right) subsets of crystals.

The position of the N_{21} atom for a fixed N-O distance is established giving the values of the N_{21}-O_{21}···O_{11} angle and the N_{21}-O_{21}···O_{11}-N_{11} dihedral. Finally, the plane on which the $O_{22}N_{22}C_2N_{21}O_{21}$ group lies is fully defined giving the C_2-N_{21}-O_{21}···O_{11} dihedral, because both the C_2-N_{21} distance and the C_2-N_{21}-O_{21} angle are fixed. Once this plane is known, the position of the N_{22} and O_{22} atoms are automatically established due to the fixed geometry of all ONCNO groups. To simplify the notation, we will identify the previous six intergroup geometrical parameters as D, A_1, A_2, T_1, T_2 and T_3 (see Figure 7 for a proper visualization).

There are no contacts in the subsets at distances shorter that 3 Å (the shortest value is 3.158 Å within the FM subset and 3.159 Å in the AFM one). The number of contacts in both subsets increases as the third power of the distance in the 3-10 Å range. The proportion of contacts in the FM and AFM subsets is nearly constant for all the distance ranges tested (in average, 44% are from the FM subset and 56% from the AFM one). These values are close to the percentage of crystals in the FM and AFM subsets (49% and 51%, respectively), although the percentage of contacts in the AFM subset is slightly larger. This result suggests that the number of ONCNO···ONCNO contacts that each NO group is making is similar in both subsets and does not strongly depend on its magnetic properties. More interesting, the ONCNO···ONCNO contacts are distributed similarly in the FM and AFM subsets. This can be appreciated plotting the position of the O_{21} atom relative to the ONCNO group for a representative sample of the FM and AFM subsets (see Figure 8, where the values of the parameters D, A_1 and T_2 are plotted for a random selection of 100 contacts within each subset). This similarity is also shown in the scattergrams of Figure 9, in which the variation of D *vs* T_2 is represented for the FM and AFM subsets. Therefore, we can safely conclude that there are no characteristic patterns present in the FM subset excluded in the AFM subset and viceversa. Instead, the two subsets present very similar *crystal packing patterns*.

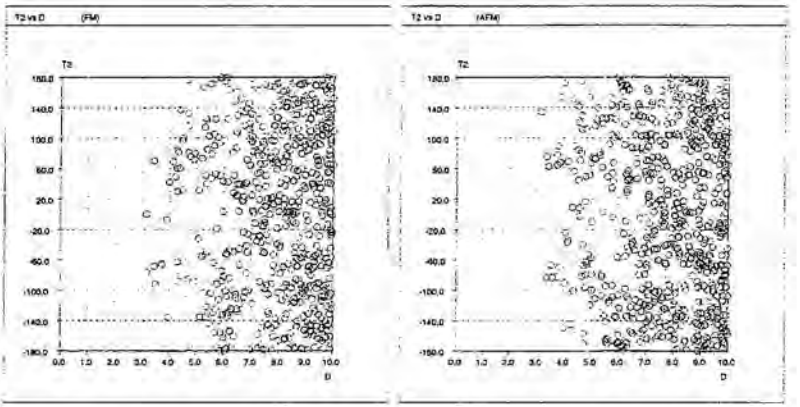

Figure 9. Scattergram of D *vs* T_2 for all the contacts of the FM and AFM subsets.

These scattergrams also show that there is no relationship between the presence of magnetism and the values of D. This is important because it goes against some commonly accepted ideas about the relationship between magnetism and crystal packing in α-nitronyl nitroxides, as the idea associating the presence of short NO···ON contacts to crystals with dominant antiferromagnetic interactions: According to the McConnell I model, when two ONCNO groups approach in such a way that their closest oxygen atoms lie in the same plane with A_1 angles between 90° and -90°, they will directly overlap the positive electron spin densities [36] of the two closest O atoms and, consequently, should give rise to a strong antiferromagnetic interaction, more important as the O···O distance gets shorter. That situation is found in our set of parameters when T_2 is equal to 0° or 180°, for values of the A_1 angles between 90° and -90°. Consequently, if the simple association between short NO···ON distance and dominant antiferromagnetic interactions is valid, one should find at these values a decrease in the number of ONCNO···ONCNO contacts in the FM subset and an increase in the contacts of the AFM subset. This is not found in the scattergrams shown in Figure 9.

We have tested if the previous conclusions were a consequence of a particular distance range employed in the analysis with no change in the conclusions: The proportion of contacts in the ferro and antiferromagnetic subsets is nearly independent on the range of distances selected. Even at very short distance ranges, where the overlap of the spin densities is maximum and the magnetic strength associated to the NO···ON contact is the largest, one also finds contacts within the FM subset. It is clear from such data the similar values of all parameters for the shortest contacts within the FM and AFM subsets. Therefore, *the presence of short NO···ON contacts, classically considered antiferromagnetic according to the McConnell I model , does not imply that the crystal has dominant antiferromagnetic interactions.* Consequently, *one should change the way in which some structure-magnetism correlation analysis of these crystals are carried out.* After a careful analysis we associate the failure in correlating the presence of expectedly large antiferromagnetic interactions with particular crystal packing patterns in these systems to the

simultaneous presence of other interactions whose strengths or number can overcome the magnetic effect of the NO···ON contact.

A correlation analysis [38] of the FM and AFM data proved in both subsets the absence of correlation for any pair of parameters employed in this study other than the expected one between A_1 and A_2. A factor analysis [39] of the two subsets showed that six is the number of parameters required to treat the geometrical data of the ONCNO···ONCNO contacts and that it is not possible to reduce this number [40]. Finally, a cluster analysis [41] of ONCNO···ONCNO contacts geometrical data on the set composed by the addition of the FM and AFM subsets, using the single linkage method as criteria to define a cluster [41], indicated that the FM and AFM sets of contacts are nearly identical and interpenetrated, *thus being indistinguishable*. Consequently, we can safely conclude that there is no statistically significant difference in the relative positions of the NO groups for the two magnetic subsets, that is, there are no different *crystal packing patterns* in these subsets for the relative positions of the NO groups.

When a similar analysis was carried out for the C(sp^3)-H···O-N and the C(sp^2)-H···O-N contacts [42], two of the main contacts responsible for the formation of hydrogen bonds within the crystals of α-nitronyl nitroxide radicals, one finds also no differences between the ferro and antiferromagnetic patterns. The contacts are spread in a smooth and in a similar way over the whole range of values represented. Consequently, there seem to be no excluded regions, specific for the crystals belonging to FM and AFM subsets. Instead, the similarity of geometries in the intermolecular contacts of the two subsets is manifested, making impossible to distinguish between the crystals showing dominant ferro- and antiferromagnetic interactions just by a direct inspection of the geometry of a particular intermolecular contact.

4. Rationalizing magnetic interactions using ab initio methods.

The previous analysis has shown that one cannot identify by simple inspection the magnetic character of a given primary packing pattern. Therefore, one has to use some kind of tool capable of associating a magnetic character to a given geometrical distribution of the molecules participating in the primary packing pattern. This has been normally done using McConnell-I model. However, as we will discuss in more detail in the next paragraph, when the McConnell-I model is applied to the PhNN and α-2OHNN crystals, the results are not completely consistent with the experimental observations. So, an obvious question can be asked: does the McConnell-I model work in identifying the magnetic character of a given intermolecular aggregate?.

The usual way of using the McConnell-I model is by looking at the overlap of the spin density for the shortest intermolecular contacts in which we have significant spin density. The electron spin density of the PhNN and α-2OHNN molecules computed at the BLYP/6-31G(2d,2p) level, a method that for these two systems gives a good description of the spin density, shows that most of it is located on the NO groups. At the same time, one find a small negative density on the C(sp^2) carbon of the five membered ring, and a spin alternation on the six membered ring. The OH oxygen of the α-2OHNN molecule has also a small positive spin density. No spin density above that value was detected by the BLYP/6-31G(2d,2p) computation in any of the hydrogen atoms, although the hyperfine coupling contact observed in the ESR spectra of the nitronyl nitroxides indicates that there is a small density in all H.

According to the previous spin density maps and McConnell-I, the most important magnetic contacts should be those involving the NO groups and the five-membered ring C(sp^2) carbon. If one looks for these type of contacts in the PhNN crystal one finds that the shortest ones in the A planes are at 5.02 Å, while in the B planes they are at 6.65 Å. At these distances

the overlaps are negligible, so no significative magnetic interaction is expected to be present along the A or B planes. If one looks at the NO···ON distances in between the planes, one finds shorter contacts: 3.68 Å in the B···B, 4.05 Å in the B···A, and 4.51 Å in the A···A interplane stackings. These contacts overlap the oxygens of the NO groups, so they are expected to be antiferromagnetic in character, according to McConnell-I. Thus, although antiferromagnetic interactions are expected along the B···B···A interplane stacking, the antiferromagnetic interactions do not propagate since the A···A antiferromagnetic interplane stacking is too weak, due to their distance. Consequently, according to the McConnell-I model, the PhNN crystals should be a paramagnet. Experimentally, the crystal is known to be an antiferromagnet. One could then resort to include other types of overlap, which although weaker according to the overlap concept, could be significative. For instace, this is the case of overlap between the NO group and the aromatic ring hydrogens. However, in doing so, the predicted magnetic behavior does not agree, once again, with the experimental one.

The α-2OHNN crystal, presents short O···O contacts of 3.97 Å for the intrachain contacts and longer contacts (of 5.50 Å) for the interchain contacts in their A planes. At the same time, the O···O distance in the A···A interplane stacking is 5.54 Å. The geometry of the contacts directly overlaps two oxygen atoms. Therefore, according to McConnell-I, these contacts should be antiferromagnetic along the planes, and the crystal should be a 1D antiferromagnet. Experimentally, the crystal is known to order ferromagnetically at 0.4 K. So, there is a clear contradiction between the predicted and experimental behavior. These results indicate, therefore, that the McConnell-I model is not working for the study of the magnetic character of the NO···ON contacts present in the family of the α-nitronyl nitroxides. We are further investigating this failure using ab initio methods, from an analytical and computational perspective, to understand the reasons for the failure and the limits of validity of the McConnell-I model.

5. Concluding remarks

The previous results illustrate how the ab initio methods can be used to study the packing and magnetic properties of purely organic molecular magnets. We have shown that they are very useful to rationalize the crystal packing patterns of these systems, following a simple procedure that we have named functional group analysis which allows to identify and energetically characterize the possible primary packing patterns present in the molecular crystals. We have illustrated the application of this method in the PhNN and α-2OHNN radical crystals. We have shown, performing an statistical analysis of magnetically well characterized ferro and antiferro α-nitronyl nitroxides, that there are no specific primary packing patterns associated to these ferro or antiferromagnetic crystals. Finally, we have shown some inconsistencies in the application of the McConnell-I model to predict the magnetic behavior of the PhNN and α-2OHNN radical crystals.

6. Acknowledgments

This work was supported by the CICYT (Grant No. MAT94-0797), the DGICYT (Projects PB92-0655-C02-02 and PB96-0862-C02-01), CIRIT (Projects GRP94-1077 and GRQ93-8028), and DGES (Project PB95-0848-C02-02). We also thank CESCA and CEPBA for generous allovations of computer time. M.D. acknowledges CIRIT for her doctoral grant. Authors also

thank Dr. S. Motherwell for providing us access to a beta version of the PREQUEST program and for the help provided in using it.

7. References and notes.

1. For a recent overview see: (a) Gatteschi, D., Kahn, O., Miller, J.S., Palacio, F, (eds.), (1991) *Molecular Magnetic Materials*, Kluwer Academic Publishers, Dordretch. (b) Iwamura, H. and Miller, J.S. (eds.) (1993) *Mol. Cryst. Liq. Cryst.* **232/233**, 1-360/1-366. (c) Miller, J.S., and Epstein, A.J. (1994) *Angew. Chem. Int. Ed. Engl.* **33**, 385-415. (d) Kahn, O. (1993) *Molecular Magnetism*, VCH Publishers, New York. (e) Rajca, A. (1994) Chem. Rev. **94**, 871-893. (f) Miller, J.S., Epstein, A.J. (eds.) (1995) *Mol. Cryst. Liq. Cryst.* **272-274**. (g) Kinoshita, M. (1994) *Jpn. J. Appl. Phys.* **33**, 5718. (h) Coronado, E., Delhaes, P., Gatteschi, D., Miller, J.S. (eds.) (1996) *Molecular Magnetism: From Molecular Assemblies to Devices*, Kluwer Academic Publishers, Dordretch. (i) Kahn, O. (ed.) (1996) *Magnetism: A Supramolecular Fucntion*, Kluwer Academic Publishers, Dordretch.

2. For molecular organic crystals with high symmetry, namely rhombic or cubic, the presence of just one intermolecular ferromagnetic interaction among the neighbor units is enough in order to guarantee the propagation of magnetic interactions along two or three spatial directions. By contrast for crystals with lower symmetries it is necessary the existence of more than one intermolecular ferromagnetic interaction for each crystallographically independent radical molecule in order to achieve a bulk ferromagnetism.

3. A lack of compensation of the magnetic moments of spins coupled antiferromagnetically can also produce a net magnetic moment -spin canting- that, when propagates over the solid, produce a spontaneous magnetization. For a recent organic example of this situation, see: (a) Banister, A.J., Bricklebank, N., Lavender, I., Rawson, J.M., Gregory, C.I., Tanner, B.K., Clegg, W., Elsegood, R.R.J., Palacio, F. (1996) *Angew. Chem. Int. Ed. Engl.* 35, 2533. (b) Palacio, F., Antorrena, G., Burriel, R., Rawson, J., Smith, J. N. B., Brickleband, N., Novoa, J. J., Ritter, C. (1997) *Phys. Rev. Lett.* **79**, 2336.

4. (a) Tamura, M., Nakazawa, Y., Shiomi, D., Nozawa, K., Hosokoshi, Y., Isjikawa, M., Takahashi, M., Kinoshita, M. (1991) *Chem. Phys. Lett.* **186**, 401. (b) Allemand, P.M., Khemani, K.C., Koch, A., Wudl, F., Holczer, K., Donovan, S., Grüner, G., Thompson, J.D. (1991) *Science*, **253**, 301. (c) Chiarelli, R., Novak, M.A., Rassat, A., Tholance, J.L. (1993) *Nature*, **363**, 147. (d) Sugawara, T., Matsushita, M.M., Izuoaka, A., Wada, N., Takeda, N., Ishikawa, M. (1994) *J. Chem. Soc., Chem. Commun.* 1081. (e) Cirujeda, J., Mas, M., Molins, E., Lanfranc de Panthou, F., Laugier, J., Geun Park, J., Paulsen, C., Rey, P., Rovira, C., Veciana, J. (1995) *J. Chem. Soc., Chem .Comm.* 709. (f) Caneschi, A., Ferraro, F., Gatteschi, D., leLirzin. A., Novak, M.A., Rentsecheler, E., Sessoli, R. (1995) *Adv. Mater.* **7**, 476. (g) Pei, Y., Kahn, O., Aebersold, M.A., Ouahab, L., Le Berre, F., Pardi, L., Tholance, J.L. (1994) *Adv. Mater.* **6**, 681. (h) Togashi, K., Imachi, K., Tomioka, K., Tsuboi, H., Ishida, T., Nogami, T., Takeda, N., Ishikawa, M. (1996) *Bull. Chem. Soc. Jpn.*, **69**, 2821 and papers cited therein.

5. In general, bulk ferromagnetism requires the presence of ferromagnetic interactions along three (or two) directions of the solid depending if there is a low (or high) magnetic anisotropy. Since organic free radicals have, in general, very small magnetic anisotropy, the requirement of the presence of ferromagnetic interactions in 3

dimensions is completely necessary for achieving such a macroscopic property. See: Palacio, F. (1991) From Ferromagnetic Interactions to Molecular Ferromagnets: An Overview of Models and Materials, Gatteschi, D. Kahn, O., Miller, J.S., and Palacio, F. (eds.) *Magnetic Molecular Materials*, Kluwer Academic Publishers, Dordrecht, p.1.

6. An important point to be developed in this field is the different ways to enhance the strengths of intermolecular magnetic interactions. Only increasing these strengths it will be possible to increase the T_C of purely organic ferromagnets that nowadays are still very low, most of them in the mK region.
7. By ab initio methods we indicate any quantum mechanical method only employs the Born-Oppenheimer approximation within the non-relativistic formulation of the time independent Schrödinger equation.
8. α-Nitronyl nitroxide is the abbreviated name most widely employed and it is here used to indicate 4,5-dihydro-4,4,5,5-tetramethyl-3-oxido-1H-imidazol-3-ium-1-oxyl, the correct IUPAC name.
9. Awaga, K. and Maruyama, Y. (1989) *J. Chem. Phys.* **91**, 2743.
10. See reference 4e
11. McConnell, H. M. (1963) *J. Chem. Phys.* **39**, 1910.
12. A motif is a pattern which extends though the crystal containing only one type of hydrogen bond.
13. Etter, M. C. (1990) *Acc. Chem. Res.* **23**, 120.
14. Bernstein, J., Davis, R.E., Shimoni, L., Chang, N.-L. (1995) *Angew. Chem. Int. Ed. Engl.* **34**, 1555.
15. Novoa, J.J., Deumal, M. (1997) *Mol. Cryst. Liq. Cryst.*, **305**, 143.
16. Desiraju, G. *Angew. Chem. Int. Ed. Engl.* (1995) **34**, 2311.
17. For a review see: Novoa, J. J. (1998) Intermolecular interactions in molecular crystals studied by ab initio methods: From isolated interactions, to patterns and crystals, Allen, F H. and Howard, J. A. K. (eds), Kluwer Academic Publishers, Dordrecht.
18. Gavezzotti A. (1994) *Acc. Chem. Res.*, **27**, 309.
19. Williams, D.E., (1983) PCK83, *QCPE* # 41.
20. (a) Ckaka, A.M., Zaniewski, R., Youngs, W., Tessier, C., Klopman, G. (1996) *Acta Cryst.*, **B52**, 165. (b) Gavezzotti A. (1991) *J. Am. Chem. Soc.*, ; **113**, 4622. (c) Gdanitz, R.J., (1992) *Chem. Phys. Lett.* **190**, 391, (d) Karfunkel, H.R., Gdanitz, R.J. (1992) *J. Comp. Chem.*, **13**, 1170.
21. The geometrical cutoff has been a controversial one. There are problems associated with the cutoff limit used: depending on which atomic radii are taken, some interactions are visualized as intermolecular bonds but slightly larger ones not. This has been discussed at length in: Jeffrey, G.A., Saenger, W. (1991) *Hydrogen Bonding in Biological Structures*, Springer Verlag, Berlin.
22. If fact, crystals grow in the practice in this way, with a nucleation and propagation steps, in which a first crystalline nucleus is formed, and then the rest of the crystal growths from it.
23. This is an extension of the ideas "Atoms-in-Molecules" concepts to intermolecular bonds in crystals, developed by Bader. For a review of them see: Bader, R. F. W. (1990) *Atoms in Molecules. A Quantum Theory*, Clarendon Press, Oxford.
24. The AIM concepts were extended to crystals in: (a) Zou, P. F. and Bader, R. F. W. (1994) *Acta Cryst.* **A50**, 714. (b) Tsirelson, V. G., Zou, P. F., Tang, T.-H., Bader, R. F. W. (1995) *Acta Cryst.* **A51**, 143.
25. Novoa, J. J., Mota, F., Perez del Valle, C., Planas, M. (1997) *J. Phys. Chem. A* **101**, 7842.

26. Novoa, J.J., Lafuente, P., Mota, F., (1998) submitted.
27. (a) Scrocco, E. and Tomasi, J. (1978) *Adv. Quant. Chem.* **11**, 115. (b) Politzer, P. and Murray, J.S. (1991) *Rev. Comp. Chem.* **2**, 273.
28. MEP maps, give information on where a positive charge is electrostatically attracted or repelled. If the interaction energy of the dimer is dominated by the electrostatic component, as is clearly the case of hydrogen bonds, for instance, then the MEP overlap analysis gives good results.
29. van Duijneveldt, F.B., van Duijneveldt-van de Rijdt, J. G. C. M., van Lenthe, J.H. (1994) *Chem. Rev.* **94**, 1873.
30. Boys, S.F., Bernardi, F. (1970) *Mol. Phys.* **19**, 553.
31. (a) Novoa, J.J., Planas, M., Whangbo, M-H. (1994) *Chem. Phys. Lett.*, **225**, 240. (b) Novoa, J.J., Planas, M., Rovira, M.C. (1996) *Chem. Phys. Lett.* **251**, 33. (c) Novoa, J.J. and Planas, M. (1998) *Chem. Phys. Lett.* In press.
32. See for instance: Deumal, M., Cirujeda, J., Veciana, J., Kinoshita, M., Hosokoshi, Y., Novoa, J.J., (1997) *Chem. Phys. Lett.* **265**, 190.
33. See, for instance: (a) Zheludev, A., Barone, V., Bonnet, M., Delley, B., Grand, A., Ressouche, E., Rey, P., Subra, R., Schweizer, J. (1994) *J. Am. Chem. Soc.* **116**, 2019. (b) Novoa, J.J., Mota, F., Veciana, J., Cirujeda, J. (1995) *Mol. Cryst. Liq. Cryst.* **271**, 79.
34. When no angular data are taken into account and only intermolecular distances are considered in a given magneto-structural correlation, one is tempted to ascribe the observed ferromagnetic intermolecular interaction to the closest contacts between atoms of the two interacting molecules that have opposite spin densities.
35. The database of crystals selected is describe in Deumal, M., Cirujeda, J., Veciana, J., Novoa, J.J., submitted. For some examples see: (a) Awaga, K., Inabe, T., Maruyama, Y., Nakamura, T., Matsumoto, M. (1992) *Chem. Phys. Lett.* **195**, 21. (b) Awaga, K., Inabe, T., Nakamura, T., Matsumoto, M., Maruyama, Y. (1993) *Mol. Cryst. Liq. Cryst.* **232**, 69. (c) Awaga, K., Okuno, T., Yamaguchi, A., Hasegawa, M., Inabe, T., Maruyama, Y., Wada, N. (1994) *Phys. Rev. B* **49**, 3975. (d) Awaga, K., Yamaguchi, A., Okuno, T., Inabe, T., Nakamura, T., Matsumoto, M., Maruyama, Y. (1994) *J. Mater. Chem.* **4**, 1377. (e) Awaga, K., Okuno, T., Yamaguchi, A., Hasegawa, M., Inabe, T., Maruyama, Y., Wada, N. (1995) *Synth. Met.* **71**, 1807. (f) Veciana, J., Cirujeda, J., Rovira, C., Vidal-Gancedo, J. (1995) *Adv. Mater.* **7**, 221. (g) Cirujeda, J., Hernàndez, E., Rovira, C., Turek, P., Veciana, J. (1994) New Organic Magnetic Materials. The Use of Hydrogen Bonds as a Crystalline Design Element of Organic Molecular Solids with Intermolecular Ferromagnetic Interactions, Seoane, C., Martin, N. (eds.) *New Organic Materials*, Universidad Complutense de Madrid, Madrid, pp. 262. (h) Cirujeda, J., Hernàndez, E., Rovira, C., Stanger, J.L., Turek, P., Veciana, J. (1995) *J. Mater. Chem.* **5**, 243. (i) Cirujeda, J., Hernàndez, E., Lanfranc de Panthou, F., Laugier, J., Mas, M., Molins, E., Rovira, C., Novoa, J.J., Rey, P., Veciana, J. (1995) *Mol. Cryst. Liq. Cryst.* 271, 1.
36. Allen, F.H., Bellard, S., Brice, M.D., Cartwright, B.A., Doubleday, A., Higgs, H., Hummelink, T., Hummelink-Peters, B.G., Kennard, O., Motherwell, W.D.S., Rodgers, J.R., Watson, D.G. (1979) *Acta Cryst.* **B35**, 2331.
37. This fact has been well documented for organic superconducting crystals, whose critical temperatures are also much lower than the room temperature. See, for instance: Williams, J.M., Ferraro, J.R., Thorn, R.J., Carlson, K.D., Geiser, U., Wang, H.H., Kini, A.M., Whangbo, M-H. (1992) *Organic Superconductors*, Prentice Hall, Englewood Cliffs. Magnetism is a different physical property than

superconductivity, although both are intimately related with the relative arrangement of molecules in the crystal. The packing properties of molecular solids and, in particular, its variation with temperature, are determined by the intermolecular contacts, characteristic of the intermolecular contact and practically independent of the electronic physical property present in the crystal.

38. Barlow R. Statistics, John Wiley and Sons, Chichester, 1989.
39. Malinowski, E.R., Howery, D.G. (1980) *Factor Analysis in Chemistry*, Wiley Interscience, New York.
40. This conclusion shows that the use of three or even two geometrical parameters, a practice performed by some authors for analyzing series of α-nitronyl nitroxide radicals, is not correct.
41. Everitt, B.S. (1993) *Cluster Analysis*, 3rd edition, Edward Arnold, London.
42. The spin density on the H atom of the four CH_3 groups is negative, whereas these on the H atoms of a phenyl ring linked to the α carbon of the five membered ring are alternated in their sign, being positive for *ortho* and *para* H atoms and negative for the *meta* ones. See: (a) Davis, M.S., Morokuma, K., Kreilich, R.W. (1972) *J. Am. Chem. Soc.* **94**, 5588. (b) Neely, J.W., Hatch, G.F., Kreilich, R.W. (1974) *J. Am. Chem. Soc.* **96**, 652. See also Ref [33].

ARTICLE 7

J. Phys. Chem. **1998**

On the Validity of the McConnell-I Model of Ferromagnetic Interactions: The [2.2]Paracyclophane Example

Mercè Deumal,[†] Juan J. Novoa,*[,†] Michael J. Bearpark,[‡] Paolo Celani,[‡] Massimo Olivucci,[§] and Michael A. Robb*[,‡]

Departament de Química Física, Universitat de Barcelona, Martí i Franquès 1, 08028, Barcelona, Department of Chemistry, King's College London, Strand, London, WC2R 2LS U.K., and Dipartimento di Chimica "G. Ciamician" dell' Universitá di Bologna, Via Selmi 2, 40126 Bologna, Italy

Received: May 15, 1998; In Final Form: July 29, 1998

A formal comparison between a rigorous implementation of a Heisenberg Hamiltonian model in a VB space with the McConnell-I model shows that the validity of the McConnell model rests upon a heuristic one-to-one correspondence between spin density products in the latter with the difference of the spin exchange density matrix elements in the former. Using a rigorous Heisenberg Hamiltonian, a numerical model computation of the singlet/quintet stability for pseudoortho, pseudometa, and pseudopara bis(phenylmethylenyl)-[2.2]paracyclophanes (modeled with the correponding singlet/triplet bis(methyl)[2.2]paracyclophanes) shows that the McConnell model makes the correct prediction of low and high spin stability only because the contributions from "closest contact" carbon atoms that are not directly aligned is rather small. In systems where the alignment is not perfect, this cancelation may not hold. The association between spin density products in the McConnell model with the difference of the spin exchange density matrix elements in the VB Heisenberg Hamiltonian is shown to be valid because the McConnell model correctly predicts the leading configuration terms in the VB expansion.

Introduction

The design of purely organic magnetic materials has been the subject of considerable recent research.[1] These materials require the presence of a persistent free radicals,[2] and the formation of crystals made of these radicals showing spontaneous magnetization below a certain critical temperature T_c. Many examples of such magnetic crystals are found in the family of the so-called α-nitronyl nitroxide radicals.[1,3] Some of them present bulk ferromagnetism, although up to now, only at low critical temperatures.

The fact that different crystal phases of the same radical give rise to different magnetic properties, suggests that molecular magnetism in a crystal is strongly related to the relative geometrical arrangement of the radicals within the crystal.[1] Thus, as a first step toward the rational design of purely organic magnetic materials with higher critical temperatures, one requires theories relating the magnetism with the crystal structure. Rational design could be founded on a model or a magnetostructural correlation, based on the observation of known structures. Once the geometrical arrangements of the molecules capable of producing ferromagnetic interactions are known, one has to learn how to control the presence of these arrangements in the packing of the crystal.

There are many models aimed at rationalizing magnetism-structure correlations and in current use.[1a,4] Many of these models are designed to explain the magnetism in polynuclear derivatives of transition metal compounds. This "through bond" magnetism was first rationalized in a qualitative form by the models of Anderson,[5] Kahn,[1b] and Hay−Thibeault−Hoffmann.[6] The latter two approaches give similar results and successfully predict the presence of ferro and antiferromagnetic interactions, and have been useful to establish qualitative magnetism-correlation relationships.[7] However, such approximations lack the electron correlation effects required to properly describe some of the properties of magnetic compounds, as those observed in dinuclear compounds made of different magnetic centers.[8] This has prompted to the development of more accurate approaches to these systems, aimed at the quantitative study of the magnetic properties. Such methods have been based on perturbation methods[9] and on configuration interaction methods such as the difference dedicated configuration interaction method.[10] The broken symmetry approach introduced by Noodleman, in the context of the density functional methodology,[11] also seems to give reasonable results in some cases.[12] Methods used to explain the high spin−low spin ordering of states in diradical molecules[13,14] are closely related.

Of particular interest are models[1,2,15−20] designed to explain the magnetism in purely organic molecular systems via the so-called "through-space" magnetism (to distinguish it from the previous "through bond" magnetism). The most widely used methods for magnetism in molecular crystals are based on the models proposed by McConnell (also known as McConnell-I[15] and -II[16] models or mechanisms). The McConnell-II mechanism is a charge-transfer model that was shown not to work in a detailed work by Kollmar and Kahn.[20] Thus, we will focus our attention in the first model.

The McConnell-I model is based on a Heisenberg spin Hamiltonian and predicts the presence of intermolecular ferromagnetic interactions only when short intermolecular contacts are found in the crystal between atoms i, j bearing considerable spin population $\rho_i\rho_j$ of opposite sign. Accordingly, the magnetic behavior of a given molecular crystal can be rationalized by

[†] Departament de Química Física.
[‡] Department of Chemistry.
[§] Dipartimento di Chimica.

S1089-5639(98)02252-X CCC: $15.00 © xxxx American Chemical Society
Published on Web 00/00/0000 PAGE EST: 8.5

computing the spin distribution on the atoms of its constituent molecules, a property available from experiment[2,21] or from theoretical computations.[21,22]

In spite of its popularity, the validity of the McConnell-I model has never been demonstrated in a rigorous theoretical way. Nevertheless, there is a good agreement between observed magnetism and the predictions of the McConnell theory, based upon accurate ab initio computations of spin densities for simple model systems.[23-24] The often quoted example is the singlet vs quintet stability of the pseudoortho, -meta, and -para [25] bis-(phenylmethylenyl)[2.2]paracyclophane isomers. Here, the predicted singlet vs quintet stability of the linked dimers is in excellent agreement with the observed ESR experiments.

However, some experimental magnetostructural relationships are difficult to explain by a straightforward application of the McConnell-I model, raising doubts on its validity and range of applicability. In this paper, we show that one may derive a rigorous Heisenberg Hamiltonian in the context of a VB wave function. Comparison with the McConnell theory, shows that the product of the spin densities $\rho_i\rho_j$ of the two molecular fragments used in the McConnell theory must be taken in one-to-one correspondence with two electron exchange density matrix elements. A numerical computation on paracyclophane compounds with the rigorous Heisenberg Hamiltonian shows that this association has numerical validity. However, this correct agreement is partly "accidental" and leads to a conceptual interpretation that is not correct. As we shall demonstrate, high spin stability is associated with the fact that "closest contact" sites are always ferromagnetically coupled and that the "closest contact" sites for the singlet state must be more strongly ferromagnetically coupled than for the triplet state.

Theory

Heisenberg Hamiltonians. A general Heisenberg spin-exchange Hamiltonian can be written as follows

$$\hat{H}^S = Q - \sum_{i,j} J_{ij}(2\hat{S}_i\cdot\hat{S}_j + {}^1/_2\hat{I}_{ij}) \qquad (1)$$

where $\hat{S}_i$ is the spin operator associated with the ith site, and $\hat{I}_{ij}$ is the identity spin operator. In the $\hat{H}^S$ operator defined in eq 1, the complexities of the wave function are absorbed into parameters Q and J_{ij} and one associates an electron with each site i [for a discussion see ref 26]. The expectation value of the spin scalar product $\langle 2\hat{S}_i\cdot\hat{S}_j\rangle$ is just $S(S+1) - {}^3/_2$. A two-electron example clarifies the meaning of eq 1. The expectation value of $\langle \hat{S}_i\cdot\hat{S}_j\rangle$ for singlet and triplet states gives $-{}^3/_4$ and $+{}^1/_4$. Therefore, from eq 1, for singlet and triplet two-electron states we have the familiar result

$$E^{S/T} = Q \pm J_{12} \qquad (2)$$

since for two electrons we have

$$-\langle(2\hat{S}_i\cdot\hat{S}_j + {}^1/_2\hat{I}_{ij})\rangle^{S/T} = \pm 1 \qquad (3)$$

In the application of Heisenberg Hamiltonians, the exchange coupling parameter J_{ij} is interpreted in terms of the electron distribution as the Heitler–London exchange

$$J_{ij} = [ij|ij] + 2s_{ij}\langle i|h|j\rangle \qquad (4)$$

where $[ij|ij]$ is the small positive two electron exchange energy, and $\langle i|h|j\rangle$ is dominated by the nuclear electron attraction being large and negative. Thus J_{ij} is negative in general. The quantity s_{ij} is the overlap of the orbitals i and j, so that J_{ij} becomes positive only when the orbital overlap becomes very small. Clearly, in making such an interpretation one is also associating an electron i on site i with an atomic orbital (AO) on center i.

At this stage one must stress the fact that eq 1 corresponds to a "model" with empirical parameters that reduces the problem of chemical binding to coupling of electron spins. There is no real physical coupling between the electron spins (except for relativistic terms which are assumed to be negligible). Thus the problem of constructing an ab initio quantum chemistry theory that yields such a model requires some careful consideration. Anderson[27a] was the first to recognize that Heisenberg Hamiltonians might be understood as effective Hamiltonians computed from an exact full CI Hamiltonian using a model space of neutral VB determinants formed from n electrons in n AO. The use of such spaces in quantum chemistry was first proposed in this context by the Toulouse School,[27] and we have successfully implemented a scheme[28] where the Q and J parameters are derived from CASSCF computations. Clearly, in a rigorous (i.e., faithful) implementation of eq 1 one must be able to associate an electron i on site i with an AO on center i. This implies that the orbitals are localized on atomic sites (i.e., localized AO). Further, $\hat{H}^S$ is only defined on a space of many electron functions spanned by a basis where the space part of all the configurations is the same and the configurations differ only in the spin part. This implies that the space on which $\hat{H}^S$ acts is the space of VB determinants where each spatial orbital occurs once (i.e., neutral VB determinants).

Now, we must write eq 1 in a form suitable for implementation in quantum chemistry. We assume that we have an orbital basis of AO that can be identified with sites i and j in eq 1. The second quantized form of eq 1 then takes the form

$$\hat{H}^S = Q - \sum_{i,j}^{N} J_{ij}\left\langle i(1)\,j(2)\left|\hat{S}(1)\cdot\hat{S}(2) + \frac{1}{4}\hat{I}(1,2)\right|i(1)\,j(2)\right\rangle a_i^+ a_j^+ a_j a_i \qquad (5)$$

where $i(1)$ and $j(2)$ are AO localized in sites i and j and a_i^+, a_i are creation and annihilation operators. For practical purposes, the Hamiltonian 5 can be rewritten [see, for example, ref 28a] in terms of the standard generators $\hat{E}_{ij}^{\sigma\sigma} = a_{i\sigma}^+ a_{j\sigma}$ of the unitary group $U(n)$ in the form where $\sigma = \alpha,\beta$

$$\hat{H}^S = Q + \sum_{i,j}^{M} J_{ij}\frac{1}{2}(\hat{E}_{ij}^{\alpha\alpha}\hat{E}_{ji}^{\beta\beta} + \hat{E}_{ij}^{\beta\beta}\hat{E}_{ji}^{\alpha\alpha} + [\hat{E}_{ij}^{\alpha\alpha}\hat{E}_{ji}^{\alpha\alpha} - \hat{E}_{ii}^{\alpha\alpha}] + [\hat{E}_{ij}^{\beta\beta}\hat{E}_{ji}^{\beta\beta} - \hat{E}_{ii}^{\beta\beta}]) \qquad (6)$$

Now eq 6 forms the basis of a quantum chemistry implementation of eq 1 since the expectation values of the bilinear forms in eq 6 are just standard two-particle density operators ("symbolic" density matrices) for a CI computation. It is also obvious that the operators in eq 6 only connect configurations where the space part of configurations is the same and the configurations differ only in the spin part. Thus, the Heisenberg Hamiltonian acts on the space of VB determinants where each spatial orbital occurs once. As we have demonstrated elsewhere,[28b] any full CI Hamiltonian can be projected onto such a space and a subset of the eigenvalues can be reproduced exactly. Therefore, the matrix representation of eq 6 on the space of neutral VB determinants forms a completely rigorous implementation of a Heisenberg Hamiltonian.

For subsequent comparison with the McConnell-I theory it is convenient to introduce the spin exchange density matrix P_{ij} [see ref 28c]. We can write the energy as the expectation value in the form

$$\langle \hat{H}^S \rangle = Q + \sum J_{ij} P_{ij} \tag{7}$$

The exchange density matrix P_{ij} can in turn be written either as

$$P_{ij} = \left\langle -\left(2\hat{S}_i \cdot \hat{S}_j + \frac{1}{2}\hat{I}_{ij}\right)\right\rangle \tag{8}$$

or (for practical purposes) as

$$P_{ij} = \left\langle \frac{1}{2}(\hat{E}^{\alpha\alpha}_{ij}\,\hat{E}^{\beta\beta}_{ji} + \hat{E}^{\beta\beta}_{ij}\,\hat{E}^{\alpha\alpha}_{ji} + [\hat{E}^{\alpha\alpha}_{ij}\,\hat{E}^{\alpha\alpha}_{ji} - \hat{E}^{\beta\beta}_{ij}] + [\hat{E}^{\beta\beta}_{ij}\,\hat{E}^{\beta\beta}_{ji} - \hat{E}^{\beta\beta}_{ii}])\right\rangle \tag{9}$$

Equation 9 is just a two-particle density matrix element [see, for example, ref 28a] that can be obtained from any CI computation. The exchange density must satisfy the relationship[29]

$$S(S+1) = \frac{1}{4}N(N-4) - \sum_{i,j} P_{ij} \tag{10}$$

where N is the number of electrons.

This exchange density P_{ij} obtained from a computation using neutral VB determinants has a simple interpretation and is indicative of the nature of the spin coupling between electrons in orbitals i and j. Using a single configuration perfectly paired VB wave function (i.e., a Rumer function[30]), the P_{ij} have values $+1$ for paired spins coupled antiparallel to a singlet, -1 for two electrons coupled parallel to a triplet, and $-1/2$ for uncoupled spins (i.e., i and j belong to *different* "spin-paired" functions) [see perfect pairing formula in ref 30]. Of course, the P_{ij} computed from eq 9 will differ from these "ideal" values because of configuration interaction. Thus, from a numerical point of view, after configuration interaction, we cannot distinguish between "triplet coupled" and "uncoupled spins". Thus from this point onward we shall refer to positive P_{ij} as "singlet coupled" and negative P_{ij} as "triplet coupled". Since J_{ij} is usually negative, the negative P_{ij} (triplet or uncoupled electrons) are obviously associated with destabilizing interactions via eq 7.

McConnell's Heisenberg Hamiltonian. In 1963, McConnell[15] suggested that the magnetic interaction between two aromatic radicals A and B could be approximated by a Heisenberg Hamiltonian of the following form:

$$\hat{H}^{AB} = -\sum_{i\in A, j\in B} J^{AB}_{ij}\,\hat{S}^A_i \cdot \hat{S}^B_j \tag{11}$$

in which J^{AB}_{ij} are two-center exchange integrals, and $\hat{S}^A_i \cdot \hat{S}^B_j$ is the product of the spin operators on atoms i, j of fragments A and B. One can easily cast this Hamiltonian into the form of eq 5. Clearly, aside from the identity operator (corresponding to a change in the zero of the energy), this Hamiltonian neglects the intrafragment terms in eq 5. *Thus the first fundamental assumption in the McConnell-I theory is that the intrafragment contributions are the same for each state on which the Hamiltonian acts.*

However, the Hamiltonian corresponding to eq 11 has never been used in this form, but is replaced by an "ad hoc" simplification given as

$$\hat{H}^{AB} = -\hat{S}^A \cdot \hat{S}^B \sum_{i\in A, j\in B} J^{AB}_{ij}\,\rho^A_i\,\rho^B_j \tag{12}$$

in which J^{AB}_{ij} are two-center exchange integrals, and ρ^A_i, ρ^B_j are spin densities on atoms i, j of fragments A and B. The $\hat{S}^A, \hat{S}^B$ are the total spin operators for fragments A, B, and the expectation value of the product is given by

$$\langle \hat{S}^A \cdot \hat{S}^B \rangle = \frac{1}{2}[S(S+1) - S_A(S_A+1) - S_B(S_B+1)] \tag{13}$$

At this stage it is important to stress that the Hamiltonian given in eq 12 acts only on a model space (usually two-dimensional) spanned by states of different spin multiplicity (e.g., a singlet and a triplet), and thus has only diagonal elements. Further, eq 12 is purely phenomenological. There is no systematic set of approximations that gives eq 12 from eq 11.

For a two-level many-electron problem (i.e., two doublets coupled to a triplet or singlet) one has $\langle \hat{S}^A \cdot \hat{S}^B \rangle^T = {}^1/_4$ and $\langle \hat{S}^A \cdot \hat{S}^B \rangle^S = -{}^3/_4$, respectively, so that

$$E^{S/T} = \begin{Bmatrix} {}^3/_4 J \\ -{}^1/_4 J \end{Bmatrix} \tag{14}$$

This result is the same as eq 2 except for the change of energy zero. The effective coupling constant J is given as

$$J = \sum_{i\in A, j\in B} J^{AB}_{ij}\,\rho^A_i\,\rho^B_j \tag{15}$$

It remains now to relate the theory suggested by eq 11 with the rigorous Heisenberg Hamiltonian model embodied in eq 1.

Comparison between McConnell-I Model with the Rigorous Heisenberg Hamiltonian Model. To make a comparison between McConnell-I model with the rigorous Heisenberg development, one must consider energy differences. An example where we consider the energy difference between a singlet and triplet clarifies the main ideas. Thus for a singlet and triplet, from eq 14 (McConnell-I model) we have

$$E^S - E^T = \sum_{i\in A, j\in B} J^{AB}_{ij}\,\rho^A_i\,\rho^B_j \tag{16}$$

In contrast, from eq 7 (Heisenberg Hamiltonian model) we have

$$E^S - E^T = \sum_{i,j} J_{ij} \Delta P_{ij} \tag{17}$$

where the ΔP_{ij} is defined as

$$\Delta P_{ij} = P^S_{ij} - P^T_{ij} \tag{18}$$

We emphasize that P^S_{ij} and P^T_{ij} are the singlet and triplet exchange density matrixes obtained from singlet and triplet eigenvectors (i.e., separate computations on the singlet and triplet state). In contrast $\rho^A_i\,\rho^B_j$ is the product of the difference of spin densities evaluated from two doublet fragments. Upon comparing eqs 16 and 17, it is clear that the McConnell relationship is valid only if we make the association

$$\Delta P_{ij} \leftrightarrow \rho^A_i\,\rho^B_j \tag{19}$$

There is no obvious reason why $\rho^A_i\,\rho^B_j$ and ΔP_{ij} should be related to each other than heuristically. This association thus constitutes the most fundamental assumption of McConnell-I model which has never been tested numerically.

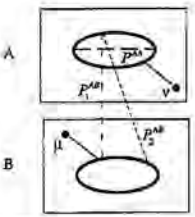

Figure 1. A schematic representation of the partition of the exchange density for two aromatic doublet structures.

For triplet stability effective coupling constant J in eq 15 must be positive. Thus, since the set of J_{ij}^{AB} are assumed to be negative, then $\rho_i^A \rho_j^B$ must be negative. *(Note that in eq 16 one MUST take the fragments A and B so that $S_z^A = {}^1/_2$, $S_z^B = {}^1/_2$).* However, there is a severe conceptual difficulty here. The case where $\rho_i^A \rho_j^B$ is negative is usually associated with "ferromagnetic coupling". As we shall see in the Results and Discussion section, a negative ΔP_{ij} (corresponding to triplet stability) for the "shortest contact" or interfragment sites arises from the case where P_{ij}^S and P_{ij}^T are both negative but $|P_{ij}^S| > |P_{ij}^T|$. Therefore, *the "shortest contact" sites in the singlet are more strongly triplet coupled than the "shortest contact" sites in the triplet. Thus the association of negative $\rho_i^A \rho_j^B$ with the concept of ferromagnetic coupling is dubious from a conceptual point of view.*

A Practical Scheme for a McConnell-Like Decomposition of the Singlet/Triplet Energy Separation. It is convenient to illustrate the approach we will use by considering the spin coupling of two doublet fragments A and B with radical centers ν and μ as shown in Figure 1. In general, there are two types of interfragment interactions, a first set which consists of the "close contact atoms" and a second set consisting of the remaining interactions. In the model shown in Figure 1, the first set corresponds to the direct interactions between aligned carbon atoms and the second to indirect interactions between nonaligned carbon atoms. This partition will be useful for the bis(phenylmethylenyl)[2.2]paracyclophane isomers we will discuss later. However, such a division must depend in general on the system being studied.

The summation in eq 16 is restricted to interfragment interactions $i \in A, j \in B$, while the summation in eq 17 extends over all atoms. Thus, to compare the predictions obtained from eq 17 with the McConnell's theory, we must partition the sum in eq 17 in which both indexes are restricted to be on the same fragment A, i.e., $\{\Delta P_{ii'}\}_{ii' \in A}$, and interfragment contributions $\{\Delta P_{ij}\}_{i \in A, j \in B}$. We now consider this point in more detail.

The P_{ij} and ΔP_{ij} in eq 18, can be divided into an intrafragment set $\{\Delta P^{AA}\} = \{\Delta P_{ii'}\}_{ii' \in A}$ and an interfragment set $\{\Delta P^{AB}\} = \{\Delta P_{ij}\}_{i \in A, j \in B}$. It is then convenient to divide the interfragment set into 3 contributions: (i) $\{P_1^{AB}\}$ and $\{\Delta P_1^{AB}\}$, the set of direct interactions between aligned carbon atoms, (ii) $\{P_2^{AB}\}$ and $\{\Delta P_2^{AB}\}$, the set of indirect interactions between nonaligned carbon atoms, and (iii) $\{P_3^{AB}\}$ and $\{\Delta P_3^{AB}\}$, the set of interfragment couplings of the radical centers ν, μ themselves together with the coupling of the radical centers ν with the centers on fragment B, and the coupling of the radical centers μ with the centers on fragment A. Thus $\{\Delta P_3^{AB}\} = \{\Delta P_{i\mu} \cup \Delta P_{j\nu} \cup \Delta P_{\mu\nu}\}_{i \in A, j \in B, j \neq \mu, i \neq \nu}$.

We now introduce some notation to simplify the presentation. We shall use $\{P_r^{AB}\}$, $\{\Delta P_r^{AB}\}$ to refer to a set of density matrix elements and density difference matrix elements of type r (r = 1,2,3). We then use P_r^{AB} and ΔP_r^{AB} to denote the sum of the quantities contained in the sets $\{P_r^{AB}\}$ and $\{\Delta P_r^{AB}\}$. The corresponding contributions to the energy will be written as ΔE_r^{AB}. For example, if $r = 3$, then

$$\Delta P_3^{AB} = \sum_{\substack{i \in A, j \in B, \\ j \neq \mu, i \neq \nu}} (\Delta P_{i\mu} + \Delta P_{j\nu} + \Delta P_{\mu\nu}) \tag{20}$$

$$\Delta E_3^{AB} = \sum_{\substack{i \in A, j \in B, \\ j \neq \mu, i \neq \nu}} (J_{i\mu} \Delta P_{i\mu} + J_{j\nu} \Delta P_{j\nu} + J_{\mu\nu} \Delta P_{\mu\nu}) \tag{21}$$

Finally we use ΔP and ΔE to denote the summation over all contributions.

With these definitions to hand, there are some approximate relationships that must hold if the McConnel-I model is to have qualitative validity. First, the intrafragment spin coupling should correspond to a doublet (i.e., the S^2 eigenvalue is ${}^3/_4$). Thus, from eq 10, the following relationship should hold approximately for fragment A (or B)

$$S_A(S_A+1) = -\frac{N_A(N_A-4)}{4} - \sum_{ii' \in A} P_{ii'} = -\frac{N_A(N_A-4)}{4} - P^{AA} \approx \frac{3}{4} \tag{22}$$

Here N_A is the number of electrons associated with fragment A. Second, the McConnell-I theory neglects the intrafragment coupling. Thus, all the elements of the set $\{\Delta P^{AA}\}$ should be approximately zero and consequently $\Delta E^{AA} = 0$. Thus, if the McConnell-I model is to have quantitative validity, the $\rho_i^A \rho_j^B$ and the ΔP_{ij} must behave in a qualitatively similar fashion and the set $\{\Delta P^{AA}\}$ must be approximately zero.

In the limit where the fragments do not interact, there are two *localized* electrons in radical centers ν and μ, these two electrons can either couple to singlet or triplet. Thus, according to the perfect pairing formula,[30] the value of $\Delta P_{\mu\nu}$ is given as

$$\Delta P_{\mu\nu} = P_{\mu\nu}^S - P_{\mu\nu}^T = 1 - (-1) = 2.0 \tag{23}$$

Further, the set of $\{\Delta P_1^{AB}\}$ and $\{\Delta P_2^{AB}\}$, and all the contributions due to $\{\Delta P_3^{AB}\}$, will be zero if there is no interaction between the fragments except those arising from $P_{\mu\nu}$ on the *localized* electrons in radical centers ν and μ. When the fragments interact, $\Delta P^{AA} = 0$ and $\Delta P^{AB} \approx 2$, we have

$$\Delta P_3^{AB} \approx 2 - \delta \tag{24}$$

and

$$\Delta P_{1+2}^{AB} \approx \Delta P_1^{AB} + \Delta P_2^{AB} \approx \delta \tag{25}$$

where δ is a small positive quantity which arises from the interaction of the fragments A, B.

However, the McConnell-I model is always used qualitatively. The individual J_{ij}^{AB} are never evaluated (but assumed to be negative) and only the $\rho_i^A \rho_j^B$ are used to make predictions. Thus, there are some additional assumptions, relating to individual J_{ij}^{AB} that are inherent in even the qualitative application of the McConnell-I model. First, the contributions from nonaligned "closest contact" sites, the $\{\Delta P_3^{AB}\}$, are completely ignored. However, the $\{\Delta P_3^{AB}\}$ are expected to be large (see eq 24) so that the validity of McConnell's approach

SCHEME 1

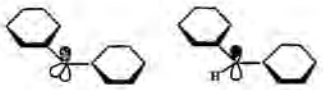

depends on all the members of the set $J_{\mu\nu},\{J_{i\mu} \cup J_{j\nu}\}_{i\in A, j\in B, j\neq\mu, i\neq\mu}$ being zero (which is reasonable provided the radical centers are far apart). Secondly, in qualitative applications of the McConnell-I theory for aromatic molecules that are pancaked on top of one another in crystals, one focuses on the contribution from the aligned centers $\{\Delta P_1^{AB}\}$ and the contribution from $\{\Delta P_2^{AB}\}$ is ignored so that McConnell's theory effectively makes a qualitative estimate of ΔE_1^{AB}. From eq 25, it is clear that ΔP_{1+2}^{AB} is a small number δ that results from sum of ΔP_1^{AB} and ΔP_2^{AB}. Thus, it is clear that ΔP_1^{AB} and ΔP_2^{AB} must have a similar magnitude but opposite sign. Therefore, qualitative applications are only valid if the corresponding J_{ij} that are combined with the $\{\Delta P_2^{AB}\}$ terms are very small. If these conditions hold, the geometry and the relative singlet/triplet ordering will be controlled by the $\{\Delta P_1^{AB}\}$ elements. Thus, if the $\{\Delta P_1^{AB}\}$ are all negative the spin coupling will be triplet in agreement with McConnell-I theory, which requires $\rho_i^A \rho_j^B < 0$. Further, the J_{ij} corresponding to $\{\Delta P_1^{AB}\}$ will be very sensitive to distance because of the direct overlap of the carbon atom p^π orbitals.

Computational Details

The [2.2]paracyclophanedicarbenes (e.g., pseudoortho, pseudometa, and pseudopara bis(phenylmethylenyl)[2.2]-paracyclophane (bPhMenyl) isomers) have been proposed to provide a reasonably good model for examining the intermolecular magnetic interaction in reference to McConnell-I model,[25] since the spin-containing benzene rings of two diphenylcarbene molecules are pancaked on top of one another in the [2.2]paracyclophane skeleton. Experimental data available for the bPhMenyl system shows that, among the three isomers with different orientation of the two phenylmethylenyl substituents, only the pseudoortho and pseudopara isomers present a quintet ground state, while the singlet is the ground state in the pseudometa stacking mode.[25] However, strictly speaking, the model is far from ideal: the two benzene rings incorporated in the [2.2]paracyclophane structure are not planar but bent into a boat form with interring distances not even (~2.8−3.1 Å), and the two rings are deeclipsed by 3.2° to avoid the ethano-type eclipsing in the side chains.[31]

A recent study[32] showed that the π-electronic structure of diphenylcarbene is very much like that of diphenylmethyl radical, as indicated in Scheme 1. The important triplet state of the carbene has one electron in the conjugated π-system. Accordingly, it is sensible to model this system with a methyl radical rather than carbene unit. Therefore, one would obtain for bis(phenylmethyl)[2.2]paracyclophanes, a singlet ground state for the pseudometa stacking mode and triplet ground state for the pseudoortho and pseudopara ones. Further, the phenylmethyl radical can be replaced by a simple methyl radical, thus giving rise to bis(methyl)[2.2]paracyclophane (namely, bMe), since the phenyl attached to the methyl is not involved in the π-electron reorganization related to singlet/triplet states.[32]

Energies and geometry optimization of the pseudoortho, pseudometa, and pseudopara bMe model systems were carried out by means of the Molecular Mechanics−Valence Bond (MMVB) method. MMVB[28] is a hybrid method, which uses the MM2 potential[33] to describe the inert molecular σ-bonded framework and a Heisenberg Hamiltonian,[27] parametrized against CASSCF computations, to represent electrons on sp^2/sp^3 carbon atoms which are involved in π-conjugation or new σ-bond formation. The Heisenberg Hamiltonian implemented in MMVB is a faithful representation of eqs 5 and 6 and acts on a basis set of neutral many-electron VB states constructed from active orbitals which are singly occupied. The P_{ij} matrix elements are obtained from the CI vectors of the MMVB Hamiltonian[28c] and provide a partition of $\hat{S}(1)\cdot\hat{S}(2)$ into interactions between these sites.

The fundamental principles behind the parametrization of MMVB via an effective Hamiltonian have been discussed in ref 28b. The important point is the exchange parameters are fitted to a CASSCF effective Hamiltonian. In ref 28b, we show that these parameters can be interpreted in terms of an expansion involving powers of the overlap. However, no overlap integrals are ever computed in pratice. Thus, eq 4 is used for interpretative purposes only. The exchange parameters contain higher powers of the overlap implicitly. Further, by construction, the CASSCF effective Hamiltonian reproduces neutral covalent states of all spin multiplicies, so there is no explict spin dependence of the paremetrization.

Results and Discussion

For the bis(methyl)[2.2]paracyclophane (later on, bMe) model system, the MMVB optimization [28] of the pseudoortho, pseudometa, and pseudopara isomers was carried out for both the singlet and the triplet states. In addition, the singlet/triplet crossing geometries were characterized and located. The geometries for minima and the singlet/triplet crossing geometries are shown in Figure 2 [Cartesian coordinates for all critical points are available in Table 1S (Supporting Information)]. At the lowest energy optimized structures (triplet in the case of the pseudoortho and -para structures, and singlet in the case of the pseudometa structure), a decomposition of the singlet/triplet energy difference was carried out in terms of the $\{\Delta P_r^{AB}\}$. These data are presented in Tables 1 and 2 [the $P_{ij}^{S/T}$ contributions to ΔP for all three bMe isomers evaluated at the ground-state geometry are listed in Tables 2S (Supporting Information), and the corresponding J_{ij} are in Table 3S (Supporting Information)].

The relative ordering of the singlet and triplet states is indicated in column 2 of Table 1 and is in agreement with that observed experimentally for the low-spin meta and high-spin ortho/para isomers of bis(phenylmethylenyl)[2.2]paracyclophane (later on, bPhMenyl).[25] The absolute value of the energy difference between singlet and triplet states at the optimized geometries is similar for all three isomers (3 kcal mol^{-1}). To confirm that the conclusions regarding triplet versus singlet stability arise mainly from the stacking orientation of the benzyl groups in the paracyclophane, we also carried out a series of computations with two planar benzyl radicals placed 3 Å apart in the ortho, meta, and para orientations. The results are qualitatively similar to the results on the optimized paracyclophanes and will not be included here.

We begin with a brief discussion of the optimized geometries in Figure 2. The geometries for the singlet and triplet states differ only by ca. 0.001−0.07 Å with respect to interfragment C−C bond lengths. Thus, the main factors that control singlet/triplet stability are electronic in origin rather than geometric. This conclusion is reinforced by a consideration of the geometries where singlet and triplet states cross. In each case, the

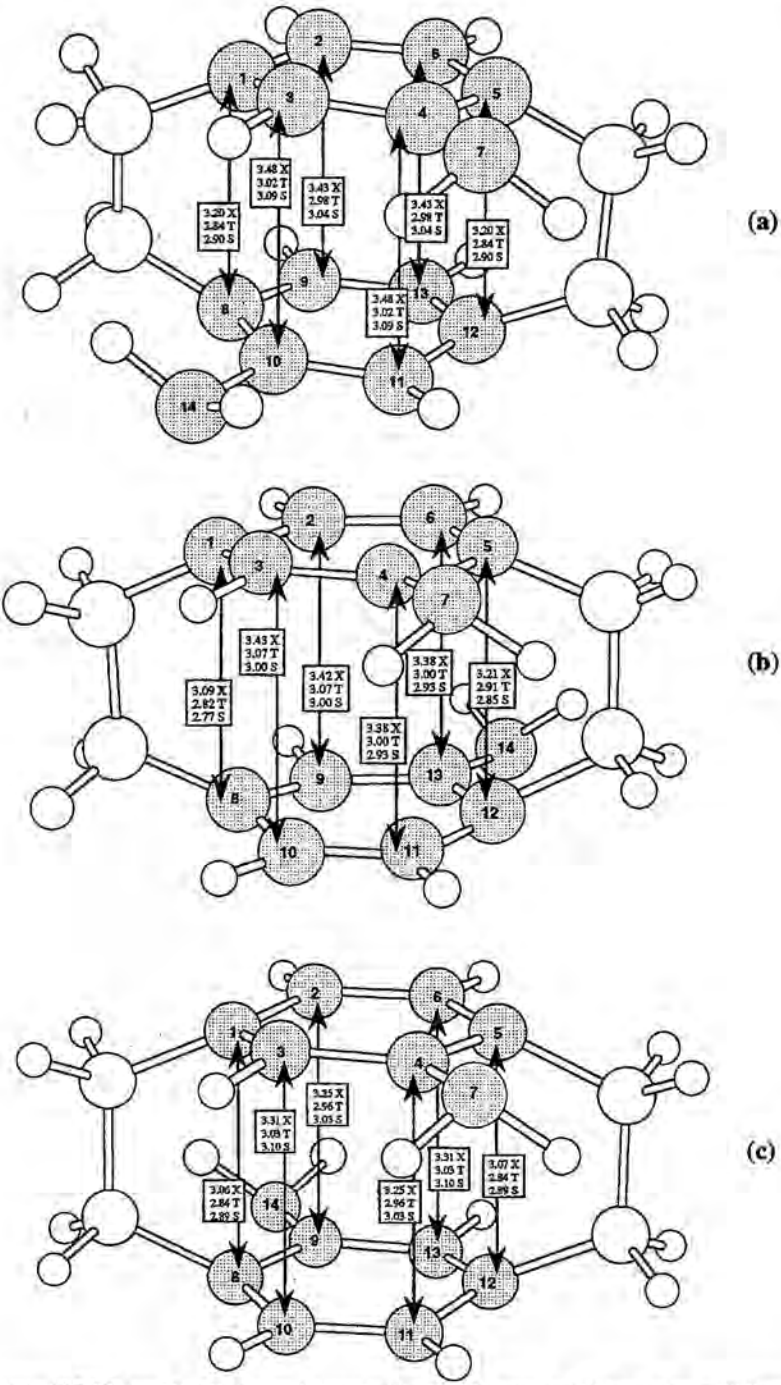

Figure 2. The optimized MMVB interfragment distances for pseudo- (a) ortho-, (b) meta-, and (c) para-bis(methyl)[2.2]paracyclophane (S = singlet, T = triplet, X = surface crossing).

crossing occurs when the interfragment bond distances are increased from ca. 2.9 Å to ca. 3.3 Å so that the interfragment J_{ij} falls to near zero. Therefore, the relative stability of singlet and triplet persists as the interfragment distances are increased

TABLE 1: Interfragment Exchange Density Matrices Differences ΔP_r^{AB} and Contributions to the Total Energy ΔE_r^{AB}. All Energy Differences in kcal mol^{-1}

isomer	stucture	ΔE^{AB}	ΔP_3^{AB} ΔE_3^{AB}	ΔP_1^{AB} ΔE_1^{AB}	ΔP_2^{AB} ΔE_2^{AB}	ΔP_{1+2}^{AB}
pseudoortho	T_{min}	2.9493	1.834	−1.355	1.508	0.153
			0.3765	3.7651	−1.1923	
pseudometa	S_{min}	−2.1963	1.666	1.264	−0.942	0.322
			−0.1255	−3.5768	1.5060	
pseudopara	T_{min}	2.6983	1.831	−1.370	1.525	0.155
			0.0000	4.0161	−1.3178	

TABLE 2: Interfragment Exchange Density Matrices Differences $\{\Delta P^{AB}\}$ for the Minima[a]

atom number	1	2	3	4	5	6	7
			(a) Pseudoortho (Triplet Minimum)				
8	***−.236***	.320	.326	−.299	.388	−.231	**.609**
9	.137	***−.198***	−.194	.175	−.231	.138	**−.356**
10	.175	−.245	***−.258***	.230	−.299	.175	**−.467**
11	−.190	.267	.273	***−.258***	.326	−.194	**.509**
12	.132	−.188	−.190	.175	***−.236***	.137	**−.352**
13	−.188	.262	.267	−.246	.320	***−.198***	**.497**
14	**−.352**	**.496**	**.509**	**−.467**	**.609**	**−.355**	**.957**
			(b) Pseudometa (Singlet Minimum)				
8	***.121***	−.172	−.171	.146	−.198	.116	**−.292**
9	−.171	***.270***	.259	−.221	.303	−.174	**.445**
10	−.172	.263	***.269***	−.225	.306	−.174	**.359**
11	.116	−.174	−.174	***.158***	−.205	.119	**−.301**
12	−.198	.307	.303	−.264	***.370***	−.205	**.531**
13	.146	−.226	−.221	.192	−.264	***.158***	**−.387**
14	**−.292**	**.452**	**.445**	**−.387**	**.531**	**−.301**	**.785**
			(c) Pseudopara (Triplet Minimum)				
8	***−.239***	.326	.329	−.305	.397	−.233	**.613**
9	.176	***−.260***	−.249	.230	−.305	.179	**−.465**
10	.137	−.192	***−.199***	.179	−.233	.137	**−.356**
11	−.190	.267	.268	***−.260***	.326	−.192	**.501**
12	.132	−.190	−.189	.176	***−.239***	.137	**−.351**
13	−.189	.268	.268	−.250	.329	***−.199***	**.503**
14	**−.350**	**.501**	**.502**	**−.465**	**.613**	**−.356**	**.948**

[a] ΔP_1^{AB} bold italic; ΔP_2^{AB} plain type; ΔP_3^{AB} bold. Atom numbers correspond to Figure 2.

until the interfragment interactions fall to zero. The interfragment−ring distances for the singlet and triplet states agree with the available experimental data (2.8 and 3.1 Å in bPhMenyl[31]). Thus, the bMe model system appears to be a good model of the bPhMenyl system (as expected since none of the phenyls attached to the methylenyl is involved in the π-electron reorganization[25]).

We now turn our attention to the analysis of the singlet/triplet energy difference ΔE^{AB} in terms of the components of ΔP^{AB} given in Table 1. The individual components of ΔP^{AB} for all the interfragment interactions are collected in Table 2. One must stress that this analysis is only sensible if $\Delta E^{AA} = \Delta E^{BB} = 0$. In all examples, this contribution computed to be less than 0.2 kcal mol^{-1}. Moreover, for each fragment, the computed intrafragment P^{AA} and P^{BB} are −6.0 (corresponding to a doublet in eq 22 with $N_A = N_B = 7$), irrespective of whether the overall spin coupling is triplet or singlet so that $\Delta P^{AA}(\Delta P^{BB})$ is zero.

The $\rho_i^A \rho_j^B$[25] are negative for the pseudoortho and -para species and positive for the pseudometa species according to the McConnell model, and thus, triplet ground states are predicted for the former and singlet for the latter. The computed values of $\{\Delta P_1^{AB}\}$ collected in the diagonal elements (bold) of Table 2 are in remarkable agreement with the qualitative model of McConnell. Thus the $\{\Delta P_1^{AB}\}$ components are negative for the pseudoortho and -para species (which have triplet ground states), and positive for the pseudo-meta species (which has a singlet ground state). Thus eq 19 appears to hold numerically.

Now let us examine some other aspects of the McConnell-I model that are necessary for reliable predictions. The $\{\Delta P_2^{AB}\}$ and $\{\Delta P_3^{AB}\}$ are ignored in the McConnell model; however, the $\{\Delta P_2^{AB}\}$ and $\{\Delta P_3^{AB}\}$ in Table 2 are clearly not zero. Rather they have large positive and negative elements. First, as predicted in eq 24, $\Delta P_3^{AB} \approx 2$. However, because the corresponding J_{ij} elements (see Table 3S) are all small we have $\Delta E_3^{AB} \approx 0.0$ (Table 1), so this term does not contribute to singlet versus triplet stability. Second, from Table 1, $\Delta P_{1+2}^{AB} \approx \delta$ (as suggested in eq 25) because ΔP_2^{AB} and ΔP_1^{AB} have opposite sign. However, ΔE_2^{AB} is not negligible. Thus, the singlet versus triplet stability results from a competition between ΔE_1^{AB} and ΔE_2^{AB}. For all the examples studied $|\Delta E_1^{AB}| > |\Delta E_2^{AB}|$, so that ΔE_1^{AB} alone gives a qualitative prediction that is in agreement with McConnell-I model. This situation arises because the magnitudes of J_{ij} (see Table 3S) that are combined with the $\{\Delta P_2^{AB}\}$ are in general smaller than the magnitudes of J_{ij} that are contracted with the $\{\Delta P_1^{AB}\}$.

Conclusions

If one compares eqs 16 and 17, it is clear that singlet/triplet stability depends on the sign and magnitude of $\rho_i^A \rho_j^B$ or ΔP_{ij}, and on the magnitude of the J_{ij} that are combined with the $\rho_i^A \rho_j^B$ or ΔP_{ij}. In this work we have included both effects on the bMe model system that is related to the bPhMenyl standard normally used to test the validity of the McConnell-I relationship. Remarkably, the predictions obtained from our Heisenberg Hamiltonian defined in eq 17, are in complete agreement with the qualitative predictions from eq 16 because of fortuitous cancelations. This agreement arises because the signs of $\rho_i^A \rho_j^B$ and ΔP_{ij} are the same and many J_{ij} are zero. We now discuss the origin of this effect in more detail.

It is clear that the agreement of the predictions of the McConnell-I model (eq 16) and our Heisenberg Hamiltonian (eq 17) arises because the partition into $\{\Delta P_1^{AB}\}$, $\{\Delta P_2^{AB}\}$, and $\{\Delta P_3^{AB}\}$ is possible, and the contribution from $\{\Delta P_1^{AB}\}$ dominates. The individual $\{\Delta P_2^{AB}\}$ and $\{\Delta P_3^{AB}\}$ are large and contain both positive and negative elements; however, this contribution is not important because the corresponding J_{ij} are very small. Thus, the McConnell-I model makes a correct prediction for our paracyclophane model by the lucky chance that $|\Delta E_1^{AB}| > |\Delta E_2^{AB}|$. In general, when the atoms are not perfectly aligned, one can expect that the ΔE_2^{AB} will not be negligible. In this case, a qualitative prediction using the McConnell model is impossible without an a priori knowledge of the J_{ij}. Further, it is clear the J_{ij} have strong orientational and directional properties. Thus, when ΔE_1^{AB} and ΔE_2^{AB} have similar magnitude (but opposite sign), the question of singlet/triplet stability will depend on subtle details of orientation manifested in the behavior of the J_{ij}.

The preceding discussion masks a severe conceptual problem. The computed "closest contact" couplings $\{P_1^{AB}\}$ (see Table 2S) are *always* negative, irrespective of whether the ground state is triplet or singlet. Thus, a negative ΔP_1^{AB} (corresponding to triplet stability) can be obtained if $|P_1^{AB}|^S > |P_1^{AB}|^T$. (In the "ideal" case where the wave function is just a simple Rumer function the P_{ij} have values −1 for two electrons coupled parallel to a triplet, and $-1/2$ for uncoupled spins, i.e., i and j belong to *different* "spin-paired" functions). Since the dominant Rumer function in the wave function must involve intrafragment

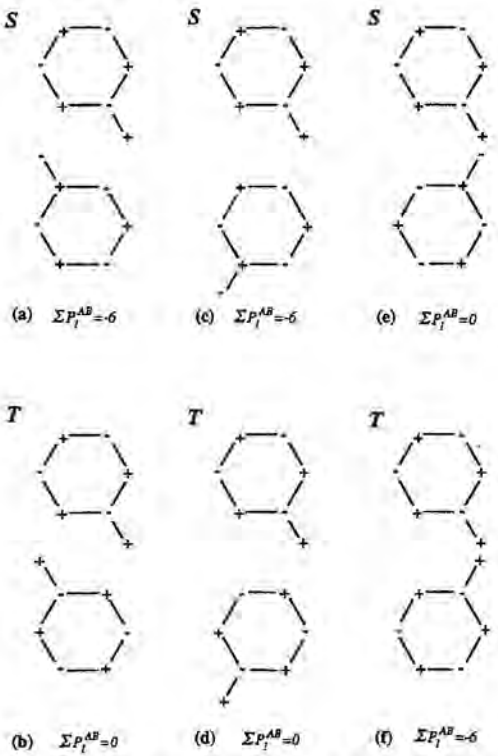

Figure 3. A schematic representation of the leading determinants in the singlet and triplet wave functions used to compute the P_{ij} for the pseudo-ortho-(a/b), para-(c/d), and meta- (e/f) bis(methyl) [2.2]paracyclophane isomers.

spin coupled pairs, the interfragment coupling is mainly that of uncoupled electrons. Therefore, we expect that the P_{ij} for the "closest contact" sites should be ca. $-1/2$. In fact, the MMVB "closest contact" couplings are all negative and range from about -0.3 to -0.6, which is in agreement with this observation. According to McConnell-I, the case where $\rho_i^A \rho_j^B$ is negative is usually associated with "ferromagnetic coupling". Similarly a negative ΔP_1^{AB} is associated with triplet stability. Thus, we are left with the difficulty of explaining why the triplet stability implies that the "closest contact" sites are more strongly ferromagnetically coupled (i.e., with a negative P_1^{AB}) in the singlet state than in triplet state for the case where the ground state is a triplet. The answer turn out to be remarkably simple as we now discuss.

In Figure 3 we show the leading determinants in the singlet and triplet wave functions that were used to compute the P_{ij}. The + and − in the figure indicate the spin (α or β) of the orbital on the corresponding site for singlet (S) and triplet (T). Remarkably, the spin arrangements for the triplet ($|S_z| = 1$) are in agreement with those suggested by the McConnell model (Figure 3b, d, f). From eq 9 for a single determinant, $P_{ij} = -1$ for electrons of same spin and $P_{ij} = 0$ for different spin. We have given the value of the sum of the ideal "closest contact" P_{ij} values as $\sum P_1^{AB}$ in Figure 3. Clearly, for the first term in the wave function the "closest contact" P_{ij} for the singlet in the case of a triplet ground state (Figure 3 a/b and c/d) are negative, while the situation is inverted for the case of the singlet ground state (Figure 3 e and f). Thus, as said before, triplet stability implies that the "closest contact" sites are more strongly ferromagnetically coupled in the singlet state than in triplet state for the case where the ground state is a triplet. Therefore, the McConnell model appears to correctly predict the stability of the leading term in the VB wave function. The magnitudes of the ΔP_1^{AB} are predictable crudely from the leading term in the wave function. However, there is no reason to expect this situation to hold in general.

Thus, the McConnell-I model gives the correct prediction of singlet/triplet stability for the bis(methyl)[2.2]paracyclophane example because many contributions are small and the association $\Delta P_{ij} \leftrightarrow \rho_i^A \rho_j^B$ is sensible. Further, the McConnell model seems to predict the leading determinants in the wave function correctly. However, the predictive value of the McConnell model must be limited in general because the orientational dependence of the model via the J_{ij} is never studied.

Finally, we believe that the methods used in this study are quite generally applicable to other related problems in magnetism. An example is the related problem of ferrimagnetism which arises form the coupling of two spins of different magnitudes in such a way, that one never has an $S = 0$ coupling. McConnell I is a through space mechanism while ferrimagnetism is often through-bond in polymetalates. But the formalism descibed in ths work is equally applicable. Another example of a through-bond mechanism is the Dougherty model.[2c] An application to this problem is published elsewhere.[34]

Acknowledgment. This work was supported (in part) by the DGES (Spain) (Project PB95-0848-C02-02). Mercè Deumal acknowledges CIRIT for her studentship.

Supporting Information Available: Cartesian coordinates for the MMVB optimized singlet, triplet, and surface crossing geometries for the ortho-, meta-, and para-bis(methyl)[2.2]-paracyclophane isomers in Table 1S, the individual $P_{ij}^{S/T}$ contributions to ΔP for all three bis(methyl)[2.2]paracyclophane isomers evaluated at the ground-state geometry in Tables 2S, and the corresponding J_{ij} in Table 3S (11 pages). Ordering information is given on any current masthead page.

References and Notes

(1) For a recent overview, see: (a) Miller, J. S.; Epstein, A. J. *Angew. Chem., Int. Ed. Engl.* **1994**, *33*, 385−415. (b) Kahn, O. *Molecular Magnetism*; VCH Publishers: New York, 1993. (c) Kinoshita, M. *Jpn. J. Appl. Phys.* **1994**, *33*, 5718. (d) Gatteschi, D., Kahn, O., Miller, J. S., Palacio, F., Eds.; *Molecular Magnetic Materials*; Kluwer Academic Publishers: Dordrecht, 1991. (e) Iwamura, H., Miller, J. S., Eds., *Mol. Cryst. Liq. Cryst.* **1993**, *232/233*, 1−360/1−366. (f) Miller, J. S., Epstein, A. J., Eds. *Mol. Cryst. Liq. Cryst.* **1995**, *272−274*. (g) Itoh, K., Miller, J. S., Takui, T., Eds. *Mol. Cryst. Liq. Cryst.* **1997**, *305−306*. (h) Coronado, E., Delhaes, P., Gatteschi, D., Miller, J. S., Eds. *Molecular Magnetism: From Molecular Assemblies to Devices*; Kluwer Academic Publishers: Dordrecht, 1996. (i) Kahn, O., Ed.; *Magnetism: A Supramolecular Function*; Kluwer Academic Publishers: Dordrecht, 1996.

(2) For a review of some stable radicals and its use in magnetism, see: (a) Lahti, P. M. In *Design of Organic-Based Materials with Controlled Magnetic Properties*; ACS Symposium Series 664; Turnbull, M. M. Sugimoto, T., Thomposon, L. K., Eds.; American Chemical Society: Washington, DC, 1996. (b) Rajca, A. *Chem. Rev.* **1994**, *94*, 871−893. (c) Dougherty, D. A. *Acc. Chem. Res.* **1991**, *24*, 88.

(3) For some recent examples of purely organic ferromagnets within this family, see: (a) Turek, P.; Nozawa, D.; Shiomi, K.; Awaga, K.; Inabe, T.; Maruyama, Y.; Kinoshita, M. *Chem. Phys. Lett.* **1991**, *180*, 327. (b) Awaga, K.; Okuno, A.; Yamaguchi, A.; Hasegawa, M.; Inabe, T.; Maruyama, Y.; Wada, N. *Phys. Rev. B* **1994**, *49*, 3975. (c) Hernández, E.; Mas, M.; Molins, E.; Rovira, C.; Veciana, J. *Angew. Chem., Int. Ed. Engl.* **1993**, *32*, 882. (d) Lanfranc de Panthou, F.; Luneau, D.; Laugier, J.; Rey, P. J. *Am. Chem. Soc.* **1993**, *115*, 9095. (e) Cirujeda, J.; Mas, M.; Molins,

E.; Lanfranc de Panthou, F.; Laugier, J.; Geun Park, J.; Paulsen, C.; Rey, P.; Rovira, C.; Veciana, J. *J. Chem. Soc., Chem. Commun.* **1995**, 709. (f) Caneschi, A.; Ferraro, F.; Gatteschi, D.; le Lirzin, A.; Rentschler, E. *Inorg. Chim. Acta* **1995**, *235*, 159. (g) Cirujeda, J.; Hernández, E.; Lanfranc de Panthou, F.; Laugier, J.; Mas, M.; Molins, E.; Rovira, C.; Novoa, J. J.; Rey, P.; Veciana, J. *Mol. Cryst. Liq. Cryst.* **1995**, *271*, 1. (h) Akita, T.; Mazaki, Y.; Kobayashi, K.; Koga, N.; Iwamura, H. *J. Org. Chem.* **1995**, *60*, 2092. (i) Lang, A.; Pei, L.; Ouohab, L.; Kahn, O. *Adv. Mater.* **1996**, *8*, 60.

(4) A short account of them is given in: Kahn, O.; Hendrickson, D. N.; Iwamura, H.; Veciana, J. In *Molecular Magnet: C Materials*; Gatteschi, D., Kahn,O., Miller, J. S., Palacio, F., Eds.; Kluwer Academic Publishers: Dordrecht, 1991; p 385.

(5) Anderson, P. W. In *Magnetism*; Rado, G. T., Shul, H., Eds.; Academic Press: New York, 1963; Vol. 1, p 25.

(6) Hay, P. J.; Thibeault, J. C.; Hoffmann, R. *J. Am. Chem. Soc.* **1975**, *97*, 4884.

(7) For instance, see: Charlot, M. F.; Kahn, O.; Jeannin, S.; Jeannin, Y. *Inorg. Chem.* **1980**, *19*, 1410.

(8) For an example, see: Kahn, O.; Galy, J.; Journaux, Y.; Morgenstern-Badarau, I., *J. Am. Chem. Soc.* **1982**, *104*, 2165.

(9) (a) de Loth, P.; Cassoux, P.; Daudey, J. P.; Malrieu, J. P. *J. Am. Chem. Soc.* **1981**, *103*, 4007. (b) Daudey, J. P.; De Loth, P.; Malrieu, J. P. In *Magneto Structural Correlations in Exchange Coupled Systems*; Willet, R. D., Gatteschi, D., Kahn, O., Eds.; Nato Advance Studies Series C140; Reidel: Dordrecht 1985. (c) De Loth, P.; Karafiloglou, P.; Daudey, J. P.; Kahn, O. *J. Am. Chem. Soc.* **1988**, *110*, 5676.

(10) (a) Miralles, J.; Castell, O.; Caballol, R.; Malrieu, J. P. *Chem. Phys.* **1993**, *172*, 33. (b) Castell, O.; Caballol, R.; Subra, R.; Grand, A. *J. Phys. Chem.* **1995**, *99*, 154.

(11) Noodleman, L.; Case, D. A. *Adv. Inorg. Chem.* **1992**, *38*, 423.

(12) (a) Ruiz, E.; Alemany, P.; Alvarez, S.; Cano, J. *J. Am. Chem. Soc.* **1997**, *119*, 1297. (b) Caballol, R.; Castell, O.; Illas, F.; de P. R. Moreira, I.; Malrieu, J. P. *J. Phys. Chem. A* **1997**, *101*, 7860.

(13) (a) Borden, W. T.; Davidson, E. R. *Acc. Chem. Res.* **1981**, *14*, 69. (b) Borden, W. T.; Iwamura, H.; Berson, J. A. *Acc. Chem. Res.* **1994**, *27*, 109.

(14) Ovchinnikov, A. A. *Theor. Chim. Acta* **1978**, *47*, 297.

(15) McConnell, H. M. *J. Chem. Phys.* **1963**, *39*, 1910.

(16) McConnell, H. M. *Proc. Robert A. Welch Found. Conf. Chem. Res.* **1967**, *11*, 144.

(17) Breslow, R. *Pure Appl. Chem.* **1982**, *54*, 927.

(18) (a) Yamaguchi, K.; Fukui, H.; Fueno, T. *Chem. Lett.* **1986**, 625. (b) Kawakami, T.; Yamanaka, S.; Yamaki, D.; Mori, W., Yamaguchi, K. In *Theoretical Approaches to Molecular Magnetism*; ACS Symposium Series 644; Turnbull, M. M., Sugimoto, T., Thompson, L. K., Eds.; American Chemical Society: Washington, DC, 1996; Chapter 3.

(19) Awaga, K.; Sugano, T.; Kinoshita, M. *Chem. Phys. Lett.* **1987**, *141*, 540.

(20) Kollmar, C.; Kahn, O. *Acc. Chem. Res.* **1993**, *26*, 259.

(21) Zheludev, A.; Barone, V.; Bonnet, M.; Delley, B.; Grand, A.; Ressouche, E.; Subra, R.; Schweizer, J. *J. Am. Chem. Soc.* **1994**, *116*, 2019.

(22) Novoa, J. J.; Mota, F.; Veciana, J.; Cirujeda, J. *Mol. Cryst Liq. Cryst.* **1995**, *271*, 79.

(23) Buchachenko, A. L. *Mol. Cryst. Liq. Cryst.* **1989**, *176*, 307.

(24) Yamaguchi, K.; Toyoda, Y.; Fueno, T. *Chem. Phys. Lett.* **1989**, *159*, 459.

(25) a) Izuoka, A.; Murata, S.; Sugawara, T.; Iwamura, H. *J. Am. Chem. Soc.* **1985**, *107*, 1786. (b) Izuoka, A.; Murata, S.; Sugawara, T.; Iwamura, H. *J. Am. Chem. Soc.* **1987**, *109*, 2631.

(26) McWeeny, R.; Sutcliffe, B. T. *Methods of Molecular Quantum Mechanics*; Academic Press, NY; 1969.

(27) (a) Anderson, P. W. *Phys. Rev.* **1959**, *115*, 2. (b) Said, M.; Maynau, D.; Malrieu, J. P.; Bach, M. A. G. *J. Am. Chem. Soc.* **1984**, *106*, 571. (c) Maynau, D.; Durand, Ph.; Daudey, J. P.; Malrieu, J. P. *Phys. Rev. A* **1983**, *28*, 3193. (d) Durand, Ph.; Malrieu, J. P. *Adv. Chem. Phys.* **1987**, *68*, 931.

(28) (a) Bearpark, M. J.; Bernardi, F.; Olivucci, M.; Robb, M. A. *Chem. Phys. Lett.* **1994**, *217*, 513. (b) Bernardi, F.; Olivucci, M.; McDouall, J. J.; Robb, M. A. *J. Chem. Phys.* **1988**, *89*, 6365. (c) Bernardi, F.; Olivucci, M.; Robb, M. A. *J. Am. Chem. Soc.* **1992**, *114*, 1606.

(29) Pauncz, R. *Spin Eigenfunctions*; Plenum Press: New York, 1979.

(30) McWeeny, R. *Spins in Chemistry*; Academic Press, Inc.: New York, 1970.

(31) (a) Brown, C. J. *J. Chem. Soc.* **1953**, 3265. (b) Lonsdale, K.; Milledge, H. J.; Rao, K. V. K. *Proc. R. Soc. London, Ser. A* **1960**, *555*, 82. (c) Cram, D. J.; Cram, J. M. *Acc. Chem. Res.* **1971**, *4*, 204.

(32) Yoshizawa, K.; Hoffmann, R. *J. Am. Chem. Soc.* **1995**, *117*, 6921.

(33) Alliger, N. L. *Adv. Phys. Org. Chem.* **1976**, *13*, 1.

(34) La Fuente, P.; Novoa, J. J.; Bearpark, M. J.; Celani, P.; Olivucci, M.; Robb, M. N. *Theoretical Chemistry Accounts*; 1998. Accepted for publication.

ARTICLE 8

Adv. Mater. **1998**

Structure–Magnetism Relationships in α-Nitronyl Nitroxide Radicals: Pitfalls and Lessons to be Learned**

By *Mercè Deumal, Joan Cirujeda, Jaume Veciana,* and *Juan J. Novoa**

The design of new, purely organic, persistent radicals with crystals capable of showing spontaneous magnetization below a certain critical temperature, has been an objective of many research groups.[1] It has been possible to obtain various crystals of purely organic radicals showing interesting magnetic properties, in some cases even bulk ferromagnetism.[2] Many examples of these magnetic crystals are found in the family of the so-called α-nitronyl nitroxide radicals.[2,3] Some of them present bulk ferromagnetism, although, up to now, only at very low critical temperatures.

One of the challenges in this research field is the rational design of persistent radicals with crystals that have ferromagnetic ordering at higher critical temperatures. This objective can only be achieved through the control of the crystal packing of the radicals[4] and a well founded structure–magnetism relationship.[1,2] To explain the relationship between the nature and strength of intermolecular magnetic interactions and the details of crystal packing, the most widely used tool has been the McConnell-I model[5] (the first of the two proposed by McConnell). This model, based on a Heisenberg spin Hamiltonian and first introduced by the author to rationalize the magnetism in planar systems with unpaired π-electrons, is capable of explaining the presence of "through space" magnetic interactions and the dependence on the relative orientation of the shortest contact molecules. It predicts the presence of intermolecular ferromagnetic interactions only when short intermolecular contacts are found in the crystal between atoms i and j bearing considerable spin populations ρ_i and ρ_j of opposite sign. Accordingly, the magnetic behavior of a molecular crystal can be established once one knows the electronic spin distribution over the atoms of the constituent molecules. This distribution can be determined by experimental[2,6] and theoretical methods.[6,7] When this analysis is done for members of the α-nitronyl nitroxide radical family, one systematically finds that most of the spin density is located on the ONCNO part of the five membered ring, being positive on the NO groups and negative in the central C(sp^2) atom.[2,6,7] Consequently, the magnetic properties of the α-nitronyl nitroxide crystals are normally rationalized by looking at the closest NO···ON and NO···C(sp^2) contacts present among the ONCNO groups of neighboring radicals. When short NO···ON contacts are found McConnell-I predicts an antiferromagnetic coupling. If these contacts dominate, one can expect this crystal to present antiferromagnetic behavior.[1,2,8] Similarly, the presence of short NO···C(sp^2) contacts is taken as a sign of ferromagnetic interactions. There are other atoms of the α-nitronyl nitroxide radicals showing much smaller spin populations, such as the carbons of the aromatic rings, the hydrogens attached to these carbons, and the hydrogens of the methyl

[*] Prof. J. J. Novoa, M. Deumal
Departament de Química Física, Facultat de Química, Universitat de Barcelona
Av. Diagonal 647, E-08028 Barcelona (Spain)
Prof. J. Veciana, Dr. J. Cirujeda
Institut de Ciència de Materials (CSIC), Campus Universitari de Bellaterra
E-08913 Cerdanyola (Spain)

[**] This work was supported by the DGICYT (Projects PB95-0848-C02-02 and PB96-0862-C02-01) and CIRIT (Projects GRP94-1077 and GRQ93-8028). We also thank CESCA and CEPBA for their generous allocations of computer time. M.D. and J.C. acknowledge CIRIT for their doctoral grants. We would like also to thank Dr. S. Motherwell from the Cambridge Crystallographic Data Center (UK) for giving us access to a beta version of the PREQUEST program.

groups of the five-membered rings.[6,7,9] The $\rho_i\rho_j$ product of such contacts are thus smaller. So, even if we extend the McConnell-I model to include σ electrons, these contacts should not play a dominant role, but their possible magnetic contribution cannot be discounted. In this Communication we are going to show that the previous structure–magnetism relationships based on the shortest NO···ON, NO···C(sp^2) and NO···C(sp^3) contacts in general do not fit the experimental magnetic behavior currently known for many α-nitronyl nitroxide radicals. We will show here that there is no statistical difference between the packing of α-nitronyl nitroxide crystals showing *dominant* ferromagnetic or antiferromagnetic behavior.[10]

One systematic and unbiased way of finding if there is a relationship between the presence of ferro- and antiferromagnetism and the relative orientation of the NO···ON contacts is by looking at the intermolecular geometrical disposition of these contacts in the known crystals of the α-nitronyl nitroxide family showing dominant ferro- or antiferromagnetic interactions. Searching in the Cambridge Crystallographic Database[11] and from our own work, or information provided by other authors, we found 143 crystals with known magnetic properties.[12] We discarded the crystals with R factors greater than 0.10, the ones with structures determined from very limited data, and those with disorder or large molecular distortions. From the remaining 117 structures, we further discarded 45 with transition metal atoms and large closed-shell organic molecules co-crystallized, since they could present magnetic pathways through the metal atoms or the closed-shell and the radical units. Finally, the remaining 72 were further trimmed by discarding those crystals that did not present clear, dominant, ferro- or antiferromagnetic interactions. This left us with a set of 47 purely organic α-nitronyl nitroxide crystals: 23 of them showing dominant ferromagnetic interactions, and 24 antiferromagnetic ones. Hereafter we will refer to these subsets as the FM and AFM subsets.

To analyze the relative orientation of the NO···ON contacts in nearby radicals of the FM and AFM subsets one has to define the relative position of the ONCNO groups of the five-membered ring involved in the contact. A previous analysis has shown that these five ONCNO atoms lie in one plane and its geometry is nearly constant.[12] Consequently, we can consider the internal geometry of these groups as fixed. Using internal coordinates, the relative positions of a N_{11}–O_{11}···O_{21}–N_{21} contact made between the O_{12}–N_{12}–C_1–N_{11}–O_{11} and O_{21}–N_{21}–C_2–N_{22}–O_{22} groups can be defined by the following six coordinates: the O_{21}···O_{11} distance, the O_{21}···O_{11}–N_{11} angle, the O_{21}···O_{11}–N_{11}–C_1 dihedral (which defines the position of the O_{21} atom), the N_{21}–O_{21}···O_{11} angle and the N_{21}–O_{21}···O_{11}–N_{11} dihedral (which define for a fixed N–O distance the position of the N_{21} atom), and the C_2–N_{21}–O_{21}···O_{11} dihedral (which defines where the C_2 atom lies when the C_2–N_{21} distance and the C_2–N_{21}–O_{21} angle are fixed). Once the O_{21}–N_{21}–C_2 plane is defined, the position of the remaining N_{22} and O_{22} atoms are also known for a fixed planar ONCNO group geometry. To simplify the notation we will identify these intermolecular parameters as

D, A_1, A_2, T_1, T_2, and T_3 (Fig. 1).

When the geometry of the N–O···O–N contacts is analyzed in the FM and AFM subsets looking for the values of the D, A_1, A_2, T_1, T_2, and T_3 parameters, the striking result is the similarity found for both subsets. We first selected the contacts with an O···O distance (D parameter) shorter than 10 Å. This gives a total of 1312 contacts, adding those in the FM and AFM subsets. The shortest value found in the FM subset is 3.158 Å while that in the AFM subset is 3.159 Å. Figure 2 shows the relative arrangement of molecules with the shortest O···O distance contacts in these two subsets. This similarity is not an exceptional situation present in only two crystals but it is a general situation. Actually, if one looks at the number of contacts in the 0–n Å range for n = 3, 4, 5, 6, 7, 8, 9, 10 Å, one sees that the number of short contacts within each distance range is similar in the FM and AFM subsets (see Table 1). The percentage of short contacts for each range present in the FM subset varies from 39 to 47 %. This number is always close to the 49 % of crystals belonging to the FM subset, therefore suggesting that the two subsets present a similar packing efficiency for the NO···ON contacts. Thus, our distance analysis reveals that the idea, that short NO···ON contacts are indicative of crystals being dominated by antiferromagnetic interactions, is not correct.

Looking only at the O···O distances is like averaging the angular distributions for each value of that distance. Thus, one should look now at the angular distribution for the NO···ON contacts. McConnell-I model predicts that short NO···ON contacts resulting from the direct overlap of two ONCNO groups can give rise to antiferromagnetic or ferromagnetic interactions, depending on the relative orientation of these ONCNO groups. When the dominant overlap comes from two NO subgroups, given the identical sign in their spins, the interaction is antiferromagnetic. However, it is possible that the dominant overlap is that between one NO subgroup and the central carbon, being then a ferromagnetic interaction.[5,8] Therefore, one should test if the angular distribution of the short NO···ON contacts present in the FM do cluster around some particular angular orientations that are excluded in the AFM subset contacts. Figure 3a shows for a selected pair of variables (D and T_2) that this is not the case and, instead, there is a remarkable similarity between the distributions of the FM and AFM subsets. To test if this similarity is an artifact of the pair of variables selected, we plotted (Fig. 3b) the position of the O_{21} atom in the O_{12}–N_{12}–C_1–N_{11}–O_{11}···O_{21}–N_{21}–C_2–N_{22}–O_{22} contacts in the 3–5 Å range for all the contacts of the FM and AFM subgroups, the most important distance range determining the magnetic properties of these crystals. Figure 3 shows two important things: that the O_{21} atom is placed all over the space, with no clustering in particular regions, and there is no difference between the spatial distribution of the FM and AFM contacts, that is, for the same distance and angle values it is possible to find short NO···ON contacts in the FM and AFM subsets. A good example of this is seen in Figure 2 for the two crystals showing the shortest contacts in the FM and AFM subsets. Summarizing, our data shows that the idea "short NO···ON

contacts are indicative of a crystal being dominated by antiferromagnetic interactions"[1,2] is not correct, even when the angular orientation of these contacts are taken into account. *Consequently, one should change the way in which some magneto–structural analyses are done, as the fundamental principle on which they are based is proved here generally to be not valid.* In another words, it is not possible to define the nature of intermolecular magnetic interactions just by looking at the geometrical disposition of the shortest NO···ON contacts.

One can wonder here if the previous conclusions are just an artifact of the coordinate set selected for the analysis. To prove that this is not the case, we carried out a factor analysis on the six internal coordinates defining the relative position of two ONCNO groups.[14,15] This analysis indicated that six is the number of independent parameters necessary and sufficient to treat this problem, and that it is not possible to reduce this number. This conclusion also shows that the use of three or even two geometrical parameters, a practice performed by some authors for analyzing series of α-nitronyl nitroxide radicals, is not correct. A cluster analysis[16] of the contact data for the FM and AFM subsets also established that the two sets of contacts are nearly identical and interpenetrated, thus being completely indistinguishable (the criteria to define the cluster was the single linkage method[16]). Thus, one can safely conclude that our main result is not an artifact of the selected coordinate set, and that the same conclusions will be obtained using other sets.

Due to the fact that most of the spin density is located in the ONCNO group,[6,7] one can assume, according with the McConnell-I model, that the intermolecular contacts relevant from the magnetic point of view are these involving the ONCNO groups. Given this fact, the previous similarity in the distribution of the NO···ON contacts within the FM and AFM subsets can only be explained if one or more of the following options are valid: the magnetic character predicted by the McConnell-I model for short NO···ON contacts is not correct; or short NO···ON contacts are not the only ones magnetically relevant. The second option can be understood looking at Figure 2. The existence of short NO···ON contacts in both crystals are a consequence of the short C-H···ON contacts (the reason being the repulsive nature of the first ones in this orientation and the attractive nature of the second ones).[17] Thus, if the C–H···ON would present a complementary magnetic role to that present in the NO···ON case and of similar size, the net character of the resulting intermolecular dimeric unit will depend in a subtle way on small geometrical changes. As indicated above, this possibility is based on the assumption that the strength of the magnetic interaction in the NO···ON and C–H···ON short contacts is similar, an assumption that goes against the usual use of the McConnell-I model, because the spin density on the hydrogens, besides being of σ type, is much smaller than on the NO groups and gives rise to very small density products. However, this weaker density product could be compensated by a stronger magnetic exchange integral J_{ij}, so it seems worth evaluating this option.

Given the potential importance of the C–H···ON contacts in understanding the structure–magnetism relationship

within the α-nitronyl nitroxides, we also analyzed the geometry of their contacts in the FM and AFM subsets. In this communication we do not give the details of the methodology or results, but just the main conclusion: no differences are found in the geometrical distribution of the C–H···ON contacts between the FM and AFM subsets, thus making impossible to distinguish between the crystals of the FM and AFM subsets just by looking at the distribution of the C–H···ON contacts. This extends what was concluded before for the NO···ON contacts. One should keep in mind here that these two types are the two main contacts determining the crystal packing of the α-nitronyl nitroxide crystals.

In conclusion, the previous statistical analysis shows that in the α-nitronyl nitroxide crystals it is not possible to define the magnetic role associated with the NO···ON or C–H···ON contacts just by looking at the local distance and geometry of one type of contacts. Statistically, crystals of the FM and AFM subsets present contacts whose geometry is distributed in a similar way over the six dimensional space of coordinates. This fact questions the validity of any magneto-structural correlation made looking at these contacts *individually*. At the same time, it indicates that the magneto–structural correlations present in the α-nitronyl nitroxide crystals must be *collective*, that is, associated with the relative disposition of *all* the magnetically active shortest contacts. In this case, the intermolecular magnetic interaction depends on the relative orientation of the two *molecules* making the short contacts as a whole (that is, their primary packing patterns[17] or synthons[18]) more than on the few particular intermolecular contacts between them. Studies in this direction are currently under way in our laboratories.

Received: ■
Final version: ■

[1] For a recent overview see: a) *Molecular Magnetic Materials*, (Eds: D. Gatteschi, O. Kahn, J. S. Miller, F. Palacio), Kluwer, Dordrecht, The Netherlands, **1991**. b) H. Iwamura, J. S. Miller, (Eds.) *Mol. Cryst. Liq. Cryst.*, **1993**, *232/233*, 1-360/1-366. c) J. S. Miller, A. J. Epstein, *Angew. Chem. Int. Ed. Engl.* **1994**, *33*, 385. d) O. Kahn, *Molecular Magnetism*, VCH Publishers, New York, **1993**. e) A. Rajca, *Chem. Rev.* **1994**, *94*, 871. f) J. S. Miller, A. J. Epstein, (Eds.) *Mol. Cryst. Liq. Cryst.*, **1995**, *272-274*. g) M. Kinoshita, *Jpn. J. Appl. Phys.* **1994**, *33*, 5718. h) *Molecular Magnetism: From Molecular Assemblies to Devices*, (Eds: E. Coronado, P. Delhaes, D. Gatteschi, J. S. Miller), Kluwer, Dordrecht, The Netherlands, **1996**. i) *Magnetism: A Supramolecular Function*, (Ed: O. Kahn), Kluwer, Dordrecht, The Netherlands, **1996**. j) K. Itoh, J. S. Miller, T. Takui, (Eds.) *Mol. Cryst. Liq. Cryst.*, **1997**, *305/306*, 1-586/1-520.

[2] a) M. Tamura, Y. Nakazawa, D. Shiomi, K. Nozawa, Y. Hosokoshi, M. Isjikawa, M. Takahashi, M. Kinoshita, *Chem. Phys. Lett.* **1991**, *186*, 401. b) P. M. Allemand, K. C. Khemani, A. Koch, F. Wudl, K. Holczer, S. Donovan, G. Grüner, J. D. Thompson, *Science*, **1991**, *253*, 301. c) R. Chiarelli, M. A. Novak, A. Rassat, J. L. Tholance, *Nature*, **1993**, *363*, 147. d) T. Sugawara, M. M. Matsushita, A. Izuoaku, N. Wada, N. Takeda, M. Ishikawa, *J. Chem. Soc., Chem. Commun.* **1994**, 1081. e) J. Cirujeda, M. Mas, E. Molins, F. Lanfrane de Panthou, J. Laugier, J. Geun Park, C. Paulsen, P. Rey, C. Rovira, J. Veciana, *J. Chem. Soc., Chem Comm.* **1995**, 709. f) A. Caneschi, F. Ferraro, D. Gatteschi, A. leLirzin, M. A. Novak, E. Rentsecheler, R. Sessoli, *Adv. Mater.* **1995**, *7*, 476. g) Y. Pei, O. Kahn, M. A. Aebersold, L. Ouahab, F. Le Berre, L. Pardi, J. L. Tholance, *Adv. Mater.* **1994**, *6*, 681. h) K. Togashi, K. Imachi, K. Tomioka, H. Tsuboi, T. Ishida, T. Nogami, N. Takeda, M. Ishikawa, *Bull. Chem. Soc. Jpn.*, **1996**, *69*, 2821 and references therein.

[3] α-nitronyl nitroxide is the abbreviated name commonly used for the compounds for which the correct IUPAC name is: 4,5-dihydro-4,4,5,5-tetramethyl-3-oxido-1*H*-imidazol-3-ium-1-oxyl.

[4] a) J. Veciana, J. Cirujeda, C. Rovira, E. Molins, J. J. Novoa, *J. Phys. I France* **1996**, *6*, 1067. b) M. Deumal, J. Cirujeda, J. Veciana, M. Kinos-

hita, Y. Hosokoshi, J. J. Novoa, *Chem. Phys. Lett.* **1997**, *265*, 190. c) J. Cirujeda, C. Rovira, J. L. Stanger, P. Turek, J. Veciana, in *Magnetism. A Supramolecular Function*; (Ed: O. Kahn); Kluwer, Amsterdam, **1996**, 219. d) J. Cirujeda, E. Hernández, F. Lanfranc de Panthou, J. Laugier, M. Mas, E. Molins, C. Rovira, J. J. Novoa, P. Rey, J. Veciana, *Mol. Cryst. Liq. Cryst.* **1995**, *271*, 1.

[5] H. M. McConnell, *J. Chem. Phys.* **1963**, *39*, 1910.

[6] A. Zheludev, V. Barone, M. Bonnet, B. Delley, A. Grand, E. Ressouche, P. Rey, R. Subra, J. Schweizer, *J. Am. Chem. Soc.* **1994**, *116*, 2019.

[7] J. J. Novoa, F. Mota, J. Veciana, J. Cirujeda, *Mol. Cryst. Liq. Cryst.* **1995**, *271*, 79.

[8] a) C. Kollmar, O. Kahn, *Acc. Chem. Res.* **1993**, *26*, 259. b) K. Yamaguchi, Y. Toyoda, T. Fueno, *Chem. Phys. Lett.* **1989**, *159*, 459. c) K. Yoshizawa, R. Hoffmann, *J. Am. Chem. Soc.* **1995**, *117*, 6921. d) P. M. Lahti, *ACS Symp. Series*, No. 644, (Eds: M. M. Turnbull, T. Sugimoto, L. K. Thompson), **1996**, Ch. 14.

[9] The spin density on the H atom of the four CH_3 groups is negative, whereas these on the H atoms of a phenyl ring linked to the α carbon of the five membered ring are alternated in their sign, being positive for *ortho* and *para* H atom, and negative for the *meta* ones. See references 5 and 6 and also: a) M. S. Davis, K. Morokuma, R. W. Kreilich, *J. Am. Chem. Soc.*, **1972**, *94*, 5588. b) J. W. Neely, G. F. Hatch, R. W. Kreilich, *J. Am. Chem. Soc.*, **1974**, *96*, 652.

[10] In this study we deliberately discarded those crystals not showing dominant magnetic interactions as they would not help to establish a clear structure–magnetism correlation. The nature of the dominant magnetic interactions is clearly manifested by the temperature dependence of the magnetic susceptibility (χ) in the 2–300 K range. Thus crystals with dominant ferromagnetic interaction have χT *vs.* T curves in which χT continuously increases when T decreases (see reference 1).

[11] F. H. Allen, S. Bellard, M. D. Brice, B. A. Cartwright, A. Doubleday, H. Higgs, T. Hummelink, B. G. Hummelink-Peters, O. Kennard, W. D. S. Motherwell, J. R. Rodgers, D. G. Watson, *Acta Crystallogr.* **1979**, *B35*, 2331.

[12] Details on the geometry of these crystals are not given here and will be presented in a full paper elsewhere.

[13] Standard deviations of the atomic distances and bond angles of this five-membered ring are smaller than 2 % of the magnitudes. See: J. Cirujeda, PhD Thesis, Univ. Ramon Llull, Barcelona, **1997**.

[14] R. Barlow, *Statistics*, John Wiley, Chichester, **1989**.

[15] E. R. Malinowski, D. G. Howery, *Factor Analysis in Chemistry*, Wiley Interscience, New York, **1980**.

[16] B. S. Everitt, *Cluster Analysis*, 3rd edition, Edward Arnold: London, 1993.

[17] a) M. Deumal, J. Cirujeda, , J. Veciana, M. Kinoshita, Y. Hosokoshi, J. J. Novoa, *Chem. Phys. Lett.* **1997**, *265*, 190. b) J. J. Novoa, M. Deumal *Mol. Cryst. Liq. Cryst.*, **1997**, *305*, 143. c) J. J. Novoa, M. Deumal, M. Kinoshita, Y. Hosokoshi, J. Veciana, J. Cirujeda, *Mol. Cryst. Liq. Cryst.*, **1997**, *305*, 129.

[18] G. Desiraju, *Angew. Chem. Int. Ed. Engl.* **1995**, *34*, 2311.

Table 1. List of ONCNO···ONCNO contacts for crystals of the FM and AFM subsets within the range of distances allowed in the analysis, which determines the contacts included in our study. Percentages of cases with intermolecular ferro- and antiferromagnetic interactions are also given.

Distance range (Å)	Total	Number of contacts (percentage) FM	AFM
[0–3]	0	0 (0)	0 (0)
[0–4]	24	10 (42)	14 (58)
[0–5]	92	36 (39)	56 (61)
[0–6]	204	90 (44)	114 (56)
[0–7]	378	167 (44)	211 (56)
[0–8]	608	274 (45)	334 (55)
[0–9]	901	416 (46)	485 (54)
[0–10]	1312	611 (47)	701 (53)

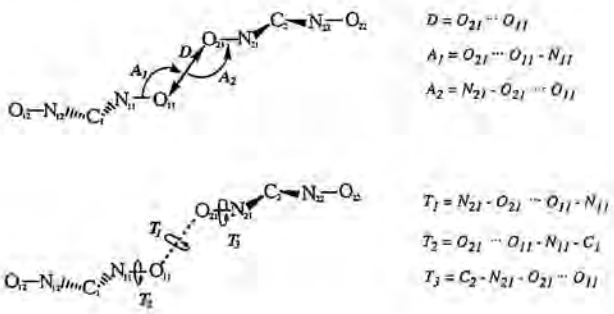

Fig. 1. Geometrical parameters used to define the relative position of two ONCNO groups.

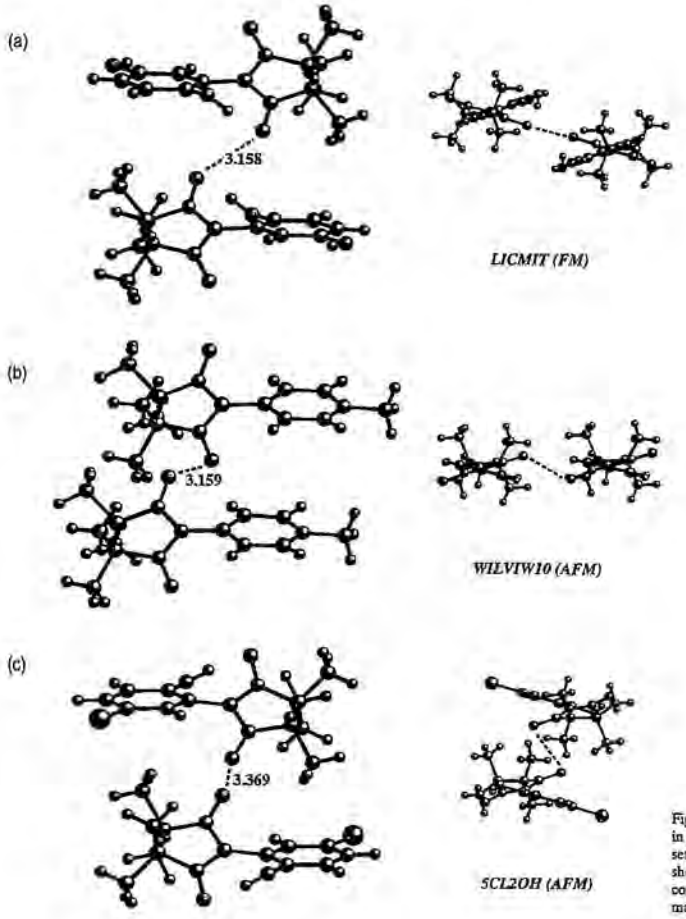

Fig. 2. Geometrical disposition of the dimers found in the two crystals of the FM (see a) and AFM subsets (see b) with the shortest NO···ON contacts. Also shown (c) is the dimer with the shortest NO···ON contact among the dimers with a head–tail conformation in the AFM subset.

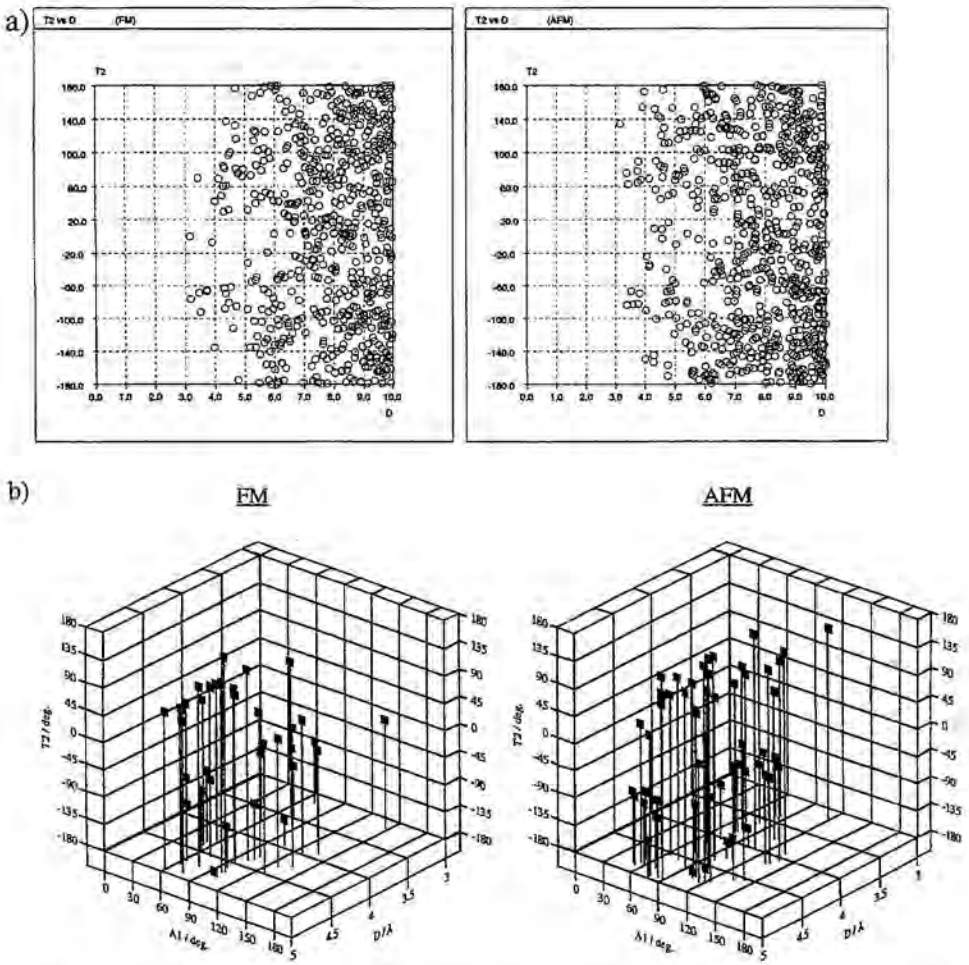

Fig. 3. a) Scattergrams of pairs of parameters characterizing the NO···ON contacts in the FM (left) and AFM (right) crystal subsets. b) Position of the O_{11} atoms relative to the O_{11}–C_{11}–C_1 group for ~~a random selection of 100~~ all the contacts of the FM (left) and AFM (right) crystal subsets in the 0–5 Å range.

ARTICLE 9

Structure-magnetism relationships in α-nitronyl nitroxide radicals

Mercè Deumal,[†] Joan Cirujeda,[‡] Jaume Veciana,[‡*] and Juan J. Novoa.[†*]

[†]Departament de Química Física, Facultat de Química, Universitat de Barcelona, Av. Diagonal 647, E-08028 Barcelona (Spain).

email: novoa@zas.qf.ub.es / fax: (+34) 93 402 1231.

[‡]Institut de Ciència de Materials de Barcelona (CSIC), Campus Bellaterra, E-08913 Cerdanyola (Spain).

email: vecianaj@icmab.es / fax: (+34) 93 580 5729

Abstract

The crystal packing of α-nitronyl nitroxide radicals showing dominant ferromagnetic or antiferromagnetic interactions is analyzed in order to test if there are characteristic orientations of their functional groups that can be associated to these magnetic interactions. From a large crystalline structural database of compounds containing α-nitronyl nitroxide radical units (143 structures), 23 representative cases showing dominant intermolecular ferromagnetic interactions, and 24 cases exhibiting dominant antiferromagnetic interactions were selected. The spatial distribution of the N-O···O-N, C(sp^3)-H···ON and C(sp^2)-H···ON contacts whose distance is smaller than 10 Å was analyzed, with special emphasis on the 0-5 Å region for the N-O···O-N contacts and 0-3.8 Å for the C-H···O-N contacts. No correspondence is found between the presence of intermolecular ferro or antiferromagnetic interactions and the geometry of any of the previous isolated contacts. Therefore, there is a need to change the way in which some structure-magnetism correlations are obtained in α-nitronyl nitroxide crystals. These results also show that the intermolecular magnetic interaction is related with the relative orientation of the nearby molecules as a whole, that is, with the collection of intermolecular contacts.

Keywords: Magnetic properties; Solid-state structures; Radicals; Crystal engineering; Noncovalent interactions; Hydrogen bonds.

Introduction

The design of purely organic magnetic materials has been the goal of many research groups during the last decade.[1] A systematic synthetic effort has provided different kinds of organic free radicals whose crystals present interesting magnetic properties, even bulk ferromagnetism in very exceptional cases.[2] The most extensively studied family of purely organic persistent radicals are the α-nitronyl nitroxide (or α-nitronyl aminoxyl) radicals,[3] whose general formula is shown in Chart 1.

-Scheme 1-

The analysis of the magnetic properties and packings in the α-nitronyl nitroxide crystals shows that the presence of bulk ferromagnetism is strongly related to the relative disposition of the radicals in the crystal. This result is consistent with the commonly accepted theoretical models about intermolecular magnetism.[1,2,4] For instance, the McConnell I model,[4] probably the one most employed today due to its simplicity, predicts the presence of intermolecular ferromagnetic interactions between neighboring molecules only when there are short contacts between atoms having a considerable atomic spin population of opposite sign (otherwise, the interaction would be antiferromagnetic or negligible).

The preparation of molecular organic crystals showing spontaneous magnetization below a certain critical temperature, T_C, is possible for persistent free radicals whose crystal packing allows for the presence of intermolecular ferromagnetic interactions propagating all over the crystal.[5,6] This is only possible if each spin containing molecule is capable of making one or more ferromagnetic interactions with its first neighbor molecules, with strengths larger than kT_C, the thermal energy at T_C.[7] Consequently, one of the most important points in this field is to recognize the relative arrangements of neighbor molecules giving rise to intermolecular ferromagnetic interactions, and those generating antiferromagnetic ones.[8] Rationalization of the crystal packing of organic molecules can be achieved in terms of *crystal packing patterns*,[9] also known as *synthons*,[10] from which the crystal can be generated by application of its symmetry operations. Patterns for radical crystals presenting dominant ferromagnetic interactions can be called *ferromagnetic patterns*. Similarly *antiferromagnetic patterns* are these present in the crystals of radicals presenting dominant antiferromagnetic interactions.

The exact geometries of these patterns are still not known, a fact that has greatly limited the design of new organic magnets and the development of *Molecular Magnetism*. Up to now, the usual way of obtaining information about the structure of the *ferro-* and *antiferromagnetic patterns* has been by a detailed inspection of the

molecular packing of individual crystals showing a well-characterized magnetic behavior. Although qualitative, several useful conclusions have been obtained using this methodology. For instance, it indicates that short NO···ON contacts are associated to *antiferromagnetic patterns*.[1,11,12] Also, some short NO···H-C contacts are indicative of *ferromagnetic patterns*.[1,11,12] This methodological approach has two major drawbacks: first of all, the structural information achieved on the *magnetic patterns* is very limited and, second, the conclusions are in many cases contaminated by preconceptions.[13] Therefore, a systematic and quantitative analysis of the crystal packing of α-nitronyl nitroxides presenting dominant magnetic interactions is required to find their structure-magnetism relationships.

In this work we try to establish the presence of magnetic patterns by looking at the geometry of the N-O···O-N contacts, the most important magnetic ones according to the McConnell-I model, and also of the $C(sp^3)$-H···ON and $C(sp^2)$-H···ON contacts, given the claims of the presence of magnetic interactions through these hydrogen bonds.[12] We have performed such an analysis on 47 α-nitronyl nitroxide crystals that clearly show *dominant* ferromagnetic or antiferromagnetic intermolecular interactions, obtained from the literature or our own work.

Methodology

A total of 143 crystal structures containing substituted α-nitronyl nitroxide radical units were used initially. The majority were retrieved from the Cambridge Structural Database (CSD),[14] and the rest from our own research, directly from the literature, or supplied by other authors. The criteria employed to select the final set of structures were as follows: (1) The 26 structures with R factors greater than 0.10, or which were determined from very limited data, or which exhibit disorder or large molecular distortions, were discarded. (2) Then, the 45 structures containing both transition metal atoms and large closed-shell organic molecules co-crystallized were discarded (thus leaving 72 purely organic crystal structures), since intermolecular magnetic interactions between radicals could be complicated in these cases by the existence of other magnetic pathways through the metal atoms or the closed-shell molecules and the radical units. (3) Finally, we also discarded all the crystals whose magnetic interactions are not clearly dominated by ferro- or antiferromagnetic interactions.[15] It is convenient to exclude all crystals with non dominating magnetic behavior because they can show both types of *crystal packing patterns* and, in consequence, it would make impossible the identification of the *ferro-* and *antiferromagnetic patterns*. The nature of the dominant magnetic interactions is clearly manifested by the temperature dependence of the magnetic susceptibility, χ, in the temperature range of 2-300 K[16]: Radicals with dominant ferromagnetic interactions,

grouped in the FM subset, show a characteristic continuous increase of χT when T decreases; Radicals with dominant antiferromagnetic interactions have the opposite trend and were collected in the AFM subset. Of the remaining 47 purely organic crystals, 23 belonged to the FM subset[17] and 24 to the AFM subset.[18] The molecular structure of the parent radicals for each crystal is shown in Schemes 2 and 3.

- Schemes 2 and 3 -

Crystals whose structures were found in the CSD (27) are located in the lower part of both Schemes. Under each drawing we have indicated the *refcode* given in the CSD database to the crystal (when more than one polymorph is present, all the *refcodes* are indicated). The equivalent information is provided in the upper part of Schemes 2 and 3 for the non-CSD crystals. In the later case, an arbitrary *refcode* was generated by us for identification purposes and for compatibility with the crystal analysis codes. The 47 crystals of the combined FM and AFM subsets belong to the following spatial groups: P-1 (3), $P2_1$ (2), Cc (2), $P2_1/c$ (25), C2/c (2), $P2_12_12_1$ (2), $Pca2_1$ (1), Ib2a (1), Pbca (4), Fdd2 (1), $I4_1/a$ (1), $P4_2bc$ (1), and P3c1 (2).

Most of the analyzed crystal structures were determined at room temperature, where the thermal energy largely overcomes the strength of the magnetic interactions. Therefore, we are trying to correlate a physical property whose magnitude is only clearly observed at low temperatures, with the crystal packing at room temperature. This is a common practice in *Molecular Magnetism* that, unfortunately, cannot be avoided since only very few crystal structures have been determined at low temperatures. At first glance such objection may look serious, but a detailed analysis of this problem reveals that it has minor consequences for our magneto-structural correlations: except for those cases where a first-order structural phase transition occur,[19] the *crystal packing patterns* of molecular crystals show only small changes with the temperature due to the thermal contraction. These changes do not turn the relative disposition of the molecules (the data of interest here) to such an extent as to reverse the nature of the dominant intermolecular magnetic interaction.[20] Therefore, it can be assumed without too much risk that the values of the distances and angles defining each contact would only change slightly with the temperature, and the differences in the geometrical distribution within the two subsets will still be of statistical significance.

One possible form of characterizing the relative positions of neighboring radicals is by looking at the relative geometry of the X···Y contacts which dominate the packing, together with those expecting to present the strongest magnetic interactions. Concerning the first type, the crystal packing of the α-nitronyl nitroxides is energetically dominated by the N-O···O-N and C-H···O-N contacts made among neighboring molecules.[21,22]

On the other hand, according to the McConnell-I model, the dominant magnetic interactions present in the α-nitronyl nitroxide crystals are expected to be directly related to the spatial orientation and proximity of the ONCNO groups (these are the atoms in which most of the electronic spin distribution is located in the α-nitronyl nitroxide radicals).[23] Therefore, we will investigate the statistical differences in the relative spatial dispositions of the N-O···O-N and C-H···O-N contacts within the FM and AFM subsets, searching for differences which later on could be used as signature for the presence of a type of magnetic interaction in other α-nitronyl nitroxide crystals.

The statistical analysis of the geometry was done using the CSD-module[14] QUEST to locate the intermolecular contacts within each crystal, and the CSD-module VISTA for the visualization and a preliminary statistical treatment of the data. The CSD-module PREQUEST was used to generate structures suitable for their posterior treatment with QUEST for the non-CSD crystals. These crystal structures were added to the α-nitronyl nitroxide crystals recovered from the CSD. The factor and cluster analysis of the data has been done using computer programs written in our laboratories. The number of intermolecular NO···ON and C(sp^2)-H···O-N contacts found in the 47 crystals of the combined FM and AFM is the following: 1312 NO···ON contacts at O···O distances smaller than 10 Å, and 6039 C(sp^3)-H···O-N and 2286 C(sp^2)-H···O-N contacts at the same H···O cutoff. These three sets are large enough to allow a statistical analysis of the geometrical distribution of the involved parameters.

Results and Discussion

Spatial distributions of the N-O···O-N contacts

A preliminary statistical analysis of the geometry of the α-nitronyl nitroxide molecules of the 47 crystals included in the FM and AFM subsets, and of other crystals with no definite, relevant, or complex magnetic behavior, showed that the spatial distribution of all the atoms present in the five-membered ring is nearly the same, and that the five ONCNO atoms lie in the same plane.[24] This behavior can be attributed to the sp^2 hybridization of the alpha C atom, which allows the delocalization of the π electrons over the five ONCNO atoms through various resonant forms. Given this fact, we do not have to worry about small distortions in the geometry of the ONCNO group and all the atoms of the imidazolidine ring, including the four methyl groups. Therefore, we can consider the internal geometry of imidazolidine ring and its ONCNO group as fixed. Consequently, given two ONCNO groups within a crystal, whose atoms are labeled as $O_{12}N_{12}C_1N_{11}O_{11}$ and $O_{22}N_{22}C_2N_{21}O_{21}$, the relative geometrical position of the N_{11}-O_{11}···O_{21}-N_{21} contact is completely defined by the following six

internal coordinates (see Figure 1): three to define the position of the terminal O_{21} atom relative to the $O_{12}N_{12}C_1N_{11}O_{11}$ group (the $O_{21}\cdots O_{11}$ distance, the $O_{21}\cdots O_{11}$-N_{11} angle, and the $O_{21}\cdots O_{11}$-N_{11}-C_1 torsion angle), two for the position of the N_{21} atom for a fixed N-O distance (N_{21}-$O_{21}\cdots O_{11}$ angle and the N_{21}-$O_{21}\cdots O_{11}$-N_{11} torsional angle), and one to fix the $O_{22}N_{22}C_2N_{21}O_{21}$ group plane (C_2-N_{21}-$O_{21}\cdots O_{11}$ torsional angle, as the C_2-N_{21} distance and the C_2-N_{21}-O_{21} angle are fixed). To simplify the notation, we will identify these six parameters as D, A_1, A_2, T_1, T_2 and T_3 (see Figure 1). There are many other possible choices for this six coordinate space, but all of them are related by linear transformations. The coordinate set selected here is the one that allows an easier visualization and clearer physical interpretation of the geometrical parameters.

-Figure 1-

The duplicities found during the geometrical analysis of the contacts and the random spatial distributions of some angular parameters were taken into account by processing the geometrical data to: (a) discard those with nearly identical parameters, and (b) force that the values of the angles A_1 and A_2 were smaller than 180° and, at the same time, to impose that $A_1 \geq A_2$. This second condition was imposed because there is no way to force one ONCNO group to be the group number 2 in the analysis carried out by using the QUEST program. No other restriction was imposed in our data analysis.

We can begin the analysis of the geometry of the NO···ON contacts in the FM and AFM subsets by looking at their number as a function of the O···O distance (D parameter). There is a similar number of contacts in both subsets in the 0-n ($n \leq 10$) Å distance range analyzed (see Table 1). Such a long cut-off value is selected to allow the inclusion in our study of patterns in which the shortest contact between the neighboring molecules involves a bulky R substituyent (like an aromatic ring) of one molecule and an O-N or other group of the second molecule. This forces the NO groups to lie far away.

The proportion of contacts in the FM and AFM subsets (see Table 1) is nearly constant for any cutoff distance within the 0-10 Å range (on average, 44% are from the FM subset, with low and high values of 39% and 47%). These values suggest that the number of ONCNO···ONCNO contacts that each NO group is making is similar in both subsets. Consequently, it is not true that the presence of short NO···ON contacts is indicative of dominant antiferromagnetic interactions, as sometimes stated in the literature.[1,11,12] This fact is better illustrated in Table 2, which gives the geometrical parameters of the FM and AFM crystals showing the shortest NO···ON contacts. Interestingly enough, the shortest NO···ON contact in the two subsets are nearly identical, 3.158 Å in the crystal of the FM subset, and 3.159 Å in that of the AFM one

(refcodes LICMIT and WILVIW10, respectively). Figure 2 shows the geometrical arrangement of the radicals in which these contacts are found The arrangement is of the up-down type in the FM case and up-up type in the AFM case, but as it is also shown in Figure 2, there are also up-down arrangements within the AFM crystals presenting very short NO···ON contacts (Table 2). Thus, *it is impossible to define the magnetic character of a crystal by looking only at the presence or absence of short NO···ON contacts.*

-Tables 1 and 2 -
- Figure 2 -

We performed also a more detailed analysis evaluating the angular dependence. Comparing only the NO···ON distance distributions is like averaging the angular distribution for each distance value (see, for instance, the angle values given Table 2). Furthermore, as mentioned before, the McConnell-I model indicates that the angular orientation between nearby ONCNO groups is important to define the magnetic nature of the interaction. We first looked at the angular distribution in the FM and AFM subsets in the short end of our distance analysis, the 3-5 Å range, as this is the most important region if the magnetic interaction is due to the direct overlap of the spin-density-containing groups (the NO groups). The scattergram of the values of D and T_2 for the FM and AFM subsets in the 3-10 Å region (Figure 3a) shows that there is a remarkable similarity in the two distributions along the 0-10 Å range. Scattergrams of other pairs of values show a similar behavior as that plotted in Figure 3a. To test if it is merely a consequence of the pair of parameters selected, we have also plotted (Figure 3b) the position of the O_{21} atom relative to the N_{11}-O_{11} group for all the contacts of the FM and AFM subsets within the 3-5 Å range. A direct observation of Figure 3b proves that: (a) the O_{21} atom is placed all over the space in the FM and AFM subgroups, and (b) there is no difference between the spatial distributions of the FM and AFM subsets.

-Figure 3-

The similarity in the geometrical distribution of the FM and AFM N-O···O-N contacts is also found when the analysis is done in the 0-10 Å range. Similar scattergrams to those in Figure 3 are obtained, but with many more points. The similarity is clearly manifested by the average values of the parameters D, A_1, A_2, T_1, T_2 and T_3: Within the 0-10 Å range, the average values of this parameters for the FM subset are 7.9 Å, 74°, 115°, 13°, 3°, -5°, while the equivalent ones for the AFM subset are 7.8 Å, 73°, 113°, 8°, -6°, 2°, differing from the previous ones in less than their standard deviation.[25] In turn, these average values differ in less than their

standard deviations with those obtained when the analysis was performed in the 0-4 Å range (in the same order, for the FM subset the values are 3.6 Å, 92°, 137°, 18°, -22°, and -37°, while for the AFM subset are 3.6Å, 88°, 93°, 32°, 44°, and 10°).

Therefore, even when the angular orientation is taken into account the presence of short NO···ON contacts does not imply that the crystal has dominant antiferromagnetic interactions. *Consequently, one should change the way in which some magneto-structural analyses are done, as it is not possible in general to define the nature of the dominant intermolecular magnetic interaction just by looking at the geometrical disposition of the closest NO···ON contacts.*

Factor and cluster analysis of the geometry of the N-O···O-N contacts

At this point, we tested if the conclusions obtained in the previous section were due to the coordinate set employed, to inconsistencies or hidden trends in the data, or to the presence of hidden variables. To discard these options, one can perform a correlation and factor analysis of the data set, constituted by the geometries of the 611 and 701 ONCNO···ONCNO contacts found in the FM and AFM subsets.[26,27] A final check could be a cluster analysis, searching for possible clusters in the geometrical distribution of the six geometrical parameters, with the help of a well-defined mathematical procedure. This procedure allows finding particular regions in the relative orientation of the NO groups in which the ferro- or antiferromagnetic contacts are grouped, regardless of their strength. These regions would be associated with the existence of ferro- and/or antiferromagnetic interactions. For such a cluster analysis, we considered the geometry of each contact as a six components vector (V), each component being one of the six parameters employed to define the N-O···O-N contact geometry, that is, $V(1) = D$, $V(2) = A_1$, and so on. The values of the V components were renormalized to have a similar weight by giving the angles in radians.

As a first step, we investigated, independently in the FM and AFM subsets, if our previous conclusions were a consequence of the coordinate set used in our study. The correlation matrix[26] was then computed. In both subsets the off-diagonal elements always have an absolute value smaller that 0.17 (their average is 0.07 and 0.06 in the FM and AFM subsets), except for the A_1 and A_2 correlation, which has a value of 0.36. Therefore, there is a small correlation between the A_1 and A_2 angles, probably due to the tendency of many of these radicals to pack as stacks of planes.[21,22] No other correlation is found for any other pair of parameters employed in this study.

We also carried out a factor analysis[27] of the 611x6 data matrix of the FM subset by computing the eigenvalues of the 6x6 covariance matrix, obtained from the data matrix by premultiplication by its transpose. The initial FM covariance matrix is nearly diagonal, thus indicating the linear independence of the coordinate set. Its

eigenvalues are 4.096, 3.479, 3.246, 2.590, 0.374, and 0.177, the first three mostly associated to the three dihedral angles, the fourth to the distance D, and the last two to the A_1 and A_2 angles. Similar conclusions are found when the factor analysis is done on the AFM subset. Furthermore, in the AFM covariance matrix the eigenvalues and eigenvectors are nearly identical to those obtained in the FM subset, an indication of the similarity of their contacts, thus confirming our previous conclusions. In summary, *these results indicate that six is the number of independent parameters needed in order to treat the NO···ON geometrical data.* Therefore, the frequent use of three, or worse, two geometrical parameters when searching for structure-magnetism relationships is not correct.

As a final test on the validity of our data we carried out a cluster analysis[28] of the ONCNO···ONCNO geometrical data. Specifically, we wanted to know whether the ONCNO···ONCNO contacts of the FM and AFM subsets are located in different regions of the six dimensional coordinate space. As clustering criterion we used the single linkage method,[28] also known as the nearest neighbor technique. Within this criterion, a cluster is defined as a set of connected elements, and one element i is said to be connected to its nearest neighbor j when the distance between both elements, d_{ij}[29] is equal or smaller than a threshold value, ε, i.e., $d_{ij} \leq \varepsilon$. This is a direct connection. If the element j is also connected to another element k, then i and k are indirectly connected and the cluster is constituted by the elements i, j, and k. Thus, a new element l is added to this cluster when the shortest distance to any element of the cluster is smaller than the threshold ε, a parameter which characterizes the cluster. If two clusters A and B are present in our data, they are characterized by two internal threshold values ε_A and ε_B, *and* the shortest distance between the elements of cluster A and cluster B must be larger than any of these two thresholds (see the upper part of Figure 4 for a graphical illustration).

-Figure 4-

To test if there are clusters of FM and/or AFM geometries, we applied the cluster analysis to the combined subsets of geometries. One can foresee three possible extreme situations, shown in Figure 4. In the first one, the FM and AFM subsets of contacts are disjoint, that is, the two sets of crystals pack in totally different forms. In the second case, there are common elements shared by the FM and AFM subsets. In the third case, the two sets of contacts are totally interpenetrated and indistinguishable, in fact forming only one set. As illustrated in Figure 4, one can mathematically differentiate among these three situations by comparing the shortest distance within the FM and AFM subsets (ε_{FM} and ε_{AFM}), with the shortest distance between the pairs of elements, one from each subset ($\varepsilon_{FM\text{-}AFM}$). The subset in which each point is included is also known. If $\varepsilon_{FM\text{-}AFM} > \varepsilon_{FM}$ and, simultaneously, $\varepsilon_{FM\text{-}AFM} > \varepsilon_{AFM}$ the two

subsets are disjoint, while if any of these two conditions are not fulfilled there is an overlap between the two sets and it is not possible to find two subsets in a cluster analysis. One can differentiate between cases 2 and 3 mentioned above in the following way. The common elements between the FM and AFM subsets are those whose $\varepsilon_{FM\text{-}AFM}$ is smaller than ε_{FM} and ε_{AFM}. If this number totals all the elements in the FM and AFM subsets, we are dealing with case 3, otherwise it is case 2.

The analysis of the FM and AFM geometrical data indicates that ε_{FM} and ε_{AFM} are 1.980 and 2.130, respectively. At the same time, $\varepsilon_{FM\text{-}AFM} < \varepsilon_{FM}$ and $\varepsilon_{FM\text{-}AFM} < \varepsilon_{AFM}$. Cluster analysis limited to NO...ON contacts shorter than 5 Å yielded the same conclusion as that done in the 0-10 Å region. Consequently, our set of contacts are distributed according to the third possibility, that is, the two sets are nearly identical, interpenetrated, and *indistinguishable*. Thus, mathematically we find that *there is no statistically significant difference in the relative disposition of the NO···ON contacts for the FM and AFM subsets*. Notice here that the previous cluster analysis does not depend on the coordinate set employed, because the Cartesian distance between two vectors is invariant to the coordinate set in which these vectors are represented.

Spatial distributions of the C(sp^3)-H···O-N and C(sp^2)-H···O-N contacts

The absence of a general connection between the geometry of the individual NO···ON contacts of neighboring molecules and the presence of dominant ferro and antiferromagnetic interactions could be easily understood if there were other relevant magnetic interactions in the α-nitronyl nitroxide crystals. There have been some reports in the literature about the possibility of magnetic interactions through hydrogen bonds[12] and the relevance of this implication in our crystals is obvious if one looks at Figure 2 for a while. Therefore, it is worthwhile the analysis of the distribution of hydrogen bonds in the α-nitronyl nitroxide crystals.

We focused our attention in the C(sp^3)-H···O-N and the C(sp^2)-H···O-N hydrogen bonds, as they constitute the majority of the H···O-N non-covalent interactions. The H atoms of CH_3 and aromatic groups posses a small amount of spin.[30] Therefore, accepting that the McConnell-I model can be extended to the H···O-N case, they are expected to give very weak magnetic interactions having a ferromagnetic nature when the spin density on the H atoms is negative and antiferromagnetic when it is positive.[1,4] Owing to their weakness, these kind of contacts are not expected to be the determinant ones in defining the dominant magnetic interaction in the crystal, although if their number is large enough, they could compensate the stronger ones.

A systematic search on the geometry of a general C-H···O-N contact requires of six independent internal coordinates. However, given the quasi-cylindrical symmetry of

the electron density around the C-H group, we can disregard two dihedrals and use the four parameters indicated in Figure 5 and 6 for the $C(sp^3)$-H···O-N and $C(sp^2)$-H···O-N contacts, respectively. They will be called as D, A_1, A_2 and T_1 for simplicity. In the $C(sp^2)$-H···O-N case, one can distinguish between *ortho*, *meta* and *para* $C(sp^2)$-H···O-N contacts relative to the *alpha* C atom of the five-membered ring. We will identify them by adding the suffix o, m and p after the name of the parameter (for instance A_{1o}, A_{1m} and A_{1p}).

-Figures 5 and 6-

All the crystals included in the two magnetic subsets have 12 hydrogens bonded to the methyl $C(sp^3)$ atoms, which have a negative spin density.[12a,30] A proportion of 49% ferro- vs. 51% antiferromagnetic $C(sp^3)$-H···O-N contacts should be expected according to the number of crystals in the FM and AFM subsets. However, not all the crystals analyzed have functionalized aromatic groups in their *R* substituyent (Schemes 1-3), and the proportion of ferro vs. antiferromagnetic $C(sp^2)$-H···O-N contacts will depend on the number of crystals having aromatic groups and on the number of hydrogens in *ortho*, *meta* or *para* positions.

-Tables 3 and 4-
- Figures 7 and 8 -

A search within the FM and AFM subsets for H···O distances smaller or equal to 3.8 Å[31] finds 364 $C(sp^3)$-H···O-N contacts and 102 $C(sp^2)$-H···O-N contacts, as indicated in Table 3, separated into *ortho*, *meta* and *para* components. Within the 364 $C(sp^3)$-H···O-N contacts, 43% belong to the FM subset and 57% to the AFM one, a similar proportion to the number of crystals in each subset. Similar proportions are found for the $C(sp^2)$-H···O-N contacts in the FM and AFM subsets for hydrogens in the *ortho*, *meta* and *para* positions. The contacts are distributed along D in a similar form for the FM and AFM subsets, as one can appreciate by comparing the values for the shortest contacts in the two subsets in Tables 4 and 5. The same fact is clearly manifested in the scattergrams shown in Figures 7 and 8 Therefore, our conclusions do not depend on the use of shorter H···O cutoffs.

A more complete idea of the distribution of these contacts in space requires the inclusion of the angular distribution. We can do so by means of the scattergrams of Figures 7 and 8 which represent views of the values of the D, A_1, and A_2 parameters for the C-H···O-N contacts in the two magnetic subsets. Similar behavior is found when one looks at other pairs of parameters. Although the number of points in Figures 7 and 8 is not large enough to allow generalizations, the $C(sp^2)$-H···O-N contacts are distributed in a similar way for the FM and AFM subsets, within the 80-180° range, for

the angles, and the 2.2-3.8 Å range for the distances. Thus, we can conclude that *no differences are found in the geometrical distribution of the C-H···O-N contacts of the FM and AFM subsets.*

Concluding remarks

Our analysis indicates that there are no statistically significant differences in the relative disposition of the NO···ON and C-H···O-N contacts found within the FM and AFM subsets. This experimental observation is consistent with the fact that the packing of α-nitronyl nitroxide radicals is driven by the same intermolecular forces in the FM and AFM crystals. Consequently, it is not possible to determine the nature (ferro or antiferromagnetic) of the dominant magnetic interaction in a crystal just by looking at the geometry of one type of intermolecular contact. This assertion breaks some accepted ideas, as that associating the dominant magnetic character of a crystal with the presence of short NO···ON distances. We have also found that six is the number of independent parameters needed to represent the NO···ON, thus invalidating the frequent use of three or two geometrical parameters when searching for structure-magnetism relationships.

Now we need to address an interesting point: if the crystals of a magnetic subset must have dominant interactions of its subset class, and these interactions clearly depend on the relative geometrical arrangement of the radicals, why are these differences not seen in the previous statistical analysis?. Two different answers can be given to this question. First, the McConnell-I model might not be valid and could be just an oversimplification of the experimental operative mechanism.[32] Second, it could be that we have looked at individual intermolecular connections, assuming that magnetism in these solids is associated to the relative position of an *individual* contact, while the experimental intermolecular interactions are *collective*, that is, associated to the relative disposition of *all* magnetically active functional groups. The second idea can be illustrated by looking at the differences in the *packing patterns* of Figure 2: the relative orientations of the NO···ON contacts are not so different in these geometrical arrangements, but the geometrical dispositions of the molecules and *all* the functional groups in the molecule is very different (that is, one is dealing with different *packing patterns*. Our statistical study does not rules out any of these options and further studies are necessary for such a task.[33]

Acknowledgments.

This work was supported by the DGES (Project PB95-0848-C02-02 and PB96-0862-C02-01) and CIRIT (Projects GRP94-1077 and GRQ93-8028). M.D. and J.C. acknowledge CIRIT for their doctoral grants. Authors thanks also Prof. M. Kinoshita (U. Tokyo), O. Kahn (Bordeaux), P. Rey (Grenoble), K. Awaga (U. Tokyo), and T. Sugawara (U. Tokyo) for providing us with some preliminary crystal data. We would like also to thank Dr. S. Motherwell (CCDC, Cambridge) for providing us access to a beta version of the PREQUEST program and for the help provided in using it. We also thank Dr. D. Amabilino for manuscript revision and valuable comments.

References and notes.

[1] For a recent overview see: a) D. Gatteschi, O. Kahn, J.-S. Miller, F. Palacio, Eds., *"Molecular Magnetic Materials"*, Kluwer Academic Publishers: Dordretch, **1991**. b) H. Iwamura, J.-S. Miller, Eds., *Mol. Cryst. Liq. Cryst.*, **1993**, *232/233*, 1-360/1-366. c) J.-S. Miller, A.-J. Epstein, *Angew. Chem. Int. Ed. Engl.* **1994**, *33*, 385-415. d) O. Kahn, *"Molecular Magnetism"*, VCH Publishers, New York, **1993**. e) A. Rajca, *Chem. Rev.* **1994**, *94*, 871-893. f) J.-S. Miller, A.-J. Epstein, Eds.; *Mol. Cryst. Liq. Cryst.*, **1995**, *272-274*. g) M. Kinoshita, *Jpn. J. Appl. Phys.* **1994**, *33*, 5718. h) E. Coronado, P. Delhaes, D. Gatteschi, J.-S. Miller, Eds., *"Molecular Magnetism: From Molecular Assemblies to Devices"*, Kluwer Academic Publishers, Dordretch, **1996**. i) O. Kahn, Ed., *"Magnetism: A Supramolecular Fucntion"*, Kluwer Academic Publishers, Dordretch, **1996**. j) K. Itoh, J. S. Miller, T. Takui, Eds. *Mol. Cryst. Liq. Cryst.*, **1997**, *305/306*, 1-586/1-520.

[2] a) M. Tamura, Y. Nakazawa, D. Shiomi, K. Nozawa, Y. Hosokoshi, M. Isjikawa, M. Takahashi, M. Kinoshita, *Chem. Phys. Lett.* **1991**, *186*, 401. b) P.-M. Allemand, K.-C. Khemani, A. Koch, F. Wudl, K. Holczer, S. Donovan, G. Grüner, J.-D. Thompson, *Science*, **1991**, *253*, 301. c) R. Chiarelli, M.-A. Novak, A. Rassat, J.-L. Tholance, *Nature*, **1993**, *363*, 147. d) T. Sugawara, M.-M. Matsushita, A. Izuoaka, N. Wada, N. Takeda, M. Ishikawa, *J. Chem. Soc., Chem. Commun.* **1994**, 1081. e) J. Cirujeda, M. Mas, E. Molins, F. Lanfranc de Panthou, J. Laugier, J. Geun Park, C. Paulsen, P. Rey, C. Rovira, J. Veciana, *J. Chem. Soc., Chem .Comm.* **1995**, 709-710. f) A. Caneschi, F. Ferraro, D. Gatteschi, A. leLirzin, M.-A. Novak, E. Rentsecheler, R. Sessoli, *Adv. Mater.* **1995**, *7*, 476. g) Y. Pei, O. Kahn, M.-A. Aebersold, L. Ouahab, F. Le Berre, L. Pardi, J.-L. Tholance, *Adv. Mater.* **1994**, *6*, 681. h) K. Togashi, K. Imachi, K. Tomioka, H. Tsuboi, T. Ishida, T. Nogami, N. Takeda, M. Ishikawa, *Bull. Chem. Soc. Jpn.*, **1996**, *69*, 2821, and papers cited therein.

[3] α-Nitronyl nitroxide is the abbreviated name most widely employed, it is used here to indicate 4,5-dihydro-4,4,5,5-tetramethyl-3-oxido-1*H*-imidazol-3-ium-1-oxyl, the correct IUPAC name.

[4] H.-M. McConnell, *J. Chem. Phys.* **1963**, *39*, 1910.

[5] In general, bulk ferromagnetism requires the presence of ferromagnetic interactions along three (or two) directions of the solid, depending on whether there is a low (or high) magnetic anisotropy. Since organic free radicals in general have very small magnetic anisotropy, the presence of ferromagnetic

interactions in three dimensions is required for achieving bulk ferromagnetism. See: F. Palacio, *From Ferromagnetic Interactions to Molecular Ferromagnets: An Overview of Models and Materials*, p.1-40 (Eds.: D. Gatteschi, O. Kahn, J.-S. Miller, F. Palacio, in *"Magnetic Molecular Materials"*,), Kluwer Academic Publishers: Dorderecht, **1991**.

[6] A lack of compensation of the magnetic moments of spins coupled antiferromagnetically can also produce a net magnetic moment -spin canting- that, when propagated over the solid, produces a spontaneous magnetization. For a recent organic example of this situation, see: A.-J. Banister, N. Bricklebank, I. Lavender, J.-M. Rawson, C.-I. Gregory, B.-K. Tanner, W. Clegg, R.R.J. Elsegood, F. Palacio, *Angew. Chem. Int. Ed. Engl.* **1996**, *35*, 2533.

[7] For molecular organic crystals with high symmetry, namely cubic, the presence of just one intermolecular ferromagnetic interaction among the neighbor units is enough in order to guarantee the propagation of magnetic interactions along two or three spatial directions. By contrast, for crystals with lower symmetries there must be more than one intermolecular ferromagnetic interaction for each crystallographically independent radical molecule in order to achieve a bulk ferromagnetism.

[8] Another important aspect to be developed in this field is the enhancement of the strengths of intermolecular magnetic interactions. On increasing these strengths it will be possible to increase the critical temperature of purely organic ferromagnets, which nowadays are still very low; most of them in the mK region.

[9] M.-C. Etter, *Acc. Chem. Res.* **1990**, *23*, 120-126; J. Bernstein, R.-E. Davis, L. Shimoni, N.-L. Chang, *Angew. Chem. Int. Ed. Engl.* **1995**, *34*, 1555-1573.

[10] G. Desiraju, *Angew. Chem. Int. Ed. Engl.* **1995**, *34*, 2311-2327.

[11] For example see: a) K. Awaga, T. Inabe, Y. Maruyama, T. Nakamura, M. Matsumoto, *Chem. Phys. Letters* **1992**, *195*, 21-24; b) K. Awaga, T. Inabe, T. Nakamura, M. Matsumoto, Y. Maruyama, *Mol. Cryst. Liq. Cryst.* **1993**, *232*, 69-78; c) K. Awaga, T. Okuno, A. Yamaguchi, M. Hasegawa, T. Inabe, Y. Maruyama, N. Wada, *Phys. Rev. B* **1994**, *49*, 3975-3981; d) K. Awaga, A. Yamaguchi, T. Okuno, T. Inabe, T. Nakamura, M. Matsumoto, Y. Maruyama, *J. Mater. Chem.* **1994**, *4*, 1377-1385; e) K. Awaga, T. Okuno, A. Yamaguchi, M. Hasegawa, T. Inabe, Y. Maruyama, N. Wada, *Synth. Met.* **1995**, *71*, 1807-1808.

[12] For example see: a) J. Veciana, J. Cirujeda, C. Rovira, J. Vidal-Gancedo, *Adv. Mater.* **1995**, *7*, 221. b) J. Cirujeda, E. Hernàndez, C. Rovira, J.-L. Stanger, P. Turek, J. Veciana, *J. Mater. Chem.* **1995**, *5*, 243-252. c) J.

Cirujeda, C. Rovira, J.-L. Stanger, P. Turek, J. Veciana, *The Self-Assembly of Hydroxylated Phenyl a-Phenyl Nitronyl Nitroxide Radicals*, pp 219-248, in *"Magnetism. A Supramolecular Function"*; (Ed.: O. Kahn); Kluwer Academic Publishers: Amsterdam, **1996**. d) J. Cirujeda, E. Hernàndez, F. Lanfranc de Panthou, J. Laugier, M. Mas, E. Molins, C. Rovira, J. J. Novoa, P. Rey, J. Veciana, *Mol. Cryst. Liq. Cryst.* **1995**, *271*, 1-12. e) M. M. Matsushita, A. Izuoka, T. Sugawara, T. Kobayashi, N. Wada, N. Takeda, M. Ishikawa, *J. Am. Chem. Soc.* **1997**, *119*, 4369.

[13] When no angular data are taken into account and only intermolecular distances are considered in a given magnetostructural correlation, one is always tempted to ascribe the observed ferromagnetic intermolecular interaction to the contacts between atoms of the two interacting molecules that have opposite spin densities and are at the closest distances. However, in some molecular layouts there could be other atoms at longer distances that interact ferromagnetically due to angular considerations.

[14] F.-H. Allen, S. Bellard, M.-D. Brice, B.-A. Cartwright, A. Doubleday, H. Higgs, T. Hummelink, B.-G. Hummelink-Peters, O. Kennard, W.D.S. Motherwell, J.-R. Rodgers, D.-G. Watson, *Acta Crystallogr.* **1979**, *B35*, 2331.

[15] When the magnetic susceptibility data show the typical signature of the presence of two competing ferro- and antiferromagnetic interactions, we considered that one of them is dominant only when its strength -deduced by the fitting of magnetic data to different magnetic models- is at least one order of magnitude larger than the other one. In cases with comparable magnitudes we discarded the crystal structure from our statistical analysis.

[16] In few cases magnetic susceptibility data down only to 4K are available.

[17] The 23 ferromagnetic crystals selected are the following ones, identified by their refcode and reference (when the crystal is not deposited in the Cambridge Structural Database we have asigned a refcode and indicate the source): 0003QN: T. Sugano, M. Tamura, M. Kinoshita, Y. Sakai, Y. Ohashi, *Chem. Phys. Lett.* **1992**, *200*, 235; 000MPY: F. Lanfranc de Panthou, PhD Thesis, Univ. J. Fourier Grenoble I (**1994**); 000PPY: K. Awaga, T. Inabe, Y. Maruyama, *Chem. Phys. Lett.* **1992**, *190*, 349; 00DPNP: Prof. M. Kinoshita, unpublished results; 00GPNP: P. Turek, K. Nozawa, D. Shiomi, K. Awaga, T. Inabe, Y. Maruyama, M. Kinoshita, *Chem. Phys. Lett.* **1991**, *180*, 327; 0PBRPH: Y. Hosokoshi, PhD Thesis, Univ. of Tokyo (**1995**); MACOPY: F.M. Romero, R. Ziessel, A. De Cian, J. Fischer, P. Turek, *New J. Chem.* **1996**, *20*, 919; MMEPYB: K. Awaga, T. Inabe, Y. Maruyama, T. Nakamura, M. Matsumoto, *Chem. Phys. Lett.* **1992**, *195*, 21; MMEPYC: K. Awaga, T. Okuno, A. Yamaguchi, M. Hasegawa, T. Inabe, Y. Maruyama, N.

Wada, *Phys. Rev. B* **1994**, *49*, 3975; HAFXOB: E. Hernández, M. Mas, E. Molins, C. Rovira, J. Veciana, *Angew. Chem., Int. Ed. Engl.* **1993**, *32*, 882; KAXHAS: K. Awaga, T. Inabe, U. Nagashima, Y. Maruyama, *J. Chem. Soc., Chem. Commun.* **1989**, 1617; LICMIT: T. Sugawara, M.-M. Matsushita, A. Izuoka, N. Wada, N. Takeda, M. Ishikawa, *J. Chem. Soc., Chem. Commun.* **1994**, 1723; PEFMES: H. Wang, D. Zhang, M. Wan, D. Zhu, *Solid State Commun.* **1993**, *85*, 685; PEYPUA: F. Lanfranc de Panthou, D. Luneau, J. Laugier, P. Rey, *J. Am. Chem. Soc.* **1993**, *115*, 9095; YISCEI: L. Angeloni, A. Caneschi, L. David, A. Fabretti, F. Ferraro, D. Gatteschi, A. le Lirzin, R. Sessoli, *J. Mater. Chem.* **1994**, *4*, 1047; YISCOS: L. Angeloni, A. Caneschi, L. David, A. Fabretti, F. Ferraro, D. Gatteschi, A. le Lirzin, R. Sessoli, *J. Mater. Chem.* **1994**, *4*, 1047; YISNIX: Y. Hosokoshi, M. Tamura, M. Kinoshita, H. Sawa, R. Kato, Y. Fujiwara, Y. Ueda, *J. Mater. Chem.* **1994**, *4*, 1219; YIWSEC: K. Awaga, A. Yamaguchi, T. Okuno, T. Inabe, T. Nakamura, M. Matsumoto, Y. Maruyama, *J. Mater. Chem.* **1994**, *4*, 1377; YODBUO: Y. Hosokoshi, M. Tamura, H. Sawa, R. Kato, M. Kinoshita, *J. Mater. Chem.* **1995**, *5*, 41; YOMYII: J. Cirujeda, M. Mas, E. Molins, F. Lanfranc de Panthou, J. Laugier, J. Geun Park, C. Paulsen, P. Rey, C. Rovira, J. Veciana, *J. Chem. Soc., Chem. Commun.* **1995**, 709; YUJNEW10: A. Caneschi, F. Ferraro, D. Gatteschi, A. le Lirzin, E. Rentschler, *Inorg. Chim. Acta* **1995**, *235*, 159; YULPOK: T. Akita, Y. Mazaki, K. Kobayashi, N. Koga, H. Iwamura, *J. Org. Chem.* **1995**, *60*, 2092; ZORHIX: A. Lang, Y. Pei, L. Ouahab, O. Kahn, *Adv. Mater.* **1996**, *8*, 60.

[18] The 24 antiferromagnetic crystals selected are the following ones, identified by their refcode and reference (when the crystal is not deposited in the Cambridge Structural Database we have asigned a refcode and indicate the source): 0000AH: Y. Hosokoshi, PhD Thesis, Univ. of Tokyo (**1995**); 0000BR: Y. Hosokoshi, PhD Thesis, Univ. of Tokyo (**1995**); 000F5P: Y. Hosokoshi, PhD Thesis, Univ. of Tokyo (**1995**); 003CLP: O. Jürgens, J. Cirujeda, M. Mas, I. Mata, A. Cabrero, J. Vidal-Gancedo, C. Rovira, E. Molins, J. Veciana, *J. Mater. Chem.* **1997**, *7*, 1723; 00NNMA: E. Hernández, PhD Thesis, Univ. of Barcelona (**1995**); 00PCLP: Y. Hosokoshi, PhD Thesis, Univ. of Tokyo (**1995**); 0PCF3P: Y. Hosokoshi, PhD Thesis, Univ. of Tokyo (**1995**); 2CLPNN: O. Jürgens, J. Cirujeda, M. Mas, I. Mata, A. Cabrero, J. Vidal-Gancedo, C. Rovira, E. Molins, J. Veciana, *J. Mater. Chem.* **1997**, *7*, 1723; 2N5OHP: J. Cirujeda, PhD Thesis, Univ. Ramon Llull (**1997**); 3CL4OH: O. Jürgens, J. Cirujeda, M. Mas, I. Mata, A. Cabrero, J. Vidal-Gancedo, C. Rovira, E. Molins, J. Veciana, *J. Mater. Chem.* **1997**, *7*, 1723; 5CL2OH: O. Jürgens, J. Cirujeda, M. Mas, I. Mata,

A. Cabrero, J. Vidal-Gancedo, C. Rovira, E. Molins, J. Veciana, *J. Mater. Chem. i***1997**, *7*, 1723; LASCAJ: D. Zhang, W. Zhou, D. Zhu, *Solid State Commun.* **1993**, *86*, 291; LEMMAR: D. Luneau, J. Laugier, P. Rey, G. Ulrich, R. Ziessel, P. Legoll, M. Drillon, *J. Chem. Soc., Chem. Commun.* **1994**, 741; PEFMAO: H. Wang, D. Zhang, M. Wan, D. Zhu, *Solid State Commun.* **1993**, *85*, 685; SUKBIJ: A. Caneschi, P. Chiesi, L. David, F. Ferraro, D. Gatteschi, R. Sessoli, *Inorg. Chem.* **1993**, *32*, 1445; SUKBOP: A. Caneschi, P. Chiesi, L. David, F. Ferraro, D. Gatteschi, R. Sessoli, *Inorg. Chem.* **1993**, *32*, 1445; WILVIW10: K. Awaga, A. Yamaguchi, T. Okuno, T. Inabe, T. Nakamura, M. Matsumoto, Y. Maruyama, *J. Mater. Chem.* **1994**, *4*, 1377; YISCIM: L. Angeloni, A. Caneschi, L. David, A. Fabretti, F. Ferraro, D. Gatteschi, A. le Lirzin, R. Sessoli, *J. Mater. Chem.* **1994**, *4*, 1047; YOMYOO: J. Cirujeda, M. Mas, E. Molins, F. Lanfranc de Panthou, J. Laugier, J. Geun Park, C. Paulsen, P. Rey, C. Rovira, J. Veciana, *J. Chem. Soc., Chem. Commun.* **1995**, 709; YOMYUU: J. Cirujeda, M. Mas, E. Molins, F. Lanfranc de Panthou, J. Laugier, J. Geun Park, C. Paulsen, P. Rey, C. Rovira, J. Veciana, *J. Chem. Soc., Chem. Commun.* **1995**, 709; YOXMAZ: T. Mitsumori, K. Inoue, N. Koga, H. Iwamura, *J. Am. Chem. Soc.* **1995**, *117*, 2467; YOXMED: T. Mitsumori, K. Inoue, N. Koga, H. Iwamura, *J. Am. Chem. Soc.* **1995**, *117*, 2467; YULPAW: T. Akita, Y. Mazaki, K. Kobayashi, N. Koga, H. Iwamura, *J. Org. Chem.* **1995**, *60*, 2092; ZIPTAT: A. Caneschi, D. Gatteschi, E. Rentschler, R. Sessoli, *Gazzetta Chim. Ital.* **1995**, *125*, 283.

[19] Such first-order transitions generally produce abrupt changes in the χT vs. T plots that are easily detected.

[20] This fact has been well documented for organic superconducting crystals, whose critical temperatures are also much lower than the room temperature. See, for instance, J.-M. Williams, J.-R. Ferraro, R.-J. Thorn, K.-D. Carlson, U. Geiser, H.-H. Wang, A.-M. Kini, M.-H. Whangbo, "*Organic Superconductors*", Prentice Hall, Englewood Cliffs, **1992**. Magnetism is a different physical property than superconductivity, although both are intimately related with the relative arrangement of molecules in the crystal. The packing properties of molecular solids and, in particular, its variation with temperature, are determined by the intermolecular contacts, but is independent of the electronic physical properties of the crystal.

[21] J. Veciana, J. Cirujeda, C. Rovira, E. Molins, J.-J. Novoa, *J. Phys. I France* **1996**, *6*, 1067-86.

[22] a) M. Deumal, J. Cirujeda, J. Veciana, M. Kinoshita, Y. Hosokoshi, J.-J. Novoa, *Chem. Phys. Lett.* **1997**, *265*, 190-199. b) J. J. Novoa, M. Deumal,

M. Kinoshita, Y. Hosokoshi, J. Veciana, J. Cirujeda, *Mol. Cryst. Liq. Cryst.* **1997**, 305, 129-141.

[23] The presence of a positive density on the O atom has been shown by experimental and theoretical methods. See for instance, A. Zheludev, V. Barone, M. Bonnet, B. Delley, A. Grand, E. Ressouche, P. Rey, R. Subra, J. Schweizer, *J. Am. Chem. Soc.* **1994**, *116*, 2019-2027; J.-J. Novoa, F. Mota, J. Veciana, J. Cirujeda, *Mol. Cryst. Liq. Cryst.* **1995**, *271*, 79-90.

[24] Standard deviations of the atomic distances and bond angles of this five-membered ring are smaller than the 2% of the respective magnitudes. See: J. Cirujeda, PhD. Thesis, Univ. Ramon Llull, Barcelona, **1997**.

[25] The standard deviation of the geometrical parameters for the FM and AFM subsets are also similar. Their values are larger for the angles than the distance D, and, among the angles, are larger for the T_i than the A_i parameters. This trend just reflects the softer form of the potential energy curves of the dihedral parameters, compared to the angles and distance stretchings.

[26] R. Barlow, "*Statistics*", John Wiley and Sons: Chichester, 1989.

[27] E.-R. Malinowski, D.-G. Howery, "*Factor Analysis in Chemistry*", Wiley Interscience: New York, **1980**.

[28] B.-S. Everitt, "*Cluster Analysis*", 3rd edition, Edward Arnold: London, **1993**.

[29] The distance between two elements, *i* and *j*, in the space defined by six dimensional coordinates space is given by:

$$d_{ij} = \sum_{k=1}^{6} \left[V(k)_i^2 - V(k)_j^2 \right]^{1/2}$$

[30] The spin density on the H atom of the four CH_3 groups is negative, whereas these on the H atoms of a phenyl ring linked to the α carbon of the five membered ring alternate in their sign, being positive for *ortho* and *para* H atoms and negative for the *meta* one. See: Ref. [23].

[31] A distance range typical in recent analysis of C-H···O hydrogen bonded contacts to avoid excluding the so called out-liers. See: G. A. Jeffrey, W. Saenger, "*Hydrogen Bonding in Biological Structures*", Springer-Verlag, Berlin, **1991**.

[32] An alternative mechanism, based on magnetic dipole-dipole interactions, has been sometimes invoked in order to explain the weak intermolecular magnetic interactions among organic radicals (see Ref [1c]). This mechanism could explain the lack of statistically significant differences in the NO···ON and C-H···O contacts. Nevertheless, some studies indicate that the magnitude of magnetic dipolar interactions are much smaller than those originating from

magnetic exchange interactions (see K. Takeda, K. Konishi, M. Tamura, M. Kinoshita, *Mol. Cryst. Liq. Cryst.*, **1995**, *273*, 57).

[33] Efforts in the theoretical and experimental directions are currently in progress in our laboratories in order to demonstrate unambigously the validity of the McConnell-I model. Some of these studies are based on looking at the similarities in the patterns present in crystals showing similar magnetic properties. Another line of research is directed towards the theoretical basis of the McConnell-I model (M. Deumal, J. J. Novoa, M. J. Bearpark, P. Celani, M. Olivucci, M. A. Robb, *J. Phys. Chem.* **1998**, *in press*)

Table 1. List of ONCNO···ONCNO contacts for crystals of the FM and AFM subsets within the range of distances indicated. Percentages of cases with intermolecular ferro- and antiferromagnetic interactions are also given.

		FM subset		**AFM subset**	
distance range (Å)	total number of contacts	number of contacts	%	number of contacts	%
[0,3]	0	0	0	0	0
[0,4]	24	10	42	14	58
[0,5]	92	36	39	56	61
[0,6]	204	90	44	114	56
[0,7]	378	167	44	211	56
[0,8]	608	274	45	334	55
[0,9]	901	416	46	485	54
[0,10]	1312	611	47	701	53

Table 2. Values of the geometrical parameters defining the ONCNO···ONCNO contact for the five crystals of the FM and AFM subsets showing the shortest D distances. The distances are given in Å and the angles in degrees. The *refcodes* of crystals in which these interactions are found are given in Schemes 2 and 3.

Refcode	D	A_1	A_2	T_1	T_2	T_3
			FM subset			
LICMIT	3.158	146.8	146.8	180.0	-0.1	0.1
ZORHIX	3.168	126.9	71.5	119.0	46.5	-76.2
MMEPYC	3.429	153.2	68.0	173.3	-40.1	70.1
000MPY	3.499	127.5	76.4	-162.1	104.2	-92.1
PEYPUA	3.719	114.6	59.0	172.9	-114.0	-66.5
			AFM subset			
WILVIW10	3.159	117.2	134.1	139.0	134.3	77.9
5CL2OH	3.369	82.6	82.6	180.0	75.6	-75.6
0000AH	3.431	120.0	75.8	-38.9	75.1	62.7
SUKBOP	3.522	77.7	77.7	180.0	-66.7	66.7
ZIPTAT	3.589	79.2	79.2	180.0	-82.7	82.7

Table 3. Number of C(sp^3)-H··· ON and C(sp^2)-H··· ON contacts (splitted into *ortho*, *meta* and *para* contributions) within the FM and AFM subsets whose O···H distances are less or equal than 3.8Å.

		FM subset		**AFM subset**	
Type of contact	total number of contacts	number of contacts	%	number of contacts	%
$C(sp^3)$-H··· ON	364	157	43	207	57
$C(sp^2)$-H··· ON					
ortho	35	20	57	15	43
meta	51	32	63	19	37
para	16	6	38	10	62

Table 4. Values of the geometrical parameters defining the C(sp^3)-H···O-N contacts for the five crystals of the FM and AFM subsets showing the shortest D distances. The distances are given in Å and the angles in degrees. The *refcodes* of crystals in which these contacts are found are also indicated.

Refcode	D	A_1	A_2	T_1
		FM subset		
HAFXOB	2.339	137.9	167.2	-145.3
YOMYII	2.382	111.9	162.2	94.9
000MPY	2.419	118.0	168.6	160.5
ZORHIX	2.582	126.8	148.1	169.2
00GPNP	2.600	124.1	132.1	-150.9
		AFM subset		
0000AH	2.295	88.9	158.0	54.5
YISCIM	2.343	162.6	161.5	-109.3
SUKBIJ	2.442	142.1	161.2	-148.0
0000BR	2.447	126.3	149.6	112.3
YOXMED	2.489	131.3	157.7	-157.8

Table 5. Values of the geometrical parameters defining the C(sp^2)-H···O-N contacts for the five crystals within the FM subset showing the shortest contact distances. The values are grouped into three different sets according to the positions (*ortho*, *meta*, and *para*) of the H atoms that make the indicated contacts. The distances are given in Å and the angles in degrees. The *refcodes* of crystals in which these contacts are found are also indicated.

FM subset

Refcode	D_o	A_{1o}	A_{2o}	T_{1o}
00GPNP	2.559	157.5	123.6	-103.3
00DPNP	2.569	158.3	123.0	118.6
KAXHAS	2.800	123.1	101.7	-82.7
YISCEI	3.067	86.3	119.3	156.7
0PBRPH	3.149	147.3	131.1	-109.0
Refcode	D_m	A_{1m}	A_{2m}	T_{1m}
YISNIX	2.239	150.7	147.8	102.0
00DPNP	2.421	132.4	130.6	-143.7
HAFXOB	2.496	143.0	128.1	-171.9
00GPNP	2.536	129.6	124.0	-149.0
YISCOS	2.592	123.7	140.5	-32.1
Refcode	D_p	A_{1p}	A_{2p}	T_{1p}
YOMYII	2.613	135.1	163.3	-92.0
LICMIT	2.892	139.2	127.4	88.1
YISCOS	2.940	112.3	118.4	156.6

Table 6. Values of the geometrical parameters defining the C(sp^2)-H···O-N contacts for the five crystals within the AFM subset showing the shortest contact distances. The values are grouped into three different sets according to the positions (*ortho*, *meta*, and *para*) of the H atoms that make the indicated contacts. The distances are given in Å and the angles in degrees. The *refcodes* of crystals in which these contacts are found are also indicated.

AFM subset

Refcode	D_o	A_{1o}	A_{2o}	T_{1o}
SUKBOP	2.645	125.8	125.1	-134.5
2N5OHP	2.698	101.6	124.9	-152.8
YOMYUU	2.791	157.9	125.5	100.7
YOMYOO	2.795	168.4	125.3	107.4
00PCLP	2.988	85.1	115.9	163.2
Refcode	D_m	A_{1m}	A_{2m}	T_{1m}
0PCF3P	2.412	140.6	137.0	120.9
3CL4OH	2.647	143.2	127.9	-95.0
YOMYOO	2.648	153.5	145.2	-131.9
2CLPNN	2.658	119.9	129.7	36.6
SUKBOP	2.693	151.4	122.4	82.4
Refcode	D_p	A_{1p}	A_{2p}	T_{1p}
5CL2OH	2.220	137.0	157.0	-95.6
YISCIM	2.325	148.2	142.7	-157.6
003CLP	2.465	152.3	127.7	179.6
YOMYOO	2.490	93.1	160.6	166.3
SUKBOP	2.645	125.8	125.1	-134.5

Chart and Figure captions

Scheme 1. General structure of α-nitronyl nitroxide radicals (R is a substituent).

Scheme 2. Chemical formulas of the R substituents for the α-nitronyl nitroxide radicals included in the FM subset. Lower part corresponds to those crystals whose structure has been deposited in the CSD.

Scheme 3. Chemical formulas of the R substituents for the α-nitronyl nitroxide radicals included in the AFM subset. Lower part corresponds to those crystals whose structure has been deposited in the CSD.

Figure 1. Geometrical parameters employed to define the relative position of two ONCNO groups.

Figure 2. Geometrical disposition of the dimers found in the two crystals of the FM (see a) and AFM subsets (see b) presenting the shortest NO···ON contacts. Also shown (c) is the dimer with the shortest NO···ON contact among the dimers presenting a head-tail conformation in the AFM subset.

Figure 3. (a) Scattergrams of the indicated pair of parameters characterizing the NO···ON contacts in the FM (left) and AFM (right) crystal subsets. (b) Position of the O_{21} atoms relative to the O_{11}-C_{11}-C_1 group for all contacts of the FM (left) and AFM (right) crystal subsets within the 0-5 Å range.

Figure 4. Types of clusters expected in our statistical analysis of FM and AFM subsets of crystals.

Figure 5. Geometrical parameters employed to define the relative position of one $C(sp^3)$-H group respect to a ONCNO group.

Figure 6. Geometrical parameters employed to define the relative position of one $C(sp^2)$-H group located in *ortho*, *meta* or *para* position of an aromatic ring respect to a ONCNO group.

Figure 7. Scattergrams of D *vs* A_1 and D *vs* A_2 for the $C(sp^3)$-H···O-N contacts of the FM (lower) and AFM (upper) subsets.

Figure 8. Scattergram of D *vs* A_1 and D *vs* A_2 for the *ortho*, *meta*, and *para* $C(sp^2)$-H···O-N contacts of the FM (lower) and AFM (upper) subsets.

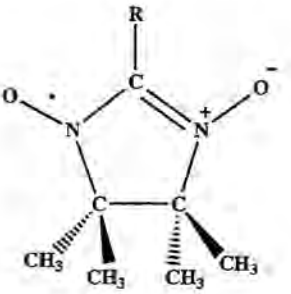

Scheme 1

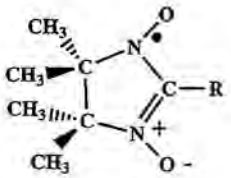

where **R ≡**

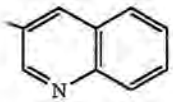

0003QN

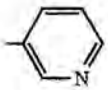

000MPY

000PPY

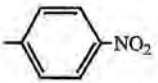

00DPNP (δ-phase)
00GPNP (γ-phase)

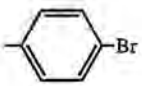

0PBRPH

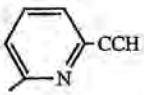

MACOPY

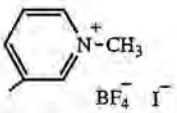

MMEPYB

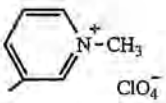

MMEPYC

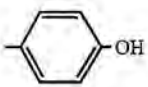

HAFXOB

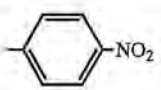

KAXHAS (β-phase)

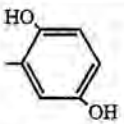

LICMIT (α-phase)

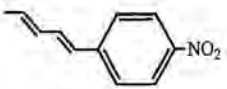

PEFMES

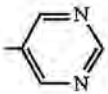

PEYPUA

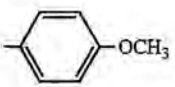

YISCEI

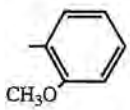

YISCOS

YISNIX

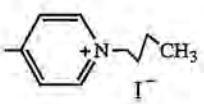

YIWSEC

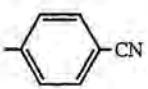

YODBUO

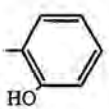

YOMYII (α-phase)

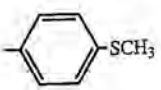

YUJNEW10

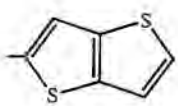

YULPOK

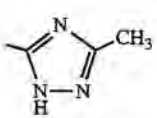

ZORHIX

Scheme 2

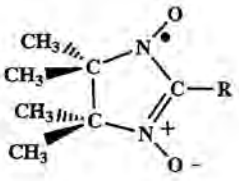

where **R ≡**

(α-phase)
0000AH

0000BR

000F5P

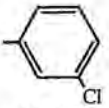

003CLP

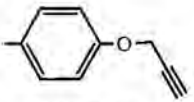

00NNMA

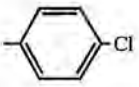

00PCLP

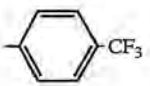

0PCF3P

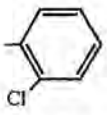

2CLPNN

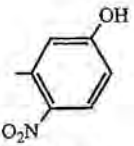

2N5OHP

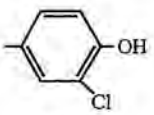

3CL4OH

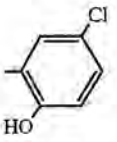

5CL2OH

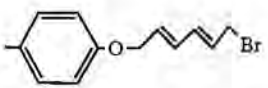

LASCAJ

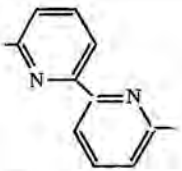

LEMMAR

PEFMAO

SUKBIJ

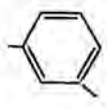

SUKBOP

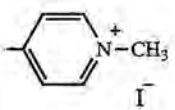

WILVIW10

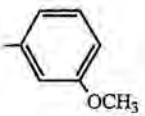

YISCIM

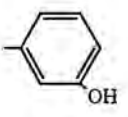

YOMYOO (β-phase)

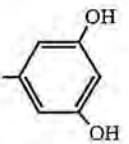

YOMYUU

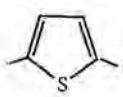

YOXMAZ

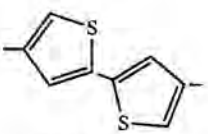

YOXMED

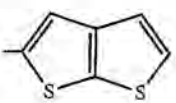

YULPAW

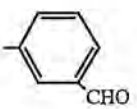

ZIPTAT

Scheme 3

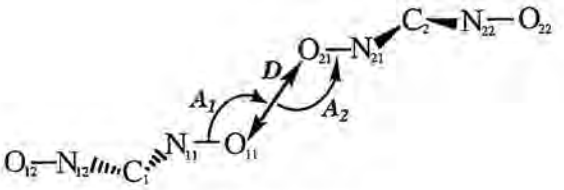

$D = O_{21} \cdots O_{11}$

$A_1 = O_{21} \cdots O_{11} - N_{11}$

$A_2 = N_{21} - O_{21} \cdots O_{11}$

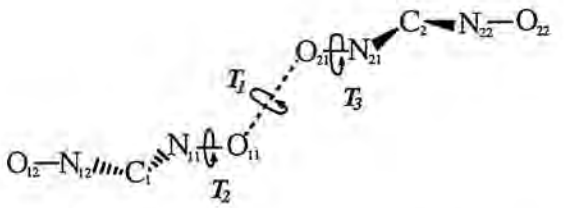

$T_1 = N_{21} - O_{21} \cdots O_{11} - N_{11}$

$T_2 = O_{21} \cdots O_{11} - N_{11} - C_1$

$T_3 = C_2 - N_{21} - O_{21} \cdots O_{11}$

Figure 1

(a)

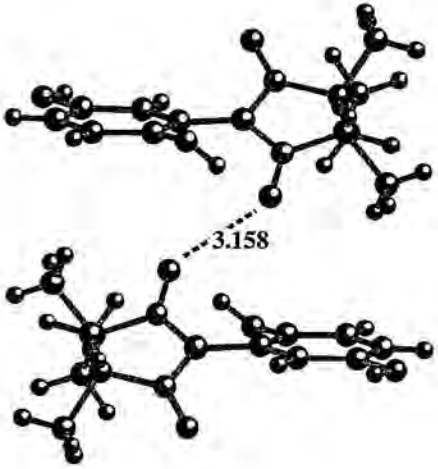

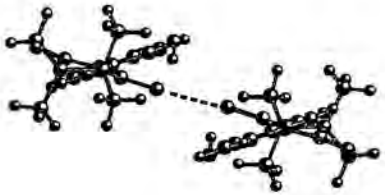

LICMIT (FM)

(b)

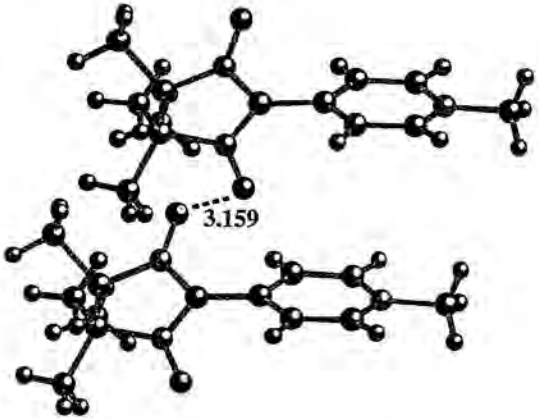

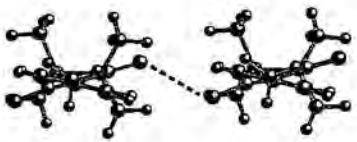

WILVIW10 (AFM)

(c)

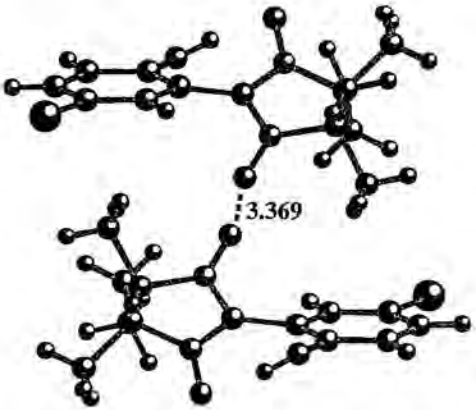

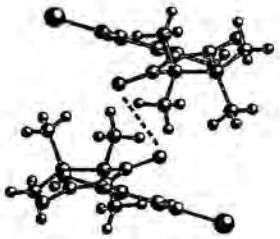

5CL2OH (AFM)

Fig. 2

(a)

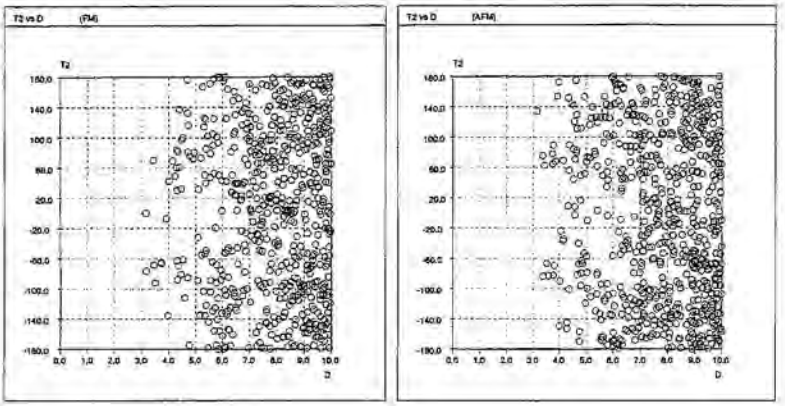

(b)

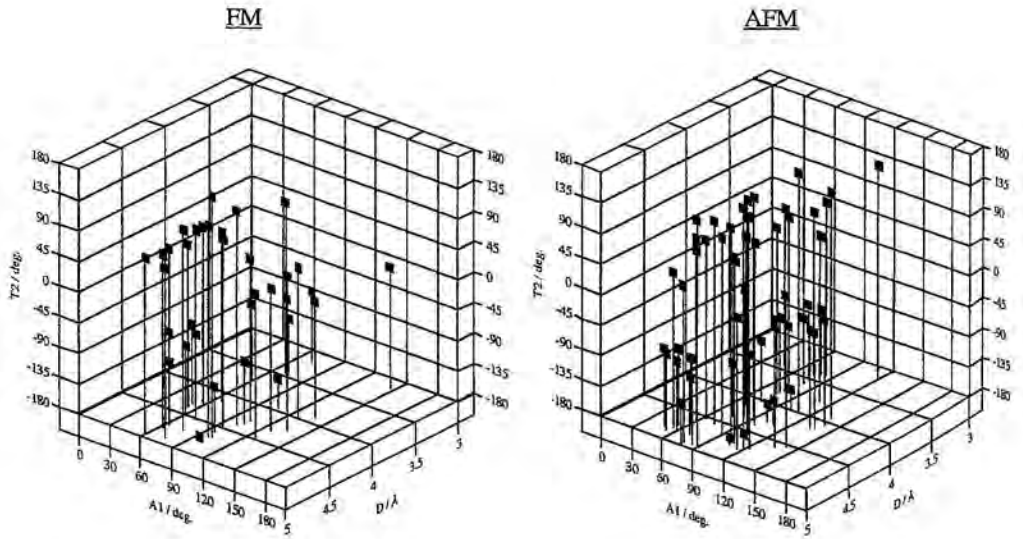

Fig. 3

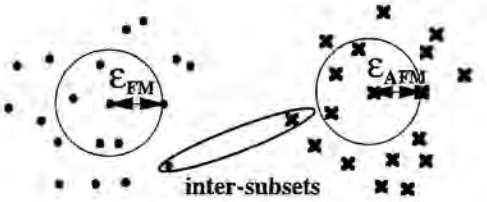

(1)

all $\varepsilon_{FM\text{-}AFM} > \varepsilon_{FM}, \varepsilon_{AFM}$

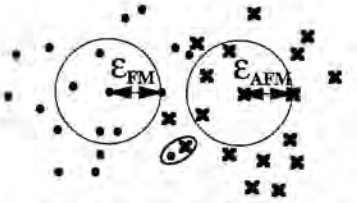

(2)

some $\varepsilon_{FM\text{-}AFM} < \varepsilon_{FM}, \varepsilon_{AFM}$

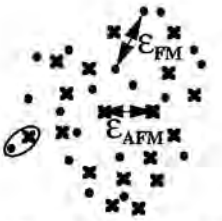

(3)

all $\varepsilon_{FM\text{-}AFM} < \varepsilon_{FM}, \varepsilon_{AFM}$

Figure 4

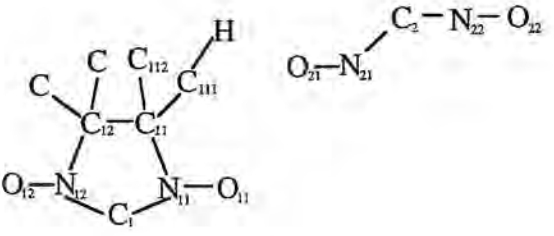

$D = H\cdots O_{21}$

$A_1 = H\cdots O_{21}\text{-}N_{21}$

$A_2 = C_{111}\text{-}H\cdots O_{21}$

$T_1 = C_{111}\text{-}H\cdots O_{21}\text{-}N_{21}$

Figure 5

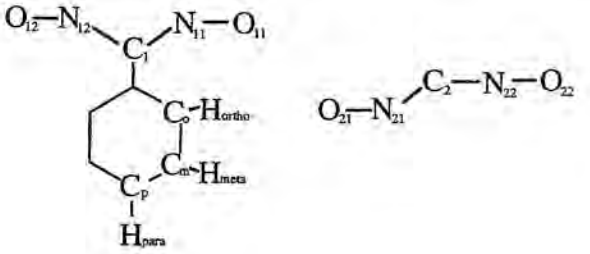

$D_i = H_j \cdots O_{21}$

$A_{1i} = H_j \cdots O_{21} - N_{21}$

$A_{2i} = C_i\text{-}H_j \cdots O_{21}$

$T_{1i} = C_i\text{-}H_j \cdots O_{21} - N_{21}$

$(i = o, m, p)$

$(H_j = H_{ortho}, H_{meta}, H_{para})$

Figure 6

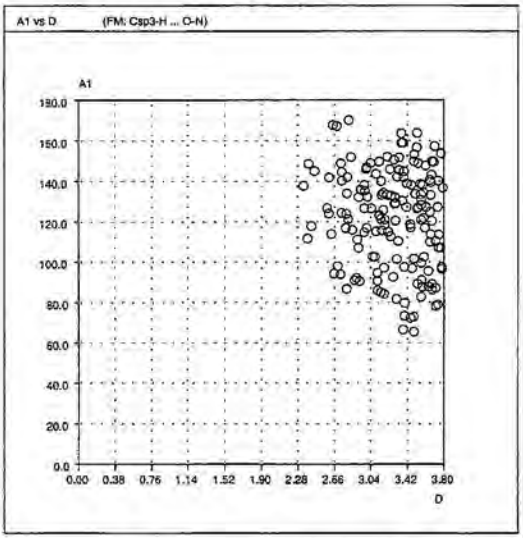
A1 vs D
(FM: Csp3-H ... O-N)
A1
180.0
160.0
140.0
120.0
100.0
80.0
60.0
40.0
20.0
0.0
0.00 0.38 0.76 1.14 1.52 1.90 2.28 2.66 3.04 3.42 3.80
D

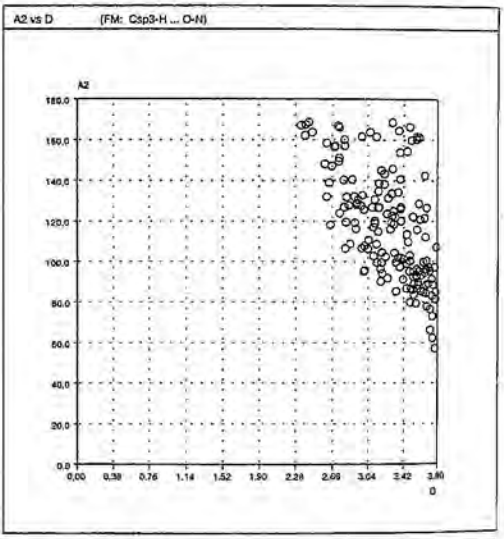
A2 vs D
(FM: Csp3-H ... O-N)
A2
180.0
160.0
140.0
120.0
100.0
80.0
60.0
40.0
20.0
0.0
0.00 0.38 0.76 1.14 1.52 1.90 2.28 2.66 3.04 3.42 3.80
D

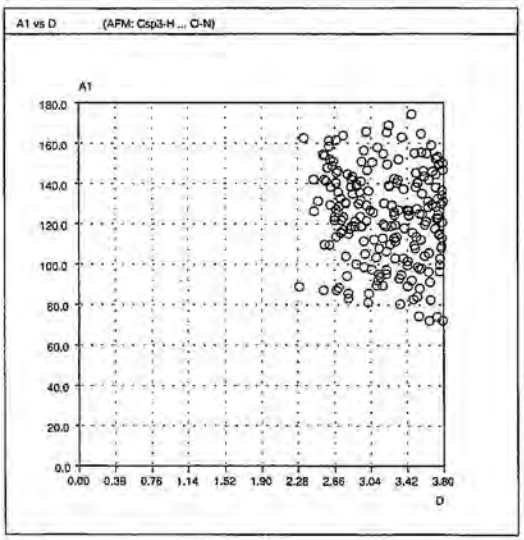
A1 vs D
(APM: Csp3-H ... O-N)
A1
180.0
160.0
140.0
120.0
100.0
80.0
60.0
40.0
20.0
0.0
0.00 0.38 0.76 1.14 1.52 1.90 2.28 2.66 3.04 3.42 3.80
D

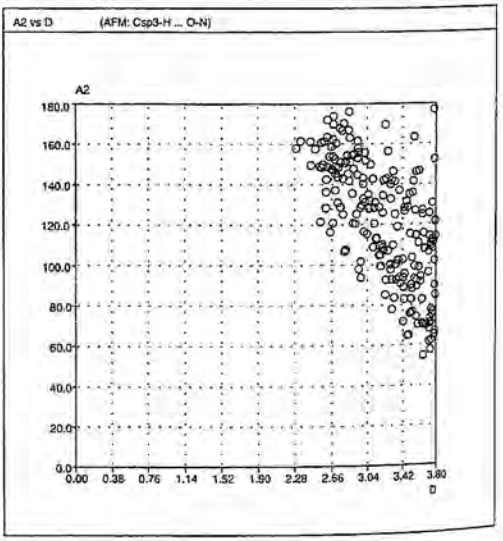
A2 vs D
(AFM: Csp3-H ... O-N)
A2
180.0
160.0
140.0
120.0
100.0
80.0
60.0
40.0
20.0
0.0
0.00 0.38 0.76 1.14 1.52 1.90 2.28 2.66 3.04 3.42 3.80
D

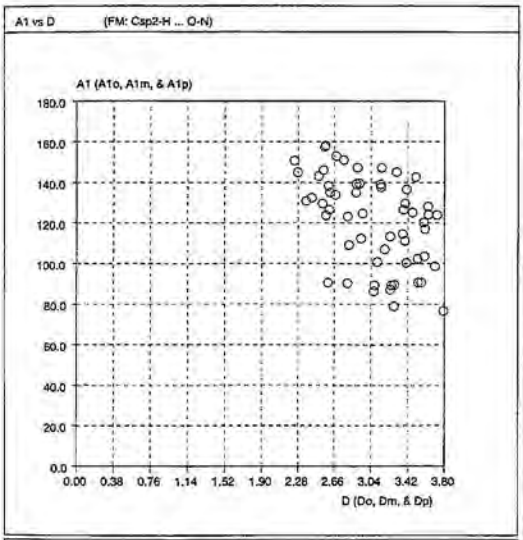
A1 vs D
(FM: Csp2-H ... O-N)
A1 (A1o, A1m, & A1p)
180.0
160.0
140.0
120.0
100.0
80.0
60.0
40.0
20.0
0.0
0.00 0.38 0.76 1.14 1.52 1.90 2.28 2.66 3.04 3.42 3.80
D (Do, Dm, & Dp)

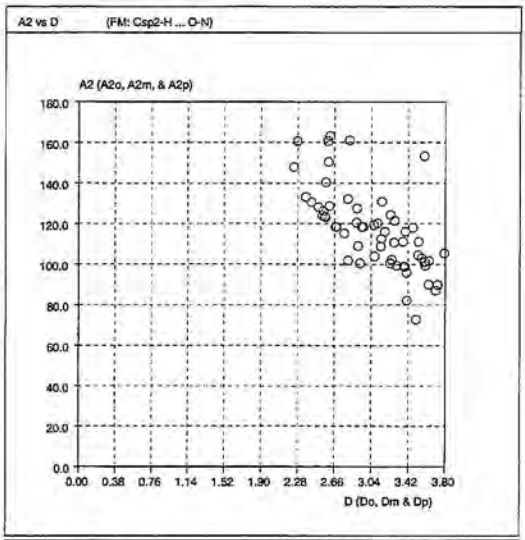
A2 vs D
(FM: Csp2-H ... O-N)
A2 (A2o, A2m, & A2p)
180.0
160.0
140.0
120.0
100.0
80.0
60.0
40.0
20.0
0.0
0.00 0.38 0.76 1.14 1.52 1.90 2.28 2.66 3.04 3.42 3.80
D (Do, Dm & Dp)

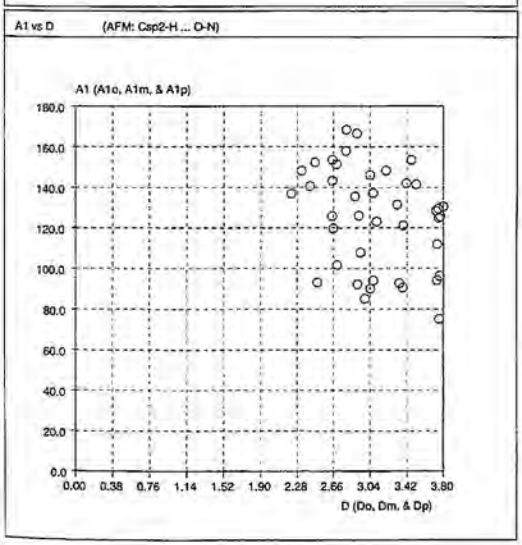
A1 vs D
(AFM: Csp2-H ... O-N)
A1 (A1o, A1m, & A1p)
180.0
160.0
140.0
120.0
100.0
80.0
60.0
40.0
20.0
0.0
0.00 0.38 0.76 1.14 1.52 1.90 2.28 2.66 3.04 3.42 3.80
D (Do, Dm, & Dp)

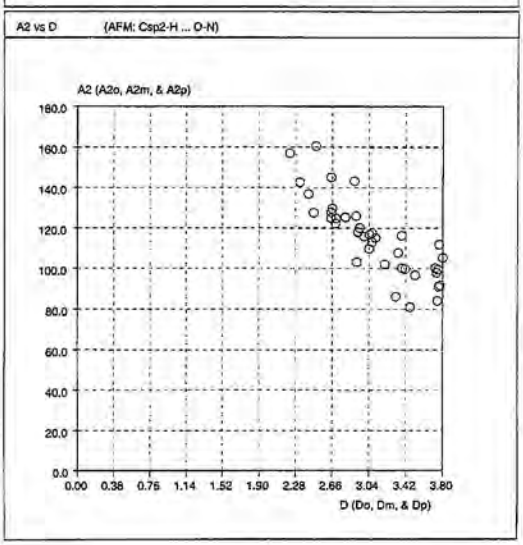
A2 vs D
(AFM: Csp2-H ... O-N)
A2 (A2o, A2m, & A2p)
180.0
160.0
140.0
120.0
100.0
80.0
60.0
40.0
20.0
0.0
0.00 0.38 0.76 1.14 1.52 1.90 2.28 2.66 3.04 3.42 3.80
D (Do, Dm, & Dp)

Graphical abstracts

The statistical analysis of the packings of all known α-nitronyl nitroxide crystals showing dominant ferro and antiferromagnetic properties shows that there are no differences in the geometrical distribution of the NO···ON, $C(sp^3)$-H···O-N and $C(sp^3)$-H···O-N contacts in these two subsets. The magnetic properties are a result of the relative orientation of the molecules, that is, of their packing patterns (or synthons) and not of the geometry of an individual contact.

ARTICLE 10

Mol. Cryst. Liq. Cryst. **1998**

Does the McConnell-I model really work?. An ab initio study of the magnetic character of some intermolecular contacts

JUAN J. NOVOA[a], MERCE DEUMAL[a], PILAR LAFUENTE[a], and MICHAEL A. ROBB[b]

[a]Departament de Química Física, Facultat de Química, Universitat de Barcelona, Av. Diagonal 647, 08028-Barcelona, Spain; [b]Chemistry Department, King´s College London, Strand, London, U.K.

The performance of the first model proposed by McConnell to rationalize the nature of the magnetic interactions in purely organic molecular crystals (the McConnell-I model) has been analyzed using ab initio methods. As a first step, we analyzed the form of deriving the basic formula of the McConnell-I model from a general Heisenberg spin Hamiltonian. We reached the conclusion that it is not possible in general, although the two show some resemblance. When the same procedure is applied to the well known example of the [2.2]paracyclophanes, we found that the agreement with the experiment comes from the fortuitous cancellation of terms which is not likely to hold in general. We then studied the high-low spin energy difference for the H_2NO dimer and the methyl-allyl radicals for different relative orientations of the two monomers using CASSCF calculations and the 6-31G(d) basis set. It is found that there are regions in which McConnell-I model does not reproduce the ab initio results. So, we can conclude that the McConnell-I does not work in general.

Keywords: molecular magnetism; McConnell-I model; ferromagnetism; ab initio computations;

INTRODUCTION

Experimentally, the presence of magnetism in a molecular crystal and its dimensionality depends on the way the crystal packs, that is, on the distance and relative spatial orientation of the molecules which constitute the crystal.[1] The rationalization of this dependence is a key step towards the controlled obtention of better molecular magnets, that is, towards the design of molecular magnets. The other needed ingredient is to know how to control the packing of the molecular radicals within the crystal.

The most widely used tool to rationalize the presence of magnetism in purely organic crystals is the McConnell-I model,[2a] so called because is the first of the two models[2b] proposed by the same author. This McConnell-I model is a qualitative model based on a Heisenberg spin Hamiltonian and predicts the presence of intermolecular ferromagnetic interactions only when the crystal presents short intermolecular contacts between atoms bearing considerable spin population of opposite sign.[2a] Accordingly, the magnetic behavior of a molecular crystal can be rationalized by computing the atomic spin population on the atoms of the radicals, a property available from experimental[3] or computational[4] studies.

In spite that the validity of the McConnell-I model has never been demonstrated in a rigorous way, that validity has been generally accepted based on two types of evidence: a) the observed relative stability of the singlet/quintet states in the pseudo-ortho, pseudo-meta, and pseudo-para [2.2]paracylophanes,[5] which follows the McConnell-I predictions, and b) the results from ab initio computations on simple model systems.[6] However, some experimental magneto-structural relationships are difficult to explain by a straightforward application of the McConnell-I model, raising doubts on its validity and range of applicability. This has prompted us to start a systematic study on the validity of the McConnell-I model, trying to answer the following question: does it really work?.

ANALYTICAL APPROACH

To find and answer to the previous question we first carried out an statistical analysis of the crystal packing of 47 α-nitronyl nitroxides (α-NN) crystals presenting dominant ferro and antiferromagnetic interactions (characterized by looking at their χT vs T plots in the 273-4 K range).[7] According to the McConnell-I model, short NO···ON contacts in the plane for N-O···O angles in the +90 to -90° range are associated to strong antiferromagnetic interactions, because these groups localize a large part of the positive atomic spin population. Therefore, these class of contacts should be only present within the crystals presenting dominant antiferromagnetic interactions. This is not what our statistical analysis[7] showed: one can find short NO···ON contacts of the previous type within the ferromagnetic and antiferromagnetic subsets with similar probability. In fact, the distribution in the space of the NO···ON contacts is nearly identical for the ferro and antiferromagnetic subsets of crystals. This is not a proof that the McConnell-I model is failing, as there are more groups in each molecule capable of magnetic interactions, and the magnetic character is the consequence of the combined set of interactions. However, the previous result clearly indicates that many structure-magnetism relationships done up to now have no statistical support: the simplified use of the McConnell-I model just looking at the NO···ON contacts is not a valid procedure. Similar conclusions are reached when the C-H···ON contacts are analyzed.[7b]

In a step forward, we studied the analytical derivation of the McConnell-I basic formula in the context of the Heisenberg spin theory.[8] The McConnell-I model is based on the application of the following spin Hamiltonian:

$$\hat{H}^{AB} = -\hat{\mathbf{S}}^{A} \cdot \hat{\mathbf{S}}^{B} \sum_{i \in A, j \in B} J_{ij}^{AB} \rho_i^A \rho_j^B \qquad (1)$$

in which J_{ij}^{AB} are two-centre exchange integrals, and ρ_i^A, ρ_j^B are spin densities on atoms i, j of fragments A and B. The $\hat{S}^A, \hat{S}^B$ are the total spin

operators for fragments A, B. The previous expression is an approximation of the general expression of a Heisenberg spin Hamiltonian, whose formula is

$$\hat{H}^S = Q - \sum_{i,j} J_{ij}\left(2\hat{S}_i \cdot \hat{S}_j + \tfrac{1}{2}\hat{I}_{ij}\right) \qquad (2)$$

in which Q is just a Coulomb shift (which is taken in many cases as zero) and $\hat{I}_{ij}$ the identity spin operator (in some cases not included). A first comparison of the properties of these two Hamiltonians can be done by looking at the energy difference between the triplet and singlet states generated from the interaction of two doublet fragments (it can be done for any high and low spin states generated from any spin fragments with the same results). In the exact Heisenberg case, the expression for the energy difference between the singlet and the triplet states is:

$$E^S - E^T = \sum_{i,j} J_{ij}\Delta P_{ij} \qquad (3)$$

where the ΔP_{ij} is defined as

$$\Delta P_{ij} = P_{ij}^S - P_{ij}^T \qquad (4)$$

being J_{ij} the exchange integrals, and P_{ij}^S and P_{ij}^T the singlet and triplet exchange density matrices obtained from singlet and triplet eigenvectors using any ab initio method. Using the McConnell-I Hamiltonian, the same energy difference is

$$E^S - E^T = \sum_{i\in A, j\in B} J_{ij}^{AB}\rho_i^A\rho_j^B \qquad (5)$$

being ρ_i^A and ρ_i^B the atomic spin populations in the atoms i and j of centers A and B, respectively. Comparing equations (3) and (5), it is clear that the McConnell-I model is valid only if we make the association

$$\Delta P_{ij} \Leftrightarrow \rho_i^A \rho_j^B \qquad (6)$$

However, there is no theoretical justification for this. Clearly $\rho_i^A \rho_j^B$ is the product of the difference of spin densities evaluated from a two doublet fragment, while ΔP_{ij} is the difference of singlet and triplet two-particle density matrices evaluated from two different supermolecule computations (one for the triplet and one for the singlet), that is, they are mathematically two type of objects. *There is no obvious reason why these two quantities should be related each other than heuristically.*

We have done a strict quantitative test of the Heisenberg and McConnell-I Hamiltonians computing the quintet-singlet energy difference for the ortho-, meta- and para- [2.2]paracyclophanes. What we found in this case is that the McConnell-I model works because of fortuitous cancellations: the agreement arises because the signs of $\rho_i^A \rho_j^B$ and ΔP_{ij} are the same and many J_{ij} are zero. However, many of the J_{ij} are zero because the perfect alignment of the C atoms in the [2.2]paracyclophanes, a fact that is not generally applicable to other systems. *Therefore, there is no reason to expect this situation to hold in general, that is, we have shown that there is no general reason for the McConnell-I model to work.*

AB INITIO COMPUTATIONS OF SOME SIMPLE SYSTEMS

To further test the validity of the McConnell-I model we studied the high spin-low spin energy difference for various orientations of two simple dimers, the H_2NO and the methyl-allyl complexes. The first one was selected because it is a simple prototype for the study of the magnetic interactions between two nitronyl groups. Therefore, the conclusions obtained in this study are of interest to understand the magnetic interactions in the α-nitronyl nitroxide crystals. The second dimer was selected because is one of the model systems taken previously to proof the validity of the McConnell-I model.[6]

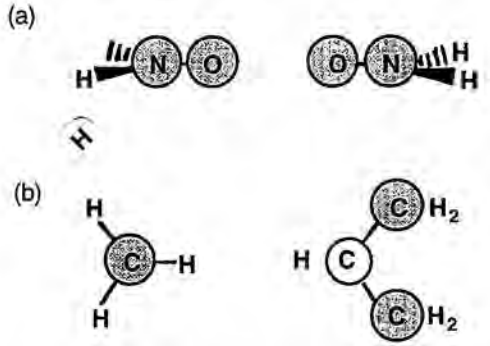

FIGURE 1. Spin densities for the isolated fragments of (a) the H_2NO dimer, and (b) the methyl and allyl radicals (shaded atoms: positive spin density, unshaded atoms: negative)

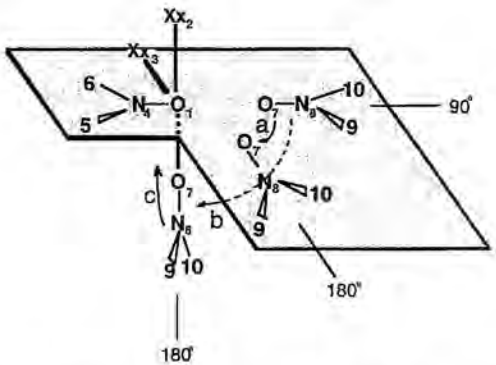

FIGURE 2. Scans carried out with the H_2NO dimer. The two extreme configurations are marked as 90 and 180 degrees.

Ab initio computations at the CASSCF and other levels with very extended basis sets (the smallest one was a 6-31+G(d) basis) give for the isolated fragments the spin distribution shown in Figure 1 (in a diagrammatic qualitative form).

We evaluated the singlet-triplet energy difference of the H_2NO dimer along the two directions of the space indicated in Figure 2: one scan is done

keeping all the atoms in the same plane (the shaded plane of Figure 2); the second scan is in the C_s plane of the fixed fragment (the left one in Figure 2) perpendicular to the shaded plane. In both cases the shortest contact is the O···O distance, kept frozen at 3Å for this study. We selected these geometrical arrangements because they are characteristic of many NO···ON orientations found in some α-nitronyl nitroxide crystals. According to the McConnell-I model, in all the points of the scans one overlaps atoms bearing atomic spin density of the same sign. Therefore, such model predicts that the most stable spin state should be always the singlet (the antiferromagnetic one).

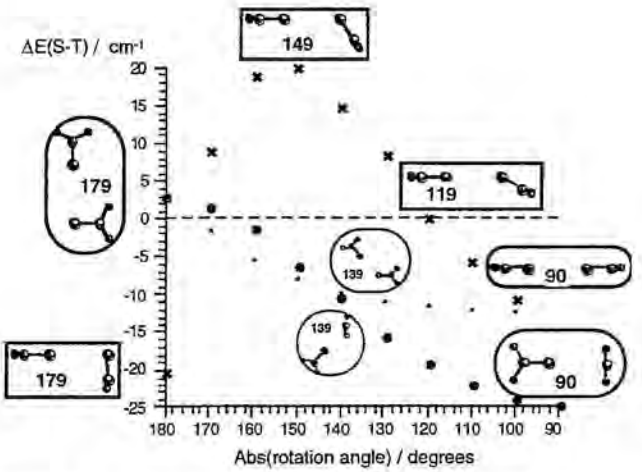

FIGURE 3. Variation of the singlet-triplet energy difference in the two scans performed on the H_2NO dimer (see text).

We computed the singlet triplet energy difference using the CASSCF method and the 6-31+G(d) basis set. The CAS space was a small (2,2) composed of two orbitals and two electrons (the two unpaired electrons of the two fragments and the π orbitals in which they are located). The singlet-triplet energy difference obtained in these computations is shown in Figure 3, along with the angle and geometrical conformation of the dimers in some

points of the curve. The scan within the shaded plane is always antiferromagnetic (the ground state is the singlet), in good agreement with the McConnell-I predictions. However, this is not the case for the scan along the plane perpendicular to the shaded one. Here *one finds a region in which the dimer behaves ferromagnetically, against the McConnell-I predictions* (the angles in the range from around 119° to 175°).

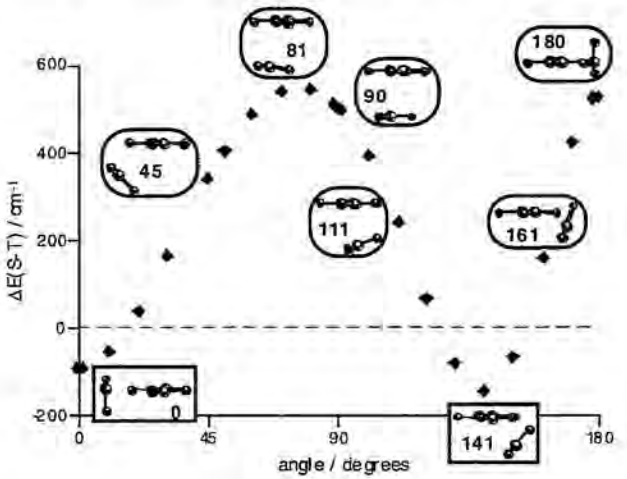

FIGURE 4. Variation of the singlet-triplet energy difference with the H-C_{allyl}···C_{methyl} angle for the methyl-allyl dimer (see text).

To test if the failure of the McConnell-I model predictions was just a exceptional behavior in the H_2NO dimer, we carried out a similar study on the methyl-allyl dimer. In this system we evaluated the singlet-triplet energy difference as the carbon methyl (C_{methyl}) rotates around the central C atom of the allyl (C_{allyl}) fragment, forcing the C_{methyl} to lye in the C_s plane perpendicular to the C-C-C plane of the allyl (see Figure 4 for some snap-shots). The angle of the variation is the H-C_{allyl}...C_{methyl} angle. At 0° C_{methyl} is in the C-C-C plane of the allyl, and sitting on the H end of the C_{2v} axis which passes through the central allyl carbon and the H atom attached to

it. At 90° the methyl and allyl are in parallel planes, with the C_{methyl} atom on top of the C_{allyl} carbon. At 180° C_{methyl} is in the C-C-C allyl plane, sitting on the C_{2v} axis, but on the C end of this axis. The $C_{allyl}...C_{methyl}$ distance was kept fixed at 3Å. All computations were carried out using the CASSCF method and the 6.31G(d) basis set. The CAS space was a (4,4), which includes all the π orbitals and electrons of the isolated methyl and allyl fragments in the active space.

According to the McConnell-I model the ferromagnetic state (the triplet) should be the ground state when $H\text{-}C_{allyl}\cdots C_{methyl} = 90°$, in good agreement with what say the ab initio results. However, the state stability should not change for small variations of the $H\text{-}C_{allyl}\cdots C_{methyl}$ angle when the distance is kept constant. Figure 4 says that this is not the case: as the angle goes to 180° the singlet becomes more stable, being the most stable state around 141°. Therefore, once more the McConnell-I model fails to explain the magnetic character in some regions of the potential energy surface.

One can argue that the regions in which the McConnell-I model has failed are out of the original proposal of McConnell, who designed its model for π-π interactions. However, as we saw before,[8] its apparent success in the π-π case comes from a fortuitous cancellation of terms associated to the high symmetry of the problem, a situation that will not hold in general. We have found enough reasons here as to stop thinking that the McConnell-I model is a good and general procedure to carry out the analysis of the magnetic properties of a molecular crystal.

Acknowledgments

This work was supported by the DGES (Project No. PB95-0848-C02-02) and CIRIT (1997SGR00072). We also thank CESCA and CEPBA for a generous allocation of computer time in their machines. M.D. and P.L. acknowledge CIRIT and MEC for their doctoral grants.

References

[1.] (a) M. Kinoshita, *Jpn. J. Appl. Phys.*, **33**, 5718 (1994) and references therein.
(b) J. S.Miller; A. J. Epstein, *Angew. Chem. Int. Ed. Engl.*, **33**, 385 (1994).
(c) O. Kahn, *Molecular Magnetism*, (VCH Publishers, New York, 1993).
(d) D. Gatteschi; O. Kahn; J.S. Miller; F. Palacio, (eds.), *Molecular Magnetic Materials* (Kluwer Academic Publishers, Dordretch, 1991).
(e) H. Iwamura; J.S. Miller (eds.), *Mol. Cryst. Liq. Cryst.*, **232/233**, (1993).
(f) J.S. Miller; A.J. Epstein (eds.) *Mol. Cryst. Liq. Cryst.*, **272-274**, (1995).
(g) K. Itoh; J.S. Miller; T. Takui (eds.) *Mol. Cryst. Liq. Cryst.*, **305-306**, (1997).

[2.] (a) H. M. McConnell, *J. Chem. Phys.* **39**, 1910 (1963)
(b) McConnell, H. M. *Proc. Robert A. Welch Found. Conf. Chem. Res.* **11**, 144(1967).

[3.] A. Zheludev; V. Barone; M. Bonnet; B. Delley; A. Grand; E. Ressouche; R. Subra; J. Schweizer, *J. Am. Chem. Soc.*, **116**, 2019 (1994).

[4.] J.J. Novoa; F. Mota; J. Veciana; J. Cirujeda, *Mol. Cryst Liq. Cryst.*, **271**, 79 (1995).

[5.] (a) A. Izuoka; S. Murata; T. Sugawara; H. Iwamura, *J. Am. Chem. Soc.*, **107**, 1786 (1985).
(b) A. Izuoka; S. Murata; T. Sugawara; H. Iwamura, *J. Am. Chem. Soc.*, **109**, 2631 (1987).

[6.] (a) A. L. Buchachenko, *Mol. Cryst. Liq. Cryst.*, **176**, 307 (1989).
(b) K. Yamaguchi; Y. Toyoda; T. Fueno, *Chem. Phys. Lett.*, **159**, 459 (1989).

[7.] (a) M. Deumal; J. Cirujeda; J. Veciana; J. J. Novoa, *Adv. Mater.* (1998) (in press).
(b) M. Deumal; J. Cirujeda; J. Veciana; J. J. Novoa, (submitted)

[8.] M. Deumal; J. J. Novoa; M. J. Bearpark; P. Celani; M. Olivucci; M. A. Robb, *J. Phys. Chem.* (1998) (in press).